Jointing and fracturing of flat-lying rock masses, Illawarra Coal Measures, southeastern Sydney Basin New South Wales, Australia

Hossein Memarian
University of Wollongong

JOINTING AND FRACTURING OF FLAT-LYING ROCK MASSES, ILLAWARRA COAL MEASURES, SOUTHEASTERN SYDNEY BASIN, NEW SOUTH WALES, AUSTRALIA.

A thesis submitted in fulfilment of the
requirement for award of the degree of

DOCTOR OF PHILOSOPHY

from

THE UNIVERSITY OF WOLLONGONG

by

HOSSEIN MEMARIAN

(M.Sc. University of Waterloo, Canada)

Department of Geology

1994

The content of this thesis are the result of original research by the author and material contained herein has not been submitted to any other university or similar institution for a higher degree.

H. Memarian

Please see print copy for image.

This thesis is dedicated to my wife.

ABSTRACT

Fracture mapping of the Late Permian Illawarra Coal Measures, between Coalcliff and Wollongong, shows that joints developed originally in extension (mode I) and were faulted in subsequent events. Conjugate joint sets are a consequence of two separate fracturing events. Extension joints developed in joint units of different size and shape, with boundaries at changes in mechanical properties. The fracture pattern of extension joints in a joint unit is related to the mechanical properties of the rock mass and loading history. Joints with regional distribution fall into two, early and late formed, groups. Group I regional joints strike N-NNE, NE and SE. These joints propagated horizontally and never interfered with each other. All the existing interactions are the result of succeeding events.

Group I regional joints were recracked subsequently. Recracking commenced with jointing and continued with lateral slip. All the faulted joints are classified as hybrid fractures. Faulted joints grew horizontally by the connection of recracked segments. En echelon arrays are the result of vertical propagation of faulted joints into intact rock. Recracking of rock also formed a set of secondary joints parallel to σ_1. The sense of movement along conjugate faulted joints and orientation of sets of secondary joints, are related to 3 compressional stress fields namely: NNE-SSW, E-W and SSE-NNW. The intensity of recracking and the amount of lateral slip is mostly related to the strength of infilling materials, the angle between the fracture and the maximum compression direction, and the number of compressional events imposed on the fracture.

In the southeastern Sydney Basin, some of the northwesterly trending normal faults were active during Late Permian deposition. Slip along these listric faults formed northwesterly trending gentle folds. A quasi-extensional regime, related to the forebulge of the Sydney Basin, reactivated appropriately oriented basement faults, which in turn, generated grabens in the cover. Group I regional joints formed after lithification and are classified as burial joints. Normal faults and dykes also developed during the Mesozoic. It is considered that the later part this episode was related to rifting that predated the opening of the Tasman Sea and its subsequent extensional history. The youngest deformational events were compressional. Group II regional joints and reactivation of pre-existing fractures occurred during these post-Early Tertiary events. Anticlockwise motion of the Australian crust, relative to the rest of the enclosing plate,

caused by the collision between the Indo-Australian and Pacific Plates, may have been responsible for the NNE-SSW compression in the eastern part of the Southern Coalfield. The E-W compression most probably postdated the NNE-SSW event.

Rock fracturing controlled the present configuration of the coastal platforms. Fractures in bedrock also governed the location of many landslips in talus along the Illawarra Escarpment. A method is presented for predicting the presence of dykes in underground coal mines, using adjacent joints.

CONTENTS

LIST OF FIGURES

LIST OF TABLES

CHAPTER 1

INTRODUCTION

1.1 OBJECTIVES

This thesis addresses structural aspects of rock fracturing, as well as some of their engineering implications, for a flat-lying sequence in the southeastern Sydney Basin (Figure 1.1). The study area extends for 20 km from Coalcliff to Wollongong (Figure 1.2), and contains the Late Permian Illawarra Coal Measures along the coast and slopes of the Illawarra Escarpment. The main aim of this research is to conduct a structural analysis and address current broad research problems concerning the jointing and fracturing of rock. Many questions about joints and their origin are still unanswered today or present answers are ambiguous (Ramsay & Huber 1987). Questions dealt with in this thesis are listed below.

1. What is the fracture pattern of the southeastern part of Sydney Basin?
2. What factors control joint orientation, size, shape, spacing, and clustering?
3. In what circumstances do joints of one set, or joints of different sets, interact with each other?
4. What is the effect of rock type, sedimentary structures, rock unit, and weathering, on rock fracturing?
5. In which part of the tectonic cycle (burial, diagenesis, tectonic compression, extension, uplift, and erosion) does each joint set form?
6. Is there any relationship between joints and adjacent structures such as folds, faults and dykes?
7. What is the significance of rock fracturing for civil and mining engineering practice?

Describing the formation of discontinuities in rock masses, which is still

poorly understood, is a major task and a very difficult topic (Aydan & Kawamoto 1990). Fortunately, as Hancock (1985) stated, the study of brittle mesostructures are most rewarding in platforms where macrostructures are rare and there has not been significant intraterrain rotations. This is the case for the southeastern Sydney Basin, where the rocks are almost horizontal.

The Late Permian Illawarra Coal Measures host economic coal seams, which are utilised in coke manufacture and power generation (Figure 1.3). The area contains more than 1700 boreholes, as well as exploratory trenches, tunnels and geophysical profiles (Hutton *et al.* 1990). Although an extensive literature is published which deals with different aspects of geology and geological engineering of the succession, no comprehensive studies of jointing and fracturing of rock have been carried out. The few previous works on jointing were mostly based on remote sensing techniques (e.g. Bowman 1974; Mauger *et al.* 1984; Lohe *et al.* 1992).

1.2 DATA BASE

The outcrops which have been studied are mostly horizontal rock platforms and adjacent vertical cliffs. The main outcrops, are numbered from 1-30 and named after each suburb or locality (Table 1.1, Figure 1.4). Field data on fractures where gathered in three different ways: (1) mapping all the outcrop, (2) mapping along scanlines, and (3) random sampling.

Sampling the orientation and distribution of vertical planes is easiest along a horizontal surface. In the study area, joints are normally vertical and horizontal surfaces of platforms are suitable places for their study. The vertical face of coastal cliffs and the seaward edge of platforms are used for examination of vertical changes in joint characteristics as well as their relation to bedding and other geological features.

In the northern platforms (Outcrops 1-9), the entire outcrop was mapped. 1:8000 and 1:4000 scale aerial photographs were enlarged to 1:1000, 1:500 and 1:250 scales and used as base maps. Data for the central platforms (Outcrops 11-25) were gathered along scanlines. All of the fractures and other structures were mapped and their characteristics were recorded along 5 to 10 m wide scanlines. Where the type of termination, bifurcation and lateral movement of a joint or its interaction with the other fractures were important, a joint was followed as far as 100 m away from the axis of the scanline. In this study, 53 scanlines with the total length of 5273 m were surveyed. A total number of 4549 joints were recorded along scanlines (Table 1.2). Directions of scanlines were selected so that the most meaningful data was gathered from the joint population, as well as other structures. Terzaghi (1965) recommended that sampling should be random, otherwise the some joint sets might be overlooked. Scanlines are fairly evenly distributed in all directions (Figure 1.5). For a few southern platforms (Outcrops 26-30), which are stratigraphically below the coal measures sequence, data were gathered from randomly spaced circles of 1-2 m in diameter, or along randomly oriented intersecting lines.

Another factor, which can influence the sampling, is the distance between outcrops. In northern parts of the study area, where the Illawarra Coal Measures are exposed, rock platforms are closely spaced and the gap between them is mostly filled by exposures along vertical cliffs.

The linear pattern of the study area, stretching along the coast from northeast to southwest, could be the most severe drawback for valid sampling. Unfortunately, outcrop of Illawarra Coal Measures is restricted to the east of the escarpment (Figure 1.2). West of the escarpment the area is mostly covered by the Triassic Hawkesbury Sandstone. In the southeastern Sydney Basin, underground workings normally follow one seam (Bulli or Wongawilli), and the cores of widely spaced drill holes could not

fulfil the requirements of the present study. Data from the few previous fracture and lineament surveys of this region (Bowman 1974; Mauger *et al.* 1984; Lohe *et al.* 1992), as well as information reported from different coal mines (Figure 1.3), were used as supporting evidence.

The linear pattern of the study area has one advantage. In the southeastern part of the Sydney Basin, most of the major structural features, i.e. folds, faults, dykes, and many joints, have a southeasterly trend. The northeast layout of the study area intersects these features at a high angle, which best reveals their characteristics.

Presentation of field data

"It is not enough to make accurate data collection; it is of equal importance to choose a simple, clear way of representation that makes a complete record of data" (Ramsay & Huber 1987). In flat-lying sequences, where joints are mostly vertical, rose diagrams are frequently used for presenting orientation data. Rose diagrams have the disadvantage that they misrepresent data by exaggerating large concentrations and suppressing small ones (Brown 1981). In many instances, where we are interested in parameters such as the spatial changes in the orientation and frequency of the joints, rose diagrams are of no help. As an alternative, the plot of fracture orientations, verses the distance along a scanline, is used. Scanline charts clearly present the orientation and frequency of each fracture set, show any changes in fracture orientation or frequency which can be related to rock type, bed thickness or other factors. Using the orientation of the scanline, the spacing of each set can be readily calculated (Fig 1.6).

Thin sections were used to study microfractures, joint infillings and host rock petrology. Coloured photographs were also taken and used to examine relationships

between fracture sets. X-ray diffraction was used for the identification of fine-grained materials, especially joint infillings.

Platform maps and the results of scanline surveys, are presented in the Appendices 3 and 4.

1.3 STRUCTURAL SETTING

Sydney Basin

The Sydney Basin, is located along the central coast of New South Wales (Figure 1.1) with an onshore area of around 36000 km^2 and a length of 380 km in a NNE direction (Mayne *et al.* 1974). It forms the southern section of the Sydney-Bowen Basin System (Lohe & McLennan 1991).

The structural history of the Sydney Basin is difficult to decipher, because there are few reliable ways for the absolute or relative dating of deformation events (Shepherd & Huntington 1981). The Sydney Basin developed in the Late Permian-Triassic as a retro-arc foreland basin (Scheibner 1976; Herbert 1980; Jones & Hutton 1984). Retro-arc basins develop behind continental magmatic arcs and exhibit a marked asymmetry. The New England Fold Belt represents the magmatic arc which bounded the Sydney Basin to the east and north (Figure 1.1). Strong crustal movements began in the Late Permian and resulted in uplift of the New England Fold Belt. These crustal movements have been termed the Hunter-Bowen Orogeny and caused significant subsidence and deposition in the Sydney Basin. The basement of the Sydney Basin consists of the Lachlan Fold Belt (Figure 1.1). The structure of the fold belt may have influenced deposition and structural patterns in the basin (e.g. Cook 1969; Clark 1992; Lohe *et al.* 1992).

Within the Sydney Basin, a thick succession of shallow marine and terrestrial strata were deposited during the Permian and Triassic periods (Mayne *et al.* 1974).

There has been some debate about the thickness of the sedimentary succession eroded from the Sydney Basin. Most recently, Faiz and Hutton (1993) proposed a maximum of 2.5 km of cover thickness over the Illawarra Coal Measures in the southeastern Sydney Basin, of which up to 2000 m has been removed by erosion.The apparently flat lying sequence of the Sydney Basin has been affected by a variety of post-depositional deformations, principally expressed by episodes of faulting (Lohe & McLennan 1991). In the Sydney Basin, deformation is more intense towards the north, adjacent to the Hunter Thrust (Figure 1.1)

Southern Coalfield

The southern Sydney Basin represents a more stable and undisturbed area. This area covers what is known as the Southern Coalfield of NSW (Figure 1.3). The terms "shelf" and "trough" have been used for areas of low and more rapid subsidence rate, respectively. Most of the southern Sydney Basin can be considered a shelf area (Bamberry 1992).

The study area is located in the eastern and coastal section of the Southern Coalfield. Structural elements of the studied area are folds, faults, joints, and dykes. In the Southern Coalfield, structural information has been obtained mostly from colliery workings, and coal, oil and gas exploration boreholes.

Folds

The dominant structure in the Southern Sydney Basin is the Camden Syncline, which trends N 5° E and plunges gently to the north at 1° or less (Figure 1.7). A series of very broad, northwesterly plunging minor folds occur on the eastern limb of the Camden Syncline (Figure 1.7). Regional dips are normally around 2° and local dips rarely exceed 5° (Wilson 1975). Some monoclines also occur in the Southern

Coalfield. Folds and their relations with brittle fractures are presented in Chapters 4 and 6.

Faults

In the southeastern Sydney Basin, faults are mostly normal and concentrated in the eastern half. Normal faults have displaced both Triassic and Permian strata. It has been suggested that reactivation of the pre-Permian basement faults has had an important influence on the fault pattern of the Southern Coalfield (Clark 1992). At the level of the coal seams, normal faults trend either N-NNE or ESE-SE. Apart from major faults with large displacements, these faults have no surface expression (Wilson *et al.* 1958). The ESE-SE faults dominate the structural map of the coalfield (Shepherd 1989). Shepherd (1990) mapped two zones of N-NNE faults close to the coast, each comprises a large number of normal faults with throws of up to 9 m (Figure 1.7).

Although lateral movements are frequent, no strike-slip faults developed initially in the study area. All strike-slip movements took place along pre-existing fractures. Faults and their relation with joints are presented in Chapter 4. The relation between faults and other structures is discussed in Chapter 6.

Joints

Very little has been published on the jointing in the southeastern part of the Sydney Basin. Bowman (1974) reported four sets of joints, striking N, NE, ESE and SE, for the Wollongong 1:50,000 Geological Map. Analysis of lineaments defined from satellite imaginary, indicates that they have similar orientations to the joints in the study area (Mauger *et al.* 1984). Among the known lineaments, the Coastal Lineament is a major structure in the area, corresponding in part to the South Coast

Warp (Figure 1.7; Mauger *et al.* 1984; Sherwin & Holmes 1986).

The study of joints is the main concern of this thesis. Most joints fall into three major orientations, namely N-NNE, NE and SE. Two groups of systematic joint sets, with regional distribution, are mapped in this part of the basin. Local joints are mostly related to monoclines or dykes. The main characteristics of joints are discussed in Chapter 2. Other aspects of fracturing of rock are covered in the rest of this thesis.

Igneous activity

The Sydney Basin succession is intruded by igneous bodies, which range in age from Late Permian to Tertiary. The igneous masses occur as dykes, sills, and volcanic plugs or necks (Branagan 1985). Dykes may occur separately or as members of swarm. Dykes were mostly injected through fractures which were propagated by magma pressure. The rocks are mostly basalt and dolerite (Bowman 1974). In the Southern Coalfield, most dykes strike ESE with other sets having strikes of NE and NNE. Dykes, and their relation to joints, are discussed in Chapter 3.

Deformational events

Fracture mapping has enabled identification of four phases of deformation active from the time of Late Permian deposition until the present. Syn-depositional mild warping and normal faulting has been recognised for the southern Sydney Basin (Wilson *et al.* 1958; Bunny 1972; Jakeman 1980) and has been confirmed by the present study. The regional joint system formed after deposition and developed in three major directions. All fracture sets were reactivated with common strike-slip movements. Chapter 5 is devoted to recracking of pre-existing fractures. The tectonic setting of this part of the basin is discussed in Chapter 6.

Mine roof conditions, gas outbursts, water inrush into working areas, gas migration, as well as slope instability along the escarpment all are mainly controlled by rock fractures and late stage compressional forces. Implications of jointing and fracturing of rock for engineering practice are presented in Chapter 7.

1.4 STRATIGRAPHY

On the eastern side of the Sydney Basin, the Late Permian Illawarra Coal Measures, overlie marine sedimentary rocks of the Shoalhaven Group. The coal measures are, in turn, overlain by alluvial sedimentary rocks of the Narrabeen Group and Hawkesbury Sandstone (Hanlon 1956a, b; Wilson 1969; Bowman 1972, 1974). The currently-accepted stratigraphic nomenclature was formalised by the Standing Committee on Coalfield Geology of New South Wales (SCCG 1971). The stratigraphy of the Southern Coalfield is summarised in Table 1.3.

Shoalhaven Group

The Shoalhaven Group consists of about 1000 m of alternating sandstone and siltstone of shallow marine origin (Lohe *et al.* 1992). The highest unit of the Shoalhaven Group is the Broughton Formation (Carr 1983), and this has been chosen as a reference for correlation of the fracturing of these deposits with the overlying Illawarra Coal Measures.

In the southern part of the study area, the upper part of the Broughton Formation consists of massive to poorly bedded grey-green volcanoclastic fine-grained sandstone (Outcrops 28-30). Igneous pebbles and boulders, up to 250 mm across, are common in fine-grained rocks (Jones & Hutton 1984). Farther to the south, and outside of the study area, this formation contains a number of tabular latite flows. A northeasterly trending volcanic chain, which was developed to the

east of the present coastline in the early Late Permian, was the source of these igneous bodies and related units in the lower Illawarra Coal Measures (Carr & Facer 1980; Jones *et al.* 1986).

Illawarra Coal Measures

The Late Permian Illawarra Coal Measures is a sequence of sandstone, siltstone, mudstone and coal with minor conglomerate and tuffaceous beds (Hutton *et al.* 1990). It has an average thickness of approximately 210 m. The thickness exceeds 500 m in the north of the coalfield and is less than 50 m thick in the south and west (Bamberry 1992). The Illawarra Coal Measures is subdivided into two subgroups, namely the lower Cumberland Subgroup and the upper Sydney Subgroup (Table 1.3; Wass *et al.* 1969).

Sedimentation within the Illawarra Coal Measures occurred in an alluvial environment with abundant peat deposition. The preservation of coal is dependent upon active subsidence of the basin of deposition to maintain such areas below ground water level. This normally happens when the tectonic activity is relatively high. This was the case for the Sydney Basin which was located on the continental side of the active New England Fold Belt (Figure 1.1).

Cumberland Subgroup

The Cumberland Subgroup, forming the lower part of the Illawarra Coal Measures, contains two formations: the Pheasants Nest Formation at the base, and the Erins Vale Formation at the top. The subgroup consists dominantly of quartzose and lithic sandstone. The Cumberland Subgroup is disconformably overlain by the Sydney Subgroup which represents the first incursion of sediment from the New England Fold Belt into the southern Sydney Basin (Jones & Hutton 1984).

The stratigraphically lower Pheasants Nest Formation consists of pebbly flat and cross-bedded volcanoclastic sandstone containing plant debris in thin silty partings. The lowermost part of the unit consists of thinly interbedded sandstone, siltstone, and claystone which contrasts with thick beds of sandstone in the top part of the underlying Broughton Sandstone (Sherwin & Holmes 1986). Stratigraphically higher in the Pheasants Nest Formation occur at least two thin, silty coal seams (Jones & Hutton 1984). The unit has a thickness of about 75 m throughout most of the area, but thickens to the northeast. In the study area, the Pheasants Nest Formation crops out south of Bellambi at Outcrops 26 and 27 (Table 1.1).

The Erins Vale Formation is essentially coal free. This unit is typically a fine-grained, quartz-lithic to lithic sandstone. The clastic particles are quartz, feldspar, volcanic rock fragments, quartzite, and chert. The matrix contains abundant carbonaceous material and secondary calcite (Bunny 1972). In the study area, this formation crops out along the coast, between Thirroul Beach and Woonona (Outcrops 22, 24 & 25).

Sydney Subgroup

The Sydney Subgroup, extends from the top of the Cumberland Subgroup to the base of the Narrabeen Group (Figure 1.8, Table 1.3). It contains the economic coal seams of the Southern Coalfield and is more extensively developed than the underlying subgroup. Details of the stratigraphy of the Illawarra Coal Measures were given by Bowman (1970, 1974), SCCG (1971), Bunny (1972), Hutton *et al.* (1990) and Bamberry (1992).

Almost all of the sandstones in the Sydney Subgroup are litharenite as defined by Folk (1968). The most abundant detritus are fine-grained and altered volcanic clasts (Bowman 1974). The sandstones generally have a clay matrix and either a

limonite or carbonate cement. The clay is mainly illite, with smaller amounts of kaolinite. Sandstones become finer grained upwards with generally better sorting at the base of each unit. Siltstone and claystone normally have organic material, which is scattered as fine material or larger fossils. The argillaceous sediments consist of illite, partially to completely degraded illite, quartz, and minor amounts of plagioclase and kaolinite (Sherwin & Holmes 1986). The economically important coal seams in the Southern Coalfield are, in descending stratigraphic order, the Bulli, Balgownie, Wongawilli, and Tongarra Coals (Table 1.3, Figure 1.8)).

The basal unit of the Sydney Subgroup is the Wilton Formation which disconformably overlies the Cumberland Subgroup. The basal Wilton Formation consists of fining upward cross-bedded sandstone overlain by horizontally interbedded fine-grained sandstone and siltstone, mudstone and coal. In coastal exposures at Thirroul (Outcrop 21), the Woonona Coal conformably overlies coarse sandstone of the lower Wilton Formation (Figure 1.8). The sequence from the Woonona Coal Member to the Tongarra Coal is laminated mudstone, siltstone and sandstone, that grades into claystone and then into the Tongarra Coal. The carbonaceous siltstone contains scattered dropstones up to 200 mm across, as well as common plant debris.

The Tongarra Coal, which occurs throughout most of the Southern Coalfield, is composed of interbedded coal, carbonaceous shale and tuffaceous claystone. In the study area, along the coastal outcrops between Woonona and Wombarra, the Tongarra Coal is composed of four coal plies separated by laterally persistent bands of light-coloured tuffaceous claystone (Hutton *et al.* 1990). The Wilton Formation is exposed in the central part of the study area (Outcrops 10-20).

Conformably overlying the Tongarra Coal is the Appin Formation, which is subdivided into the lower Bargo Claystone and the upper Darkes Forest Sandstone Members (Table 1.3). The Appin Formation forms a thick coarsening upward

sequence recognised throughout the Southern Coalfield. The Bargo Claystone Member, which overlies the Tongarra Coal, consists of mid-grey to black claystone, siltstone and sandstone (Sherwin & Holmes 1986). A sandstone interbedded with siltstone, named the Austinmer Sandstone Member, is present near the base of this unit (Bowman 1974). The outcrop of this sandstone is generally poor and highly weathered. The boundary between Bargo Claystone and the overlying Darkes Forest Sandstone Member is often transitional. It consists of light-grey, fine-grained, quartz lithic sandstone with interbedded siltstone, which becomes coarser upward. This unit is generally highly weathered, resulting in poor outcrop.

The Allans Creek Formation consists of two (or more) carbonaceous and coaly intervals separated by an interbedded sequence of claystone, siltstone and fine to medium-grained lithic sandstone (Hutton *et al.* 1990). Rapid lateral variation is typical, but the unit commonly commences and ends with coaly sequences separated by an interval of essentially non-coaly, clastic strata (Sherwin & Holmes 1986). The upper seam or coaly unit, immediately below the Kembla Sandstone, is referred to as the American Creek Coal Member (Fig. 1.8). A sharp and slightly disconformable boundary (Jakeman 1980) separates the Allans Creek Formation from the overlying Kembla Sandstone. This formation, along with Allans Creek Formation, is exposed at the base of the escarpment north of the Scarborough Fault (Outcrops 5 to 7).

Overlying the Allans Creek Formation is the Kembla Sandstone, which is one of the most persistent clastic units in the Southern Coalfield. It is generally a fine to medium-grained, light grey, lithic sandstone which becomes very fine-grained near the top (Sherwin & Holmes 1986). This unit combined with the upper Wongawilli Coal, represents a useful marker interval over most of the coalfield (Hutton *et al.* 1990).

The Wongawilli Coal, which conformably overlies the Kembla Sandstone,

consists of 9 to 11 m of coal, carbonaceous shale and claystone bands (Figure 1.8). The light-coloured claystone bands are thought to have a tuffaceous component. Approximately 6 m above the base of the Wongawilli Coal occurs a 1 m bed of tuffaceous claystone to sandstone, which persists over most of the Southern Sydney Basin (Clark 1992).

Within the Eckersley Formation, which conformably overlies the Wongawilli Coal, Jones and Hutton (1984) defined three main fining-upward sequences each ending with a coal member. The Eckersley Formation changes greatly in thickness, and to a lesser extent in rock type, but is persistent over the entire Southern Coalfield (Clark 1992). In coastal outcrops, between Coalcliff and Clifton, the unit is generally between 20 and 40 m thick and consists predominantly of sandstone (Figure 1.8). In cliffs near Scarborough and Clifton, Hanlon (1956b) formally named the Balgownie, Cape Horn and Hargrave Coal Members and the Lawrence Sandstone Member. Along the coast the Hargrave and Cape Horn Coal Members consist of coal and carbonaceous mudstone, with their thickness 0.3 and 1 m respectively. The Balgownie Coal Member, which is approximately 1 m thick, is separated from the overlying Bulli Coal by 5-15 m of coarse to fine-grained sandstone and minor claystone and sandstone (Outcrops 3, 4).

The Eckersley Formation is overlain gradationally by the Bulli Coal which is the uppermost formation of the Illawarra Coal Measures (Sherwin & Holmes 1986). The Bulli Coal consists of well banded coal and carbonaceous shale. The thickness of the Bulli Coal is greatest in the northern part of the coalfield, and decreases to the south.

Narrabeen Group

The Triassic sedimentary sequence consists of the Narrabeen Group, Hawkesbury

Sandstone and Wianamatta Group (Table 1.3), and forms a significant thickness of overburden for the Illawarra Coal Measures. The Early Triassic Narrabeen Group consists of thick interbedded sandstone and claystone layers. The Narrabeen Group was derived from the north, due to uplift of the New England Fold Belt (Herbert 1980). In contrast, the Hawkesbury Sandstone was derived from a western and southern source (Jones & Hutton 1984).

The lowermost rock unit of the Narrabeen group is the Coal Cliff Sandstone. This unit is chosen as a reference for comparison of fracturing of the Illawarra Coal Measures with younger units. At Coalcliff (Outcrops 1, 2) the Coal Cliff Sandstone forms a low coastal cliff, slightly above sea level. South of the Clifton Fault this unit is about 60 m above sea level. This unit, which is around 10 m thick in the study area, consists of a homogeneous, medium to coarse-grained lithic sandstone with a number of pebbly bands and a few beds of grey shale and brown clay ironstone. Intraclasts are common and overbank deposits are thin and ferruginized (Jones & Hutton 1984).

CHAPTER 2

DEVELOPMENT OF SYSTEMATIC JOINTS

2.1. INTRODUCTION

The fracture pattern of the Sydney Basin is remarkably complex for relatively flat-lying sedimentary rocks and a better understanding of this pattern is of importance, to coal mining and civil engineering works (Shepherd & Huntington 1981). Most data on lineaments, fractures, and joints in the southern Sydney Basin, have come mainly from satellite imagery and air photo interpretation with some collection of fracture data from coal mines (see Connelly 1970; Bowman 1974; Mauger *et al.* 1984). Very little has been published on the jointing in the southeastern part of Sydney Basin.

Shepherd and Huntington (1981) studied a large geological and geophysical data base, in order to obtain an overview of fracture systems and stress fields of the Sydney Basin. They emphasised that overall structure and origin of the Sydney Basin is still poorly known, and that the interpretation of the fracture pattern is so far at an early stage. Their synthesis demonstrated that the basin has undergone numerous tectonic and magmatic events, the spatial and temporal relationships of which are still partly unknown. The most recent work on the fracture pattern of the Sydney Basin was conducted by Lohe *et al.* (1992).

Definitions: Brittle fractures that occur in rock have been defined differently within the geological literature. The following section briefly defines nomenclature which is used throughout the present work. A 'fracture' is a planar or curviplanar discontinuity in a rock body caused by strain (Gabrielsen 1990). It includes cracks, joints, veins, dykes and faults. 'Joints' and 'cracks' are fractures of geological origin along which no appreciable movement has occurred (Hodgson 1961a; Price 1966; Ramsay & Huber

1987).

A joint can be closed, open or filled with minerals or fluids. A group of parallel or subparallel joints form a 'joint set' (Hodgson 1961a; Ramsay & Huber 1987). A 'joint system' is a pattern of joints consisting of two or more sets symmetrically arranged with respect to each other (Dunne & Hancock 1994). A 'conjugate system' comprise two sets enclosing an acute angle.

A planar joint belonging to a regularly oriented set is called a 'systematic joint', while nonparallel joints that are generally nonplanar are 'nonsystematic joints'. 'Cross joints' are a group of roughly planar nonsystematic joints that extend across the interval between systematic joints (Hodgson 1961a, b). Cross joints should not be confused with cross strike joints (Badgley 1965; Hancock & Engelder 1989) which are vertical joints that cut fold hinges at a high angle.

Joints are categorised as either regional or local. Engelder (1982) used regional joints for those that persist from outcrop to outcrop over a broad region. For the present study 'regional joints' are defined as those that are well developed over the study area and can be traced beyond it, both horizontally and vertically. 'Local joints' have a limited distribution and are normally related to a particular structure, such as a dyke or a monocline.

Objectives: This chapter presents a data base gathered during extensive field work, on 30 selected outcrops, along the coast between Coalcliff and Wollongong. Six regional joint sets have been recognised in this area. The present joint pattern has formed cumulatively through time and all of the fracture sets were propagated as extension joints (mode I). Regional and local joints, even those with similar orientations, were differentiated. The role of rock type or pre-existing sedimentary structures, on the development of the fracture pattern are discussed and the concept of 'jointing units' is

introduced. Based on cross cutting and overprinting relations the joints with regional distribution have been placed into early and late formed groups.

2.2. ORIENTATION AND DISTRIBUTION OF JOINTS

One approach to joint analysis is to combine a large amount of data gathered from different outcrops and then identify preferred orientations. In this method, much valuable information could be lost (Nelson 1985). Another method is to interpret the data at each station, or outcrop, prior to regional statistical treatment (Stearns 1969). The later method was used for the present study. All the local joints were separated from the data set before any regional interpretation was attempted.

Different characters of fractures were noted and measured in the field, among them: orientation, spacing, persistence, planarity, termination, surface features, openings, infillings, lateral movement and interactions with other fractures. Displacements along joints as little as 0.5 mm were recorded. More than 10,000 fractures were surveyed during the course of this study. Methods used for gathering field data include mapping of entire outcrops, scanline surveys and random sampling. A total of 5160 m of scanline, 5-10 m wide, was mapped during the course of this study. The orientation of scanlines were chosen in a way to reduce biased sampling (see Priest & Hodgson 1981) (Figure 1.5).

Previous work

Study of joints and other fractures at the surface in the southeastern part of Sydney Basin has been mostly based on Landsat imaginary and air-photo interpretation (Bowman 1974; Mauger *et al.* 1984). The results of these studies usually reflect fracturing of the Hawkesbury Sandstone, which covers most of the Southern Coalfield. Similar studies in underground coal mines are limited to working coal seams and their adjacent roof

and floor strata. For the southeastern Sydney Basin, Bowman (1974) reported four sets of joints with mean directions of 005°, 055°, 105°, and 155°. He arranged these four sets in two systems, each with two sets at near right angles with each other. Analysis of lineaments, defined from satellite imaginary, demonstrated their similarity to trends of the previously reported joints in the area (Mauger *et al.* 1984).

General characteristics

The studied joints are either systematic or nonsystematic (in the sense of Hodgson 1961a). A well developed systematic joint is normally planar and rectangular in shape, with its upper and lower terminations bounded the by upper and lower limits of a single mechanical layer (in the sense of Narr & Suppe 1991) (Figure 2.1). The length of an original joint is generally a few times its height. Joints are principally vertical and developed normal to bedding interfaces (Figure 2.2). Locally joints are non-vertical, but are still steeply dipping. They normally break through irregularities such as clasts, pebbles and fossils.

Systematic joints are segmented, both horizontally and vertically (joint zones in the sense of Hodgson 1961)(Figures 2.3, 2.5). The length of segments ranges between 1 cm up to more than 10 m. In places, segments are connected and a single joint can be traced for more than 100 m (e.g. Scanline 22-CC' or Figure 2.3). Joints are either closed and sealed with calcite and/or siderite or opened. Open members are much longer than closed joints. Some of the joints, show more than one phase of infilling, which indicates subsequent reworking. The open members frequently show dextral and/or sinistral movements of 1-50 mm along their strike. Two adjacent joints might show opposite displacements (see Chapter 5). Systematic joints occur in sets of parallel or sub-parallel fractures (Figures 2.3, 2.4). The distribution of these joints is either regional or local.

Major orientations

Figure 2.6a is a rose diagram of 6967 systematic joints measured all over the study area. These joints are developed in three major orientations, namely N-NNE, NE and SE. Still some other directions occur with a smaller number of joints of regional or local distribution. The study area is divided into the northern, central and southern zones, by the Scarborough and Thirroul Faults. The orientation data for the northern zone, located to the north of the Scarborough Fault, is presented in Figure 2.6b. The lower most part of the Narrabeen Group and the upper parts of the Illawarra Coal Measures are exposed in these outcrops. Figure 2.6c shows the joint pattern of the central part of the study area, which consists of flat laminated siltstones and fine-grained sandstones of the upper Wilton Formation. The southern zone comprises outcrops of the Cumberland Subgroup and the uppermost part of the Shoalhaven Group (Figure 2.6d). Orientation data for different outcrops in these zones are presented in Figures 2.7, 2.8, 2.9 and Table 2.1.

N-NNE joints: N-NNE joints strike between 355° and 020°. Locally, they are subdivided into two N and NNE subsets (Figure 2.6). These joints are most frequent in the northern parts of the study area (Figure 2.6b). Some N-NNE fractures have a vertical component of displacement, ranging between 1 mm and up to 100 cm (see Chapter 4). Joints in this direction have formed during different deformation events (see Chapters 3, 4, 5).

NE joints: The average strike of the NE joints is 043°. A set of 060° striking joints are locally developed in the central zone (Figure 2.6c). Similarly, another set, striking 070°, occur in the southern zone (Figure 2.6d). At Coalcliff, the general characters of

the NE joints are similar to those of the N-NNE joints, except the NE joints are slightly concave towards the SE, both at the platform scale (Figure 2.3b) and at a small scale (Figure 2.4b).

SE joints: The SE joints are best developed in the upper Wilton Formation of the central zone, where they strike 120-130°. In this zone the SE joints are normally very straight and fine. Another subset of these joints, which strike 140°, are locally developed in the central zone (Figure 2.6c). To the north of the Scarborough Fault, SE joints are absent in thick sandstone beds, but strike 135-140° in thin beds of fine to medium-grained sandstone.

Other systematic joints: In addition to N-NNE, NE and SE joints, which comprises both regional and local joints, other directions of joint formation exist. Among them are E and SSE joints which are short and less frequent (Figure 2.10). These joints also have a regional distribution (see Chapter 5). One or more of the regional joint sets may be absent in a single outcrop (Figures 2.7, 2.8, 2.9).

Nonsystematic joints: In the southeastern Sydney Basin, nonsystematic joints are generally open and curved, both in plan and section. The length of these fractures changes considerably. Larger scale nonsystematic joints are developed in thick sandstone beds (Figure 2.3c). These fractures have a tendency to break around inhomogeneities such as pebbles. The frequency of these fractures is not uniform, even in one outcrop (Figures 2.3, 2.4). Nonsystematic joints are not present in all outcrops.

Non-systematic joints terminate at, but do not cross, pre-existing fractures as has been recognised elsewhere (e.g. Babcock 1973; Kulander *et al.* 1979; Gross 1993). These fractures normally connect members of systematic sets (cross joints in the sense

of Hodgson 1961a). They mostly initiate in the mid-region between neighbouring joints and propagate towards them. With pre-existing nonsystematic and systematic joints, as well as bedding surfaces, they form at 90° angles creating T-intersections and H-shaped patterns (Figures 2.1c, 2.3, 2.4, 2.11; Hancock 1985; Gross 1993). Segments of nonsystematic joints which grow toward each other interact (Figure 2.11). Spacing between nonsystematic joints is controlled by distances between pre-existing open joints.

Discussion

In the southeastern Sydney Basin, regional and local joints are often parallel or subparallel to each other, even in a single outcrop. The number of joints in a particular direction is not necessarily an indicator of a regional joint set. Abundances of local joint sets frequently surpasses the regional joints. For example, in Outcrop 19 the most dominant joint set strikes 140° and is locally developed in conjunction with a dyke of similar orientation (Figure 2.8/19). Regional joints are barely recognisable in the joint rosette of this locality. One frequently used technique is to weight the joints of different sets by their length (Bowman 1974). This technique gives misleading results in the southeastern Sydney Basin, where some regional joints were selectively enlarged due to subsequent events (see Chapters 4, 5). One solution to this problem, which was successfully used during the course of the present study, was to filter the local joints from the data set (Figure 2.10).

Six regional joint sets have been recognised in the study area (Figure 2.10). These sets can be categorised into two groups, based on their nature, frequency and age. Group I include the N-NNE, NE and SE regional joint sets, and are older, more dominant and widespread, while Group II, include the NNE, E and SSE regional joints and are less frequent, very short and normally abut against the members of the first group (Table 2.2). Group II joints are dealt with in more detail in Chapter 5.

No significant change in joint pattern is recorded throughout the succession, from the upper Shoalhaven Group, through the Illawarra Coal Measures and into the lower part of the Narrabeen Group (Figure 2.10). Almost all of the regional sets which occur in the basal parts of the succession (southern zone), are present in the upper parts (central and northern zones, Figures 2.6., 2.10). This suggests that the regional joints were mainly formed after deposition of the succession. Changes do occur in the joint pattern between different locations unrelated to stratigraphic position. Figures 2.6b and 2.10 show that in the north of the study area, the N-NNE joints are more frequent and more variable in strike. Another notable example is a 6-10° decrease in mean orientation of N-NNE, NE and SE regional sets in the central zone compared to the northern zone (Table 2.3, Figure 2.10).

In some outcrops, the NE and SE regional joints are almost normal to each other (Table 2.4). It has been argued that an orthogonal joint system may form alternatively (Hancock 1985; Pollard & Aydin 1988; Rives *et al.* 1994). Apart from the 90° dihedral angle, no other firm evidence was found to support this relationship.

On the other hand, a genetic relation exists between systematic and nonsystematic joints. Nonsystematic joints frequently developed subnormal to one of the systematic sets, which for most parts of the study area is the NE set (Figures 2.3, 2.4). Based on the physical characters of nonsystematic joints in the Colorado Plateau, Hodgson (1961a) concluded that these joints were formed under inhomogeneous stresses of possibly local nature. These fractures, despite their nonsystematic nature, have a relatively fixed orientation, which is subparallel to the SE and normal to the NE regional joints (Figure 2.11). Curving perpendicular abutting relations of nonsystematic joints against each other and other pre-existing fractures suggests that they formed sequentially (Gross 1993). Cross-cutting relations indicate that the nonsystematic joints are the youngest natural fractures developed in the southeastern part of the Sydney Basin. Bedding-

parallel horizontal joints are uncommon in the study area and where they exist, they have formed from unloading and more recent weathering.

2.3. ORIGIN OF JOINTS

Mode of formation

Joints are kinematically puzzling structures and their interpretation has generated controversy. In many instances, the origin of an identical set of joints is suggested as either extension or shear fracturing. Joint sets in the Appalachian Plateau (New York area) were interpreted by Engelder and Geiser (1980) and Engelder (1982) as tension fractures, and by Muehlberger (1961) and Scheidegger (1982) as shear joints (see also Bergerat *et al.* 1992 for a similar example in the Colorado Plateau). Conjugate patterns of systematic sets in some outcrops, and the sense of shearing along their strikes, are the main factors used to indicate a shear origin for jointing. Hancock (1985) classified joint sets as extension, hybrid or shear fractures. He suggested 10 different criteria for differentiating between these three types of joints in the field. In this study, joint infillings, lateral displacement, surface marking and conjugate patterns have been found to be the most useful of these criteria for establishing the mode of joint initiation.

Infillings: Subhedral crystals of calcite cover some fracture walls and indicate that the fracture was open at depth (Lorenz & Finley 1991). The infilling also demonstrates that joints were filled with fluids at the time of fracturing, although the infillings themselves may have crystallised from other fluids that subsequently flowed through the fracture system (Wheeler & Holland 1978). The presently sealed calcite filled joints are normally undeformed and show no shear offset (Figure 2.12a).

Some fractures are filled or their walls are stained with brown minerals which have been determined by XRD, on samples from the Coalcliff-Scarborough area, to be

mostly siderite and ankerite. In some fractures more than one phase of calcite infilling is visible (Figure 2.12b). Where both calcite and siderite are present, siderite forms a fine film adjacent to joint walls suggesting that it was the first phase precipitated followed by calcite.

Lateral displacement: Offsets of grain boundaries or fossil fragments along a joint are regarded as evidence for a shear origin of a fracture (Engelder 1982). Figure 2.12a shows a 045° joint which cuts pebbles of a conglomeratic bed, exposed at Outcrop 2. The joint is sealed with a 2 mm thick undeformed calcite vein. No significant shear offset is visible in the plane of this joint (Figure 2.12a). Both in hand specimen and under the microscope, no original lateral movements are visible in closed and/or sealed joints with only one phase of infilling.

Surface marking: Mode of formation and the propagation history of joints can be inferred from their surface markings (see Kulander *et al.* 1979; Bahat & Engelder 1984; Bahat 1986, 1987a, b). In the southeastern Sydney Basin, surface markings are not abundant, probably due to subsequent lateral movements along the joints and also from the more recent destructive effects of wave action and weathering. Surface ornaments are more common in fine-grained, competent and homogeneous rocks, such as medium to fine-grained sandstone.

Some well developed surface markings are exposed along the cliff face at Scarborough. Figure 2.13 shows a long, vertical, rectangular joint, striking 033°. The main joint face, which is located in the upper one third of a sandstone bed, is terminated above by a 3 mm thick mudstone band located 10 cm below the upper boundary of the sandstone bed. A fringe zone is developed in the lower two thirds of the bed, separated from the main face by a well defined shoulder. Here, the fringe zone

consists of a set of closely spaced en echelon cracks (twist hackle faces) connected by abutting steps (twist hackle steps). The en echelon segments strike 026-028°. These segments show a second-order plume structure indicating that their propagation was normal to the direction of propagation of the main joint face, i.e. downward. Figure 2.14 shows an elliptical joint face developed in the lower two thirds of the sandstone bed. This joint is also vertical and strikes 003°. A narrow fringe zone is developed in the lower part of the elliptical joint (Figure 2.14).

The direction of joint propagation of the main joint face was usually horizontal and parallel to the bedding. Propagation of the joint in Figure 2.13 was from left to right, while in Figure 2.14 the joint propagated both to the left and right of its nucleation point. Nucleation points of joints were normally small clasts or some other type of inhomogeneity.

Surface markings, such as plumes, are attributed to an extensional joint origin (Bahat & Engelder 1984; Kulander & Dean 1985; DeGraff & Aydin 1987). Plumose patterns indicate that the joint formed while the main motion was normal to the joint face (opening mode). The bilateral plumose morphology in Figures 2.13 and 2.14 indicate that these joints were opened by propagation away from the central horizontal axis (Engelder 1982).

Conjugate pattern: The size of the dihedral (2θ) angle between conjugate joint sets is another criteria for differentiating between extension and shear joints. Classical interpretations state that conjugate joints intersect at the axis of intermediate stress (σ_2), with the axis of the greatest principal stress (σ_1) bisecting the acute angle (2θ) between the conjugate fractures (Davis 1984). Hancock (1985) suggested the following classification, assuming an angle of internal friction (ϕ) of 30° for the rock. A 2θ angle of less than 10° indicates that the joints formed by extension, while a 2θ angle of 11-

50° suggests that the joints are hybrid. The continuum of orientations enclosing the range of 2θ angles of 10-50° is a joint spectrum comprising extension and hybrid joints. Dihedral angles in excess of 50° indicate a shear origin for the conjugate sets (for more detail see Chapter 5).

Accepting Hancock's classification, the shear origin for the conjugate NNE and NE joint sets at Coalcliff (Figure 2.3), with a dihedral angle around 35°, is rejected. This leaves the extension and hybrid options. Two sets of conjugate joints, with almost identical orientations and a similar 2θ angle with the conjugate set at Coalcliff, are developed in the Scarborough area (Figure 2.14c). Here, members of both sets show surface markings which indicate an extensional origin, as described above. Conjugate joint sets in the Coal Cliff-Scarborough area, with a 2θ angle of less than 40°, are considered the result of two separate extensional events with different orientations.

Discussion

Differential stresses (σ_1-σ_3) in the upper 2 km the of the crust rarely exceed the shear strength of rock (Engelder 1982). Study of joints, unaffected by subsequent recracking (see Chapter 5), showed that the relative displacement across these joints was normal to the joint surfaces indicating that they were formed as dilatant fractures (Segall & Pollard 1983; Engelder 1985; Lorenz *et al.* 1991). Undeformed infillings, lack of original shearing and/or lateral displacement as well as distinctive surface markings also support an extensional origin for the regional joint sets of the study area. These fractures formed from one of: a remote tension normal to the joint face, an internal fluid pressure or a combination of these factors (Secor 1965; Segall 1984; Pollard & Aydin 1988; Dunne & Hancock 1994). Elevated fluid pressures would enable tensile stresses at the depth of burial to overcome the weak tensile strength of rock and produce joints (Lorenz & Finley 1991).

Regardless of the origin of the causative stress fields, extension joints developed parallel to the maximum compression direction (Pollard & Aydin 1988). Nonsystematic joints which frequently developed sub-normal to extension joints are the result of unloading and subsequent stress release (Gross 1993). This relationship is well preserved in a fracture pattern formed due to an artificial explosion. In Figure 2.15 (Brickyard Point, Outcrop 17), a group of radiating fractures and abutting curved, sub-normal, short fractures have developed around a hole during blasting associated with rock excavation. The radial fractures formed parallel to the maximum compression direction (σ_1), while the shorter abutting fractures are the result of subsequent stress relief. The pattern in Figure 2.15 developed relatively rapidly, while in geological environments extension joints, and associated tensional nonsystematic joints (Figure 2.11), usually form over a longer time span.

2.4. ROCK TYPE AND JOINTING

Changes in rock type may exert control on both joint occurrence and variations in joint orientation and spacing, although these relations are not fully understood (Pollard & Aydin 1988). Babcock (1973) studied joints of different ages in parts of southern Alberta and found that no regional variation in joint orientation was attributable to rock type or stratigraphic position. Holst (1982) also reported no correlation between local mean orientation of joint sets with rock type, rock age or location. On the other hand, some reports have documented control of joint patterns by rock type (e.g. Kulander *et al.* 1979; Lorenz *et al.* 1991). The present section discusses the influence of rock type on jointing.

Coarse-grained rocks

Joints are well developed in homogeneous regularly bedded sandstone (Figure 2.3). In

a single outcrop, the orientation of joints are similar in jointed conglomerate and sandstone, although joint surfaces are normally rougher in conglomerate. Two elongated conglomeratic units developed in a N-S direction at Outcrop 2, show almost the same pattern of jointing as thick neighbouring sandstone beds (Figure 2.3). The only difference is the spacing, which is less in the conglomerate owing to its thinner bedded nature. At Thirroul, jointing of a thick medium-grained sandstone bed at the uppermost part of Erins Vale Formation is not as regular as at Coalcliff (Scanline 21-AA').

Fine-grained rocks

The following examples have been selected to demonstrate that joint spacing and orientation are controlled by the nature of fine-grained rock types, both in horizontal and vertical sections.

Horizontal variation of jointing: Differences in joint orientation, frequency and pattern are related to lateral changes in rock type across a platform at Coalcliff (upper Coal Cliff Sandstone, Outcrop 1, Figure 2.16). Based on the fracture pattern, the platform is divided into 3 zones (Figure 2.16). In zone 1 occurs a main set of NNE joints (000-010°), and a second set of NE joints, in medium to coarse-grained sandstones up to 2 m thick. Zone 2 has mainly the NNE joints, which in the northern part are regularly spaced, long and straight, and in the southern part are shorter and less frequent. The rock type in zone 2 is composed of thin beds of grey siltstone and mudstone. In zone 3, the joint pattern is far more changeable with individual joints being irregular, rough and open. Zone 3 consists of coarse-grained sandstone beds up to 1 m thick (Figure 2.16).

The influence of lateral facies changes is also illustrated by fine-grained rocks of the upper Eckersley Formation at Scarborough (Outcrop 4). One major fracture set

of very long, 017° striking joints occur with a spacing of about 1-3 m. In the centre of the platform, these fractures terminate at the margins of an elliptical joint-free area (40x70 m). The joint-free area consists of mudstone in contrast to siltstone and fine-grained sandstone in the remainder of the platform (Figure 5.8).

These examples illustrate that changes in grain size were responsible for differences in mechanical properties between rocks. Scanline charts were found useful in documenting relationships between changing joint patterns and rock types. Figure 2.17 demonstrates additional examples of different joints patterns related to changes in rock type.

Vertical variation of jointing: Joints are best developed in laminated siltstone and fine-grained sandstone. In laminated units, each joint crosses many laminations, but is arrested at thin claystone bands or at interfaces with neighbouring sandstone layers (Figure 2.13). Pure claystone is rare in the succession, and where it occurs is joint free and normally forms a mechanical boundary between jointed units. Even a 2 mm thick claystone band terminates a set of systematic fractures in a neighbouring sandstone bed (Figure 2.13).

In the example presented in Figure 2.13, an 032° striking joint consists of an upper main joint face, developed in a mechanically distinctive upper sub-layer of medium grained sandstone. It has a lower fringe zone with an en echelon array of twist hackles, developed in the lower two thirds of the same sandstone layer, except that this part of the layer contains laminations of carbonaceous material and is mechanically separate from the upper part. This is also demonstrated by the two neighbouring 005° striking joints which nucleated and propagated independently in the two mechanically distinctive sub-layers of the same layer (Figure 2.14). Formation of the twist hackles is probably related to either a local rotation of the stress field induced by a difference

in rock type or reflects subsequent recracking (see Chapter 5).

Coal

Fractures in coal are classically divided into an orthogonal system comprising a set of systematic joints, called face cleat, and a second set of nonsystematic joints, called cross or butt cleat (Nickelsen & Hough 1967). In general, the study of fractures in coal in the study area was more difficult due to limited exposures and the subsequent effects of weathering. At Clifton, bright bands in Bulli Coal show more joints than dull bands (Figure 2.18a). Spacing of joints in coal changes from less than a millimetre to several centimetres. Due to the development of more than two sets of fractures in the coal, it breaks into long prisms perpendicular to bedding (see also Nickelsen & Hough 1967). Cleats terminate at shale or clay partings. The spacing of joints changes sharply at the interface between coal and neighbouring strata (Figure 2.18a). Some coals are almost joint free, as seen in a 10 cm thick coal bed exposed to the north of platform No. 7 (Figure 2.18b).

The origin of cleat in coal has been related to compaction, coalification, and more frequently to tectonic forces (Ver Steeg 1944; Nickelsen & Hough 1967; McCulloch & Deul 1974). In the study area, coal cleats were formed from the same processes as caused fractures in other rock types. For example, the Tongarra Coal, at Bell Point (Austinmer) contains a dominant joint set with strike of 013° and a less dominant set, striking 111° which correspond to the 003° and 120° fractures in neighbouring laminated mudstone and fine-grained sandstone (Figure 2.19b). The 10° difference in strike, is related to changes in rock type and mechanical properties.

Plant fragments and clasts

Clasts, pebbles, nodules and fossils, with a different rock type to their host have their

own joint patterns. Fractures in 37 silicified leaves and plant fragments, up to 50 cm long, were measured at Coledale (Outcrops 13-15). At all locations, the dominant joint set strikes 130-135°, compared to the 125-130° strike of SE joints in siltstone and fine-grained sandstone (Figure 2.20). At Wombarra (Outcrop 11), the main joint set which occurs in plant fragments strike 135°, while the strikes of the same set in surrounding rocks is 127°. The difference in composition of petrified plant fragments and neighbouring rocks is responsible for an up to 10° range in strike of SE joints.

Well jointed ironstone bands, 1-10 cm thick, as well as ironstone intraclasts, 1-40 cm in diameter, occur in the Coal Cliff Sandstone in the Coalcliff-Clifton area and contain two NNE and NE joint sets (cf. Eidelman & Reches 1992). These joint sets are almost identical with those of adjoining thick sandstone beds (Figures 2.1c, 2.3, 2.4, 2.11a).

Discussion

The frequency, orientation and pattern of fractures changes according to rock types both at a regional and local scale (see also Kulander *et al.* 1979). A more than 10° range in strike of a joint set occurs mainly due to changes in rock type. Petrophysical properties of rock, in part, control the susceptibility of fracturing. With respect to joints, strata are classed as either brittle or relatively ductile (Narr & Suppe 1991). Brittle beds, which are hard and more cohesive, include: conglomerate, sandstone, siltstone, and some mudstone and shale. These rocks normally contain a well developed joint pattern. In ductile rocks, such as claystone and some mudstone and shale, joints are less well developed or are even absent. Patterns of joints in coal are normally masked by subsequent weathering and fracturing.

Joint frequency differs in adjacent rock types within the same outcrop. In layers of similar thicknesses, joint frequency is greater in coal than in shale or mudstone. The

lowest joint frequency occurs in sandstone beds. The strike of fractures in coarse-grained lenticular and/or poorly bedded units is commonly more variable than the strike of fractures in fine-grained, regularly bedded, and homogeneous rocks (see also Hodgson 1961a; Babcock 1973). However, fracture orientation is more susceptible to change where subtle differences occur in rock type, such as a decrease in grain size. A slight change in either chemical composition or induration of the rock, can have a pronounced effect on fracturing. For example, Outcrop 2 at Coalcliff has a uniform conjugate joint pattern (Figure 2.3), while in the next platform to the north, the fracture pattern is somewhat irregular (Figure 2.16). This difference is mainly due to rock type with thick sandstone beds uniformly exposed in the southern platform, while the northern platform has laterally changing thick sandstone and thin fine-grained rocks (Figure 2.16).

Joints are normally developed in one bed or in several beds consisting of the same rock type. Where joints extend across contacts between different rock types they most probably have been subsequently enlarged by recracking processes (see Chapter 5).

It has not been possible to quantify the relation between rock type and jointing. Although fracture orientation and frequency change in differing rock types, these characteristics are also influenced by other factors, such as changes in bed thickness.

2.5. EFFECTS OF BED THICKNESS

In the southeastern Sydney Basin, joint frequency increases within progressively thinner beds of the same rock type. Joint sets with curving strikes and changing frequency or regularity, are also found to have been influenced by changes in bed thickness.

Curving strikes

In beds, where the rock type or thickness changes continuously, strikes of the joints may

change gradually. For example, some elongated lensoidal medium-grained sandstone bodies occur sporadically between fine-grained rocks in the central part of Outcrop 1, at Coalcliff (Figure 2.21). A set of very long 010° joints, with a spacing of 1-2 m, is developed in this part of the platform. Within the lensoidal bodies, the strike of these joints changes to less than 005° and their spacing decreases to 10-50 cm. Two other joint sets, striking 035-040° and 145-150°, also occur in the sandstone bodies (Figure 2.21). Strikes of joints in the sandstone bodies are slightly curved. These changes in strikes are related to a gradual thickening of the sandstone body (Figure 2.21b).

In some small ironstone intraclasts of the Coal Cliff Sandstone, joints are curving probably in response to increasing thickness of the jointed body (Figure 2.22a-c). In another example, a petrified log in rock platform No. 4 (Figure 2.22d) has one set of curved joints with a strike of 010-030°, while the dominant joints in the surrounding, regularly bedded, sandstone are straight and strike 020°. Curving of joint sets in these examples, reflects gradual reductions in the thicknesses of the jointed bodies.

Joint spacing

In the southeastern Sydney Basin, spacing between the members of a specific set, ranges between 1 mm (Figure 2.20) and several metres (Figure 2.3). Regularity of spacing also changes from place to place. The frequency and distribution of fractures in heterogeneous beds are irregular, which is related to spatial changes in the mechanical behaviour of the rock.

Increasing bed thicknesses are associated with an increase in joint spacing in different rock types. At Coalcliff the spacing of both NNE and NE joint sets is 2-4 m in 1-2 m thick sandstone beds and 2-5 cm in 1-2 cm thick ironstone bands (Figures 2.3, 2.4). A similar relationship exists in ironstone intraclasts, except here, because of a rapid change in thickness, the spacing is not as regular as in thin ironstone bands

(Figure 2.22a). It has been frequently reported that joint spacing is less than bed thickness, which corresponds to a fracture spacing index of more than 1 (Narr & Suppe 1991; Lorenz *et al.* 1991; Gross 1993). On a plot of thickness of a jointed layer against joint spacing, the slope of the best-fit line is referred to as the fracture spacing index (FSI, Narr 1991). Ladeira and Price (1981) suggested that FSI is a function of rock type. Narr (1991) and Narr and Suppe (1991) reported a single FSI of 1.3 for all the fractures in different rocks and structural locations over a substantial region of the Monterey Formation in California. This is in contrast to the Coalcliff-Scarborough area, where the FSI is normally less than 1.

No significant difference exists between the spacing of NNE and NE sets at Coalcliff (Figures 2.3, 2.4). In contrast, other parts of the study area have joints sets with different spacing. For example, scanline charts of Figure 2.23 display joint patterns from 3 localities in the upper Wilton Formation and show that the joint spacing and the joint regularity within joint sets differs at each locality.

Where a sandstone layer is partly divided to two sublayers, by a thin shale or ironstone band, joint spacing decreases proportional to the thickness of each sub-layer (Figure 2.24a). Decreasing joint spacing with decreasing bed thickness is well illustrated in one example, where a gradual and linear decrease in thickness of a lens of cross-bedded sandstone is accompanied by the development of new joints in between the previous ones (Figures 2.21b, 2.24b).

Pre-existing open fractures such as dykes, faults or joints, arrest further propagation of newly formed extension joints. The stress field is locally perturbed near these shear stress free surfaces, causing newly formed joints to change direction either parallel to or normal to the free face. Interaction between newly formed joints and existing open fractures is discussed in Chapter 5.

Discussion

Spacing of joints in flat-lying sedimentary rocks is a result of layer parallel extension. In general, fracture spacing and consistency of orientation are influenced by rock properties, such as elastic moduli, which themselves are a function of rock type (Lorenz & Finley 1991). Based on a model presented by Hobbs (1967), a single joint confined to a layer, only releases stresses for a short distance (d) along the layer normal to the joint, which is proportional to the bed thickness (Figure 2.25). The rest of the layer remains at a stress close to the fracture stress and susceptible to jointing. Far field extensional strain increases with time and the next joint forms most probably mid-way between existing joints. This process continues until the bed is saturated with joints (Figure 2.25). Laboratory experiments have shown that early stages of compressive deformation of rock are accommodated by formation of many small fractures (Bieniawski 1967; Lorenz *et al.* 1991). These microscopic flaws, and other inhomogeneities, weaken the jointed bed at essentially random sites along its length, and act as nucleation points for joints (Narr & Suppe 1991). Two joint sets with different spacing, occurring in one bed (Figure 2.23c), are related to different degrees of saturation of each set. Similarly, the FSI of less than 1 for joints in the Coalcliff-Scarborough area may be partly attributed to the local lack of joint saturation.

In the southeastern Sydney Basin, the average spacing of joints decreases proportionally with increasing bed thickness. In general, spacing is a function of: (1) thickness of jointed units, (2) the rock type and contrast between the jointed unit and adjacent beds, and (3) loading (Price 1966; Hobbs 1967; McQuillan 1973; Ladeira & Price 1981; Huang & Angelier 1989; Narr & Suppe 1991; Rives *et al.* 1992; Gross 1993). The variation in thickness of the jointed units can also influence the orientation of the joints; this effect is more pronounced in fine-grained rocks (Figure 2.22).

2.6. AGE OF JOINTING

One of the controversial topics in rock fracturing is the time of joint formation in flat-lying sedimentary rocks. Some authors have suggested that systematic joints could develop in unlithified or semilithified sediments (Cook & Johnson 1970; McQuillan 1973; Nickelsen 1976; Moelle 1977; Winsor 1979; Shepherd & Huntington 1981; Hancock 1985; Shepherd 1989).

Cook and Johnson (1970) reported early syn-depositional jointing in ironstone intraclasts embedded in the Coal Cliff Sandstone at Scarborough. Joints in intraclasts and neighbouring sandstone layers were thought to have differed only in orientation. According to Cook and Johnson (1970) the jointed ironstone layers were eroded, broken into intraclasts in a high energy fluvial environment and deposited in sandstone layers that were subsequently jointed due to the contemporaneous stress field.

Variation in orientation of fractures in some intraclasts, reported by Cook and Johnson (1970), is very local and mostly due to the rapid changes of thickness of intraclasts and because some of the slab-shaped intraclasts are inclined or near vertical. Random variation of joints in intraclasts was only reported from one site, which occurs in the ceiling of an overhanging part of the Coal Cliff Sandstone, and can only be studied at a distance of about 4 m. One of the joint sets reported is nonsystematic. Other fractures appear to be identical with the regional joints in the Scarborough area, as determined for more accessible ironstone intraclasts in the same area (Figures 2.6b, 2.7/2-5).

The most dominant joint sets in the Coalcliff-Scarborough area strike NNE and NE (Figure 2.26). Orientation of joints in ironstone intraclasts and enclosing sandstone beds are identical and range between 005-020° for the NNE and 040-050° for the NE joints (Figure 2.26a, b). The similarity between joints in ironstone intraclasts, ironstone bands and thick sandstone layers indicates that the joints formed regionally after

deposition of the Coal Cliff sandstone.

In the southeastern Sydney Basin, jointing was initiated in the succession after lithification enabled brittle deformation. This is shown by the widespread occurrence of plume structures and the consistent regional orientation of joints throughout the succession (see Lorenz *et al.* 1991). In this part of the basin, the only syn-depositional fractures with regional distribution are growth faults and related fractures. At Scarborough, a group of subparallel shear fractures were developed in conjunction with normal faulting during deposition of the Illawarra Coal Measures and the Narrabeen Group (see Chapter 4).

Relative age of joints

The fracture pattern of the southeastern Sydney Basin is cumulative (in the sense of Nickelsen 1976), and not the result of a single fault or jointing event. A major problem is to separate the various elements of the pattern into a chronological sequence (Shepherd & Huntington 1981). Different criteria have been established for determining the relative ages of joints (See Hancock 1985; Bergerat *et al.* 1992; Dunne & Hancock 1994). The most frequently used criteria is that younger joints abut older joints (Engelder 1982), although application of this criteria is not always straight forward (Figure 2.27).

In the case of two joint sets, 'A' and 'B', if the number of abutting of A against B is significantly higher than B against A, it can be concluded that A is younger than B. In Figure 2.27b the number of 070° joints abutted against 030° joints is 9, while the number of 030° joints terminated against 070° joints is 7 which is not significantly different. Similar comparisons between other sets shows that this technique cannot establish a valid relative age between joint sets at this locality. Repeating the techniques and procedure presented in Figure 2.27, for the other parts of the study area,

showed that the relative ages of N-NNE, NE and SE regional joints cannot be established. Therefore no age relation has been determined between the N-NNE, NE and SE regional joint sets.

The cross-cutting criterion was used successfully to establish a time relation between Group II regional joints and Group I regional joints (N-NNE, NE and SE sets), where joints of the Group II were formed universally after the joints of the Group I. An example is presented in Figure 2.28. Among the six joint sets presented in this figure, the short and fine 018°, 095° and 165° joint sets generally abut against the 040° joints, but the reverse relation is absent. Extension joints belonging to the first group (000°, 040°, 125°) left no meaningful interactions or cross-cutting relations with each other. The second group of extension joints (018°, 095°, 165°) developed later, when the members of the first group were opened and acted as free surfaces preventing further propagation of Group I joints.

Discussion

Propagating extension joints abutted against other fractures, only when the pre-existing fracture was opened and acted as a free surface. Members of each regional set were healed before the next set started to propagate. Hence, each new regional set was formed, as it was propagating into intact rock, leaving no meaningful cross-cutting relations with pre-existing joint sets. The opening, enlargement and lateral displacement of pre-existing joints are the result of subsequent events in the history of the basin, which destroyed any early formed cross-cutting relations. All mapped cross cutting relations are considered to have formed from late deformational events (see Chapter 5).

Using the cross-cutting and overprinting data, systematic joint sets with regional distribution in the southeastern Sydney Basin are divided into two groups: an older one (Group I) and a younger one (Group II). Group I joints strike N-NNE, NE and SE

(Figures 2.6a, 2.10, Table 2.2). These joints are frequent, straight, long to very long and segmented. Some of these joints were subsequently opened and displaced along their strike. Group II joints strike NNE, E and SSE (Figure 2.28, Table 2.2). These joints are less frequent, straight to slightly curved, short and fine (see Chapter 5).

Other systematic joint sets developed locally in different parts of the study area. These joint are mostly related to local structures, such as dykes (see Chapter 3), monoclines and normal faults (see Chapter 4) and were mostly formed in between the two major groups (see Chapters 6). The last group of natural fractures are nonsystematic. These joints are curved and opened and most frequently formed subnormal to the NE regional joints. Cross-cutting and overprinting relations show that the nonsystematic joints were the youngest fractures developed in this part of the basin.

All joints that occur in the same direction are not necessarily similar in age. For example, two groups of regional joints as well as local joints were formed in the NNE direction, and only careful inspection can differentiate between them.

2.7 DEVELOPMENT OF JOINT PATTERNS

Joint patterns change, even in single outcrops, due to factors such as rock type, bed thickness and pre-existing discontinuities. These variables affected mechanical properties, such as the elastic moduli. Extension joints normally developed in competent rocks with higher moduli, while in more ductile rocks these joints are rare or absent. Another factor influencing the development of joint patterns is the history of loading.

During a tectonic cycle, joints could propagate at different times such as during burial, diagenesis, tectonic compression, uplift and erosional unloading (Engelder 1985). The magnitude and orientation of stress fields have repeatedly changed, both locally and regionally, through the history of the region. In each stress field, extension joints formed parallel to σ_1, in suitable rocks. High pore water pressures enabled extension

joints to form at relatively low levels of stress (Secor 1965). Each newly formed joint set cross cut pre-existing discontinuities that were already sealed with minerals. The degree of anisotropy of stresses during fracturing controlled the planarity of fractures (Olson & Pollard 1988, 1989; Lorenz *et al.* 1991). A larger deviatoric stress normally produce straighter fractures.

Later in the history of the region, compressional forces refractured the pre-existing joints and enlarged them both horizontally and vertically (Chapter 5). The vertical enlargement of joints, extended them to the unjointed neighbouring rock bodies. Reworking of the joints, as hybrid or shear fractures, destroyed all meaningful joint relations that existed in the rock, and extended the fractures into ductile strata, where extension joints are normally absent (Figure 2.1a).

In general, the joint pattern which cumulatively developed through time in this part of the Sydney Basin, is a function of the mechanical properties of a rock mass and its loading history. Mechanical properties of rock masses are mostly influenced by the mechanical properties of intact rock (Suppe 1985), bed thickness (Ladeira & Price 1981; Narr & Suppe 1991) and pre-existing discontinuities such as joints, dykes and faults (Rawnsley *et al.* 1992). The following section briefly discusses criteria for differentiating rock masses with different joint patterns.

Jointing units

Joint spacing or frequency is normally discussed with respect to bed thickness, but as it was mentioned earlier, joints might develop in one part of a bed (Figures 2.13, 2.14), terminate at the bedding interface (Figure 2.1) or propagate vertically across a few beds (Figure 2.2). Narr and Suppe (1991) introduced the concept of 'mechanical layer' for a planar body of jointed rock which corresponds to the 'jointing layer' of Pollard and Segall (1987). The term 'layer' was used to avoid stratigraphic implications (Gross

1993). Boundaries of a mechanical layer are thin and discrete layers of ductile materials, such as claystone, and range in thickness from a fraction of a millimetre to a few millimetres.

The jointed mass of rock is not necessarily planar in shape. At Coalcliff-Clifton area, lensoidal sandstone bodies (Figure 2.21), rounded or elliptical clasts (Figure 2.22a, 26b) as well as plant fragments of any shape (Figure 2.20) are jointed, and in most cases their joint patterns are significantly different from the surrounding rocks. In general, joints developed in mechanical units of different sizes and shapes are defined here in as 'jointing units', that is a unit of rock behaves homogeneously under an applied stress. Extension joints normally terminate at the boundaries of a jointing unit. Two adjoining jointing units are differentiated from each other by: (a) absence of systematic joints in one unit, (b) differences in number and orientation of joint sets, (c) up to 10° change in orientation of one set, and (d) difference in joint density or planarity.

In general, boundaries of a mechanical unit occur at a change in mechanical properties, which are mainly related to changes in rock type (Gross 1993). Several types of boundary have been recognised for jointed units.

(a) Sharp boundaries separating the jointed unit from a neighbouring joint free body of ductile rock of any thickness. Even a 1 mm thick claystone band can act as a ductile boundary (Figures 2.1a, 2.13, 2.14 and 2.24).

(b) Sharp boundaries occurring between two brittle units of different elastic moduli. In Figures 2.20, 2.22, 2.26b both intraclasts and the neighbouring rocks are jointed. They are in direct contact with each other, but each has its own joint pattern.

(c) Gradual boundaries exist where the change in joint patterns is transitional. This happens where mechanical properties of a jointing unit gradually change in one direction. For example, in fine-grained deposits, a jointed siltstone changes laterally

to a joint free mudstone (Figure 5.8).

(d) Fracture-controlled boundaries include open joints, faults, dykes or nonsystematic joints. Open fractures are barriers to the passage of stress concentration and inhibit propagation of new joints. These shear stress free boundaries are different from rock-controlled boundaries (Figure 2.29), as no change in elastic properties necessarily exists across them. Compressive stress can be transmitted across an interface which can be a pre-existing joint or a bedding surface (Rives *et al.* 1994).

Groups of related joint units form a 'jointing domain'. Joints of neighbouring domains differ considerably in pattern or strike (Martel *et al.* 1988; Pollard & Aydin 1988). A domain might be restricted to a geological structure, such as a monocline. Contacts between domains have been designated on the bases of geographic boundaries, lithologic contacts (Nickelsen & Hough 1967), structural subdivisions, age of rock formation and a combination of these and other factors (Davis 1984).

Relation between jointed units

Nucleation points of joints are located either inside the jointing unit or at their boundaries. In the Appalachian Plateau, nucleation points of joints in layered siltstone and shale are almost always located at bedding interfaces (Helgeson & Aydin 1991). In sandstone, siltstone and mudstone of the southeastern Sydney Basin, nucleation points of regional joints are normally located away from the interfaces, usually in the mid-region of the homogeneous mechanical unit (Figures 2.13, 2.14). The horizontally lying elliptical arrest lines of the regional joints (Figure 2.14), indicate that they were propagated horizontally. A propagating joint terminates at the boundaries of its mechanical layer, but is able to grow horizontally for a distance, before it is arrested. This results in a rectangular joint face, with its height controlled by the thickness of the mechanical layer, and its length typically several times its height (Figures 2.1, 2.2).

The orientation of an identical joint set might be different in two adjoining units. In the case of Figure 2.21, the NNE joints strike 010° in the lower mechanical unit and 005° in the upper lensoidal sandstone bodies. In this case, each unit was fractured independently and joints of adjoining units only have one point in common (Figure 2.29a, c). In Figure 2.13, the long 033° joint face in the upper unit has changed to an array of en echelon joints in the lower unit. Surface markings indicate that the nucleation point of each en echelon segment is located at the mechanical boundary. A contact line between joints of neighbouring units, as well as plumose markings indicate that the joint was extended from the upper unit to the lower one (Fig, 2.29b). The en echelon extension of joints to the neighbouring units are frequently the result of subsequent deformational events (see Chapter 5).

2.8. CONCLUSIONS

In the southeastern Sydney Basin, systematic joints were initiated by brittle deformation in the succession after lithification had occurred. The regional orientation of joints is consistent throughout the Late Permian-Early Triassic succession, which indicates that they were formed after the deposition of this sequence. The presence of plumose structures, undeformed infillings and the lack of original shearing all demonstrate that the joints originally developed as extension fractures (mode I). Conjugate joint sets are the consequence of two separate fracturing events of different orientations, with each set formed in the direction of prevailing σ_1.

The present fracture pattern formed cumulatively from the Late Permian to the Present. Not all joints occurring in the same direction are of similar age. Following the deposition and lithification of the Illawarra Coal Measures, the region was fractured repeatedly forming Group I regional joints. These joints are vertical, straight, long and segmented. Each joint set was sealed and filled with calcite or siderite following its

formation. New regional sets were propagated in intact rock, leaving no meaningful cross-cutting relations with pre-existing joints. Most of these joints have lost their original characteristics due to subsequent deformations, which usually have enlarged them dramatically, both horizontally and vertically. Presently observed cross-cutting relations between fracture sets, mostly developed during the succeeding deformations.

Group II regional joints were formed later in the history of the region. These joint sets, which strike NNE, E and SSE, are less frequent, straight to slightly curved, short, mostly closed and fine. Locally developed systematic joints are generally related to local structures, such as dykes, monoclines or faults. The nonsystematic fractures formed mainly normal to the NE joints. Local systematic joints were formed mostly in the time span between the two groups of regional joints, while the nonsystematic joints are the youngest group of natural fractures developed in this part of the basin.

Joints are well developed in sandstone, laminated siltstone and some mudstone, while relatively less data were obtained from claystone or coal. Coal cleats were formed due to the same processes which formed the fractures of the other rock types. The orientation and frequency of a joint set might change, even in a single outcrop, mostly due to changes in rock type.

A direct relation exists between bed thickness and joint spacing, with more joints formed in thinner beds. This relation could not be quantified due to the effect of other influencing factors, such as rock type. Each fracture set in a given rock type may have a different spacing-bedding thickness relationship. Gradual changes in thickness or rock type, account for the formation of joint sets with curving strike.

Extension joints develop in jointing units with different sizes and shapes. The major factors defining the pattern of the extension joints in a unit are the mechanical properties of the rock mass and the loading history. Boundaries between jointing units are at changes in mechanical properties, which are mainly related to changes in rock

type. Boundaries are also marked by a pre-existing open fracture. Regional joints normally initiated in the middle of each mechanical unit and propagated horizontally. In this part of the Sydney Basin, the spacing of joints is frequently more than the thickness of the jointed unit.

The strike of a set of joints may differ in two adjoining mechanical units. Where the strike differs sharply at the interface then the joints in each unit were formed independently. In these cases, nucleation points were located away from the interface. Where the joints have extended vertically from one unit to the adjoining unit with a different rock type, then the strikes are slightly changed . To accommodate this, the main joint face has segmented, twisted and formed an array of en echelon fractures. Nucleation points of each en echelon segment is located at the interface, and the direction of propagation was vertical.

Where joints extend across contacts between different rock types, they commonly have been enlarged by subsequent events. Arrays of en echelon fractures often are the result of subsequent propagation of a pre-existing joint into a neighbouring mechanical unit (see Chapter 5).

CHAPTER 3

DYKE INJECTION AND DYKE RELATED JOINTS

3.1 INTRODUCTION

Mafic dykes have intruded the subhorizontal, Late Permian Illawarra Coal Measures of the southern Sydney Basin. Regionally, igneous activity is contemporaneous with sedimentation in the Late Permian (upper Shoalhaven Group) and continued until the Tertiary (Mayne *et al.* 1974). Based on K-Ar dating, three long-lived episodes of intrusive and volcanic activity have been recognised in the Sydney Basin and include: the Permian (250 Ma ago), Jurassic (180 Ma ago) and Eocene (50 Ma ago)(Carr & Facer 1980; Embleton *et al.* 1985).

Field relationships between dykes and neighbouring joints have been mapped along the coastal section between Coalcliff and Wollongong. Cross-cutting relationships, and other kinematic indicators, between sets of fractures in the vicinity of the injected dykes, are used to determine the sequence of brittle deformation before, during and after dyke emplacement.

Propagating magmas either fracture intact rock and intrude it, or fill pre-existing fractures. Dykes formed from intrusion along pre-existing fractures are not necessarily related to the prevailing stress field. Relationships between joints and dykes indicate that one set of fractures developed during dyke formation. Only those joints that are related to dyke formation reflect the prevailing stress field (Baer & Beyth 1990).

Dyke orientations are available both from surface mapping and also from colliery workings. These data are compared to infer a regional pattern for dyke distribution and orientation. The significance of dyke orientation for inferring palaeo-stress fields is also considered.

3.2 GENERAL CHARACTERISTICS OF DYKES

Dykes exposed at the surface are vertical to sub-vertical, and normally basaltic to doleritic in composition (Bowman 1974). They are generally less than 1.5 m in thickness, and have various lengths (less than 3 m to 15 km). Dykes are rarely in a fresh state, and most of the thinner dykes are altered to clay (Bowman 1974). In impermeable host rocks, such as siltstone and mudstone, dykes are mostly fresh, for example, at Red Point (Port Kembla) they consist of fresh basalt and the host rock is an impermeable sandstone of the upper Shoalhaven Group. In less cemented and more permeable rock types, such as in the Illawarra Coal Measures or the Narrabeen Group, the dyke material is weathered to clay, and in most cases forms negative features on the land surface (Figure 3.1).

Table 3.1 summarises field characteristics of dykes in the study area. These dykes are vertical to subvertical and are mostly planar surfaces, but locally are segmented (e.g. Bulli Point-1 and Red Point at Port Kembla, Figure 3.2). Dykes are relatively thin (10-200 cm) and their lengths always extend beyond the limits of the rock platforms. They occur either separately, as at Austinmer, or in swarms, as at Red Point (Port Kembla).

Dyke orientation

The distribution and orientation of dykes in the southeastern Sydney Basin is shown in Figure 3.3. A significant southward increase occurs in dyke frequency along a coastal traverse between Stanwell Park and to the south of Gerringong. A rose diagram from this traverse shows that most dykes have a 100-120° orientation (Figure 3.3a). From all over the Southern Coalfield, including the coastal traverse, a rose diagram shows a similar ESE-SE maxima, as well as at least three, less

significant, N-S, NE-SW and E-W maxima (Figure 3.1b).

A more comprehensive data set exists for the dykes encountered at the mining level. Most of these dykes have no surface expression. Rixon and Shepherd (1988) compiled all the available structural data at the level of working seams, i.e. Bulli and Wongawilli Coals, in five 1:25,000 sheets. A histogram of 347 dykes measured from these maps shows 4 maxima at 018°, 045°, 118° and 160° (Figure 3.4a). Dykes in the northeastern part of the coalfield, which occur in the Metropolitan, West Cliff, Coal Cliff and the northern part of the Bulli Collieries (sheet 1 of Rixon & Shepherd 1988), have a dominant NNE set (Figure 3.4b). The rest of the dykes are scattered in other directions, with less preferred maxima. In Figure 3.4c, data for the northeastern part of the coalfield, have been excluded from the data set. The dominant NNE set of the northeastern part (Figure 3.4b) is absent from the reminder of the coalfield. The three dyke orientation maxima in Figure 3.4c are similar to those for the whole of the region (Figure 3.4a).

The number of dykes in each direction, may not be the best tool for inferring their preferred regional orientation. For example, should a 15 km long dyke be weighted similar to another dyke only a few metres in length? In Figure 3.4d, the cumulative length of dykes encountered in each direction are plotted and the most important set strikes ESE, while the 160° striking dykes are less significant. Other peaks in this diagram are almost identical with Figure 3.4a.

Regional dyke orientations are best determined from the subsurface as a more comprehensive data base exists for the mining level than for surface data, which is mainly restricted to the coastline or limited exposures inland. Data presented in Figures 3.3 and 3.4 shows that the dykes in the Southern Coalfield are oriented in five major directions: NNE, NE, E, ESE and SSE. The ESE group, which strike between 100-120°, are the most dominant, both in size and number, but are absent

from the northeastern part of the coalfield (Figure 3.4b). The NE dykes strike between 040-050° and are regionally developed. The E-W (085-095°) and the SSE (150-160°) dykes, although widespread, are less dominant. NNE and SSE dykes have short lengths (compare Figure 3.3a, b, c with d). NNE (010-030°) dykes are restricted to the northeastern part of the Southern Coalfield where other sets are rare or absent (Figure 3.4b).

Structures associated with dykes

Several dykes were studied in detail along 5-10 m wide scanlines at a high-angle to the trend of the dyke (Table 3.1). Joints of the host rock in the vicinity of each dyke, are classified after Delaney *et al.* (1986) as one of adjacent, local and regional. 'Adjacent joints' develop parallel to some dykes and their frequency increases toward the dyke. 'Local joints' are present within a distance comparable to the outcrop length of the dyke, and finally 'regional joints' are present over distances much greater than the dyke length (see Chapter 2).

A set of adjacent joints occur parallel to most of the studied dykes (Figures 3.1, 3.5). The spacing between these joints increases from 3 mm adjacent to the dyke walls, to more than 100 cm before they vanish. Adjacent joints are developed over zones from less than 1 m to more than 50 m (Figure 3.5). These joints are normally vertical, straight, and their length changes from a few centimetres to a few metres. They are either filled with a thin film of calcite or are open.

Locally, dykes are parallel to regional joints (Table 3.1). At Brickyard Point, NNE regional joints are parallel to a 003° striking dyke (Table 3.1, Figure 3.6) and it is assumed that magma followed a pre-existing joint. Along the strike of the dyke, a limited number of adjacent joints occur, but only where the dyke has fractured intact rock that occurred between pre-existing joint segments. Similarly at

Coledale, a 010° striking dyke is controlled by pre-existing fractures along part of its exposed length (Figures 3.6c, 3.7).

Spacing and size of adjacent joints is dependent on rock type (see Chapter 2). At Austinmer (Outcrop 19), the upper part of the platform is 10-30 cm of laminated siltstone and is underlain by 10-20 cm of dark grey, soft claystone, which in turn is underlain by a 10 cm thick white tuffaceous layer. Here, dyke parallel joints are restricted to the upper siltstone beds, and the underlying strata are barren. Similarly at Red Point (Port Kembla), adjacent joints are well developed in an upper medium-grained sandstone bed, while almost no dyke parallel joints occur in a lower fine-grained sandstone layer (Figure 3.8).

The frequency of dyke parallel joints, while generally decreasing away from the dyke, locally contain zones with closely spaced joints. At Austinmer (Outcrop 19), joint zones occur to the south of a 140° striking dyke (Figure 3.5). Another example was mapped at the Red Point (Port Kembla) associated with some 120° striking dykes.

At Austinmer and also at Bulli Point, dyke parallel joints are divided into two subsets: (1) adjacent joints formed ahead of propagating magma, and (2) release fractures which are confined to a narrow band adjacent to the dyke walls, and formed after the emplacement of the dyke. The latter formed due to the cooling and contraction of the dyke and adjacent heated host rock. These fractures are relatively short, very closely spaced and slightly curved, and are readily differentiated from the longer and straighter adjacent joints, which typically extend to a greater distance away from the dyke.

At Wombarra the 110° adjacent joints are subparallel to a set of 120°-125° striking regional joints (Figure 3.1c, d). Here, adjacent joints have the characteristic changing spacing and cross the regularly spaced, mostly closed, regional joints.

These features indicate that these two sets were formed at different time and due to different processes. Dykes and dyke parallel joints have been subsequently recracked and accommodated lateral movement (see Chapter 5). Right-stepped en echelon gashes, filled with calcite, occur inside a 022° striking dyke at Bulli Point (Figure 3.2c). 50 cm of dextral movement has occurred along another dyke, striking 040° at the Bulli (see Chapter 5, Figures 5.3, 5.22). At Austinmer, adjacent joints, striking 140°, are displaced dextrally along their strike (see Figure 5.22). Finally, at Bulli Point, the walls of a 025° striking dyke are filled with 5-10 mm of secondary calcite.

3.3 DISCUSSION

Dyke induced fractures

Two main models have been proposed for dyke injection: (1) magma invasion along pre-existing faults and joints (Billings 1972), and (2) magma intrusion produces its own fractures by hydraulic fracturing (Anderson 1951). When suitably oriented fractures are absent from the host rock, advancing magma generates its own fractures. In unfractured rock, a propagating dyke is treated as a Griffith Crack, i.e. a very planar fluid-pressurised elliptical hole (Suppe 1985). The tensile stress at the tip of this crack is at a maximum if the crack is oriented perpendicular to least principal stress. When magma pressure is more than the resolved component of the far-field compressive stress acting perpendicular across the dyke plane, it generates tension in the host rock, beyond the dyke tip and propagates a new fracture ahead of the migrating magma.

Both dykes and most joints, are believed to be natural hydraulic tensile fractures, which involve magma and water respectively (Suppe 1985). In laboratory tests, carried out on rock specimens, a region of decreased cohesion, several

millimetres in radius, is detected around the tip of extension fractures, several centimetres in length (Pollard & Segall 1987). This damaged region, which is called the 'process zone', contains numerous microcracks. Growth of the process zone with the parent crack, produces a narrow band of rock on either side of the main fracture, which contains a dense array of microcracks (Delaney *et al.* 1986).

Adjacent joints near dykes are analogous to microcracks formed near the tips of parent cracks during tensile loading in laboratory test specimens. Pollard and Segall (1987) described the similarity between extension fractures formed in the laboratory and igneous dykes. In both of these structures the cohesion of the rock is reduced in a tabular zone. This is achieved by the formation of microcracks and adjacent joints associated with extension joints and dykes, respectively. These fractures are very small compared to their parent structures. In both cases, the loss of cohesion is apparently localised near the tip of the joint or dyke and propagates to form a process zone of weakened rock, subsequently cut symmetrically by the parent structure (Delaney *et al.* 1986).

The amount of energy required for crack propagation is related to the surface energy of the fracture, as given by the Griffith energy criterion for brittle elastic materials (Pollard and Segall, 1987). The fracture energy required to propagate a dyke is claimed to be much greater than that necessary to propagate an extension fracture. A dyke needs enough energy to propagate a set of adjacent joints, each of which in turn contains a process zone with numerous small microcracks (Delaney *et al.* 1986).

Maximum tension occurs in front of the dyke tip, with local maxima of tension gradually decreasing in magnitude either side of the dyke plane. Pollard and Segall (1987) suggested that joints formed in areas of maximum tension, and concluded that as the dyke continues to propagate, it bisects the jointed rock, leaving

a set of joints adjacent to the dyke contact. The number of adjacent joints increases towards the dyke due to an increase in tensile stress magnitude towards the dyke tip.

Local zones with higher frequencies of adjacent joints away from the parent dyke could indicate a buried dyke. At Outcrop 19 (Figure 3.5), adjacent joints are associated with a 140° striking vertical dyke. 20 and 25 m south of the dyke, occur two joint zones parallel to the dyke; each zone is presumably a set of adjacent joints propagated ahead of an underlying dyke tip (Figure 3.5). Figures 3.9 and 3.10 summarise processes of dyke injection and formation of adjacent joints in a sequence of alternating competent and incompetent flat lying layers.

Different factors contribute to the number and frequency of adjacent joints. Among them are differences in driving stress caused by the advancing magma, tensile strength of the host rock, resolved component of far-field stress normal and parallel to dyke, depth of emplacement, and dyke length (Delaney *et al.* 1986). Mechanical properties of the host rock are greatly influenced by rock type, bed thickness and the presence of pre-existing fractures (see Chapter 2). For dykes on the coast, the rock type of the host rock, plays the most important role. Adjacent joints are more frequent in competent rocks, such as sandstone and siltstone, rather than in less competent shale or mudstone (Figures 3.9, 3.10). Absence of adjacent joints in an outcrop, is sometimes misleading. In two neighbouring layers, one might develop adjacent joints, while the other is barren primarily due to differences in mechanical properties (Figure 3.10).

Bed thicknesses also affect the frequency of adjacent joints and their distances of development from the dyke. As noted for regional joints (see Chapter 2), in the same rock type, the number of adjacent joints increases as the bed thickness decreases. Widths of dykes is a less significant factor. At Bundeena, south of Sydney, a vertical dyke more than 4 m thick and striking 130°, intruded thick

bedded Triassic Hawkesbury Sandstone. In spite the size of this dyke, only a few widely spaced adjacent joints occur parallel to the dyke, due to the large thicknesses of sandstone beds. In contrast, at Austinmer (Figure 3.5), adjacent joints are developed in less than 30 cm thick alternating layers of fine-grained sandstone and siltstone more than 50 m away from a dyke, which is only 80 cm across.

One of the main differences between the adjacent joints and the regional joints described in Chapter 2 is in their propagation direction. Regional joints mainly propagated horizontally, while adjacent joints were propagated vertically upward through the sequence.

Relative age of dykes

Although some absolute dating is available for larger igneous bodies, little is known about the exact age of dykes in the southeastern part of the Sydney Basin. This is mainly because dykes, especially those hosted by the Illawarra Coal Measures, are too strongly altered for K-Ar radiometric dating. As most of the dykes intrude both Permian and Triassic rocks, they are probably Jurassic or younger in age (Bowman 1974; Ray 1986).

Relative dating of joints can constrain the relative timing of dyke formation. For each dyke, two stages of joint formation are recognised with joints formed before and after magma intrusion. Most of the dykes in the study area, are not members of regional joint sets. Adjacent joints cut through all pre-existing regional joints (Figure 3.1c, d). In a few cases magma has injected along, and therefore postdated, the NNE regional joints. Dykes and adjacent joints were recracked, and displaced laterally during the late stage compressional events and therefore they predated the Group II regional joints of inferred mid to late Tertiary age (see Chapters 2 & 5).

Dykes and stress fields

Dykes are injected most easily along previous open fractures that lie perpendicular to σ_3, as this orientation requires the least work (Anderson 1951). When a dyke intrudes a pre-existing fracture, magma pressure only has to exceed the normal component of regional stress resolved on the fracture plane. Regional stress directions acting at the time of intrusion are not necessarily orthogonal to the pre-existing fractures, and hence, dyke orientation need have no relationship to the contemporary stress field.

The present study shows that, in the southeastern part of the Sydney Basin, early joints were relatively small, mostly disconnected, mineral filled and closed (see Chapter 2). Dyke injection in the direction of these joints normally refractured them, or fractured intact rock, and produced a set of adjacent joints. Each of these dykes and their associated adjacent joints, indicate the orientation of the local stress field at the time of dyke injection. The strike of dykes along the coast, between Coalcliff and Wollongong (Table 3.1), are either N-NE or ESE-SE, which are identical with the orientation of dykes in the rest of the Southern Coalfield (Figures 3.3b, 4a).

Relatively long-lived stretching(s) from the NNE-NE, were responsible for formation of most of the ESE-SE normal faults and dykes in the southeastern part of Sydney Basin. The N-NNE dykes occur mostly in the northeastern corner of Southern Coalfield, and were injected along faulted members of at least two fracture zones with the same orientation (see Rixon & Shepherd 1988; Lohe *et al.* 1992, see also Chapters 4 & 6).

Tectonic and related igneous activity in eastern Australia from the Jurassic to late Cretaceous is related to the breakup of Australia and the Lord Howe Rise with subsequent formation of the Tasman Sea (Carr & Facer 1980; Embleton *et al.* 1985;

Middlemost *et al.* 1992). In the southeastern Sydney Basin stress fields and associated dykes were probably largely controlled by this relatively long-lived extensional regime (see Chapter 6).

3.4 CONCLUSIONS

Dykes intruded into the Illawarra Coal Measures, along the coast of the Southern Coalfield, are mostly injected along magma induced fractures and have an associated set of dyke parallel joints (adjacent joints). These joints were the result of hydraulic fracturing of intact rock during magma injection. Spacing of adjacent joints decreases away from the dyke. The frequency and the extent of development of these joints are higher in sandstone and siltstone and lower in mudstone. Adjacent joints are absent in incompetent rock types, such as claystone, and some mudstone. The number and frequency of adjacent joints increases with decreasing bed thickness. Shorter, slightly curved and very closely spaced joints, which occasionally develop in the immediate contact with the walls of some dykes, are release joints and are related to subsequent cooling of the dyke and host rock. Where magma intruded along an open fracture, adjacent joints did not develop. Orientations of dykes that are not injected into pre-existing fractures reflect the prevailing contemporary stress field.

At a regional scale over the Southern Coalfield, the most dominant set of dykes strikes ESE (100-120°) and reflects a relatively long-lived tension, acting from the NNE-NE. The second most important set of dykes, which are developed regionally, strike NE. NNE striking dykes are developed locally in the northeastern part of the coalfield and are parallel to N-NNE normal faults. Dykes, and their related joints, have formed in the interval between the formation of two groups of regional joints and possibly are related to extensional events predating rifting that

subsequently formed the Tasman Sea.

CHAPTER 4

FAULTS AND RELATED STRUCTURES

4.1 INTRODUCTION

Southeasterly oriented normal faults and gentle folds are the most pronounced structural features of the Southern Coalfield. Shepherd (1990), using data from coal mines, recognised two major groups of normal faults in the Southern Coalfield, which were characterised by differences in trend, throw versus length behaviour and slip direction (Figure 4.1). These faults, which strike SE and N-NNE, are more frequent on the eastern side of the coalfield. In the coastal strip, some branches of the southeast faults strike east-southeast (Figure 4.2).

Southeasterly trending normal faults are up to 10 km long with throws of up to 75 m (Shepherd 1990). The dips of these faults are between 50° and 70° at the Bulli Coal level. Apart from some faults with large displacement, these structures typically have no surface expression (Wilson *et al.* 1958; Bowman 1974). Shepherd (1990) mapped three zones of N-NNE faults close to the coast, each comprises a large number of normal faults with throws of up to 9 m (Figure 1.7). In the Southern Coalfield, strike-slip faults occur in a number of orientations but principally ESE. Maximum lateral displacement along these faults is reported to be about 2 m (Shepherd 1989).

Different authors have discussed the timing of formation of structural elements of the Southern Coalfield, and proposed that some of these structures, such as minor folds and normal faults, might have been active during the deposition of the Illawarra Coal Measures and Narrabeen Group (Hanlon 1956; Wilson *et al.* 1958; Wilson 1969; Cook 1969; Bunny 1972; Bowman 1974; Jakeman 1981; Clark 1992).

The orientation and major characteristics of faults mapped along the coastal exposures of the Illawarra Coal Measures, and neighbouring rock units, is presented in

this chapter and the results have been correlated with data from coal mines. A new chronology of fault formation is discussed. The relationship between faults and folds (anticlines and monoclines), both at a local and regional scale, is also considered.

4.2 ESE-SE NORMAL FAULTS

The most pronounced normal faults of the study area strike ESE (Hanlon 1956). These faults are either major with a single break or minor and zonal. Few ESE striking major faults are exposed north of the study area. Figure 4.2 shows four of these faults exposed along the coast, and displacing the Coal Cliff Sandstone and the underlying Bulli Coal.

The Harbour Fault, is located at the southern edge of the Outcrop 2 at Coalcliff (Figure 4.2). The throw at the coast is estimated at 18 m and decreases to 15 m to the west of the Lawrence Hargrave Drive and dies out in that direction. West of the road, the fault, is a clean break dipping 70° to the south. Slickenlines occur on the fault surface and indicate pure dip slip (Figure 4.3b).

The Jetty Fault occurs north of the old Coal Cliff adit and is a clean break with its northerly dip increasing upward from 50° to 75°. The Bulli Coal is exposed at sea level, on the downthrown side of the fault (Figure 4.2b). The fault dies out rapidly, both westward and upward. Throw decreases from 9 m at the top of Bulli Coal to 8.3 m at the top of the Coal Cliff Sandstone (Hanlon 1956; Cramsie 1964). The fault terminates in the Scarborough Sandstone of the Narrabeen Group, west of the road.

The Clifton Fault cuts the northern edge of the coastal platform (Outcrop 5) at Clifton (Figure 4.2a). The Bulli Coal occurs at sea level on the northern side of the fault, while on the southern side, the Allans Creek Formation forms the coastal platform. The displacement along this fault is estimated at 60 m. At an outcrop along a gully, west of the platform, the fault strikes 110°, dips 60° to the north, with the northern

block downthrown. Fault dip locally decreases in mudstone and claystone. At this locality, fine-grained strata on the downthrown side bend in towards the fault plane, forming a small anticline. The limbs of this flexure dip between 5° and 15°, and its axis plunges 12° towards 300°. No flexure occurs on the upthrown side. The fault surface is filled with 10 cm of gouge and fault breccia.

Several small normal faults, with displacement up to 5 cm, occur in the Coal Cliff Sandstone adjacent to the Clifton Fault (Figure 4.4). Microscopic studies of these fault surfaces show no brittle deformation of sand grains and indicate that the faults affected unlithified strata. Fractures dipping 70° to the north have a similar orientation to the Clifton Fault (Figure 4.4). Another, less developed, conjugate set dips at 60° to the south. One of the fractures accommodated up to 4 cm of normal displacement. The sedimentary sequence on the downthrown side of this fault (point A of Figure 4.4b) is thicker than on the upthrown side (point B), indicating that faulting was active during sedimentation. This, and similar structures at Jetty Fault, or faults located beyond the study area (e.g. at Garie North), indicate the syn-depositional nature of some of the ESE-SE normal faults.

The Scarborough Fault is not exposed in the study area. A throw of up to 50-60 m is reported for this fault from coal mines, where the dip is estimated to be about 60° to the north (Hanlon 1956).

Notable examples of minor southeast striking faults occur in the Austinmer area (Figure 4.5). Here, a group of southeasterly striking normal faults have displaced horizontal beds, up to 200 cm. Throw diminishes rapidly, both horizontally and upward, similar to the major ESE faults farther north. A normal fault with a throw of 2 m (point a of Figure 4.5) changes laterally to a vertical fracture with zero normal displacement, in less than 30 m. At point a in Figure 4.5, the dip of the fault is 30° in the coal and laminated mudstone and increases to 55° in the upper sandstone beds.

In some of these faults, beds are dipping away from the fault on the downthrown side (point c of Figure 4.5). These normal faults at Austinmer could be branches or splays developed near the end point of a major normal fault to the west of, or below, this platform.

Another group of minor ESE normal faults is exposed in the cutting to the north of Bulli Railway Station. These faults strike 110-130°, dip 75-90° to the southwest and have displacements of less than 5 cm. Unlike the Scarborough and Austinmer areas, displacements along these faults are relatively constant and they result from normal slip along recracked fractures.

Relative age

Evidence for the syn-depositional nature of ESE faults includes: thicker strata on downthrown sides and decreasing throw up the sequence (Hanlon 1956; Wilson *et al.* 1958; Cramsie 1964; Cook 1969; Wilson 1975). Comparing coal seam structure maps (Rixon & Shepherd 1988) with geological maps (Bowman 1974; Sherwin & Holmes 1986), indicates that many of the faults recognised in colliery workings were not identified at the surface. This reflects diminishing movement up the faults into Triassic strata, as shown by the Harbour, Jetty and Clifton Faults. Locally, a 30-60 m range in stratigraphic thickness has been recorded on the opposite sides of these faults (Hanlon 1956), which is much more than that expected from differential compaction. The syn-depositional mesoscopic faults adjacent to the Clifton Fault support the inferred syn-depositional nature of some of the ESE faults.

No systematic joint sets were mapped parallel to any of these ESE faults. The average strike of the SE regional joint set in this part of the basin is 135° which differs from the 100-110° strike of the ESE normal faults (Table 2.1, Figures 2.6b, 2.7). Lack of brittle joint formation accompanying development of these normal faults is considered

a reflection of the syn-depositional nature of faulting, as the strata were too poorly lithified to undergo pervasive joint formation (see Chapter 2).

Development of slickensides along some ESE normal faults (Figure 4.3b) indicate that some of these structures were active after the succession became lithified. It is concluded that the ESE normal faults were the only fractures formed during deposition of the Late Permian sequence in this part of the basin, followed by the formation of regional joint sets in competent rocks.

4.3 N-NNE NORMAL FAULTS

A group of N-NNE faults are mapped mostly in the northern and central parts of the study area. These faults, although numerous, show only small displacements (2 mm to 10 cm). The strike of these faults is between 000° and 025°, and their dips are mostly between 75° and 90°. Either eastern or western sides of these faults are downthrown.

The N-NNE faults usually occur as zones associated with a parallel set of vertical joints. An example of this relationship is seen in thick beds of the Coal Cliff Sandstone, exposed along the cliff face north of the Coalcliff adit (Figures 4.6). Here, the smaller faults with 2-20 mm of displacement are restricted to sandstone layers. They terminate at sandstone contacts with more ductile interbedded mudstone and coal. A normal fault with 100 cm of throw, crosses these ductile beds (point 1 of Figure 4.6, Figure 4.7a). The joint set, developed parallel to these faults, were originally closed and filled with a thin film of calcite. These joints also occur in the one sandstone layer and terminate at the upper mudstone beds and the lower coal seam.

A similar situation is observed at Wombarra (Outcrop 17), where a group of N-S striking minor faults is exposed over the coastal platform. Vertical displacements along the members of this fault zone are between 20 and 100 mm. The normal faults, which are usually more than 20 m long, are parallel to a set of 3-10 m long vertical

joints (Figure 4.8).

The throw of NNE faults are constant along strike, in contrast to most of the ESE faults. Most of the N-NNE faults display secondary dextral movement along their strikes. The N-NNE normal faults are less frequent south of the Scarborough Fault (compare Figures 4.1a, b with c).

In coal mines, a major NNE fracture zone, and related normal faults and dykes, has been mapped inland at 500 m to 1 km west of the coastline (Shepherd 1989; Rixon & Shepherd 1988; Lohe *et al.* 1992). Numerous N-NNE fractures with small normal displacements in the northern part of the study area occur parallel to this major fracture zone and presumably reflect the same deformation event(s).

Relative age

Overprinting between N-NNE faults and ESE faults has not been established (Shepherd 1990). Lohe and McLennan (1991) suggested that movement along the N-NNE faults predated the ESE faults. The present study shows that while some of the ESE faults were active during the deposition of the Illawarra Coal Measures, all of the N-NNE faults are post depositional, and formed after similarly oriented sets of N-NNE joints. In competent rock types, such as sandstone beds, the NNE faults follow the course of previous vertical N-NNE joints (Figures 4.6, 4.7, 4.8), while in incompetent layers, such as claystone and some mudstones, fault parallel joints are absent and the fault dip is between 55°-80° (point d of Figure 4.5). This is mainly due to differences in mechanical properties of the rocks (see Chapter 2). The competent beds were already jointed when the N-NNE normal faults started to propagate. It should be added that there are still another group of NNE joints which are much younger and postdate the earlier group of NNE regional joints and the accompanied faults and dykes. These joints are the result of a late-stage NNE-SSW compression (see Chapter 5).

4.4 STRIKE-SLIP FAULTS

No true strike-slip fault were mapped in the study area. Numerous dextral and sinistral movements measured in this study are due to slip along pre-existing fractures (i.e. faults, dykes and joints). These lateral displacements are mostly in the range of 1-20 mm. More than 50 cm of dextral displacement was measured along the strike of one dyke in the Bulli area.

Cross-cutting relationships between different sets of fractures indicate that these movements have postdated the extensional episodes which were responsible for the formation of normal faults and dykes (see Chapter 3). As an extensional regime was still active in the early Tertiary (Carr & Facer 1980; Embleton *et al.* 1985), strike-slip movements along the strike of the regional fracture sets, related to compressional episodes, are therefore most likely of post early Tertiary age. This is consistent with the timing of the strike-slip faults in the Southern Coalfield as proposed by Lohe *et al.* (1992). These strike-slip movements and their causative stress fields are discussed in Chapter 5.

No thrust faults have been mapped during the course of present study, and they have been rarely reported from the adjacent coal mines. Suitably oriented normal faults could have been reactivated (inverted) due to late-staged compressional events (see Chapter 6).

4.5 FAULT-RELATED MONOCLINES

Two monoclines have been mapped along the coast at Coledale and Scarborough. At the southern end of Outcrop 16 (Coledale), a small monocline, with a 055°-060° trend, is exposed on the coastal platform (Figure 4.9). In this structure, beds within the middle limb of the monocline dip 4°-12° toward the southeast (Figure 4.9a). Parallel

to the trend of the monocline are a set of rough, slightly curved, calcite-filled fractures, dipping 60°-90° toward the northwest. Their fracture spacing is between 50 to 150 cm. Some of these 060° fractures have normal offset, mostly of 2-10 cm. All the fractures show dextral displacement in the range 2-55 mm. Larger faults are have up to 2 cm wide zones of fault breccia.

The 060° fractures are local and are most probably related to the formation of monocline. Other joint sets mapped in this outcrop strike N, NNE, NE and E (Figure 4.9b). Unlike the 060° fractures, these joints are straight, fine and partly closed. The regional joints have been displaced by normal movement along the 060° fractures, indicating that these fractures and the related monocline are younger. Scanlines 16-CC', 16-DD', and 16-DD'2 traverse this structure (Appendix 4).

In the Scarborough area, a larger monocline is exposed along the coast. The axis of this monocline trends southeasterly parallel to the Scarborough Fault, which forms the southern boundary of the structure (Figure 4.2). The top of the Kembla Sandstone, which is slightly above sea level at Outcrop 8, rises 10 m towards the north, in less than 400 m (Figure 4.2).

A set of joints occur subparallel to the monocline at Scarborough and are considered members of the SE regional joints to the north of the Scarborough Fault (Table 2.1, Figure 2.6b). In contrast to the local joints associated with the monocline at Coledale, the joints parallel to the monocline at Scarborough are straight, fine, filled only with calcite and contain no gouge.

Discussion

Monoclines are one of the characteristic features of the southern and western part of the coalfield. The southern members have a SE trend and dip towards the NE, farther to the northwest, monoclines swing to a N-S direction, and dip towards the east (Figure

1.7; Wilson 1975). The exact location and geometry of these structures is unknown (Lohe *et al.* 1992).

It has been suggested that these monoclines probably represent folds formed above normal faults emerging from the basement (Lohe & McLennan 1991). They have been also related to high-angle reverse faults, formed from NE-SW compression (Lohe *et al.* 1992). Branagan (1975) and Bishop *et al.* (1982), amongst others, proposed that much of the deformation on these structures probably occurred during the uplift of the Eastern Highlands.

Laboratory experiments have shown that monoclines are either formed by movements along underlying reverse faults (Davis 1978) or normal faults (Withjack *et al.* 1990). The classic monoclines in the Colorado Plateau of the western United States are formed above reactivated faults in Precambrian basement (Davis 1984; Suppe 1985). Recent laboratory modelling showed that monoclines can develop as extensional forced folds above buried normal faults (Figure 4.10; Patton 1984; Vendeville 1987; Withjack *et al.* 1990). In a single-layer clay model, tested by Withjack *et al.* (1990), monoclines developed above normal faults, with curved anticlinal axial surfaces dipping in the same direction as the underlying master normal fault, while the synclinal axial surface is relatively planar and dips in the opposite direction to the underlying normal fault. A reverse relationship was found between the width of each monocline and the dip of the buried normal fault. In general, with steeper dips of the normal fault, the fold width decreases and the limb dip increases. Earlier tests carried out by Patton (1984), who used limestone and chalk, and Vendeville (1987), who used dry sand and silicon putty as modelling materials, both reached similar conclusions to those of Withjack *et al.* (1990).

Despite the differences in modelling materials, all these experiments formed widening upward monoclines above steeply dipping buried normal faults. Secondary

normal faults formed near the master normal fault and steepen upwards. When the dip of master fault is 75° or more, the secondary faults have reverse dip-slip at shallow depths (Figure 4.10).

Similar features have been reported from the field or inferred from seismic data. Many monoclines have been mapped along the margin of Gulf of Suez which were reported to have formed above normal faults (Coffield & Schamel 1989; Withjack *et al.* 1990). In the Haltenbanken area of offshore Norway, seismic data show monoclines formed above underlying master normal faults (Withjack *et al.* 1988, 1989, 1990). The experiments and field examples illustrate that monoclines are not necessarily compressional features, and have formed above normal faults. Locally, reverse faults have formed under these conditions, due to the upward inversion of the dip of normal faults (Figure 4.10).

The small monocline at the southern end of Outcrop 16, is undoubtedly fault related, and normal displacement along a steeply dipping buried fault developed this structure (Figure 4.10). Stretching and lengthening of strata in the central limb of the monocline is accommodated by a set of inclined normal faults striking parallel to the axis of the fold (Figure 4.10). The structural configuration of this monocline closely matches those produced by laboratory tests on clay models (cf. Figures 3-10 of Withjack *et al.* 1990).

The situation is less straight forward for the larger monocline mapped in the Scarborough area. The axial trace of this structure is subparallel with ESE faults, all showing clear normal displacement (Figure 4.2). If an underlying reverse fault was responsible for the formation of this monocline, then this structure would represent the only manifestation of this compressional event. No reverse faults, or related compressional structures, have been mapped during the course of present study nor are they reported from the coal mines located in the eastern proximity of the study area (see

Lohe *et al.* 1992). Alternatively, if a southward dipping underlying normal fault was responsible for the formation of this monocline, then lengthening of the strata should have occurred, as seen in the smaller monocline at Coledale. Apart from a set of 135° striking joints which are partly opened, no other sign of stretching was recorded. Strain induced by the formation of these regional joints was very small, and most probably less than 1% (see Ramsay & Huber 1987; Rawnsley *et al.* 1990). According to the results of laboratory experiments on clay models (Withjack *et al.* 1990), the type of buried normal fault that could have formed this structure, should be gently dipping (compare figures 3, 7 of Withjack *et al.* 1990 with Figure 4.2b).

The monocline at Scarborough could have developed from rollover on the downthrown side of the Scarborough Fault (see below). Similar rollovers play a significant role in formation of fault-bound anticlines in other parts of the southeastern Sydney Basin. Monoclines of the Southern Coalfield are probably fault related, and formed by rollover in the hanging wall and/or flexing of strata above a buried normal fault.

4.6 FAULT-BOUND ANTICLINES

ESE-SE trending normal faults and gentle folds, as well as N-NNE fracture zones are the dominant structural elements of the eastern part of the Southern Coalfield. Locations of some of these structures have not been accurately established. Clark (1992) compared structures described by Wilson *et al.* (1958), Bunny (1972), Wilson (1975) and Jakeman (1980, 1981) and found considerable variation between locations of the main structural features proposed by these authors. In the Southern Coalfield, most of the available data are from colliery workings and therefore axial traces of folds were drawn at the level of the floor of the Bulli Coal (R.J. Wilson, pers. comm. 1993).

Figure 4.11a shows the fluctuation of a marker horizon (Bulli Coal) due to

displacement along ESE-SE normal faults. South of the Scarborough Fault, the Bulli Coal is sub-horizontal. Tongarra Coal is located about 6 m above sea level between Wombarra (Outcrop 10) and south of Austinmer (Outcrop 19). Towards the north, between the Scarborough and Clifton Faults, the Bulli Coal is 60 m above sea level and dips at 1°-6° south. Bulli Coal is at sea level in the hanging wall of the Clifton Fault. Farther north, the seam continues to dip to the south at 2°-3°, up to the Jetty Fault (Figure 4.2b). In the hanging wall of the Jetty Fault, the Bulli Coal is once again at sea level. North of this fault, the coal seam has a northerly dip of about 3° (Figure 4.2b). Finally, in the footwall of the Harbour Fault the top of the Bulli Coal is 1 m below sea level and to the north of this fault it dips 1°-3° towards the north.

In Figure 4.2b, in the hanging walls of the Harbour, Clifton and Scarborough Faults, beds are dipping gently towards the fault plane (see also Figure 4.11a). The exception is the small Jetty Fault. Here, dips of the Bulli Coal define an anticline with its hinge approximately at the Jetty Fault. This anticline could be the eastwards continuation of the Coal Cliff Anticline, recognised west of the escarpment (Figure 4.11b).

Several very gently, northwesterly plunging folds are inferred from the structural maps of the working seams; these structures are subparallel to the southeast-trending normal faults (the ESE normal faults in the study area; Figure 1.7). Grabens formed by pairs of these normal faults invariably contain anticlines (Shepherd 1990). For example, the Bulli and the Coal Cliff Anticlines are bounded by two normal faults which dip towards the cores of both folds (Figure 4.10, Table 4.1). Farther to the north, the Waterfall Anticline is bounded between the Metropolitan Fault and a zone of normal faults that occur 1 km to the northeast. In West Cliff Colliery, a gentle anticline occurs between two normal faults which diverge from each other towards the northwest. A similar pattern exists southeast of this structure (Table. 4.1, Figure 1.7).

Structural maps of the Bulli Coal (e.g. Rixon & Shepherd 1988) show that the Coal Cliff Anticline does not extend eastwards to the coastline (Lohe *et al.* 1992). If this structure is projected eastwards along its axial trace, it intersects coastal exposures midway between the Scarborough and the Clifton Faults. No anticline crest was located in this area during the course of the present study. In contrast to the fault-bounded Coal Cliff Anticline (Figure 4.11b), on the coast the Scarborough and Clifton Faults both dip to the north (Figures 4.2b, 4.11a). Along the coast, the crest of the anticline has shifted to the north and is located south of the Harbour Fault, where faults on either side dip towards the core of anticline (Figure 4.2b).

All of the anticlines listed in Table 4.1 are confined, totally or partially, by normal faults that dip towards the fold cores; this also occurs along the coast between Coalcliff and Scarborough. One exception is the Woronora Anticline of Bunny (1972), at West Cliff Colliery where only the southeastern part of this structure is bounded by normal faults dipping towards each other.

In the southeastern Sydney Basin, anticlines are separated by synclines which are normally several times wider than neighbouring fault-bounded anticlines. Novice, Cataract and South Bulli Synclines are examples of this type of structure (Figures 1.7, 4.11b). Horizontal strata south of the Scarborough Fault, between Wombarra and Austinmer, represent a typical very broad syncline in this part of the basin.

Discussion

In the northern half of the Southern Coalfield at the Bulli Coal level, anticlines are bounded by inward dipping normal faults, while the synclines are normally devoid of major faults. On the downthrown side of faults, dips are towards the fault plane. This phenomena is called reverse drag or rollover and is typical of listric faults. Movement along a listric normal fault results in tilting of strata in the downthrown block towards

the fault. Rollover is defined by Xiao and Suppe (1992) as folding of strata in the hanging wall of the fault by bending or collapse in response to slip on nonplanar, commonly listric normal faults.

In the Southern Coalfield the ESE-SE faults mostly dip in the range 50°-70° (Shepherd, 1990). Vertical profiles of these faults, are not well established, as coal mining proceeds along single seams (Bulli or Wongawilli) and most of the faults encountered at the mining level do not have surface expression. The listric nature of growth faults (Dennis 1987), as well as some exposed examples of fault surfaces, suggests that dips of ESE-SE faults decrease downwards through the stratigraphic sequence. These faults also change dip with rock type. Since these faults were active during sedimentation, they have been affected by compaction. Mud compacts much more than sand, so that after compaction fault dips in shales are less steep than fault dips in adjacent sandstone (Figure 4.12a; Shelton 1984; Dennis 1987).

Rollovers formed on the downthrown side of the faults were responsible for the formation of anticlines in the associated grabens. The origin of the northwesterly plunging anticlines and synclines in the southeastern part of Sydney Basin, will be treated in more detail in Chapter 6.

It is considered that the fault-bound anticlines were reactivated. The gentle dip of strata away from the fault plane on the downthrown side (e.g. point c of Figure 4.5) is not attributable to rollover effects and could reflect minor inversion of the pre-existing normal faults.

4.7 CONCLUSIONS

Faults of the study area are normal and strike ESE and N-NNE. The ESE faults occur as single breaks or as zones of minor faults. The throw of these faults rapidly decreases upwards and along strike. The N-NNE faults developed in zones, where each

fault has a small normal slip. They are always accompanied by a set of similarly oriented, mostly vertical, joints. In more brittle rocks, like sandstones, the faults recracked vertical joints, while in less competent rocks the fault dip decreases. The N-NNE faults are restricted to the northern and central parts of the study area. No strike-slip faults were mapped during the course of the present study. All of the measured lateral movements have been accommodated along either faulted joints or pre-existing dykes and normal faults.

Delicate mesoscopic normal faults, with no gouge, are diagnostic of soft sediment faulting in the hanging wall of the Clifton Fault, and indicate the syn-depositional nature of some of the ESE normal faults. The N-NNE faults are post depositional and postdated development of similarly oriented joints. Strike-slip movements are the results of the youngest deformations in this part of the basin. The northwest plunging minor folds originated during deposition of the Illawarra Coal Measures.

Folds are mainly fault related. In the southeastern Sydney Basin, the southeast striking normal faults are mostly concentrated around anticlines, while synclines lack major faults. Anticlines are located in narrow grabens. The width of each fault-bound anticline is much less than the width of neighbouring synclines. Fault-bound anticlines are formed by rollover on the downthrown side of inward dipping listric normal faults, and the monoclines are either forced folds formed above buried normal faults or are the result of rollover developed in the downthrown side of the major faults.

CHAPTER 5

RECRACKING OF JOINTED ROCK MASSES

5.1 INTRODUCTION

Fractures in rock might have formed in more than one stage of deformation. The present study shows that in the southeastern part of the Sydney Basin all joints formed in extension (see Chapter 2), and were recracked with accompanying lateral slip due to subsequent events. The term 'recracking' is restricted to breaking of pre-existing fractures. Many pre-existing fractures in the southeastern Sydney Basin, have been healed by the introduction of a cement. Recracking occurs when a second rupture follows the original crack, either by propagating through the cement or by following the cement-intact rock boundary. The term recracking was first used by Engelder (1987) as the re-starting of a rupture after it has come to a complete halt. Joint-zone growth (Hodgson 1961), crack seal growth (Ramsay 1980), and intermittent growth (Bahat & Engelder 1984) are major types of recracking. Faulted joints are the end products of recracking (Zhao & Johnson 1992). Faulted joints are formed in mode I and subsequently slipped in modes II or III.

Slip on pre-existing fractures has been reported from different geological settings. For example refracturing has occurred along a set of joints in granodiorite of the Sierra Nevada (Segall & Pollard 1983, Martel *et al.* 1988). In this area, small sinistral faults occur parallel to joints within the same outcrop. Zhao and Johnson (1991, 1992) described the evolution of a system of small strike-slip faults in the porous Entrada Sandstone of Arches National Park, Utah. Here, a group of strike-slip faults, with only a few centimetres of lateral slip, were subsequently opened as joints and then were sheared with a sense opposite to that of the original faults. Other fractures in the same area started as joints and were subsequently sheared. Cruikshank *et al.* (1991)

recognised several types of minor cracks associated with subsequent lateral slip along joints.

The nature of reactivation of extension fractures in flat-lying strata of the southeastern Sydney Basin, as well as the stress fields responsible for their recracking are discussed in the present chapter. Most of the 30 studied rock platforms illustrate subsequent recracking of pre-existing fractures in the Late Permian Illawarra Coal Measures and the lower Narrabeen Group. Sets of laterally slipped fractures as well as secondary extension joints were mapped throughout the study area. Outcrop 2 has been selected as an example to demonstrate field relations associated with recracking. Data from other outcrops have been used to support the main conclusions about recracking from Outcrop 2. Selected fracture maps as well as scanlines of all the 30 outcrops are presented in Appendices 3 and 4.

The study area was subjected to more than one compressional deformation. Each deformation gave rise to a resolved lateral shear stress on pre-existing joints. These stresses were sufficient to recrack many of the joints, cause lateral slip on some, and produce conjugate sets of faulted joints. The sense of movement along the faulted joints, as well as the orientation of a set of short fractures formed during compression were used to infer the direction of compression responsible for each episode of recracking. At least three compressional stress fields are recognised as active during the Cainozoic in this part of the basin.

5.2 CONJUGATE FRACTURE PATTERN AT COALCLIFF

Outcrop 2 is the southern member of twin coastal platform at Coalcliff, 35 km south of Sydney (Figure 1.4). This platform contains the Coal Cliff Sandstone, which is 10 m thick and consists of a homogeneous, medium to coarse-grained lithic sandstone with a number of pebbly bands and a few beds of grey mudstone and brown clay ironstone.

Sandstone beds are normally 1-2 m thick. Brown clay ironstone (siderite claystone) generally occur in beds usually less than 5 cm thick. These beds grade into grey shale at the base and are sharply overlain by either additional shale or sandstone (Ward 1971). Coal Cliff Sandstone disconformably overlies the Bulli Coal, and forms the basal formation of the Narrabeen Group.

An enlarged airphotograph (1:250) was used for preparing the base map and tracing the longer open joints, which in turn were used as references for field mapping of the smaller fractures and related features. At this scale many of the larger and open fractures are visible on the aerial photograph. Almost all of the fractures, except some minor ones, are shown in Figure 5.1. The location of individual fractures are accurate to within 10-50 cm.

Two distinctive regional fractures sets were measured in this platform and strike NNE and NE. All of the systematic joints are vertical, and normally straight. The NNE joints strike 5°-15° with a mean direction of 13° and the NE joints strike between 35° and 50°, with a mean direction of 46° (Figure 5.1).

The widths of individual fractures range from 2 to 20 mm. Many fractures are filled with calcite. The length of fractures ranges from 1 m to around 100 m. Each fracture is composed of segments, 1-20 m long (Figure 5.1). Segments are parallel with the overall trend of the fractures. Fractures are mostly planar. The average spacing in thicker sandstone beds is about 2-8 m. Spacing changes locally due to differences in rock type or bed thickness. In some thin ironstone bands the spacing is 2 cm or even less. The vertical dimension of fractures is much less than their horizontal extent.

Conjugate patterns are frequent in the study area. At Austinmer (Outcrop 18) the acute angle between two sets of NNE and SE striking recracked joints is about 60° (Figure 4.5). At Wombarra two recracked fracture sets are almost normal to each other.

Conjugate Faulted Joints

At Coalcliff, both NNE and NE joints were recracked and slipped laterally in a subsequent event and produced faulted joints. Figure 5.1 shows the original joints (dotted lines) as well as faulted joints (solid lines). Original joints are dilated and filled with undeformed calcite. Recracking is more frequent in the NE set (Figure 5.1). Lateral movement was dextral for NNE and sinistral for NE fractures. Lateral movements along faulted joints are small and generally have accommodated less than a few millimetres of slip. The typical width of a faulted joint is less than 1 cm (Figure 5.2). The vertical slip is zero. These fractures have grown by amalgamation of recracked segments. This is also illustrated in Figure 5.3 which shows the structure of a long, SE striking, faulted joint at Bulli (Outcrop 22). In this example, the length of segments are between 2 to more than 10 m and they have been linked due to subsequent sinistral movement along the 120° striking fracture.

No slickenlines occur on fracture walls. This is partly due to the small size of displacements and subsequent weathering and wave action, which destroyed all possible structures on fracture surfaces. Erosion has been able to exploit healed joints where they were reactivated by recracking. Weathering and wave action have increased the openings of the faulted joints dramatically to more than 30 cm.

The strike-slip movements along the faulted joints are easily measured where they are cut by markers such as older joints (Figure 5.2). The amount of sinistral and dextral slip is proportional to length and continuity of each faulted joint. In short disconnected segments the displacements are small, sometimes less than 1 mm. In some places the amount of lateral slip along a recracked joint cannot be distinguished. In longer faulted joints the displacements is mainly in the range 2-3 cm.

Lateral displacements have also been recorded along normal faults and dykes. At Bulli (Scanline 22-CC'), a long 120° striking joint was cut by a 040° striking and

80 cm thick vertical dyke (56 m mark of Figure 5.3). Dextral slip along the dyke surface has displaced the 120° joint for approximately 50 cm (Figure 5.3). At the commencement of compressional events, dykes and normal faults were continuous compared to the joints which were relatively short, disconnected and mostly healed with calcite. All the studied dykes (Table 3.1) show some sort of lateral displacement, which is generally more than the corresponding slip along neighbouring faulted joints. In general, one major factor controlling the size of lateral displacement is the length of a faulted segment.

5.3 RECRACKING AND JOINTING

Movement upon pre-existing planes of weakness is a major deformation mechanism in low strain environments. Wherever a set or sets of suitably oriented fractures are present in rock, they potentially control nucleation and growth of faults (Segall & Pollard 1983). Even in the southeastern Sydney Basin, where fractures were healed by calcite, the strength of fracture infillings were less than the surrounding rock and fractures were capable of nucleating faults.

Horizontal recracking

Recracking normally took place along pre-existing infilled and closed joints (Figures 5.1, 5.2, 5.3). When a horizontally propagating front reached the end of an existing joint, it occasionally continued and fractured intact rock, before it terminated or began out-of-plane growth. The recracking front comes to a halt wherever it reaches a shear-stress free surface. In the case of conjugate joints, the horizontally propagating recracking front might follow the course of a member of the other set at an intersection. In Figure 5.4a a 045° open fracture has abutted against a through-going 013° joint. Recracking followed the 045° joint and when it reached the intersection, it took the

course of the 013° joint. A similar pattern has developed in Figure 5.4b.

Recracked fractures have enlarged horizontally by connecting segments of the parent joints. As a result of horizontal fracturing, disconnected short segments link and form long continuous open fractures. This process has dramatically increased the horizontal extent of the parent joint (Figure 5.1).

In general, when the recracking front reached the end of the pre-existing joint it either terminated or continued to grow in-plane or out-of-plane of the parent joint. The fracture tilts or twists from the parent joint orientation to a new direction which minimises shear and maximises tensile stress at the fracture tip (Engelder 1987; Olson & Pollard 1988, 1989). Further horizontal or vertical propagation of a fracture into the intact rock developed the wide range of secondary cracks (see below).

Vertical recracking

Vertical enlargement normally extends to the boundaries of mechanical units. Fractures propagating in sandstone terminated when they encountered mudstone or claystone beds (Chapter 2). In Figure 5.5 an open vertical fracture, striking northeast, penetrated for about 3 cm into a lower conglomerate bed, before it bifurcated and flattened its dip to become parallel to the interface between sandstone and conglomerate.

Segall and Pollard (1983) reported that in granodiorite of the central Sierra Nevada, the recracking front of a faulted joint did not propagate into the intact rock in its own plane, instead, it deviated and started to grow out of the plane of the main fracture. In contrast, in the study area, some fractures continued to grow beyond the tip of the parent fracture without any deviation. An example is presented in Figure 5.6, where an 013° striking open fracture is parallel to a closed joint. The question arises as to why the fracture in Figure 5.6 did not follow the course of the neighbouring joint? Close study of fractures at this locality, and similar patterns elsewhere, both in vertical

and horizontal sections, showed that the vertical extent of a pre-existing joint in two adjacent beds, was not necessarily aligned (Figure 5.6b). When the recracking front in the lower bed reached the contact, it penetrated the upper bed, simply by fracturing the overlying intact rock. This mostly happened when two adjacent competent beds are separated by a very thin incompetent layer. In Figure 5.6 two sandstone beds are separated by a 1-2 mm mudstone band.

In the vertical direction and at the edge of a pre-existing joint, the propagating front may do one of the following: (1) terminate, (2) proceed and fracture intact rock, (3) form an array of short en echelon cracks (see below).

The major parameters that control joint propagation across interfaces are: strength of the interface, geometric and material properties of the layers on the either side of the interface and loading (Helgeson & Aydin 1991). A strong contact between two similar layers, (e.g. the two sandstone layers of Figure 5.6) will not fail, and the recracking front will continue across the contact without any change in direction. A weaker contact will fail and the propagating front either ceases, bends or twists, before it terminates as for the contact in Figure 5.5.

Using cyclic loading, Prost (1988) modelled the behaviour of joints at rock contacts. His laboratory experiments showed that joints can cross an interface in one of the following situations: (1) existence of large compressive stress normal to the interface, (2) shearing along the fracture forming a microfault and (3) concentration of tensile stress at the contact along pre-existing cracks. All of these factors could have contributed to the vertical enlargement of the recracked joints in Figure 5.6.

5.4 FORMATION OF SECONDARY JOINTS

At Coalcliff, recracking of rock and development of faulted joints, also formed a new group of fractures, which developed at the tip, along the sides, or in between pre-

existing NNE and NE joints. These dilatant fractures (mode I) are called secondary fractures (Segall & Pollard 1983), splay cracks (Martel *et al.* 1988), and pinnate or feather joints (Hancock 1985). Secondary cracks formed as a result of small slips along faulted joints. In plan view, the traces of these fractures are straight or curved and compared to the parent joints, they are short (5 cm to 2 m). They are subvertical and strike 20°-30° at Coalcliff (Figure 5.1b). Several types of secondary cracks have been recognised in association with recracking, among them are those that form at the termination points or along the sides of the pre-existing fractures. Secondary cracks develop either by horizontal or vertical growth of the parent joint.

Horizontally grown secondary cracks

One of the most common group of secondary cracks are those that form at the termination points of faulted joints in response to shearing along them. These fractures are either straight and bend abruptly from the termination point (kinked in the sense of Cruikshank *et al.* 1991), or are curved and sometimes branched and resemble the hairs in a horse-tail. For example in Figure 5.7, the ends of two faulted segments of a 045° joint have bent counter clockwise for about 17°, and grown towards each other. One of these secondary cracks grew 10 cm while the other extended for 50 cm before they ceased to propagate.

A group of horse-tail fractures developed at the termination points of a set of long 017° striking fractures at Clifton (Outcrop 4, Figure 5.8). The original 017° joints had terminated due to a lateral facies change from sandstone to mudstone and claystone. Horse-tail fractures formed subsequently at the termination point of each recracked 017° joint. These secondary cracks are curved and their average strike is 033°.

Horse-tail fractures always grow out of the plane of the host fracture. Their clockwise or counter clockwise bending indicates the sense of shearing and the direction

of maximum tension (Segall & Pollard 1983). Horse-tail fractures represent the location where the slip terminates along the host fracture, the sense of faulting accommodated by the host fracture, and the direction of maximum tension (Davies & Pollard 1986).

Similar short fractures can occur anywhere along the length of a faulted joint (e.g. Figure 5.9). These cracks occur on either side of the parent joint but normally do not cross it. Some of the secondary fractures are wedged open due to slip on the host faulted joint. The width of opening of these secondary cracks decreases away from the parent faulted joints (Figure 5.9). Secondary cracks are more frequent near the end of each sheared segment or near the termination points of a faulted joint. Where the spacing between two parent fractures is relatively small, the secondary cracks, which have initiated from one fracture, terminate against the second one and form an en echelon pattern. These short fractures are more frequent at the area of two overlapping segments of a faulted joint (Figure 5.8b).

Secondary fractures frequently connect overlapping steps between neighbouring faulted segments. Figure 5.10 shows a 022° secondary fracture which connects two segments of a 177° faulted joint. The secondary crack has formed by clockwise bending of one segment towards the other, and finally abutting against it (Figure 5.10b). Calcite has filled the rhombohedron shaped cavity which formed due to dextral slip along the 177° fracture.

In a horizontally propagating front, the fracture tip tilts uniformly about an axis in the fracture plane but normal to the direction of propagation (Engelder 1987). All horizontally propagating secondary cracks occur in the extensional quadrants of a faulted segment (Figure 5.11). These two quadrants undergo net dilation during slip on small faults (Segall & Pollard 1983). Repeated movements at different locking points lead to the formation of secondary cracks on both sides of the faulted joint (Hancock 1985). This also happens when compressional events of different orientations developed

differently oriented sets of secondary cracks.

Vertically grown secondary cracks

Some of the recracked joints show an array of small en echelon cracks at their termination points. These cracks also form along the length or besides other fractures. En echelon cracks are different from horse-tail fractures; they are not connected with the host fracture in plan view. For example, in the southwestern part of Outcrop 15 at Coledale, each member of a group of 175° fractures, is overlain by an array of en echelon fractures (Figure 5.12). These en echelon fractures are secondary cracks which were formed after recracking of the 175° joints of the lower layer (Figure 5.12a).

During vertical recracking of a joint which terminated at an interface, when the propagating front reached the end of the pre-existing joint, it was under a combination of mode I and mode III deformation but instead of twisting as a unit it subdivided into en echelon secondary cracks by rotating about a vertical axes in the fracture plane (Pollard *et al.* 1982; Pollard & Aydin 1988; Engelder 1987; Cruikshank *et al.* 1991). This process is illustrated in Figure 5.13 and explains the en echelon array shown in Figure 5.12. Here, a single 175° fracture in the lower bed (b) breaks into multiple fracture segments in the upper bed (d). During vertical propagation, the joint was subjected to a NNE far-field compression which caused mode I loading as well as dextral shear (mode III) on the fracture tip (c). Above the interface, the newly formed extension fracture was oriented parallel to the direction of compression, and as it could not twist as a single unit, it broke into segments (Figure 5.13d). In some places where a set of joints existed in the upper layer (e), the subsequently formed en echelon segments were bounded by two neighbouring joints (Figure 5.13f, g).

The complex fracture array in Figure 5.14 contains both en echelon cracks, that have formed from vertical propagation of an underlying fracture (see Fig. 5.13) and

horse-tail cracks, which have grown from horizontal propagation of fractures. Development of this pattern is summarised below. (1) The en echelon array was formed in intact rock above a recracked joint (Figure 14b/II). (2) Further slip along the parent faulted joint fractured the intact rock, between the en echelon segments (Figure 5.14b/IV). The resulting short fractures, were subparallel with the parent faulted joint and were connected with it. (3) Further dextral slip along this system was responsible for growth of some of the en echelon segments as horse-tail fractures (Figure 5.14b/V).

It is concluded that, all of the en echelon arrays of secondary cracks in the field area are the result of vertical enlargement of faulted joints into upper or lower intact rock. They are small extension fractures and are aligned in the compression direction. They also show the same sense of shearing as the parent fracture.

Interactive secondary cracks

There are other secondary cracks which abut against a nearby fracture with a 90° angle. Examples are shown in Figure 5.15. In this example, the recracking front propagated out-of-plane of the parent joint when it reached the proximity of a nearby open fracture, and abutted against it at a normal angle. The curving perpendicular geometry is the result of the interaction of the recracking front with a nearby through-going free surface. Curving parallel secondary cracks are another product of the interaction between a propagating fracture and a free face.

The state of stress for fracture propagation changes as neighbouring cracks start to interact (Cruikshank *et al.* 1991; Pollard *et al.* 1990). When a recracking front grows towards an already opened fracture, the stress field systematically rotates and changes due to the presence of the open joint (Dyer 1988). At the free surface, one of the principal stresses is perpendicular to the fracture face and its magnitude is zero (Figure 5.16). To minimise the resolved shear on the propagating crack tip, the approaching

fracture curved and become perpendicular, or less frequently parallel, to the free surface. Each point on the path of this type of secondary crack, is roughly perpendicular to the least compressive local stress (Pollard *et al.* 1990). As these sigmoidal patterns developed due to the rotation of σ_1 near a free surface of any orientation, they are not indicators of far-field stress, nor can they be used to infer the sense of displacement along a faulted joint.

Summary

Secondary cracks are either far-field stress indicators or not. The first type can also be used as a tool to infer the sense of movement along the faulted joints. In the horizontal direction, those secondary cracks which turn clockwise with respect to the direction of the main joint, is the result of right-lateral shear, and those that turn counter clockwise are the result of left-lateral shear. Secondary fractures also indicate the direction of maximum horizontal compression. In these fractures, the far-field minimum principal stress, σ_3, is normal to the fracture surface. Figure 5.17a illustrates different types of secondary cracks which can be used to infer the direction of causative compression and also the sense of displacement along the faulted joint. Figure 5.17b demonstrates some exceptional secondary cracks which form due to the local re-orientation of the stress field. In the vertical direction, the recracking front either terminates at the boundary of a mechanical unit or crosses it. En echelon arrays are one result of jointing of intact rock beyond the tip of a recracked joint in a vertical direction (Figure 5.18).

5.5. FAULTED JOINTS WITH MULTIPLE DISPLACEMENTS

In most cases, the sense of displacement inferred from the orientation of secondary cracks and the actual slip measured along fractures support each other, i.e. both are

either sinistral or dextral. Contradictions occur locally, where one member of a fracture set shows a sinistral movement and another a dextral slip. The following examples demonstrate different aspects of this problem.

(a) At Wombarra (Outcrop 12), a set of E-W striking secondary fractures, which propagated from a NE faulted joint, bend and approached the adjacent open fracture at a 90° angle (Figure 5.19a). While the orientation of these secondary cracks suggest a dextral movement for the parent fracture, a 10 mm sinistral slip has been recorded for this faulted joint.

(b) In a few places both sinistral and dextral displacements have been measured for a single set of faulted joints. For example, in Outcrop 15 at Coledale, two adjacent 005° faulted joints occur and one has 10 mm of sinistral slip, while the other has 20 mm of dextral slip. Another example from this locality is illustrated in Figure 5. 19b, where two neighbouring NE fractures show 20 and 2 mm of dextral and sinistral slip respectively.

(c) Frequently, more than one set of secondary cracks occur along the sides of a parent fracture (see examples in Figure 5.20). Two sets of secondary fractures form a feather-shaped pattern at the ends of some faulted joints at Scarborough (Figure 5.20c). These secondary fractures are straight to slightly curved and up to 5 m long. A similar pattern is developed at Wombarra South (Figure 5.20d). Development of the feather pattern at the end of a recracked fracture suggests that each side of the termination point of the faulted joint has experienced tension.

In all of these examples, a single event cannot explain the formation of two differently oriented sets of secondary cracks. Opposite senses of strike-slip displacement along faulted joints of the same set have also been reported from the Garden Area of Arches National Park, Utah. Cruikshank *et al.* (1991) have related them to inhomogeneous deformation within the region. In the southeastern Sydney Basin, some

fractures have been affected by more than one episode of lateral shearing, frequently with an opposite sense of slip. The model presented in Figure 5.21 shows the evolution of NNE striking faulted joints at Coledale (Outcrop 15), where two neighbouring fractures show 4 and 2 mm of sinistral and dextral slip, respectively. Based on frequent observations, it is concluded that measured lateral slips on many faulted joints presented in this chapter, are probably the result of more than one deformational event which in many cases acted against each other.

5.6 EPISODES OF RECRACKING

Following lithification of the Illawarra Coal Measures several sets of extension joints were formed and sealed with calcite (see Chapter 2). Later in the history of the basin the orientation and probably the magnitude of the stress field changed. In the new stress field, resolved shear stresses on properly oriented pre-existing joints resulted in recracking and lateral slip. Mode I secondary cracks were formed during recracking and initiated at roughness elements and irregularities along a faulted joint, where the rock was subjected to tension during slippage and faulting (see Davies & Pollard 1986; Cruikshank *et al.* 1991). No lateral displacements have been recorded along the length of surveyed secondary cracks. Both, faulted joints and secondary cracks may have been sealed with calcite. Only faulted joints show more than one episode of infilling (see Figure 2.11b).

Secondary cracks in Outcrop 2 form a set of extension joints striking 020-028°. The secondary cracks mapped in the other parts of the study area do not fall into a single orientation. At Bulli (Outcrop 22), most of the secondary cracks strike 100-105° (Figures 5.3, 5.22). In some places, as stated previously, more than one set of secondary cracks are present. For example, at Scarborough (Outcrop 7) two dominant sets of secondary cracks strike 090° and 165° (Figure 5.20c). Secondary joints

measured throughout the study area fall into three main orientations, namely NNE, E and SSE (Figure 5.23). In Figure 5.23g the orientation of 430 secondary fractures measured in different rock units of the Illawarra Coal Measures, and the Coal Cliff Sandstone of the Narrabeen Group, is presented. Each of three fracture sets of Figure 5.23g represents an episode of compressional deformation.

NNE-SSW compressional event

At Coalcliff, the compression that acted from the NNE was responsible for the formation of secondary cracks that have a mean orientation of 023° (Figure 5.23a). This compression can be traced all over the study area, although its orientation changes slightly due to local geological variations. Pre-existing N-NNE and NE fractures have been reactivated by this compressional event. Dextral movements along N-NNE joints, normal faults and dykes and sinistral slip along NE fractures are all related to this event. SE joints, dykes and normal faults are least affected by this deformation. The mean orientation of NNE secondary cracks measured between Coalcliff and Bulli, is 024° (Figure 5.23g) and is regarded as the mean orientation of the NNE compression.

E-W compressional event

A well defined set of 85-105° striking secondary cracks developed in most parts of the study area (Figure 5.23). The mean orientation for this set is 097°. E-W compression caused sinistral shear on SE fractures as well as dextral shear on NE oriented fractures (Figures 5.3, 5.22). This compression had almost no effect on N-NNE oriented fractures.

At Coalcliff, recracking is more frequent along NE fractures (Figure 5.1). Different factors might have contributed to this phenomena. (1) If the causative compression formed a smaller angle with the NE fractures, it could have caused a larger

shear stress along these joints. At Coalcliff, the orientation of secondary cracks indicates that the angles between the NNE compression and the 010° and 045° joint sets were identical at about 15° and therefore this factor is not relevant. (2) Another factor is the different nature of the fracture surfaces and their infilling materials. Although no distinct difference has been recorded between two sets of conjugate joints in Coalcliff, understanding of the original strength of fracture infillings is minimal, due to subsequent weathering. (3) The last factor which could have produced more recracking on the NE fracture set is the effect of more than one compressional event. NE fractures have been affected by major NNE-SSW as well as E-W compressions, while this is not the case for NNE joints, which were sub-normal to the E-W compression and only affected by NNE compression.

SSE-NNW compressional event

The third set of secondary cracks has a mean orientation of 163° (Figure 5.23g). These fractures are the least important, both in size and number. The compressional event responsible for the formation of these fractures caused sinistral shear along N-NNE and NE fractures as well as a dextral shear along SE fractures. For example, at Austinmer, conjugate sets of 000-010° and 120° joints, both show dextral slip (Figures 4.5, 5.24). The dextral slip along SE fractures as well as the formation of a set of 160° striking secondary cracks at Austinmer are due to SSE compression, while the dextral slip along the 000-010° joints is related to the NNE compressional event (Figure 5.24a). At this locality, the short secondary fractures sometimes formed in intact rock with no connection with neighbouring fractures (Figure 5.24a inset 1, and its photograph in b), while in other places, they form along the sides or at the end of the faulted joints (Figures 5.24a, inset 4, 5.20c, d). Dextral displacements of two sets of conjugate faulted joints form small rhombohedric cavities (Figure 5.24a, inset 3). These relations

indicate that the displacement along NNE fractures was prior to lateral slip along the SE fractures.

Relative age of compressional events

The principal criteria for determining the sequence of fracturing are abutting and overprinting relationships and the offset of one structure by another (Hancock 1985). Different indicators, namely the recracking of, and slippage along, pre-existing joints dykes and faults, as well as the wide range of secondary cracks, have been used to establish age relations between compressional events and major structural features in the study area. The following is a brief review of time relations between compressional events and regional joints, dykes, faults and monocline.

Regional joints: Compressional events are younger than Group I regional joints. In the southeastern Sydney Basin, recracking and lateral displacements, which are the products of compressional events, always occur along pre-existing regional joints (Figures 5.1, 5.2, 5.3).

Normal faults: Compressional events postdate the ESE and N-NNE normal faults (see Chapter 4). ESE normal faults started to form during the deposition of Illawarra Coal Measures and hence are much older than the compressional events.

Some of the N-NNE normal faults show a horizontal component as well as a normal slip. N-NNE normal faults formed along pre-existing closed joints (see Chapter 4). The N-NNE joints, are typically open and show a few millimetres of lateral slip while their vertical displacements are zero. An example is the N striking joints and normal faults at Brickyard Point (Scanline 17-DD'), where both joints and normal faults have dextrally slipped, while faulted joints have zero vertical slip. If the lateral slip due

to the NNE compression predated normal faulting then dip-slip movement should have occurred along all open fractures and not just the normal faults. This implies that the compressions which caused lateral slip along the N striking faults and joints are younger than the normal slip that occurred along the faults (Figure 5.25).

Dykes: Compressional events are invariably younger than dykes. All studied dykes (Table 3.1), and their related adjacent joints, have been recracked and displaced by subsequent compressions.

Figure 5.22 shows the right lateral offset of a long 125° striking faulted joint by displacement along a 025° striking dyke at Bulli (25 m mark of Scanline 22-FF'). This pattern indicated that the dyke was injected prior to the commencement of the compressional event. Movement along strike of this dyke is about 16 cm, while the movement on dyke-parallel joints, where detected, is in the order of 1-10 mm. This is due to the fact that at the commencement of the compressional events, the dyke walls were two continuous weak planes, with relatively low cohesion, while the dyke parallel joints where relatively short and disconnected, both horizontally and vertically. Therefore, the strain induced by compressions are more significant along the dykes. Dyke-parallel joints have been displaced laterally in few places (e.g. Figure 5.26).

Monocline: The 060° fracture set, which developed locally parallel to the axis of a small monocline at Brickyard Point has a dextral component of 5-50 mm (Scanline 16-CC'). Vertical displacement along the 060° fractures was responsible for the formation of the monocline (see Chapter 4). The dextral slip, which is a product of a E-W compressional event, postdated formation of 060° fractures and the normal slip along them (see Chapter 4).

Compressional events: Establishing a relative age between the compressional events and the time of formation of regional joints, normal faults and dykes is much easier than finding the time relations between the compressional episodes. Overprinting relations between compressional episodes are uncommon. The following indicate the relative age of these compressional events.

1. All over the study area, the 90-100° secondary cracks occur most frequently along the NE fractures, and less frequently along the SE fractures. The dihedral angle between the E-W compression direction and the SE joints is about 30°, which is less than its 45° dihedral angle with the NE joints. Thus the E-W compression must have caused a larger shear stress on the SE joints compared to the NE joints. Why should have the E striking secondary cracks occurred more commonly besides the NE joints?

At Wombarra (Figure 5.20a) the 095-100° secondary cracks developed along the sides and in between NE fractures. The NE fractures had sinistral displacement along their strike with the NNE secondary cracks developed at the ends of and in between NE fractures. This pattern suggests that the 040° joints had already opened and slipped due to the NNE compressional event, and therefore predated the E-W compression that formed the 095-100° secondary cracks. In another example, also from Wombarra (Figure 5.19a, Scanline 12-GG'), 100° striking secondary joints started from a 040° fracture and approached the next 040° fracture at a 90° angle. It is concluded that sinistral movement on the 040° fracture, recracked it, before the commencement of E-W compression which developed the 100° joints.

2. At the 20 m mark of Scanline 12-BB', 090° secondary cracks cut 040° joints without any lateral displacement, but sinistral displacement along the same 040° joint has displaced a Group I fracture striking 115° (Figure 5.27a). Sinistral slip of the 040° fracture is related to the NNE compression. This configuration suggests that at this locality the NNE compression, which was responsible for the sinistral slip along the

040° fracture, was active earlier than the E-W compression, which formed the 090° secondary cracks

3. At the 210 m mark of Scanline 11-HH', sinistral slip of a 140° fracture has displaced two parallel 010° secondary fractures. E-W compression is responsible for this sinistral movement, while the 010° cracks are the product of NNE compression (Figure 5.27b). Once again, it is concluded that the NNE compression was older than E-W one.

4. At Austinmer (Outcrop 18), both the NNE and SE fractures have a dextral component. Cross-cutting relations in inset 2 of Figure 5.24a demonstrate that the dextral movement along the 005° fracture, which was due to the NNE compression, was earlier than similar movement along the 120° fractures. The SSE-NNW compression was responsible for the later displacement.

The compressional episodes were the last group of deformational events in this part of the Sydney Basin. Overprinting relations suggest that the NNE-SSW compression predated the E-W compression but the relative age of the SSE-NNW compressional event to these is unknown.

5.7 MECHANISMS OF RECRACKING

Mode of fracturing

Fractures formed in intact rock are classified as extension, hybrid and shear (Hancock 1985). The Coulomb-Mohr failure envelop (Figure 5.28a) predicts that shear failure occurs along conjugate planes with a progressively smaller dihedral angle (2θ) as the confining pressure (σ_3) is decreased (Engelder 1987). Normal stresses decrease and even become tensile as the dihedral angle becomes smaller (Figure 5.28a, b). Under tensile normal stress an oblique hybrid extension-shear fracture is formed (Hancock 1985, 1986; Dunne & Hancock 1994).

At Coalcliff (Figure 5.1), two sets of conjugate 010° and 045° fractures were formed separately as extension joints (see Chapter 2), and were recracked during the subsequent compressive event. The sense of slip along these fractures and the direction of secondary cracks indicate that the direction of regional compression was contained within the dihedral angle. The dihedral angle at Coalcliff is 35°, which lies in the range proposed by Dunne and Hancock (1994) for hybrid fractures (10-50°). Figure 5.28 shows that conjugate fractures enclosing a dihedral angle of less than 45°, have a component of dilation which kept the fracture open while it was propagating.

Directions of recracking in Figure 5.1 were controlled by the orientation of pre-existing fractures, which did not necessarily coincide with the orientation of hybrid fractures that would have formed in intact rock. Pre-existing fractures formed planes of weaknesses in the rock mass. The tensile strength of fracture infilling is considered less than the tensile strength of intact rock, as recracking, almost universally, has initiated and propagated along pre-existing fractures. Differential stresses needed for the formation of hybrid fractures are much less than that needed for shear fracturing (Figure 5.28). The recracked sets of joints at Coalcliff are considered a conjugate set of hybrid fractures reactivated from pre-existing planes of weakness.

This is also valid for the other parts of the study area, where the dihedral angles between the recracked conjugate sets are less than 60°. Comparison between the directions of the compressional events and the strike of recracked sets showed that pre-existing joints at a 10-30° angle to the direction of each compression have been most frequently recracked. Where the angle between two sets of fractures was between 60 and 90°, each set was recracked by a separate compressional event with σ_1 at a 10-30° angle to the recracked set. A typical example is Outcrop 18 at Austinmer where two sets of 005° and 120° fractures (2θ = 65°), both show a dextral displacement (Figures 4.5, 5.24a). At this locality, recracking and lateral slip of the 005° joints was

due to a NNE compression, while a SSE compression recracked and dextrally displaced the SE joints. Each of these faulted joint sets formed a 15-25° angle with the corresponding compression direction. It should be noted that an already recracked set could be reactivated by a subsequent compression even if the acute angle between the contemporary compression and the pre-existing faulted joint was more than the 30° limit for closed fractures.

In the southeastern Sydney Basin, recracking of pre-existing fractures and formation of faulted joints has occurred under a mixed mode, comprising both an opening component (mode I) and a shearing component (mode II or III). The absence of slickenlines or gouge along the faulted joints reflects their hybrid nature and that they were open during their formation. Gouge does not form during shear displacement along hybrid fractures (Engelder 1987).

There have been some efforts to estimate the amount of opening of faulted joints at the time of their formation. Cruikshank *et al.* (1991), using the straight secondary cracks formed at the end of some faulted joints, have related the amount of opening to their lateral slip. They concluded that the opening width of a refractured joint was greater than or equal to the amount of slip across the faulted joint at the time it was faulted in response to mode II loading. The technique proposed by Cruikshank *et al.* (1991) is not applicable in the southeastern Sydney Basin where the measured displacements are the resultant of more than one recracking event.

Sequence of recracking

Different parts of a faulted joint were not fractured simultaneously, nor were different fractures of a set or members of conjugate systems formed at the same time. The following examples demonstrate the sequence of recracking in the Illawarra Coal Measures due to the compressional events.

(a) Figure 5.15 demonstrates the formation of two conjugate faulted joints striking 045° and 010°. First the 045° fracture was recracked, followed by recracking of both segments of the 010° joint. The 010° joint segments, as they approached the 045° through-going joint, gradually bent and finally abutted against the 045° fracture at a 90° angle. The curving normal segments are in fact secondary cracks, propagated out of the plane of the recracked joint. Two short segments of the original 010° joint have been left closed (Figure 5.15).

(b) Similar configurations have been mapped in the other parts of the study area. For example three joint sets striking 003°, 035° and 155° developed in a 5 cm thick, medium-grained sandstone at Outcrop 1 (Figure 5.29). Joints are partly opened, and the recracked segments of different fractures are connected with each other. Figure 5.29 demonstrates that recracked segments developed alternatively. It also shows that recracking along a single joint can initiate from more than one place and that the direction of propagation of segments can be either the same or opposite (Figure 5.29).

(c) The previous examples show that secondary cracks propagate from or abut against pre-existing fractures. In some places, a group of secondary fractures have been mapped which cut through neighbouring fractures without any interaction. In Scanline 19-AA' at Austinmer, 160° striking, secondary cracks abut against 010° fractures or are sinistrally displaced by them. Other 160° secondary fractures cut the 010° joints without abutting (Figure 5.30). A compression from SSE (160°) was responsible for the recracking and sinistral slip of 010° joints. Extension joints, formed before recracking of neighbouring 010° joints, cut through them without interfering. Later in the compressional episode, more 010° joints were recracked. The sinistral movement along these fractures displaced the already formed secondary cracks (Figure 5.30c). The 160° cracks, which were formed later, have abutted against the 010° fractures (Figure 5.30d). Study of similar patterns in over 10 different places have shown that through-going

secondary cracks were formed when the pre-existing fractures were closed.

Traces of faulted joints are segmented and segments are fractured sequentially. Segments form with an alternate sequence of fracturing of different segments in the same group of closely spaced joints. Segments of one fracture, or two conjugate sets, interfered with each other when a recracking joint approached an already opened fracture. As a result of recracking, a network of connected open segments developed in rock which accommodate lateral slip along faulted joints. These observations on faulted joints are almost identical with those that have been reported for strike-slip faults developed in sandstone (Zhao & Johnson 1991) and strike-slip faults formed during the laboratory tests on clay models (Reches 1988).

Recracking and deviatoric stress

Each extension joint set developed in rock, represents a unique stress field (Engelder 1987; Dyer 1988). In some outcrops the fracture pattern consists of two or more regional extension joint sets. It is expected that each new, differently oriented, stress field may cause shear stresses on pre-existing fractures. Two extension joint sets mapped in the Coalcliff (Figure 5.1), or similar sets mapped in the other parts of the study area have not interfered with each other. Why has no sign of shearing occurred along older extension joints during a subsequent extension of a different orientation? In contrast, why have shear stresses later in the history of the region recracked the pre-existing joints?

Extension joints form under a small deviatoric stress (Hancock 1985; Engelder 1987; Lorenz & Finley 1991) (Figure 5.28). During the formation of Group I regional joints (Chapter 2), the small value of deviatoric stress could not overcome the strength of fracture infillings. Thus the pre-existing fractures were not planes of weakness in the rock mass. In compressional regimes, such as those responsible for the recracking

of the pre-existing joints in the study area, the stress difference was higher thus the differential stress could overcome the strength of fracture infillings and recrack them. The other major controlling factors are overburden and pore water pressure. The role of pore water pressure, which was significant during the formation of the Group I of regional extension joints (Chapter 2), was probably less important during the more recent compressional events.

5.8 CONCLUSIONS

In the Late Permian Illawarra Coal Measures of the southeastern Sydney Basin, joints and faulted joints occur parallel with each other. The joints are dilated and filled with undeformed calcite, while the faulted joints are mostly opened with evidence of lateral slip along them. All measured strike-slip displacements were nucleated along the pre-existing joints, faults and dykes. Faulting commenced with jointing and continued by lateral slip.

As a result of shearing along recracked joints, secondary cracks developed. These fractures are systematic and regional, and form sets of relatively short dilatant joints. Secondary cracks form at the end, along the sides and in between faulted joints or cut through closed joints. They may be opened but show no sign of subsequent shearing. Secondary cracks are the youngest systematic fractures formed naturally in the southeastern part of Sydney Basin.

Some fractures continued to grow beyond the tip of the parent joint without any deviation, while others terminated or tilted and twisted away from the host fracture. The faulted joints grow horizontally by the connection of recracked segments with secondary cracks. En echelon arrays are the result of vertical propagation of faulted joints into intact rock. Fracturing fronts came to a halt when they reached a shear stress free surface.

The amount of displacement is proportional to the length and continuity of the faulted segment. More than 50 cm of dextral slip has been measured along one dyke, while the lateral slip on faulted joints is in the range of 0-20 mm. Various amounts of slip occur along a single fault. Lateral slip along one set of faulted joints might be dextral, sinistral or both. Some long faulted joints show exceptionably small displacements. These fractures have been affected by more than one episode of lateral slip, acting in opposite directions.

Conjugate sets of laterally slipped faulted joints are used to infer the general direction of causative compression. Results from this method are inconclusive where rocks have been affected by compressions from more than one direction. In such cases the orientation of secondary cracks define a more reliable direction of maximum compression. The only exceptions are curving normal, or curving parallel secondary cracks, which are the result of the local stress field.

All recorded lateral displacements over the study area are readily interpreted as related to 3 compressional stress fields namely: NNE-SSW, E-W and SSE-NNW. Each of these compressions were responsible for recracking and lateral slip along suitably oriented pre-existing fractures and formation of one set of secondary cracks parallel to the compression direction. The remarkably consistent direction of secondary cracks indicates that the far-field stress field was roughly uniform for each episode of compression in this part of the basin.

All the faulted joints are classified as hybrid fractures. During each event, the pre-existing sealed fractures which formed a 10-30° angle with σ_1, have been recracked with lateral slip along their strike. Recracked joints may have been subsequently reactivated by a later compression of a different orientation. The angle between the direction of the later compression and the strike of the reactivated faulted joints could exceed the 30° limit for the recracking of a sealed joint. The result of the alternative

recracking of conjugate set(s) is a network of connected recracked segments which have accommodated shear displacement caused by different compressions.

The intensity of recracking and the amount of lateral slip is mostly related to the strength of infilling materials, the angle between the fracture and the maximum compression, and the number of compressional events imposed on the fracture. Extension joints formed under a small deviatoric stress which could not overcome the strength of fracture infillings along pre-existing joints. Thus different sets of regional joints were formed without interfering with each other. During subsequent compressional events, the deviatoric stress was high as it could overcome the strength of fracture infillings and recracked them. Interactions started when a recracking front reached the vicinity of an already recracked (opened) fracture.

Regional joints, normal faults and dykes were formed before the commencement of the compressional events. Establishment of a valid time relations between three mapped compressional events is not straight forward. The existing evidence suggests that the NNE-SSW compressional episode developed prior to the E-W compressional event. The relative age of the SSE-NNW compressional event compared to the other recracking events is unknown.

CHAPTER 6

TECTONIC DEVELOPMENT OF THE SOUTHEASTERN SYDNEY BASIN

6.1 INTRODUCTION

The southern Permian-Triassic Sydney Basin is characterised by very mild deformation, in contrast to the more deformed northern parts. The southern Sydney Basin has a unique structural pattern (Figure 1.7). Some of the main structures in this part of the basin include: (1) the Camden Syncline, which is the southern extension of a broad N-S syncline forming the overall structure of the Sydney Basin, (2) the western limb of this syncline has N-S and NNW-SSE trending monoclines, (3) the eastern limb has several NW trending gentle folds (warps), and (4) southeasterly trending syn-depositional normal faults forming grabens that contain anticlines.

The structural pattern of the Southern Coalfield evolved through several deformational events. For the earliest event, a quasi-extensional model is presented to account for the formation of syn-depositional SE trending normal faults and gentle folds. Several very mild compressional events are proposed to explain reworking of pre-existing structures during the Tertiary. Based on these models, a scenario is formulated to describe the tectonic history of the southeastern Sydney Basin.

6.2 PERMIAN-TRIASSIC TECTONIC HISTORY OF THE SYDNEY BASIN

The Sydney Basin forms the southern part of the Sydney-Bowen Basin system, which lies west of the Palaeozoic-Early Mesozoic New England Fold Belt (Figure 6.1). The basin contains an Early Permian to mid-Triassic sedimentary and volcanic succession, which unconformably overlies deformed Palaeozoic rocks of the Lachlan Fold Belt (Figure 6.1; Mayne *et al.* 1974). In the southern Sydney Basin the 2.5 km thick sedimentary sequence is only slightly deformed. The thickness increases to more than

6 km adjacent to the New England Fold Belt, where the sequence is more noticeably folded and faulted. The succession also thickens from west to east.

Different models have been suggested for formation of the Sydney-Bowen Basin System. The most feasible model proposes an early extensional phase followed by a retroarc foreland setting, for both the Sydney Basin (Mallett *et al.* 1989; Lohe *et al.* 1992; Tye & Fielding 1994) and the Bowen Basin (Hammond 1988; Baker *et al.* 1993). Based on this model, the tectonic history of the Sydney Basin is divided into three successive phases.

(1) An Early Permian extensional phase, which formed a series of major rifts, mostly at the northern part of the basin. In the Sydney Basin the fill of these rifts is still poorly documented, but in the south may include fluvial-deltaic deposits of the Talaterang Group (Tye & Fielding 1994). Mafic and/or silicic volcanism occurred at or near the base of the Sydney Basin succession (Lohe *et al.* 1992).

(2) A late Early Permian to early Late Permian subsidence phase due to post-rift cooling and lithospheric contraction. This subsidence resulted in major transgression across the entire basin. In the southern Sydney Basin, the lower part of the Shoalhaven Group was deposited during this phase. These strata are alluvial and conglomeratic in the west adjacent to their source, while in the centre and east they are shallow marine siltstone and sandstone (Pebbly Beach, Snapper Point and Wandrawandian Formations; Table 1.3; Tye & Fielding 1994; Fielding & Tye 1994).

(3) A Late Permian-Early Triassic foreland setting associated with flexural downwarping induced by thrust and magmatic loading in the adjoining New England Fold Belt (Figure 6.2). Thick successions of terrestrial and marine rocks were deposited during this phase (Lohe *et al.* 1992). In the southern Sydney Basin, deposition of the Late Permian-Early Triassic fluvial-deltaic Illawarra Coal Measures and Narrabeen Group occurred during this stage.

In the early Late Permian, strong crustal movements, known as the Hunter-Bowen Orogeny, began to affect the New England Fold Belt with formation of Hunter-Mooki Thrust system (Figure 6.1; Collins 1991). This orogeny produced synchronous molasse sedimentation and marine regression (Lohe *et al.* 1992). At the end of the Permian, the fold belt began to subside, and the foreland began to rise gently (Jones *et al.* 1984). The New England Fold Belt presumably extended southward, under the present continental shelf to the east of the southern Sydney Basin (Figure 6.1) (Currarong orogen of Jones *et al.* 1984, see also Glen & Beckett 1989a, b; Migliucci & Evans 1991; Veevers *et al.* 1993).

Major volcanic activity occurred during the Late Permian in the southeastern Sydney Basin. This igneous activity is shoshonitic in character (Carr & Facer 1980) and anomalous in its tectonic setting within a retroarc foreland basin. Shoshonitic extrusions, that occur around the boundary between the Illawarra Coal Measures and the lower Shoalhaven Group, were derived from the NE trending Gerringong volcanic chain, that existed to the east of the present coastline (Mayne *et al.* 1974; Facer & Carr 1979; Herbert 1980; Bembrick *et al.* 1980; Jones 1990).

6.3 POST-TRIASSIC TECTONIC HISTORY OF THE SYDNEY BASIN

Within the southern Sydney Basin no major tectonic activity occurred between deposition of the Sydney Basin succession and the extensional episode responsible for the formation of the Tasman Sea (Late Cretaceous). Structures, such as the regional joint sets described in this thesis, although locally impressive in their development, at most, represent only mild tectonic activity. They are not indicative of major tectonic events as recognised in more strongly deformed belts.

Igneous activity has been reported for different parts of the Sydney Basin during the Mesozoic era. In the Southern Coalfield, igneous activity occurred, with three

periods of maximum activity at 250, 180 and 50 Ma ago (Facer & Carr 1979; Carr & Facer 1980; Embleton *et al.* 1985). Igneous activity during the Jurassic to Early Cretaceous is related to a tensional regime that existed throughout the Australian continent during the Mesozoic (Embleton *et al.* 1985). At the beginning of the Mesozoic era, Australia was enclosed within the supercontinent of Pangaea, but by the Tertiary period Australia had drifted away from India, the Lord Howe Rise and Antarctica (Veevers *et al.* 1991).

The youngest sedimentary rocks preserved in the Sydney Basin are the mid-Triassic Wianamatta Group. Although no direct evidence for Late Triassic, Jurassic or Cretaceous strata have been recorded in the onshore basin area (Herbert 1980), the rank of coal laminae in the Wianamatta Group suggests that they may have been buried by more than 1000 m of overlying Mesozoic strata. Accepting that the eroded cover existed, then the area must have been mildly subsiding during part of the Late Triassic and Jurassic.

Late Cretaceous to Early Tertiary (96-56 Ma) rifting and sea floor spreading in the Tasman Sea (Veevers *et al.* 1991) must have had some influence on the structural evolution of the southern Sydney Basin. Rifting began prior to sea floor spreading (drifting) at 96 Ma (Dumitru *et al.* 1991; Veevers *et al.* 1991). Towards the end of Paleocene (57.5 My), spreading terminated in the Tasman Sea (Veevers *et al.* 1984).

Compressional events occurred during the late Tertiary in the Sydney Basin and this is consistent with the modern-day compressional state of stress characteristic of the Australian continent (Worotnicki & Denham 1976; Gray 1982). The relatively high seismicity recorded for Australia, considering its stable tectonic intraplate setting, is also compatible with the high stresses that have been measured in the Australian continental crust (Shepherd & Huntington 1981; Gray 1982; Lohe *et al.* 1992). This compressional setting contrasts to the extensional activity in eastern Australia at the time

of formation of the Tasman and Coral Seas and perhaps reflects the northward motion and continuing collision of the Indian-Australian plate with Eurasia and the Pacific plate during the last 50 Ma.

Uplift

A major tectonic event is the uplift of southeastern Australia. The Eastern Highlands extend along the length of the eastern Australia, roughly parallel to the coastline and die out inland (Ollier 1982; Bishop 1988; Dumitru *et al.* 1991). They are 0.3-1.6 km high and over 400 km wide.

The uplift of the Eastern Highlands formed due to a combination of tectonic uplift and isostatic rebound. No general agreement exists about the timing and mechanism of uplift. The location of basaltic lava in valleys indicate that most of the uplift in southeastern Australia occurred before the mid-Cainozoic (Wellman 1987). Lambeck and Stephenson (1986) proposed that the present highlands are the erosional residue of Late Paleozoic or Early Mesozoic mountain building process. In the Sydney Basin, sedimentary rocks as young as mid-Triassic (Wianamatta Group), occur in parts of the highlands, at 1.2 km altitude, indicating that uplift, in these areas, is mostly post mid-Triassic (Wellman 1987). The total amount of eroded strata from the top of Wianamatta Group, has been estimated at less than 1 km (Branagan 1983) and up to 2 km (Faiz & Hutton 1993). If either of these estimates are correct, then the uplift was initiated no earlier than the Late Triassic.

The proximity and parallelism of the highlands and the continental margin in NSW, suggests some sort of link in their history. A marked change in sedimentation pattern and tectonics at the Cenomanian (95 Ma ago) is proposed by Jones and Veevers (1983), as the time of initiation of the Eastern Highlands. The Cenomanian was at the end of a period of subsidence and basin tilting in eastern Australia, and was also

marked by the termination of andesitic volcanoclastic sedimentation in Queensland and the Bass Strait region (Jones & Veevers 1983; Wellman 1987). Tectonically, the margin of Australia, east of the Sydney Basin, changed from an oblique-slip boundary to a passive margin, after crustal extension and initiation of sea floor spreading (Jones & Veevers 1983). The uplift has been related to a phase of high heat flow and extensional tectonics preceding the main oceanic rifting event (Lohe *et al.* 1992). Lister *et al.* (1986) suggested that extension of lithosphere prior to sea floor spreading was by formation of a gently dipping detachment fault with a normal fault system developed in the hanging wall. Movement on the detachment removed the lower lithosphere from beneath the highlands (an upper plate margin in the sense of Lister *et al.* 1986). The consequence of this process was production of a thermal anomaly beneath the upper plate margin with massive crustal underplating and replacement of the lower lithosphere. Thermal uplift associated with rifting of the continent would be expected to decay with time resulting in elimination of any thermal uplift up to 50 Ma after the rifting event. In the model of Lister *et al.* (1986), however, crustal underplating thickens the lithosphere and thereby provides a mechanism whereby the uplift is maintained over a much longer interval.

In the study area, the coastal escarpment is the best manifestation of the uplift. The escarpment is an erosional feature, and its present location is not a fault line scarp (Ollier 1982). Kooi and Beaumount (1994) presented a model for the formation of high elevated rifted margins. In this model, the formation of escarpments is partly related to the existence of an erosion-resistant caprock, which in this case, is the thick competent Hawkesbury Sandstone. The NE direction of the Illawarra Escarpment, which is parallel to the coastline, and the trend of the continental shelf margin, formed by Tasman Sea rifting, suggests that the initial location of the escarpment, to the east of the present coastline, was controlled by a pre-existing discontinuity (Ollier 1982).

6.4 SYN-DEPOSITIONAL STRUCTURAL MODEL FOR THE SOUTHERN COALFIELD

Development of syn-depositional structures, such as northwesterly plunging minor folds, have been related to either syn-depositional subsidence (Wilson 1969; Cook & Johnson 1970; Bowman 1974) or short-lived compaction and erosion (Shibaoka & Bennett 1975, 1976).

Owing to thicker sedimentation in the troughs of synclines, it has been concluded that the NW plunging gentle folds of the Southern Coalfield were active during Late Permian sedimentation. For example, Cook (1969), using trend surface analysis, was able to show that the Bulli Coal is thicker in the troughs of the northwesterly plunging synclines. Bunny (1972) showed that this relationship also occurs in the overlying Triassic sequence. Jakeman (1980), using regression techniques, demonstrated that during deposition of the Permian-Triassic sequence in the Southern Coalfield, sedimentation was controlled by contemporaneous basement subsidence rather than subsidence by compaction. It is concluded that the short-lived compaction-induced subsidence is not a controlling factor for the formation of structures in the southeastern Sydney Basin.

The mild gentle folds formed during deposition of the Illawarra Coal Measures have been attributed to compression (Wilson *et al.* 1958; Bowman 1974). A 2% lengthening has been measured for an area along the coast, between Coalcliff and Scarborough (Figure 4.2). Both the lengthening of the strata and syn-depositional normal faulting indicate a mild extensional deformation, rather than a mild compression, during the Late Permian.

Quasi-extensional model

In the eastern part of the Southern Coalfield, the development of a series of southeasterly oriented normal faults (grabens) and similarly oriented gentle folds, all bounded by marginal monoclines, forms a zone of collapse (Figure 1.7). At least some of these SE trending fractures are growth faults (see Chapter 4).

Growth faults are common in deltaic successions, where they are listric and normally accompanied by rollover anticlines (Miall 1990). These failure surfaces developed as a result of sediment loading and basinward creep of the sediment pile (Crans *et al.* 1980). The thickness affected by these faults is often 1-7 km and throw can be as much as 1 km (Reading 1986). Displacement changes from almost zero at the top of the fault to a maximum at some mid-point at depth.

Typical deltaic growth faults, as occur in the Niger Delta (Reading 1986; Miall 1990), have limited lateral persistence, are curved in plan view (concave seaward) and develop parallel to the shoreline (Weber & Dakoru 1975). In contrast, the SE striking growth faults of the fluvial-deltaic Illawarra Coal Measures are long, straight, and form as narrow grabens oblique to the shoreline.

In the southeastern Sydney Basin, simultaneous faulting and sedimentation has resulted in thicker sedimentation in the hanging wall of the faults. Anticlines are fault-forced folds, formed by rollover of strata on the downthrown side of two inward dipping listric faults which bound the narrow grabens (Figures 6.3, 6.4; see also Mitra 1993, figures 15b, c).

The exact nature of monoclines, which developed along the edge of the basin, is uncertain (Lohe *et al.* 1992). The Illawarra Coal Measures thins out in the vicinity of these monoclines (Bowman 1974). All the monoclines in the Southern Coalfield have central limbs dipping towards the centre of the basin, in the southern monoclines these limbs dip to the NE and in the western monoclines they dip to the east (Figure

1.7).

A SE-NW extension (or a tension from the NE), active at the time of deposition of the Illawarra Coal Measures, and presumably the Narrabeen Group, accounts for the formation of southeasterly oriented normal faults and grabens. In this model, anticlines formed inside the narrow grabens, synclines developed between widely spaced grabens and monoclines formed above buried normal faults. The corresponding detachment for listric faults in the southeastern Sydney Basin, was not necessarily located at the boundary between basement rocks and the cover sequence. Each of the several thick, fine-grained units of the Shoalhaven Group could have served as detachment horizons (Figure 6.5).

Recent laboratory modelling has shown that extensional forced folds, i.e. anticlines and monoclines, can form above underlying master normal faults (see Mitra 1993, figures 4b, 9b). In these experiments, narrow graben developed near the axial surfaces of the induced anticlines (Patton, 1984; Vendeville 1987; Withjack *et al.* 1990). Similar conditions have been reported from the field and inferred from seismic data, for example, in the Haltenbanken area of offshore Norway, seismic data reveal forced folds above master normal faults (Figure 6.6). Withjack *et al.* (1990) have found narrow graben developed near the axial surfaces of some of these anticlines (Figure 6.6).

Origin of extensional stress: The special pattern of structures in the southeastern Sydney Basin is related to a minor extensional stress field developed during uplift formed away from the loaded area of the subsiding foreland basin (see Molnar & Lyon-Caen 1988; Plint *et al.* 1993). Because of the elastic properties of lithosphere, the load stress of the mountain belt produces a depression that extends beyond the limits of the mountain range itself. The elastic upbending at the edge of the depressed part produces an uplift at the margin of the depression (Walcott 1970; Miall 1990). In a foreland

basin, such as the Sydney Basin, as the underthrusting plate bends downward, the outer arc of the elastic portion of the plate is extended (Figure 6.7) (Molnar & Lyon-Caen 1988; Coward 1994). This deflection is called a forebulge, foreswell, flexural bulge, flexural upwarp and/or peripheral bulge (Figure 6.7). Development of a forebulge produces tangential longitudinal strain along the outer arc of the bulge and a quasi-extensional stress field is locally formed in the foreland regime.

Sedimentological evidence supports identification of the northern part of the Southern Coalfield as a forebulge. Bunny (1972) identified the Woronora Anticline (Figure 1.7) as a depositional hinge. North of this structure the Bulli Coal loses its identity, and the sedimentary sequence thickens. This anticline, together with the continuing southeastern structure, the Bulli Anticline, are regarded by Bunny (1972), as the most significant structures in relation to deposition in the southern part of Sydney Basin. This hingeline effectively separates shelf and trough areas of the basin, with more rapid subsidence to the northeast of the structure (Bembrick *et al.* 1973; Bamberry 1992; Lohe *et al.* 1992). In the Southern Coalfield, the direction of the forebulge is ESE, which differs from the anticipated N-S direction of a forebulge for the whole Sydney-Bowen Basin System. The anomalous structural pattern of the Southern Coalfield thus related to the local orientation of the forebulge in this part of the basin.

The effect of basement structures: Tangential longitudinal strain developed normal to the trend of the forebulge may have reactivated appropriately oriented pre-existing faults in the basement.

The structural fabric of the sedimentary sequence of the southern Sydney Basin is frequently related to configuration of the basement (Cook 1969; Jakeman 1980; Gray 1982; Mauger *et al.* 1984; Shepherd 1990; Hutton *et al.* 1990; Lohe & McLennan 1991). Details of this pattern are not well documented, because of the inaccessibility

of these structures. The study of lineaments and fracture zones in adjoining Palaeozoic rocks of the Lachlan Fold Belt, which forms the basement of southern Sydney Basin, is one approach that may indicate the orientation of structures beneath the basin.

Studies by Mauger *et al.* (1984) and Lohe *et al.* (1992) have shown that ESE-SE lineaments in the southern Sydney Basin are continuous with lineaments in the Lachlan Fold Belt, thereby indicating that they originated from the basement structures (Figure 6.8). Clark (1992) used aeromagnetic data to argue that basement faulting with normal slip had effected the succession during deposition. Powell *et al.* (1985) reported a group of ESE megakinks in basement rocks of the Lachlan Fold Belt, to the west of Sydney Basin. These structures, which have nucleated along strike of pre-existing ESE lineaments, most probably continue eastward into the basement rock under the Sydney Basin (Figure 6.8; C.McA. Powell 1994, pers. comm.).

One of the major lineaments of the Lachlan Fold Belt is the ESE Lachlan River Lineament, which extends from the Darling River to the coast (Scheibner 1974). One segment of this fracture zone runs through the centre of the Bathurst Granite, before entering the Sydney Basin and finally cuts the coast in the vicinity of Botany Bay (Figure 6.8). Another segment runs through the Tertiary Canobolas volcanic complex (Figure 6.8). The Cainozoic volcanic activity at Mt Canobolas and the emplacement of the Late Carboniferous Bathurst Granite along the Lachlan River Lineament indicate that these lineaments may have controlled Late Palaeozoic and younger features.

Older faulting along these ESE lineaments has been documented in the Lachlan Fold Belt, at their NW termination in the Cobar region, 500 km NW of the southern Sydney Basin. Here, the ESE-SE Crowl Creek (Scheibner 1974), Buckambool and Winduck Lineaments are basement faults, which were active in the Devonian and then reactivated in the Carboniferous (Glen 1987). These, and similarly oriented lineaments are segments of the Lachlan River Fracture Zone (Scheibner 1974). Thus it appears that

this zone of lineaments has been active from the Devonian onwards and could conceivably have been reactivated in the Late Permian to form the anomalous ESE-SE trends of structures in the southeastern Sydney Basin.

The ESE basement faults, which were active since the Devonian, are subparallel to the normal faults, grabens and the southern group of monoclines in the Southern Coalfield (Figures 1.7, 6.8). These basement faults were reactivated due to upward flexing of the forebulge of the Sydney Basin during the Late Permian. The immediate result of this reactivation was the formation of broad synclines above basement grabens (Figures 6.4, 6.6). The normal faults, which bound the narrow grabens, were not necessarily the continuation of basement faults (Figures 6.4, 6.5, 6.6). Downwarping of synclines, imposed some tensions on neighbouring areas. These tensions were responsible for the initiation of growth faults and grabens in the elevated parts of the cover (Figures 6.4, 6.5, 6.6). Anticlines formed by rollovers as a result of the listric movement of these growth faults, and finally monoclines either originated above peripheral buried normal faults or were the result of rollover along listric normal faults (Figures 4.10, 6.4).

6.5 POST-DEPOSITIONAL STRUCTURAL MODELS FOR THE SOUTHERN COALFIELD

Mesozoic-Early Tertiary extensional episodes

Sets of joints and dykes, as well as normal faults, formed during the Mesozoic time. In the southeastern Sydney Basin, all systematic joints originally formed as extension fractures. Extension joints have been reported to form in response to different processes, such as earth tides, seismicity, desiccation, uplift, erosional unloading, thermal contraction, high pore pressure, chemical weathering, regional extension and variation of unconsolidated or semi-consolidated materials over uneven basement blocks (Prost

1986). Formation of extension joints begins early in the history of a basin and continues through uplift and unloading (see Engelder 1985).

In the southeastern Sydney Basin, jointing has been previously considered to be contemporaneous with sedimentation (Cook & Johnson 1970; Moelle 1977) or folding (Bowman & Mullard 1986). The present study indicates that the systematic joints in southeastern Sydney Basin are post-depositional (see Chapter 2). Bowman (1974) reported four sets of joints with mean directions at 005°, 055°, 105°, and 155° for this part of the basin. He arranged these four sets in two systems, each with two sets at near right angles to each other and concluded that they are parallel to and perpendicular to prevailing fold axes in the southern Sydney Basin (bc and ac respectively), which strike N-S and SE-NW. Joints sets that symmetrically enclose fold hinge lines are not necessarily related to folding, and in the southeastern Sydney Basin, these sets are pairs of unrelated extension joints (see Chapter 2; see also Engelder & Geiser 1980). The present study indicates that minor northwest plunging folds in this part of the basin are not compressional features, as previously proposed (e.g. see Bowman & Mullard 1986). Small strain due to mild warping is unlikely to be responsible for the formation of a well developed conjugate joint sets. Furthermore, the northeast plunging folds originated syn-depositionally, whereas the systematic joint sets are post-depositional.

The exact time and depth of formation of Group I regional joints is not completely understood. These joints must have developed after the mid-Triassic as they occur in strata of Late Permian to mid-Triassic age. Cross-cutting relations of these joints with other fractures (Chapters 2 & 5) indicate that Group I regional joints predate the post-Early Tertiary compressional events and the dykes which precede these compressional events. Maximum burial of the Illawarra Coal Measures probably occurred during the Late Triassic-Jurassic and this is tentatively regarded as the time of formation of the Group I regional joints. Therefore, the timing of formation of the

Group I regional joints, in addition to their general characteristics (see Chapter 2), are consistent with them being burial joints in the sense of Bahat (1991).

The broad, N-S trending Camden Syncline is not necessarily the result of E-W compression as reported in the past (e.g. Gray 1982; Bowman & Mullard 1986). No convincing evidence has so far presented to support formation of this syncline during Late Permian deposition. Another alternative is that the Camden Syncline is post-depositional and probably related to the uplift of the Illawarra Escarpment. The parallelism of the axis of this structure with the general trend of the escarpment supports this idea.

The present study indicates post-depositional formation of N-NNE faults (see Chapter 4). During the Mesozoic, especially in the Late Cretaceous-Early Tertiary Tasman Sea extension and rifting, more normal faults may have formed in the SE direction and pre-existing faults may have been reactivated. Normal faults and dykes with other orientations, have also been also correlated with this event (Lohe *et al.* 1992). In the Southern Coalfield, dykes are mostly ESE-SE, or NNE-NE. Cross-cutting relations, between dykes, dyke-related joints and other fractures, indicate that these structures were mostly formed in between Group I and II regional joints. Initiation of most of the dykes is correlated with the Late Cretaceous-Early Tertiary Tasman Sea rifting (Carr & Facer 1980; Branagan 1985), which was active between 95 and 57.5 Ma ago (Jones & Veevers 1984).

Zones of N-NNE trending normal faults and dykes, in the northern part of the Southern Coalfield (Figure 1.7, see also Chapter 4), are broadly parallel to the Tasman Sea rift margin, and oblique to the NE direction of the Tasman sea extensional tectonism (Figure 6.9; Lohe *et al.* 1992). Pre-existing N-NNE discontinuities in the crust, similar to the Coastal Lineaments (Scheibner 1974) and the Helensburgh Lineament (Mauger *et al.* 1984), have been suggested to have influenced the location

and orientation of the rift zone (Lohe *et al.* 1992), as well as formation of zones of N-NNE faults and dykes in the cover sequence (Figures 1.7, 6.9; Rixon & Shepherd 1988). NNE fault zones and lineaments are also generally parallel to the coastline, and the trend of the continental shelf margin generated by the Tasman Sea rifting (Lohe *et al.* 1992). It is conceivable that rather than controlling the NNE trend of the initial rift system, these structures were actually generated during the rift itself, perhaps utilising the N-NNE regional joint set.

Late-stage compressional events

Group II regional joints were formed by compression. In this study, three late-stage compressional events are recognised, during post-early Tertiary time, with NNE-SSW, E-W and SSE-NNW directions for σ_1. The most important effects of these compressions in the study area are the recracking of joints and formation of faulted joints (See Chapter 5), as well as displacement along pre-existing normal faults and dykes. The anomalous dip of strata away from the faults on the footwall side (see Figure 4.5 point c), is regarded as an indication of the subsequent very mild inversion of these faults.

Cross-cutting relations between fracture sets indicate that these compressional events postdated formation of normal faults, monoclines and dykes. Hence, the compressional events are considered to have post-dated rifting in the Tasman Sea. The compressional events are the youngest deformations recorded in the studied sequence. The relative age of these compressional events are not yet established, although, cross-cutting relationships suggest an older age for the NNE-SSW compression relative to the E-W one (see Chapter 5). Nonsystematic joints of the study area are classified as unloading joints. These joints formed due to thermal-elastic contraction developed during uplift and erosion (see Engelder 1985). The nonsystematic joints postdated the formation of Group II systematic joint sets.

Origin of compressional stress: Lohe *et al.* (1992) discussed the late stage N-S and E-W compressional events in the Sydney Basin which they tentatively dated as Oligocene-Miocene and Miocene-Holocene, respectively. Blayden (1971) suggested that the folding event that formed the Macquarie Syncline, in the northern Sydney Basin, occurred in the Tertiary. Compressional forces, active after the cessation of extension in the Late Cretaceous-Early Tertiary, have been reported from other parts of eastern Australia (e.g. see Hoffmann 1989; Lohe *et al.* 1992)

The collision between the Indo-Australian and Pacific Plates in the Tertiary generated an anticlockwise motion of the Australia relative to the rest of the enclosing plate and was responsible for the development of dextral shear at the edges of the continent (Veevers & Powell 1984). The effect of this deformation, which started no earlier than 30 Ma ago, has been reported from a few places along the margin of the Australian continent. The direction of E-W echelon folds and faults in Neogene sediments of the Gippsland Basin (Davidson 1980), at the southeast margin of the continent, is consistent with dextral or anticlockwise motion of Australia at this time (Figure 6.10). At the northeastern margin of the continent, in the Carnarvon-Dampier Basin, Miocene and younger NE trending en echelon folds, were formed by dextral shear (Evans 1981, 1982).

In the Illawarra region, the dextral shear developed parallel to the continental margin and generated a NNE compression direction. This is consistent with the stress field associated with the most pronounced recracking event established during the present study (Figure 6.10). If this model is correct, then the NNE compression in southeastern Sydney Basin is post-Oligocene.

6.6 DEFORMATION HISTORY

The following scenario is established for the sequence of formation of the major structural features of the southeast Sydney Basin.

1. Late Permian-Early Triassic: ESE-SE normal faults and similarly oriented fault-forced folds were initiated during the deposition of the Illawarra Coal Measures and the Narrabeen Group.

2. Jurassic-Early Tertiary: Group I regional joints, striking N-NNE, NE and SE, were formed in three separate events. These fractures are classified as burial joints. NNE and more ESE-SE normal faults and dykes were developed. Local joints, which are mostly related to dykes also formed during this stage. It is assumed that this episode was terminated at the end of extension related to opening of the Tasman Sea.

3. Post-Early Tertiary-Present: Pre-existing fractures were recracked and slipped along their strike, due to 3 compressional events, namely NNE-SSW, E-W, and SSE-NNW. Group II extension joints, were formed. Monoclines and SE trending folds were reactivated. Finally, nonsystematic cross joints were formed and opened fractures were widened due to unloading, weathering and surficial movements.

6.7. CONCLUSIONS

Incipient extension was responsible for formation of SE trending anticlines and grabens during deposition of the Illawarra Coal Measures and the lower part of the Narrabeen Group. A Late Permian-Early Triassic quasi-extensional stress field was developed by formation of a forebulge in the northern part of the Southern Coalfield. This stress field may have reactivated appropriately oriented basement faults. Downwarping of the sedimentary sequence occurred above basement grabens, generating tension in neighbouring areas, and propagating grabens. Anticlines are mostly the result of rollover on the downthrown sides of inward dipping growth faults. Major normal faults which

bound the grabens, are not necessarily the continuation of basement faults. Detachment horizons for these listric faults may be located in fine-grained units of the Shoalhaven Group.

Joints are post-depositional and cumulatively formed during burial, uplift and unloading. Group I regional joints, formed during burial and show no apparent genetic relation with SE trending minor folds. Additional normal faults and related dykes were formed during the Mesozoic, and probably developed during extensional events related to the Late Cretaceous-Early Tertiary rifting of the Tasman Sea. Structures such as Camden Syncline are most probably post-depositional and probably related to the uplift of the Illawarra Escarpment.

The only compressional events recorded in this part of the basin, are post-early Tertiary in age. All lateral displacements recorded in the study area are interpreted as related to three compressional stress fields namely: (1) NNE-SSW, (2) E-W, (3) SSE-NNW. Group II regional joints were formed during these compressional events. These events are also responsible for formation of N-NNE and ESE strike-slip faults, very mild inversion of pre-existing normal faults and development of thrust faults of the Southern Coalfield.

Tentatively, the NNE compression is related to the collision between the Indo-Australian and Pacific Plates, which generated an anticlockwise motion of Australia relative to the rest of the enclosing plate. In the Illawarra region, this dextral motion generated a NNE compression direction. The E-W compressional event most probably postdated the NNE event. The SSE compression is less pronounced and its relative age is not established.

CHAPTER 7

SOME GEOMORPHOLOGICAL AND ENGINEERING IMPLICATIONS OF ROCK FRACTURING

7.1 INTRODUCTION

Discontinuities in a rock mass usually control its overall behaviour. Rock mass deformability, stability of underground excavations and flow of fluid depend significantly on the intensity, the degree of interconnection, and the characteristics of the fracture network (Ghosh & Daemen 1993).

In this chapter, the relation between rock fracturing and the development and geometry of rock platforms is discussed for the Wollongong-Coalcliff area. Relaxation of the rock mass, due to unloading and relief from high horizontal stress, has played a notable role in the opening of fractures. Excessive pore water pressure, developed after heavy rains, as well as the mechanical behaviour of claystone and talus materials, are reported to be the main causes of instability along the slopes of the Illawarra Escarpment (Bowman 1972; Chowdhury & Young 1987). The present chapter also discusses the previously underestimated role of fracturing of underlying rock masses in developing landslips on talus materials in the Coalcliff and Scarborough area. The latter part of the chapter presents a technique for predicting the occurrence of dykes in either underground coal mining or civil engineering works.

7.2 THE FORMATION AND RECESSION OF ROCK PLATFORMS

The eastern Australian continental margin has several unusual characteristics, including an exceptionally narrow continental shelf and coastal lowlands backed by the Great Escarpment (Jenkin 1984). In the southeastern Sydney Basin, the coastline is composed of horizontal strata (normally less than 5° dipping) forming rock platforms, separated

by embayments and narrow beaches. Platforms are normally backed by a cliff or headland, and have a break at their seaward edge, called the 'low tide cliff'. Rock platforms are more frequent in the central and northern parts of the study area. Platform length ranges from 100 to 1250 m, with widths ranging between 20 and 200 m. Some platforms are partly covered by coastal sediments. The size and shape of sediment accumulation changes through the year.

Although the strata are subhorizontal and the geology is simple, slight changes in geological conditions have a pronounced effect on formation and recession of platforms. Rock platforms occur above mean tide level (MTL) and their mean frontal elevation ranges between 0 and 1.5 m above Australian Height Datum (AHD; Brooke 1993). The changes in height are mostly related to geological conditions, such as rock type and faults. Platform surfaces normally follow bedding. In some platforms, such as at Outcrops 1 and 2 (Figure 7.1), the frontal height changes from north to south, while in others (e.g. Outcrops 12, 13) it is almost uniform. The depth of water in front of the low tide cliff relates to the thickness of strata capping the platform, with greater depths in front of thicker beds (Outcrop 2, Figure 7.1; Brooke 1993). A thin layer of water covers most of the platforms at high tide. Some platforms, such as Outcrops 4 and 7, are only exposed at low tide.

Development of rock platforms

The coastal zone is the product of interaction between marine and terrestrial processes. In the southeastern Sydney Basin, where the sub-horizontal sequence is composed of alternating soft and hard rocks, platforms have formed where competent, mostly sandstone, beds crop out above sea level. For some platforms, this situation developed due to tilting of strata by faulting. Major faults in the study area are sub-normal to the coast and are usually clean breaks that lack thick gouge or fault breccia (see Chapter

4). Due to the listric nature of these growth faults (see Chapter 4), strata dip toward the fault plane on the downthrown side. In contrast, strata dip away from the fault on the upthrown side which reflects slight inversion of the faults in the Tertiary (see Chapter 6). The mismatch of dip on either side of the faults, plays an important role in the development of rock platforms. Platforms develop where the tilted sandstone beds are exposed at sea level. Examples of this relationship are: Outcrops 1 and 2 and the Harbour Fault (Figure 7.1), Outcrop 8 and 9 and the Scarborough Fault, Outcrops 21 and the Bulli Pass Fault, and Outcrop 25 and the Woonona Fault (Figure 1.4). The fault related platforms are relatively short and their length is less than 400 m.

Embayments or beaches have formed between platforms, where either incompetent beds occur at sea level (Figure 7.1), or erosion was facilitated by intense fracturing. An example is the embayment between Outcrops 4 and 5, which is controlled by a major 015° open fracture.

Between Wombarra and Austinmer (Outcrops 10-19), platforms and adjacent headlands consist of alternating thin beds of sandstone, siltstone and mudstone of the upper Wilton Formation. In this area, where the strata are horizontal and no fault-related tilting has occurred, platforms are long. Examples are a 1250 m long platform at Wombarra (Outcrops 11, 12), and a 850 m long platform at Coledale (Outcrops 13-15). In the same area, where the strata are locally tilted, platforms are either short or suddenly truncated. The short platform at Brickyard North is terminated at its southern side by the sudden southward descent of strata caused by a small monocline (Figure 4.9). Similarly, the platform at Bell Point (Austinmer, Outcrop 18) is relatively short due to tilting of strata caused by few SE trending normal faults (Figure 4.5).

Platform recession

Platforms erode when the assailing force of waves exceeds the resisting force of rocks

(Sunamura 1992). The study area experiences a low tidal regime, moderate swell conditions and infrequent storms (Brooke 1993). Tides are mostly about 1 m and rarely exceed 2 m.

Platform width is mainly controlled by relative rates of recession of seaward and backward cliffs (Trenhaile 1987). In the study area, platform widths change considerably in short distances (e.g. Brickyard Point), suggesting that wave energy is not the only factor influencing the erosion of platforms (see also Sunamura 1992). In addition to waves and tides, other factors influencing erosion and recession, as well as the height, of platforms are: rock type, geological structures (such as bedding planes, faults, folds and joints), susceptibility to weathering, degree of exposure to wave assault, availability of abrasive tools and possible minor relative changes in land and sea level (Gill 1972; Hills 1972; Kirk 1977; Sunamura 1992). Erosion can take place along low tide cliffs, surfaces of platforms, as well as at the base of the headland at the back of platforms.

Surfacial Erosion: Weathering as well as the wearing effect of sediments transported by waves, gradually erode the surface of platforms. The surfacial downwearing for platforms at Austinmer and Wombarra is measured from the wearing down of artificial features to be about 0.15-0.19 mm per year (Brooke 1993).

Geological defects facilitate downwearing (Figure 7.2a). In an area between Wombarra and Austinmer South (Outcrops 10-19), where the platforms consist of alternating thin beds of sandstone, siltstone and mudstone, commonly a stepped topography has developed (see also Brooke 1993), due to the combined effect of vertical joints and thin bedding (Figure 7.2b). In platforms with thicker capping sandstone beds, such as Outcrops 1, 2 and 21, vertical open joints are widened, up to 30 cm, mostly due to weathering and wave action (Figures 7.2c, 5.15). In general, surface

downwearing is slow, but major fractures, dykes and faults erode more easily and form narrow channels on the surface of platforms (Figures 3.1, 7.2b). Closed joints might resist erosion, leaving a raised joint infilling (Figure 7.2d).

Recession of low-tide cliff: Geology, in addition to wave and tides, controls the rate and shape of recession of the low tide cliff (Sunamura 1992). Due to the alternating competent and incompetent nature of the horizontal sequence, undermining of the stronger rocks is the dominant erosional mechanism. The combined effect of the conjugate pattern of vertical joints and bedding planes forms cubical, platy or rhombohedral blocks of various sizes, which either topple or are washed away upon undermining (Figure 7.3a). At Coalcliff (Outcrop 2), the zig-zag edge of the platform is dictated by 010° and 045° striking joints. Similarly at Wombarra and Brickyard Point, the platform geometry is controlled by jointing (Figure 7.4). Due to variations in wave energy and geological conditions, the rate of recession is not uniform even in a single platform. An example is Outcrop 2 at Coalcliff, where the southernmost part of the platform is receding much faster than the other parts (Figures 7.1, 7.3a).

Recracking of joints and strike-slip movement along them (see Chapter 5) formed a network of interconnected open joints. Weathering and wave action widened these open fractures and minimised cohesion between adjacent blocks. These blocks are easily detached from the rest of rock mass upon undermining (Figure 7.3).

The depth of water in front of platforms with thicker undermined caprock, is more than the thickness of thin-bedded units. An increase in depth raises the assailing force of waves (Sunamura 1992). In some places, such as Outcrops 1 and 2, blocks of rock, have been separated from the edge of the low tide cliff and transported back to the surface of the platform by occasional high energy waves (Figure 7.1; Brooke 1993). At the intervening embayment, composed of less competent materials, the locally derived

small deposit of shingles has developed a gentle slope occasionally covered by boulders (e.g. between Outcrops 4, 5; see also Figure 7.5a).

Erosion of headlands: The accumulation of talus deposits at the toes of some headlands and cliffs, parallel with thin layers of coastal sediments covering parts of platform, suggests that erosion of the headland is not due to marine process (Figure 7.5). From observations over three years in the study area (1991-1994), it appears that where erosion and recession of the seaward edges and surface of the platforms is noticeable, the marine erosion of the toe of adjacent headlands is not significant. This is in accordance with similar observations by Brooke (1993). As the low tide cliff of these platforms appears to be eroding faster than the landward headland, it seems that the platforms are gradually eroding away.

Age of rock platforms

Five levels of relict rock platforms 2-30 m above present sea level, have been reported for the coast to the south of Sydney, and dated to be Late Quaternary to mid-Tertiary in age (Bryant *et al.* 1992; Young & Nanson 1982). For the southern Sydney Basin, which is tectonically stable, these levels appear to be eustatic (Young 1993). The latest rise is related to the Holocene transgression, which reached its maximum height 1 m above present sea level at about 6500 years before the present (Sunamura 1992; Bryant *et al.* 1992).

The relative rate of erosion of cliffs at the back and front of platforms indicates whether they were formed by present sea level or are the relict of an older higher sea level (Sunamura 1992). In most of the studied platforms, the erosion and recession of the low tide cliff is evident, while the landward cliff shows no signs of current marine erosion (Figure 7.5). This observation suggests that the headlands are the product of

the higher Pleistocene sea level.

7.3 BEDROCK FRACTURES AND INSTABILITY OF TALUS SLOPES

Mass movement is regarded as the most severe geological hazard in the northern Illawarra region of the southeastern Sydney Basin (Bowman & Mullard 1986). Numerous historic and recent landslides, rock falls and mud flows have been recorded for this area. It has been estimated that over 150 major slope failures occurred between Wollongong and Stanwell Park during the present century (Young 1978; Bowman & Mullard 1986).

In the coastal plain between Coalcliff and Wollongong, instability is related to residual soil, talus materials, as well as the Late Permian strata of the Sydney Subgroup of the Illawarra Coal Measures which underlies most of the foothill ridges. Higher risks occur at Mt Ousley Road, Bulli Pass and in the Austinmer-Coledale area. For example, after the heavy rains of 1973-74, frequent failure occurred and 11 houses were destroyed and at least 12 others were damaged in the Austinmer-Coledale area (Young 1978). Towards the north, where the high cliffs meet the sea, the instability is mostly related to talus and the Early Triassic strata of the Narrabeen Group.

Illawarra Escarpment

The most important physiographic feature of the study area is the Illawarra Escarpment. At Coalcliff, where the escarpment meets the sea, its height is 350 m. Towards the south, the distance between the escarpment and the sea increases, and a narrow coastal plain is developed. Very steep slopes exist along the coastline and the Illawarra Escarpment. Thick beds of the resistant Hawkesbury Sandstone which cap the escarpment (Figure 7.6), are underlain by alternating sandstone, siltstone, mudstone and claystone of the Narrabeen Group (Table 1.3). Two major terraces exist near the base

of the Narrabeen Group. The upper terrace formed on the Stanwell Park Claystone and the lower on the Wombarra Shale (Figure 7.6). These benches are poorly drained and crossed by many small wandering shallow channels (Young 1977, 1978). Benching of the escarpment is related to differential erosion. Shale weathers faster and develops gentle slopes, whereas sandstone, especially thick units, break along joints and form sub-vertical cliffs. Landslips and rock falls from these cliffs are a major threat to the railway line and road in the northern part of the study area.

Materials transported from the upper cliffs generally cover the more gentle slopes. Weathering of these materials, as well as the upper part of the bedrock, forms a talus-type soil which is thicker above less resistant strata (Young 1977). Talus is composed of sandstone blocks in a matrix of fine-grained, mostly clayey, soil. The ratio of clay, silt, sand and coarser sized particles in talus changes from place to place (Chowdhury 1976).

Factors effecting slope instability: Surface and groundwater as well as rock type, and its weatherability, are the major factors controlling the instability of talus along the slopes of the Illawarra Escarpment. Vertical open fractures in the underlying rock mass and the existence of high horizontal stresses are other factors that contribute to slope instability.

A close relation exists between rainfall and slope failure. The Illawarra region has a moderate climate and the average annual rainfall is about 1200-1400 mm, with no distinct wet or dry season. A peak rainfall of 800 mm in 48 hours has been reported for this area (Young 1978). Slope failures occur immediately after extensive precipitation, but are not related to a particular season.

The distribution of the landslips of the Illawarra Escarpment is also closely linked to changes in topography and rock type. Mudstone, claystone and coal weather more

rapidly than sandstone and siltstone. Weathering of less competent claystone and mudstone units undermines overlying sandstone beds. Where sandstone is thick bedded and intact, the overhung part is stable. An example is an up to 3 m overhung part of the Coal Cliff Sandstone at Clifton (Outcrop 4). Along the escarpment, overhanging is frequent at the contact between the Wombarra Shale and the Scarborough Sandstone, and also between the Stanwell Park Claystone and the Bulgo Sandstone.

Finally, a close relation exists between faults, faulted joints, jointed faults and ground instability. Examples are slumps which developed adjacent to the ESE trending Harbour, Jetty and Clifton Faults, or frequent failures of undermined sandstone blocks along the vertical open joints. Weathering enlarges fractures by dissolving the wall material in percolating water or by the presence of expanding clays and/or tree roots growing in fractures.

Contemporary stress: The study area is under a relatively high horizontal stress. The direction of contemporary horizontal stress can have a considerable effect on engineering structures, because extra measures have to be taken to overcome or relief the stress or the resulting strain effects (Gray 1982). High horizontal stress has been responsible for many gas outbursts in underground coal mines of the Southern Coalfield (Shepherd & Creasey 1979; Shepherd & Gale 1982; Shepherd *et al.* 1981a, b; Hanes *et al.* 1983). A ratio of 1.6-2 to 1 has been reported for the horizontal stress components (Enever *et al.* 1989).

Two stress measurements, at the Corrimal and Coal Cliff Collieries, indicate a general N-S to NE-SW maximum horizontal stress along the coast (Worotnicki & Denham 1976), while another study by Enever *et al.* (1989) suggested a NE to E direction for σ_1.

Fault orientation and occurrence of fractures and gutters are used to infer the

contemporary stress field in the collieries of the Southern Coalfield (Shepherd & Huntington 1981). In several collieries, guttering and roof failure is found to be more frequent in roadways driven in particular orientations. It is empirically established that the drivages parallel to σ_1 have less failure problems compared to those which occur normal to the direction of maximum horizontal compression. Similarly in boreholes, swelling and failure has been reported in a direction normal to σ_1. Based on these observations, it has been inferred that σ_1 is generally N-S at Coalcliff Colliery and E-W in the Westcliff Colliery (Peter Lamb 1994, pers. comm.).

In-situ measurements, seismic studies of recent earthquakes (Robertson 1961, Burrarorang 1973), as well as geological observations on dam sites and coal mines suggest a high component of horizontal stress, striking either N-S, NE-SW or E-W for the Southern Coalfield (Cleary 1963; Doyle *et al.* 1968; Gray 1975, 1976; Worotnicki & Denham 1976; Scheibner 1976; Mills & Fitch 1977; Denham *et al.* 1979; Fitch 1976; Denham 1980; Shepherd & Huntington 1981; Gray 1982; Enever *et al.* 1989). These differences, reported for the contemporary stress directions, either are due to local changes in the stress field or reflect the inadequacy of the data base.

Faulted joints are presently open. In the northern part of the study area, open fractures mostly strike N-NNE or NE, which is broadly parallel with the direction of the Illawarra Escarpment. These openings can be partly related to stress release caused by unloading due to receding of the escarpment. A similar situation has been reported from North America, where the E-W trending Niagara Escarpment in western New York and southern Ontario is capped by flat-lying strata of the Palaeozoic Lockport Dolomite. Four vertical joint sets are developed in this unit (Memarian 1975; Williams *et al.* 1985; Gross & Engelder 1991); among them one set, strikes ESE and is sub-parallel to the Niagara Escarpment. The frequency of ESE joints increases toward the escarpment. These joints are neotectonic (in the sense of Hancock & Engelder 1989) and appear to

have formed near the Earth's surface in response to low tensile stresses developed in bedrock adjacent to the retreating escarpment (Gross & Engelder 1991).

In the southeastern Sydney Basin, the N-NNE and NE regional joints, are subparallel to the Illawarra Escarpment. The opening of these joints is normally more than SE striking joints. Elimination of high σ_1, caused by cliff cutting, and the westward recession of the escarpment, is partly responsible for the present day openings of those fractures, which are subparallel to the cliff face. Widening of open fractures is also related to wave action and weathering.

Major recent landslips

The section of the Lawrence Hargrave Drive and railway line between Coalcliff and Scarborough, has had a long history of slope instability. The road is founded on the Wombarra Shale, which is normally blanketed with a few metres of talus. The instability of this part of the road goes back to the last century when the railway track was situated along the present road. In 1920 the track was moved uphill, to its present site, partly due to frequent rock slides and landslips (Hanlon 1956a, b, 1958). During the period 1950-51 the road was severely damaged by numerous slides that occurred immediately after heavy rainfall.

The landslips along the Lawrence Hargrave Drive have been mostly related to lubrication of the talus/bedrock interface and saturation of overlying talus and soil (e.g. see Bowman 1972; Bowman & Mullard 1986). The higher areas of the escarpment act as catchment, leading water to the lower parts (Amaral 1975). The talus blanket, which is more permeable than the underlying mudstone bedrock, develops perched water tables after heavy rains, rather than being influenced by a rise in the regional water table (Young 1978, 1983). The increase in pore water pressure reduces the shear strength of the talus material.

The most recent major slides, along this section of the road, occurred after the heavy rainfall in late April 1988. One of these slides developed to the east of the road at Moronga Park (Figures 7.7, point 2 & 7.8a). Hutton *et al.* (1989) described it as a composite slide comprising a slump and two earth flows. This slide has remained active. Within a week after the heavy rain, the main scarp was 1-2 m high. Three to four weeks later it was 4-5 m high and ten months later it was 10 m high (Hutton *et al.* 1989). The main scarp is presently about 12 m high. The slide developed in talus that rested on the Illawarra Coal Measures. The basal shear surface of the slide occurs along the top of a sandstone unit (Figure 7.9a). Material at the base of the slide dropped over the edge of the resistant sandstone to the platform below, where finer particles were subsequently washed away by wave action.

The northern flank of the slide partly coincides with the ESE trending Clifton Fault, which is steeply dipping to the north (Figure 7.8). Uphill and farther west of the main scarp, zones of en echelon tension fractures developed aligned with the direction of the Clifton Fault (Hutton *et al.* 1989). These tension fractures formed from dextral shear and indicate that the zone of instability extended above the main scarp of the slide.

Air photographs taken one month after the slide incident shows that the crest line of the slide at Moronga Park is straight and strikes 015° (Figure 7.9a). The crest line coincided with an open fracture in the bedrock which is traced south into the lower parts of the cliff (Figure 7.7).

At 500 m north of the Moronga Slide, the road was undercut and collapsed by a 50 m long slide (Figures 7.8, point 1 & 7.9b). Air photographs taken shortly after sliding showed that the main scarp of the slide, located along the road, was composed of straight segments striking 015°. The main scarp also coincided with a very long open fracture, which is followed along the coastal rock platform to the south (Figure

7.8).

A third slide developed to the south of the Moronga Park slide, 100 m south of the Clifton Hotel (Figures 7.7, point 3 & 7.9c, point 3). This slide is about 50 by 50 m in area, and developed in gently sloping talus materials along the road. The slide crest is located near the contact between the Wombarra Shale and the Scarborough Sandstone, and its base is truncated by the Coal Cliff Sandstone. Water seepage occurs at the base of the slide which is still active. In June 1993, the recently paved road was fractured and vertically displaced 3 cm along a 018° striking fracture. The northern end of this fracture curved clockwise and then bifurcated, before it terminated. Towards the south, the fracture passes below the only house on this part of the road and then forms the edge of the lower cliff.

The 1988 slide, south of the Clifton Hotel, is in fact the relict of an older slide. Chowdhury and Young (1987) presented data for the previous activity of this, and two other slips which were initiated through the development of a series of cracks along the 350 m length of the road between the Clifton Hotel and Scarborough (Figure 7.9c). These slides, were investigated during 1984, using both site and laboratory techniques. Site work included geological mapping, seepage observations, seismic runs, drilling of 15 boreholes and the installation of standpipe piezometers. Laboratory work consisted of classification, Atterberg limits and triaxial testing to determine shear strengths. The depth of talus mantle is less than 8 m, and the contact between bedrock and the talus mantle was shown to be the slip surface. Tension cracks developed along the road, represented the crests of these slides and strike 015-020°. These tension cracks also coincide with fractures in the underlying bedrock (see Chapter 2).

For rectification of these slides, a series of subsoil drains have been positioned to lower the water table by 4-5 m. Also a few trenches were dug and covered with geotextile and filled with slag. Piezometers and alignment/settlement stakes were the

major methods recommended for continuous monitoring of the slides. The remedial works have not stabilised the slope totally (Figure 7.9c, point 3).

All the studied landslips occur in talus and immediately followed heavy rains. Tension cracks developed at the crest of these slides were straight and strike 015-020°, which coincides with the direction of the NNE joints in the bedrock (Figure 2.6b). Frequent rock falls, which occur along the Lawrence Hargrave Drive, are also partly controlled by rock fractures. An example is a large (500 tonnes) rock fall which blocked the road after the heavy rain of April 1988 (see the road on the lower part of the Figure 7.1). This fall was composed of slabs as large as 2 m in diameter along with smaller blocks and weathered rock and clay particles mainly detached from the cliff face (Hutton *et al.* 1989). The sources of these falls are thick-bedded sandstones. Vertical fractures, and release joints control the size and shape of blocks.

Bedrock fractures and talus failure

In the Coalcliff-Scarborough area, crests and main scarps of slumps are parallel to and coincide with vertical open fractures in underlying bedrock. There are 2 options to explain why the bedrock fractures have controlled the location and orientation of the slumps. The slumps have formed either by: (1) a slide surface developed at least partly in bedrock (Figure 7.10a), or (2) the slide surface occurs along the contact of the talus with the bedrock (Figure 7.10b). In both cases, opening or movement of 015-020° striking vertical fractures in bedrock stretched overlying talus, forming cracks which mark the crests of slides. Although the rock experiences a high horizontal stress, the faults and fractures are not active, and no earthquakes have been reported to be related to any of the faults of the study area. Hence, any movement along fractures must be purely gravitational.

It is possible that at least some segments of a rupture surface may pass through

the upper part of the bedrock, which is generally weathered and has a relatively lower strength than intact bedrock. Slight lateral spreading of blocks of bedrock along lubricated bedding planes, can widen bedrock fractures at the back of blocks, which in turn stretches the overlying soil and forms tension cracks at the surface (Figure 7.10b). Downhill movement of blocks of rock is caused by forces exerted by expanding clays, which fill these open fractures, as well as a sudden rise of cleft water pressure after heavy rains.

More frequently, the slip surface is the contact between bedrock and talus (Bowman 1972; Chowdhury & Young 1987). The step-like topography of the bedrock, with steps dropping at vertical fractures, form wedges of talus soil (Figure 7.10). The base of a wedge has a general downslope dip and the back of it is marked by a fracture wall. In dry seasons water, which flows along the contact between talus and bedrock, drops at the steps and washes away finer grains, reducing the cohesion between the soil and the bedrock.

After a heavy rain, the water table rises sharply, reducing the shear strength of the talus material. The weight of saturated soil has a downhill component. Slight downhill movement of soil can develop a tabular gap at the back of wedge which in turn stretches the overlying soil. The resulting cracks mark the crest of landslip (Figure 7.10).

7.4 DYKE PREDICTION IN UNDERGROUND MINING

Dykes are readily recognised at the surface, because the physical characters of dykes are rarely identical with the host rock. This difference is magnified by subsequent weathering and alteration. Dykes that are softer than the host rock produce negative features, while a harder dyke stands higher in outcrop. This is not the case in underground mining, where dykes are unpredictable and encountering a dyke might be

troublesome. Large dykes can significantly change the host rock physical characters, which in case of coal seams can be disadvantageous or costly in terms of providing proper support for weakened areas. Dykes can also cause water inrushes into underground workings. Geophysical surveys or exploratory holes are among techniques currently used, where the prediction of dykes is needed. Most of these techniques, although accurate, are time consuming and costly.

Rickwood (1985) proposed the following features as signs of increasing proximity to an igneous intrusion in underground coal mines: coking or cindering of coal and localised hardening or bleaching of shales; abnormal hardening, fracturing, weathering, columnar jointing or iron oxide filling of joints in sandstone; and finally, abnormal flow of water to subsurface excavations, which is usually related to abnormal fracturing.

Adjacent joints and dyke prediction

Where dykes are formed by magma pressure and hydraulic fracturing of bedrock, a set of adjacent joints is developed parallel to the dyke (Figure 7.11a, also see Chapter 3). The spacing of these joints systematically decreases towards the dyke (see Figure 3.6). Where the rock is competent and capable of jointing, adjacent joints are well developed up to 100 m away from the dyke. Adjacent joints can be used to predict dykes in places where the ground surface is partly covered by water or overburden or the dyke is not exposed at the surface.

Figure 2.23a demonstrates joint orientation along the Scanline 11-HH', at Wombarra. Here, the systematic joints sets strike 015°, 040°, 110° and 125°. From the 230 m mark, a fifth set striking 155°-160°, is introduced. The spacing of these joints is more than 3 m, where they commence, but decreases to about 1 m at the end of the scanline. This scanline is terminated at the seaward edge of the platform. The unexpected introduction of 160° joints, with increasing frequency toward the edge of the

platform, and the absence of similar joints in other parts of this platform or the neighbouring outcrops, suggests that a dyke may be expected, not far from the edge of the platform.

Figure 3.5 is another example showing the joint pattern along Scanline 19-EE'. The dominant set in this scanline is 040°. Two dykes, striking 040°, are encountered at the 28 and 35 m marks. Adjacent joints are developed parallel to dykes with decreasing spacing toward each dyke (Figure 3.5). Between the 60 and 63 m marks, the frequency of adjacent joints is abnormally increased, developing some joint zones. These small joint zones most probably are developed ahead of some propagating dykes, which did not reach the present elevation of the platform. Existence of a similar joint zone, beyond the termination point of the dyke at the 28 m mark, supports this hypothesis.

In conclusion, adjacent joints can be used as a tool for the prediction of the location of dykes, both at the surface and underground. At the surface, this technique is especially useful, where the dyke is buried under soil, water or bedrock, or where application of geophysical methods is not feasible. Dykes in the Illawarra Coal Measures are usually weathered to clay materials, which do not respond efficiently to the magnetic method.

In underground coal mining, or civil engineering practice, a routine scanline survey along a progressing tunnel or working face, and plotting the results on a scanline chart, should show the introduction of any new group of joints. Where the spacing of a newly introduced set is decreasing, a dyke with a similar orientation, can be anticipated farther ahead. Introduction of a new joint set in a scanline may also be related to other structures, such as monoclines. In the latter case, spacing of the newly introduced joint set should not be reducing systematically (Figure 7.11b).

CONCLUSIONS

Between Coalcliff and Wollongong, rock platforms formed where more resistant beds, especially sandstone, emerged above sea level. Movement along listric normal faults, and related tilting of strata, frequently control the exposure of competent rocks at sea level. The length to width ratio of platforms, containing tilted strata, is between 1 and 4. In contrast, those platforms which are not structurally controlled, have a uniform frontal height and the ratio between their length to width is between 5 and 15.

Joints, and other fractures, control the present geometry of platforms. Platforms recede from their low tide cliff, by undermining of vertically jointed sandstone or siltstone. Surfaces of platforms are gradually worn down by wave action and weathering. The effect of present marine processes in recession of headlands is less significant. Platforms formed before the present sea level was established and are currently eroding away.

Vertical open fractures play an important role in formation of both rock falls and landslips. In a section of the Lawrence Hargrave Drive, between Coalcliff and Scarborough, cracks formed at the crest of landslips are straight and strike 015-020°. Surfacial cracks in talus are normally located above vertical open fractures in the bedrock.

Relaxation caused by the removal of the high contemporary σ_1 due to cliff cutting and erosion of the escarpment played an important role in opening of those fractures which are subparallel to the escarpment. Slight outward spreading of jointed blocks, caused by excessive cleft water pressure, which developed after heavy rains, or forces exerted by expanding clays, as well as the step-like surface of the bedrock contribute to the development of tension cracks in overlying talus mantle and its subsequent slip. The role of bedrock fractures in propagation of talus slumps, must be considered in any future planning for rectification or monitoring of the rock mass in this area.

In underground coal mining, dykes might be hazardous as they may cause instability problems as well as inrush of water into the working area. Adjacent joints can be used as a tool for predicting approaching dykes. Routine scanline survey of the joints of a progressing tunnel or excavation can indicate the introduction of a new set of joints. Where the spacing of these joints is systematically decreasing, a dyke is expected further ahead.

CHAPTER 8

SUMMARY OF CONCLUSIONS

8.1 JOINTS

Frequent plumose structures and lack of original shearing demonstrate that almost all joints of the Illawarra Coal Measures originally developed as extension fractures (mode I). Conjugate joint sets are the result of two separate fracturing events of different orientations. The fracture pattern has formed cumulatively from the Late Permian to the Present.

Two distinct groups of regional joints occur in this area. Following deposition and lithification of the Illawarra Coal Measures, the region was fractured repeatedly forming N-NNE, NE and SE, joint sets (Group I regional joints). These joints are vertical, straight, long and segmented. Each joint set was sealed and filled with calcite or siderite following its formation. Group I regional joints never interfere with each other. Cross-cutting relations show that Group II regional joints were formed later in the history of the region. These joint sets, which strike NNE, E and SSE, are less frequent, straight to slightly curved, short, mostly closed and fine. Local joints are related to other structures, such as dykes or monoclines. Regional and local joints are often parallel or subparallel to each other, even in a single outcrop. Nonsystematic fractures (cross joints) formed mainly normal to the NE joints.

Competent rocks like sandstone, laminated siltstone and some mudstone are jointed, while relatively less data were obtained from claystone or coal. The orientation and frequency of a joint set may change, even in a single outcrop, mostly due to changes in rock type. More joints formed in thinner beds. This relation could not be quantified due to the effect of other influencing factors, such as rock type. Each fracture set in a given rock type may have a different spacing-bedding thickness

relationship.

Extension joints develop in mechanical units of varying shape and size, defined here as jointing units. Boundaries between jointing units are at changes in mechanical properties, which are mainly related to changes in rock type, or marked by a pre-existing open fracture. The major factors defining the pattern of extension joints in a unit are the mechanical properties of the rock mass and the loading history. In the southeastern Sydney basin, Group I regional joints normally nucleated in the middle of each mechanical unit and propagated horizontally. The spacing of these joints is frequently more than the thickness of the jointed unit.

Gradual changes in thickness or rock type, account for the formation of joint sets with curving strike. The strike of a set of joints may differ in two adjoining mechanical units. Where the strike differs sharply at the interface, joints in each unit were formed independently, each with nucleation points located away from the interface. Where the joints have extended vertically from one unit to the other, the main joint face has slightly twisted, then segmented and formed an array of en echelon fractures, with nucleation points at the interface.

8.2 FAULTS AND DYKES

In the southeastern Sydney Basin, faults are generally normal and strike ESE-SE and N-NNE. The ESE-SE faults are either major and consist of a single break or are minor and zonal. Their throw decreases rapidly both horizontally and vertically. The downthrown block is either to NE or SW. A notable characteristic of these faults, consistent with a listric geometry, is the dip of strata, which is towards the fault plane, on the downthrown side.

The N-NNE faults occur mainly in the northern and central parts of the study area. Their characteristics include: a strike of 000-025°, a dip between 70-90°,

downthrow either to the east or west, occurrence in groups of subparallel fractures, small normal components and an associated parallel set of joints. In more brittle rocks, like sandstones, these faults are subvertical faulted joints while in more ductile rocks fault dip is less. Although lateral movements are frequent, no strike-slip faults developed initially in the study area.

In the Southern Coalfield, most of the dykes strike ESE (100-120°) with another regional set with a NE strike. NNE striking dykes are developed locally in the northeastern part of the coalfield and are parallel to N-NNE normal faults. Dykes were mostly injected through fractures which were propagated by magma pressure. Tension responsible for dyke formation, usually propagates a joint zone with one of its central members intruded by magma. The spacing of these adjacent joints decreases away from the dyke. Where magma intruded along a pre-existing open fracture, adjacent joints did not develop. Orientations of dykes that are not injected into pre-existing fractures reflect the prevailing contemporary stress field.

8.3 FAULT-FORCED FOLDS

In the southeastern Sydney Basin, NW plunging gentle folds are generally fault related. ESE-SE striking normal faults are mostly concentrated around anticlines, forming grabens, while synclines lack major faults. Synclines are much wider than the fault-bounded anticlines. Anticlines formed by rollover on the downthrown side of the inward dipping listric normal faults. Monoclines are also the result of rollover developed in the downthrown side of major faults, or are forced folds formed above buried normal faults.

8.4 FAULTED JOINTS

Joints and faulted joints occur parallel with each other. All measured strike-slip

displacements are the result of recracking of pre-existing joints, faults and dykes. Faulting commenced with recracking (jointing) and continued by lateral slip. A recracking front might have: (1) continued to grow beyond the tip of the parent joint without any deviation, (2) terminated, or (3) tilted and twisted away from the host fracture. Recracking grew horizontally by the connection of joint segments. En echelon arrays are the result of vertical propagation of faulted joints into neighbouring mechanical units. A fracturing front terminated at an intersection with an open joint.

Lateral movements along recracked joints have produced systems of conjugate pairs of faulted joints. Slip along a faulted joint might be dextral, sinistral or both. Displacement is generally proportional to the length and continuity of the faulted segment. Some long faulted joints, which demonstrate small displacements, have been affected by more than one episode of lateral displacement, acting in opposite directions.

Recracking of rock also formed a new set of short secondary cracks which are developed either at the tip, at the sides or in between pre-existing fractures. Secondary joints are straight to slightly curved and relatively short, and form sets of relatively short dilatant joints which are systematic and regional. They may be opened but show no sign of subsequent shearing. In the southeastern Sydney Basin, secondary joints, strike NNE, E and SSE, and form the Group II regional joints.

Conjugate sets of recracked joints as well as the orientation of secondary cracks over the study area are readily interpreted as related to 3 compressional stress fields namely: (1) NNE-SSW, (2) E-W and (3) SSE-NNW. During each compression, suitably oriented fractures recracked and had lateral slip along them. Additionally, a set of secondary cracks formed aligned with σ_1. The consistent orientation of secondary cracks over the study area, signifies that the stress field was approximately uniform for each compressional event.

Faulted joints are hybrid fractures, resulting from recracking and lateral slip along

those pre-existing joints which formed a 10-30° angle with contemporary σ_1. Suitably oriented faulted joints have been reactivated by subsequent compressions. The angle between the direction of the later compression and the strike of pre-existing faulted joints could be more than 30°, which is the limit for the initial recracking of a closed joint. The outcome of multiple recracking of conjugate set(s) of joints is a network of connected open fractures which accommodate shear displacement caused by compressional events.

Factors such as strength of infilling materials, angle between fractures and σ_1, and the number of compressional events imposed on each fracture, control the intensity of recracking and the amount of lateral slip. Group I regional joints formed without interfering with each other. The small deviatoric stress responsible for the formation of these joints could not overcome the strength of fracture infillings along pre-existing joints. The deviatoric stress developed during the compressional episodes was high, as it could overcome the strength of fracture infillings and recracked them. Group II regional joints interacted with those members of Group I regional joints that had been previously recracked.

8.5 RELATIVE AGES OF STRUCTURES

Although it is possible to assign a relative age for each joint set at a particular location, it is difficult, and probably unwise, to generalise it regionally. Most of the Group I joints have lost their morphological features due to subsequent deformation, which usually has enlarged them dramatically, both horizontally and vertically. Subsequent deformation has also destroyed cross-cutting relations that presumably existed between neighbouring fractures. Preserved cross-cutting relationships, presently observed between fracture sets, mostly developed in succeeding deformations. Joints formed during burial, uplift and unloading of the Late Permian sequence. Group I regional joints, formed

during burial and show no apparent genetic relation with SE trending minor folds. Locally developed systematic joints were formed mostly in the time span between the Group I and Group II regional joints. Nonsystematic joints (cross joints) are the youngest natural fractures and formed after Group II joints.

The only fractures which formed during deposition were local normal faults. For example, several small normal faults with displacements up to 5 cm occur in the Coal Cliff Sandstone adjacent to the Clifton Fault. They have an identical orientation to the Clifton Fault. Microscopic study of these fault surfaces shows no brittle deformation of sand grains and indicates that the faults affected unlithified strata. This is confirmed by the presence of growth fault controlled deposition with thicker strata preserved in the downthrown blocks.

ESE-SE normal faults have increased, both in size and number, during the younger extensional episodes, which were active up to the Early Tertiary. The present study also shows that the N-NNE faults are post depositional and postdated development of similarly oriented joints.

Cross-cutting relationships indicate that all dykes are post depositional and developed after the formation of regional joint sets and most of the normal faults of the study area. In the Southern Coalfield, igneous activity was active from the Late Mesozoic to Early Tertiary. No dykes formed after the commencement of the compression in the Tertiary.

Recracking with strike-slip movements along pre-existing fractures and the formation of secondary joints developed from compressions which are the last significant deformation events in this part of the basin. Cross-cutting relations between fracture sets indicate that these compressional events postdate formation of dykes. Cross-cutting data suggests that the E-W compressional event most probably postdated the NNE event. The SSE compression is less pronounced and its relative age is not established.

8.6 TECTONIC HISTORY

The following scenario is established for the sequence of formation of the major structural features of this part of the basin:

(1) Early quasi-extensional regime (Late Permian)

This episode is marked by the initiation of ESE-SE normal faults and similarly oriented minor folds during deposition of the Illawarra Coal Measures and the Narrabeen Group. A quasi-extensional regime was responsible for the formation of these structures. This stress field was developed by formation of a forebulge in the northern part of the Southern Coalfield, and may have reactivated suitably oriented basement faults. Downwarping occurred above basement grabens, generating tension in adjoining areas, which in turn propagated grabens in the sedimentary succession. Mild anticlines (warps) are fault-forced folds and are mostly the result of rollover on the downthrown sides of inward-dipping listric faults. Normal faults are not necessarily the continuation of basement faults. Fine-grained units of the Shoalhaven Group may have acted as detachment horizons for these listric faults.

(2) Intermediate regime (Mesozoic-Early Tertiary)

Group I regional joints were formed during this time. Additional normal fault and related dykes, monoclines and local joints were also formed during the Mesozoic, especially during extensional events related to the Late Cretaceous-Early Tertiary rifting of the Tasman Sea and the rifting between Australia and New Zealand. Structures such as Camden Syncline are most probably post-depositional and probably related to the uplift of the Illawarra Escarpment. This episode was possibly terminated at the end of extension related to the opening of the Tasman Sea.

(3) Late compressional regime (Post-Early Tertiary-Present)

Recracking of pre-existing fractures with lateral slippage along them, and formation of Group II extension joints, are the major products of this episode in the study area. Compression would not be expected during Tasman Sea rifting (95-55 Ma) and hence, the late compressional episodes are probably post-Tasman Sea formation or post-earliest Tertiary. The NNE compression is tentatively related to the collision between the Indo-Australian and Pacific Plates. Due to this collision, Australia rotated anticlockwise relative to the rest of its enclosing plate. This dextral motion generated a NNE compression direction in the Illawarra region.

Formation of non-systematic cross joints and widening of open fractures, as well as formation and recession of coastal platforms and headlands, are due to unloading and more recent weathering, wave action and surfacial movements.

8.7 IMPLICATIONS OF ROCK FRACTURING

In the southeastern Sydney Basin, coastal platforms formed when the competent sandstone beds emerge at sea level. This frequently happened due to tilting of strata, caused by movement along listric faults (see above). Platforms containing tilted strata are relatively short, in contrast to the longer platforms with almost horizontal strata. Rock platforms were formed at a higher sea level, and vertical fractures are one of the prime factors which control their present geometry. Platforms receded from their low tide cliff, mostly by undermining of jointed blocks. Surfacial erosion and weathering widens open fractures and develops channels. As marine erosion of headlands is not significant, rock platforms are gradually eroded away.

Frequent landslips, which occur along the slopes of the Illawarra Escarpment, are related to heavy rains and the mechanical behaviour of both talus material and

underlying bedrock. The present study shows the relation between landslips and bedrock fractures. Along the Lawrence Hargrave Drive, landslips were found to contain tension cracks developed at their crests that are aligned with open fractures in underlying bedrock.

Due to alternating hard and soft strata, bedrock topography is step-like. After heavy rains, slight downhill movement of a wedge of soil in front of a step section of a step, forms a tabular gap at the back of a wedge, which in turn generate tension cracks in overlying talus. Where the slip surface is inside the bedrock, cleft water pressure or forces exerted by expanding clays filling fractures, slightly moves the block of rock downhill. Opening of the fracture at the back of block, stretches the overlying talus and forms tension cracks, which mark the main scarp of the immediate slide.

Dykes cause problems in underground coal mining and civil engineering practice. Adjacent joints are a useful tool for predicting the location of dykes in progressing tunnels or working faces. Continuous fracture mapping and plotting of the results on a scanline chart can reveal any newly introduced joint sets. Where the frequency of these joints increases a dyke might be expected ahead.

REFERENCES

AMARAL R. 1975. Special instability problems in the Illawarra and Warringah Shire area of New South Wales. *Proceedings of the 2nd Australia-New Zealand Conference on Geomechanics*, pp. 319-325. Brisbane.

ANDERSON E. M. 1951. *The Dynamics of faulting and dyke formation with application to Britain,* 2nd ed. Oliver and Boyd, Edinburgh.

AYDAN Q. & KAWAMOTO T. 1990. Discontinuities and their effect on rock mass. *In* Barton N.R. and Stephansson O. eds *Rock Joints*, pp. 149-156. A.A. Balkema, Rotterdam.

BABCOCK E. A. 1973. Regional jointing in Southern Alberta. *Canadian Journal of Earth Sciences* **10**, 1769-1781.

BADGLEY P.C. 1965. *Structural and Tectonic Principles*. Harper and Row, New York.

BAER G. & BEYTH M. 1990. A mechanism of Dyke segmentation in fractured host rock. *In* Rickwood P.C. and Tucker eds *Mafic Dykes and Emplacement Mechanisms*, pp. 3-11. A.A. Balkema, Rotterdam.

BAHAT D. 1986. Criteria for the differentiation of en echelons and hackles in fractured rocks. *Tectonophysics* **121**, 197-206.

BAHAT D. 1987a. Jointing and fracture interactions in Middle Eocene chalks near Beer Sheva, Israel. *Tectonophysics* **136**, 299-321.

BAHAT D. 1987b. Correlation between fracture surface morphology and orientation of cross-fold joints in Eocene chalks around Beer Sheva, Israel. *Tectonophysics* **136**, 323-333.

BAHAT D. 1991. *Tectonophractography*. Springer Verlag, London.

BAHAT D. & ENGELDER T. 1984. Surface morphology on cross-fold joints of the Appalachian Plateau, New York and Pennsylvania. *Tectonophysics* **104,** 299-313.

BAKER J. C., FIELDING C. R., CARITAT P. D. & WILKINSON M. M. 1993. Permian evolution of sandstone composition in a complex back-arc extensional to foreland basin: the Bowen Basin, eastern Australia. *Journal of Sedimentary Petrology* **63**, 881-893.

BAMBERRY W. J. 1992. Stratigraphy and sedimentology of the Late Permian Illawarra Coal Measures, southern Sydney Basin, New South Wales. PhD

thesis, University of Wollongong, Wollongong (unpubl.).

BEMBRICK C. S., HERBERT C., SCHEIBNER E. & STUNTZ J. 1973. Structural subdivision of the New South Wales portion of the Sydney-Bowen Basin. *Geological Survey of New South Wales, Quarterly Notes* **11**, 1-13.

BEMBRICK C. S., HERBERT C., SCHEIBNER E. & STUNTZ J. 1980. Structural subdivision of Sydney Basin. *In* Herbert C. and Helby R. eds *A Guide to the Sydney Basin*, pp. 2-9. Geological Survey of New South Wales Bulletin 26.

BERGERAT F. BOUROZ-WEIL C. & ANGELIER J. 1992. Paleostresses inferred from macrofractures, Colorado Plateau, western U.S.A. *Tectonophysics* 206, 219-243.

BIENIAWSKI Z. T. 1967. Mechanism of brittle fracture in rock (part I); theory of fracture processes (part II); experimental studies (part III); fracture in tension and long term loading. *International Journal of Rock Mechanics and Mining Science* **4**, 395-430.

BILLINGS M. P. 1972. *Structural Geology*. Prentice Hall, Englewood Cliffs, New Jersy.

BISHOP P. 1988. The Eastern Highlands of Australia: the evolution of an intraplate highland belt. *Progress in Physical Geography* **12**, 159-182.

BISHOP P. HUNT P. & SCHMIDT P. W. 1982. Limits to the age of the Lapstone Monocline, NSW: a palaeomagnetic study. *Journal of the Geological Society of Australia* **29**, 319-438.

BLAYDEN I. 1971. On the structural evolution of the Macquarie Syncline. PhD thesis, University of Newcastle, Newcastle (unpubl).

BOWMAN H. N. 1970. Palaeoenvironment and revised nomenclature of the upper Shoalhaven Group and Illawarra Coal Measures in the Wollongong-Kiama area, New South Wales. *Records of the Geological Survey of New South Wales* **12**, 163-182.

BOWMAN H. N. 1972. The geology and natural slope stability of the city of the Greater Wollongong, MSc thesis, Sydney University, Sydney (unpubl.).

BOWMAN H. N. 1974. *Geology of the Wollongong, Kiama, and Robertson, 1:50,000 Sheets (9029-11, 9028-I & IV)*. Geological Survey of New South Wales, Sydney.

BOWMAN H. N. & MULLARD B. W. 1986. Structural Geology. *In* Sherwin L. and Holmes G.G. eds *Geology of the Wollongong and Port Hawking 1:100,000* Sheets 9029, 9129. Geological Survey of New South Wales,

Sydney.

BRANAGAN D. F. 1975. Further thoughts on the Lapstone structures. *Proceedings of 10th Symposium on Advances in the Study of the Sydney Basin*, pp. 22-23. Department of Geology, University of Newcastle, Newcastle.

BRANAGAN D. F. 1983. The Sydney Basin and its vanished sequence. *Journal of the Geological Society of Australia* **30**, 75-84.

BRANAGAN D. F. 1985. An overview of the geology of the Sydney Region. *In* Pells P. J. N. ed. *Engineering Geology of the Sydney Region*, pp. 3-46. A. A. Balkema, Rotterdam.

BROOKE B. P. 1994. Shore Platforms of the Northern Illawarra. BSc (Hons) thesis, Geography Department, University of Wollongong, Wollongong (unpubl.).

BROWN E. T. (ed.) 1981. *Rock Characterisation, Testing and Monitoring, ISRM Suggested Methods*. Pergamon Press, Oxford.

BRYANT E. A., YOUNG R. W., PRICE D. M., SHORT S. A. 1992. Evidence for Pleistocene and Holocene raised marine deposits, Sandon Point, New South Wales. *Australian Journal of Earth Sciences* **39**, 481-493.

BUNNY M. R. 1972. *Geology and coal resources of the Southern Catchment Coal Reserve, Southern Sydney Basin, New South Wales*. Geological Survey of New South Wales Bulletin **22**.

CARR P. F. 1983. A reappraisal of the stratigraphy of the upper Shoalhaven Group and the lower Illawarra Coal Measures, southern Sydney Basin, New South Wales. *Linnean Society of New South Wales* **106**, 287-297.

CARR P. F. & FACER R. A. 1980. Radiometric ages of some igneous rocks from Southern and Southwestern Coalfields of New South Wales. *Search* **11**, 382-383.

CHOWDHURY R. N. 1976. Mechanism of natural slope failure in the Greater Wollongong area of New South Wales. *Search* **7**, 396-397.

CHOWDHURY R. N. & YOUNG A. R. M. 1987. Field Guide to slope instability in the Wollongong-Picton-Nattai Region of New South Wales. *5th International Conference and Field Workshop on Landslides*. University of Wollongong, Wollongong.

CLARK B. R. 1992. Depositional environment of the Bulli Coal and its effect on quality characteristics. MSc thesis, University of Wollongong, Wollongong (unpubl.).

CLEARY J. R. 1963 Near earthquake studies in southeastern Australia. PhD thesis,

Australian National University, Canberra (unpubl.).

COFFIELD D. Q. & SCHAMEL S. 1989. Surface expression of an accommodation zone within the Gulf of Suez, Egypt. *Geology* **17**, 76-79.

COLLINS W. J. 1991. A reassessment of the Hunter-Bowen Orogeny: tectonic implications for the southern New England Fold Belt. *Australian Journal of Earth Sciences* **38**, 409-423.

CONNELLY M. A. 1970. A geological structural assessment at Appin Colliery with reference to roof failure and directional mining. *Proceedings of the Australian Institute of Mining and Metallurgy* **234**, 17-26.

COOK A. C. 1969a. Trend surface analysis of structure and thickness of the Bulli Seam, Sydney Basin, New South Wales. *Mathematical Geology* **1**, 53-78.

COOK A. C. 1969b. Contemporaneous structures in the Southern Coalfield, New South Wales. *Australian Journal of Science* **32**, 257-258.

COOK A. C. JOHNSON K. R. 1970. Early joint formation in sediments. *Geological Magazine* **107**, 361-368.

COWARD M. 1994. Continental collision. *In* Hancock P.L. ed. *Continental Deformation*, pp. 264-289. Pergamon Press, Oxford.

CRAMSIE J. N. 1964. Sedimentation and structure in the Illawarra Coal Measures. MSc thesis, University of Sydney, Sydney (unpubl.).

CRANS W., MANDL G. & HAREMBOURE J. 1980. On the theory of the growth faulting: a geomechanical delta model based on gravity sliding. *Journal of Petroleum Geology* **2**, 265-307.

CRUIKSHANK K. M., ZHAO G. & JOHNSON A. M. 1991. Analysis of minor fractures associated with joints and faulted joints. *Journal of Structural Geology* **13**, 865-886.

DAVIDSON J. K. 1980. Rotational displacements in southeastern Australia and their influence on hydrocarbon occurrence. *Tectonophysics* **63**, 139-153.

DAVIES R. K. & POLLARD D. D. 1986. Relations between left-lateral strike-slip faults and right-lateral monoclinal kink bands in granodiorite, Mt. Abbot Quadrangle, Sierra Nevada, California. *Pure and Applied Geophysics* **124**, 177-201.

DAVIS G. H. 1978. The monocline fold pattern of the Colorado Plateau. *In* Matthews V. ed. Laramid Folding Associated with Basement Block Faulting in the Western United State. *Geological Society of America, Memoir* **151**, 215-233.

DAVIS G. H. 1984. *Structural geology of rocks and regions*. John Wiley, New York.

DEGRAFF J. M. & AYDIN A. 1987. Surface morphology of columnar joints and its significance to mechanics and direction of joint growth. *Geological Society of America, Bulletin* **99,** 605-617.

DELANEY P. T., POLLARD D. D., ZIONY J. I. & MCKEE E. H. 1986. Field relations between dykes and joints: emplacement processes and paleostress analysis. *Journal of Geophysical Research* **91,** 4920-4938.

DENHAM D., ALEXANDER L. G. & WOROTNICKI G. 1979. Stresses in the Australian crust: evidence from earthquakes and in-situ stress measurements. *BMR Journal of Australian Geology and Geophysics* **4,** 289-295.

DENHAM D. 1980. The 1961 Robertson earthquake - more evidence for compressive stress in southeast Australia. *BMR Journal of Australian Geology and Geophysics* **5,** 153 156.

DENNIS J. G 1987. *Structural Geology: an introduction*, Wm. C. Brown Publishers, Iowa.

DOYLE H. A., CLEARY J. R. & GRAY N. M. 1968. The seismicity of the Sydney Basin. *Journal of the Geological Society of Australian* **15,** 175-181.

DUMITRU T. A., HILL K. C., COYLE D. A., DUDDY I. R., FOSTER D. A., GLEADOW A. J. W., GREEN P. F., KOHN B. P., LASLETT G. M. & O'SULLIVAN A. J. 1991. Fission track thermochronology: application to continental rifting of southeastern Australia. *APEA Journal* **31,** 131-142.

DUNNE W. M. & HANCOCK P. 1994. Paleostress analysis of small-scale brittle structures. *In* Hancock P. ed. *Continental Deformation*, pp. 101-120. Pergamon Press, Oxford.

DYER R. 1988. Using joint interactions to estimate paleostress ratios. *Journal of Structural Geology* **10,** 685-699.

EIDELMAN A. & RECHES Z. 1992. Fractured pebbles, a new stress indicator. *Geology* **20,** 307-310.

EMBLETON B. J. J., SCHMIDT P. W., HAMILTON L. H. & RILEY G. H. 1985. Dating volcanism in the Sydney Basin: evidence from K-Ar ages and palaeomagnetism. *In* Sutherland F. L., Franklin B. J. and Waltho A. E. eds *Volcanism in Eastern Australia,* pp. 59-72. Geological Society of Australia, New South Wales Division, Publication 1.

ENGELDER T. 1982a. Is there a genetic relationship between selected regional joints and contemporary stress within the lithosphere of North America? *Tectonics* **1,**

161-177.

ENGELDER T. 1982b. Reply to a comment by A.E. Scheidegger on "is there a genetic relationship between selected regional joints and contemporary stress within the lithosphere of North America?", by T. Engelder. *Tectonics* **1**, 465-470.

ENGELDER T. 1985. Loading paths to joint propagation during a tectonic cycle: an example from the Appalachian Plateau, USA. *Journal of Structural Geology* **7**, 459-476.

ENGELDER T. 1987. Joint and shear fractures in rock. *In* Atkinson B.K. ed. *Fracture mechanics of rock*, pp. 27-69. Academic Press, London.

ENGELDER T. & GEISER P. 1980. On the use of regional joint sets as trajectories of paleostress fields during the development of the Appalachian Plateau. *Journal of Geophysical Research* **85**, 6319-6341.

EVANS P. R. 1981. The petroleum potential of Australia. *Petroleum Geology* **4**, 123-146.

EVANS P. R. 1982. The age distribution of petroleum in Australia. *APEA Journal* **22**, 301-310.

EVANS P. R. & MIGLIUCCI A. 1991. Evolution of the Sydney Basin during the Permian as a foreland basin to the Currarong and New England Orogens. *Proceedings of 25th Symposium on Advances in the Study of the Sydney Basin*, pp. 22-29. Department of Geology, University of Newcastle, Newcastle.

FACER R. A. & CARR P. F. 1979. K-Ar dating of Permian and Tertiary igneous activity in the southeastern Sydney Basin, New South Wales. *Journal of the Geological Society of Australia* **26**, 73-79.

FAIZ M. M. & HUTTON A. C. 1993. Two kilometres of post-Permian sediment - did it exist? *Proceedings of the 27th Symposium on Advances in the Study of Sydney Basin*, pp. 221-228. Department of Geology, University of Newcastle, Newcastle.

FIELDING C. R. & TYE S. C. 1994. Stratigraphy of the Talaterang and Shoalhaven Groups in the southernmost Sydney Basin. *Proceedings of the 28th Symposium on the Advances in the Study of the Sydney Basin*, pp. 212-219. Department of Geology, University of Newcastle, Newcastle.

FITCH T. J. 1976. Source of Picton Earthquake, 9th March 1973, a seismic review of the source. *Bureau of Mineral Resources Geology and Geophysics, Bulletin* **164**, 11-14.

FOLK R. L. 1968. *Petrology of Sedimentary Rocks*. Hemphills, Austin.

GABRIELSEN R. H. 1990. Characteristics of joints and faults. *In* Barton N. R. and Stephansson O. eds *Rock Joint*, pp. 11-17. A. A. Balkema, Rotterdam.

GHOSH A. & DAEMEN J. J. K. 1993. Fractal characteristics of rock discontinuities. *Engineering Geology* **34**, 1-9.

GILL E. D. 1972. The relationship of present shore platforms to past sea level. *Boreas* **1**, 1-25.

GLEN R. A. 1987. *Geology of the Wrightville 1:100,000, Sheet 8034*. New South Wales Geological Survey, Sydney.

GLEN R. A. & BECKETT J. 1989a. Coal in a thrust belt: the Hunter Coalfield of New South Wales. *Proceedings of the 23rd Symposium on Advances in the Study of the Sydney Basin*, pp. 15-28. Department of Geology, University of Newcastle, Newcastle.

GLEN R. A. & BECKETT J. 1989b. Thin-skinned tectonics in the Hunter Coalfield of New South Wales. *Australian Journal of Earth Sciences* **36**, 589-593.

GRAY D. R. 1975. Structure and jointing in Permian rocks near Ravensworth, New South Wales, northern Sydney Basin. *Journal and Proceedings of the Royal Society of New South Wales* **108**, 16-28.

GRAY N. M. 1976. Geological appreciation of the seismicity of the southern portion of the Sydney Basin. *In* Denham D. ed. Symposium on Seismicity and Earthquake Risk in Eastern Australia. *Bureau of Mineral Resources Geology and Geophysics, Bulletin* **164**, 9-10.

GRAY N. M. 1982. Direction of Stress, southern Sydney Basin. *Journal of the Geological Society of Australia* **29**, 277-284.

GROSS M. R. 1993. The origin and spacing of cross joints: examples from the Monterey Formation, Santa Barbara coastline, California. *Journal of Structural Geology* **15**, 737-751.

GROSS M. R. & ENGELDER T. 1991. A case for neotectonic joints along the Niagara Escarpment. *Tectonics* **10**, 631-641.

HAMMOND R. L. 1988. Geological structure of the Bowen Basin. *In* Mallett C. W., Hammond R. L., Leach J. H. J., Enever J. R. & Mengel C. eds *Bowen Basin - stress, structure, and mining conditions assessment for mine planning*. pp. 10-38. Final Report, National Energy Research Development and Demonstration Council, Report Project 901, Canberra.

HANCOCK P. L. 1985. Brittle microtectonics: principles and practice. *Journal of*

Structural Geology **7**, 437-457.

HANCOCK P. L. 1986. Joint spectra. *In* Nicol I. and Nesbitt R. W. eds *Geology in real world- The Kingsley Dunham Volume*. pp. 155-164. Institution of Mining and Metallurgy, London.

HANCOCK P. L. & ENGELDER T. 1989. Neotectonic joints. *Geological Society of America, Bulletin* **101**, 1197-1208.

HANES J., LAMA R. D. & SHEPHERD J. 1983. Research into the phenomenon of outbursts of coal and gas in some Australian Collieries. *In 5th International congress on Rock Mechanics, Melbourne*, pp. E79-E85. A. A. Balkema, Rotterdam.

HANLON F. N. 1956a. Geology of the southern Coalfield, Illawarra District. *New South Wales Department of Mines, Annual Report for 1952*, 95-104.

HANLON F. N. 1956b. Southern Coalfield, geology of the Stanwell Park-Coledale area. *New South Wales Department of Mines, Technical Report* **1**, 20-35.

HANLON F. N. 1958. Presidential address. Part II. Geology and transport, with special reference to landslides on the near South Coast of New South Wales. *Journal and Proceedings of the Royal Society of New South Wales* **92**, 2-15.

HELGESON D. E. & AYDIN A. 1991. Characteristics of joint propagation across layer interfaces in sedimentary rocks. *Journal of Structural Geology* **13**, 897-911.

HERBERT C. 1980. Depositional development of the Sydney Basin. *In* Herbert C. and Helby R. J. eds A Guide to the Sydney Basin. *Geological Survey of New South Wales, Bulletin* **26**, 10-52.

HILLS E. S. 1972. Shore platforms and wave ramps, *Geological Magazine* **109**, 81-88.

HOBBS D. W. 1967. The formation of tension joints in sedimentary rocks: an explanation. *Geological Magazine* **104**, 550-556.

HODGSON R. A. 1961a. Regional study of jointing in Comb Ridge - Navajo Mountain area, Arizona and Utah. *American Association of Petroleum Geologists, Bulletin* **45**, 11-38.

HODGSON R. A. 1961b. Classification of structures on joint surfaces. *American Journal of Science* **259**, 439-502.

HOFFMANN K. L. 1989. Tectonic setting and structural setting of the southern Eromanga Basin, Queensland. *Queensland Department of Mines, Record* 1989/15.

HOLST T. B. 1982. Regional jointing in the northern Michigan Basin. *Geology* **10**, 273-277.

HUANG Q. & ANGELIER J. 1989. Fracture spacing and its relation to bed thickness. *Geological Magazine* **126**, 355-362.

HUTTON A. C., FERGUSSON C. L. & JONES B. G. 1989. Landslip in the northern Illawarra Coalfield. *Proceedings of the 23rd Symposium on Advances in the Study of Sydney Basin*, pp. 37-44. Department of Geology, University of Newcastle, Newcastle.

HUTTON A. C., JONES B. G., BAMBERRY W. J. ODINS P. & CLARK B. 1990. *The Distribution and Evolution of Coal in the Southern Sydney Basin.* National Energy Research Development and Demonstration Program, Project 1019, Canberra.

JAKEMAN B. L. 1980. The relationship between formation structure and thickness in the Permo-Triassic succession of the Southern Coalfield, Sydney Basin, New South Wales, Australia. *Mathematical Geology* **12**, 185-212.

JAKEMAN B. L. 1981. Quantitative analysis of sedimentation and structure relating to the Permian-Triassic succession of the Southern Sydney Basin. PhD thesis, University of Wollongong, Wollongong (unpubl.).

JENKIN J. J. 1984. Evolution of Australian coast and continental margin. *In* Than B. G. ed. *Coastal Geomorphology in Australia*, pp. 23-42. Academic Press, Sydney.

JONES B. G. 1990. The Shoalhaven Group: implications for subsequent coal measures deposition in the southern Sydney Basin. *In* Hutton A.C. and Depers A.M. eds *Proceedings of the Workshop on Southern and Western Coalfields of the Sydney Basin*, pp. 11-18. University of Wollongong, Wollongong.

JONES B. G. & HUTTON A. C. 1984. Fluvio-deltaic and coal sequences in the northern Illawarra District, NSW. 7th Australian Geological Convention, Excursion Z2, Notes, University of Wollongong, Wollongong.

JONES J. G., CONAGHAN P. J., MCDONNELL K. L., FLOOD R. H. & SHAW S. E. 1984. Papuan Basin analogue and a foreland basin model for the Bowen-Sydney Basin. *In* Veevers J. J. ed. *Phanerozoic Earth History of Australia*, pp. 243-262. Clarendon Press, Oxford.

JONES B. G., GOSTIN V. A. & DICKINS J. M. 1986. *Sydney Basin.* 12th International Sedimentological Congress, Excursion 1c, Notes.

JONES J. G. & VEEVERS J. J. 1983. Mesozoic origins and antecedents of

Australia's Eastern Highlands. *Journal of the Geological Society of Australia* **30,** 305-322.

JONES J. G. & VEEVERS J. J. 1984. Eastern Highlands. *In* Veevers J.J. ed. *Phanerozoic Earth History of Australia,* pp. 115-143. Clarendon Press, Oxford.

KIRK R. M. 1977. Rates and forms of erosion on intertidal platforms at Kaikoura Peninsula, South Island, New Zealand. *New Zealand Journal of Geology and Geophysics* **20,** 571-613.

KOOI H. & BEAUMOUNT C. 1994. Escarpment evolution on high-elevation rifted margins; insights derived from a surface processes model that combines diffusion, advection and reaction. *Geophysical Abstracts in Press.*

KULANDER B. R., BARTON C. C. & DEAN S. L. 1979. *The application of fractography to core and outcrop fracture investigations.* Technical Report, US Department of Energy, METC/SP-79/3. Morgantown Energy Technology Centre.

KULANDER B. R. & DEAN S. L. 1985. Hackle plume geometry and joint propagation dynamics. *In* Stephansson O. ed. *Fundamentals of Rock Joints,* pp. 85-94. Lulea University Technology, Sweden.

LADEIRA F. L. & PRICE N. J. 1981. Relationship between fracture spacing and bed thickness. *Journal of Structural Geology* **3,** 179-183.

LAMBECK K. & STEPHENSON R. 1986. The post-Paleozoic uplift history of south-eastern Australia. *Australian Journal of Earth Sciences* **33,** 253-270.

LISTER G. S., ETHERIDGE M. A. & SYMONDS P. A. 1986. Detachment faulting and the evolution of passive continental margin. *Geology* **14,** 246-250.

LOHE E. M. & MCLENNAN T. P. T. 1991. An overview of the structural fabrics of the Sydney Basin, and a comparison with the Bowen Basin. *Proceeding of the 25th Symposium on Advances in the Study of the Sydney Basin,* pp. 12-21. Department of Geology, University of Newcastle, Newcastle.

LOHE E. M., MCLENNAN T. P. T., SULLIVAN T. D., SOOLE K. P. & MALLETT C. W. 1992. *Sydney Basin geological structure and mining conditions, assessment for mine planning.* National Energy Research Development and Demonstration Council, Project 1239, Canberra.

LORENZ J. C., Teufel L. W., Warpinski N. R. 1991. Regional fractures I: a mechanism for the formation of regional fractures at depth in flat-lying reservoirs. *American Association of Petroleum Geologists, Bulletin* **75,** 1714-1737.

LORENZ J. C. & FINLEY S. J. 1991. Regional fractures II: fracturing of Mesaverde Reservoirs in Piceance Basin, Colorado. *American Association of Petroleum Geologists, Bulletin* **75**, 1738-1757.

MALLETT C. W. HAMMOND R. L. & SULLIVAN T. D. 1988. The implications for the Sydney Basin of upper crustal extension in the Bowen Basin. *Proceedings of the 22nd Symposium on Advances in the Study of the Sydney Basin,* pp. 1-8. Department of Geology, University of Newcastle, Newcastle.

MARTEL S. J., POLLARD D. D. & SEGALL P. 1988. Development of strike-slip fault zones, Mount Abbot quadrangle, Sierra Nevada, California. *Geological Society of America, Bulletin* **100**, 1451-1465.

MAUGER A. J., CREASEY J. W. & HUNTINGTON J. F. 1984. *The use of pre-development data for mine design. Sydney Basin fracture pattern analysis.* National Energy Research Development and Demonstration Council, Final Report on Project 343, Canberra.

MAYNE S. J., NICHOLAS E., BIGG-WITHER A. L., RASIDI J. S. & RAINE M. J. 1974. Geology of the Sydney Basin: a review. *Bureau of Mineral Resources Geology and Geophysics, Bulletin* **149**, 229 pp.

MCCULLOCH C. M. & DEUL M. 1974. Cleat in bituminous coal beds. *U.S. Bureau of Mines, Report of Investigation,* No 7910.

MCQUILLAN H. 1973. Small scale fracture density in Asmari Formation of southwest Iran and its relation to bed thickness and structural setting. *American Association of Petroleum Geologists, Bulletin* **57**, 2367-2385.

MEMARIAN H. 1975. Past and present stability and evolution of the Niagara Gorge in the vicinity of Niagara Geln, Niagara Falls, Ontario. MSc thesis, University of Waterloo, Waterloo, Ontario, Canada (unpubl.).

MIALL A. D. 1990. *Principles of Sedimentary Basin Analysis* (2nd edition). Springer Verlag, New York.

MIDDLEMOST E. A., DULHUNTY J. A. & BECK R. W. 1992. Some Mesozoic igneous rocks from northeastern New South Wales and their tectonic setting. *Journal and Proceedings of the Royal Society of New South Wales* **I**, 1-11.

MIGLIUCCI A. & EVANS P. R. 1991. Clay model of the northern Sydney Basin and southern Tamworth Belt, New South Wales. *Proceedings of the 25th Symposium on Advances in the Study of the Sydney Basin,* pp. 122-127. Department of Geology, University of Newcastle, Newcastle.

MILLS J. M. & FITCH T. J. 1977. Trust faulting: a crust-upper mantle structure in

east Australia. *Geophysical Journal of the Royal Astronomical Society* **48**, 251-384.

MITRA S. 1993. Geometry and kinematic evolution of inversion structures. *American Association of Petroleum Geologists, Bulletin* **77**, 1159-1191.

MOELLE K. H. R. 1977. On a geometrical relationship between some primary sedimentary structures and diagenetically formed fracture systems. *In* Sin G.C. and Chow C. L. eds *Fracture Mechanics and Technology*, pp. 381-392.

MOLNAR P. & LYON-CAEN H. 1988. Some simple physical aspects of the support, structure, and evolution of mountain belts. *In* Clark P., Burchfiel B. C. and Suppe J. eds Processes in Continental Lithospheric Deformation. *Geological Society of America, Special Paper* **218**, 179-207.

MUEHLBERGER W. R. 1961. Conjugate joint sets of small dihedral angle. *Journal of Geology* **69**, 211-219.

NARR W. 1991. Fracture density in the deep subsurface: techniques with application to Point Arguello oil field. *American Association of Petroleum Geologists, Bulletin* **66**, 1231-1247.

NARR W. & SUPPE J. 1991. Joint spacing in sedimentary rocks. *Journal of Structural Geology* **13**, 1037-1048.

NELSON R. A. 1985. Analysis of Naturally Fractures Reservoirs. *Contributions in Petroleum Geology and Engineering* **1**, 1-27. Gulf Publishing Company, Houston, Texas.

NICKELSEN R. P. 1976. Early jointing and cumulative fracture patterns. *In*: Hodgson, R.A. ed. *Proceedings of the First International Conference on New Basement Tectonics*, pp. 193-199. Utah Geological Association Publication, Salt Lake City.

NIKELSEN R. P. & HOUGH V. N. D. 1967. Jointing in the Appalachian Plateau of Pennsylvania. *Geological Society of America, Bulletin* **78**, 609-630.

OLLIER C. D. 1982. The great escarpment of eastern Australia: tectonic and geomorphic significance. *Journal of the Geological Society of Australia* **29**, 13-23.

OLSON J. & POLLARD D. D. 1988. Inferring stress state from detailed joint geometry. *In* Cundall P. A., Sterling R. L. and Strafield A. M. eds *Key Questions in Rock Mechanics*, pp. 159- 167. A. A. Balkema, Rotterdam.

OLSON J. & POLLARD D. D. 1989. Inferring paleostress from natural fracture patterns: a new method. *Geology* **17**, 345-348.

PATTON T. L. 1984. Normal fault and fold development in sedimentary rocks above a pre-existing basement normal fault. PhD thesis, Texas A & M University, College Station, Texas (unpubl.).

PLINT A. G., HART B. S. & DONALDSON W. S. 1993. Lithospheric flexure as a control on stratal geometry and facies distribution on Upper Cretaceous rocks of the Alberta foreland basin. *Basin Research* **5,** 69-77.

POLLARD D., SEGALL P. & DELANEY P. T. 1982. Formation and interpretation of dilatant echelon cracks. *Geological Society of America, Bulletin* **93**, 1291-1303.

POLLARD D. D. & SEGALL P. 1987. Theoretical displacements and stresses near fractures in rock: with applications to faults, joints, veins, dykes, and solution surfaces. *In* Atkinson, B. K. ed. *Fracture Mechanics of Rock,* pp. 277-349. Academic Press, London.

POLLARD D. D. & AYDIN A. 1988. Progress in understanding jointing over the past century. *Geological Society of America, Bulletin* **100**, 1181-1204.

POLLARD D. D., ZELLER S. & OLSON J. 1990. Understanding the process of jointing in brittle rock masses. *In* Hustrulid W. and Johnson G. A. eds *Rock Mechanics, Contribution and Challenges*, pp. 447-454. A. A. Balkema, Rotterdam.

POWELL C. McA., COLE J. P. & CUDAHY T. J. 1985. Megakinking in the Lachlan Fold Belt, Australia. *Journal of Structural Geology* **7,** 281-300.

PRICE N. J. 1966. *Fault and Joint Development in Brittle and Semi-brittle Rock.* Pergamon Press, Oxford.

PRIEST S. D. HUDSON I. A. 1981. Estimation of discontinuity spacing and trace length using scanline surveys. *International Journal of Rock Mechanics, Mining Sciences and Geomechanics Abstract* **18,** 183-197.

PROST G. L. 1986. Jointing in relatively undeformed strata: relation to basement and exploration implication. PhD thesis, Colorado School of Mines, USA (unpubl.).

PROST G. L. 1988. Jointing at rock contacts in cyclic loading. *International Journal of Rock Mechanics, Mining Sciences and Geomechanics Abstract* **25,** 263-272.

RAMSAY J. G. 1980. The crack-seal mechanism of rock deformation. *Nature* **284**, 135-139.

RAMSAY J. G. & HUBER M. I. 1987. *Modern Structural Geology. Volume 2: Folds and Fractures*. Academic Press, London.

RAWNSLEY K. D., HENCHER S. R. & LUMSDEN A. C. 1990. Joint origin as a

predictive tool for the estimation of geotechnical properties. *In* Barton N. R. and Stephansson O. eds *Rock Joints*, pp. 91-96. A. A. Balkema, Rotterdam.

RAWNSLEY K. D., RIVES T. & PETIT J. P. 1992. Joint development in perturbed stress fields near faults. *Journal of Structural Geology* **14**, 939-951.

RAY H. N. 1986. Igneous rocks. *In* Sherwin L. and Holmes, G.G. eds *Geology of the Wollongong and Port Hacking 1:100,000 sheets 9029, 9129*, pp. 51-56. Geological Survey of New South Wales, Sydney.

READING H. G. 1986. *Sedimentary Environments and Facies*. Blackwell Scientific Publication, Oxford.

RECHES Z. 1988. Evolution of fault patterns in clay experiments. *Tectonophysics* **145**, 141-156.

RICKWOOD P. C. 1985. Igneous intrusions of the Greater Sydney Region. *In* Pells, P. J. N. ed. *Engineering Geology of the Sydney Region*, pp. 215-307, A. A. Balkema, Rotterdam.

RIVES T., RAZAK M., Petit J. P. & Rawnsley K. D. 1992. Joint spacing: analogue and numerical simulations. *Journal of Structural Geology* **14**, 925-937.

RIVES T., RAWNSLEY K. D. & PETIT J. P. 1994. Analogue simulation of natural orthogonal joint set formation in brittle varnish. *Journal of Structural Geology* **16**, 419-429.

RIXON L. K. & SHEPHERD J. 1988. *Southern Coalfield of New South Wales seam structures (6 maps).* ACIRL Geotechnical Engineering Group, York Road, Bellambi, New South Wales.

SCHEIBNER E. 1974. Fossil fracture zones, segmentation, and correlation problems in the Tasman Fold Belt System. *In* Denmead A. K., Tweedale G. W. and Wilson A. F. eds *The Tasman Geosyncline: a Symposium*, pp. 65-96. Geological Society of Australia, Queensland Division, Brisbane.

SCHEIBNER E. 1976. *Explanatory notes on the Tectonic Map of New South Wales.* Geological Survey of New South Wales, Sydney.

SCHEIDEGGER A. E. 1982. Comments on "is there a genetic relationship between selected regional joints and contemporary stress within the lithosphere of North America?" by T. Engelder. *Tectonics* **1**, 463-464.

SECOR D. T. 1965. Role of fluid pressure in jointing. *American Journal of Science* **263**, 633-646.

SEGALL P. 1984. Formation and growth of extensional fracture sets. *Geological Society of America, Bulletin* **95**, 454-462.

SEGALL P. & POLLARD D. D. 1983a. Joint formation in granitic rock of the Sierra Nevada. *Geological Society of America, Bulletin* **94**, 563-575.

SEGALL P. & POLLARD D. D. 1983b. Nucleation and growth of strike-slip faults in granite. *Journal of Geophysical Research* **88**, 555-568.

SHELTON J. W. 1984. Listric normal faults: an illustrative summary. *American Association of Petroleum Geologists, Bulletin* **68**, 801-815.

SHEPHERD J. 1989. Behaviour of some faults in Sydney Basin coal seams. *Proceedings of the 23rd Symposium on Advances in the Study of the Sydney Basin*, pp. 225-230. Department of Geology, University of Newcastle, Newcastle.

SHEPHERD J. 1990. Coal-seam faults in the Southern Coalfield of NSW. In Hutton A. C. & Depers A. M. eds *Proceedings of the Workshop on Southern and Western Coalfields of the Sydney Basin*, pp. 92-108. University of Wollongong, Wollongong.

SHEPHERD J. & GALE W. 1982. Colliery roof stability and the role of geology - a review. *Australian Journal of Coal Mining Technology and Research* **1**, 47-67.

SHEPHERD J. & CREASEY J. W. 1979. Forewarning of faults and outbursts of coal and gas at Westcliff Colliery, Australia. *Colliery Guardian International* **227**, 13-22.

SHEPHERD J. & HUNTINGTON J. F. 1981. Geological fracture mapping in coalfields and the stress fields of the Sydney Basin. *Journal of the Geological Society of Australia* **28**, 299-309.

SHEPHERD J., HUNTINGTON J. F. & CREASEY J. W. 1981a. Surface and underground geological prediction of bad roof conditions in collieries of the Western Coalfield, New South Wales, Australia. *Transactions of the Institute of Mining and Metallurgy* **90**, B1-B14.

SHEPHERD J., RIXON L. K. & GRIFFITHS L. 1981b. Outbursts and geological structures in coal mines: a review. *International Journal of Rock Mechanics and Geomechanics Abstract* **18**, 267-283.

SHERWIN L. & HOLMES G. G. (eds) 1986. *Geology of Wollongong and Port Hacking, 1:100,000 Sheets 9020 9129*. Geological Survey of New South Wales, Sydney.

SHIBAOKA M. & BENNETT A.J.R. 1975. Geological interpretation of ply structure of the Bulli Seam, Sydney Basin, New South Wales. *Journal of the*

Geological Society of Australia **22**, 327-343.

SHIBAOKA M. & BENNETT A.J.R. 1976. Use of swelling-index profiles of the Bulli Seam in New South Wales, and their general application in coalfield geology. *Fuel* **55**, 99-104.

STANDING COMMITTEE ON COALFIELD GEOLOGY OF NEW SOUTH WALES (SCCG) 1971. Report of combined sub-committees for the Southern and South-Western Coalfields. *Geological Survey of New South Wales*, Record **13**, 115-130.

STEARNS D. W. 1969. Certain aspects of fractures in naturally deformed rocks. *In* Riecker R. E. ed. *Rock Mechanics Seminar*, pp. 97-118. Air Force Cambridge Research Laboratory, Bedford, Massachussetts,

SUNAMURA T. 1992. *Geomorphology of Rocky Coasts*. John Wiley and Sons, Brisbane.

SUPPE J. 1985. *Principles of Structural Geology*, Prentice Hall, Englewood Cliffs, New Jersey.

TERZAGHI R. D. 1965. Sources of error in joint surveys. *Geotechnique* **15**, 287-304.

TRENHAILE A. S. 1987. *The Geomorphology of Rock Coasts*. Oxford University Press, Oxford.

TYE S. C. & FEILDING C. R. 1994. Sedimentology of the Talaterang and Shoalhaven Groups in the southernmost Sydney Basin. *Proceedings of the 28th Symposium on the Advances in the Study of the Sydney Basin*, pp. 220-227. Department of Geology, Newcastle University, Newcastle.

VEEVERS J. J. & POWELL C. McA. 1984. Dextral shear within the eastern Indo-Australia Plate. *In* Veevers J. J. ed. *Phanerozoic Earth History of Australia*, pp. 102-105. Clarendon Press, Oxford.

VEEVERS J. J., POWELL C. McA. & ROOTS S. R. 1991. Review of sea floor spreading around Australia. I. Synthesis of the patterns of spreading. *Australian Journal of Earth Sciences* **38**, 373-389.

VEEVERS J. J., CONAGHAN P. J. & SHAW S. E. 1993. Permian and Triassic New England Orogen/Bowen-Gunnedah-Sydney Basin in the context of Gondwanaland and Pangea. *In* Flood P. G. and Atkinson J. C. eds *New England Orogen, eastern Australia*, pp. 31-51. Department of Geology and Geophysics, University of New England, Armidale.

VENDEVILLE. B. 1987. Champs de failles et tectonique en extension: modelisation

experimental. PhD thesis, University de Rennes, Rennes, France (unpubl.).

VER STEEG K. 1942. Jointing in coal beds of Ohio. *Economic Geology* **37,** 503-509.

WALCOTT R. I. 1970. Isostatic response to loading of the crust in Canada. *Canadian Journal of Earth Sciences* **7**, 716-727.

WARD C. R. 1971. Mesozoic sedimentation and structure in the southern part of the Sydney Basin, the Narrabeen Group. PhD thesis, University of New South Wales, Sydney (unpubl.).

WASS R. E., WOOD K. G., BUNNY M. R. & GOLDBERY R. 1969. A review of some recent studies in the Sydney Basin, *In* Brown D. A. ed. Proceedings of Specialists Meeting. *Geological Society of Australia Special Publication* **2,** 7-12.

WEBER K. J. & DAUKORU E. M. 1975. Petroleum geological aspects of the Niger Delta. *Journal of Mining and Geology* **12**, 9-22.

WELLMAN P. 1987. Eastern Highlands of Australia; their uplift and erosion. *BMR Journal of Australian Geology and Geophysics* **10**, 277- 286.

WHEELER R. L. & HOLLAND S. M. 1978. Style element of systematic joints: an analytic procedure with a field example. *In* O'Leary D. W., Earle J. L. eds *Proceedings of the Third International Conference on New Basement Tectonics*, pp. 393-404. Basement Tectonic Committee, Durango, Colorado

WILLIAMS H. R., CORKERY D. & LOREK G. 1985. A study of joint and stress-release buckles in Paleozoic rocks of the Niagara Peninsula, southern Ontario. *Canadian Journal of Earth Sciences* **22**, 296-300.

WILSON R. G., WRIGHT E. A., TAYLOR B. L. & ROBERT D. H. 1958. Review of the geology of the Southern Coalfield, NSW. *Australasian Institute of Mining and Metallurgy Proceedings* **187**, 81-104.

WILSON R. G. 1969. Illawarra Coal Measures: Southern Coalfield. *In* Packham, G. H. ed. Geology of New South Wales. *Journal of the Geological Society of Australia* **16**, 370-379.

WILSON R. G. 1975. Southern Coalfield. *In* Travis D. M. and King K. eds Economic Geology of Australia and Papua New Guinea. *Australasian Institute of Mining and Metallurgy, Monograph* **6**, 206-218.

WINSOR C. N. 1979. The correlation of fracture directions with sediment anisotropy in folded rocks of the Delamerian fold belt at Port Germein gorge, South Australia. *Journal of Structural Geology* **1**, 245-254.

WITHJACK M. O., MEISLING K. E. & RUSSELL L. R. 1988. Forced folding and basement detached normal faulting in the Haltenbanken area, off-shore Norway. *American Association of Petroleum Geologists, Bulletin* **72**, 259.

WITHJACK M. O., MEISLING K. E. & RUSSELL L. R. 1989. Forced folding and basement detached normal faulting in the Haltenbanken area, off-shore Norway. *In* Tankard A. J. and Balkwill H. R. eds Extensional tectonics and stratigraphy of the North Atlantic margins. *American Association of Petroleum Geologists, Memoir* **46**, 567-575.

WITHJACK M. O., OLSON J. & PETERSON E. 1990. Experimental models of extensional forced folds. *American Association of Petroleum Geologists, Bulletin* **74**, 1038-1054.

WOROTNICKI G. & DENHAM D. 1976. The state of stress in the upper part of the Earth's crust in Australia according to measurements in mines and tunnels and from seismic observations. *In Symposium on the Investigation of Stress in Rock*, pp. 71-82. International Society of Rock Mechanics.

XIAO H. & SUPPE J. 1992. Origin of rollover. *American Association of Petroleum Geologists, Bulletin* **76**, 509-529.

YOUNG R. M. 1977. The characteristics and origin of coarse debris deposits near Wollongong, New South Wales, Australia. *Catena* **4**, 289-307.

YOUNG R. W. 1978. The influence of debris mantles and local climatic variations on slope stability near Wollongong, Australia. *Catena* **5**, 95-107.

YOUNG R. W. 1983. Block gliding in sandstones of the southern Sydney Basin. *In* Young R. W. and Nanson G. C. eds Aspects of Australian Sandstone Landscapes. *Australian and New Zealand Geomorphology Group Special Publication* **1**, 31-38.

YOUNG R. W. BRYANT E. A. 1993. Coastal rock platforms and ramps of Pleistocene and Tertiary age in Southern New South Wales, Australia. *Zeitschrift fur Geomorphologie* **37**, 257-272.

YOUNG R. W. & NANSON G. C. 1982. Terrace formation in the Illawarra region of New South Wales. *Australian Geographer* **15**, 212-219.

ZHAO G. & JOHNSON A. M. 1992. Sequence of deformations recorded in joints and faults, Arches National Park, Utah. *Journal of Structural Geology* **14**, 225-2236.

ZHAO G. & JOHNSON A. M. 1991. Sequential and incremental formation of conjugate sets of faults. *Journal of Structural Geology* **13**, 887-895.

ACKNOWLEDGEMENTS

I would like to thank Dr C.L. Fergusson of the Department of Geology at the University of Wollongong for his valuable comments and supervision of this study. I also acknowledge discussion with other academic members of the Department of Geology: Associate Professor B.G. Jones, Dr P.F. Carr, Dr C. Murray-Wallace, Dr L.E.A. Jones, Dr A.C. Hutton and Mr A.M. Deepers.

The assistance of the clerical and technical staff of the Department of Geology, University of Wollongong is acknowledged. I especially mention Barbara McGoldrick, Max Perkins, David Carrie and David M. Martin. I would like to thank the assistance of Richard Miller of the Department of Geography, University of Wollongong.

I would like to the following for fruitful discussions: Professor C.McA. Powell of the University of Western Australia, Dr D.F. Branagan, and Dr. J. Shepherd of Shepherd Mining and Geotechnics.

I wish to express my appreciation to the following organisations and individuals: Peter Lamb of Kembla Coke and Coal Company, Wollongong; Brian Lafoe and Peter Beattie of the Road and Traffic Authority (RTA), Wollongong; B. Hogan, District Engineer of the City Rail, Wollongong; Bruce Adie of the Cartographic Section of B.H.P. Engineering Department; Dr John Bamberry of the Department of Mineral Resources; Barry Clark and John Hanes of Cordeaux Colliery; and Dr R.G. Wilson.

I acknowledge discussions with colleagues during the progress of this study, particularly M. Faiz, M.H. Dehghani and B. Brooke. Finally, I deeply appreciate the members of my family, without their cooperation this study could not have been completed satisfactory.

FIGURES
&
TABLES

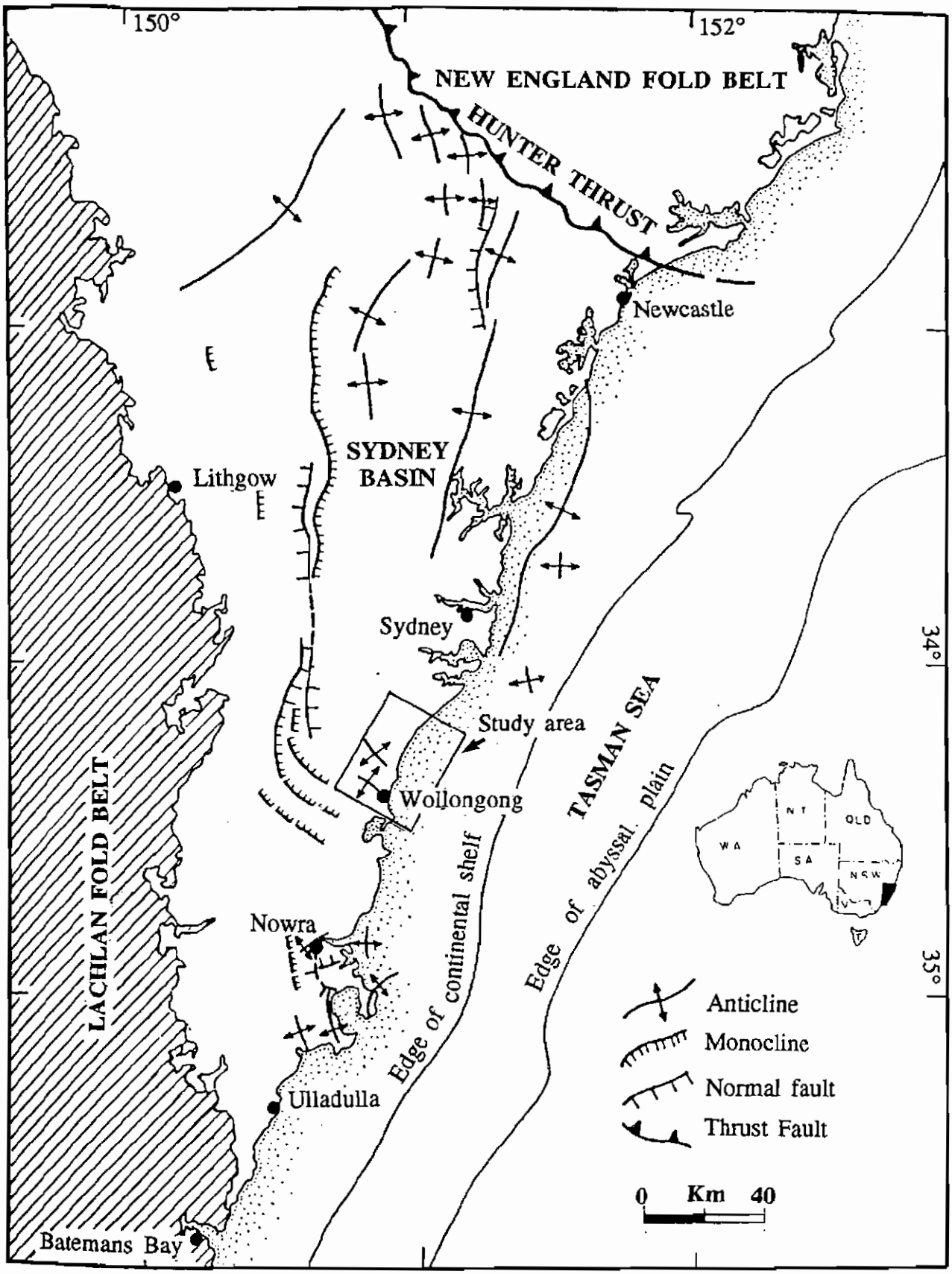

Figure 1.1 Simplified structural elements of the Sydney Basin (after Jones *et al.* 1986).

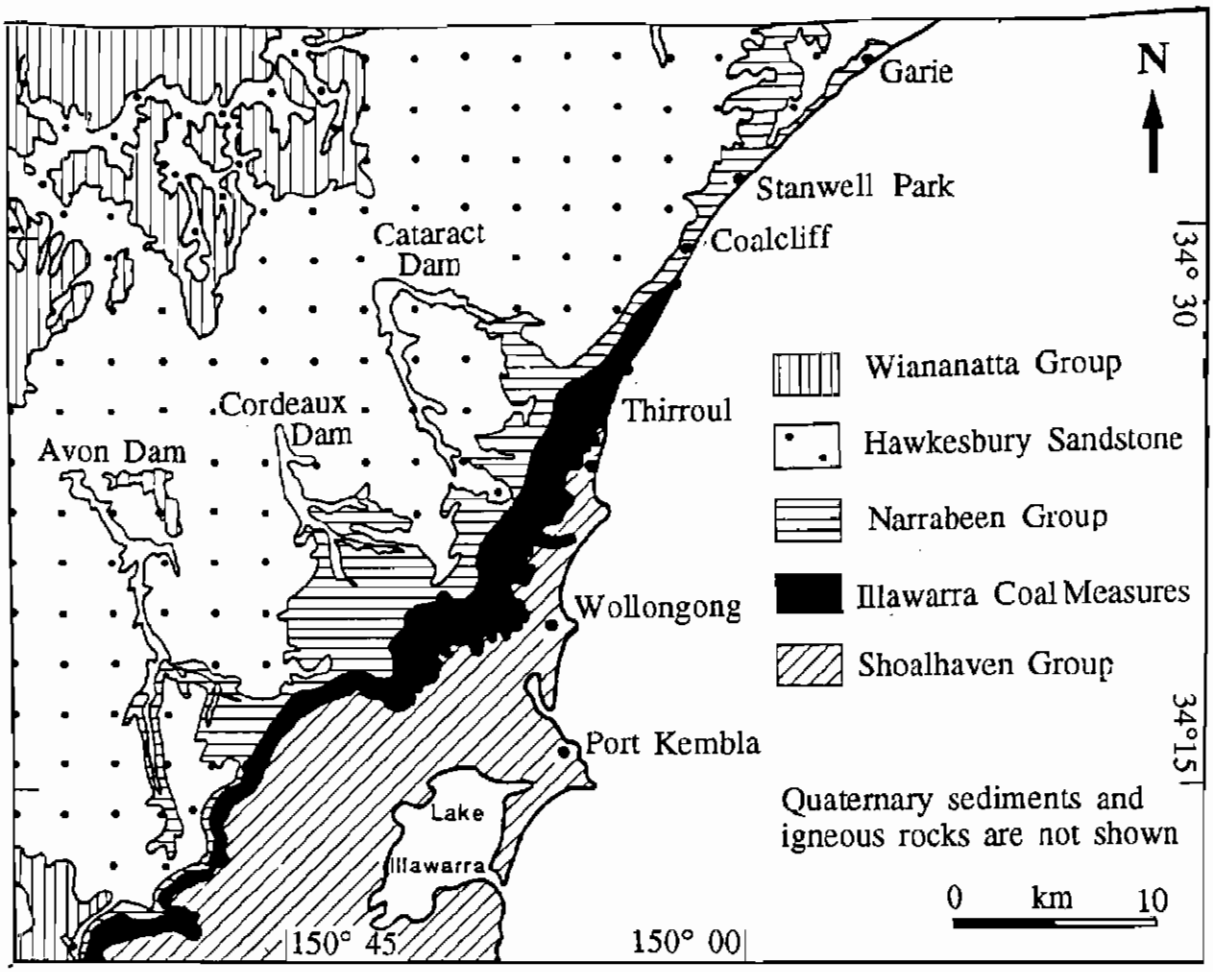

Figure 1.2 Simplified geological map of the southeastern Sydney Basin (after Jones & Hutton 1984).

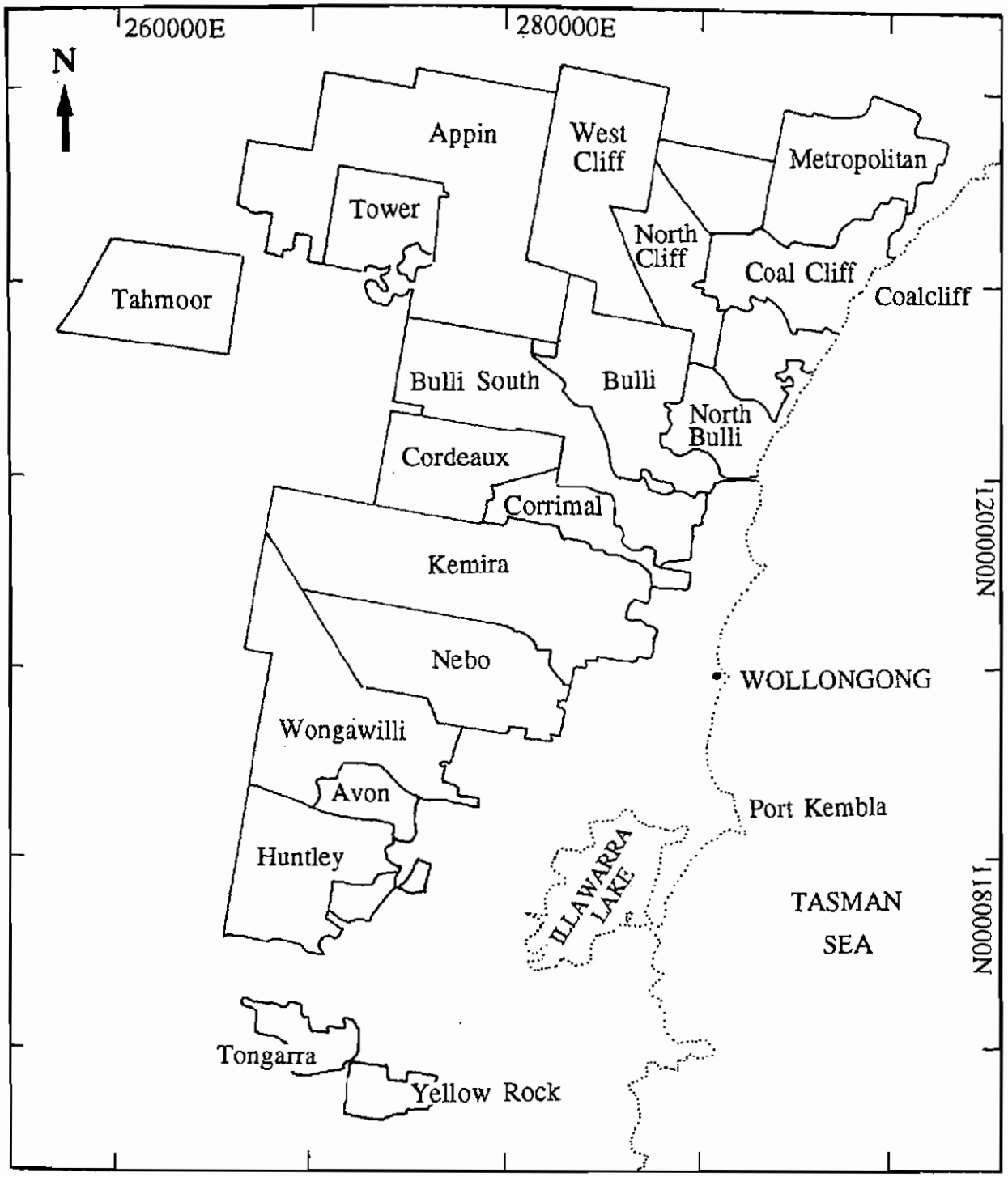

Figure 1.3 Lease boundaries of coal mines of the Southern Coalfield (after Clark 1990).

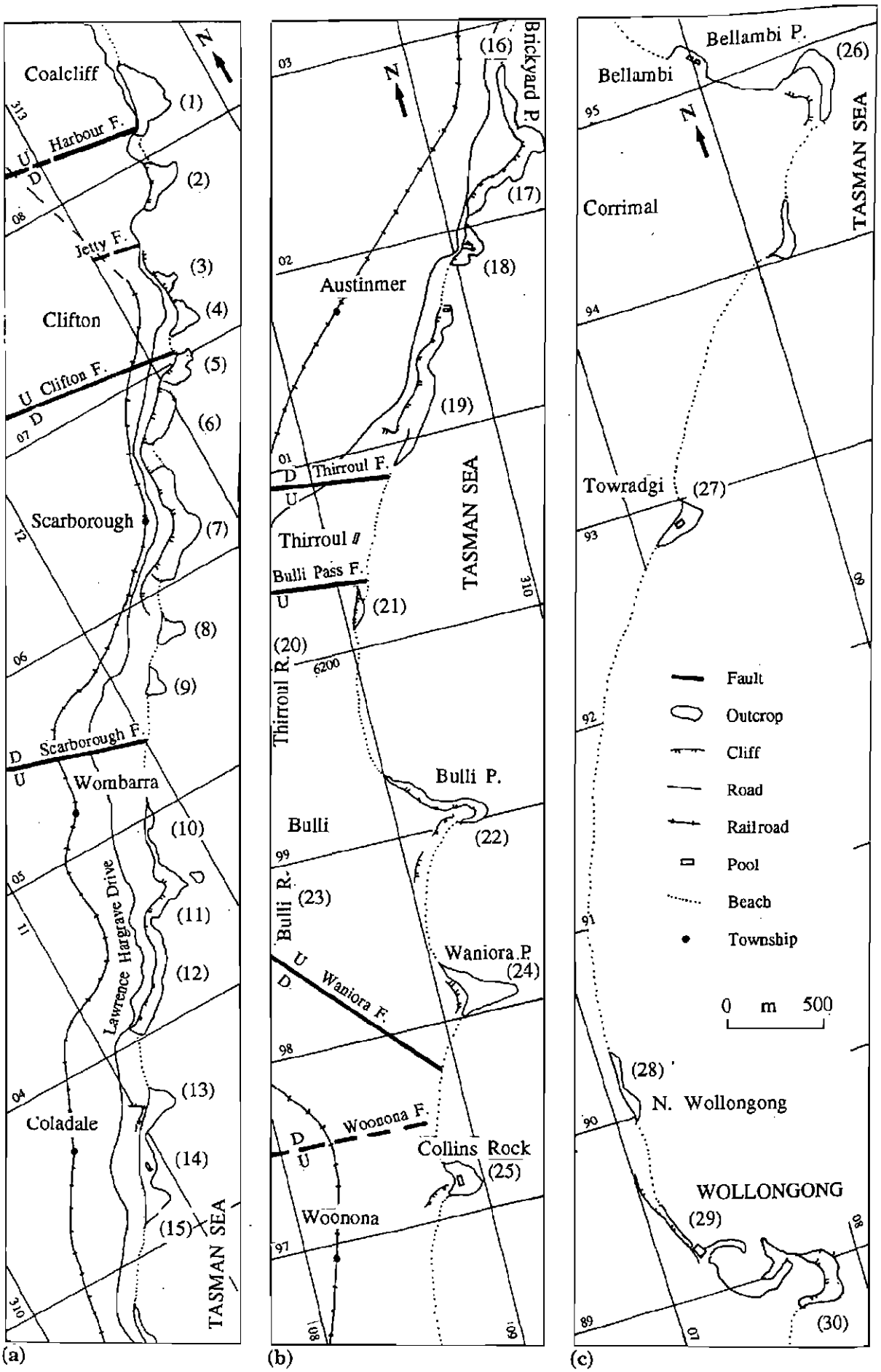

Figure 1.4 Location map of the studied outcrops. Northern (a), central (b) and southern (c) outcrops.

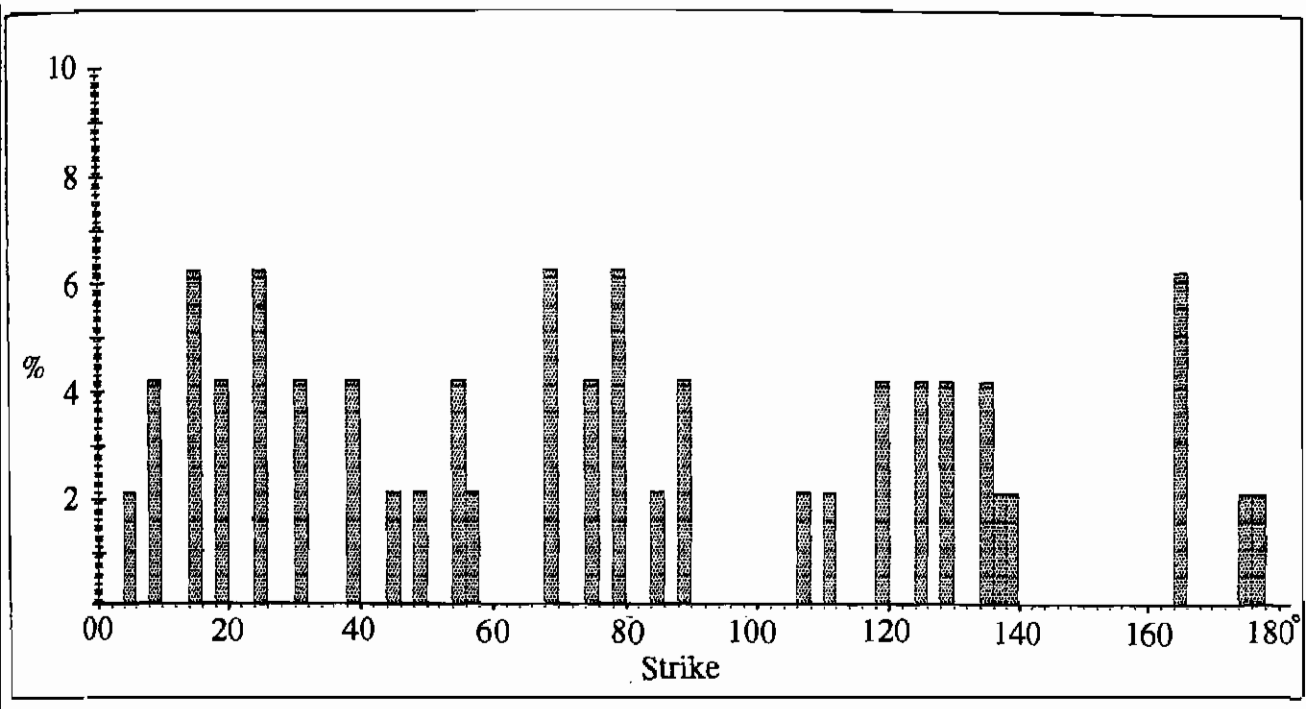

Figure 1.5 Distribution of the orientation of 57 surveyed scanlines.

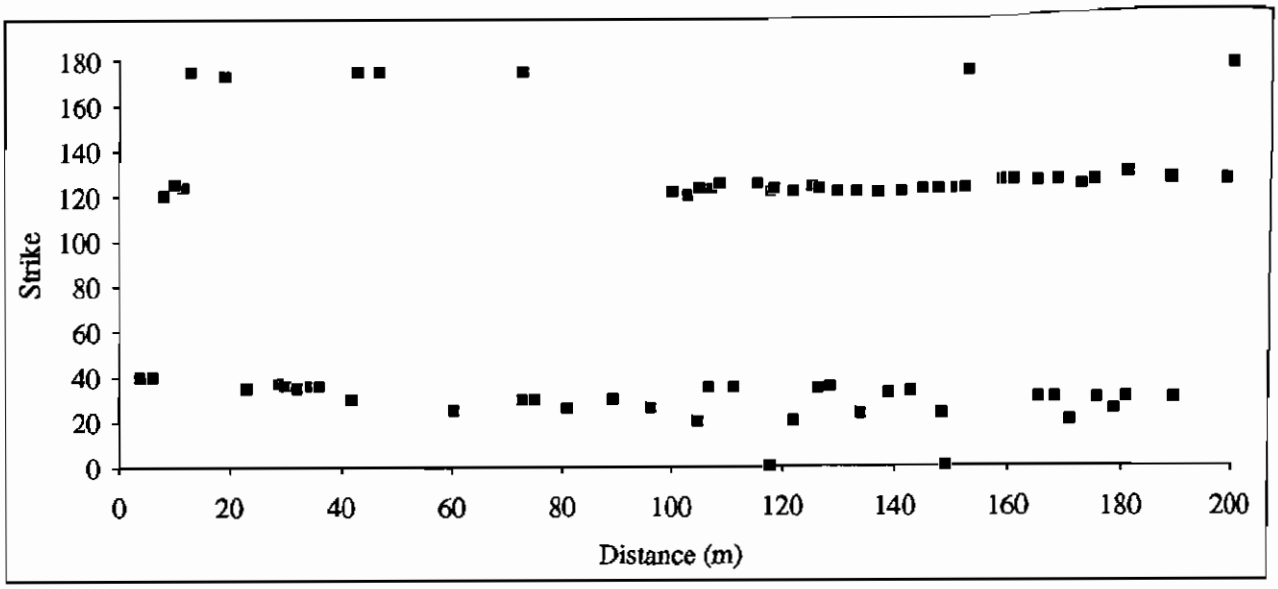

Figure 1.6 Scanline chart of rock fractures, for scanline 14-II', at Coledale, with 200 m length and a 010° trend. The following are some information which can be extracted from this chart. Of three systematic N, NE and SE sets, the latter is more frequent and less scattered. Surprisingly, this set is not developed between the 10 and 100 m mark. The N joints (175-180°) are the least frequent. The NE joints are divided into two subsets, striking 040° and 030°, especially after the 100 m mark. The true spacing of each set (sp), is easily calculated from this chart, using the following simple formula:

$$\sin d = sp / a \qquad (1.1)$$

where d is the difference between the orientation of scanline, here 10°, and the strike of the chosen set (when d is bigger than 90° it should be subtracted from 180°), and a is the average spacing of the same set measured from the scanline. The spacing of the NW (120°) set, between the 122 m and 152 m marks is 3.1 m (sin 180-110° = sp / 3.3).

Please see print copy for image.

Figure 1.7 Major structural elements of the southeastern Sydney Basin, mostly based on mining data (Rixon & Shepherd 1988; Lohe *et al.* 1992).

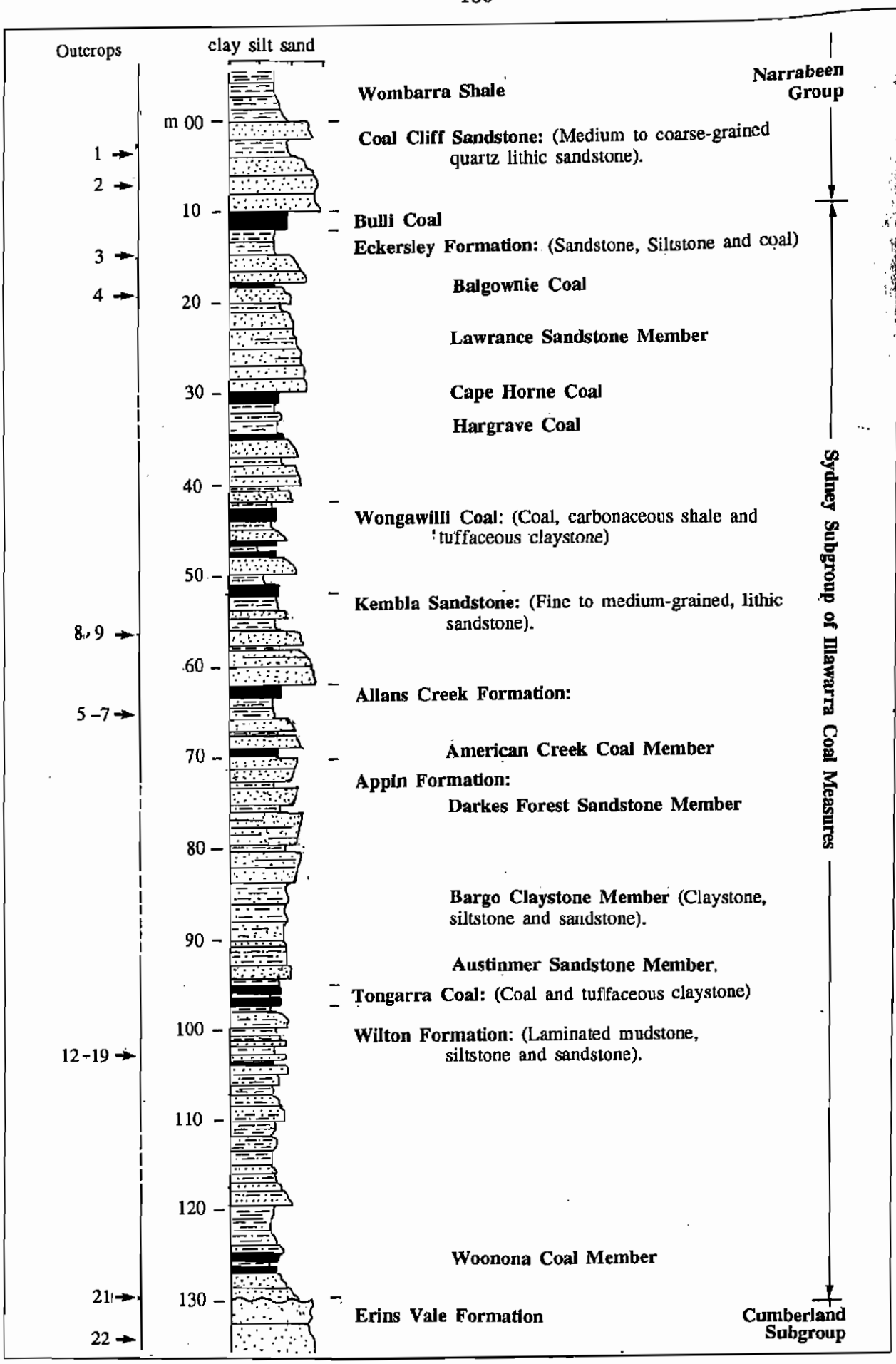

Figure 1.8 Simplified stratigraphic column of the Sydney Subgroup of the Illawarra Coal Measures in the southeastern Sydney Basin.

(b)

(d)

(a)

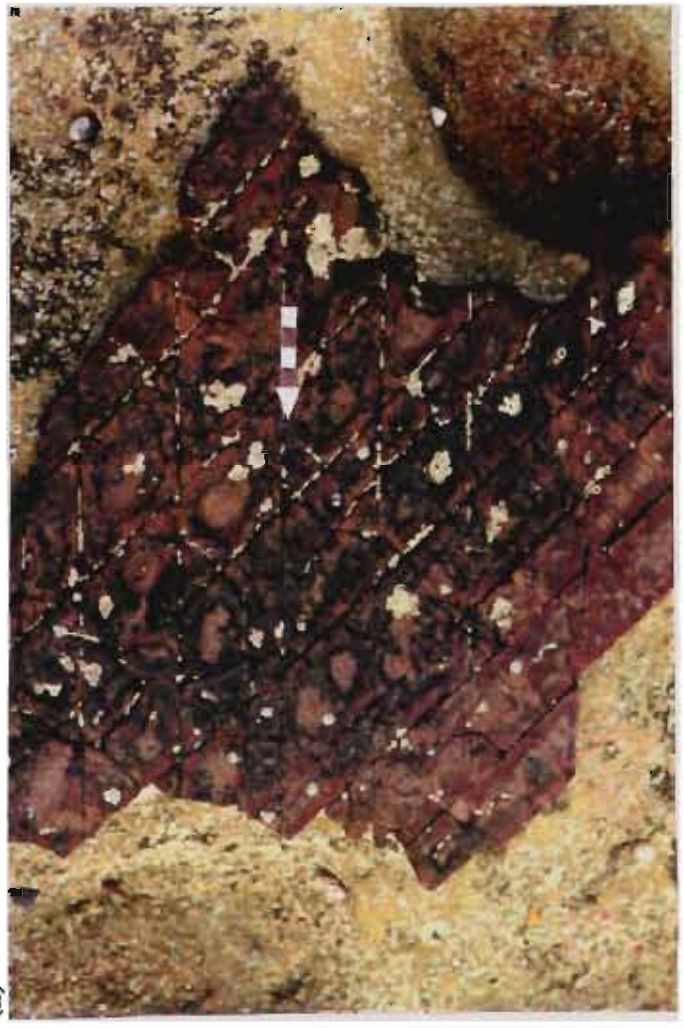

(c)

Figure 2.1 Vertical propagation of joints in one or more beds. (a) Long 033° joints and some slightly curved 022° fractures developed in fine-grained sandstone. The lower mudstone bed (foreground) is joint free, except for one major 033° fracture which cuts through it (Outcrop 8, looking towards the south). Hammer 33 cm long. (b) Remnants of two beds of medium-grained sandstone, 40 cm thick, with 3 vertical joint sets striking 000, 055, 135°, above a joint free, laminated siltstone and mudstone (Outcrop 1, bar scale - 10 cm). (c) Conjugate joint sets, striking 000 and 045°, in a 1 cm thick sideritic mudstone band overlying the thick sandstone beds of Outcrop 2 (point i of Figure 2.3e). The nonsystematic joints are subnormal to the NE joints. Arrow 5 cm long. (d) 020° joints developed in 2 cm thick grey siltstone beds, interbedded with joint free fine-grained sandstone and siltstone beds with a red weathered surface. The spacing of the 020° joints is 10 cm. Few of these joints penetrate into the neighbouring beds (Outcrop 6 at Scarborough).

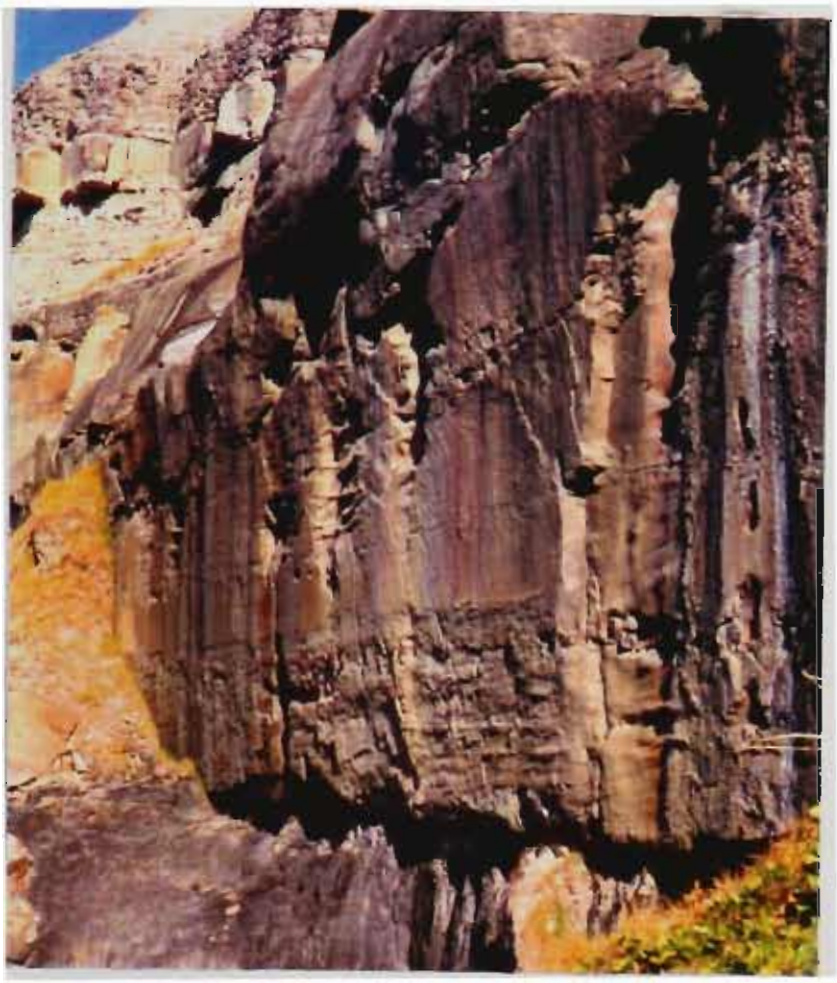

(a)

(b)

Figure 2.2 (a) Vertical extent of a 010° striking joint with surface markings in sandstone beds of the lower part of the Coal Cliff Sandstone. The joint is terminated at the top by a thin shale bed and at the base by the Bulli Coal. The axis of the plumose marking is parallel to bedding. The sandstone unit is 5 m thick. (b) A set of 020° joints developed in sandstone beds of different thickness, interbedded with mudstones. Note the closer spacing of joints in thinner sandstone beds (Outcrop 6, Scarborough). Hammer 33 cm long.

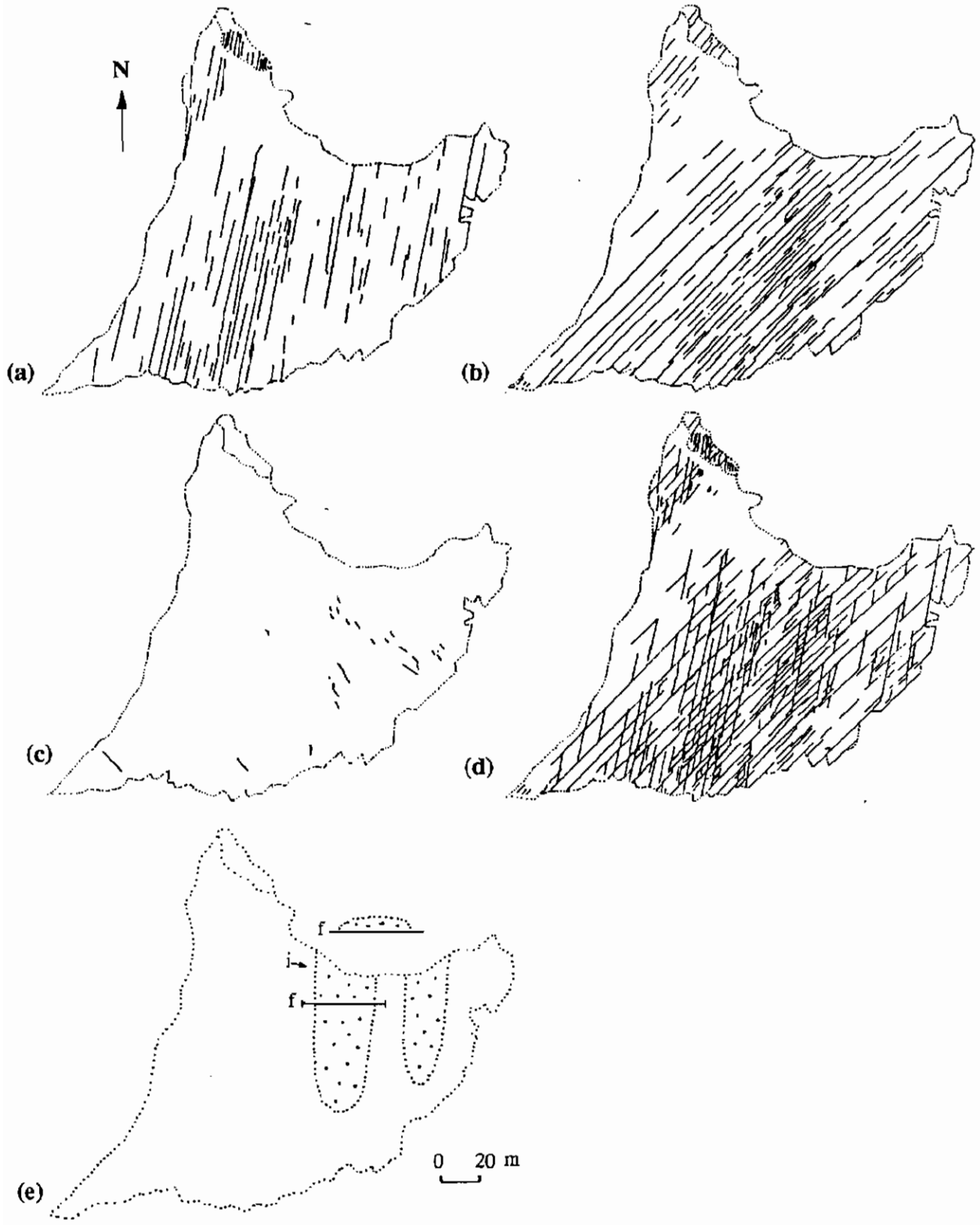

Figure 2.3 Open NNE (a) and NE (b) joints forming a conjugate pattern (d) in thick sandstone beds, at Coalcliff (Outcrop 2). The NE joints are slightly concave towards the SE. Nonsystematic joints are sub-normal to the NE joints (c). Long NNE and NE joints cross the elongated conglomeratic units (e) with minimum deviation in their strike (a)-(b).

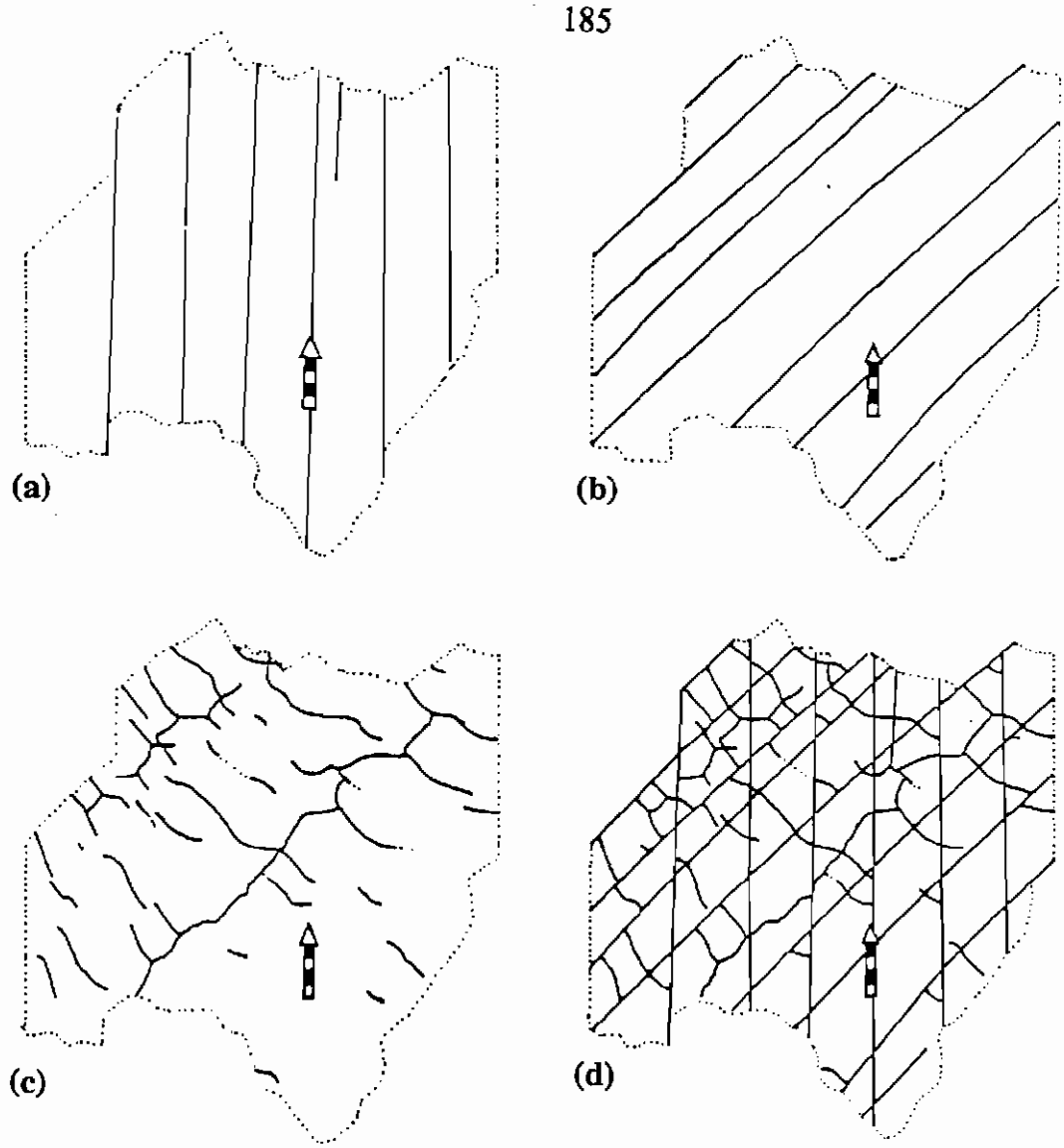

Figure 2.4 Fracture pattern of a 1 cm thick sideritic mudstone band (Figure 2.1c), exposed at point i on Figure 2.3e. The conjugate sets are identical to joints throughout the platform (cf. Figure 2.3d). The NNE (a) and NE (b) sets show similar characters, except the NE joints which are slightly concave towards the SE. Nonsystematic joints (c) are mainly sub-normal to NE joints. North arrow scaled in centimetres.

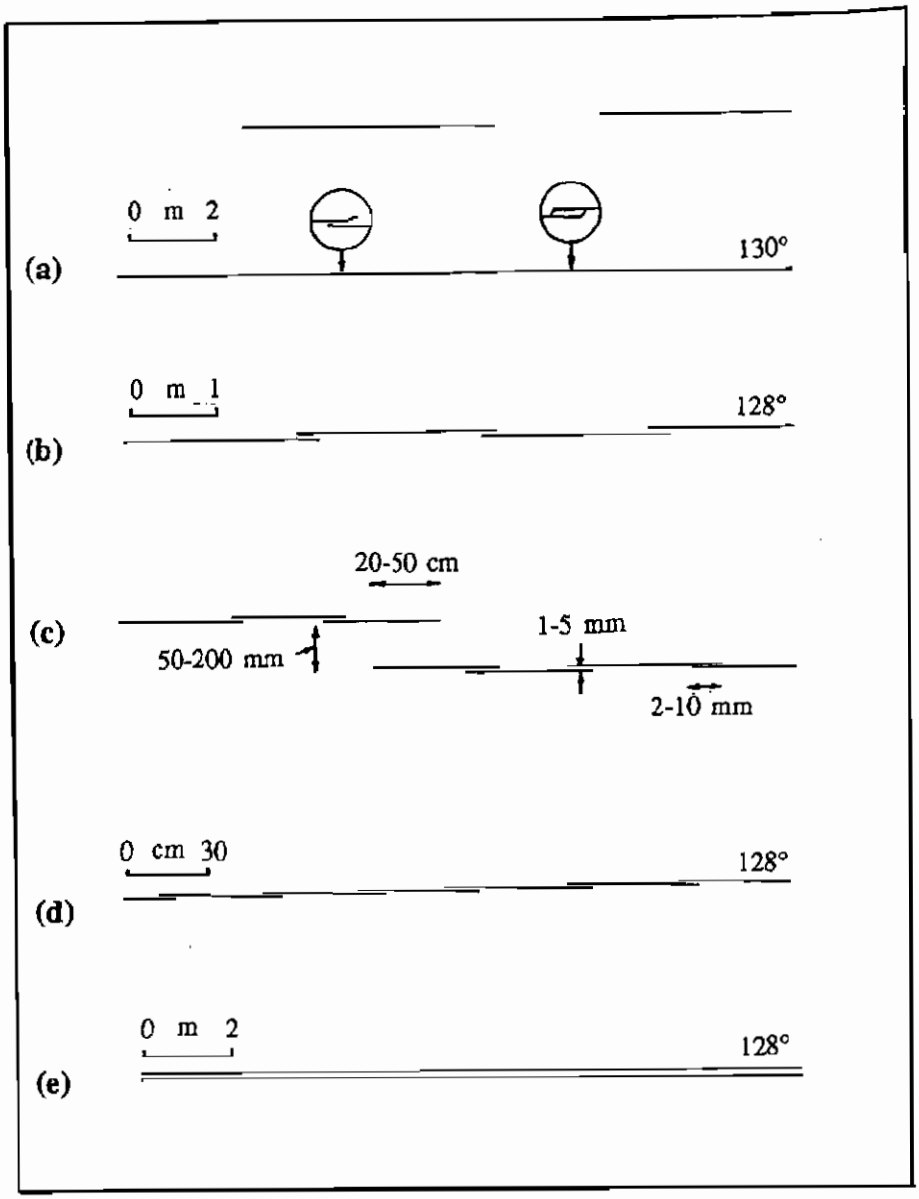

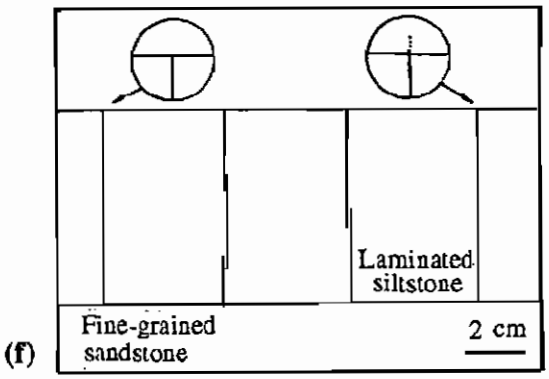

Figure 2.5 Horizontal and vertical traces of the SE joints. (a) Hair like and closed joints (Coledale). (b) Segmented and overlapped joints sealed with less than 1 mm of calcite (40 m mark of Scanline 11-HH' at Wombarra). (c) Joint with two orders of segmentation and overlap (Scanline 11-HH' at Wombarra). (d) En echelon traces (75 m mark of Scanline 17-AA' at Brickyard Point). (e) A very long (more than 20 m), open (up to 5 mm) joint at Bulli (Scanline 22-CC' at Bulli). (f) Vertical extent of segmented SE joints in laminated siltstone and their termination at the interface with medium to coarse-grained sandstone. Locally, the joint slightly (1-3 mm) penetrates to the other side of the interface before termination (Scanlines 13-FF' & 14-II' at Coledale).

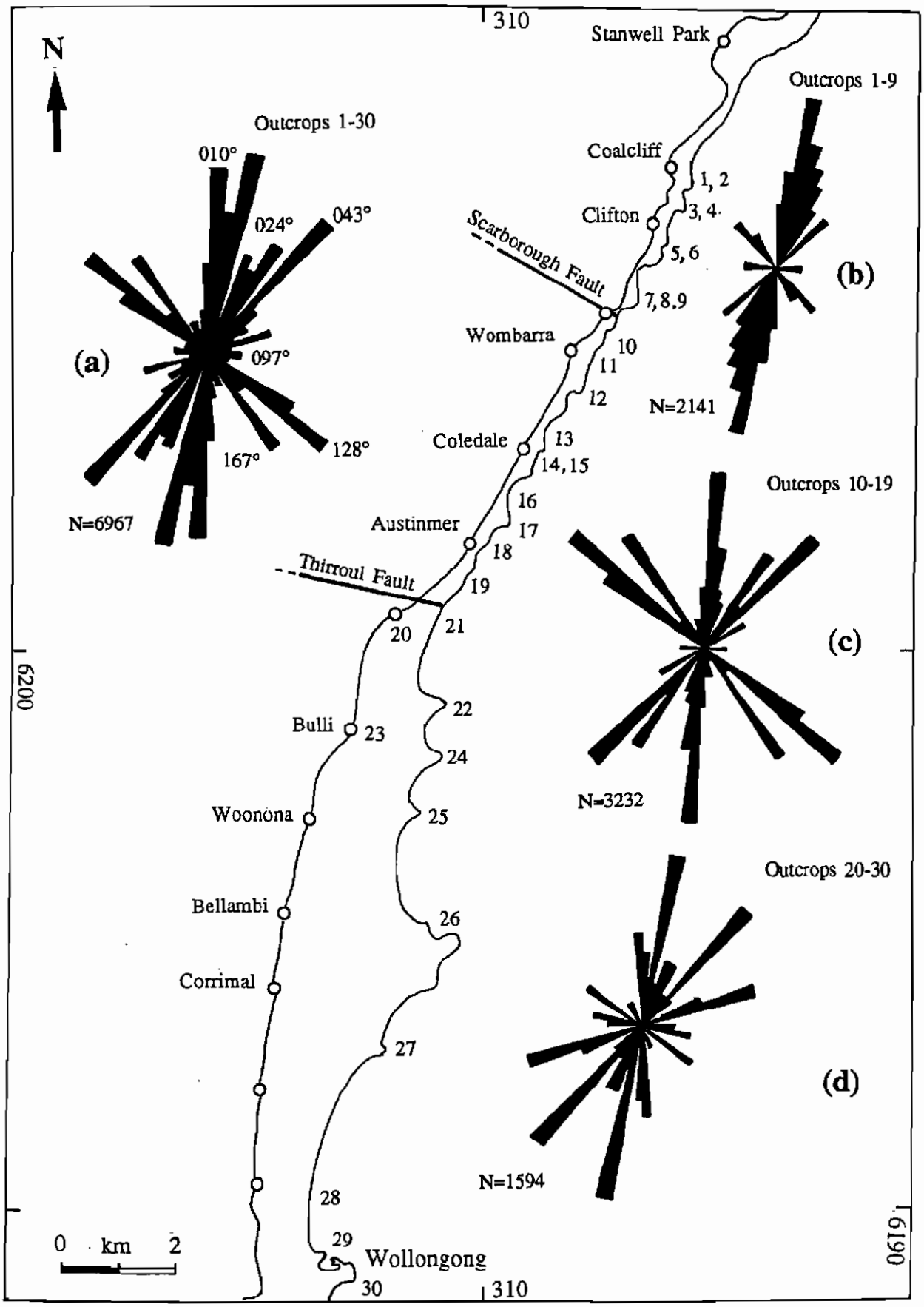

Figure 2.6 Orientation of systematic joints in southeastern part of the Sydney Basin. (a) Rose diagram of 6967 joints measured in this part of the basin with three dominant sets (NNE, NE and SE), as well as three less frequent sets (NNE, E and SSE). (b) Jointing of the northern zone, which comprises the 9 outcrops to the north of the Scarborough Fault. (c) Jointing of the 10 central outcrops. (d) Jointing of outcrops south of the Thirroul Fault.

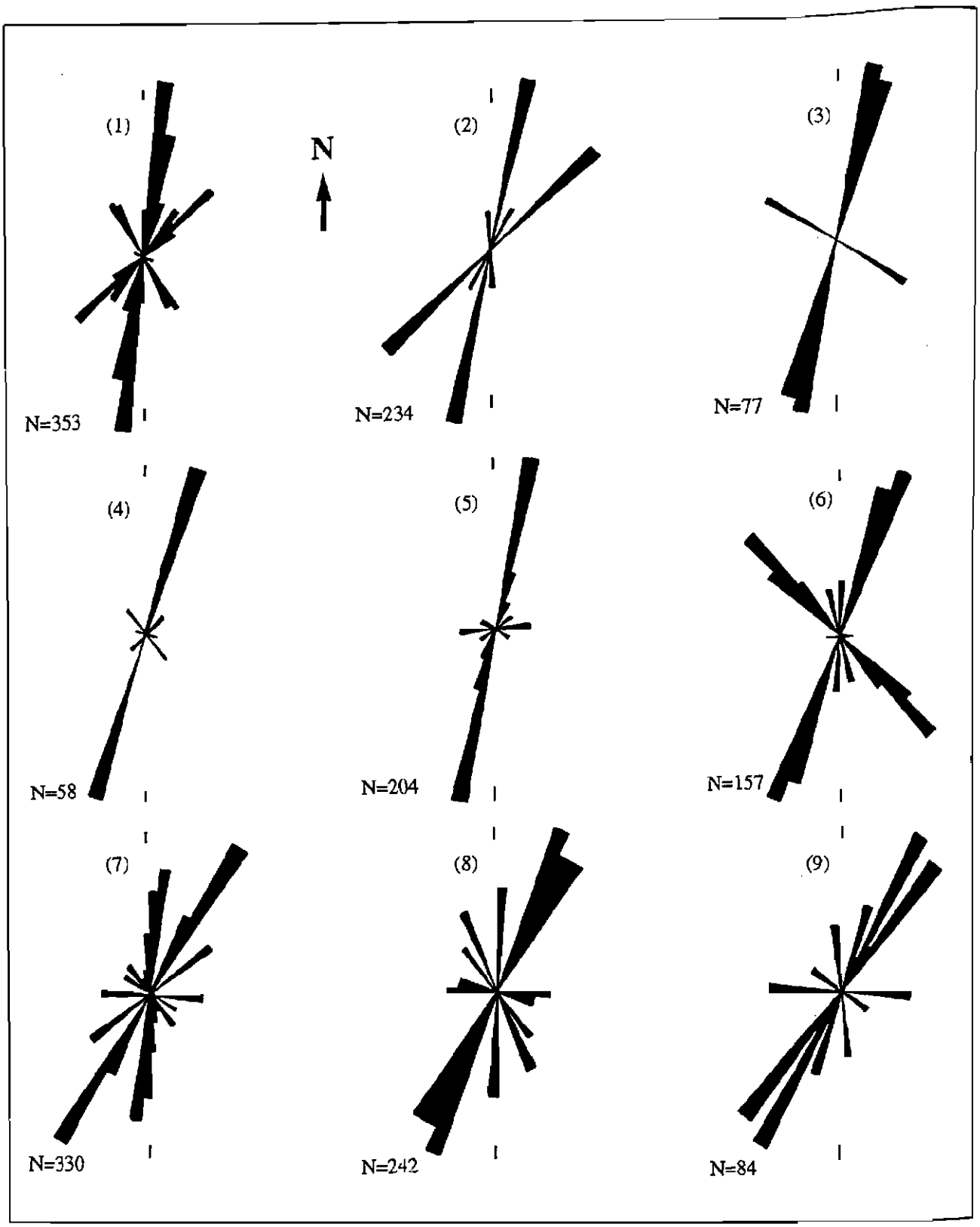

Figure 2.7 Regional and local joint sets of 9 outcrops to the north of the Scarborough Fault. Outcrops 1 and 2 consist of the Coal Cliff Sandstone of the Narrabeen Group, while the rest are part of the upper Illawarra Coal Measures. The combined fracture pattern of these 9 outcrops is shown in Figure 2.6b.

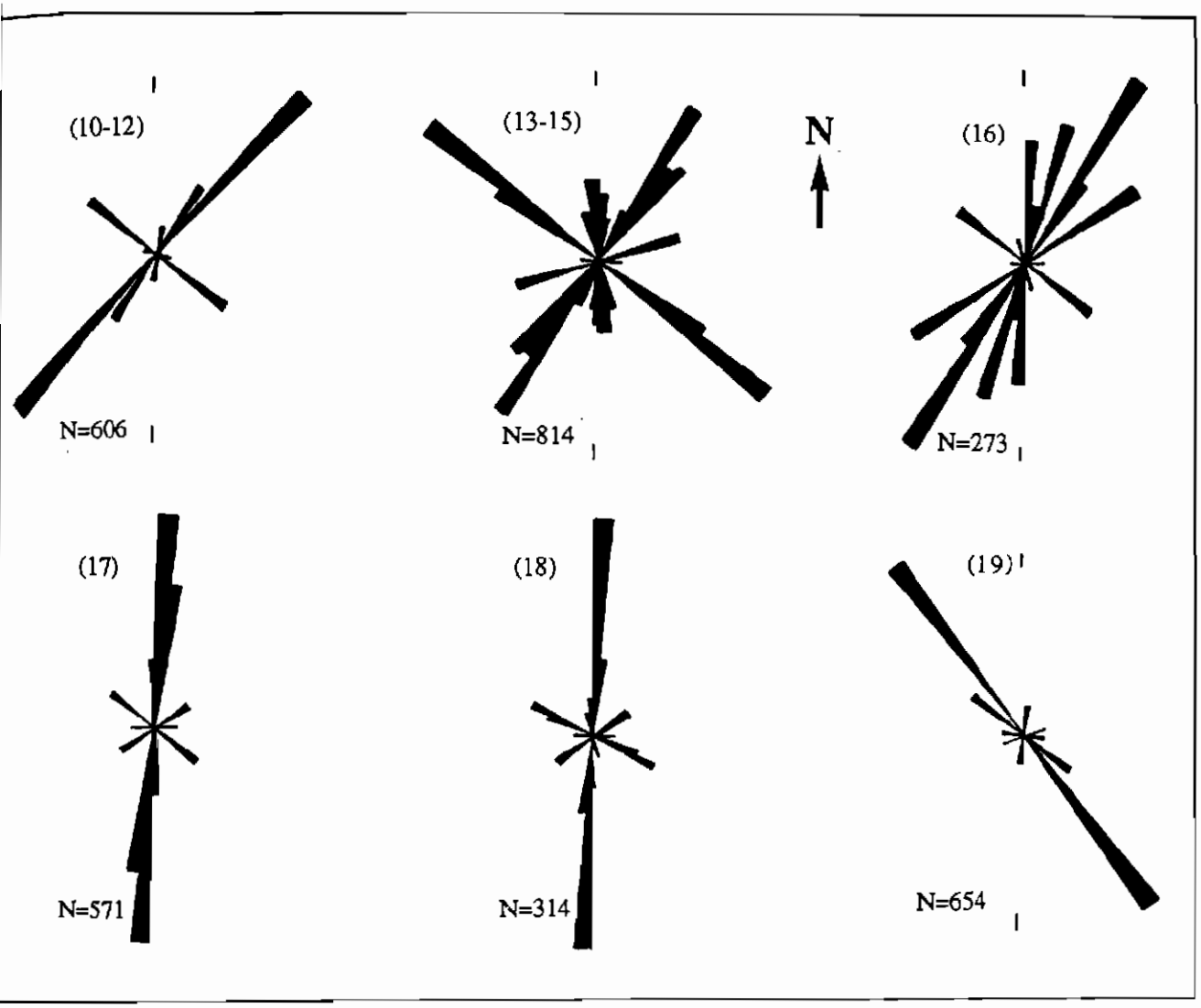

Figure 2.8 Orientation of joints in the central zone (Outcrops 10-19). The combined fracture pattern of this zone is presented in Figure 2.6c.

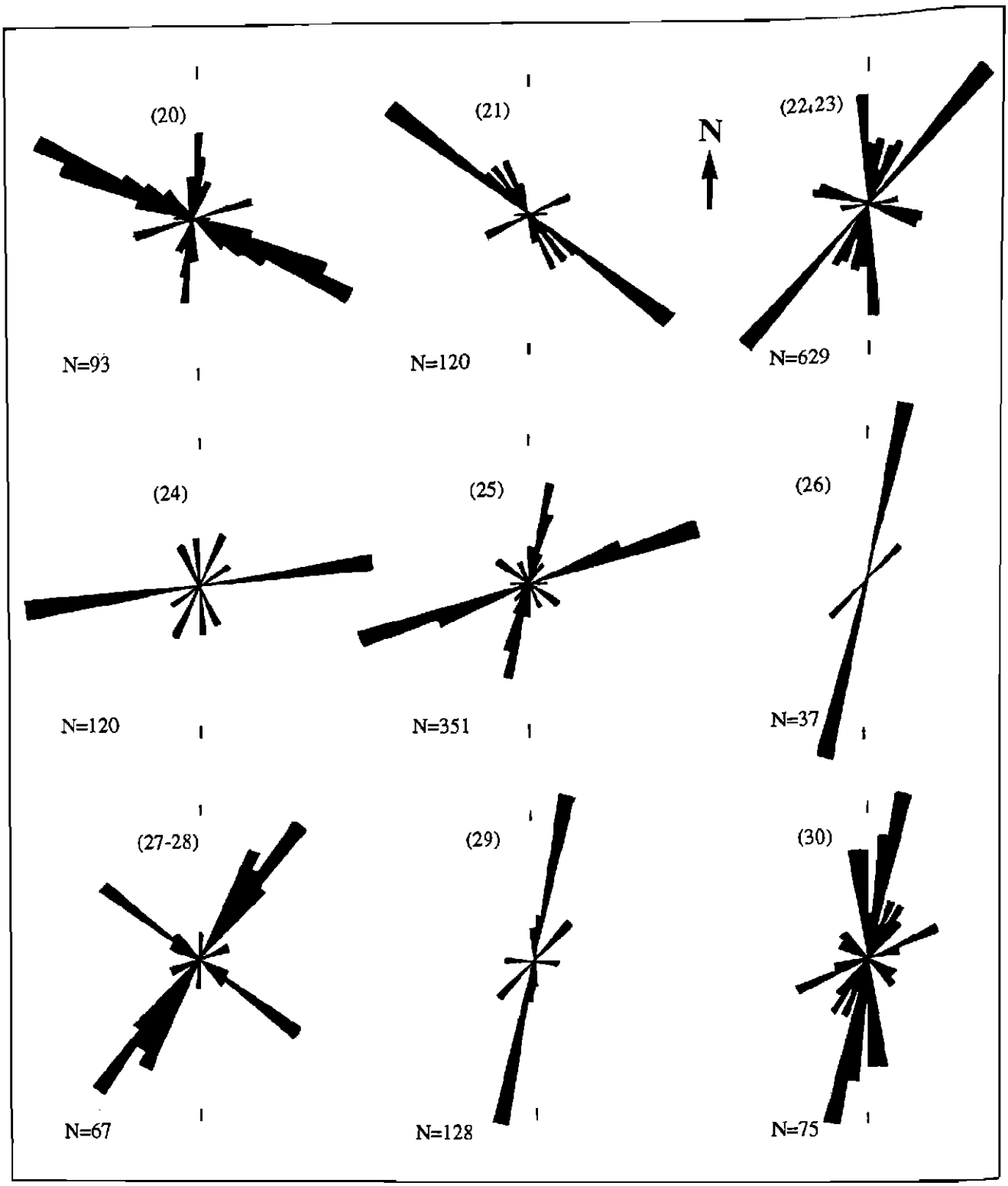

Figure 2.9 Fracture sets of the outcrops to the south of the Thirroul Fault (Outcrops 20-30). The overall fracture pattern of this zone is presented in Figure 2.6d.

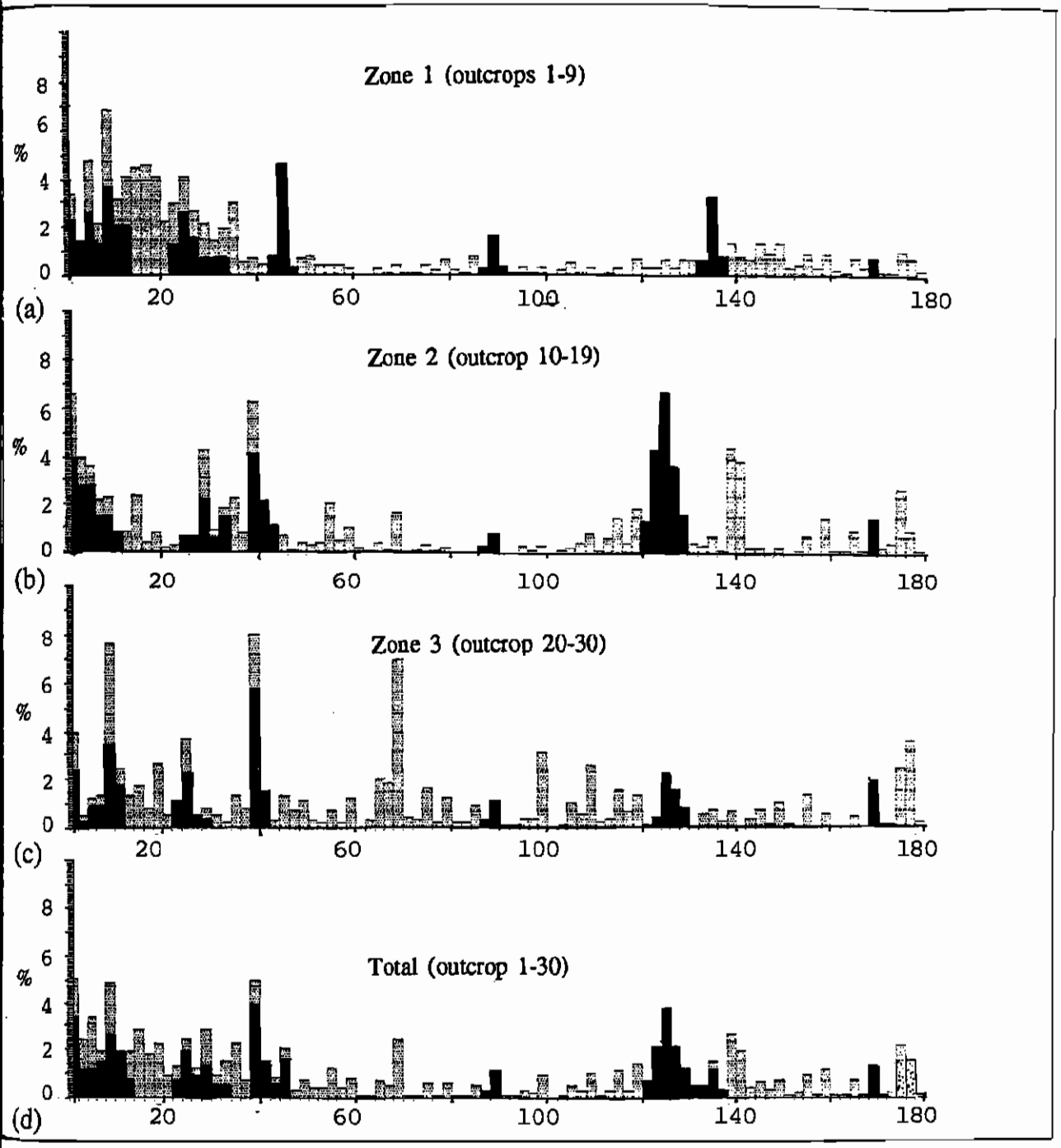

Figure 2.10 Histograms of joint orientation in northern (a), central (b) and southern (c) parts of the study area. Six set of regional joints (black) are recognised in each of these zones. The rest of the joints (grey) are local or unidentified. Local joints are related to either dykes (e.g. 140° of zone 2) or a monocline (e.g. 053° - zone 2). Note that both regional and local joints are developed in N-NNE direction. The data for all the 30 outcrops is presented in (d).

(a)

(b)

Figure 2.11 Nonsystematic cross joints. (a) NE extension joints and a set of nonsystematic cross joints in a 2 cm thick ironstone band at the southern most part of Outcrop 2. (b) Cross joints developed in a siltstone layer, normal to a 020° joint set at Scarborough (north arrow is scaled in centimetres).

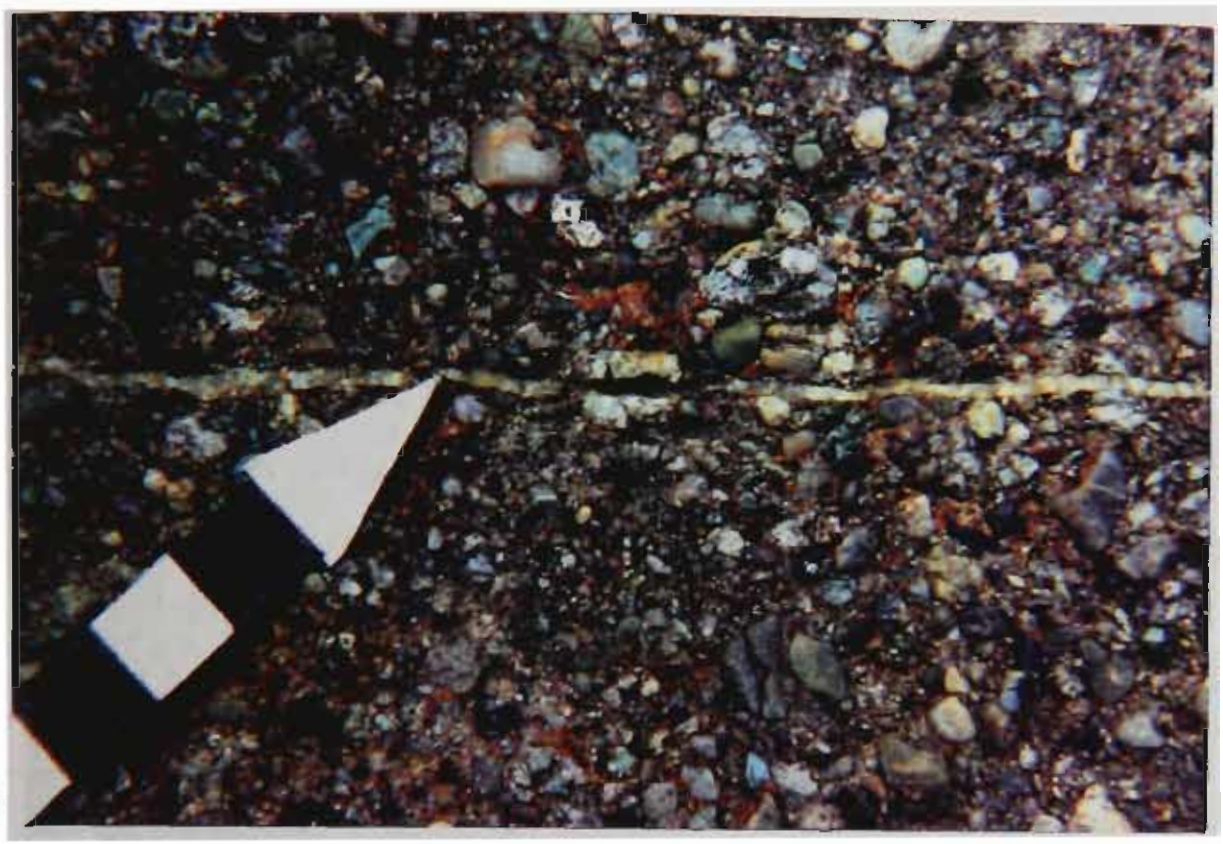

(a)

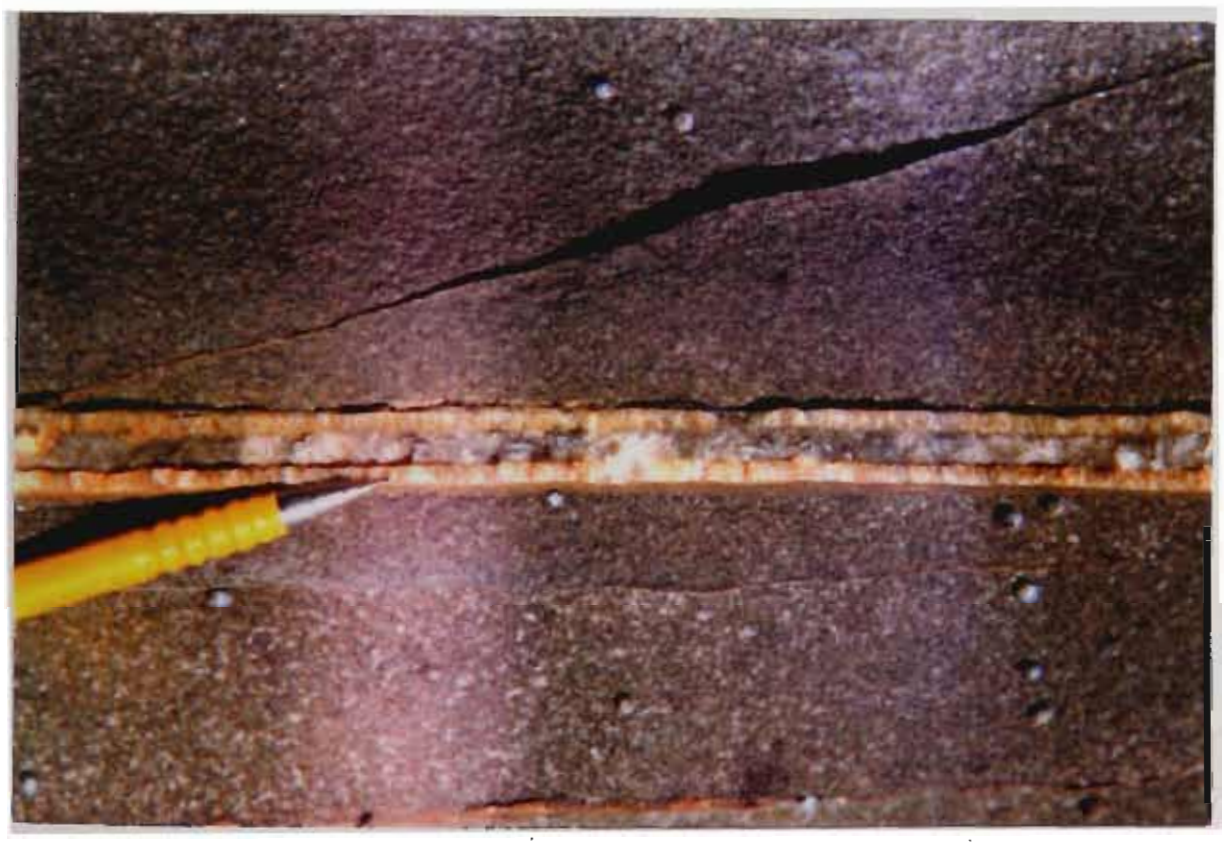

(b)

Figure 2.12 (a) A 045° vertical joint, cuts pebbles of a conglomerate at Coalcliff (Figure 2.3e). The joint, which is filled with 2 mm of calcite, has cut clasts which show no sign of lateral shearing. North arrow is scaled in centimetres. (b) A NNE vertical fracture with a double phase of calcite infilling. Calcite crystals, which grew away from the joint walls, show no sign of shearing or lateral displacement. Pen tip (5 cm long) points to north (Outcrop 2).

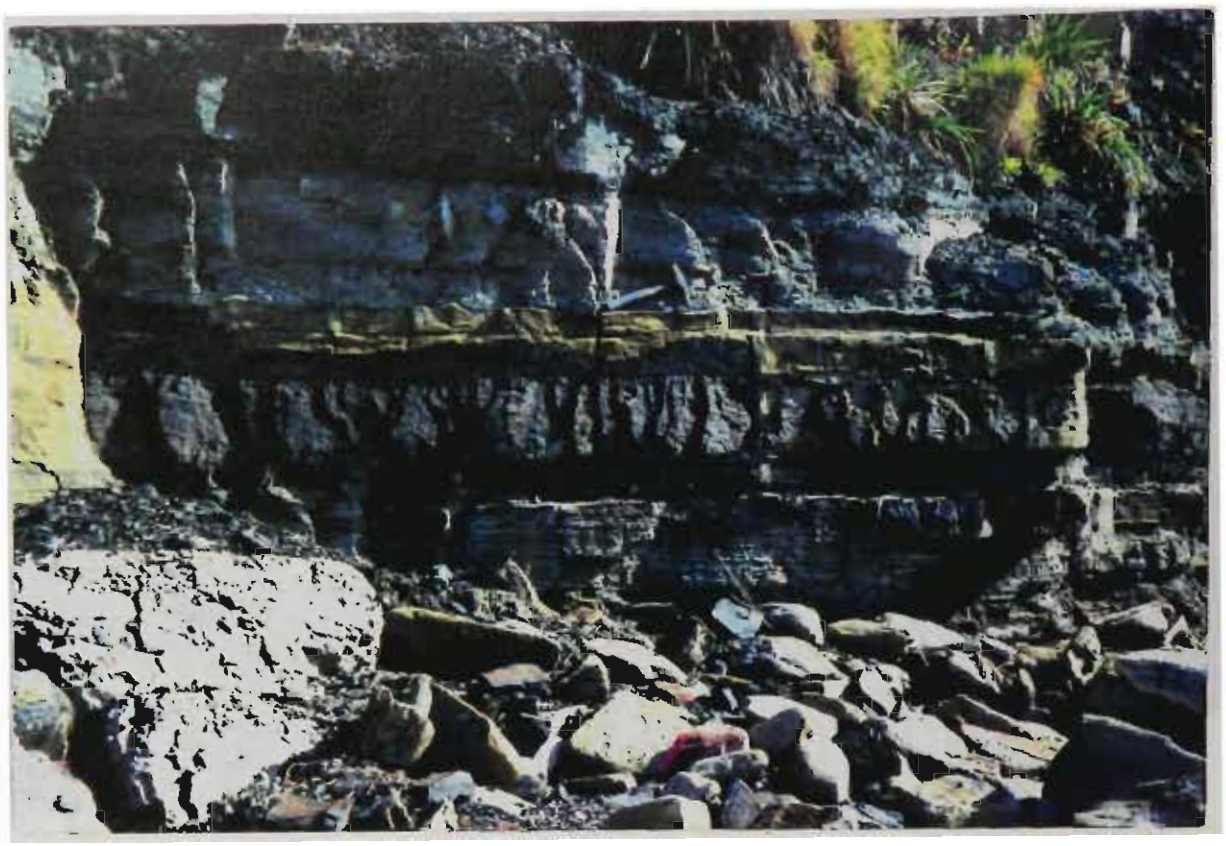

(a)

(b)

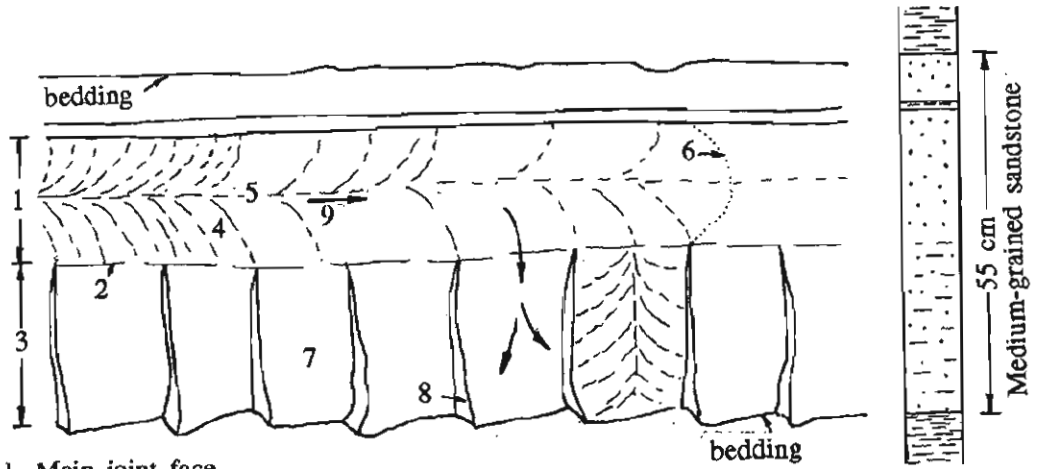

1. Main joint face
2. Shoulder
3. Fringe zone (twist hackle fringe)
4. Plume structure (plumose marking, hackle plume or barbs)
5. Plume axis
6. Arrest line
7. Twist hackle face (f-joint) with second order plumose marhing
8. Twist hackle step (c-joint)
9. Direction of joint propagation.

Figure 2.13 Photograph (a) and sketch (b) of surface marking on a 032° striking joint developed in a medium-grained sandstone bed of the Kembla Formation at Scarborough. The sandstone bed is overlain by a grey mudstone and underlain by laminated mudstone and fine-grained sandstone. The main joint face is terminated by a 3 mm thick claystone band occurring in the upper part of the bed. The lower two thirds of the sandstone bed contains flat laminations of carbonaceous material. The joint surface is iron stained (see text for more explanation). Hammer 33 cm long.

(a)

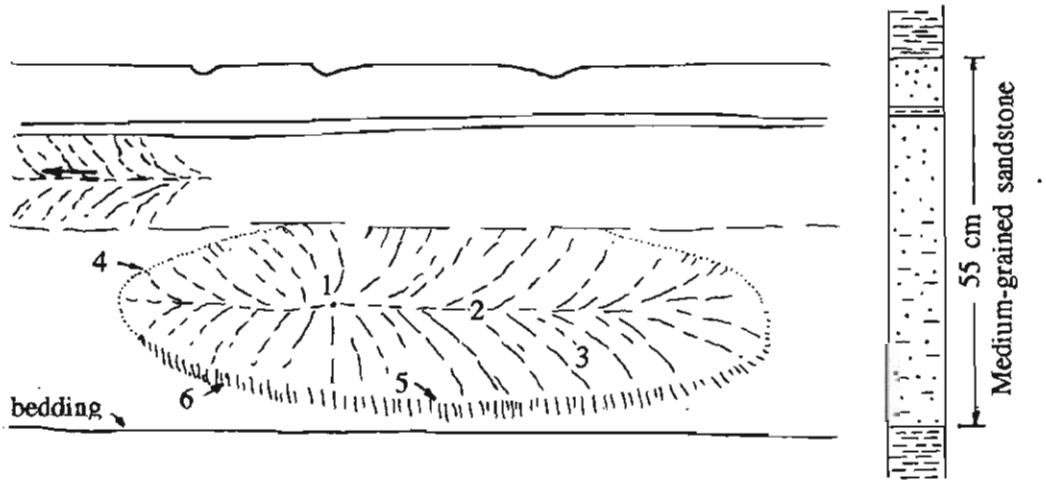

(b)

1. Nucleation point (origin)
2. Plume axis
3. Plume structure
4. Arrest line
5. Sholder
6. Fringe zone

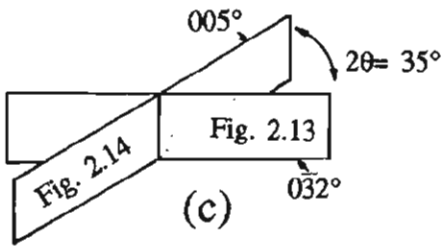

(c)

Figure 2.14 Photograph (a) and sketch (b) of an elliptical vertical joint developed in the lower two thirds of the medium-grained sandstone in Figure 2.13. This joint strikes 005° and has propagated bilaterally both to the left and right of its nucleation point. Hammer 33 cm long. (c) Relative location of joints in Figures 2.13 and 2.14a, b.

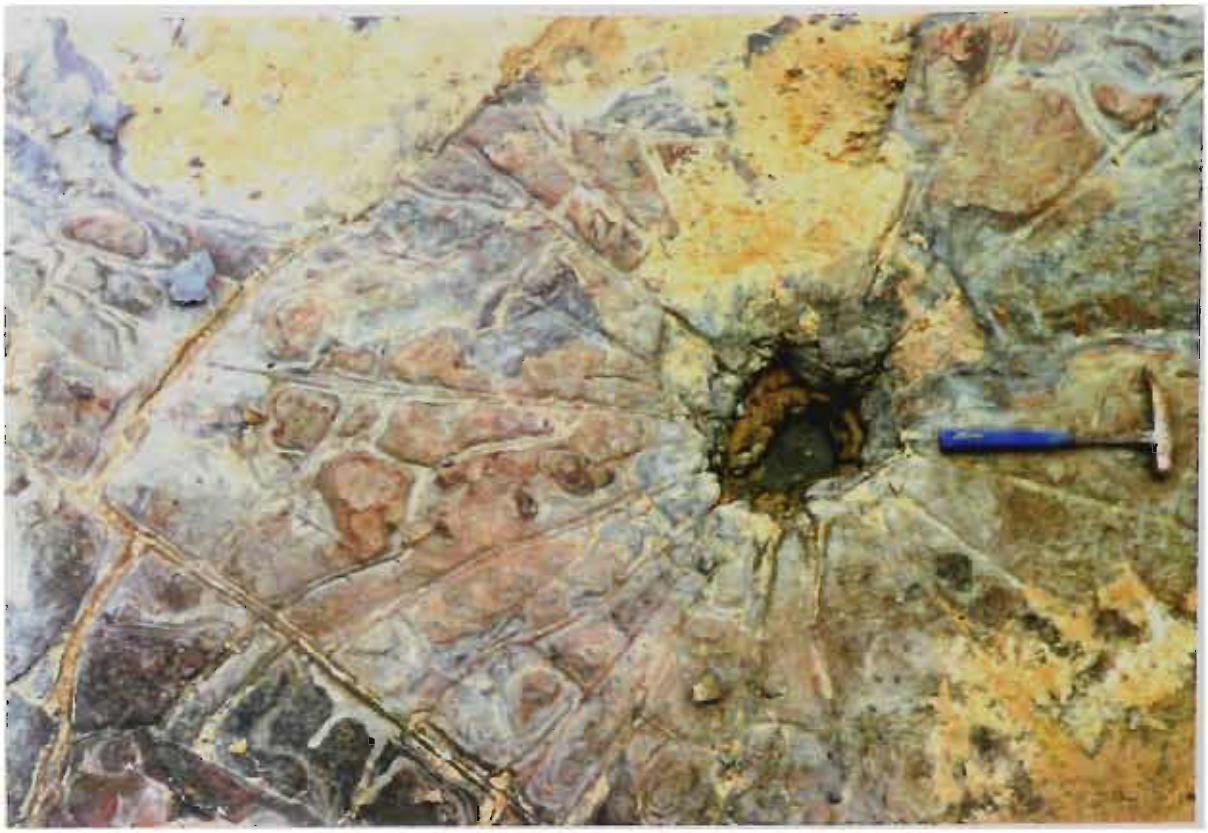

Figure 2.15 Fracture pattern resulting from a dynamite explosion in shallow vertical holes at Brickyard Point (5 m mark of Scanline 17-cc'). Note the termination of extension fractures along the sides of an open 040° fracture at the bottom left of the picture (north to the right). Hammer 33 cm long.

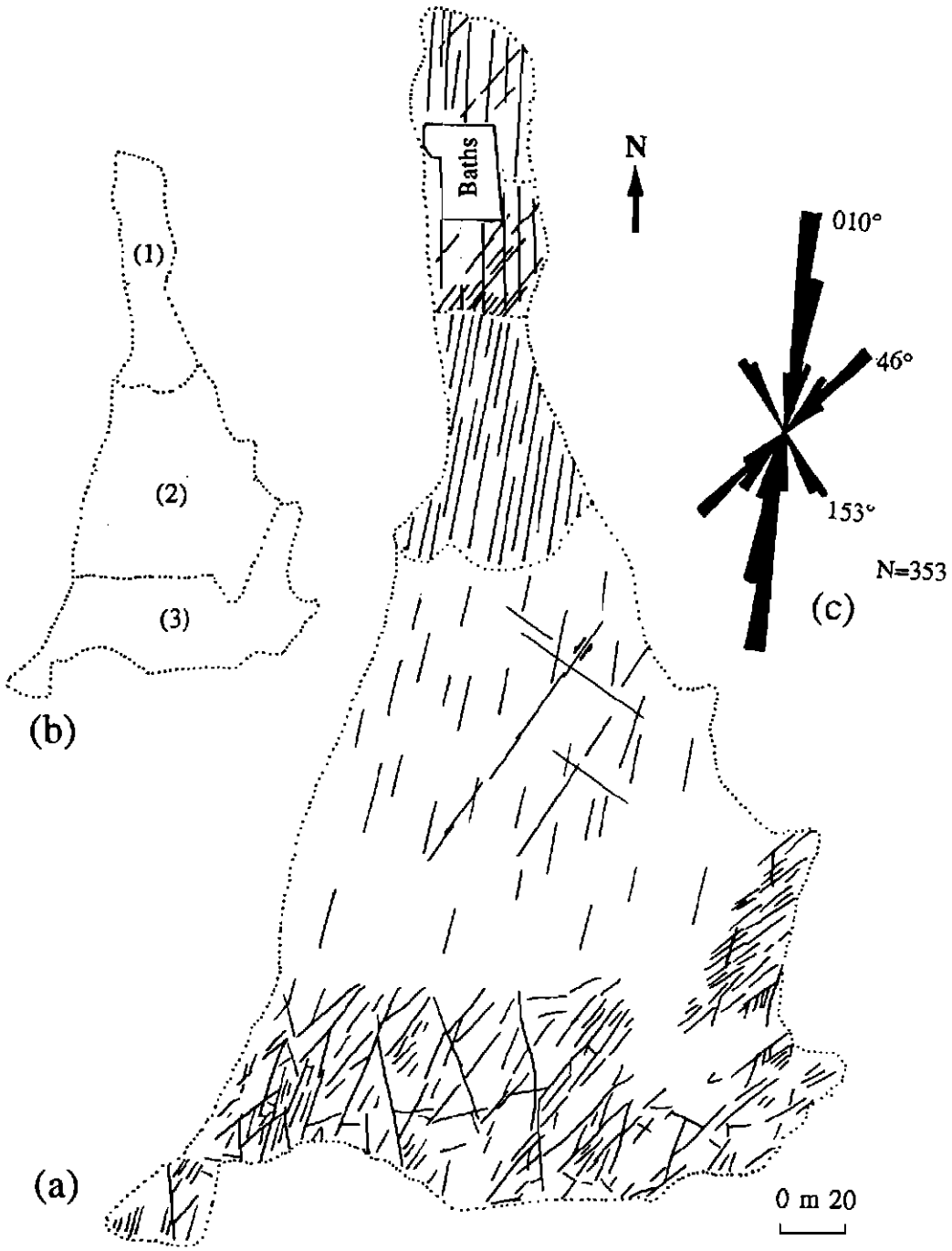

Figure 2.16 Relation between rock type and fracture pattern. (a) Simplified fracture pattern of Outcrop 1, at Coalcliff. (b) Subhorizontal thick sandstone beds occur in the northern (1) and southern (3) parts of this platform, while the central part (2) is made of thin beds of siltstone and mudstone. (c) Joint rosette for the platform.

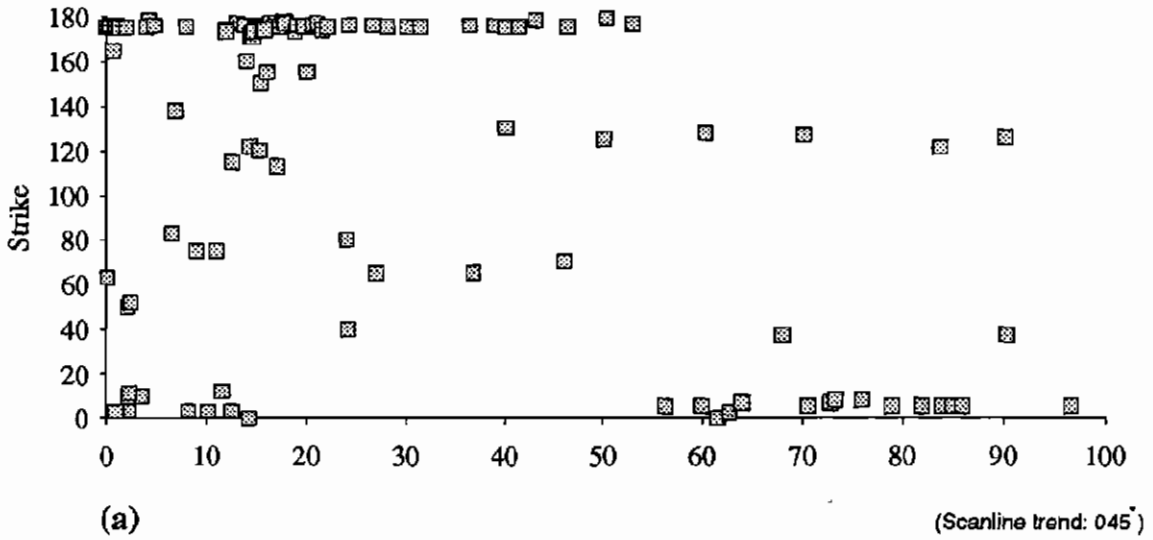

(a) (Scanline trend: 045°)

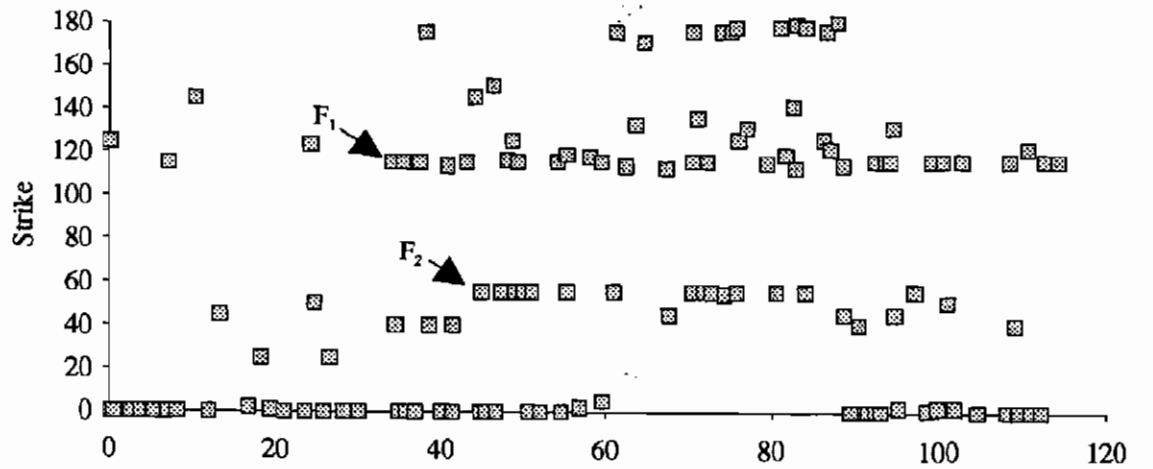

(b) (Scanline trend: 070°)

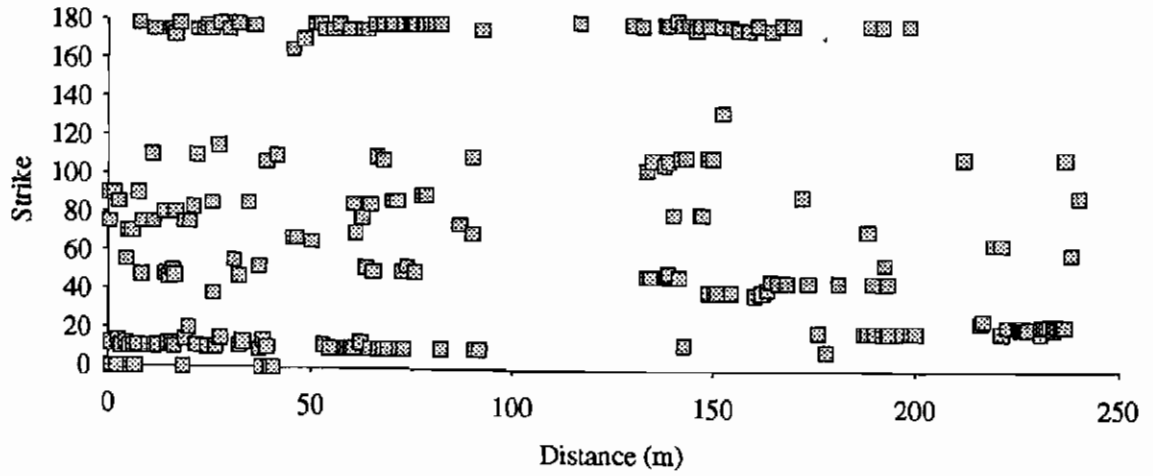

(c) (Scanline trend: 135°)

Figure 2.17 Scanline charts, demonstrating the influence of rock type on frequency and orientation of joints. (a) Change of orientation of 000° joints to 005° at 55 m mark is due to a N-S striking normal fault, with 15 cm of vertical displacement and downthrown to the east. Fine-grained sandstone occurs to the west and laminated siltstone to the east of the fault, respectively (Brickyard Point, 17-DD'). (b) The change of strike and frequency of a NE joint set (44 m mark) and a SE joint set (37 m mark), are primarily due to normal faults (F_1, F_2) juxtaposing different rock types. The change of strike from 000° to 175°, in the 60-90 m interval is due to the scanline crossing onto an overlying medium-grained sandstone bed (Austinmer, 18-CC'). (c) The absence of the joints in the interval between 95 and 131 m is due to a 10 cm descent of the scanline from a jointed, medium-grained sandstone bed to a less competent sandstone bed with more clay material (Bulli, 22-AA').

(a)

(b)

Figure 2.18 (a) Fracture pattern of Bulli Coal in a vertical exposure at Clifton (Outcrop 4). Joints in coal are much more abundant than in neighbouring mudstone and sandstone. Hammer 33 cm long. (b) A 10 cm thick, almost joint free, coal seam, exposed at Scarborough (Outcrop 7).

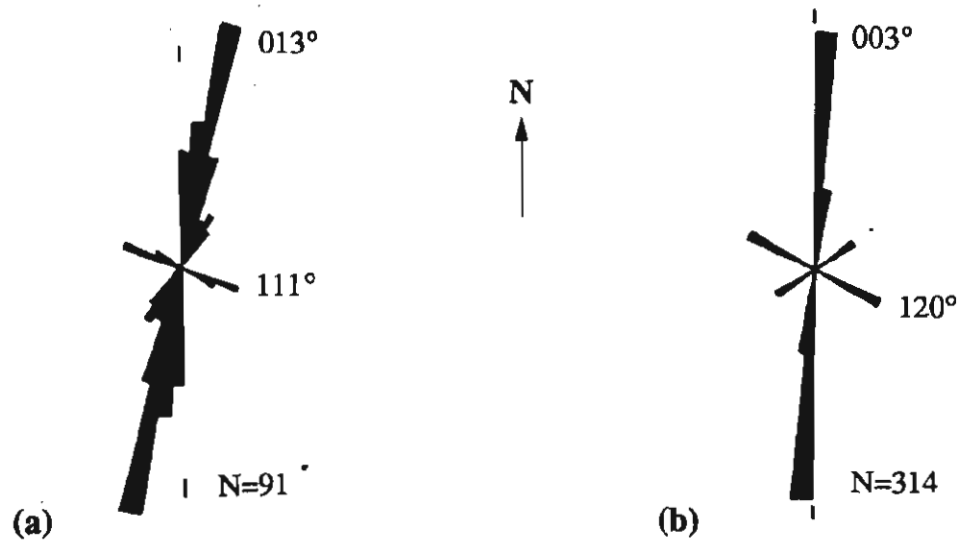

Figure 2.19 (a) Fractures in the Tongarra Coal at Bell Point, Austinmer (Outcrop 18). The dominant set strikes 013°, while a second minor set, strikes 111° (face and butt cleats respectively, in the sense of Nickelsen and Hough 1967). (b) Rose diagram of 314 joints measured in Outcrop 18. Note the similarity between joints in the coal (a) and the rest of the platform (b).

Figure 2.20 Fracture pattern of a silicified plant fragment at Coledale (48 m mark of Scanline 13-AA'). The dominant joint set, strikes 135° with a spacing of 1-2 mm. The second set, which strikes 035-040°, is nonsystematic and abuts against the first set. Coin has 1 cm radius.

(a)

(b)

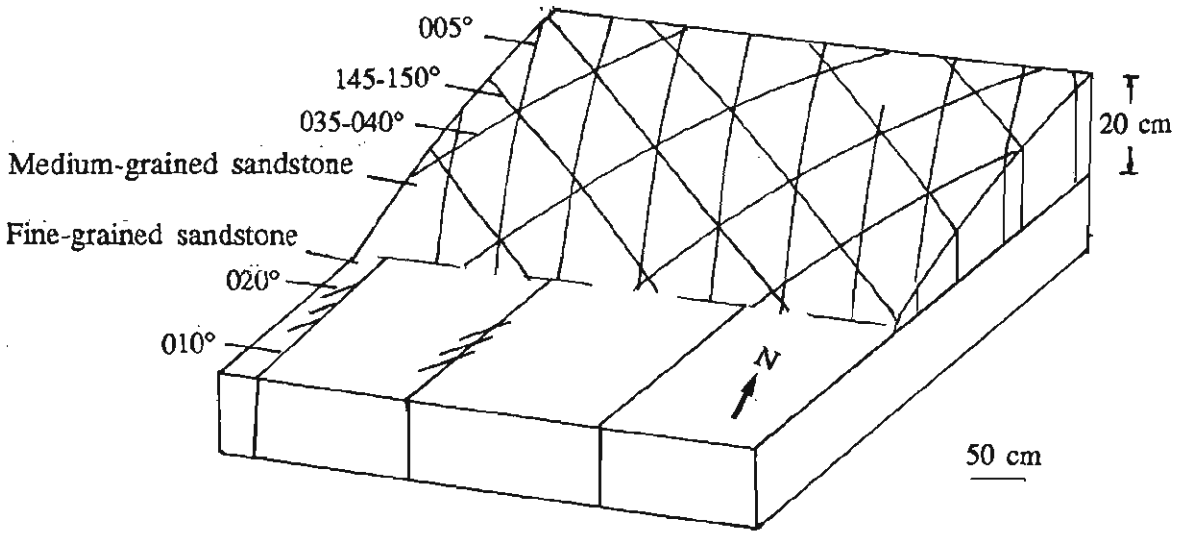
005°
145-150°
035-040°
Medium-grained sandstone
Fine-grained sandstone
020°
010°
N
20 cm
50 cm

(c)

Figure 2.21 The effect of bed thickness and rock type on jointing. Photograph (a) and sketch (b) of long 010° joints in fine-grained sandstone changing to a strike of 005° in an upper medium-grained lensoidal sandstone. Note that spacing has also decreased from 2 m to about 0.5 m and that all the joints in the lensoidal body are slightly curved (Outcrop 1). Hammer 33 cm in length. (c) Vertical section of a coarse-grained, cross-bedded, lensoidal sandstone at Scarborough (Outcrop 7). Note the close relation between the thickness of the jointed unit and the spacing. Hammer 33 cm long.

(a)

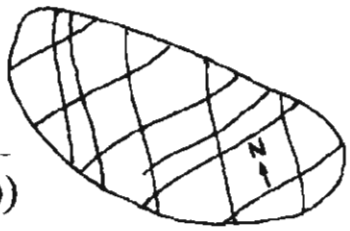

(b)

(c)

(d)

Figure 2.22 Gradual change in strike, due to an increase in thickness of the jointed body. (a) Slight bending of traces of the NNE and NE joint sets in an ironstone intraclast at Coalcliff (Outcrop 2). The intraclast is half-ellipsoidal in shape with an upper flat surface. Pen tip 5 cm long. Plan (b) and block (c) sketches of the intraclast. (d) Fracturing of a southeasterly oriented petrified log at Clifton (Outcrop 4). Only one set of 010-030° joints, with spacing between 2 and 5 cm, is developed in the log. North arrow is scaled in centimetres.

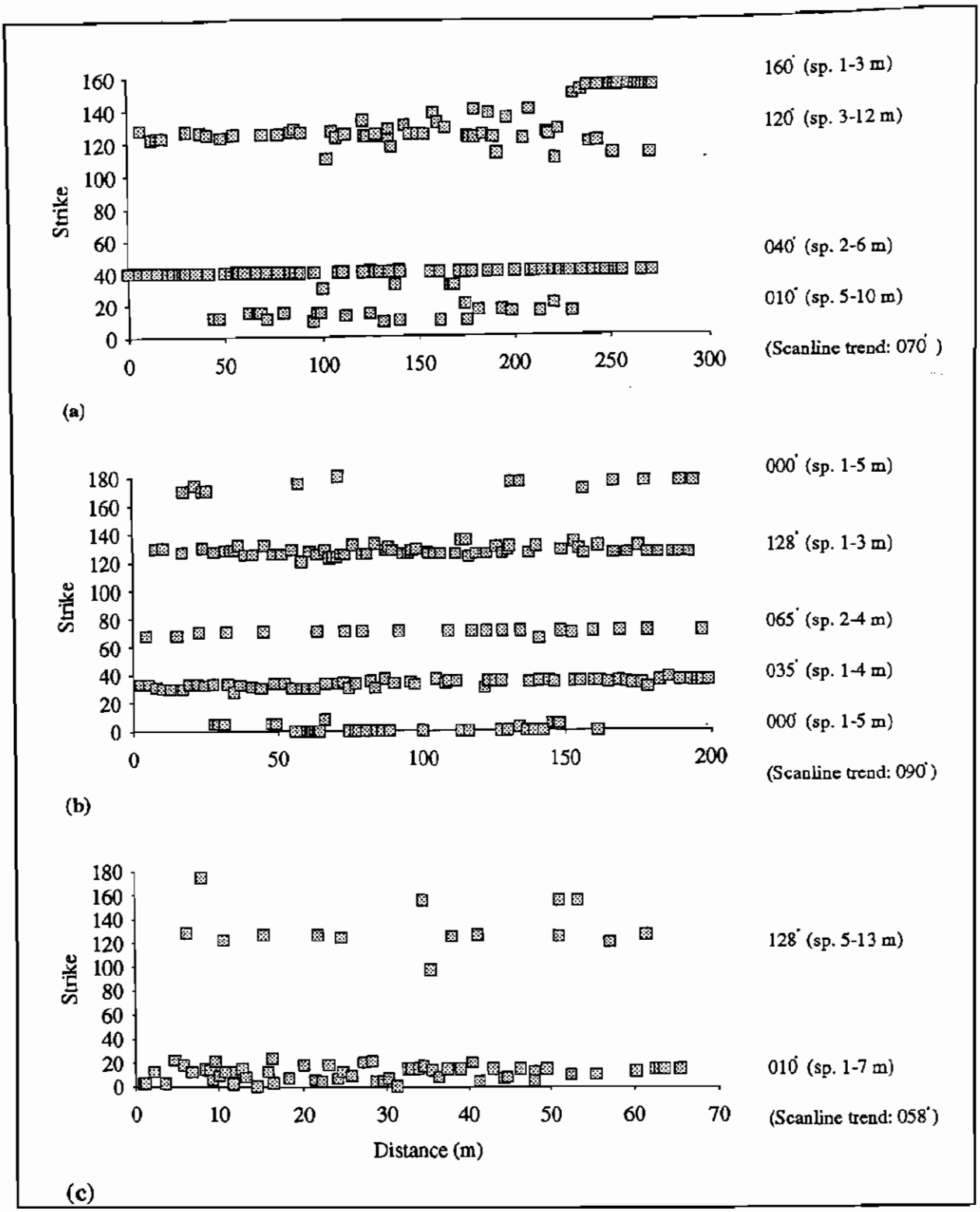

Figure 2.23 Scanline charts showing the difference in frequency and strike of systematic joint sets in similar rock types. The values in the right hand column are the average strike of each set and the range of spacing (sp. = spacing). (a) The 040° joint set is more consistent in strike and more frequent than the 010°and 125° joint sets. The 160° set is local and occurs only from the 230 m mark onwards (Wombarra, 11-HH'). (b) 005, 035, 070 and 125° joints with almost similar spacing and variation around the mean strike (Coledale, 15-JJ'). (c) The frequency of the 125° joint set is much less than the 010° joints (Brickyard N., 16-CC'). Spacing is determined using the data on scanlines (Appendix) and the formula presented in Chapter 1 (Figure 1.6).

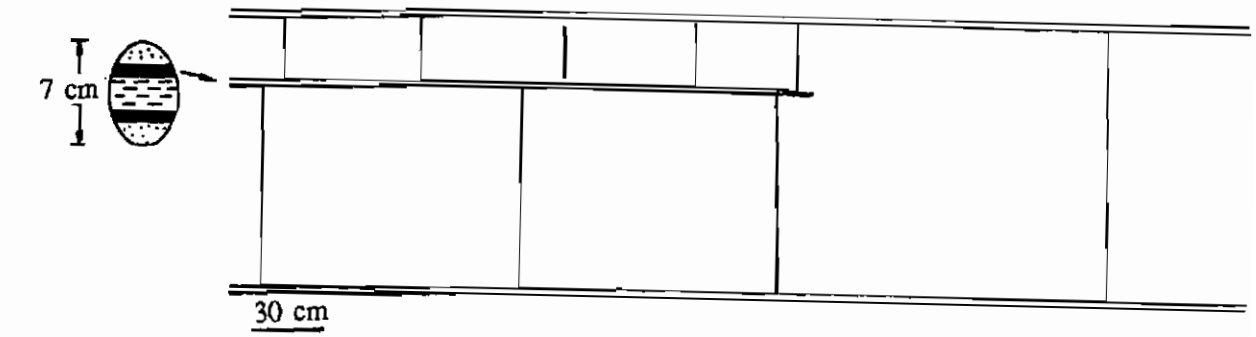

(a)

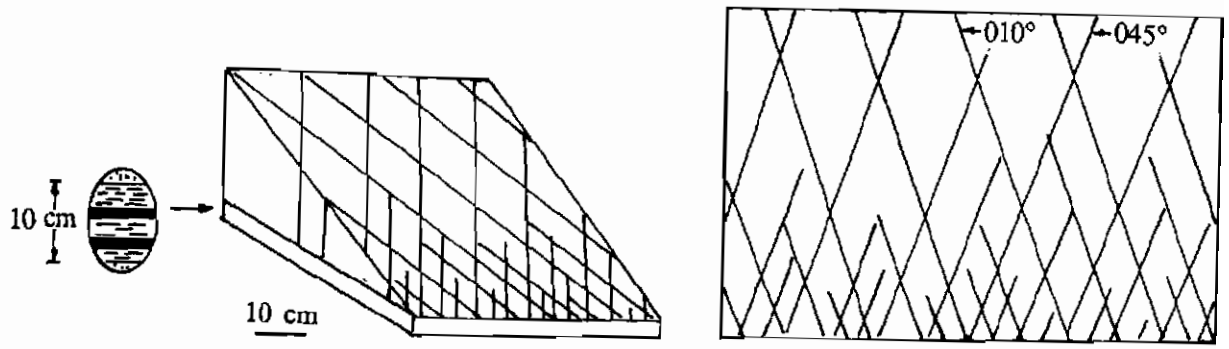

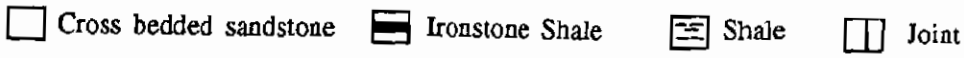

(b)

Figure 2.24 The effect of bed thickness on frequency of joints at Coalcliff. (a) Sandstone beds partly divided by thin bands of shale and ironstone. (b) Termination of some members of the NNE and NE joint sets due to a gradual increase in thickness of cross-bedded sandstone, from 2 cm at the front to 50 cm at the back of the block diagram. The spacing is 5-10 cm at the front and increases to about 50 cm at the back.

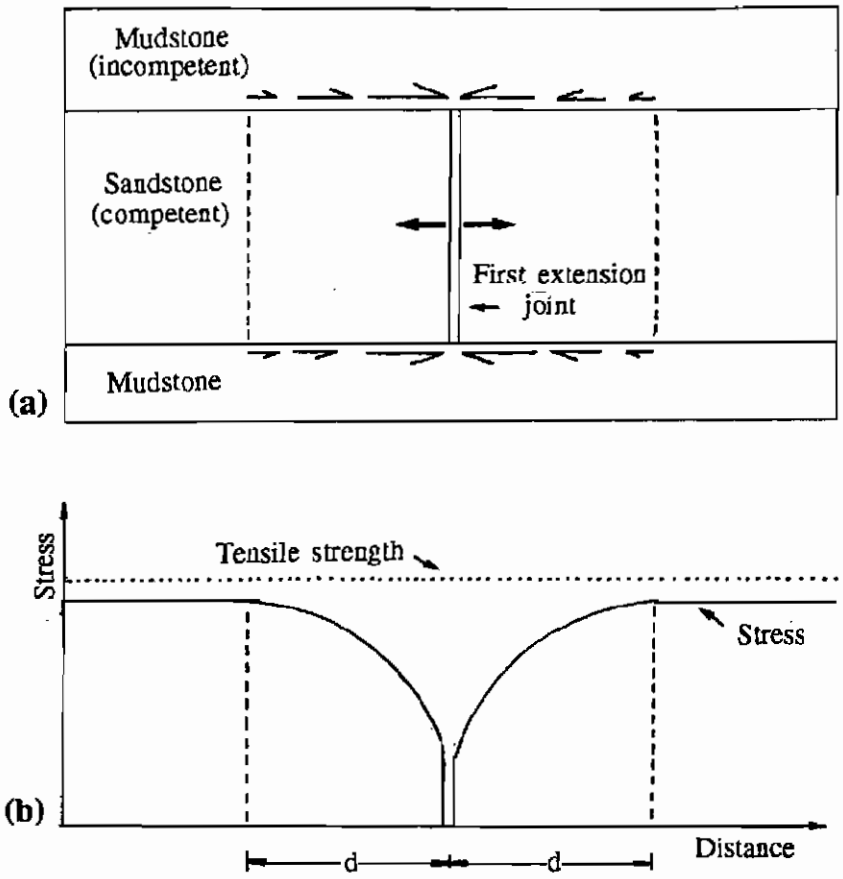

Figure 2.25 Hobbs (1967) model for spacing of joints in sedimentary rocks. In a competent (higher-modulus) bed in between two incompetent (lower modulus) beds, shear stresses develop along the interfaces, due to layer parallel extension. Formation of the first joint only releases stress for a short distance (d). The rest of the layer remains at the stress level close to the fracture stress. The next joint forms at a distance equal or greater than to 'd' from the first joint. This process continues until the jointed unit is saturated with joints.

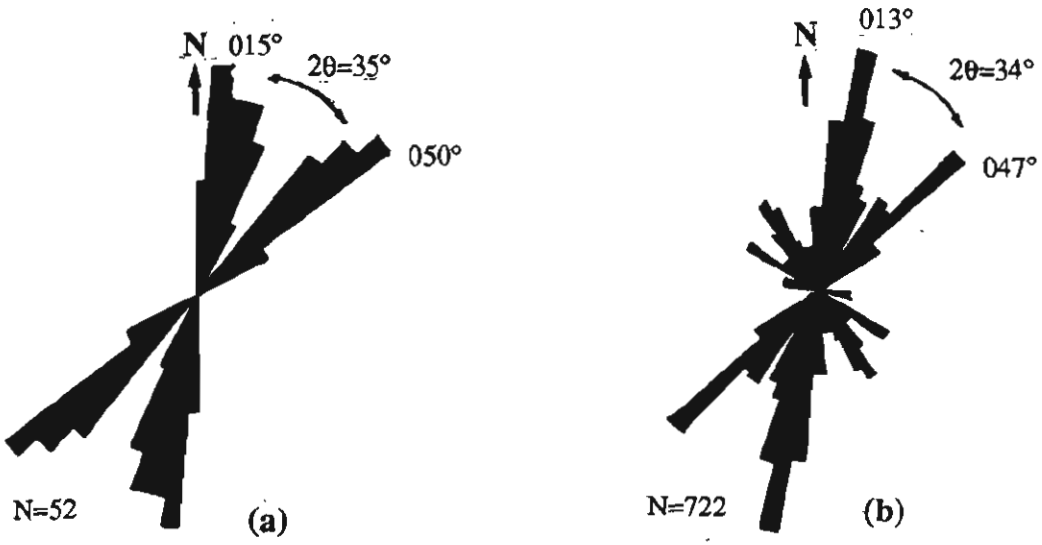

(c)

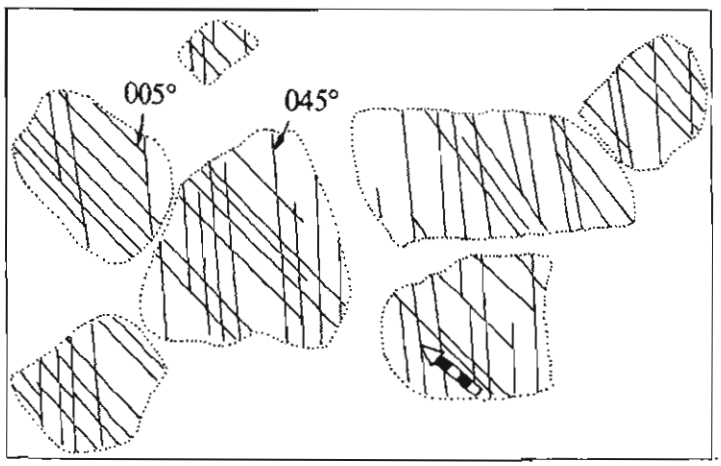

(d)

Figure 2.26 Similarity between the orientation of fractures in ironstone intraclasts of 1-40 cm diameter (a) and the enclosing 1-2 m thick sandstone layers (b), in the Coalcliff-Scarborough area. Not the dihedral angle, which is almost identical in both cases. These fractures are straight and almost always vertical (c, d). North arrow is scaled in centimetre.

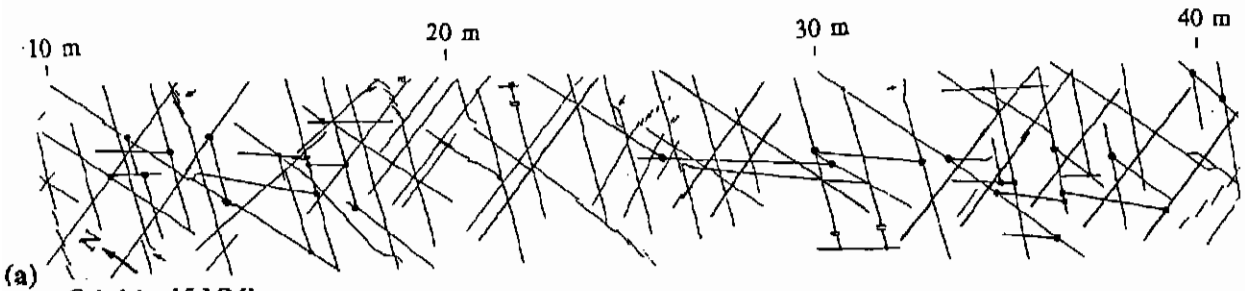

(a) Coledale, 15-MM'

(b)

	030°	070°	125°	175°
030°	–	9	0	6
070°	7	–	1	8
125°	0	3	–	1
175°	5	10	0	–

Figure 2.27 Cross cutting relationships between 4 sets of systematic fractures. (a) 50 abutting points (dots) mapped between 10 and 40 m marks of Scanline 15-MM' at Coledale. (b) A matrix demonstrating the frequency of abutting of fractures against each other for the same area. The top row and the left hand column show the mean strike of different joint sets. The other numbers are the frequency of abutting of a younger set (top right rows) against an older set (bottom left rows). (For example, the number of 175° striking joints that abut the 030° joints is 6, while the number of 030° joints abutting 175° is 5.)

(a)

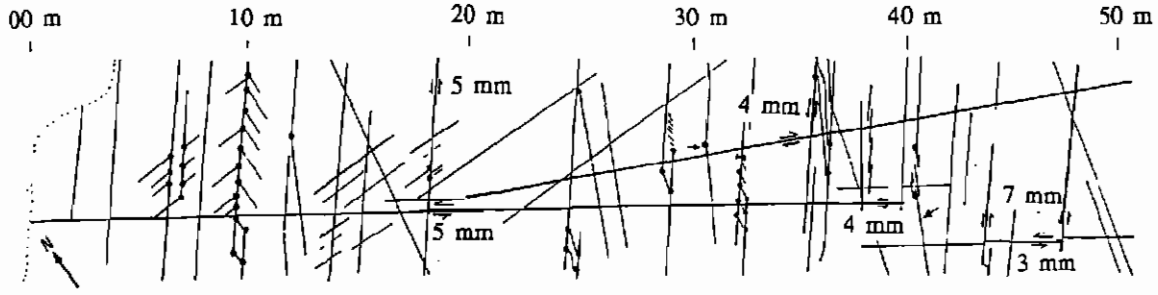

Wombarra S., 12-BB'

(b)

	018°	040°	090°	165°
018°	—	0	0	0
040°	7	—	14	17
090°	0	1	—	0
165°	0	0	0	—

Figure 2.28 Cross-cutting relationships between 6 sets of joints (000°, 018°, 040°, 095°, 125°, 165°) at Wombarra (0-40 m marks of Scanline 12-BB'). (a) Fracture pattern consist of 44 abutting (dots). (b) The abutting frequency of a younger joint (top right rows) against an older joint (bottom left rows). Cross-cutting relations show that the 000°, 040° and 125° are older than the 018°, 095° and 165° joints. The number of relations for abutting 000° and 125° joints, are zero and are excluded from the matrix.

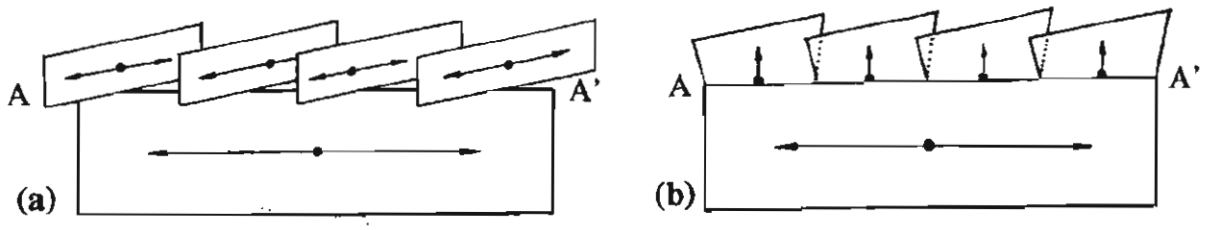

A A' = Mechanical layer boundary

(c)

Figure 2.29 Change of orientation of one joint set formed in two adjoining mechanical units. (a) Joints in each units were formed independently. (b) Horizontally propagating joint in the lower unit cross the interface, and the en echelon segments propagated vertically in the upper unit. Dots locate the nucleation point of joints. (c) An example of independent formation of joints in jointing layers at the cliff face at Scarborough (Outcrop 7)(cf. (a)).

(a)

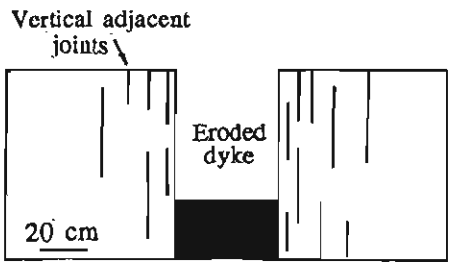

(b)

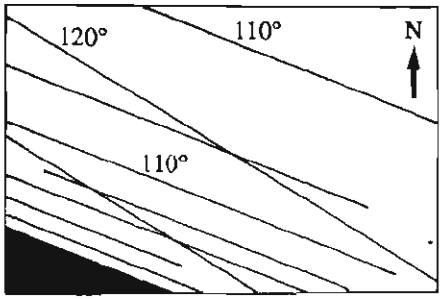

(c)

(d)

Figure 3.1 (a) Adjacent joints parallel to a 110° striking, partly eroded dyke, at Wombarra (Outcrop 11). Width of dyke is 40 cm. (b) Profile sketch of dyke in (a). (c) Plan sketch of dyke in (a). Note that the frequency of adjacent joints decreases rapidly away from the dyke. These joints cross closed 120-125° regional joints with no interaction. (d) Photograph of central portion of sketch in (c). Pen (15 cm long) rests on a 120° joint.

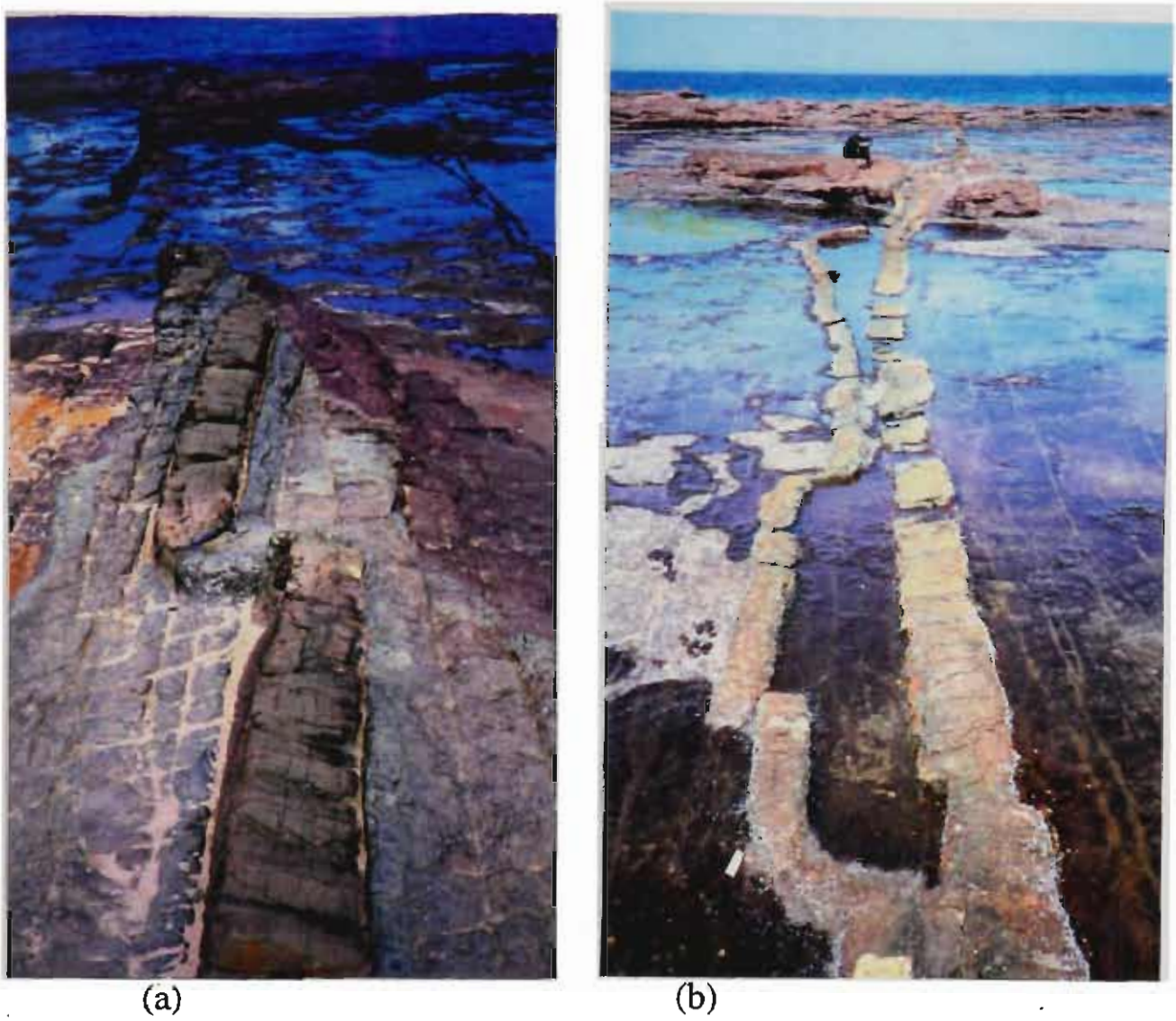

Figure 3.2 (a)-(b) 120° striking, nearly vertical segmented dykes, in subhorizontal sandstone layers, at Red Point (Port Kembla). Note the decrease in spacing of adjacent joints away from the dykes. Dykes are 40-50 cm in width. (c) A segmented, 023° striking dyke and related adjacent joints at Bulli (Outcrop 22). An up to 2 cm vertical offset of the dyke and adjacent joints (inset), is due to the dyke crossing a contact, from a lower layer (1), to an upper layer (2). En echelon gashes, as well as longitudinal fractures, are filled with up to 3 cm of calcite, and indicate subsequent recracking of the dyke.

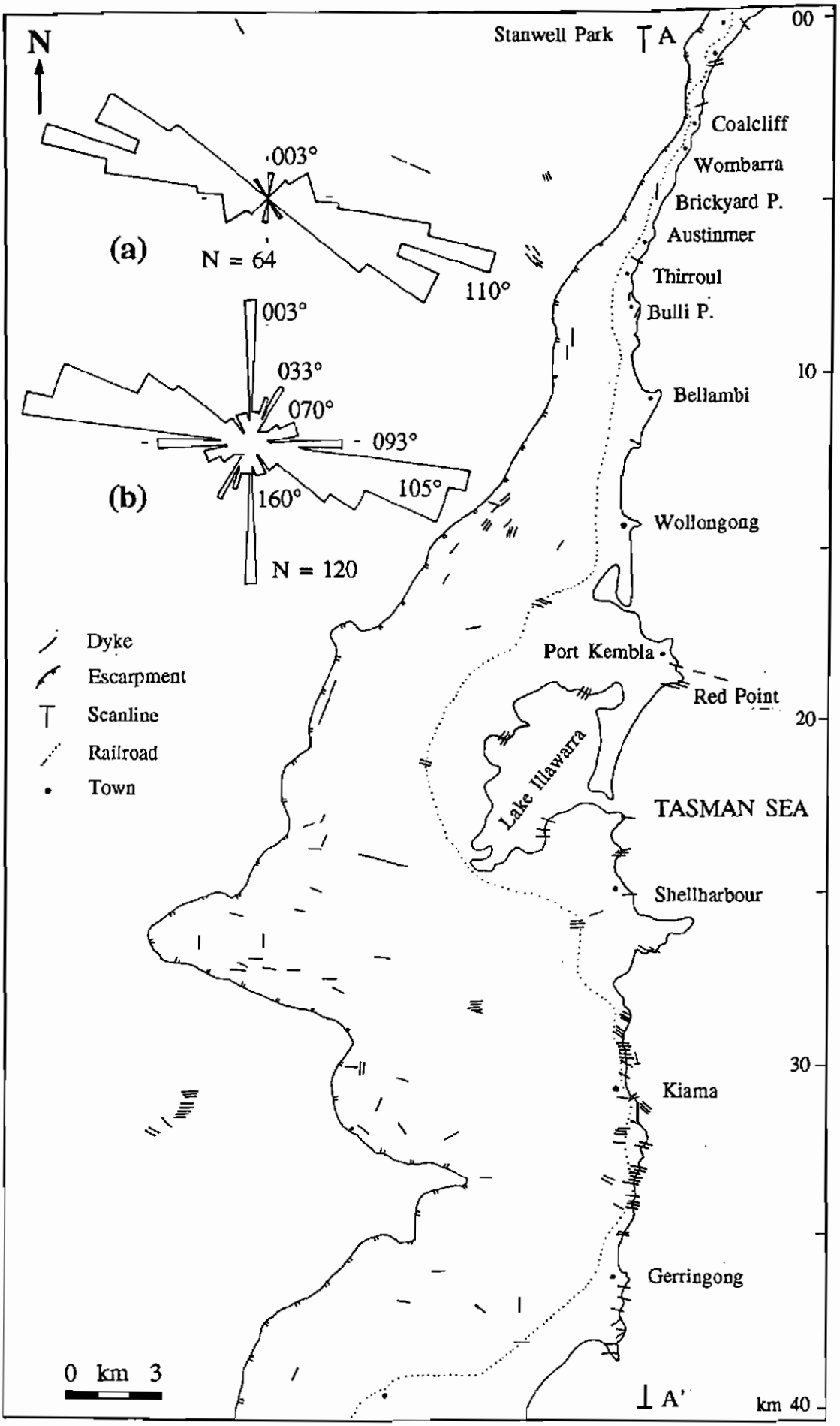
N
Stanwell Park
A
00
Coalcliff
Wombarra
Brickyard P.
Austinmer
Thirroul
Bulli P.
10
Bellambi
Wollongong
003°
(a)
N = 64
110°
003°
033°
070°
093°
(b)
160°
105°
N = 120
Dyke
Escarpment
Scanline
Railroad
Town
Port Kembla
Red Point
20
Lake Illawarra
TASMAN SEA
Shellharbour
30
Kiama
Gerringong
0 km 3
A'
km 40

Figure 3.3 Distribution and orientation of dykes in the Southern Coalfield of NSW. (a) Rose diagram of 64 dykes form a 40 km traverse along the coast, between Stanwell Park and to the south of Gerringong (AA'). The mean direction of the main dyke cluster is 106°. (b) Rose diagram of 120 dykes mapped over the Southern Coalfield of NSW, including the dykes of 3.1a. Most of the dykes strike ESE (100-120°), with a mean direction of 109°. Other significant orientations are N-S, E-W, and NE-SW. The class interval for both diagrams is 5°. Data from Harper (1915), Bowman (1974), and the present study.

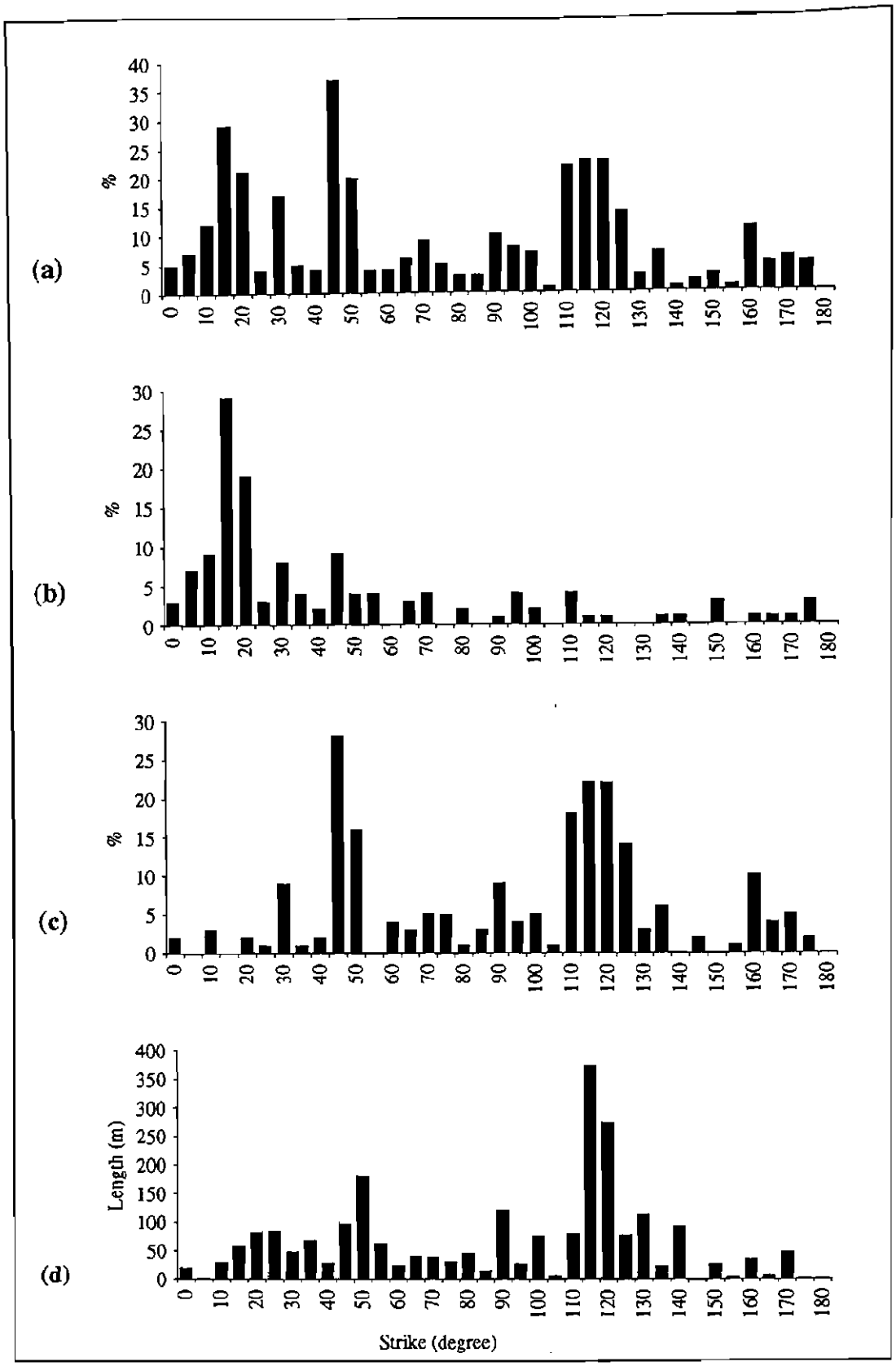

Figure 3.4 Histograms of the orientation of dykes from the Southern Coalfield at the level of coal mining (data from Rixon & Shepherd 1988). (a) 347 dykes encountered at different collieries. (b) 135 dykes of the northeastern section of the Southern Coalfield (sheet 1 of Rixon & Shepherd 1988). (c) Similar to (a), except dykes of (b) are subtracted from the data base (sheets 2-5, Rixon & Shepherd 1988). (d) Cumulative length of 347 coal seam dykes of the Southern Coalfield.

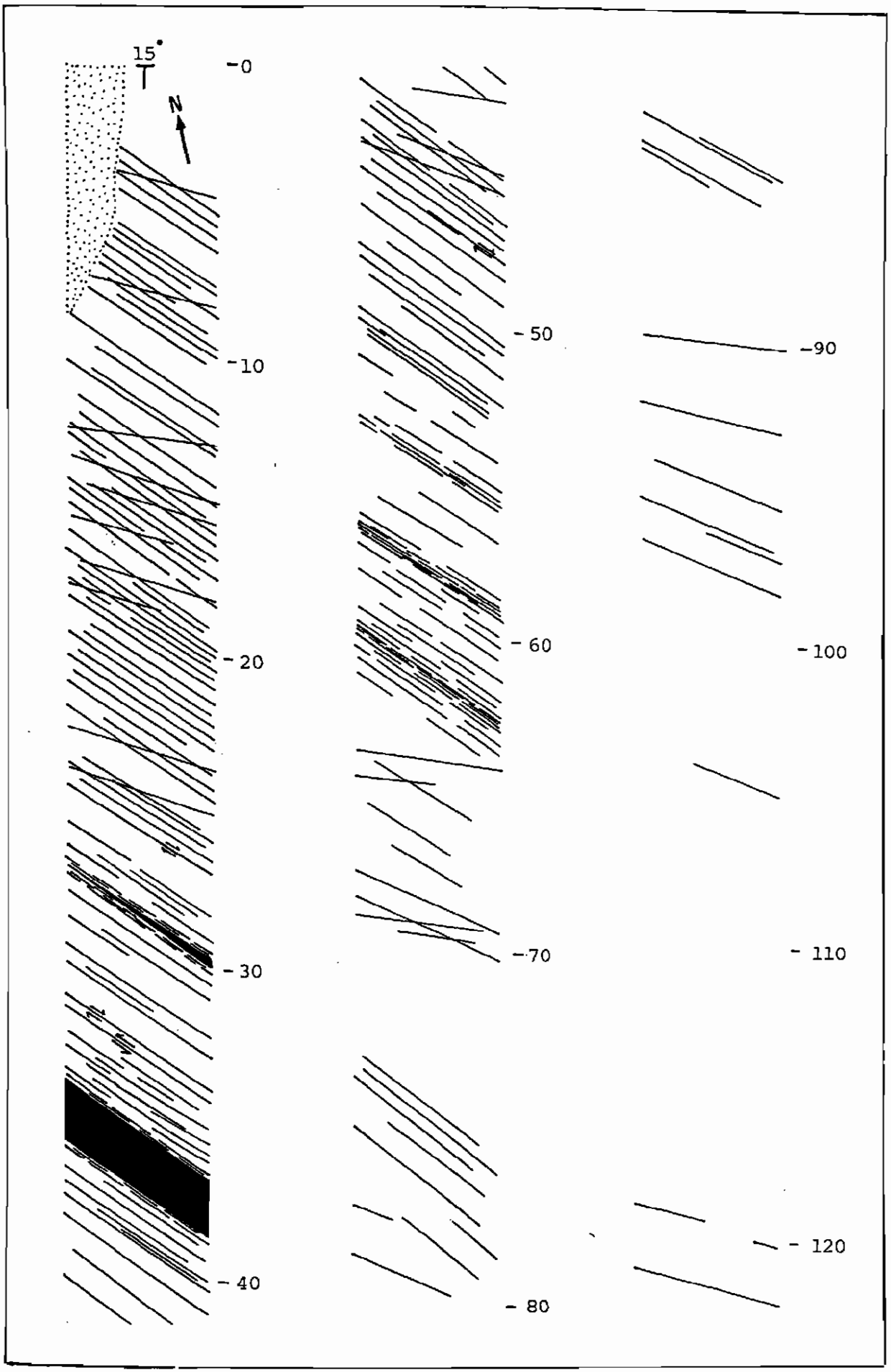

Figure 3.5 Distribution of a set of adjacent joints along a 15° trending scanline (19-EE') at Austinmer. Two dykes are exposed at the 28 and 36 m marks. Except for a set of subparallel regional joints striking 125°, regional and local joints are omitted from this scanline (see text for more detail).

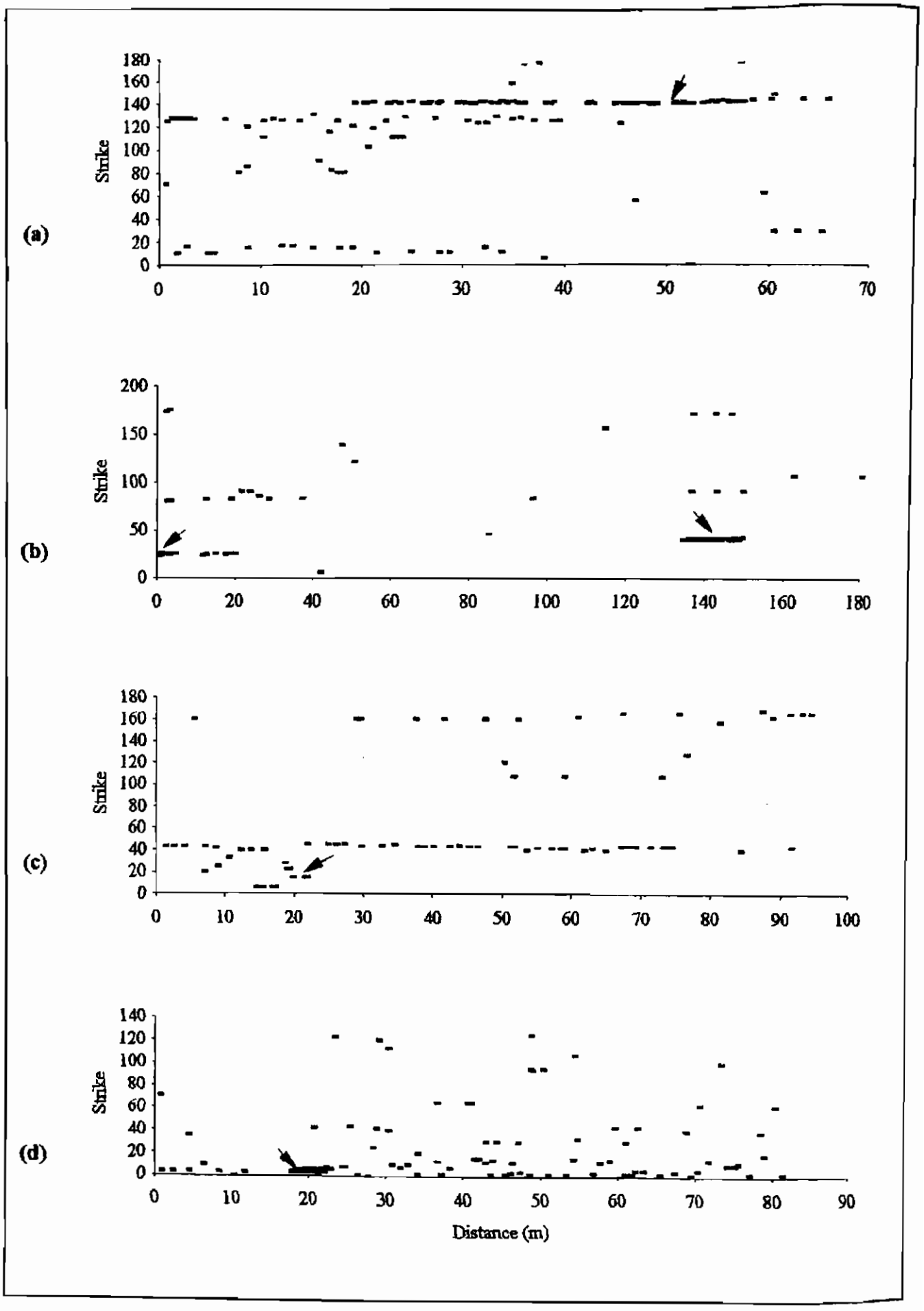
(a)
Strike
180
160
140
120
100
80
60
40
20
0
0
10
20
30
40
50
60
70
(b)
Strike
200
150
100
50
0
0
20
40
60
80
100
120
140
160
180
(c)
Strike
180
160
140
120
100
80
60
40
20
0
0
10
20
30
40
50
60
70
80
90
100
(d)
Strike
140
120
100
80
60
40
20
0
0
10
20
30
40
50
60
70
80
90
Distance (m)

Figure 3.6 Scanline charts showing the relationship between adjacent joints and the other local or regional joints. (a) A 140° striking dyke is exposed at the 50 m mark of Scanline 19-DD' at Austinmer S. The frequency of adjacent joints, which start at the 18 m mark, increase towards the dyke. No interaction was recorded between the dyke related joints and the 120° regional joints. (b) Adjacent joints developed as far as 10 m away from two, 023° and 040° striking, dykes, exposed at the 0 and 140 m marks of Scanline 22-BB' at Bulli. (c) A limited number of short adjacent joints developed along some parts of 010° striking dyke at Coledale (22 m mark of Scanline 13-GG'). Two other joint sets at this locality strike 040° and 160°. The 040° set is regional and formed before magma emplacement as the dyke partly follows these fractures (see Figure 3.7). The 160° joints are absent in the vicinity of the dyke, which suggests that they formed later. (d) A 003° dyke exposed at the 18 m mark of the Scanline 17-BB' at Brickyard point. A set of regional joints occur parallel to the dyke. As magma has invaded an open regional joint, the adjacent joints are absent.

Figure 3.7 A NNE striking vertical dyke follows pre-existing conjugate NNE and NE joints (Outcrop 13 at Coledale, Figure 3.6c). The dyke is 150 cm wide and the dyke has weathered to pale clay. The host rock is laminated siltstone and medium to fine-grained sandstone of the upper Wilton Formation. A late fault along the trend of the dyke has had 30 cm of dextral displacement.

(a)

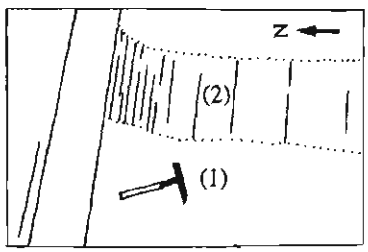

(b)

Figure 3.8 Photograph (a) and sketch (b) of the effect of rock type on development of adjacent joints parallel to a 120° striking dyke at Red Point (Port Kembla). Adjacent joints are well developed in the upper medium-grained sandstone bed near the water in (a) and point 2 in (b), while in the lower fine-grained sandstone, these joints are absent (in the vicinity of the hammer ——— ———.

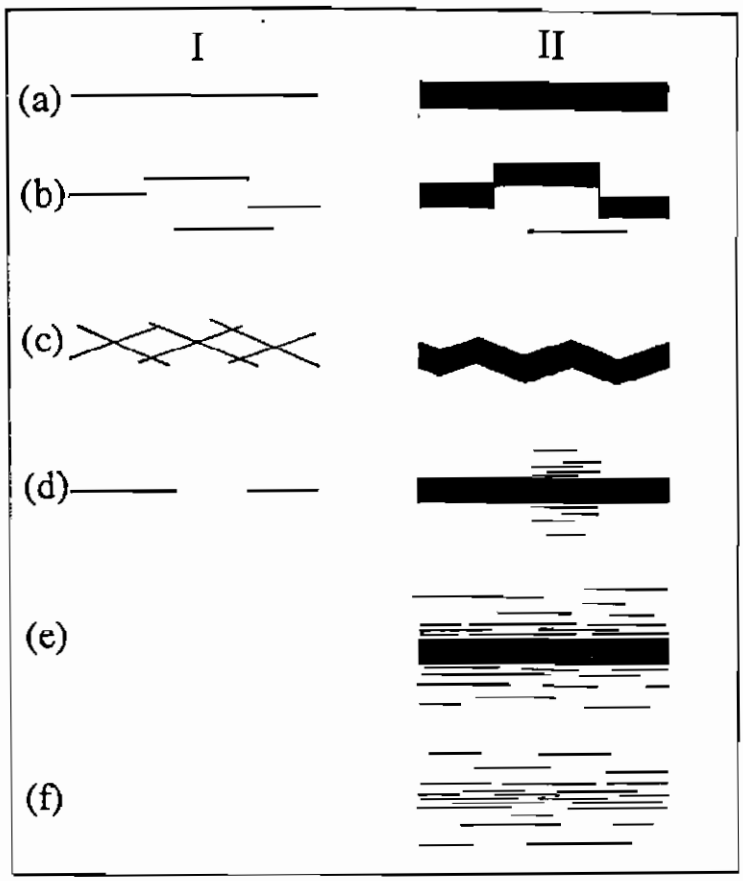

Figure 3.9 Development of adjacent joints. Adjacent joints are absent where magma invades pre-existing fractures (a), (b) and (c). Adjacent joints are developed where the dyke cuts intact rock either partially (d) or totally (e) along its length. These joints also develop ahead of propagating magma in competent layers (f). Adjacent joints are absent in incompetent layers (see Figure 3.10).

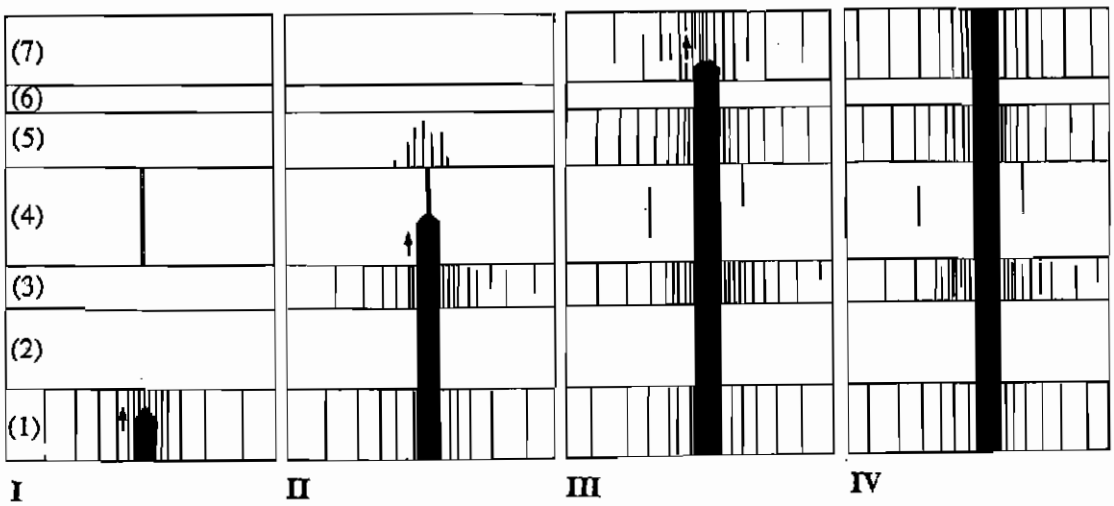

Figure 3.10 Process of magma injection into a sequence of competent (1, 3, 4, 5, 7) and incompetent (2, 6) layers. Adjacent joints develop ahead of the propagating magma in competent layers. This does not occur in layer 4, where the magma invaded a pre-existing open fracture. The joint zone shown in III at the surface is formed due to the wedging action of the ascending magma.

Figure 4.1 (a, b, c) Rose diagrams of fault orientations at the level of the coal seams, north (a, b) and south (c) of the Bulli Fault (Shepherd 1990). (d) Rose diagram showing the orientation of faults in the southeastern Sydney Basin (from Wollongong 1:50,000 geological sheet, Bowman 1974). (e) The fracture pattern for the southeastern Sydney Basin traced from air photographs (Bowman 1974). (f) Landsat and air photograph fracture trace trend for the Sydney Basin (Mauger *et al.* 1984).

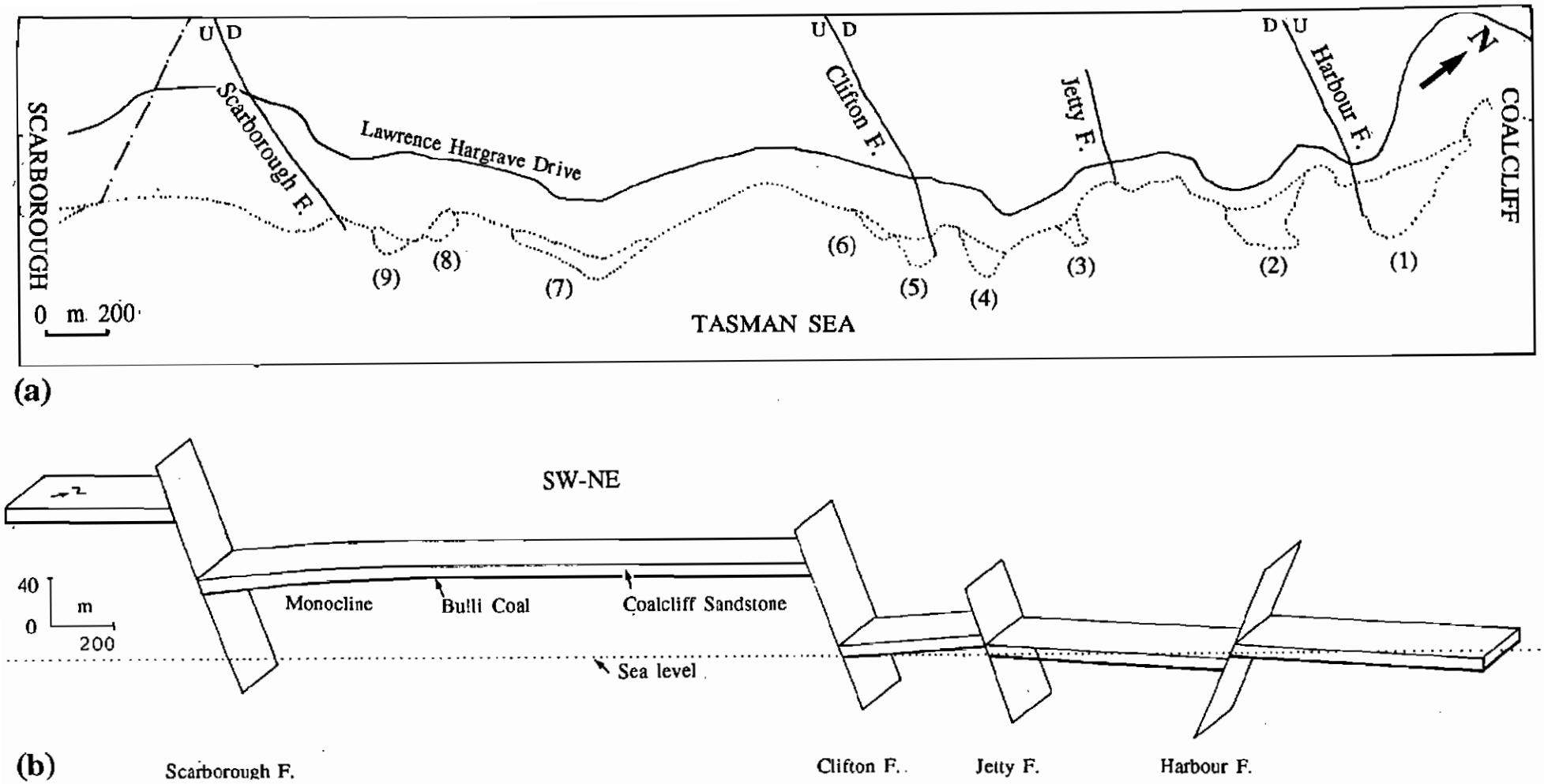

Figure 4.2 (a) Simplified map of the ESE faults in the northern part of the study area (numbers in brackets refer to outcrops). (b) NE-SW three dimensional diagram along the coast between Coalcliff and Clifton, showing the normal displacements of the ESE normal faults. To demonstrate the slight changes in dip of the strata, the vertical scale is almost five times exaggerated. The effect of this exaggeration on faults dip has been ignored.

(a)

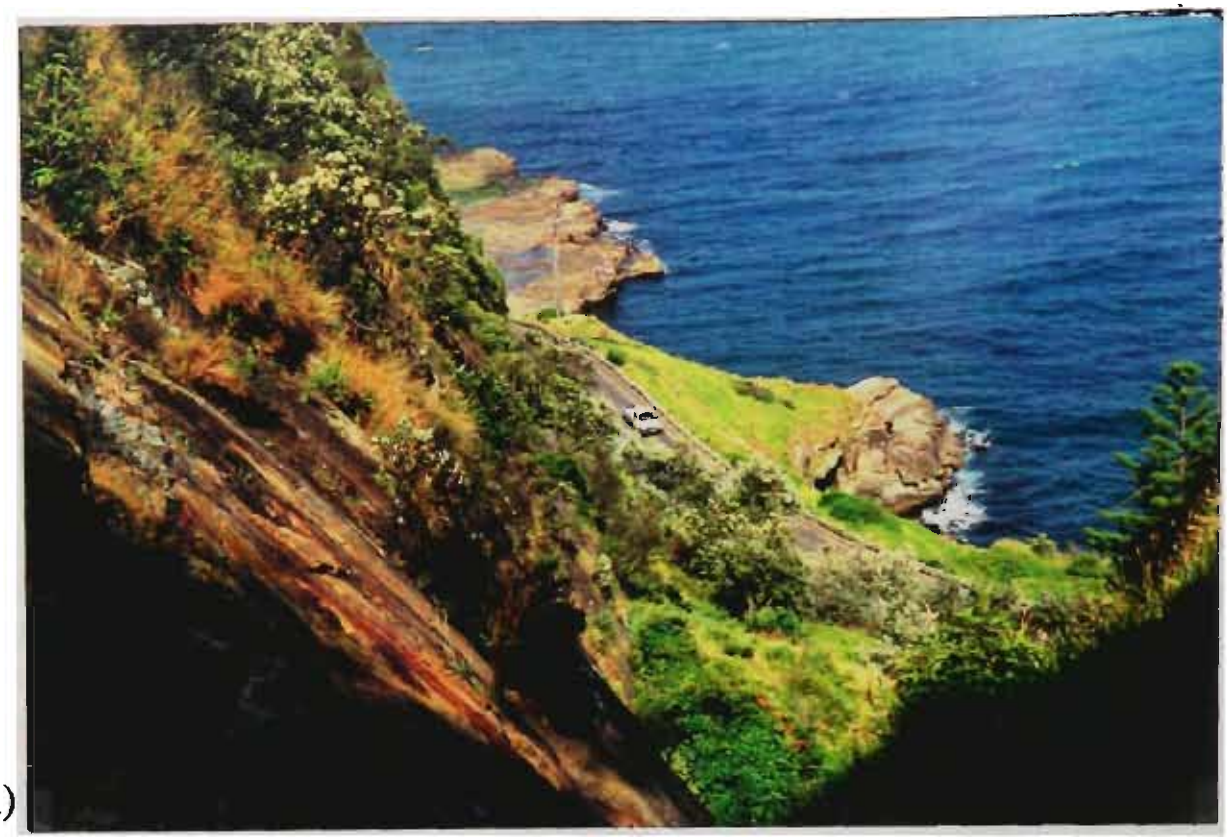

(b)

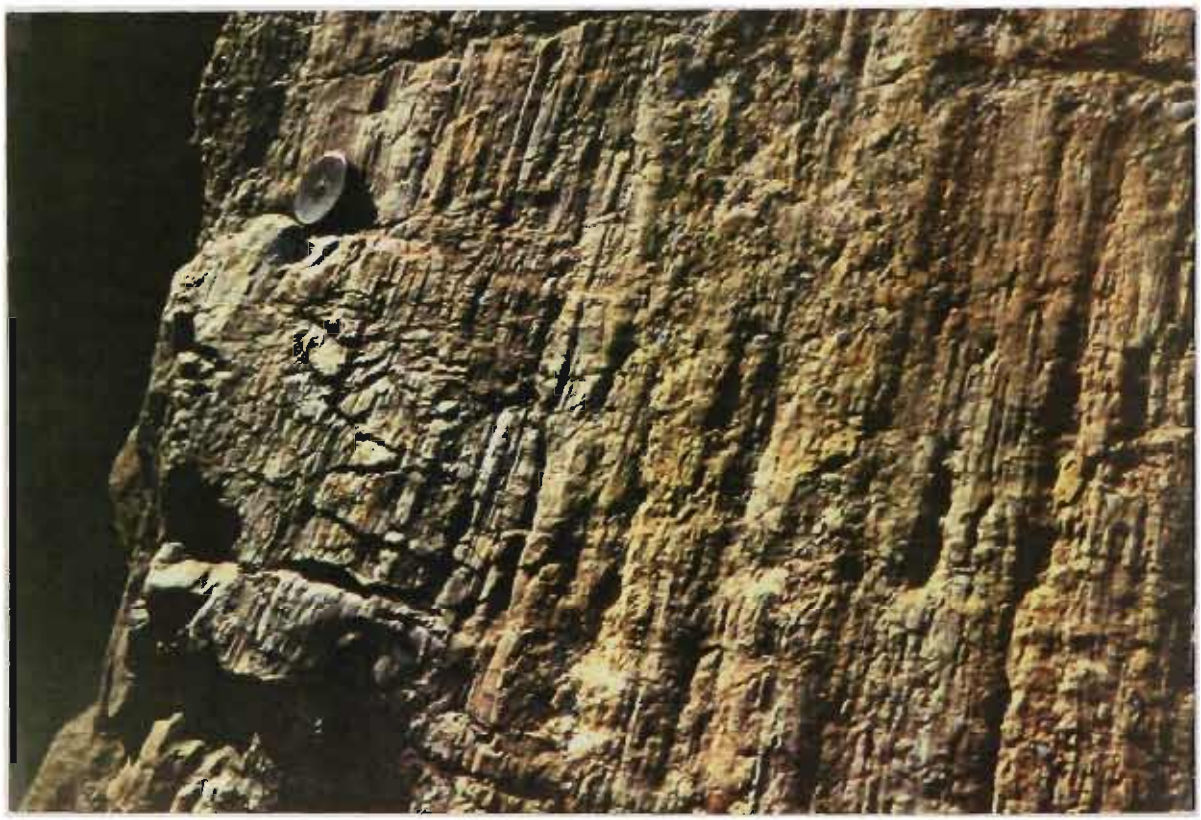

Figure 4.3 Post-depositional normal slip on the Harbour Fault. (a) Steep, south dipping fault surface (bottom left of the photo), that crosses the road at approximately the location of the white car and cuts the southern edge of the coastal platform in the background. (b) Slickensides on the surface of this fault indicate that the last movement was pure dip slip, and occurred in lithified strata (camera cap is 5.3 cm in diameter).

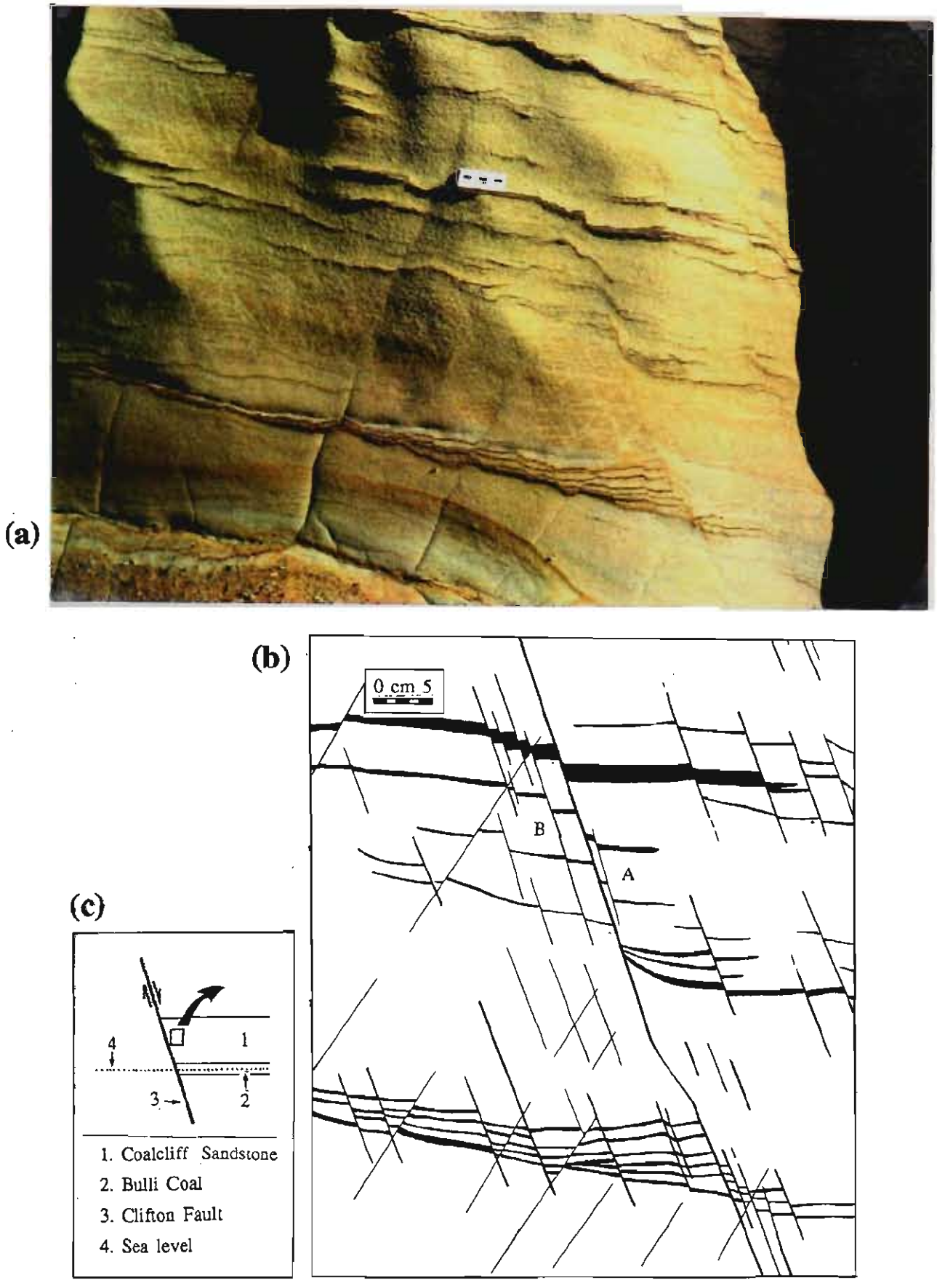

Figure 4.4 (a) Soft sediment structures in the Coal Cliff Sandstone, exposed on the downthrown side of the Clifton Fault, at Clifton (Outcrop 5). Two sets of conjugate 110° striking fractures occur parallel to the Clifton Fault. The northerly dipping set is dominant. (b) Magnified sketches of the central part of (a). (c) The location of (a) and (b) in respect to the Clifton Fault (see text for more detail).

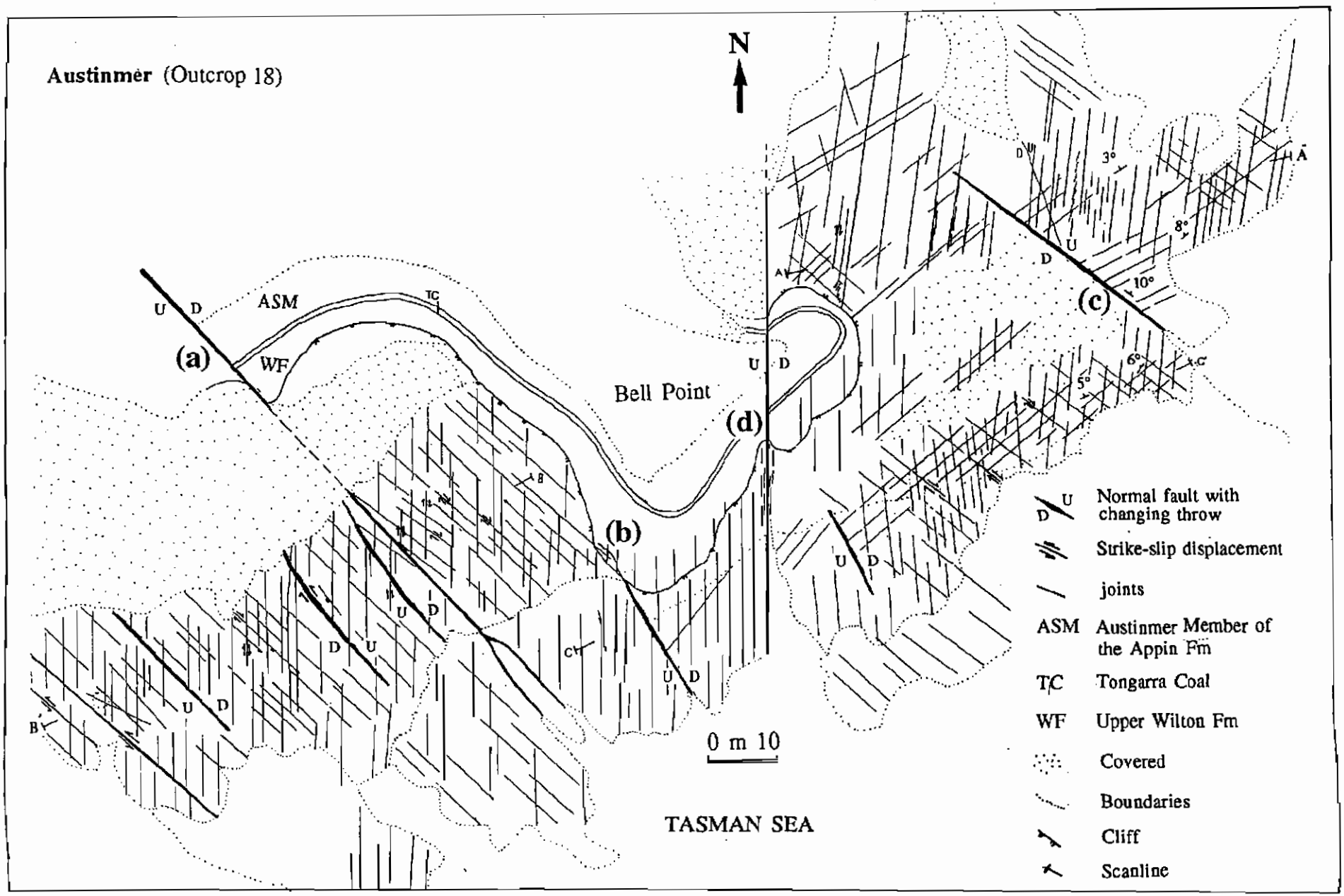
Austinmer (Outcrop 18)
N
(a)
(b)
(c)
(d)
U D
ASM
TC
WF
Bell Point
3°
8°
10°
6°
5°
0 m 10
TASMAN SEA
Normal fault with changing throw
Strike-slip displacement
joints
ASM Austinmer Member of the Appin Fm
T/C Tongarra Coal
WF Upper Wilton Fm
Covered
Boundaries
Cliff
Scanline

Figure 4.5. A group of 120-145° striking and 45-60° dipping, normal faults at Bell Point Austinmer (Outcrop 18). The throw of these faults rapidly decreases both along strike and upward. One 140° fault terminates as a 120° joint at (b). The N-S normal fault at (d) is parallel to a set of joints. This fault is subvertical in sandstone and siltstone of the Wilton Formation, but its dip decreases upward in the Tongarra Coal. Both joints and faults have been subsequently slipped sinistrally or dextrally along their strike (see text for more details).

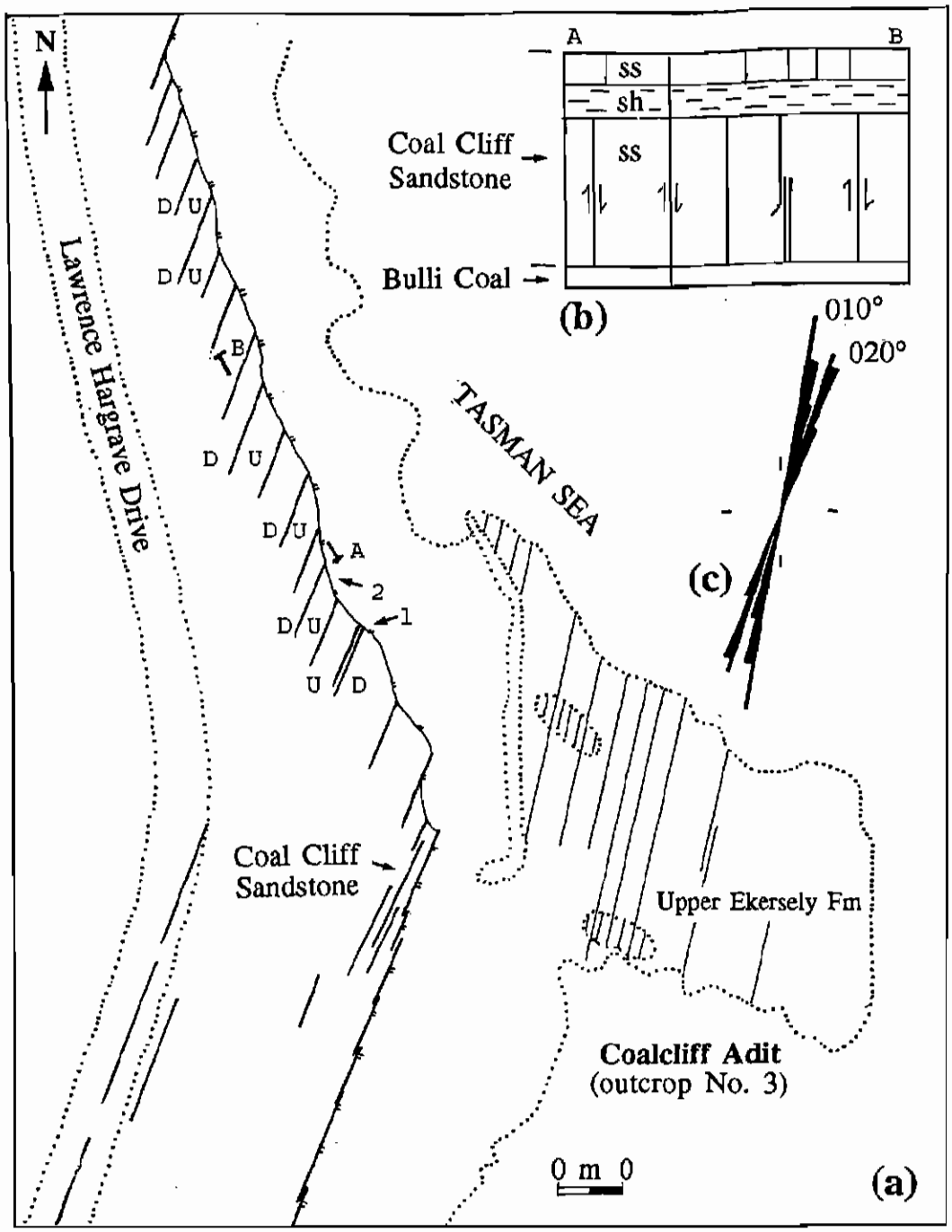

Figure 4.6 (a) A set of NNE (020°) vertical joints, some of which show subsequent normal displacement (Coal Cliff Adit, Outcrop 3). The maximum normal slip is 100 cm (point 1), and the downthrow is to the east (see also Figure 4.7a). Other displacements are minor (2-20 mm) and are downthrown to the west. The faulted joints are open, while those which have no displacement were left closed. (b) Fractures with normal displacement are frequent in sandstone beds (inset b). (c) Rose diagram of fractures of Outcrop 3.

(a)

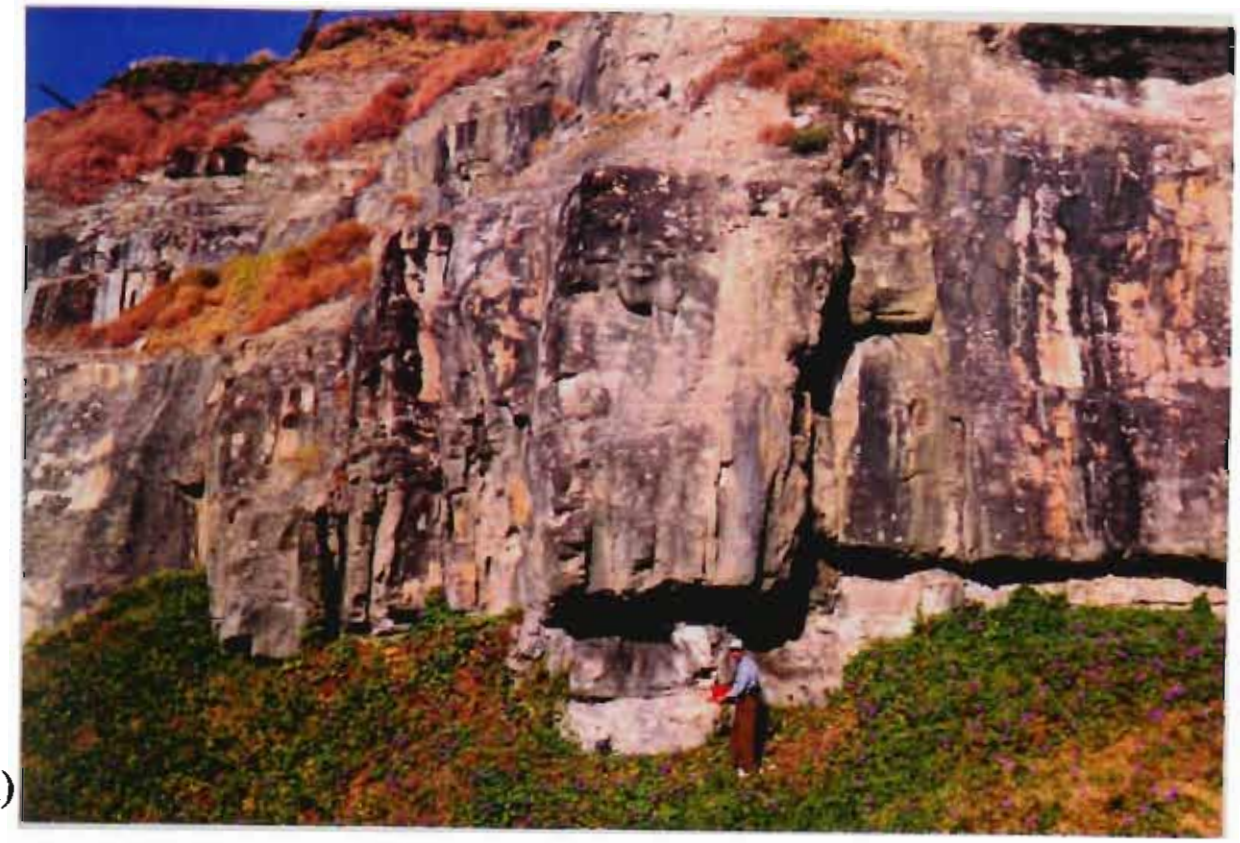

(b)

Figure 4.7 (a) A 020° striking subvertical normal fault with eastern side (left side) dropped 1 m in the Coal Cliff sandstone (point 1 of Figure 4.6). Mr Dehghani for scale. (b) A 015° striking fault with 50 cm of normal displacement (downthrown to the west - left side). The fault is almost vertical in the upper sandstone beds and dips 75° to the west, in the lower coal (Scarborough, in gully between Outcrops 5 and 6). Hammer 33 cm long for scale.

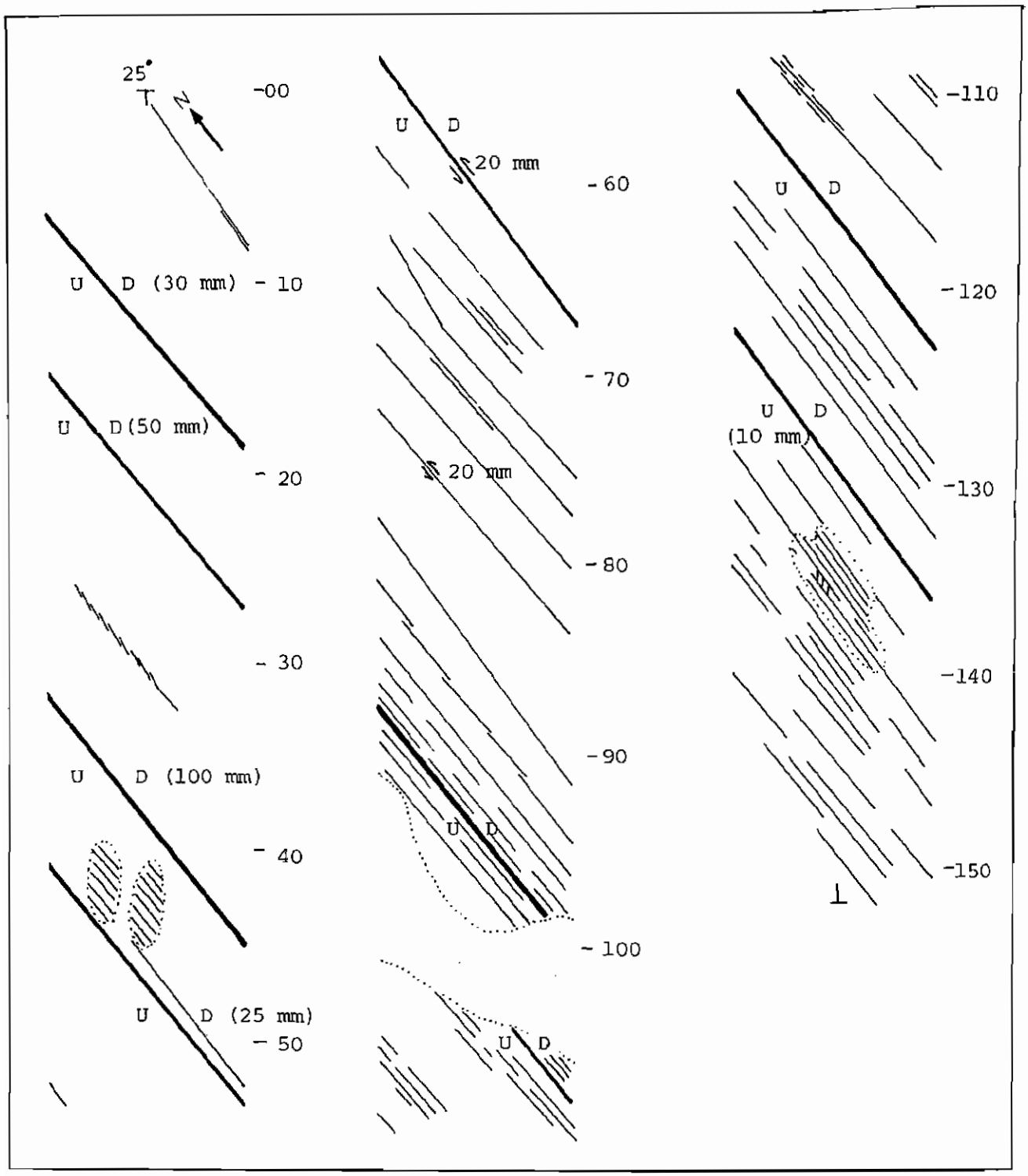

Figure 4.8 Distribution of N-S fractures along a 150 m long and 025° striking scanline at Wombarra (17-EE'). The platform consists of laminated mudstone, siltstone and thin beds of sandstone of the Wilton Formation. Some of these joints have a dip slip component of 10-50 mm, downthrown to the east. To reduce complexity, the fractures of other directions have eliminated from this scanline.

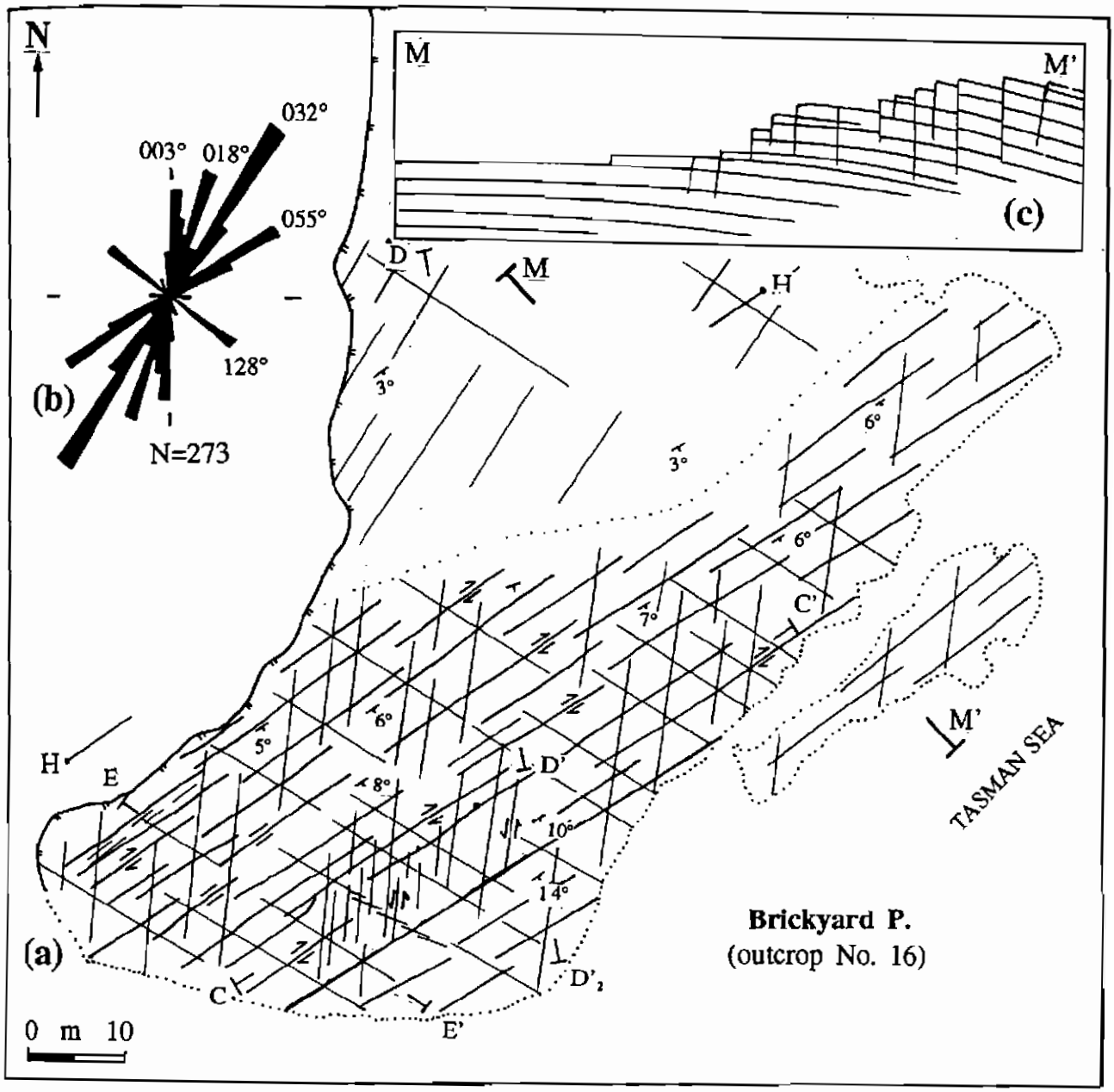

Figure 4.9 A fault related monocline at Coledale (Outcrop 16). The coastal platform contains laminated mudstone, siltstone and thin beds of sandstone of the upper Wilton Formation. A set of fractures striking 060° occur parallel to the axial trace of the monocline. These fractures terminate north of the anticlinal hinge of the monocline (north of HH'). Some of these fractures show a normal component and also a subsequent dextral slip.

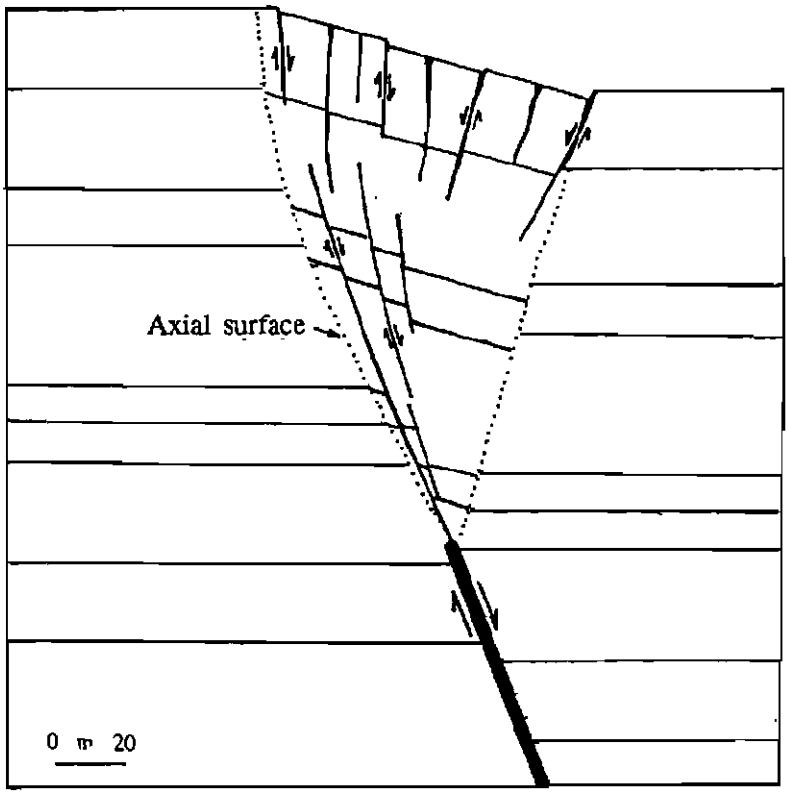

Figure 4.10 A cross section demonstrating the relationship between a small monocline at Coledale (Outcrop 16) with an assumed underlying normal fault (see text for more description).

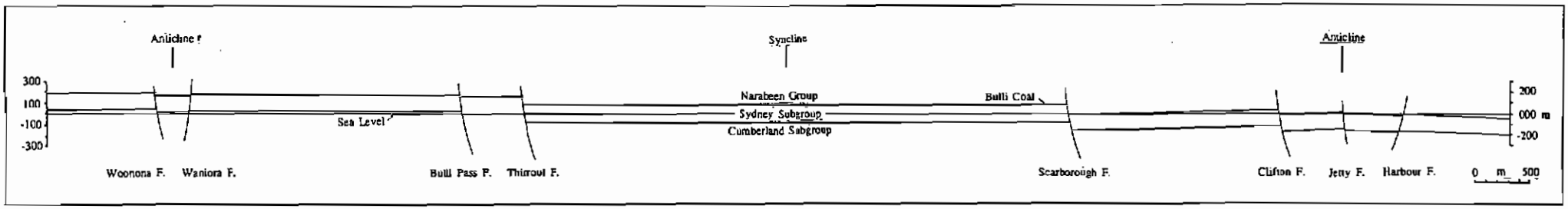

(a)

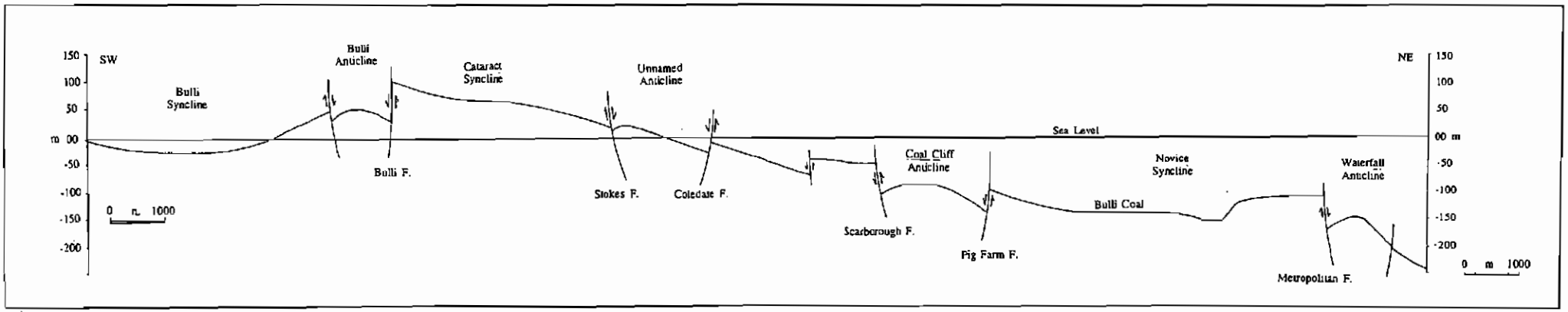

(b)

Figure 4.11 (a) NE-SW cross section along the coast between Coalcliff and Woonona. Between the Scarborough and Thirroul Faults the strata are almost horizontal (vertical and horizontal scales are identical). (b) NE-NW cross section of the Southern Coalfield (AA' of Figure 1.7), at the level of the Bulli Coal (data from Rixon and Shepherd 1988). Four anticlines (Bulli, Coal Cliff, Waterfall and unnamed) in this section are bounded by inward dipping normal faults (Vertical exaggeration x 10).

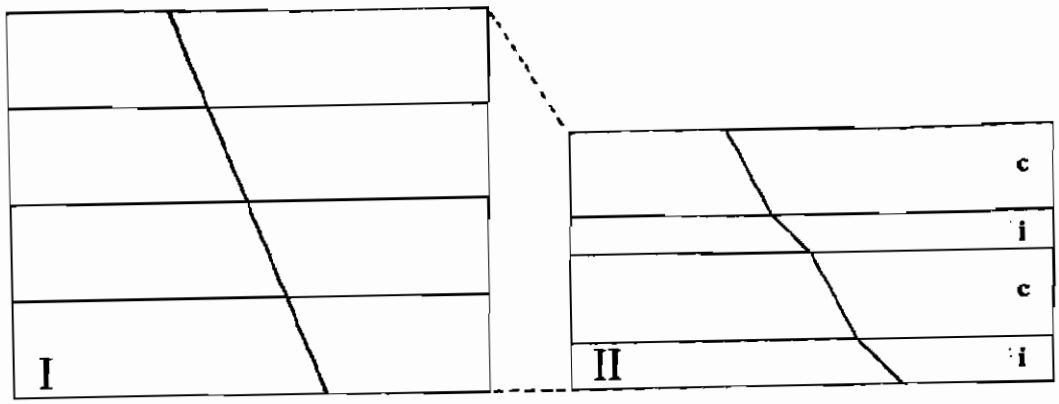

(a)

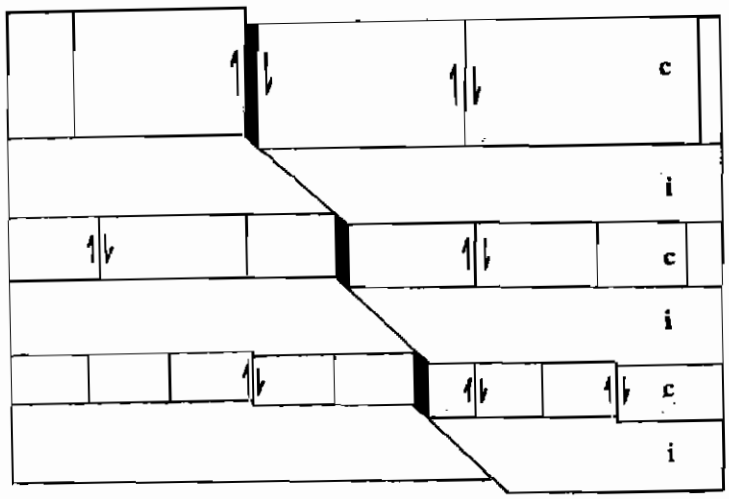

(b)

Figure 4.12 (a) Local variation in dip of ESE growth faults due to differential compaction of the strata. (b) The post-depositional N-NNE faults follow the pre-existing vertical joints of similar orientation in competent layers. The dip of these faults is less in adjoining incompetent layers (c=competent, i=incompetent).

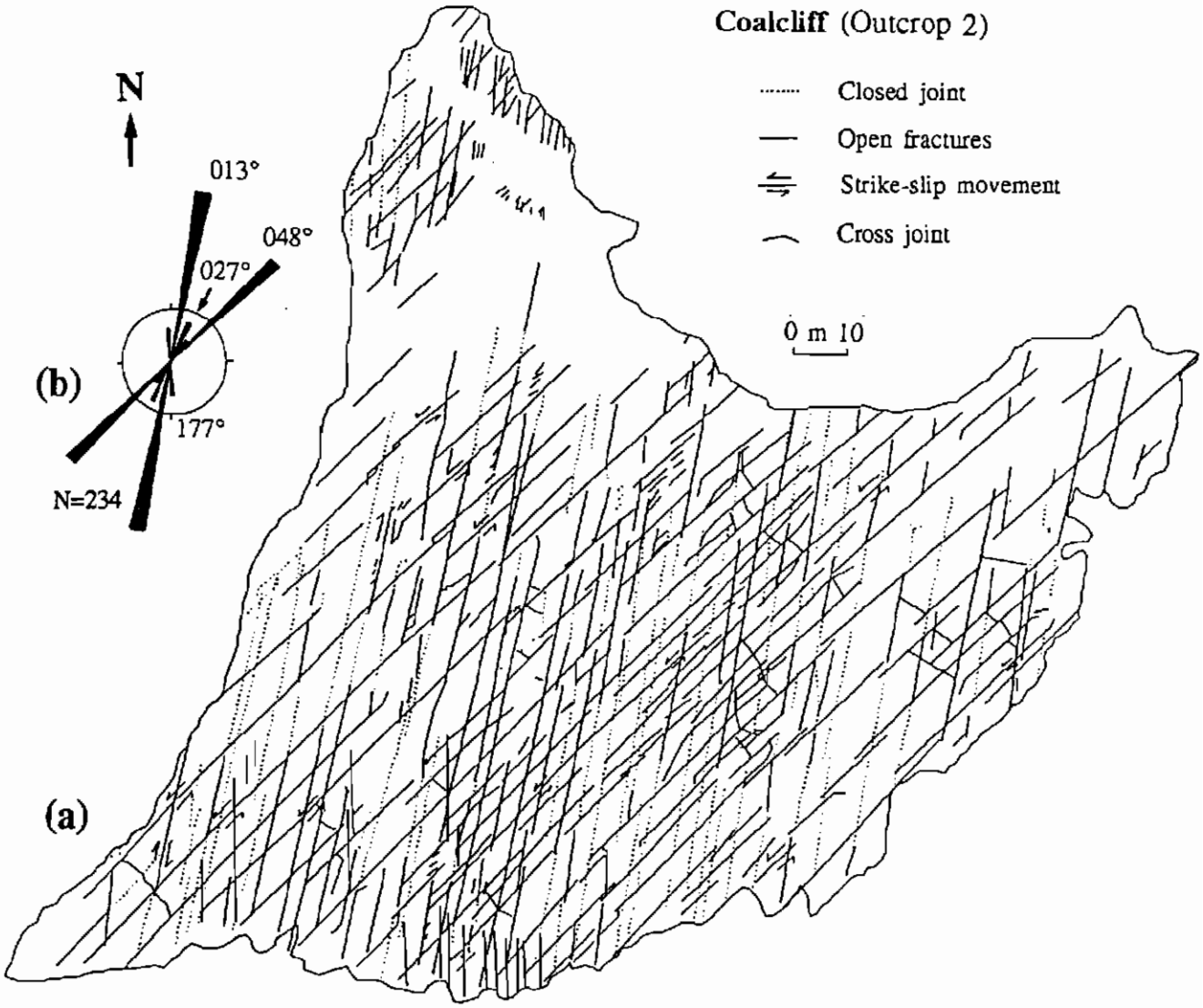

Figure 5.1 (a) Fracture pattern of Coalcliff Sandstone at Coalcliff, NSW (Outcrop 2). (b) Rose diagram of 234 fractures of this platform (see text).

Figure 5.2 A 2 mm dextral movement along a 010° faulted joint which has displaced a 045° joint. The joint infilling is calcite (arrow scale is 5 cm and points to the north).

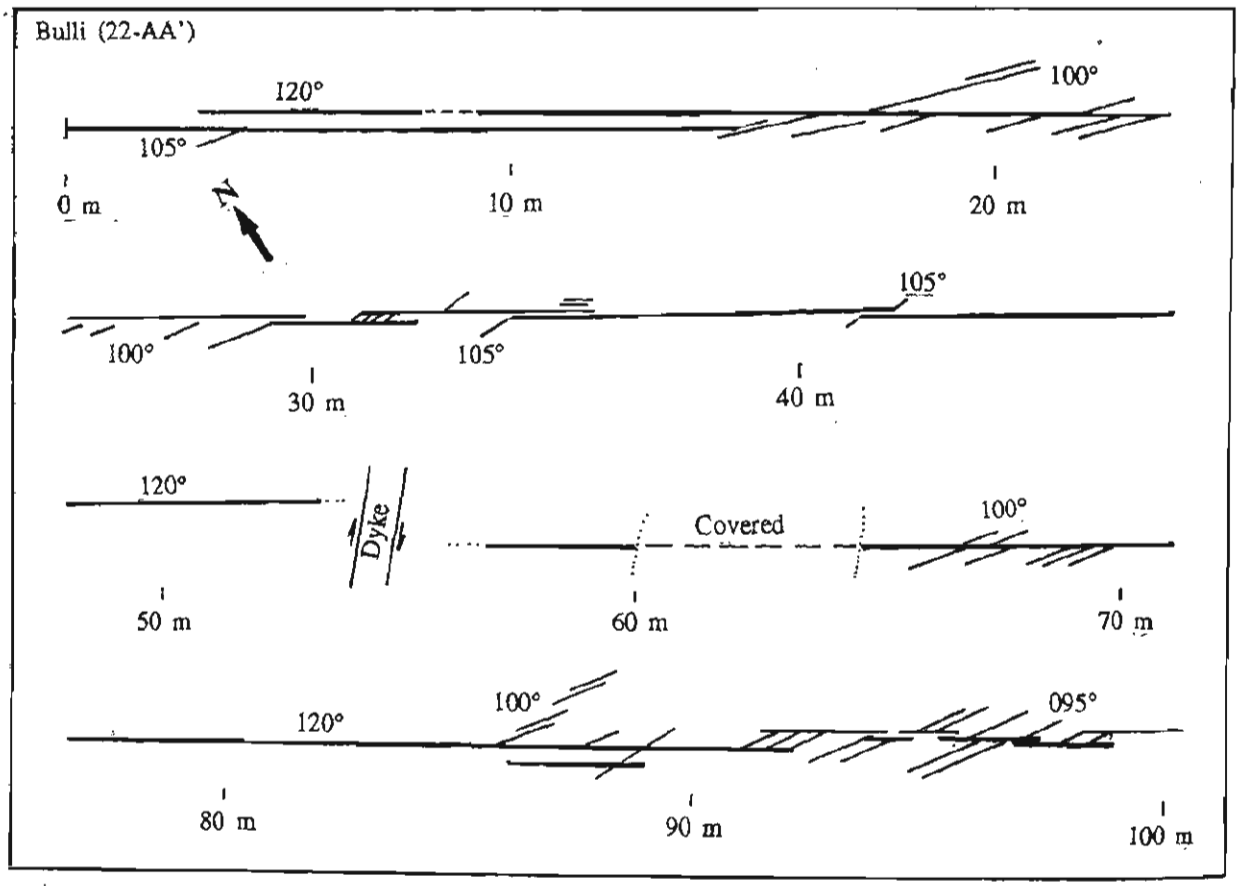

Figure 5.3 Structure of a long recracked 120° striking joint at Bulli (Scanline 22-CC'). The segments are 2-15 m long. Short 095-105° secondary fractures indicate sinistral shear along the parent fracture. Dextral slip along the dyke at the 54 m mark displaced the 120° joint for approximately 50 cm.

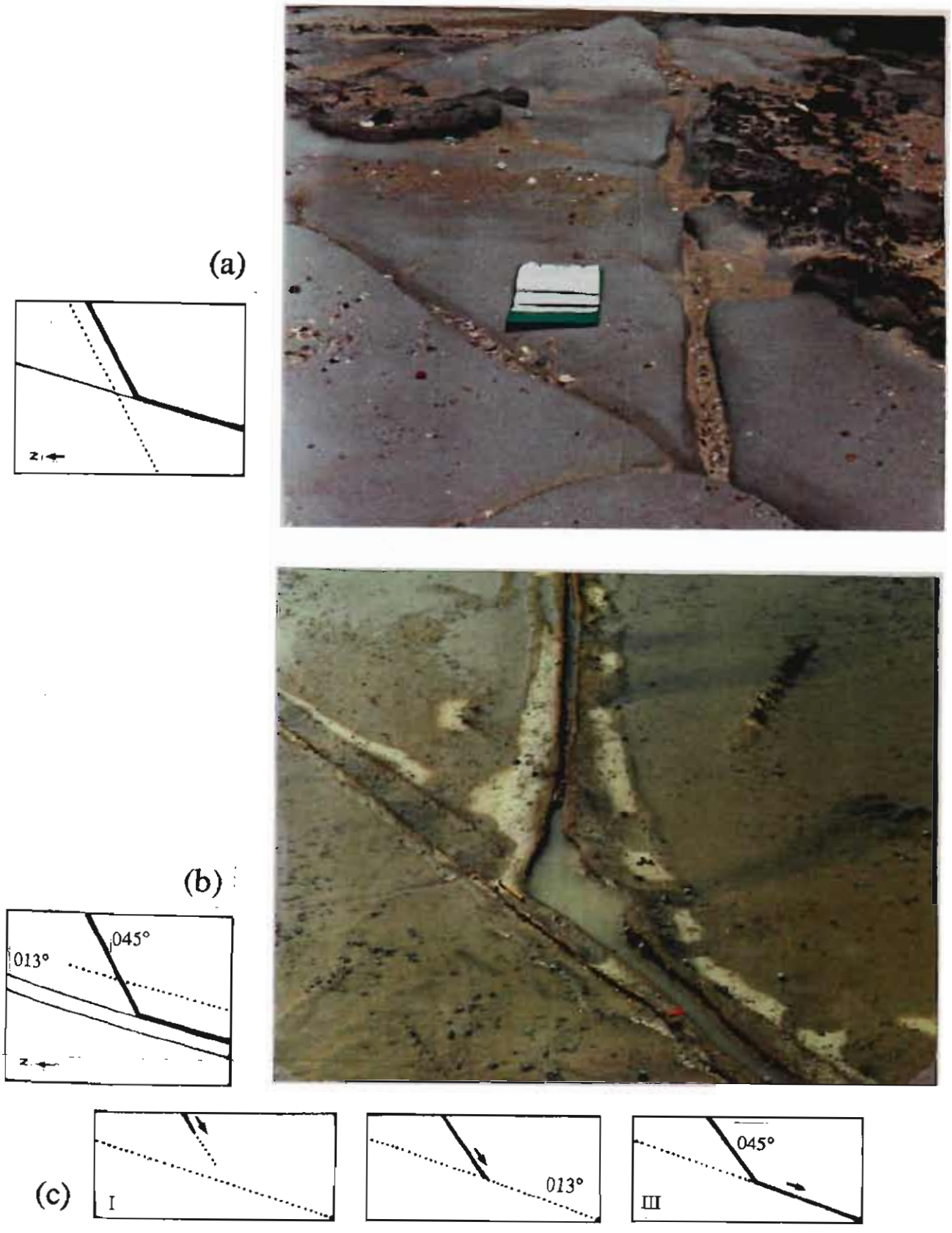

Figure 5.4 (a) Abutting of a 045° fracture against a 013° fracture, while a second 045° joint cuts through the 013° fracture without any interaction (paper pad is 23 cm wide). (b) Another example of abutting of an 045° fracture against a 013° fracture. (c) In both of these examples recracking started from the 045° joint and when the propagating front reached the intersection, it diverted to the 013° joint. Outcrop 2, Coalcliff (pen is 15 cm long).

(a)

(b)

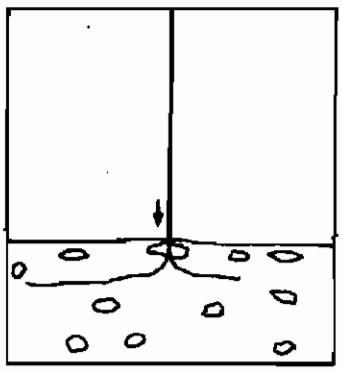

Figure 5.5 Photograph (a) and sketch (b) of the termination by branching of a vertical NE joint after it penetrated about 3 cm into the lower conglomeratic bed. The branches are 20 and 30 cm long and are subparallel to bedding. Both vertical fracture and horizontal branches are open. Note how the white pebble , to the left of the pen tip, has fractured without any vertical slip (pen is 15 cm).

(a)

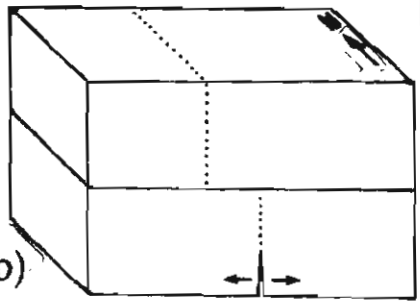

(b)

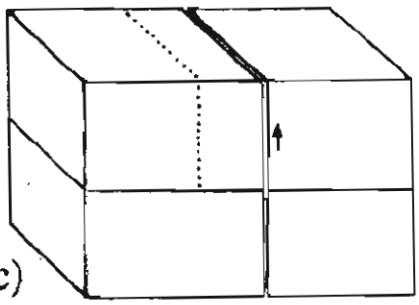

(c)

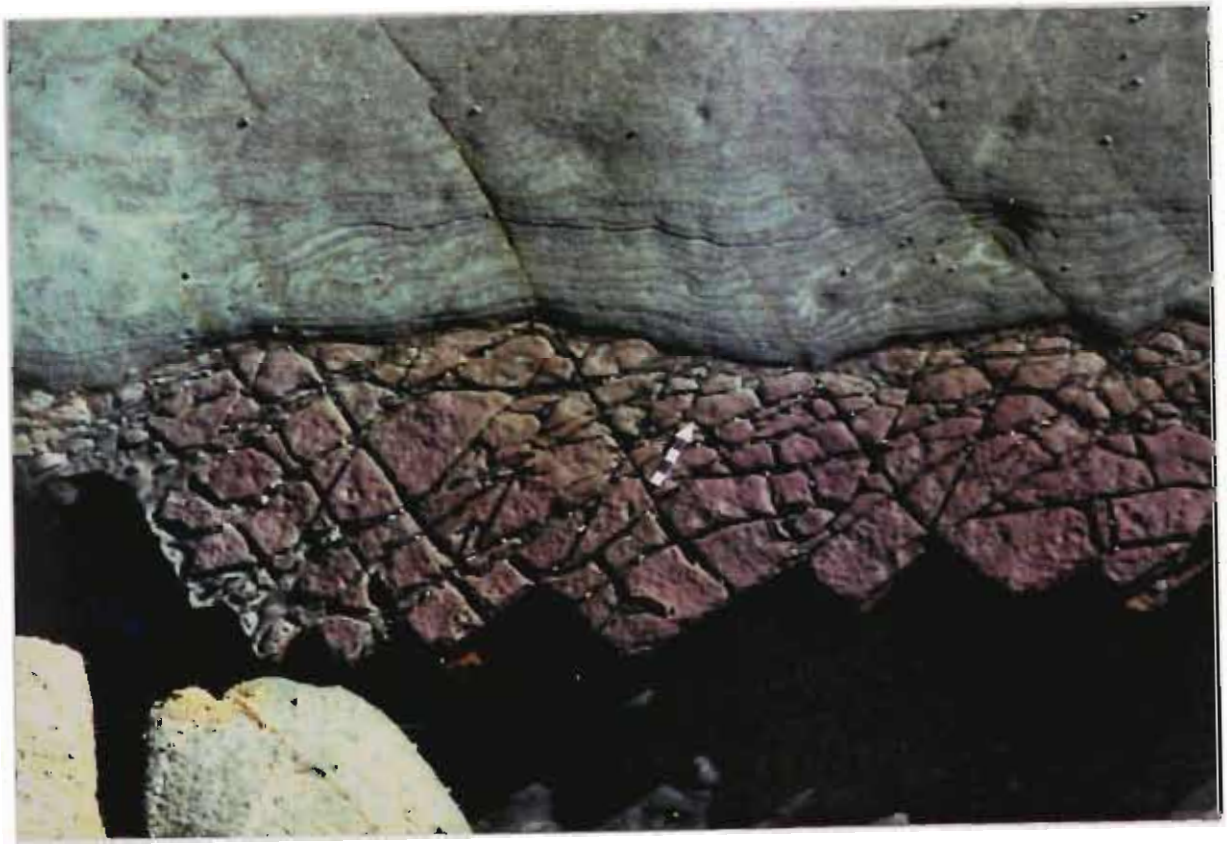

(d)

Figure 5.6 (a) An open vertical fracture, striking 013°, developed parallel to a closed joint with a similar orientation. The closed 013° joint, as well as a through-going 045° joint, show no signs of lateral slip, while the open fracture has a faint dextral movement (compass arm to the south). (b, c) Sketches showing the development of this pattern (see text). (d) Selective in-plane penetration of SE joints from the lower siltstone bed to the upper laminated fine-grained sandstone, due to subsequent recracking (Outcrop 7 at Scarborough) (north arrow is 5 cm).

(a)

(b)

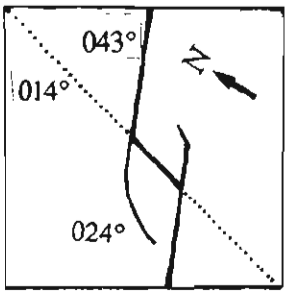

Figure 5.7 Photograph (a) and sketch (b) of a 025° striking secondary crack formed at the end of two segments of a NE (043°) faulted joint. One secondary crack bends abruptly but the other is curved. Another through-going joint, which strikes NNE (014°), is mostly closed and filled with 5 mm of calcite (compass arm points to the north). (Outcrop 2, Coalcliff).

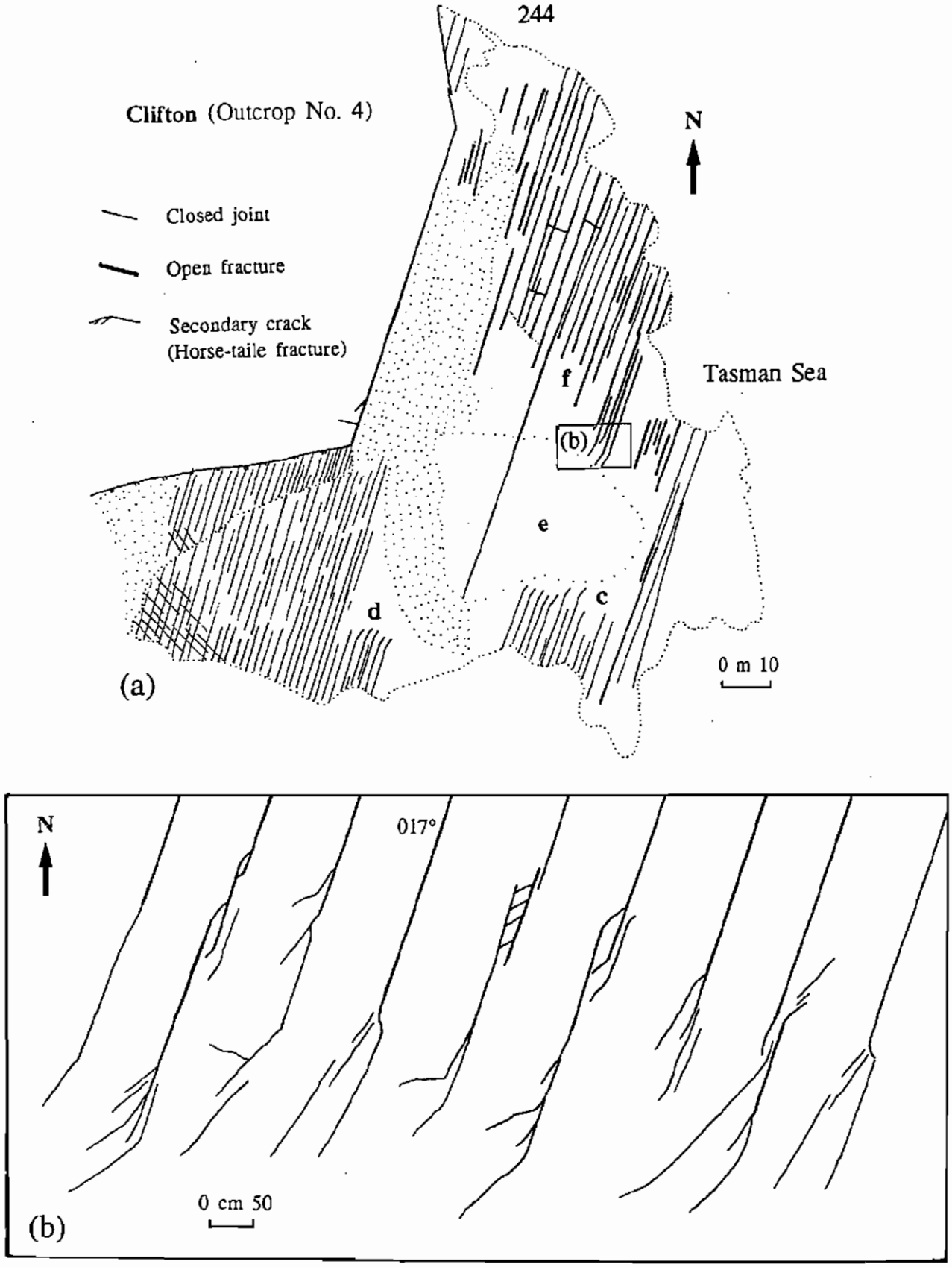

Figure 5.8 (a) NNE striking horse-tail fractures at Clifton (Outcrop 4). A set of long 017° fractures which developed in fine-grained sandstones of upper Eckersley Formation (locality c) have terminated due to the lateral facies change from sandstone (at f) to mudstone and claystone (at e). (b) Horse-tail fractures that have formed at the termination points of pre-existing 017° fractures. The average strike of secondary cracks is 033°. Similar patterns exist at localities c and d.

(a)

(b)

Figure 5.9 (a) A group of 100° striking secondary cracks which developed along one side of a 128° open fracture. Secondary cracks are straight and 30-40 cm long. They were subsequently connected with cross joints. The width of secondary fractures increase toward the through-going fracture. Hammer 33 cm long and hammer handle to the north. (b) Vertical profile of a set of 025° striking secondary cracks (at hammer pick), developed along a 040° joint (Outcrop 12 at Wombarra).

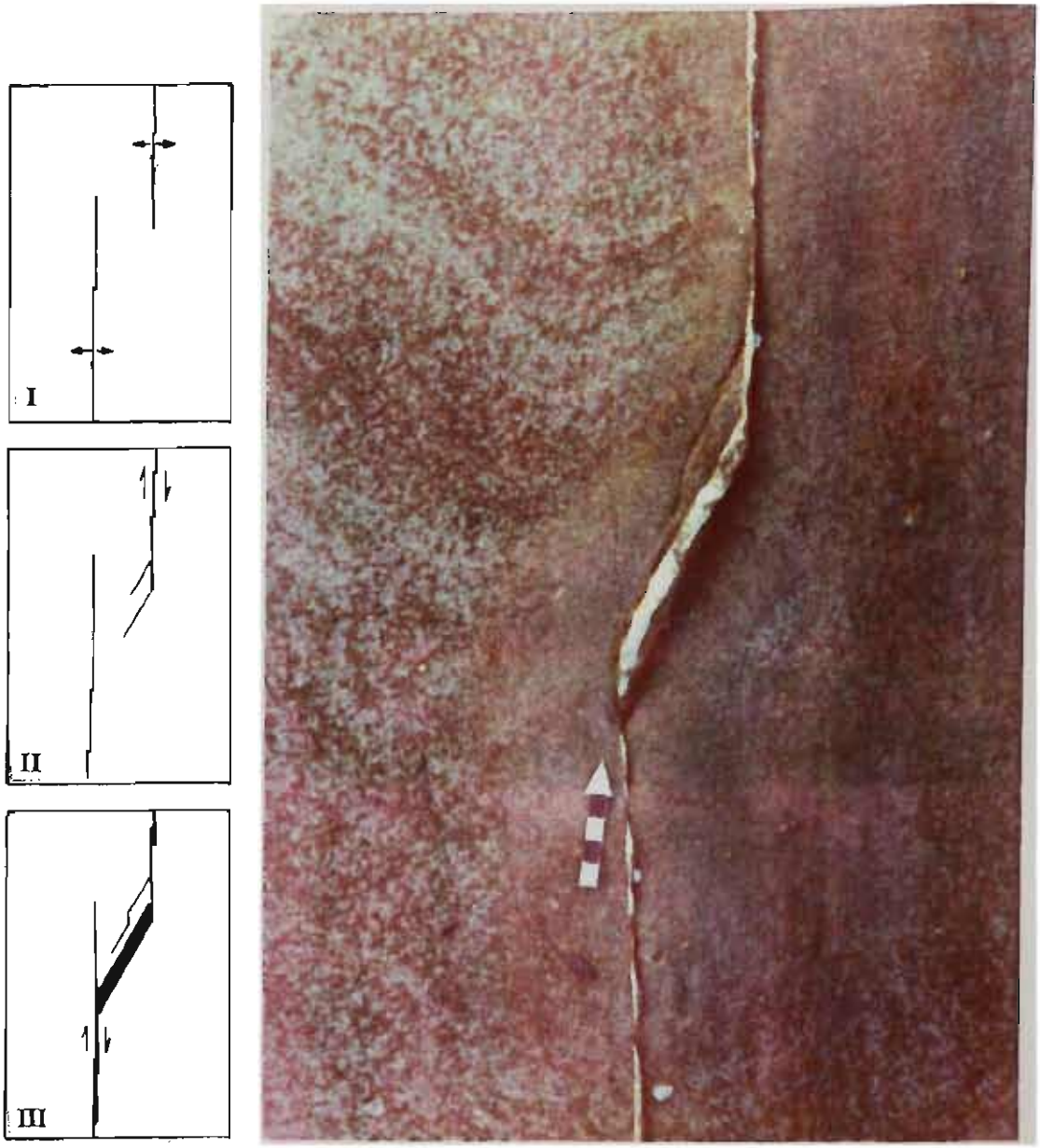

Figure 5.10 Sketches (a) and photograph (b) showing development of a secondary fracture, striking 022°, connecting two segments of a 177° joint and accommodating dextral slip. The amount of slip is 16 mm, which is equal to the thickness of calcite, measured parallel to the strike of the faulted joint. Outcrop 2 at Coalcliff. Arrow scale is 5 cm and points to the north.

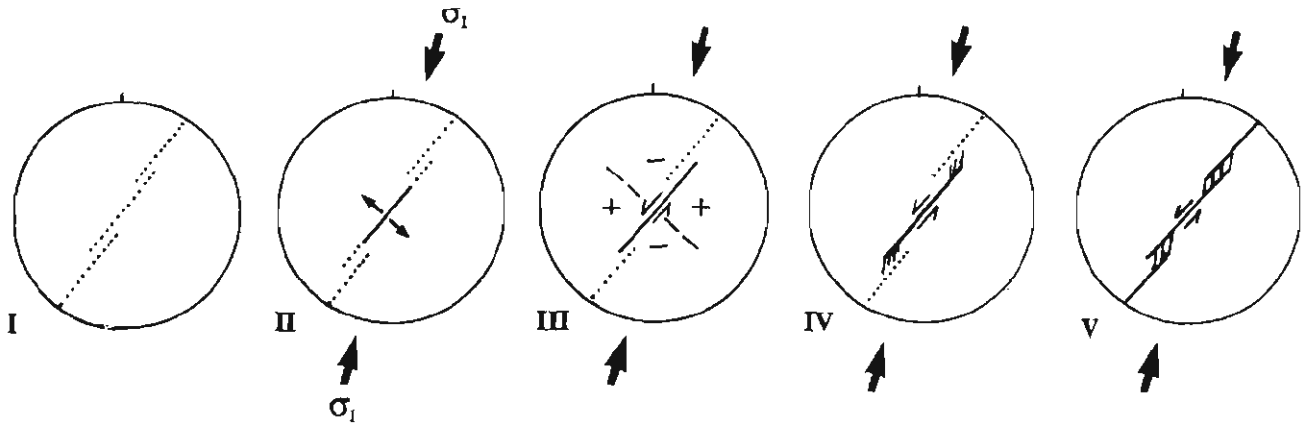

Figure 5.11 Recracking and horizontal enlargement of a segmented NE joint (I). Due to a NNE horizontal compression one segment started to recrack (II), and slipped (III). Secondary cracks developed at the tension quadrants of the faulted segment (III) and (IV). The next segments recracked and linked by secondary cracks and bridge fractures (V).

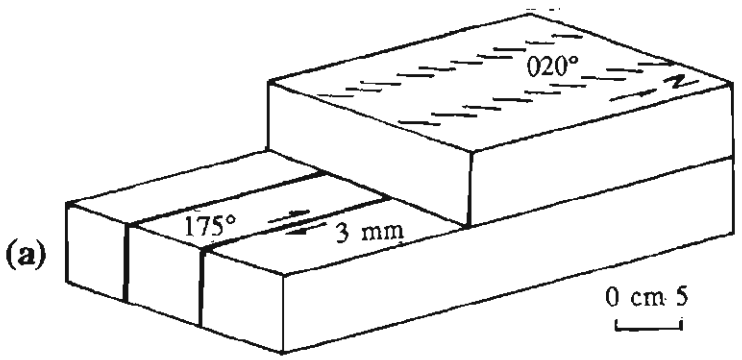

(b)

Figure 5.12 Three dimensional view (a) and photograph (b) of en echelon arrays at the Coledale (Outcrop 15). A set of 175° fractures, some with up to 3 mm of dextral slip, occur in the lower sandstone bed. Each of these fractures are overlain by an array of en echelon cracks formed in the upper sandstone bed. The strike of en echelon segments are 020-025°.

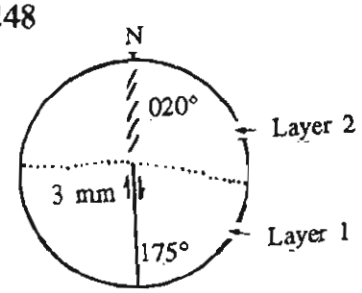
N
020°
Layer 2
3 mm
Layer 1
175°

(a)

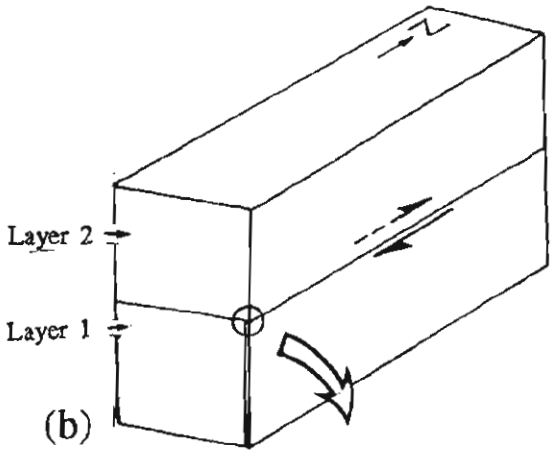
Layer 2
Layer 1

(b)

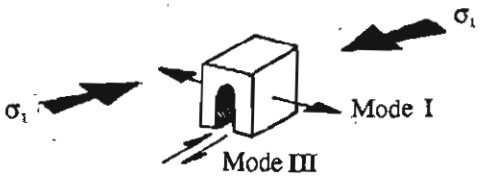
σ1
σ1
Mode I
Mode III

(c)

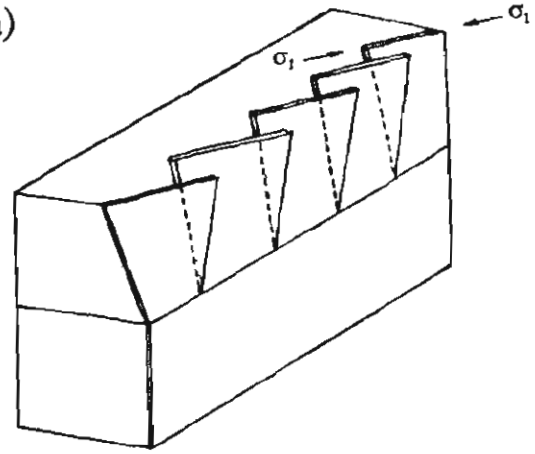
σ1
σ1

(d)

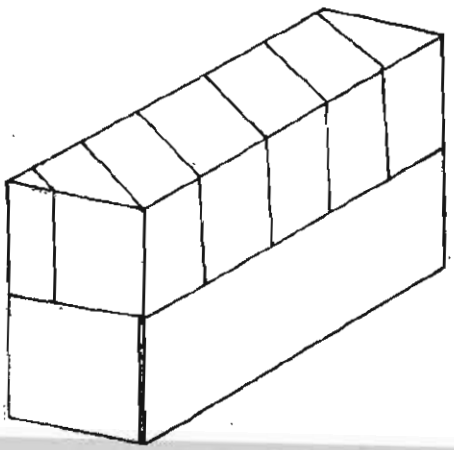

(e)

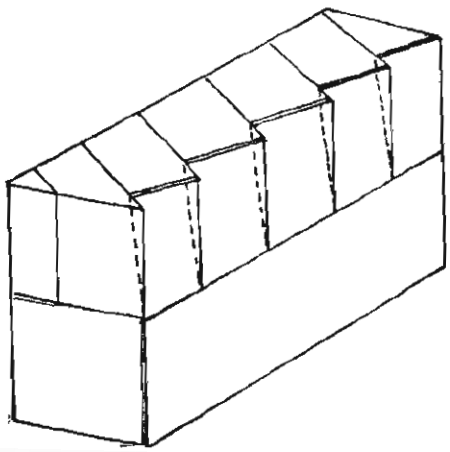

(f)

(g)

Figure 5.13 Development of an array of echelon fractures due to the vertical propagation of a recracking front (a). In a two layer sequence, the pre-existing 177° joint at the lower layer (b) reactivated due to a NNE horizontal compression (Figure 5.12, southwest of Outcrop 15, Coledale). At the interface the edge of recracked joint was under mode I (opening) and mode III (twisting) (c). The propagating front subdivided into blades, and these have twisted and aligned with the direction of compression, i.e. 022° (d). When the upper bed contains a set of joints (e), each en echelon segment is bounded by two neighbouring joints (f) and (g). North arrow in (g) is 5 cm.

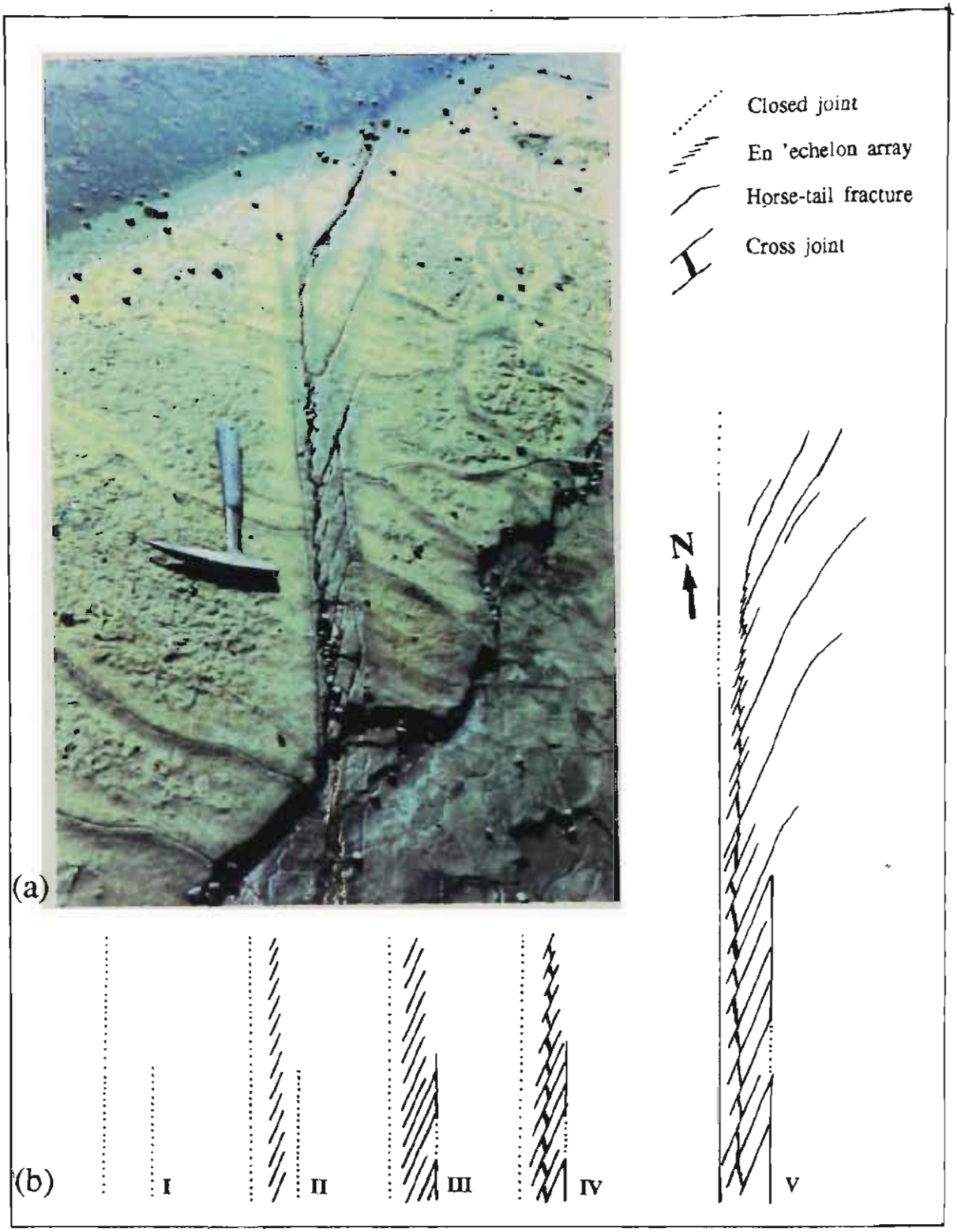

Figure 5.14 (a) A complex zone of secondary fractures developed at the termination points of two closely spaced 010° joints at Outcrop 1. The zone is in a 5 cm thick, medium-grained sandstone underlain by a slightly finer grained sandstone. An array of left-stepped en echelon fractures occurs parallel to and in between these joints. Echelon segments are at a clockwise 10-15° angle with the 010° joints. In the lower part of the figure, parallel en echelon cracks abutted against part of the parent joint, while towards the end of this structure (top of figure) most became progressively shorter. Some segments are exceptionally longer, partially curved, and resemble horse-tail fractures. A group of short and open cracks, subparallel with the host joint, have subsequently connected the en echelon segments. (b) Sequence of formation (see text for more details).

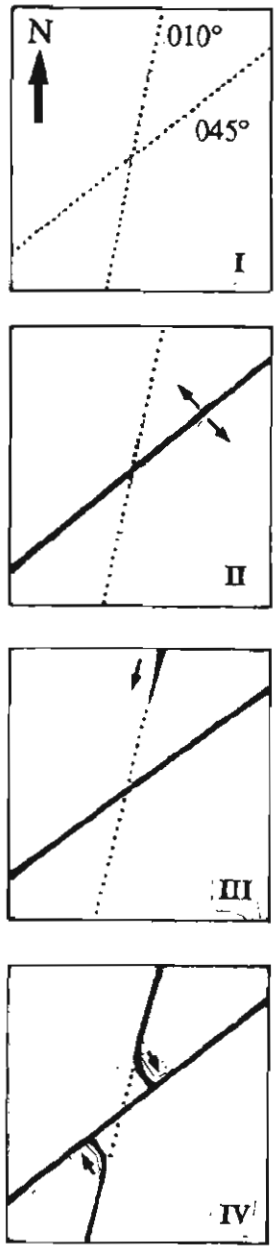

(a) (b)

Figure 5.15 Sketches of the sequence of formation (a) and photograph (b) of the interaction between two conjugate faulted joints. The NNE (010°) fracture bends where it approaches the through-going NE (045°) fracture. Two short segments of the NNE fracture are left closed. Weathering and wave action have dramatically enlarged the open fractures. The curving perpendicular form of abutting indicates the sequential nature of recracking. See text for more details.

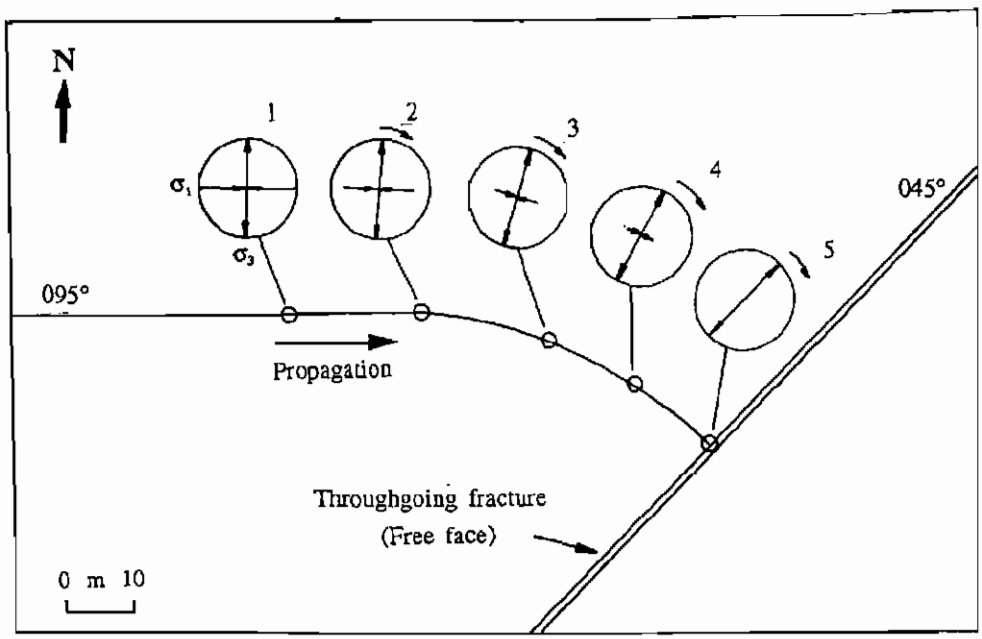

Figure 5.16 Secondary crack formed due to the rotation of stress field near a free surface (Wombarra South, Figure 5.19a). The 095° fracture propagated from left to right due to a compressive far-field stress (1). The propagating front was perturbed and deflected near the through-going NE fracture and terminated against it at a 90° angle (Dyer 1988). At the free surface, σ_1 was zero and σ_3 was parallel to the through-going fractures (5). Along the path, σ_3 was always normal to the propagating fracture and σ_1 was progressively decreasing (2, 3 and 4). The curving perpendicular secondary cracks represent the state of local stress and the direction of far-field stress, cannot be inferred from them.

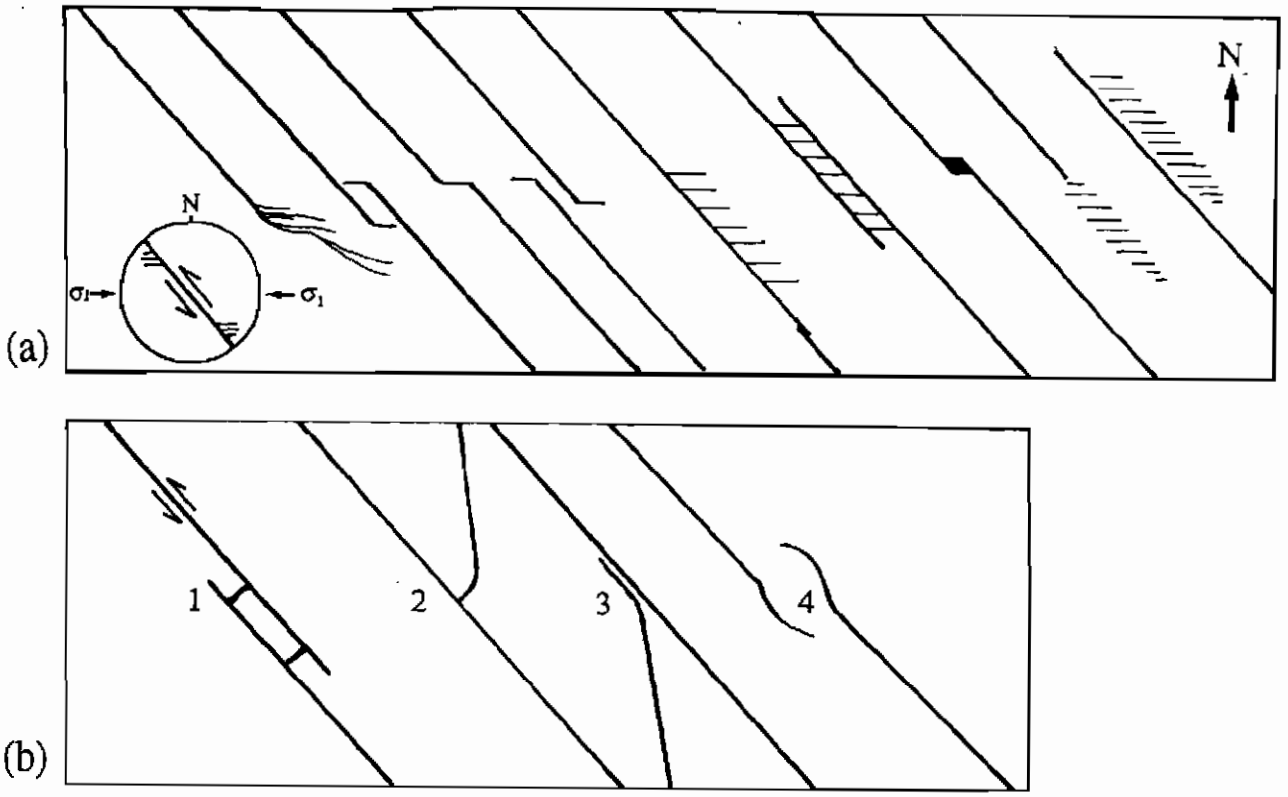

Figure 5.17 Classification of secondary cracks. (a) Secondary cracks which indicate the orientation of far-field stress and the sense of slip along the faulted joints. Circular inset indicates the E-W direction of far-field compressive stress, responsible for the sinistral shearing and formation of secondary cracks. (b) Secondary fractures which form due to the local reorientation of stress field: bridge fractures (cross joints, 1), curving perpendicular (2) and curving parallel (3) fractures, and interaction between two segments of a same fracture propagating towards each other (veers in the sense of Cruikshank *et al* 1991) (4).

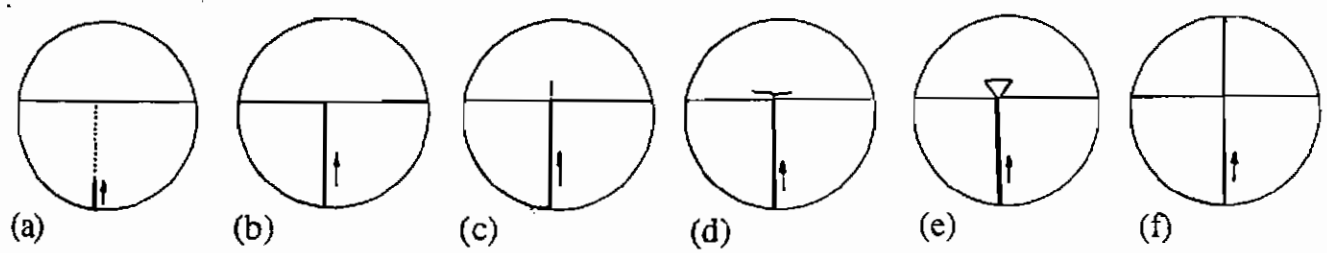

Figure 5.18 Vertical growth of a NE joint (a) across an interface (mechanical boundary) due to a NNE striking horizontal compression. The recracking might come to a halt at the interface (b) or cross it for few millimetres to few centimetres before it stopped propagating (c). The interface might fail and the recracking front bifurcate and become subparallel with the interface (d). The propagating front might break into segments, and the growing segments swing and form an en echelon array of short fractures (e). The echelon segments are aligned with the direction of maximum compression. The recracking front occasionally ignored the interface and fractured intact rock (f).

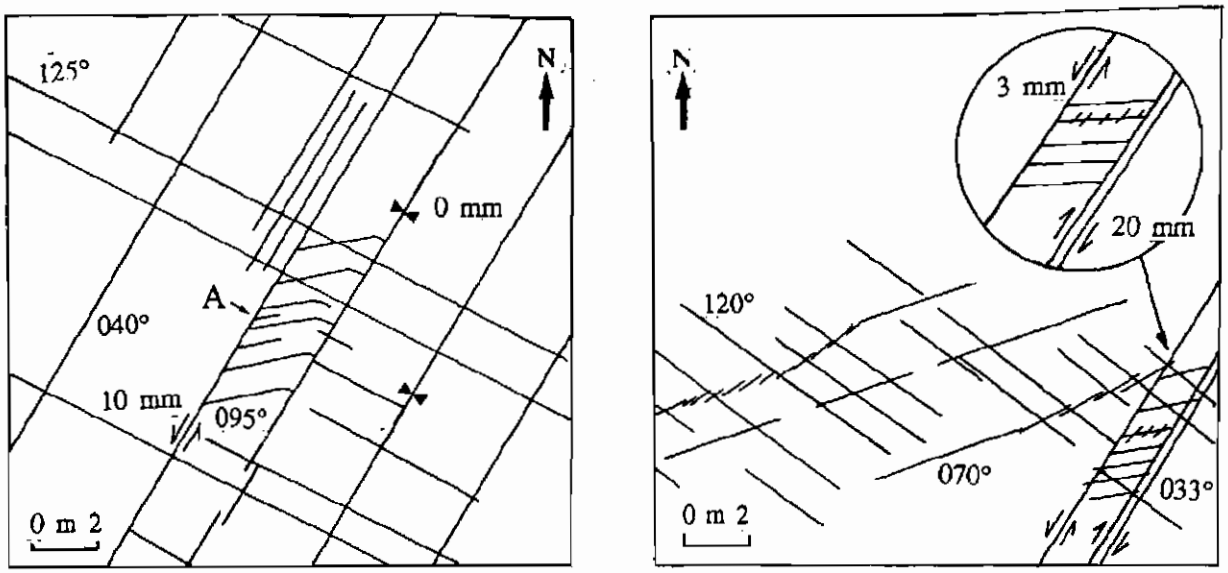

Figure 5.19 Multiple slip along faulted joints. (a) Opposite direction of inferred and measured horizontal displacement along a NE faulted joint. The secondary cracks along the NE fracture 'A' suggest a dextral slip, while a 10 mm sinistral slip is measured for this fracture (Wombarra South, Scanline 12-GG', 10-30 m marks). (b) Opposite direction of displacement along two NE striking faulted joints (Coledale, Scanline 15-JJ', 120-140 m marks).

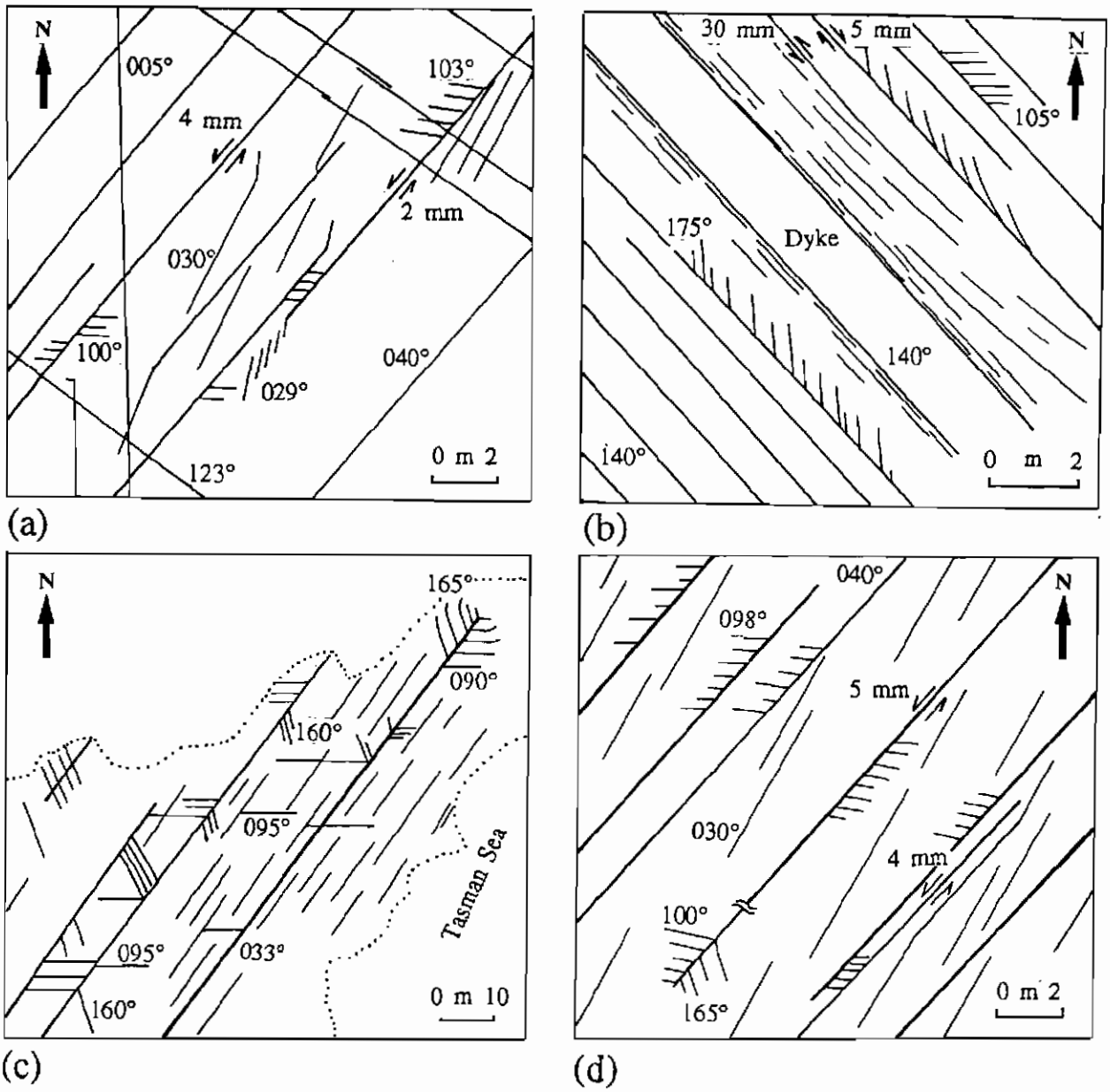

Figure 5.20 Development of multiple sets of secondary cracks along faulted joints. (a) NNE and E-W oriented secondary cracks formed along a set of NE faulted joint (Wombarra South, Scanline 12-DD', 30-50 m marks). (b) 160-180° as well as 090° secondary fractures formed along adjacent joints of a 140° dyke (Austinmer South, Scanline 19-EE', 30-45 m marks). (c) - (d) Feather patterns formed by two sets of 090° and 160° secondary cracks near the termination points of faulted joints. Southwest corner of Outcrop 7 at Scarborough (c) and 10-45 m mark of Scanline 12-AA' at Wombarra South (d).

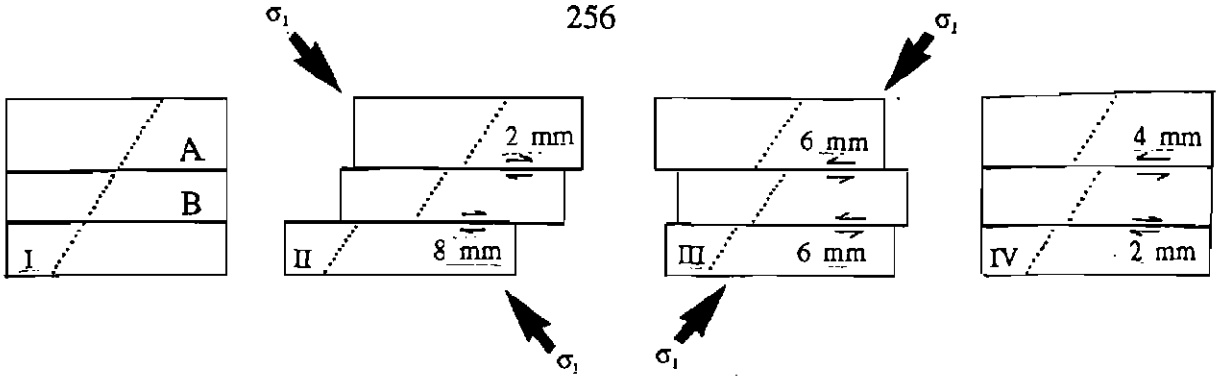

Figure 5.21 Model for development of opposite senses of lateral slip in two neighbouring, NNE striking, faulted joints at Coledale. In the first deformation, dextral slip along two fractures, A and B (I), has been for 2 and 8 mm respectively (II). The difference in lateral slip is due to the different lengths of faulted segments and the variation in strength of infilling materials. In a subsequent event, both fractures have been slipped sinistrally along their strike for 6 mm (III). The outcome has caused an overall different sense of displacement for A and B, which is therefore attributed to 2 deformations (IV).

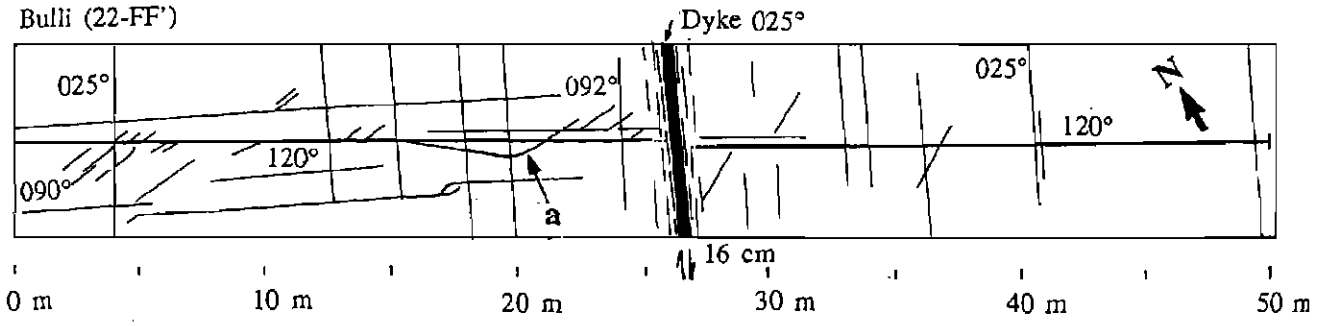

Figure 5.22 A 16 cm dextral displacement of a 020° striking vertical dyke at Bulli (Scanline 22-FF'). Short secondary cracks formed along the sides of a long 120° joint. At the 20 m mark the recracked joint swings clockwise for 5 m and then swings back counterclockwise and strikes 100° before it terminates.

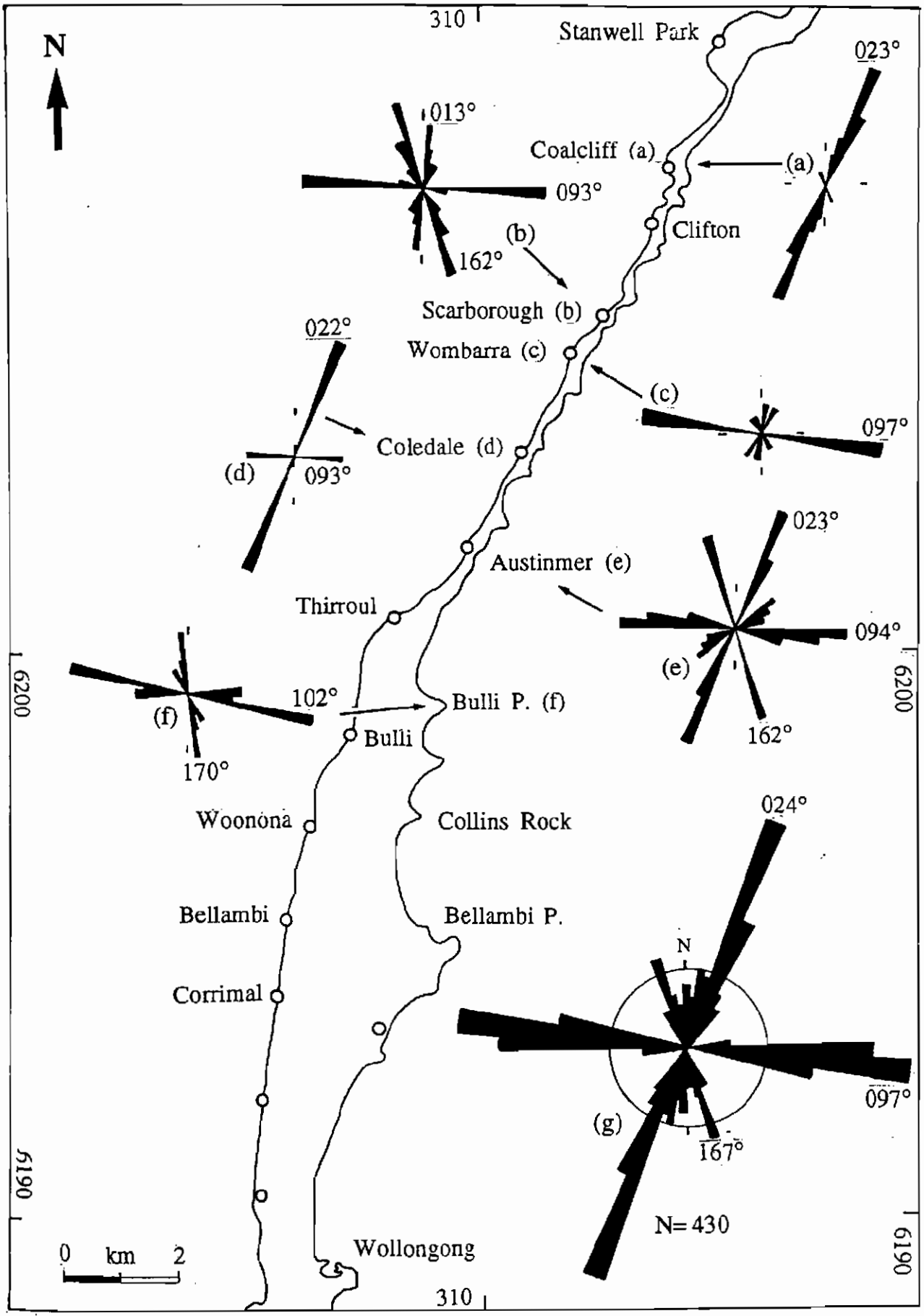

Figure 5.23 Rose diagram (5° intervals) with the orientation of secondary cracks in the southeastern Sydney Basin. (a) Coalcliff (Outcrops 1, and 2), (b) Scarborough (Outcrops 6-9), (c) Wombarra (Outcrops 10-12), (d) Coledale (Outcrops 13-16), (e) Austinmer (Outcrops 17-19), (f) Bulli (Outcrops 21-22), (g) 430 secondary cracks measured in Illawarra Coal Measures and lower Narrabeen Group, between Coalcliff and Bulli.

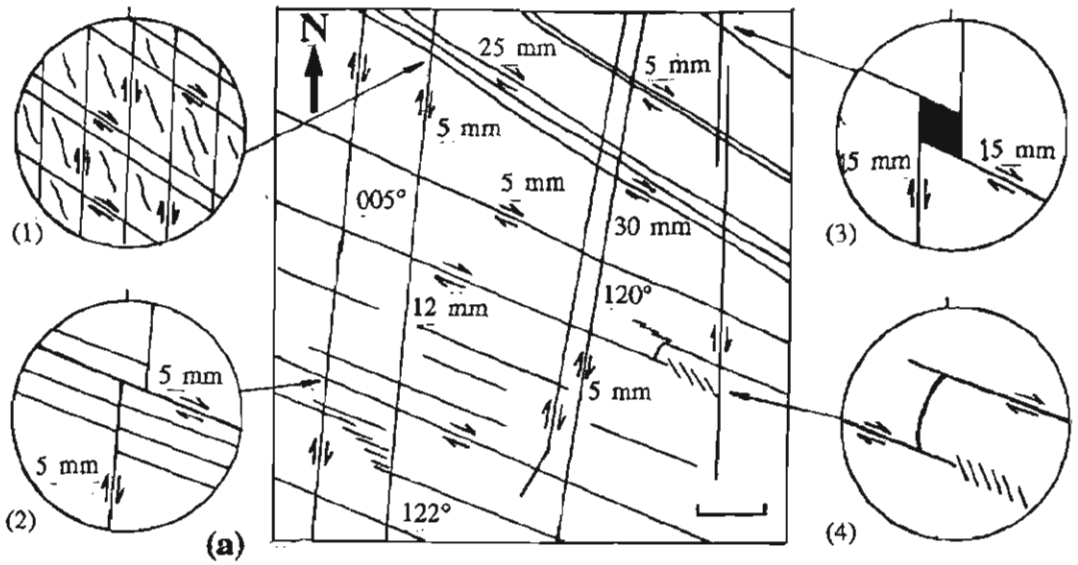
N
25 mm
5 mm
5 mm
5 mm
005°
30 mm
12 mm
120°
5 mm
122°
(1)
(2)
5 mm
5 mm
(3)
15 mm
15 mm
(4)
(a)

(b)

(c)

Figure 5.24 Fracture map (a) and photographs (b)-(c) demonstrating the relation between secondary cracks and lateral displacement in laminated siltstone and fine-grained sandstone of the Wilton Formation (Scanline 18-BB' at Austinmer). Short, slightly curved, 160° striking secondary cracks (insets 1-4 of a and photograph b) represent the direction of SSE compression which was responsible for the dextral slip along the 120° joints at this locality (inset 4 of a). Dextral slip on 000-005° fractures is due to the NNE compression. The amount of lateral slips ranges between 0 and 30 mm. Small rhombohedric cavities are the results of dextral slip on both sets (inset 3 of a, photograph c). Inset 2 of (a) suggests that the slip along the NNE joints was prior to slip along SE fractures. North arrow in (b) is 4 cm.

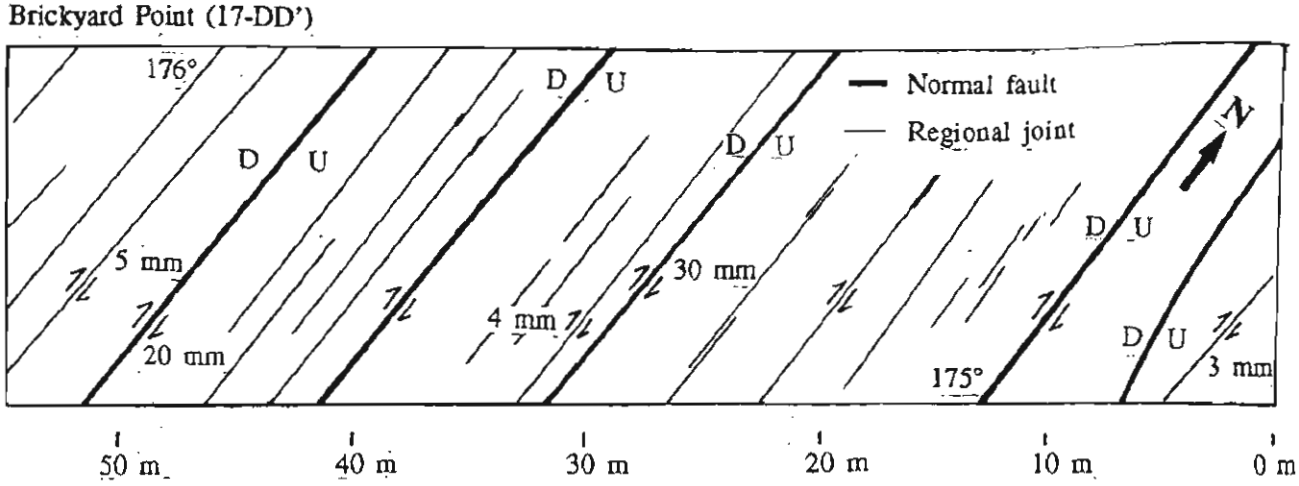

Figure 5.25 A set of N striking regional joints and normal faults both with a component of dextral slip, along the first 50 m of Scanline 17-DD' at Brickyard Point. Vertical displacement along recracked joints is zero. Fractures with other directions are not shown on the Scanline.

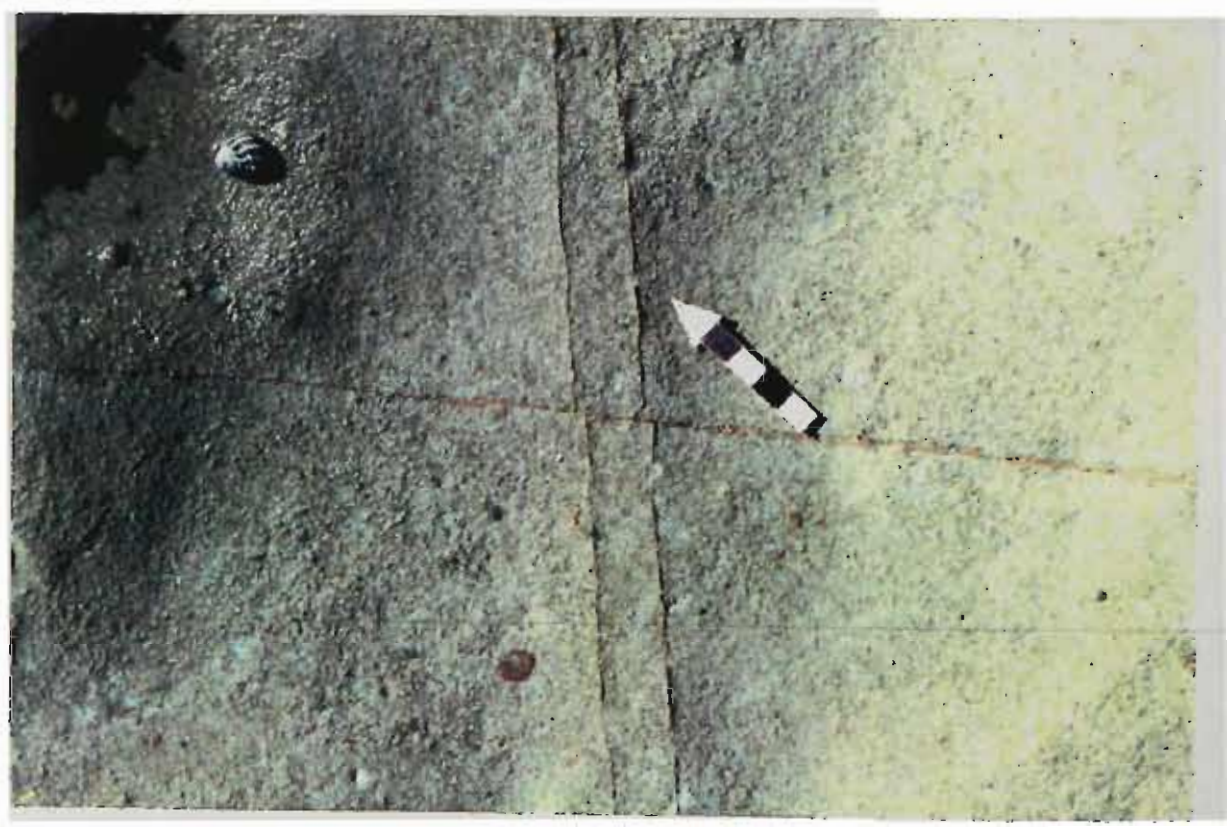

Figure 5.26 3 mm sinistral movement along a 140° striking joint, which displaced the 040° striking dyke parallel joints. This proves that the dyke, and its related joints, are older than E-W compressional forces responsible for sinistral movement (Bulli, Scanline 22-BB'). North arrow is 5 cm.

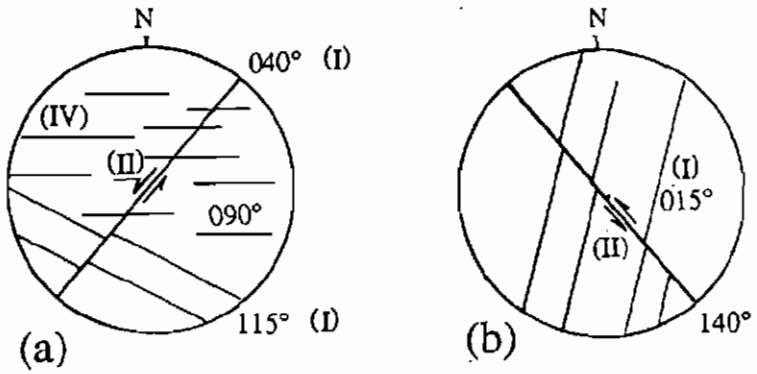

Figure 5.27 Sequence of deformation events at Wombarra:

(a) Formation of 040° and 115° fractures (I), sinistral displacement of 040° fracture due to the NNE-SSW compression (II), healing of the NE fracture (III), formation of through-going 090° secondary cracks due to the E-W compression (IV) (Scanline 12-BB', 20 m mark).

(b) Formation of 015° secondary fractures due to NNE-SSW compression (I), sinistral displacement of 140° fracture due to E-W compression (II) (Scanline 11-HH', 210 m mark).

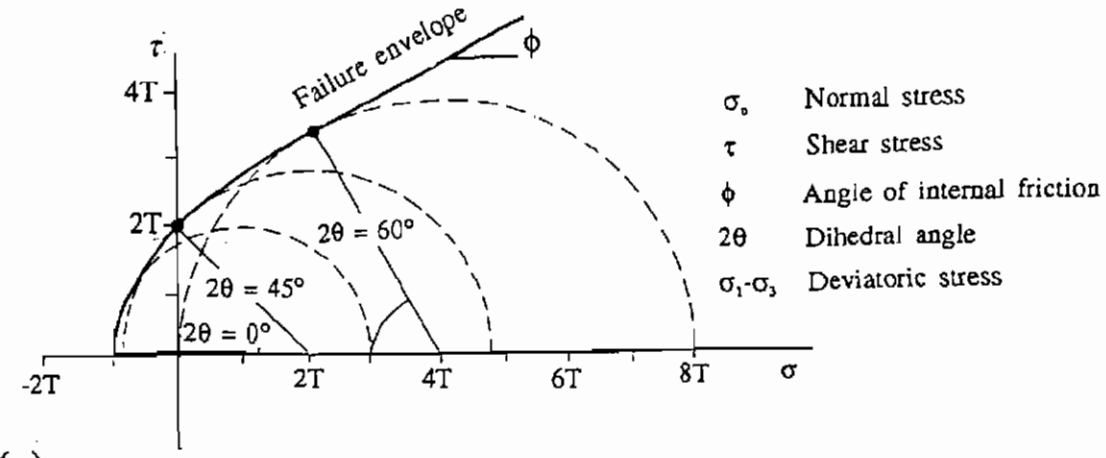

(a)

Class	2θ	σ_n	σ_3	σ_1-σ_3	
Extension	0°	-	-	<4T	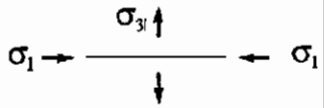
Hybrid	1-44°	-	-	4T-5.66T	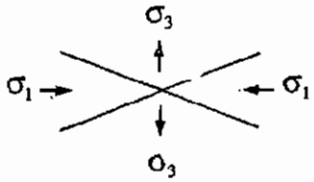
	45°	0	-	5.66T	
	45-59°	+	-	5.66T-8T	
Shear	>60°	+	0 or +	>8T	

(b)

Figure 5.28 Stress conditions during the formation of fractures in intact rock (after Hancock 1985, 1986, Dunne & Hancock 1994). (a) Coulomb-Mohr failure envelop with Mohr circles constructed for dihedral angle (2θ) of 0°, 45° and 60°. T, tensile strength of rock and ϕ = 30°. (b) The relationship between 2θ, σ_n, σ_3, (σ_1-σ_3) and T with three types of fractures. Note that σ_3 is negative for extension and hybrid fractures.

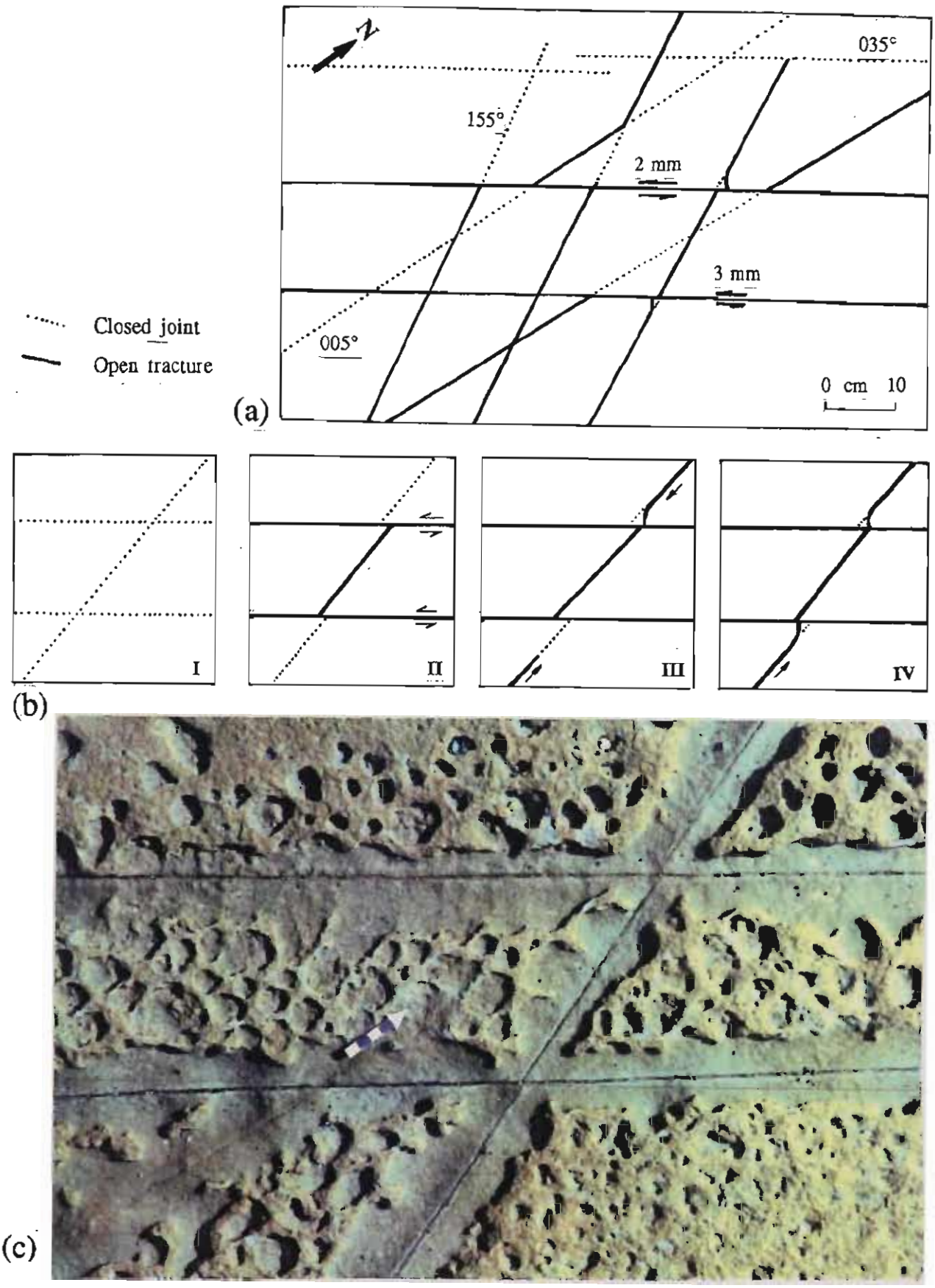

Figure 5.29 (a) Alternative recracking of three sets of vertical joints striking 005, 035, and 155° in a 5 cm thick, medium-grained sandstone bed at Outcrop 1. Each fracture consist of both open and closed segments. (b) Stages of recracking in the central part of (a). Recracking was sequential and for a single joint, the propagation was from either side toward the free surfaces (b). (c) Photograph of (b). North arrow is 5 cm.

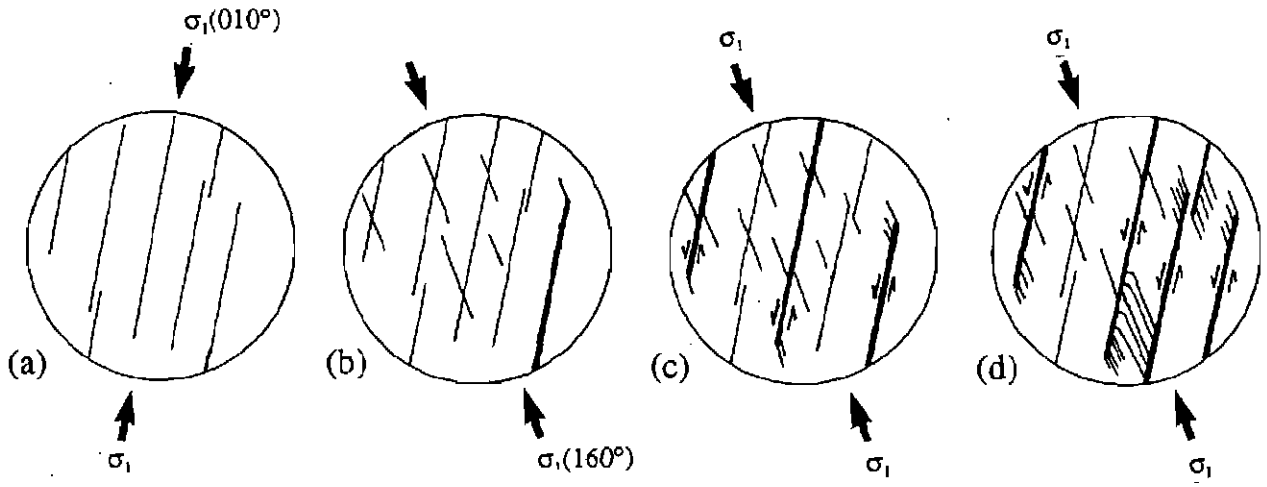

Figure 5.30 Sequential development of through-going, abutting and offsetting secondary cracks (Austinmer, Scanline 19-AA'). After formation of 010° joints (a), the orientation of stress field changed and a new set of extension fractures formed parallel to the contemporary σ_1 , i.e. 160° (b). Resolved shear stress on 010° joints recracked one of these joints. Small secondary cracks form parallel to σ_1 at the termination point of this joint. Later in the compressional episode, more 010° joints recracked and sinistral slips along them displaced the already existing 160° joints (c). Finally, more secondary cracks formed where the faulted segments were under tension (Austinmer, Scanline 19-AA').

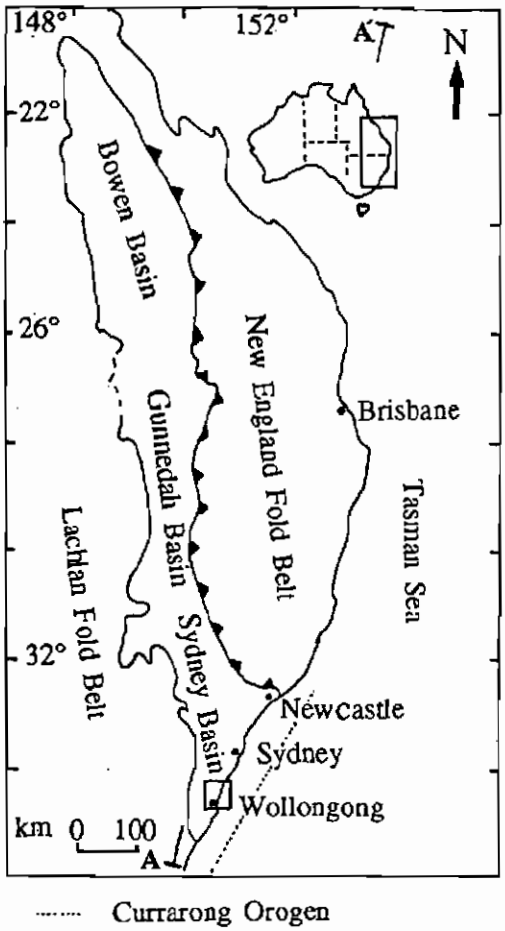

Figure 6.1 Sydney-Bowen Basin System and neighbouring fold belts.

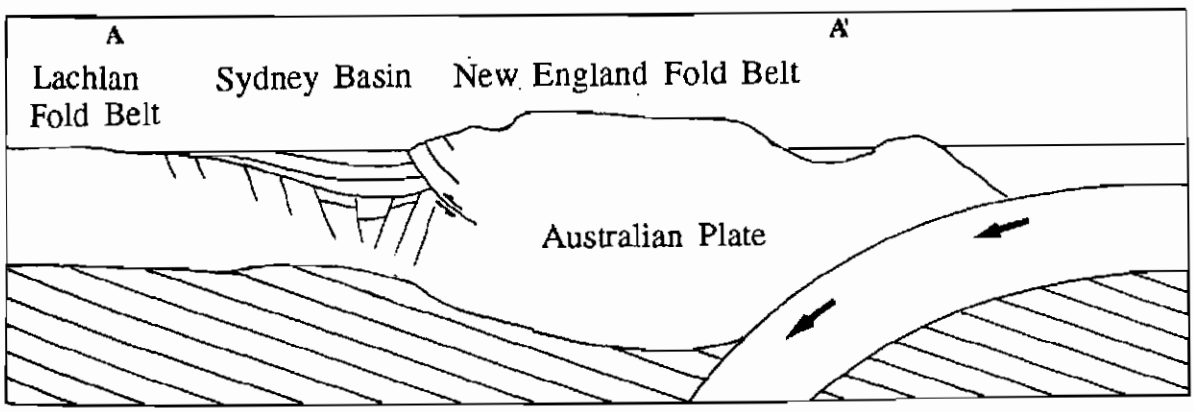

Figure 6.2 Schematic cross section of the Sydney Basin and adjacent areas (AA' in Figure 6.1). The section is not drawn to scale.

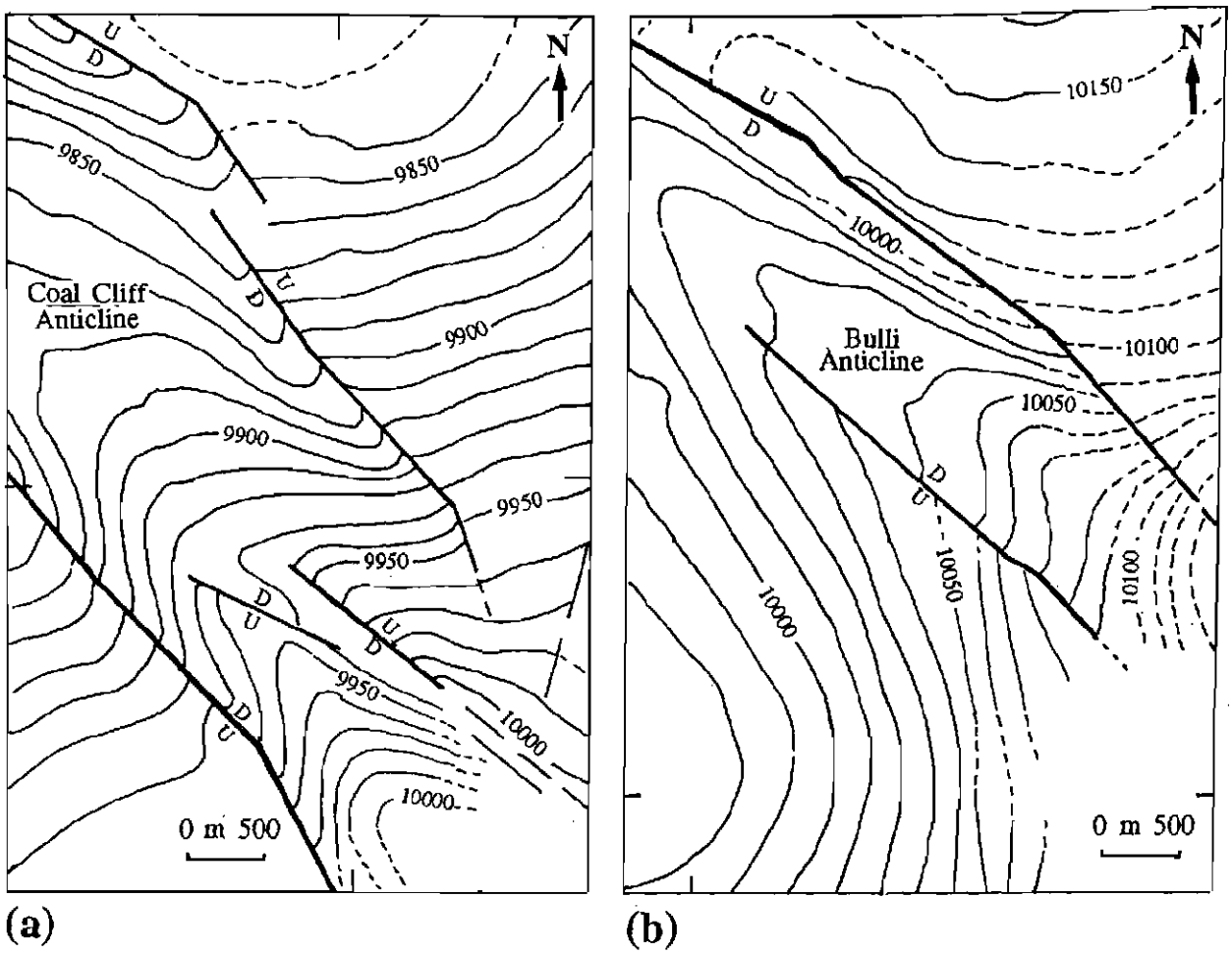

Figure 6.3 Fault-forced anticlines at Coal Cliff (a) and Bulli (b) Collieries (from Bulli Coal structure map of Rixon & Shepherd 1988). Datum is 10,000 m below Australian Height Datum.

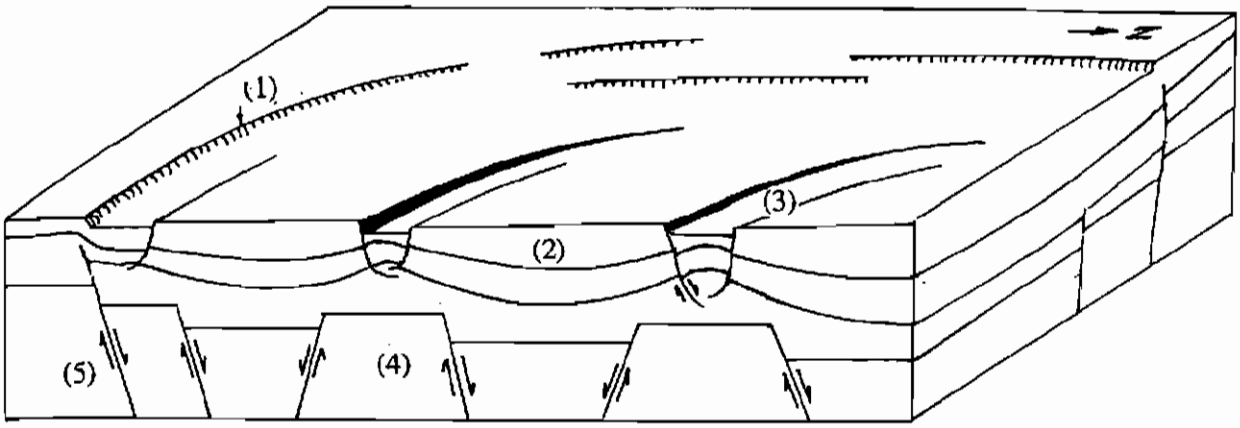

Figure 6.4 Syn-depositional structural model of the Southern Coalfield during the Late Permian deposition of the Illawarra Coal Measures. Monocline (1), syncline (2), graben and fault forced anticline (3), basement rock (4), basement normal fault (5). A SE-NW extension, may have been responsible for reactivation of appropriately oriented basement faults. Synclines formed above basement lows, while narrow grabens grew above basement highs. Anticlines are fault forced folds. Monoclines mark the edges of the disturbed area and formed above buried normal faults.

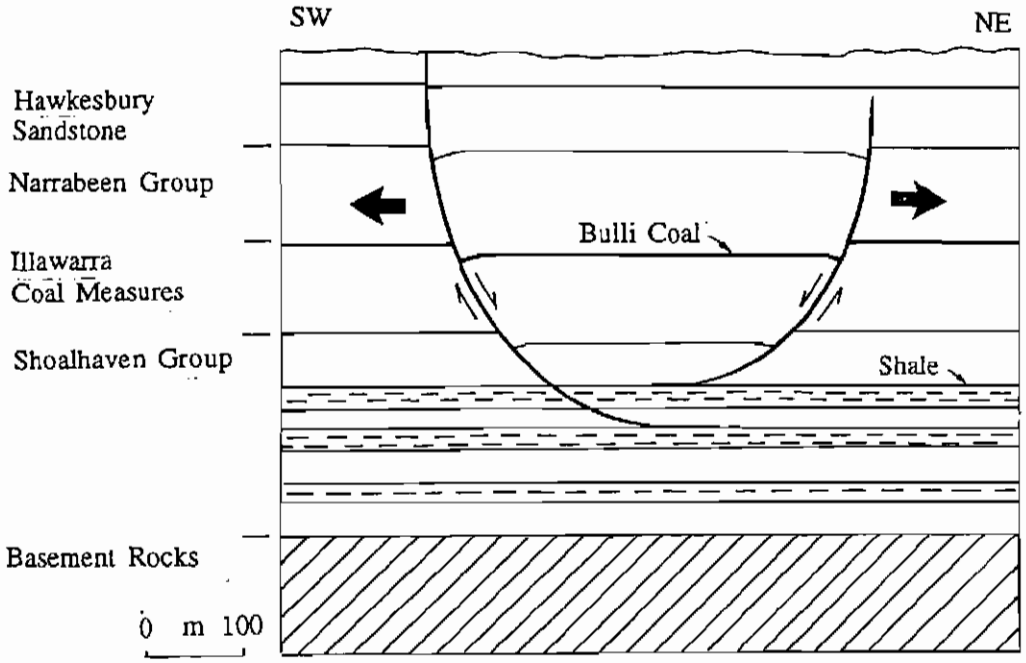

Figure 6.5 A model for the formation of fault forced anticlines of the Southern Coalfield. Movement along two inward dipping listric faults produced rollovers on the hanging walls, which forms a gentle flat-topped anticline. Fault dip is 60-70° at the Bulli Coal level. The detachments for these faults occurs in one of the fine-grained units of the Shoalhaven Group.

Please see print copy for image.

Figure 6.6 Formation of extensional forced folds and narrow grabens due to movement on an underlying normal fault. Note that the normal faults in the cover sequence are not necessarily the continuation of the basement fault. (a) Experimental laboratory model. An upper layer of homogeneous dry sand represents brittle sedimentary rocks and a lower layer of silicone putty represents ductile sedimentary rocks (Vendeville 1987). (b) Interpreted line drawing of seismic data from the Haltenbanken area, offshore Norway. Base of Cretaceous unconformity (1), Triassic/Jurassic coal (2), top of Jurassic fault (3)(Withjack *et al.* 1990).

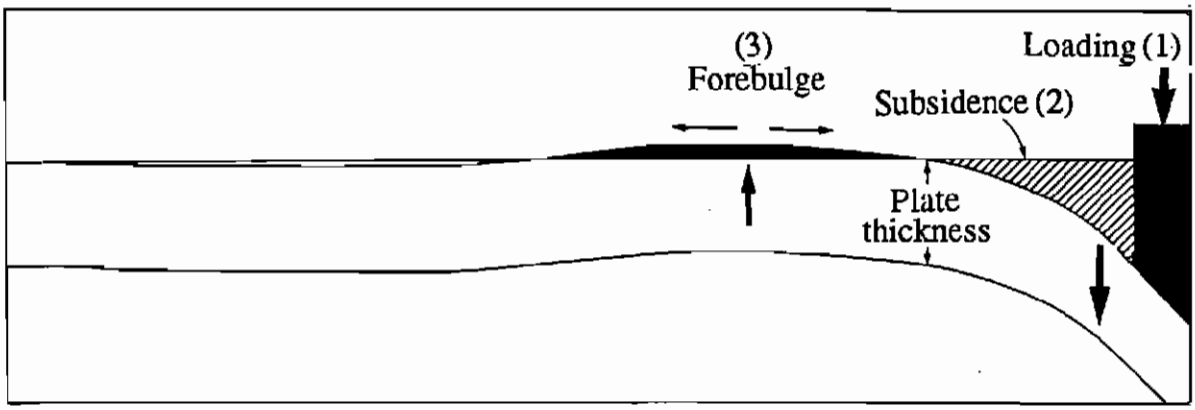

Figure 6.7 Schematic cross section demonstrating the development of tensional forces due to formation of a forebulge, away from the loading front in foreland basins (after Molnar & Lyon-Caen 1988). New England Fold Belt (1), subsiding Sydney Basin (maximum subsidence adjacent to the loading front, i.e. Hunter-Mooki Thrust) (2), elastically deflecting plate and the forebulge formed in the northern part of the Southern Coalfield (3).

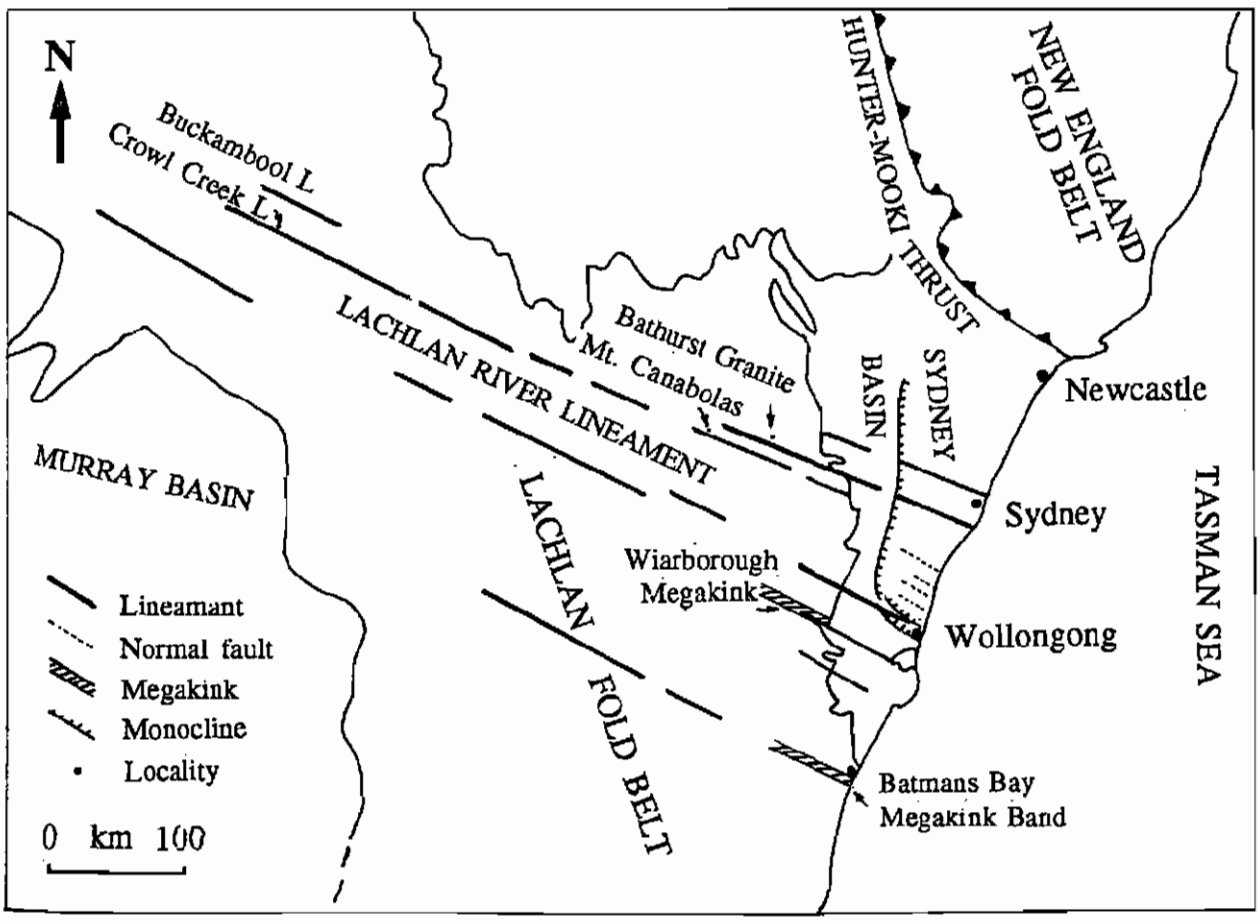

Figure 6.8 Major ESE lineaments in the southern Sydney Basin and the adjacent Lachlan Fold Belt (data from Scheibner 1974; Mauger *et al.* 1984; Powell *et al.* 1985; Lohe *et al.* 1992). See text for more detail.

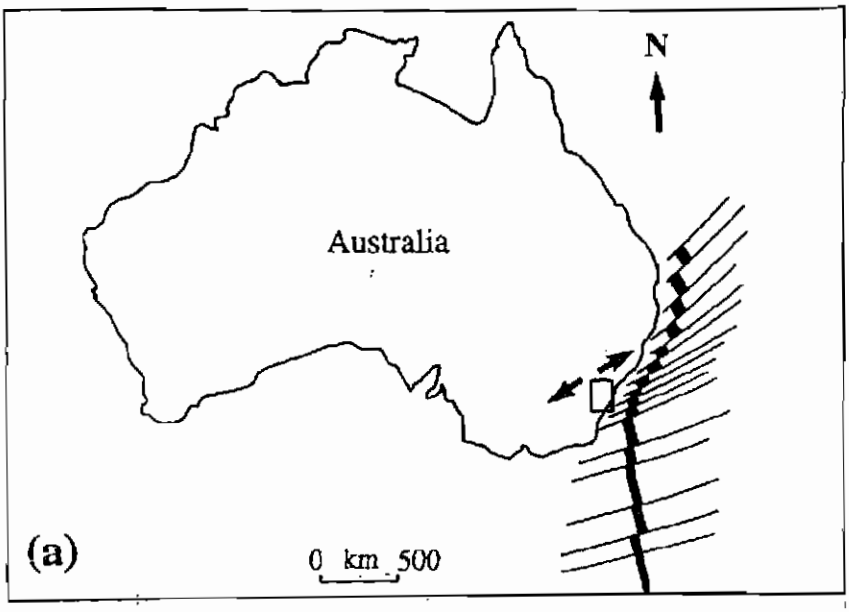
N
Australia
(a)
0 km 500

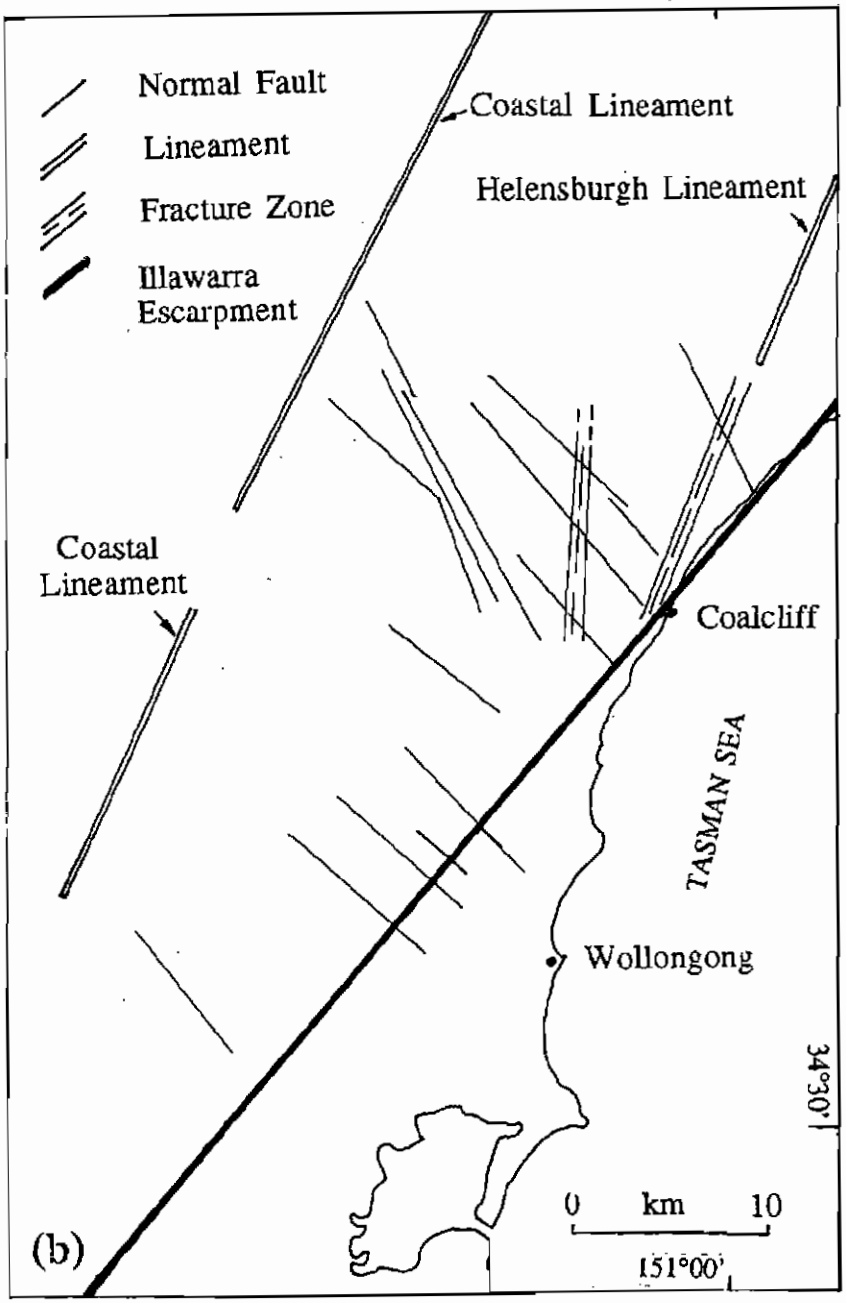
Normal Fault
Lineament
Fracture Zone
Illawarra Escarpment
Coastal Lineament
Helensburgh Lineament
Coastal Lineament
Coalcliff
TASMAN SEA
Wollongong
34°30'
(b)
0 km 10
151°00'

Figure 6.9 (a) The pattern and orientation of sea floor spreading in eastern Australia in the early Paleocene (64 Ma ago) (after Veevers & Powell 1991). (b) In the southeastern Sydney Basin, the NE-ENE direction of tension reactivated pre-existing SE trending faults, and also formed new faults and dykes of similar orientation. The NNE direction of the rift margin is sub-parallel to the zones of N-NNE fractures and dykes as well as some lineaments.

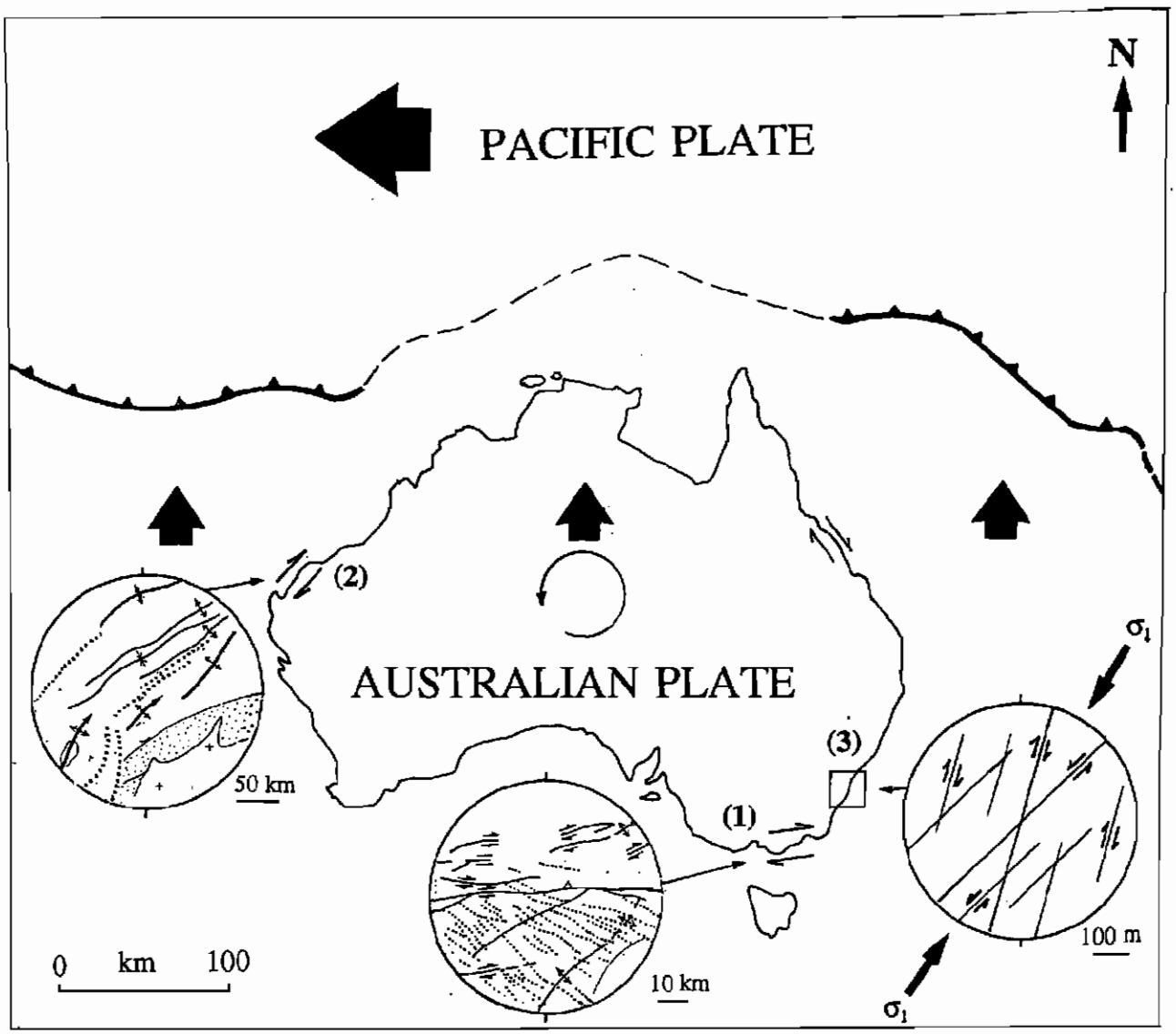

Figure 6.10 Origin of the post-early Tertiary NNE compressional forces in the southeastern Sydney Basin. Northward movement of the Australian Plate, and its collision with the westward moving Pacific Plate, caused anticlockwise motion of the continent, which generated dextral shear along the edge of the continent. Dextral shear in Gippsland Basin (1), dextral shear in Carnarvon-Dampier Basin (2), NNE compression developed in the Illawarra region of the Southern Coalfield, due to dextral shear (3). (Insets 1 & 2 from Veevers & Powell 1984; inset 3 Outcrop 2 at CoalCliff, see Figure 5.1.)

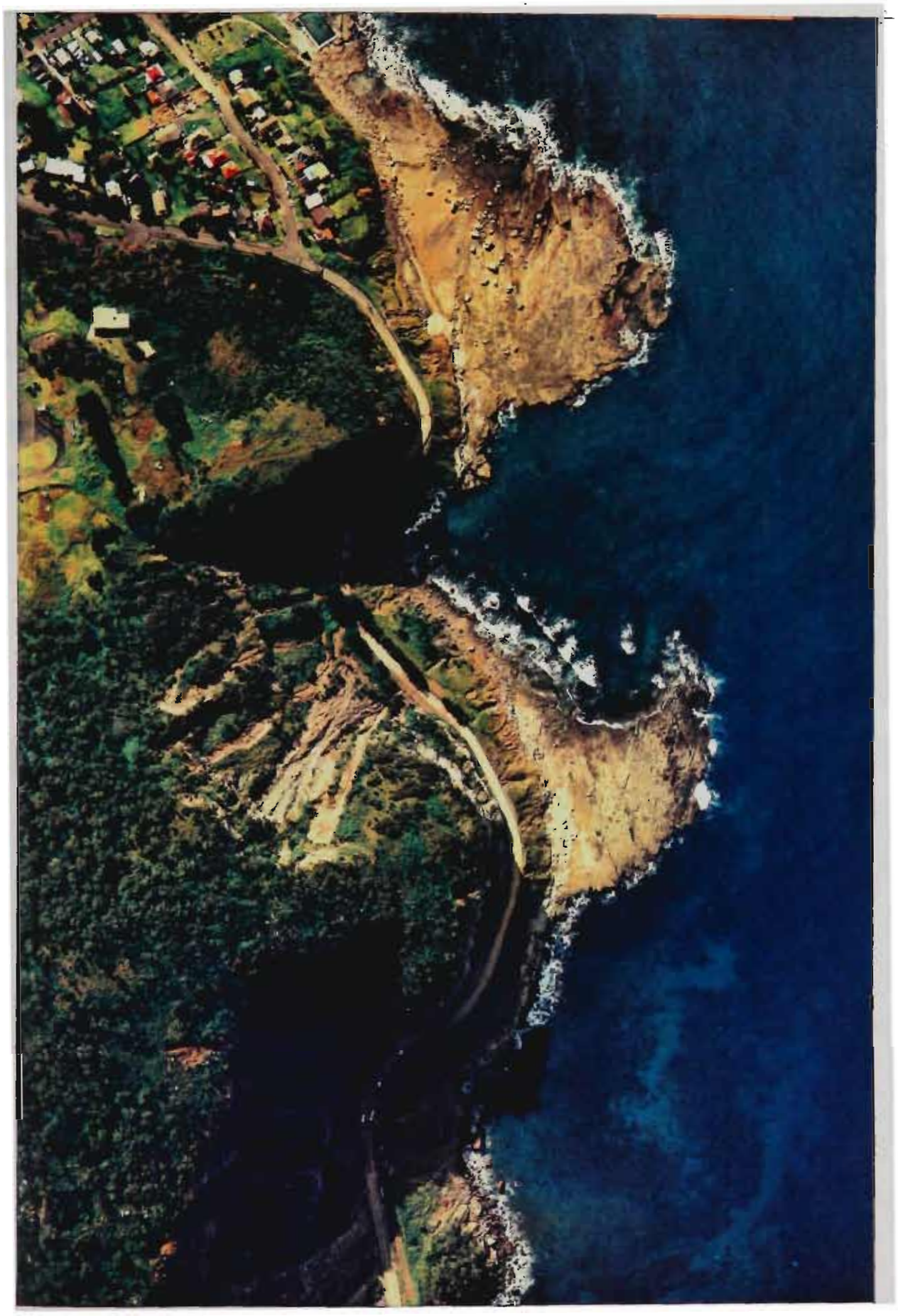

Figure 7.1 Two rock platforms at Coalcliff (Outcrops 1 at the top, and 2 at the base) consisting of the Coal Cliff Sandstone. In each case, the frontal height increases from 0 to 1.5 m from north to south. The embayment between the two platforms developed due to tilting caused by the Harbour Fault, which forms the southern edge of the northern platform.

The photograph was taken one month after the heavy rain of April 1988. Parts of the Lawrence Hargrave Drive, south of Outcrop 2, were still closed due to rain triggered landslips and rock falls (the road is 6 m wide).

(a)

(b)

(c)

(d)

Figure 7.2 Influence of fracturing on surface weathering and erosion. (a) V-shape wearing of recracked parts of joints (5 cm wide and deep) in a 20 cm thick sandstone bed (northern part of Outcrop 7 at Scarborough, north arrow scaled in centimetres and inches). (b) Stepped topography on a thin-bedded and vertically jointed sequence of competent and incompetent rock layers. The deeply eroded vertical fracture strikes 028° (Outcrop 15 at Coledale; looking to the south; the back pack is 40 cm wide). (c) Deep erosion of 040° joints and nonsystematic fractures normal to them, in the remnant of a sandstone bed (Outcrop 7, hammer handle is 33 cm). (d) Raised joints formed due to differential weathering and erosion (Outcrop 24 at Waniora Point, north arrow is 5 cm long).

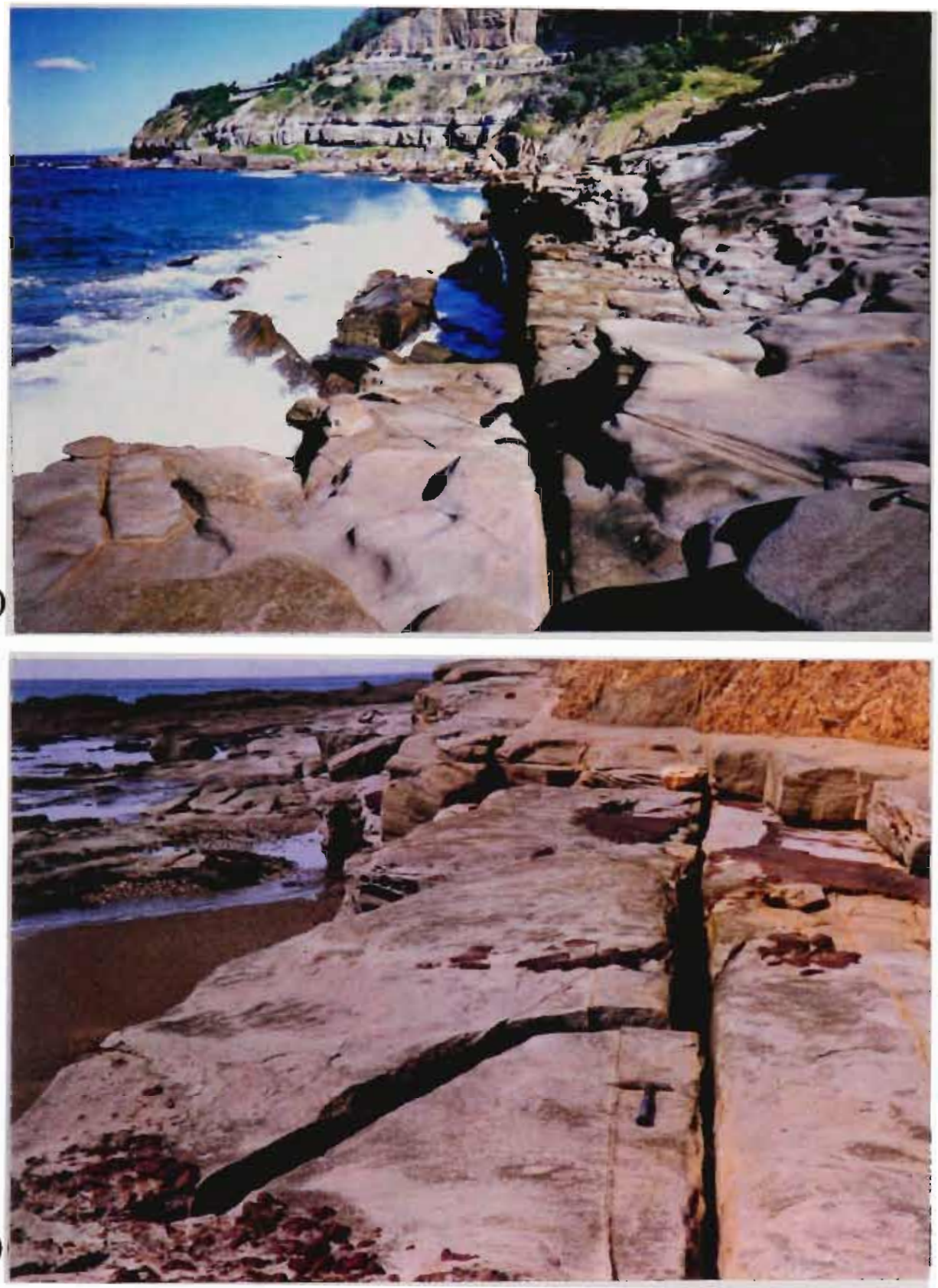

Figure 7.3 (a) Collapse of sandstone blocks along an 045° open fracture at the face of a low tide cliff at the southern end of Outcrop 2 at Coalcliff (looking to the southwest). This locality is also shown in the southernmost part of the lower platform in Figure 7.1. (b) Slight lateral spreading of a block of sandstone detached from the base of the cliff along a 005° vertical fracture (Outcrop 2, hammer handle is 33 cm and points to the north).

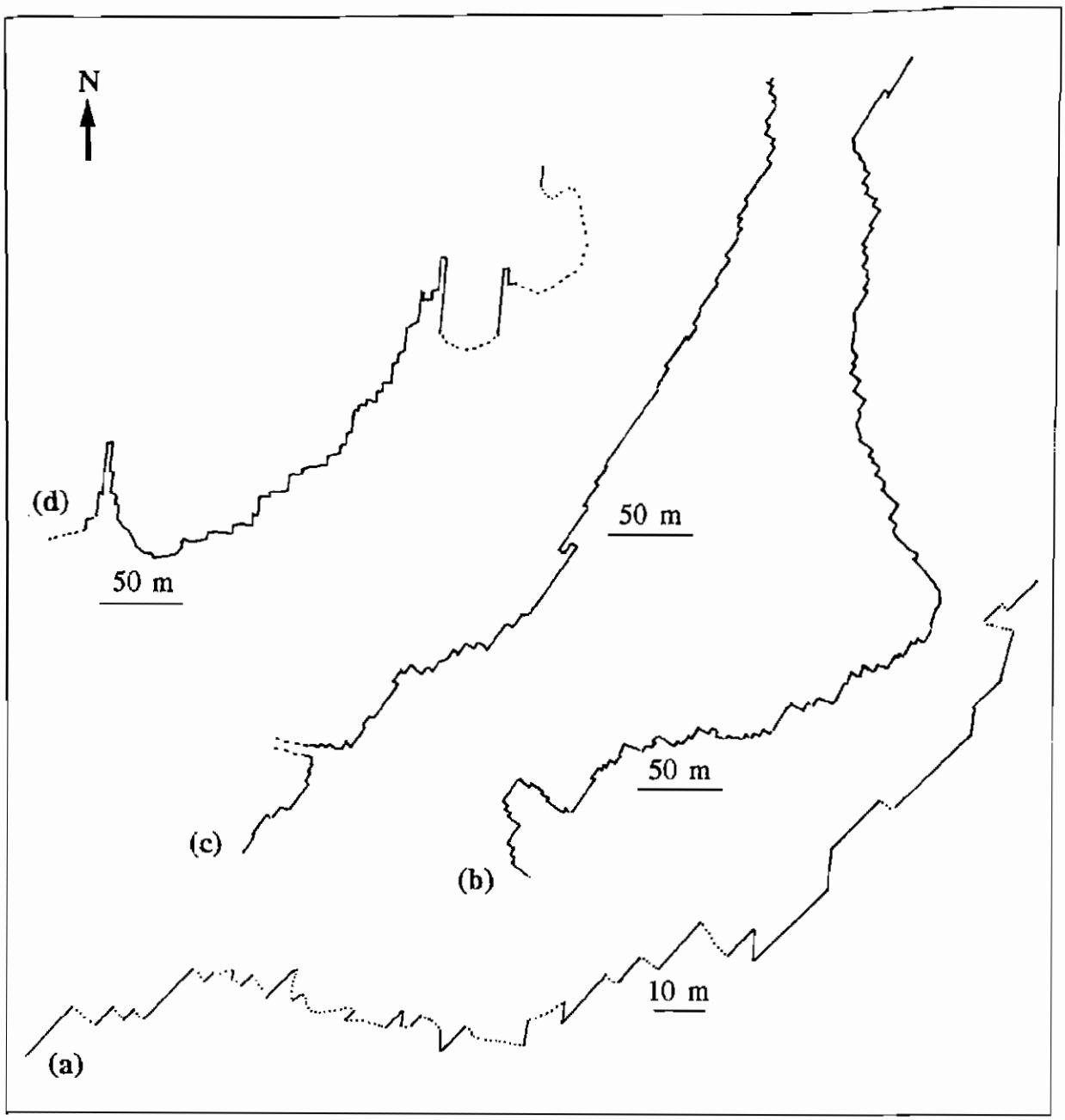

Figure 7.4 Fractures controlling the geometry of platforms. (a) NNE and NE joints (solid lines) as well as nonsystematic joints (dashed lines) forming the seaward edge of the platform at Coalcliff (Outcrop 2). The thickness of sandstone beds are 1-2 m. (b)-(c) NE joints as well as orthogonal nonsystematic joints, forming the outer edges of the platform at Wombarra (Outcrops 11, 12). (d) N-NNE joints, dykes and normal faults forming the edges of the platform at Brickyard Point.

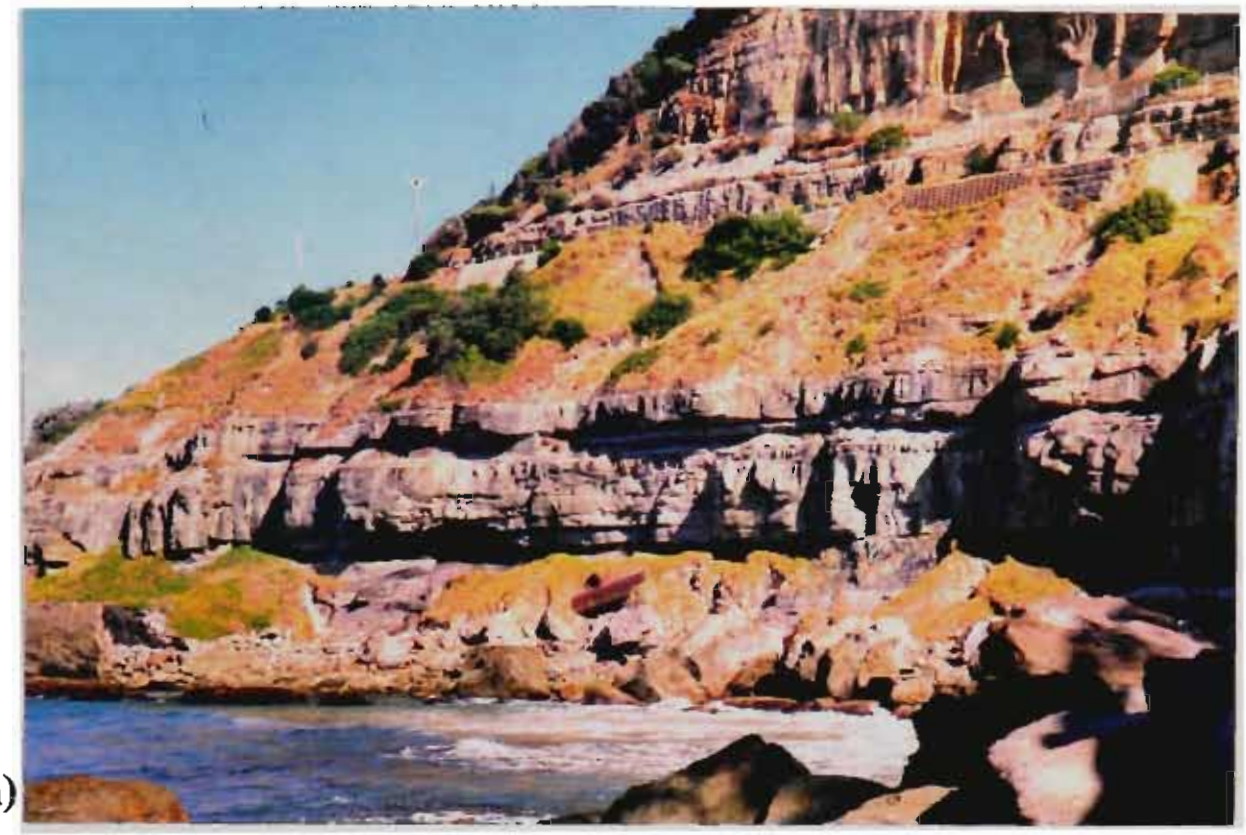

(a)

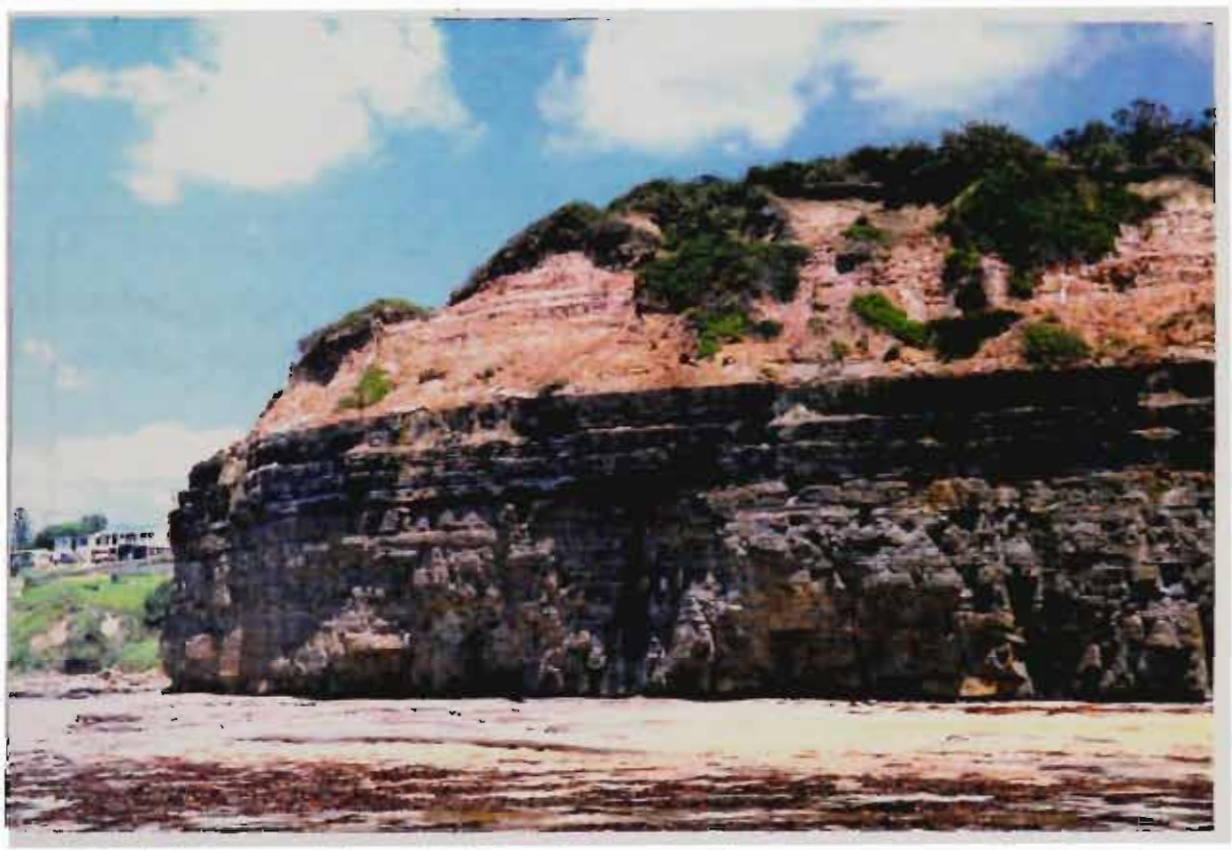

(b)

Figure 7.5 (a) Accumulation of fallen blocks and debris mantle, resulting from both marine and terrestrial processes, at the toe of the cliff near the Coalcliff adit. These fallen blocks reduce the effects of wave action. The road is the Lawrence Hargrave Drive. (b) Platform with horizontal rock partly covered by marine sediments. Undermining at the toe of the headland occurs in a thin carbonaceous claystone. At this locality, recession of the headland due to marine processes, is not significant (Outcrop 12 at Wombarra).

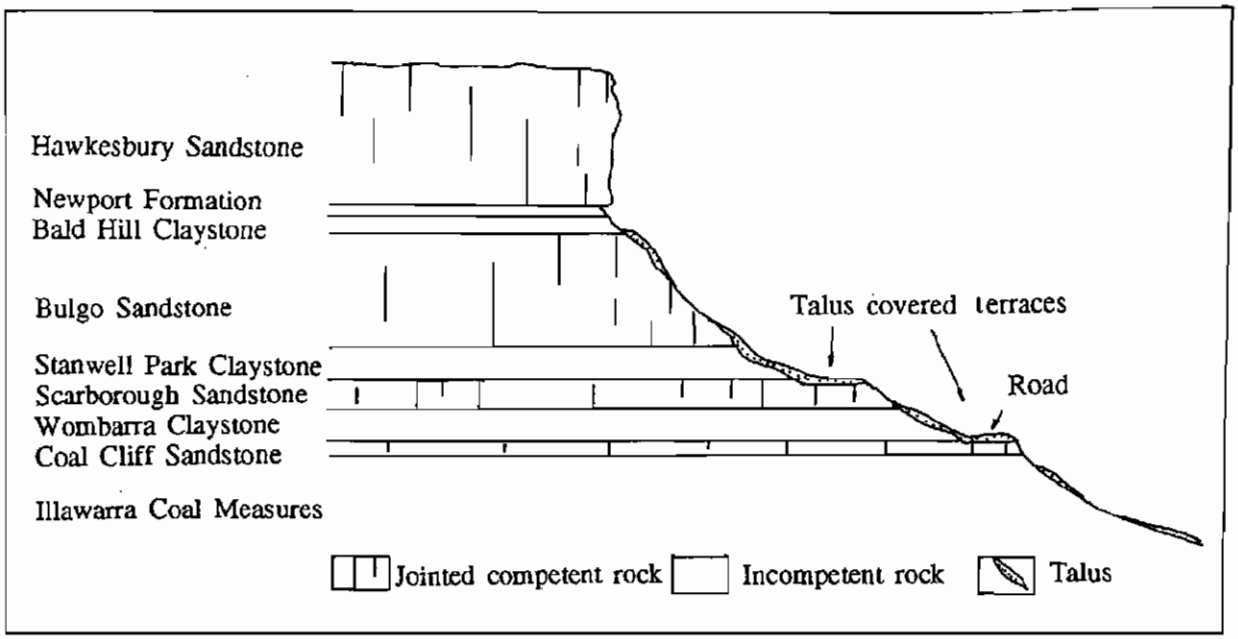

Figure 7.6 Schematic E-W cross section of the Illawarra Escarpment near Scarborough.

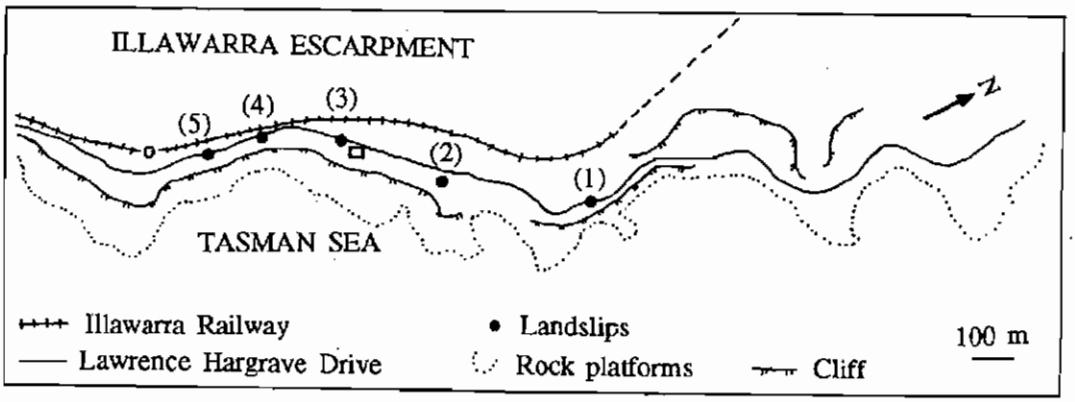

Figure 7.7 Location map for landslips cited in the text.

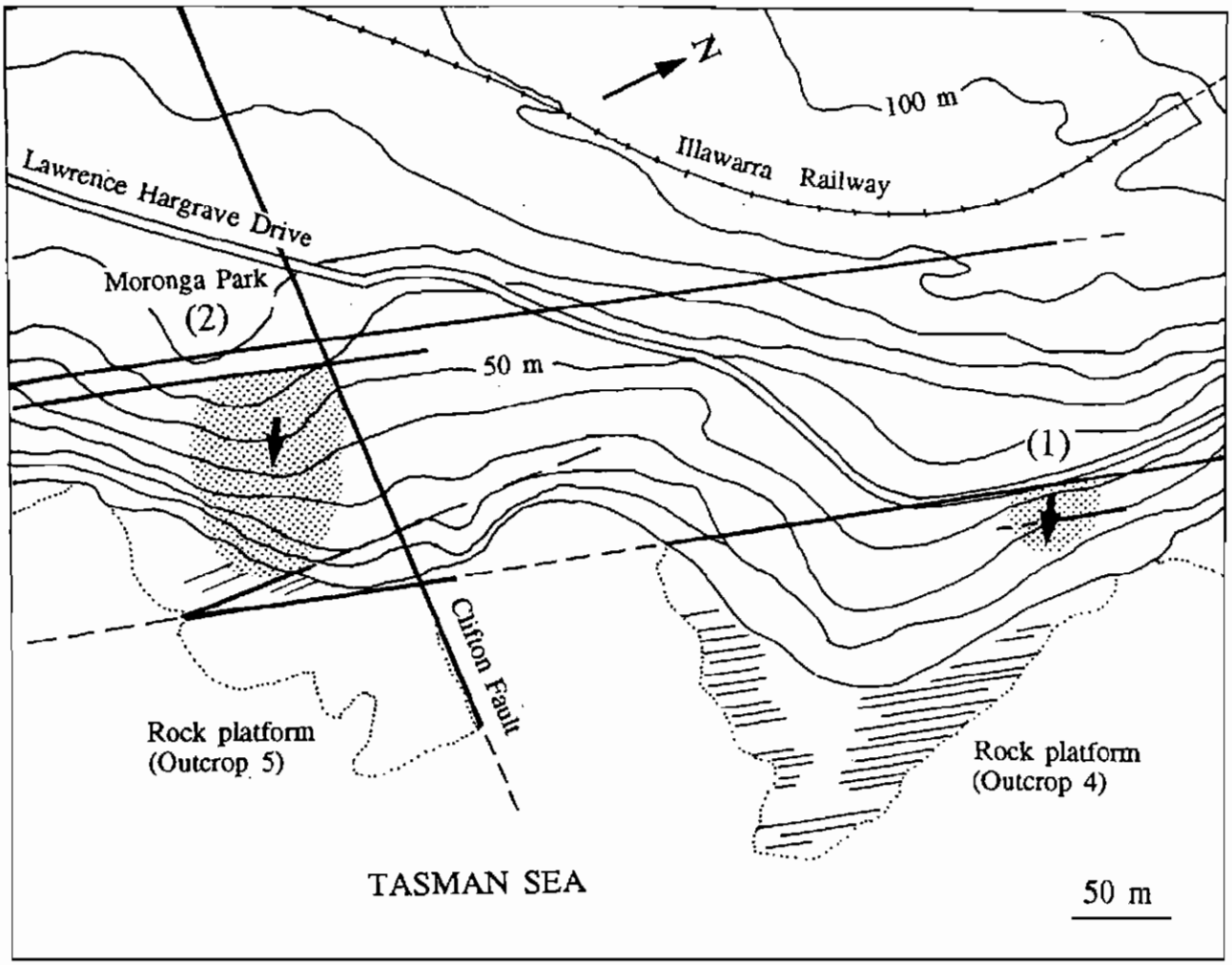

Figure 7.8 Two landslips along the Lawrence Hargrave Drive (1), and at Moronga Park (2), caused by heavy rain of late April 1988. In both cases cracks developed at the crest of slides and coincided with an open fracture in the bedrock.

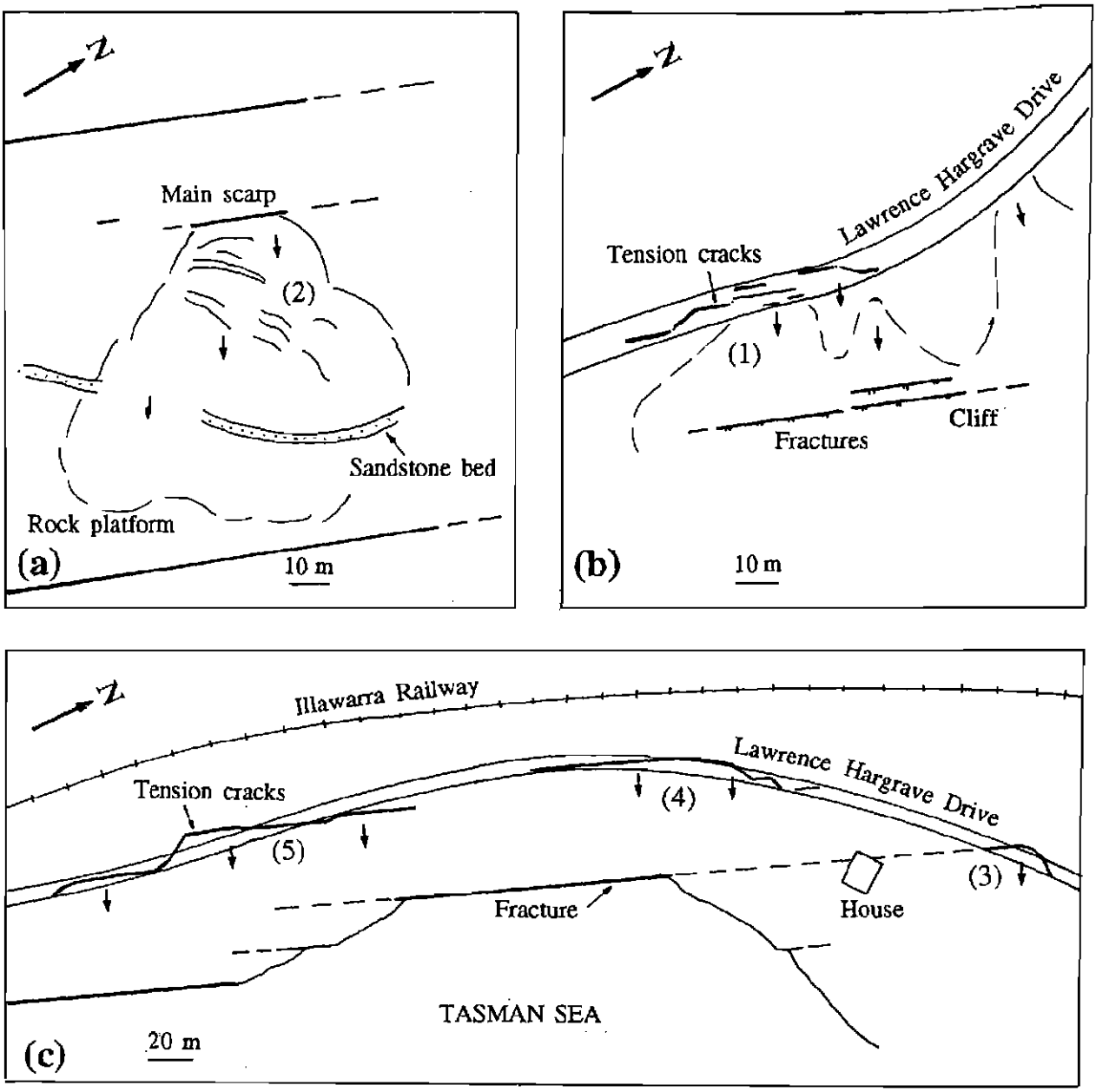

Figure 7.9 The relation between landslips and bedrock fractures. (a)-(b) Landslips at Moronga Park and along the Lawrence Hargrave Drive (point 1 and 2 of Figure 7.8, respectively). (c) Landslips along the section of the road, to the south of the Clifton Hotel.

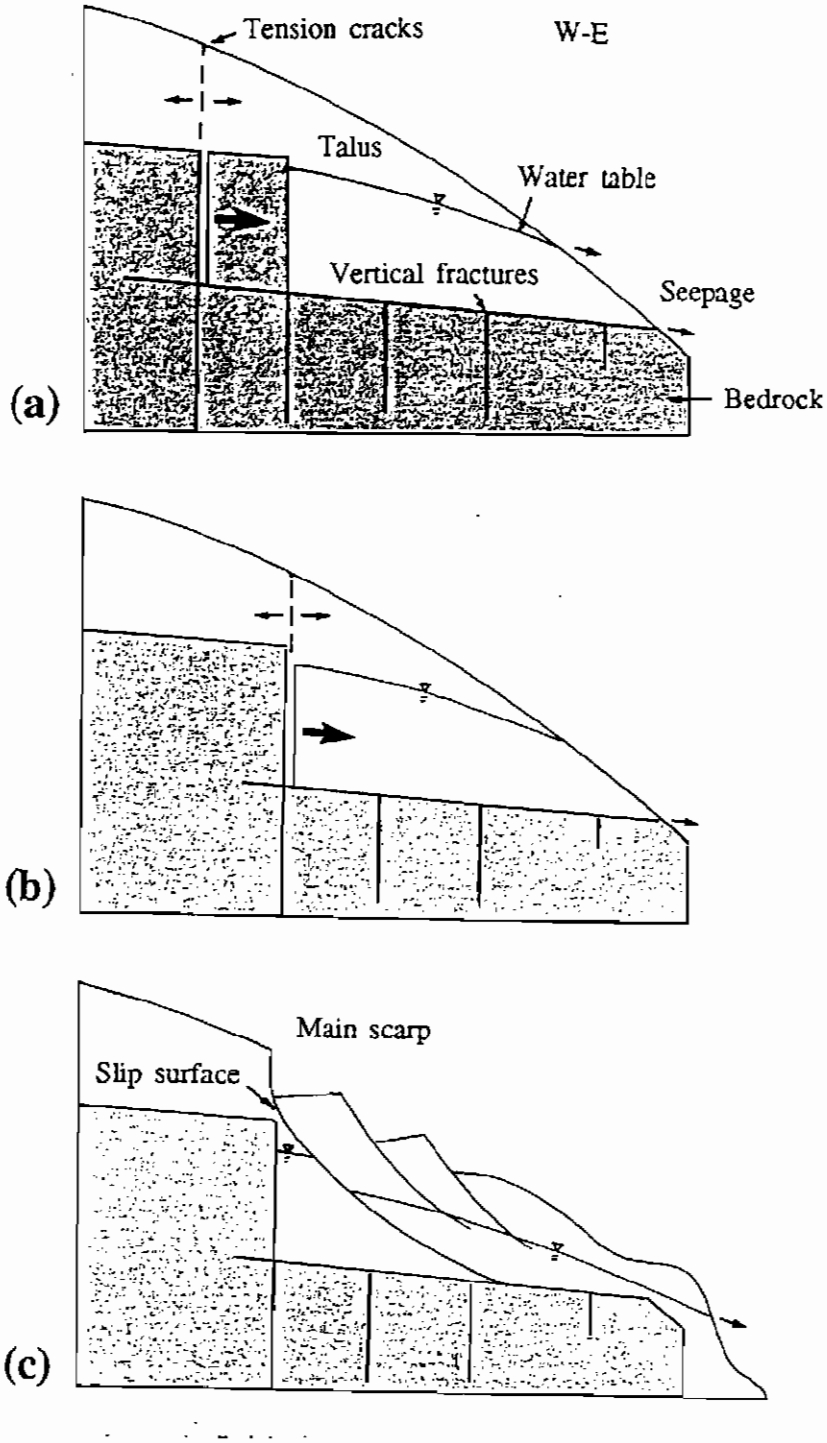

Figure 7.10 (a) Initiation of tension cracks in talus and their relation to vertical fractures in bedrock. Slip surfaces, partly or totally, pass through bedrock. Downslope movement of blocks of rock widens the vertical fractures, which in turn stretches the overlying soil and forms tension cracks. (b) Slip surface at the contact between bedrock and talus. A wedge of soil is developed in front of a drop in bedrock which is the wall of a 015-020° joint. The weight of the wedge has a downhill component. After heavy rain the water table rises in the wedge and reduces the shear strength of talus material. The wedge detaches from bedrock at its back. (c) The tabular, vertical gap forming between the bedrock and the soil stretches the soil above, and forms NNE oriented fractures which mark the crest of future slides.

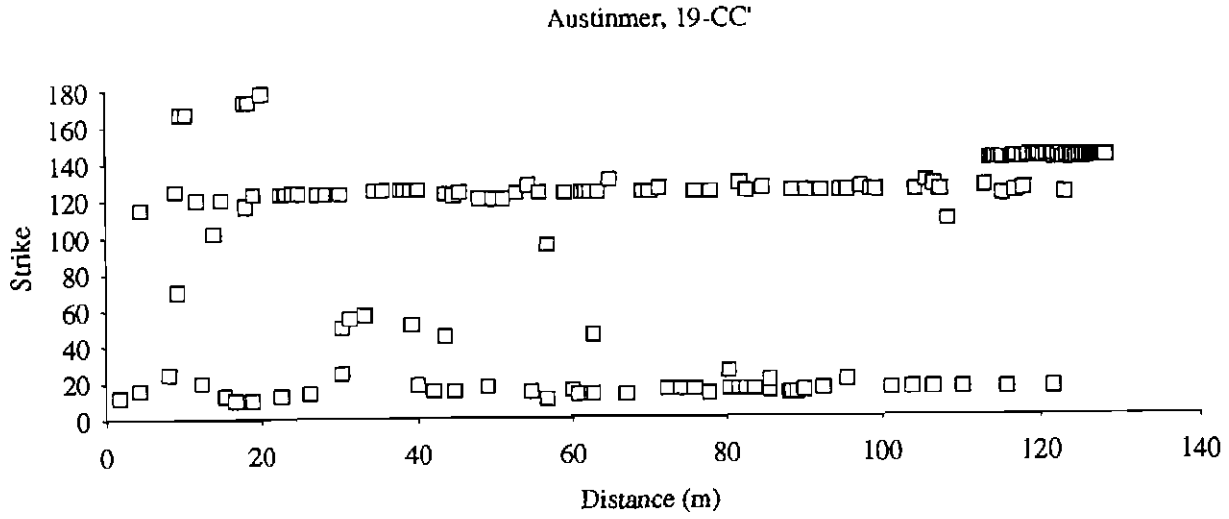

(a)

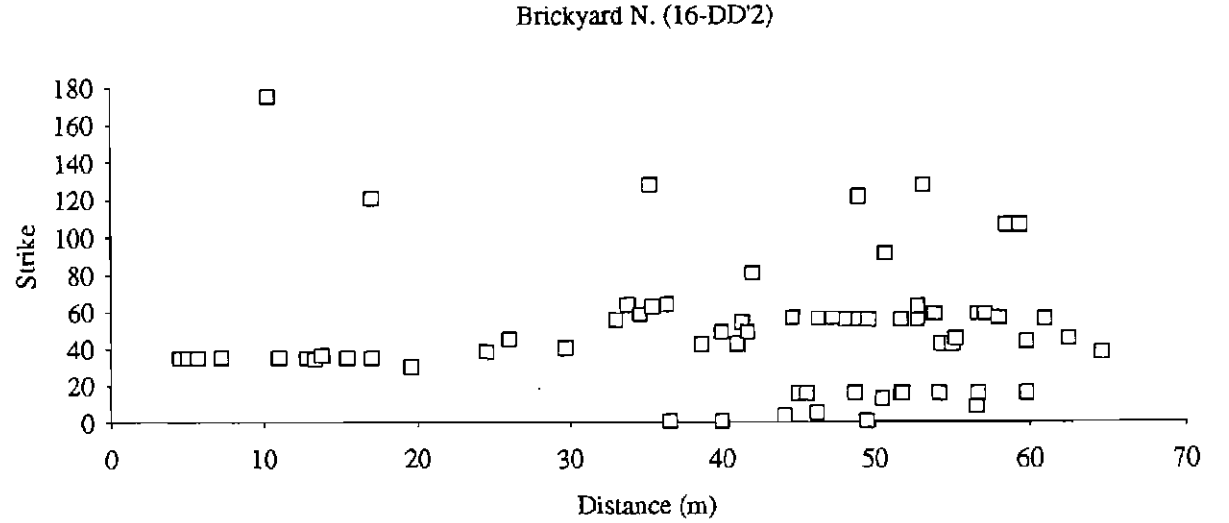

(b)

Figure 7.11 (a) Distribution of joints mapped along the scanline 19-CC', at Austinmer South. Two dominant joint sets in this chart strike 018° and 120°. A third set, strikes 140°, starts at the 110 m mark. Spacing of 140° joints decreases toward the end of the scanline where a dyke with a similar orientation is exposed. (b) Introduction of a 060° striking set at the 34 m mark of scanline 16-DD'2 at Brickyard North. The spacing of this set is almost uniform. These joints are formed in conjunction with a small monocline (see also Figure 4.9).

Table 1.1 Studied outcrops

Outcrop No.	Outcrop Name	Locality	Rock Unit	P*	C*
1	Coalcliff N.	Coalcliff	Coal Clff Sandstone	x	x
2	Coalcliff S.	Coalcliff	Coal Cliff Sandstone	x	x
3	Coalcliff Adit	Clifton	Upper Eckersley Formation	x	x
4	Clifton N.	Clifton	Upper Eckersley Formation	x	x
5	Clifton	Clifton	Allans Creek Formation	x	x
6	Clifton S.	Clifton	Allans Creek Formation	x	x
7	Cape Horn	Scarborough	Allans Creek Formation	x	x
8	Scarborough S.	Scarborough	Kembla Formation	x	x
9	Scarborough S.	Scarborough	Kembla Formation	x	
10	Wombarra N.	Wombarra	Wilton Formation	x	
11	Wombarra Reef	Wombarra	Wilton Formation	x	x
12	Wombarra S.	Wombarra	Wilton Formation	x	x
13	Coledale N.	Coledale	Wilton Formation	x	x
14	Coledale Pool	Coledale	Wilton Formation	x	x
15	Coledale S.	Coledale	Wilton Formation	x	x
16	Brickyard N.	Austinmer	Wilton Formation	x	x
17	Brickyard Point	Austinmer	Wilton Formation	x	x
18	Bell Point	Austinmer	Wilton Formation	x	x
19	Austinmer S.	Austinmer	Wilton Formation	x	x
20	Thirroul Rail	Thirroul	Erins Vale Formation		x
21	Thirroul	Thirroul	Erins Vale Formation	x	x
22	Bulli Point	Bulli	Erins Vale Formation	x	x
23	Bulli Rail	Bulli	Erins Vale Formation		x
24	Waniora Point	Bulli S.	Erins Vale Formation	x	x
25	Collins Rock	Woonona	Erins Vale Formation	x	
26	Bellambi Point	Bellambi	Pheasant Nest Formation	x	
27	Towradgi	Towradgi	Pheasant Nest Formation	x	
28	Wollongong N.	Wollongong	Broughton Formation	x	
29	Wollongong	Wollongong	Broughton Formation	x	x
30	Wollongong S.	Wollongong	Broughton Formation	x	x

* Orientation of studied outcrops: P=horizontal platform, C=cliff face.

Table 1. 2 Scanline data

Number	Name	Location	Direction	Length	Measured	Coordinate (begining)		Coordinate (end)	
			(deg)	(m)	Fractures	mE	mN	mE	mN
1	11-HH'	Wombarra N.	70	279	157	311550	6204520	311815	6204620
2	11-II'	Wombarra N.	5	182.5	55	311740	6204710	311760	6204020
3	12-AA'	Wombarra S.	130	45.5	44	311240	6204050	311280	6204020
4	12-BB'	Wombarra S.	125	57	46	311285	6204110	311335	6204075
5	12-CC'	Wombarra S.	135	47	33	311385	6204180	311420	6204150
6	12-DD'	Wombarra S.	55	300	156	311195	6204020	311440	6204190
7	12-EE'	Wombarra S.	20	87	21	311445	6204195	311480	6204280
8	12-GG'	Wombarra S.	175	139	84	311555	6204380	311545	6204515
9	13-AA'	Coledale	80	44.7	54	311125	6203650	311080	6203635
10	13-BB'	Coledale	80	52	43	311085	6203620	311035	6203610
11	13-CC'	Coledale	80	40	30	311030	6203595	310995	6203590
12	13-DD'	Coledale	80	51.5	38	311155	6203435	311115	6203625
13	13-EE'	Coledale	80	79	50	311220	6203640	311150	6203625
14	13-FF'	Coledale	80	29.3	23	311060	6203740	311030	6203735
15	13-GG'	Coledale	130	100	82	311145	6203705	311220	6203640
16	13-HH'	Coledale	40	40	36	311200	6203695	311175	6203665
17	14--II'	Coledale	10	206	73	310995	6203590	310960	620395
18	15-JJ'	Coledale	90	199	195	310940	6203190	310745	6203150
19	14-KK'	Coledale	20	100	41	310880	6203410	310850	6203320
20	14-LL'	Coledale	75	57.6	31	310890	6203330	310825	3203315
21	15-MM'	Coledale	165	170.4	119	310880	6203160	310835	3203325
22	16-AA'	Brickyard N.	177	95.5	32	310450	6202590	310445	6202690
23	16-BB'	Brickyard N.	137	54	31	310440	6202635	310480	6202600
24	16-CC'	Brickyard N.	58	65.5	74	310435	6202500	310490	6202535
25	16-DD'	Brickyard N.	165	97.4	58	310440	6202615	310465	6202525
26	16-DD'2	Brickyard N.	165	64.6	69	310405	6202565	310470	6202505
27	16-EE'	Brickyard N.	125	37.2	9	310460	6202500	310425	6202520
28	17-AA'	Brickyard	32	200	266	310530	6202370	310415	6202200
29	17-BB'	Brickyard	107	81	118	310530	6202370	310605	6202345
30	17-CC'	Brickyard	70	21	28	310390	6202210	310365	6202200
31	17-DD'	Brickyard	45	96.5	84	310370	6202225	310300	6203155
32	17-EE'	Brickyard	25	151	117	310220	6202165	310145	6202030
33	18-AA'	Austinmer	75	75	84	310125	6201885	310195	6201900
34	18-BB'	Austinmer	55	78	105	310085	6201850	310020	6201805
35	18-CC'	Austinmer	70	114	125	310095	6201835	310200	6201880
36	19-AA'	Austinmer S.	50	47	63	309910	6201560	309870	6201530
37	19-BB'	Austinmer S.	25	134	85	309865	6201570	309810	6201450
38	19-CC'	Austinmer S.	40	128	164	309715	6201295	309630	6201195
39	19-DD'	Austinmer S.	32	67	163	309665	6201230	309630	6201175
40	19-EE'	Austinmer S.	15	136	170	309635	6201220	309600	6201095
41	20-AA'	Thirroul Rail	165	83	95	308190	6199635	308165	6199715
42	21-AA'	Thirroul	15	132	120	309115	6200250	309070	6200115
43	22-AA'	Bulli	135	240	256	309010	6199300	309180	6199130
44	22-BB'	Bulli	112	180	85	309165	6199135	309345	6199060
45	22-CC'	Bulli	120	109	98	309210	6199125	309350	619908
46	22-DD'	Bulli	90	29.5	71	309350	6199080	309380	619980
47	22-EE'	Bulli	25	10	28	309380	6199080	309375	6199065
48	22-FF'	Bulli	120	49.5	60	309435	6199070	309480	6199040
49	23-AA'	Bulli Rail	15	143	93	308235	6199200	308195	619905
50	25-AA'	Woonona	86	125	200	308805	61976100	308925	6197110
51	25-BB'	Woonona	10	45.7	54	308895	6197170	308900	6197215
52	25-CC'	Woonona	15	49.8	96	308930	6197115	308940	6197165
53	26-AA'	Bellambi	140	28	37				
			Total	5273.7	4549				

* Coordinates from orthophoto maps , 1:4000

Table 1.3 Stratigraphy of the Southern Coalfield (Bowman 1974; Bamberry 1992).

Table 2.1. Mean orientations of systematic joint sets in different outcrops in degrees.

Zone	Outcrop No.	Location	0		45		90		135		180
			N	NNE	NE	ENE	E	ESE	SE	SSE	
	1	Coalcliff N.	10	20	46				120	153	
	2	Coalcliff S.	175	13, 24	46						
	3	Coalcliff Adit		14					122		
	4	Clifton N.		18	38		100		140		
Northern	5	Clifton		13, 25			87		135		
zone	6	Clifton S	5	20			88		138	167	
	7	Scarborough N.	7	33	52		92		140	163	
	8	Scarborough	3	23			90		140	158	
	9	Scarborough S.	175	18, 28	37		92		128	170	
	10,11	Wombarra N.		18	40		87		125	164	
	12	Wombarra	0	13	30,40		90		122	167	
	13	Coledale N.	5	20	40		108		127	167	
	14	Coledale	0	28	37				123		
Central	15	Coledale S.	0		36	70	90		127		
zone	16	Brickyard N.	3	18	32	55	90		128	162	
	17	Brickyard	0	13		56	90		128		
	18	Austinmer	0			57	94		118	162	
	19	Austinmer S.		13		60	90		128, 140	160	
	20	Thirroul R.	8	28		75	98		118, 126		
	21	Thirroul				68	88		128	159	
	22	Bulli	0	13	40		90	113		170	
Southern	23	Bulli R.		13		73	100		120		
zone	24	Waniora		25		57	80			158	
	25	Woonona		13	38	73	100		128	158	
	26	Bellambi		11	38						
	27,28	Wollongong N.		13	40	70			128		
	29	Wollongong		13	38		98				
	30	Wollongong S.		13, 20	33	68			128	170	

Table 2.2. Major joint sets with regional distribution, southeastern Sydney Basin, NSW.

Group	Orientation	Range of strike (degree)	Average (degree)	General characteristics
I	N-NNE	350-20	10	(Numerous, straight, vertical, segmented, long, early formed, filled with calcite or siderite, sinistral or dextral displacement along strike)
	NE	38-48	43	
	SE	122-130	128	
II	NNE	15-30	24	(Rare, straight or slightly curved, vertical, short, young, fine, mostly closed, terminate against members of the first group).
	E	90-100	97	
	SSE	160-167	167	

Table 2.3 Comparison between orientation of regional joints in northern and central zones.

	N-NNE	NE	SE
Northern zone	13	48	138
Central Zone	5	42	128
Difference	8	6	10

Table 2.4. Mean orientations of the NE and SE joint sets in different outcrops, and the dihedral angle between them.

Outcrop No.	Mean strike		Dihedral angle (degree)
	NE set	SE set	
1	48	150	78
2	46		
3		122	
4		140	
5		113	
6		137	
7	32	122	90
8	50	140	90
9	38	128	90
10, 11, 12	43	125	82
13, 14, 15	33	127	86
16	33	128	85
17	58	128	70
18	58	118	60
19	75	142	70
20	70	118	48
21	68	127	59
22	43	113	70
23	73	123	50
24, 25		131	
26	45		
27, 28	42		
30	33	123	90

Table. 3.1 Dykes exposed along the coast between Stanwell Park and Port Kembla

Location	Strike (degree)	Dip (degree)	Rock type	Thickness cm	Host rock		Adjacent joints (deg.)	Regional joints (deg.)	Refrence (scanline No.)
					Formation	Rock type			
Stanwell Park		90	Basalt	80	Bulgo Fm	Sandstone	25		
Wombarra	110	90	Washed away	40	Wilton Fm	Laminite*	110	NE (40) NW (125)	12-DD'
Coledale	10	90	Weathered to clay	150	Wilton Fm	Laminite*	5 to 14 (rare)	NE (10) NW(120)	13-GG'
Brickyard	3	90	Weathered to clay	50	Wilton Fm	Laminite*	0-10 (rare)	N (5) NE (50) NW (125)	17-BB'
Austinmer South	140	90	Weathered to clay	180	Wilton Fm	Laminite*	140	NNE (10) NW (125)	19-DD' 19-EE'
Bulli Point-1	23	85W	Diorite	5 to 10	Erins Vale Fm	Sandstone	20 to 25	N (175) NNE (10) NE (50)	22-AA'
Bulli Point-2	40	90	Weathered to clay	80	Erins Vale Fm	Sandstone	40	N (175) NW (120)	22-BB' 22-CC'
Bulli Point-3	25	90	Weathered to clay	40	Erins Vale Fm	Sandstone	22-25	NW (120)	22-FF'
Red Point (Port Kembla)	100-120 swarm	90	Basalt	50-300	Broughton Fm	Sandstone	100 to 125		

* Thin bedded and laminated sandstone, siltstone and mudstone.

Table 4.1 Map-scale anticlinales and related normal faults in southeastern Sydney Basin.

	Anticline			Neighboring normal faults					
	Name	Colliery	Axial trend	Fault name	Strike	Dip	Throw	Length	Coments
1	Woronora	West Cliff		Scarborough	NW	NE	57 m		Major fault zone
				Pig Farm	NW	SW	35 m	3 km	Fault zone
2	Waterfall	Metropolitan	WNW-NW	Unnamed	140-150	SW	30 m		Fault zone
				Metropolitan	160	NE	70 m		Major fault zone
3	Coal Cliff	Coal Cliff	NW	Pig Farm	NW	SW	35 m	3 km	Falt zone
				Coal Cliff	NW	SW	65 m		Fault zone
				Scarborough	NW	NE	57 m		Major fault zone
4	Unnamed	West Cliff	NW	Four Mile	NW	SW	60 m	15 km	Major fault
				Unnamed	130	44-85	21 m	5 km	
5	Unnamed	Bulli	NW	Coledale	155	SW	60 m	5 km	
				Stokes	155	NE	30-40 m	15 km	
6	Bulli	Bulli	NW	Bulli	NW	SW	20-90	6 km	Fault zone
				Unnamed	NW	NE	10 m	3 km	
7	Kemira Dome	Kemira	W-NW						
8	Cordeaux Dome	Nebo	NW-NNW						
9	Unnamed	Wongawilli		Unnamed zone	NW	SW			
				Wongawilli	NW	NE	22-50 m	5 km	

* For the first 6 structures the data are from Bulli seam level and for the last 2 from the Wongawilli seam level.

* Data from Acril (1989) and Lohe et al (1992)

APPENDICES

APPENDICES

(1) Symbols used in maps and scanlines

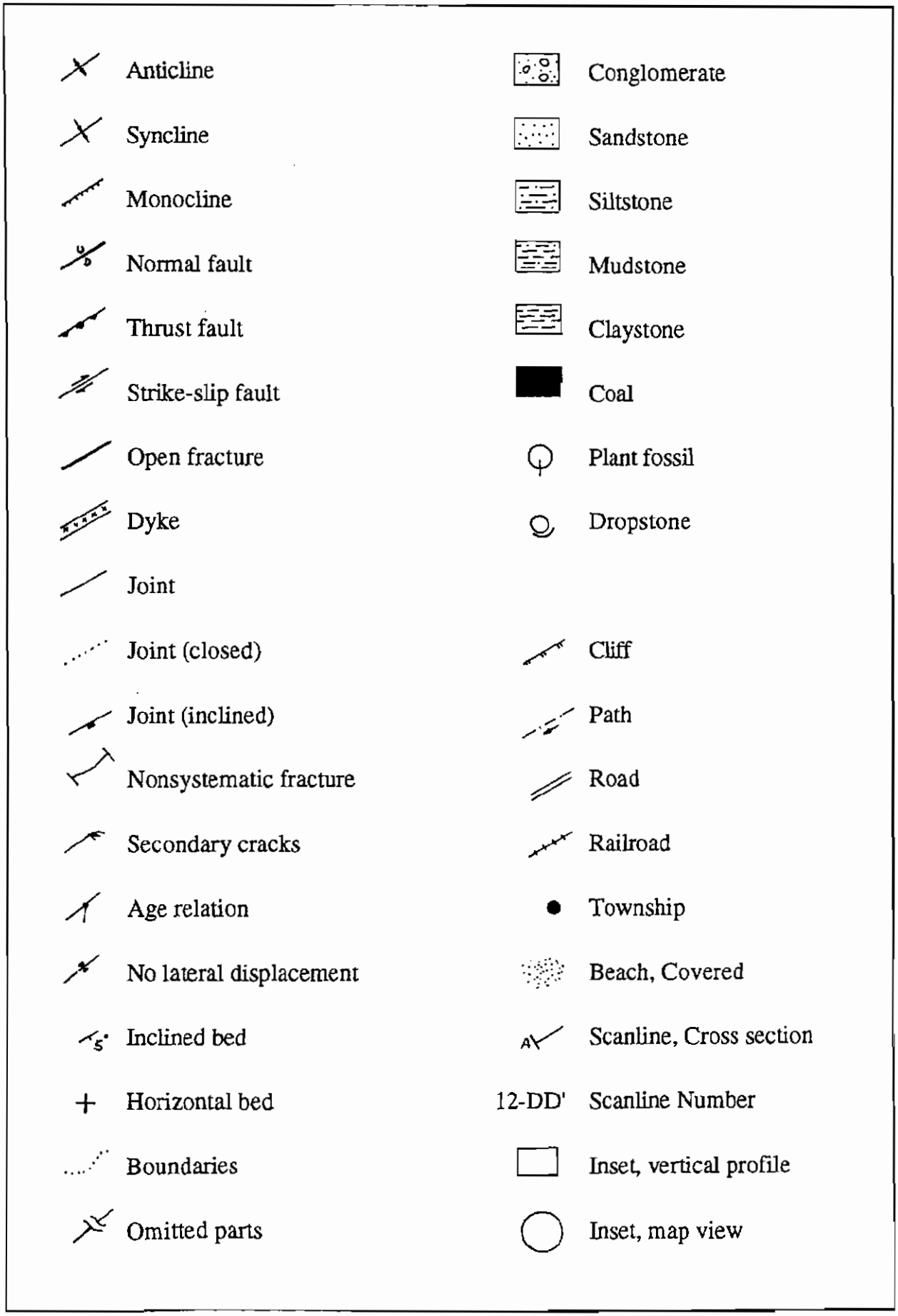

(2) Location maps of outcrops and scanlines

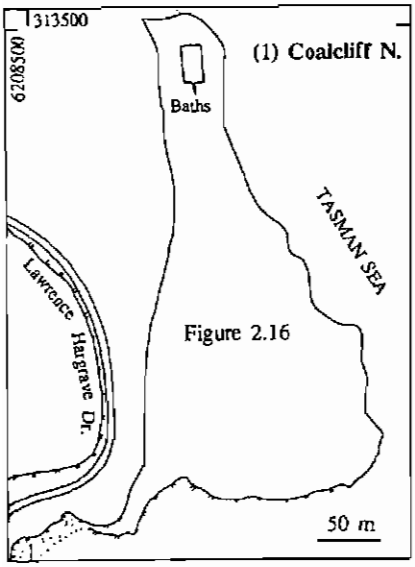

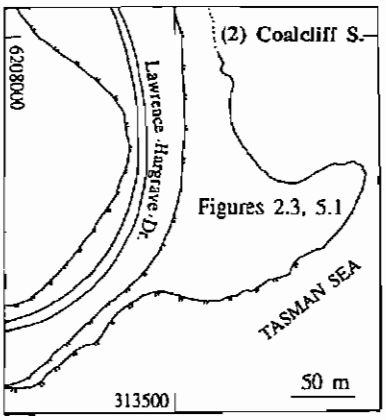

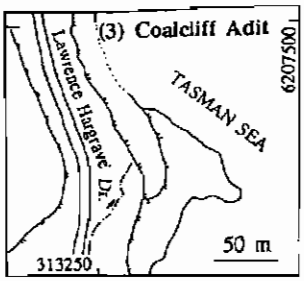

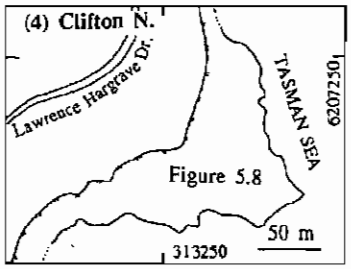

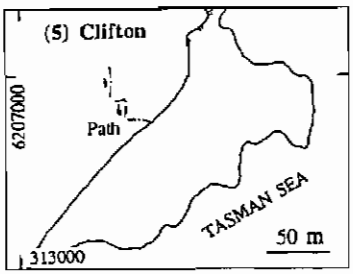

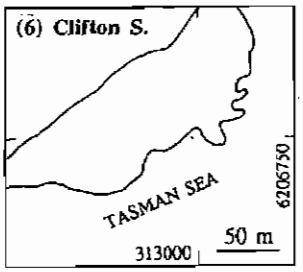

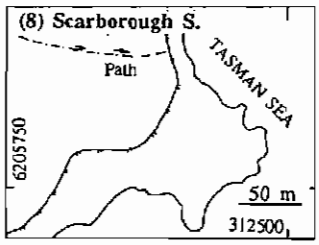

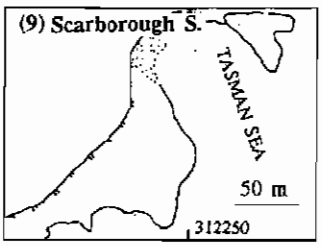

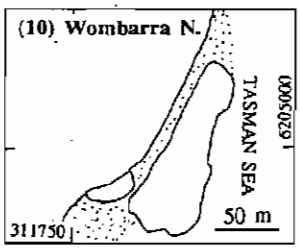

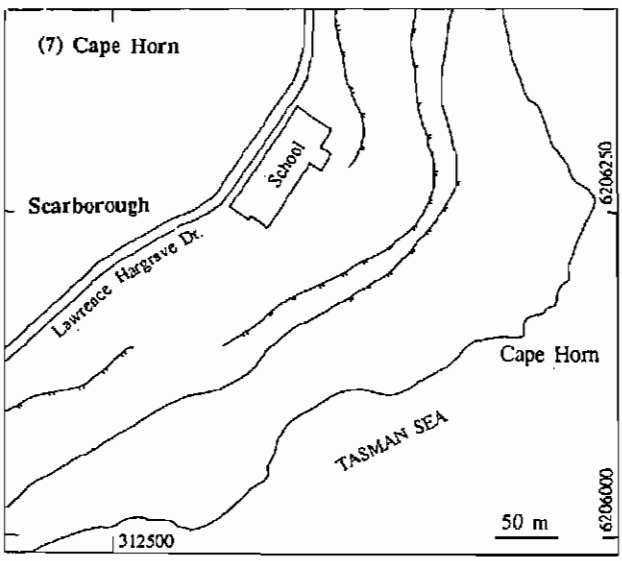

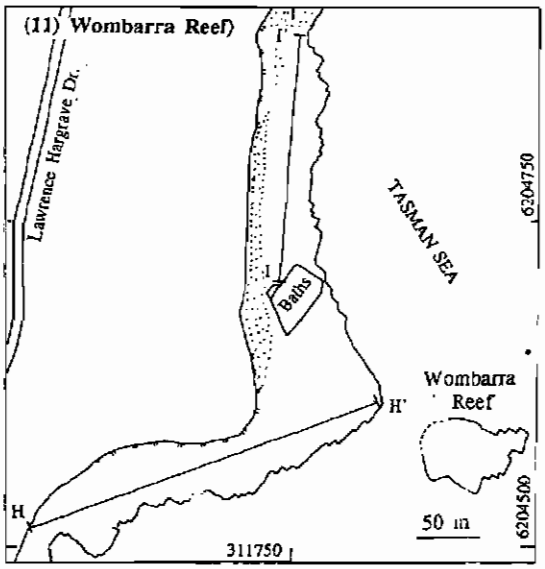

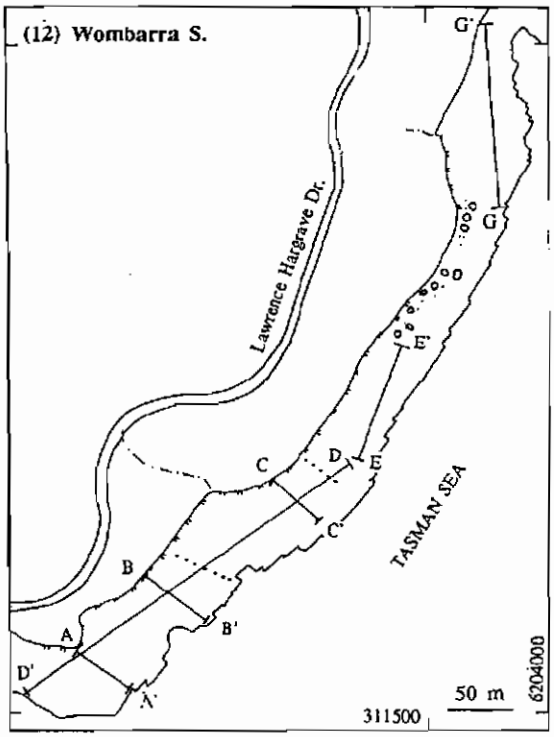
(12) Wombarra S.
Lawrence Hargrave Dr.
TASMAN SEA
50 m
311500
6204000

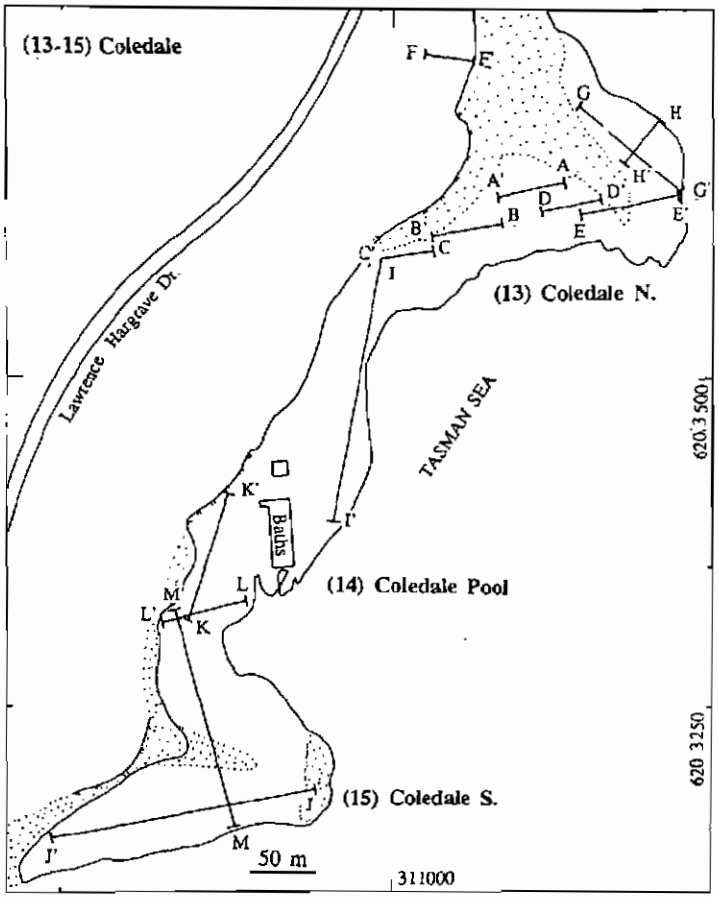
(13-15) Coledale
(13) Coledale N.
(14) Coledale Pool
(15) Coledale S.
Lawrence Hargrave Dr.
TASMAN SEA
Baths
50 m
311000
620 3500
620 3250

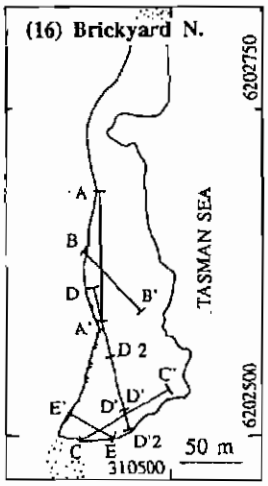
(16) Brickyard N.
TASMAN SEA
50 m
310500
6202750
6202500

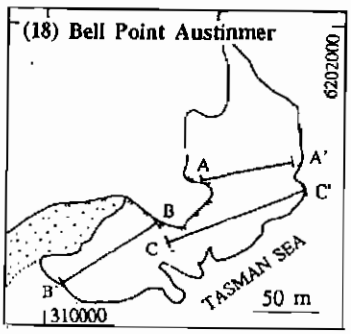
(18) Bell Point Austinmer
TASMAN SEA
50 m
310000
6202000

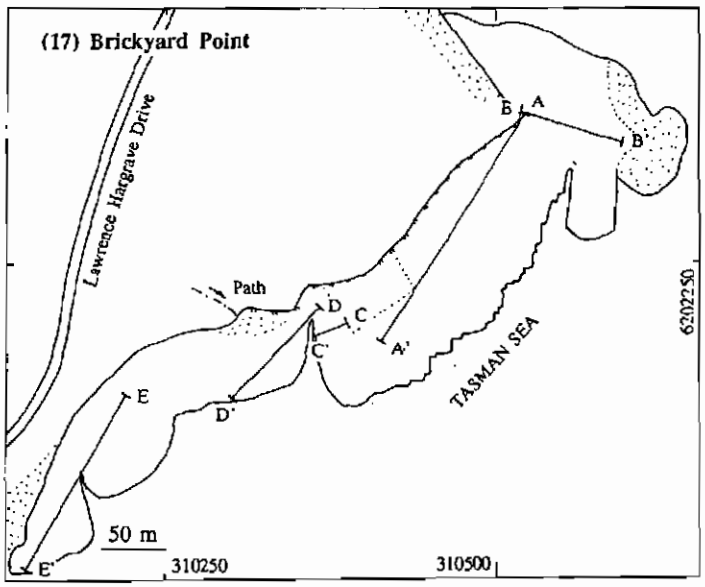
(17) Brickyard Point
Lawrence Hargrave Drive
Path
TASMAN SEA
50 m
310250
310500
6202250

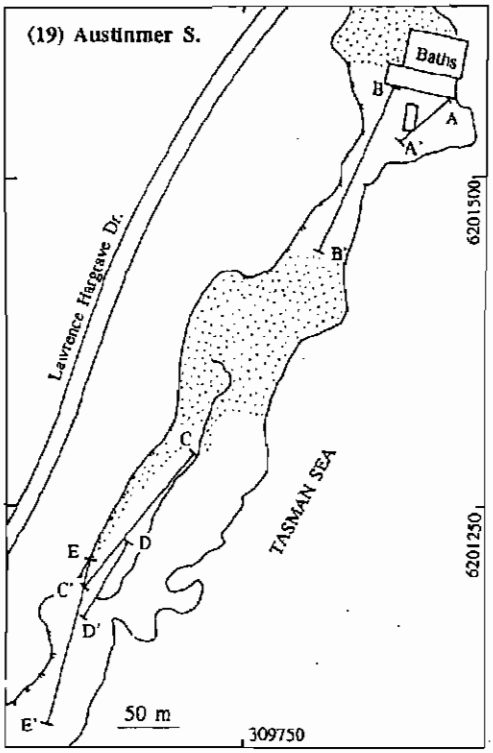
(19) Austinmer S.
Baths
Lawrence Hargrave Dr.
TASMAN SEA
6201500
6201250
309750
50 m

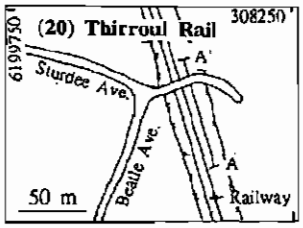
(20) Thirroul Rail
308250
6199750
Sturdee Ave.
Beatle Ave.
Railway
50 m

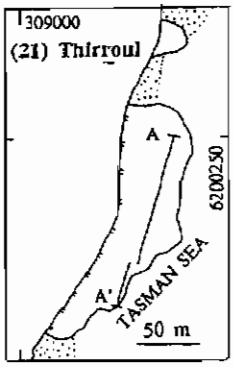
309000
(21) Thirroul
6200250
TASMAN SEA
50 m

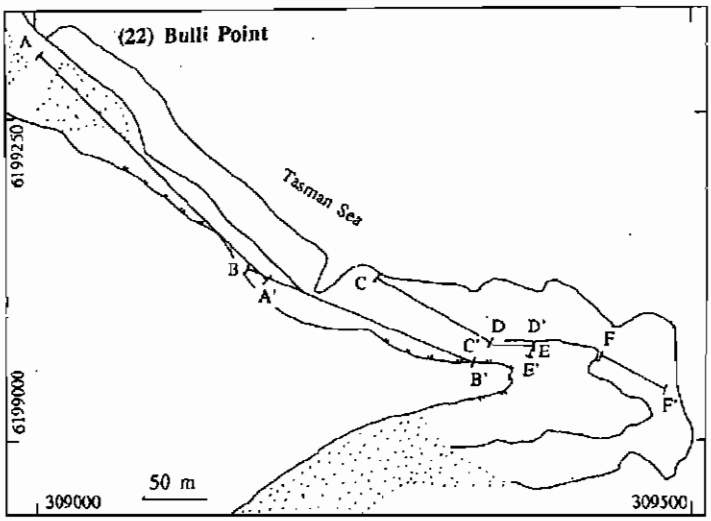
(22) Bulli Point
6199250
Tasman Sea
6199000
309000
309500
50 m

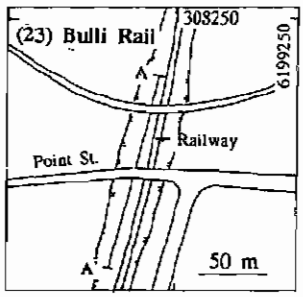
(23) Bulli Rail
308250
6199250
Railway
Point St.
50 m

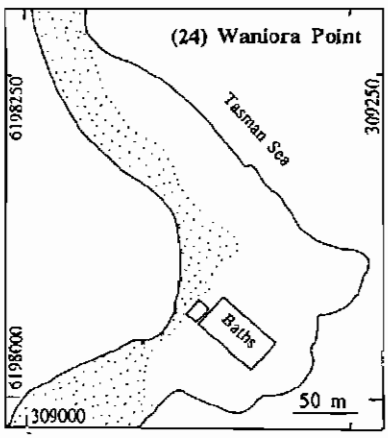
(24) Waniora Point
6198250
309250
Tasman Sea
Baths
6198000
309000
50 m

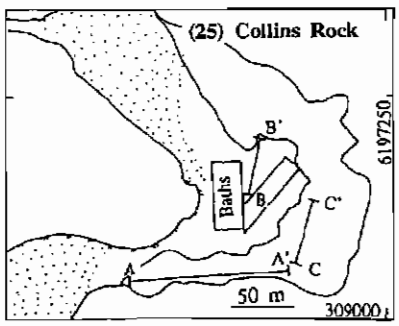
(25) Collins Rock
6197250
Baths
50 m
309000

(3) Fracture maps of selected outcrops

Coalcliff North (Outcrop 1)

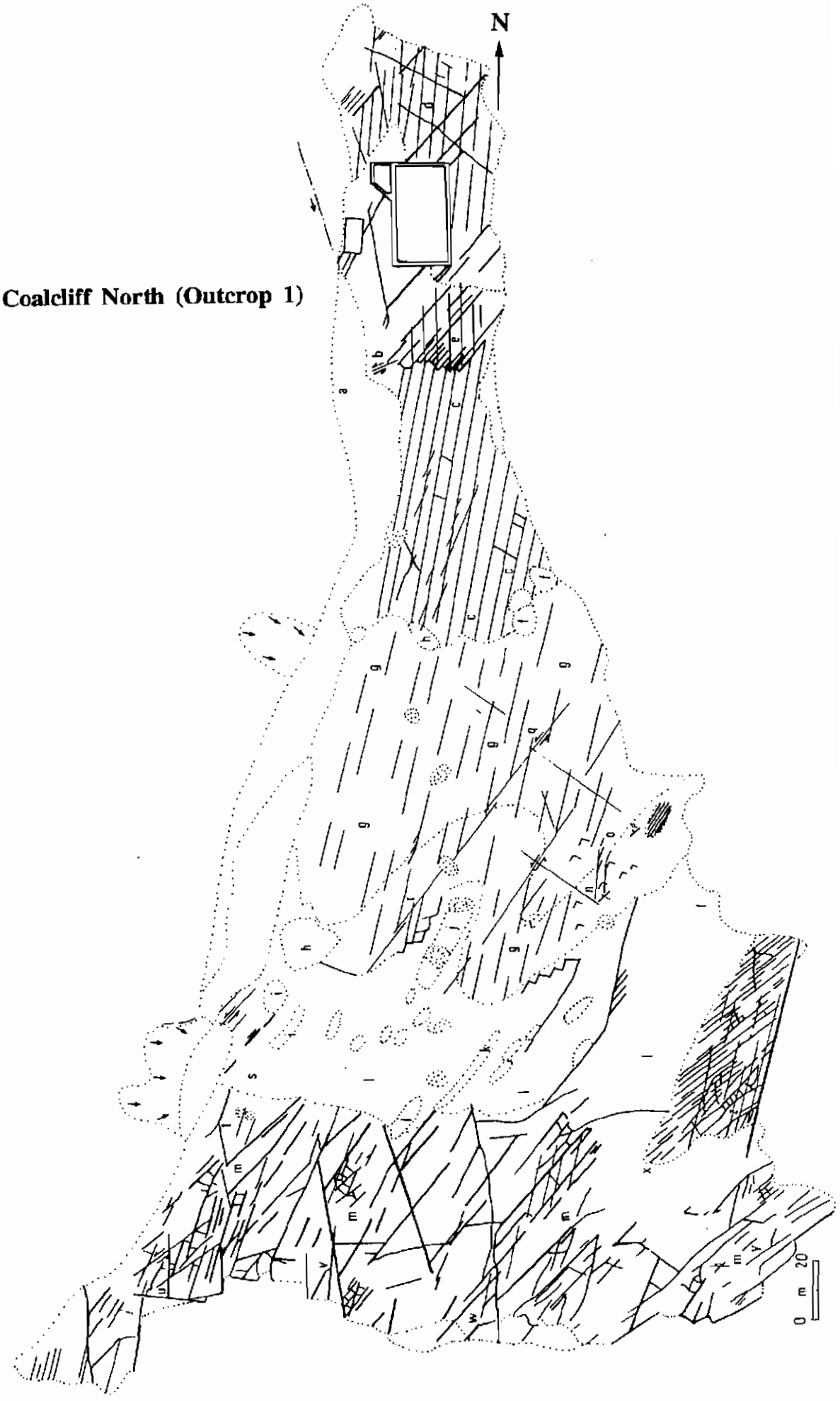

Coalcliff N. (Outcrop 1)

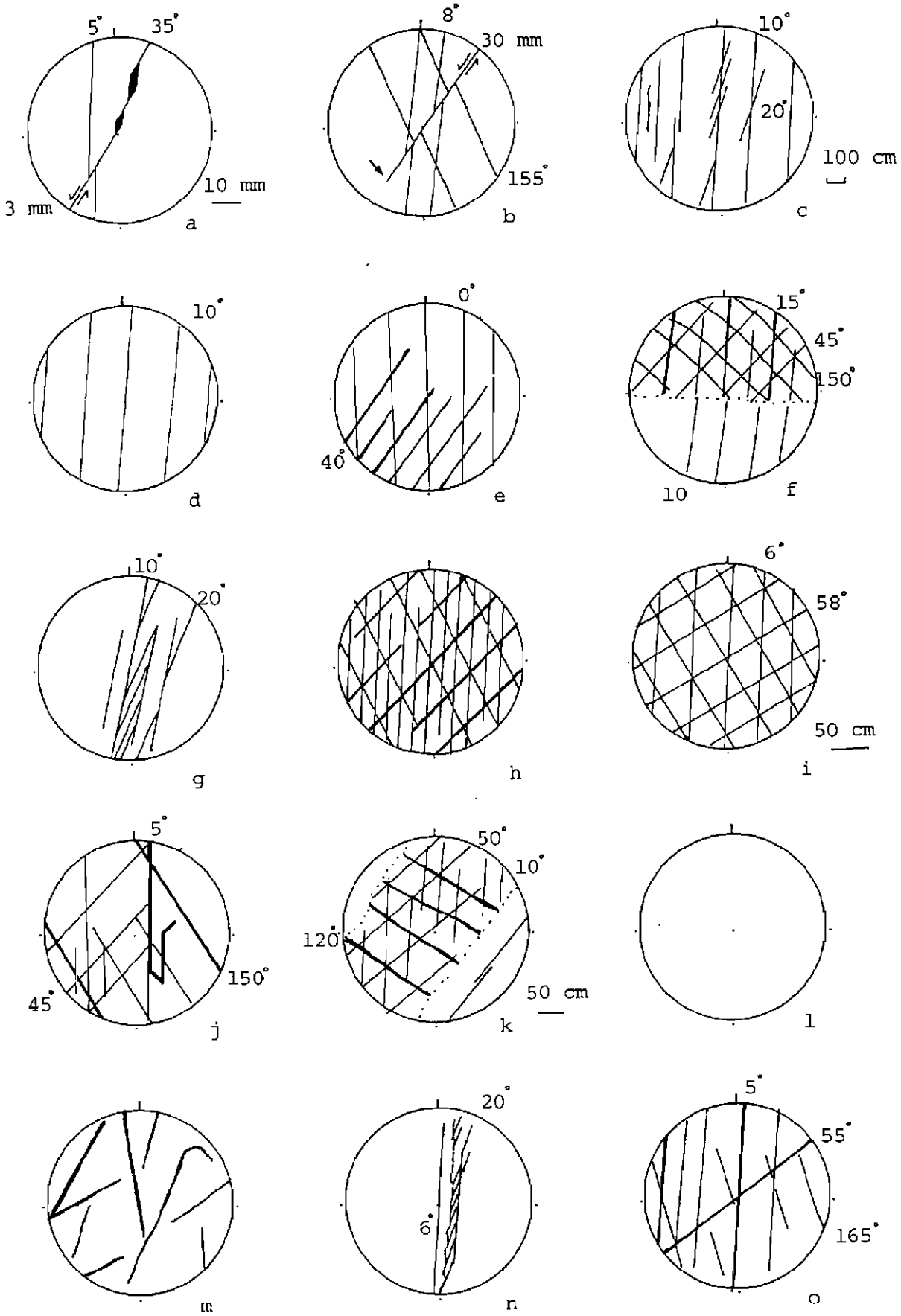

Coalcliff N. cont.

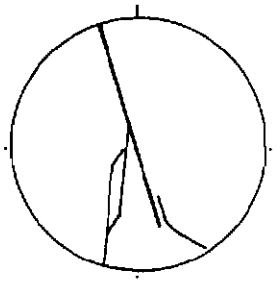
p

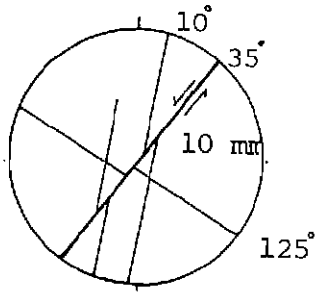

q

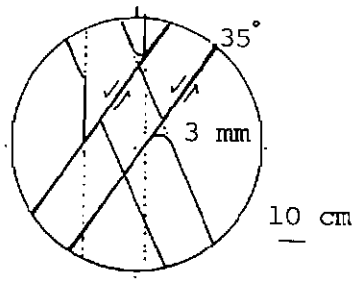

r

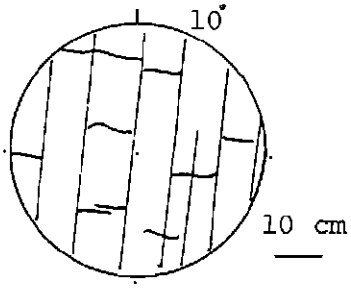

s

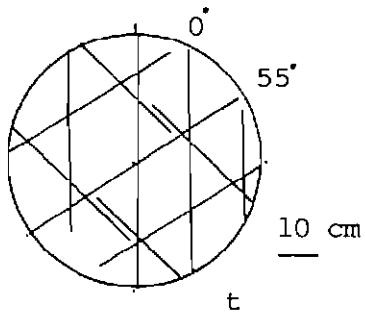

t

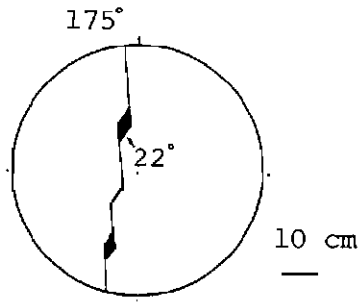

u

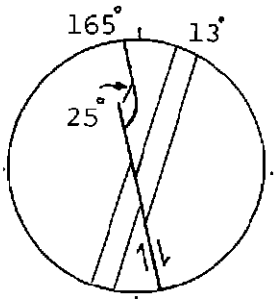

v

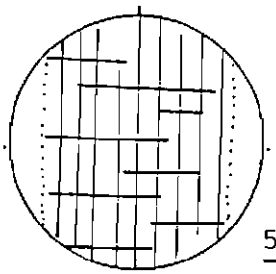

w

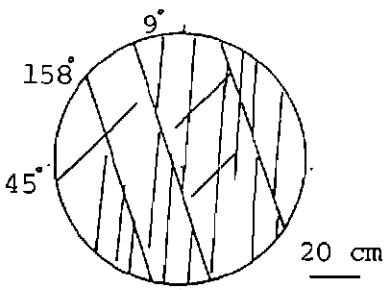

x

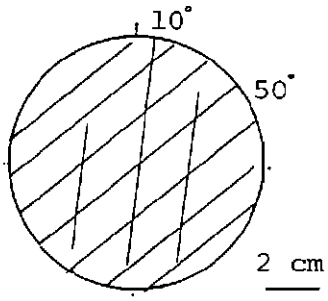

y

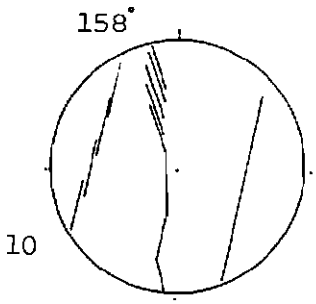

z

Coalcliff South (Outcrop 2)

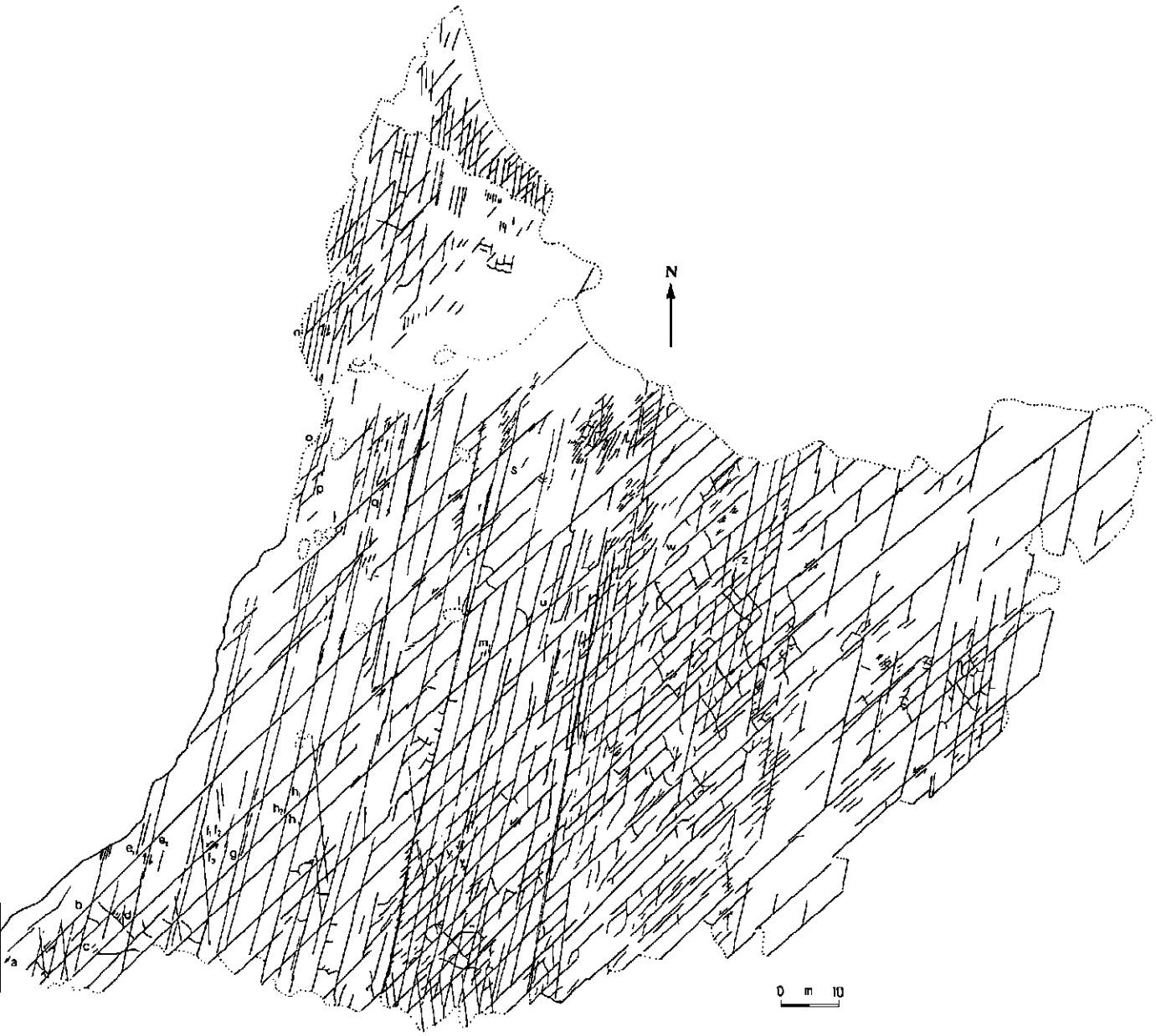

Coalcliff S. (Outcrop 2)

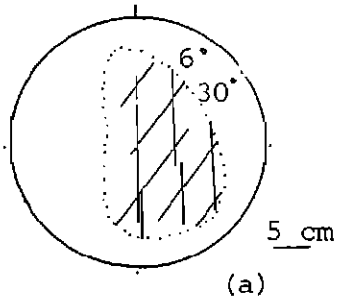

(a)

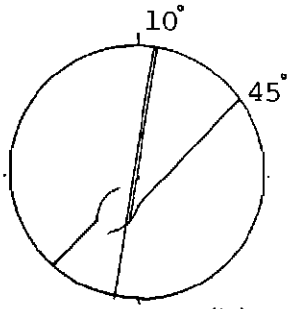

(b)

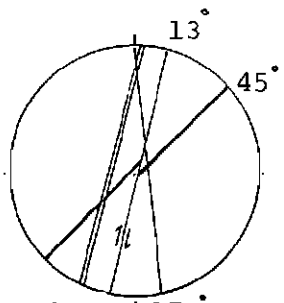

(c)

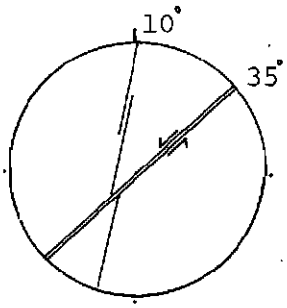

(d)

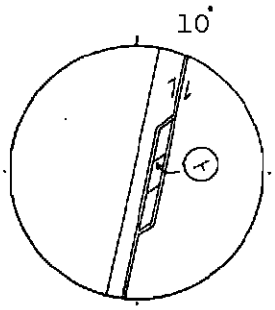

(e1)

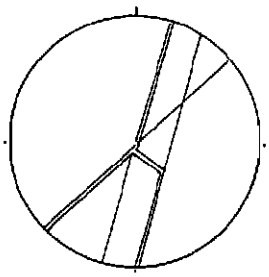
(e2)

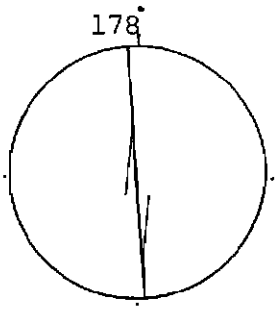

(f1)

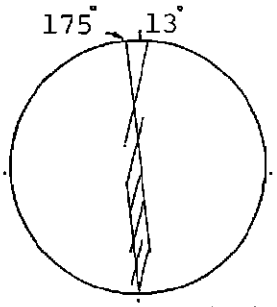

(f2)

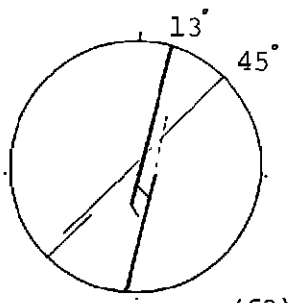

(f3)

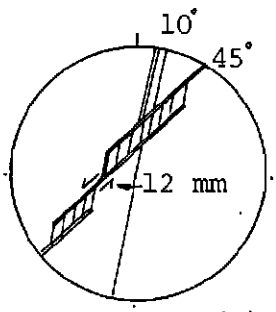

(g)

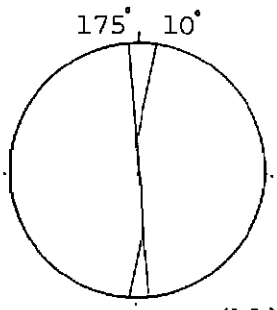

(h1)

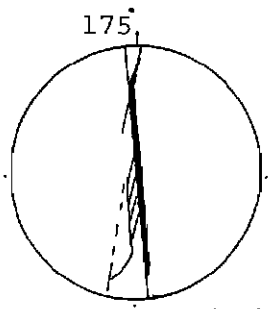

(h2)

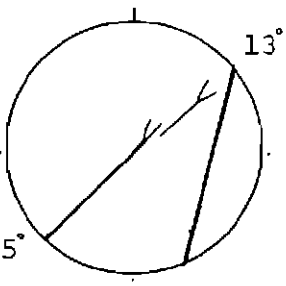

(i1)

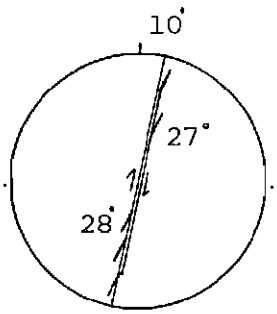

(i2)

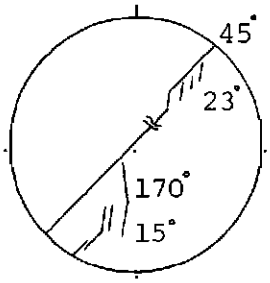

(j)

Coalcliff S. cont.

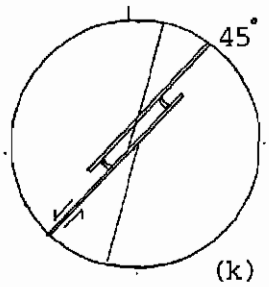

(k)

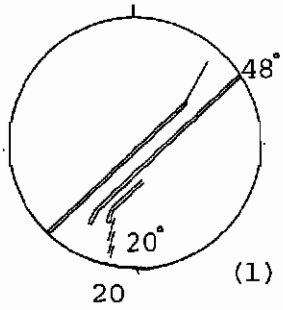

(l)

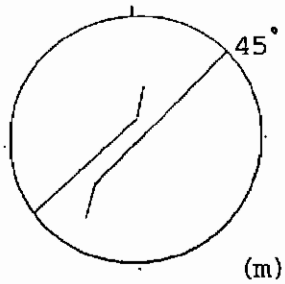

(m)

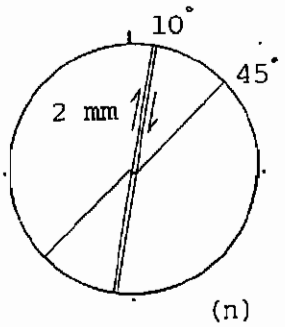

(n)

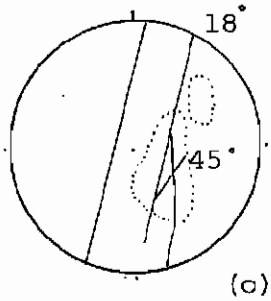

(o)

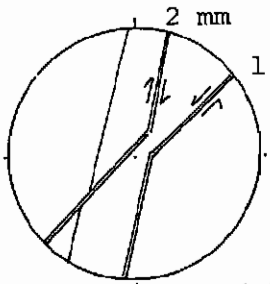

(p)

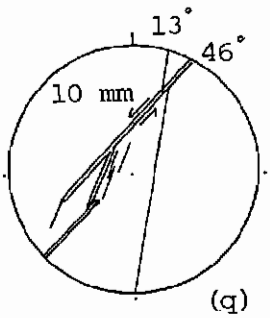

(q)

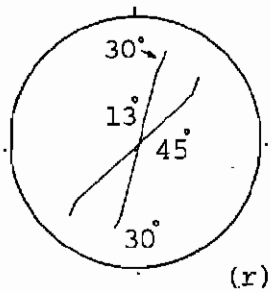

(r)

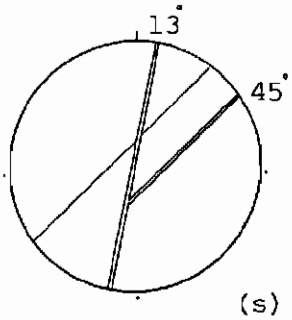

(s)

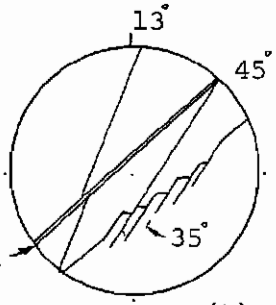

(t)

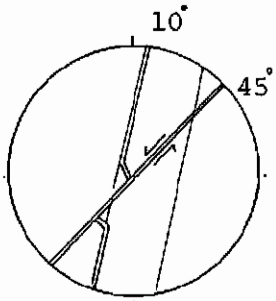

(u)

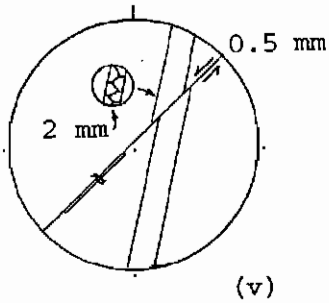

(v)

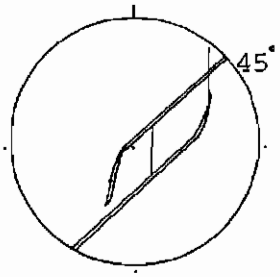

(w)

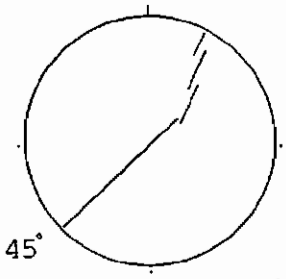

(x)

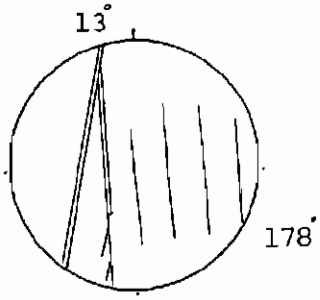

(y1)

Clifton (Outcrop 5)

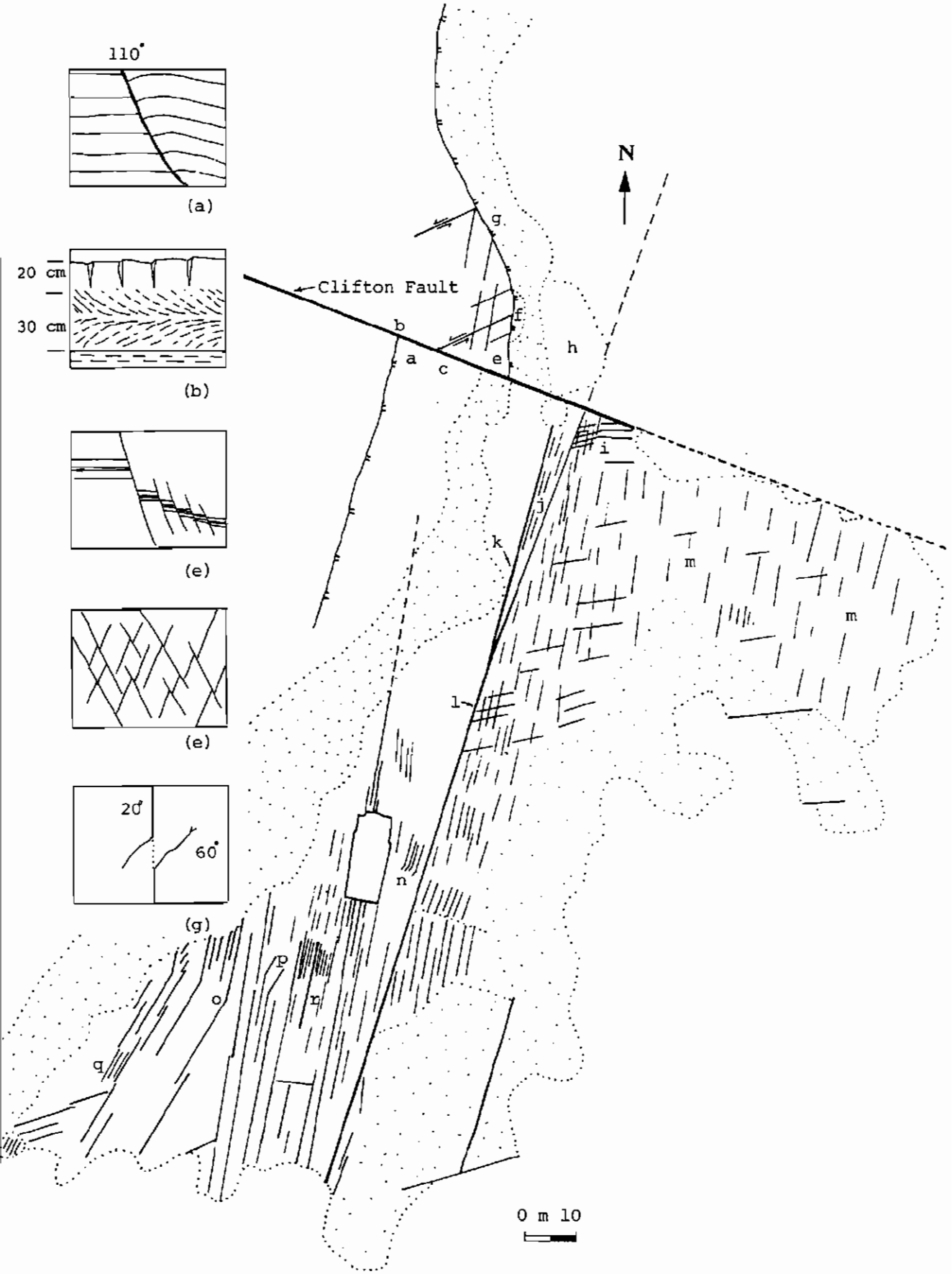

Clifton (Outcrop 5)

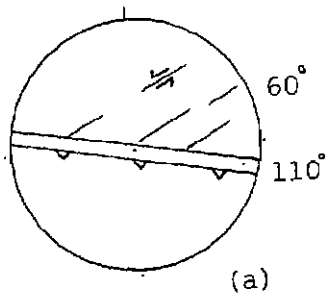

(a)

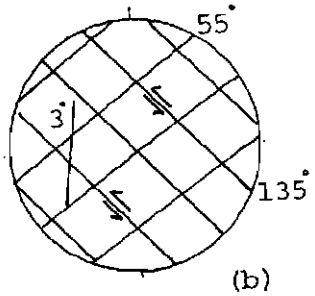

(b)

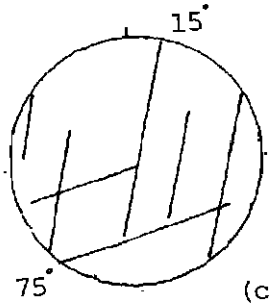

(c)

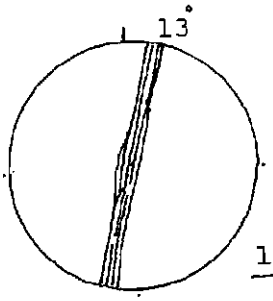

(d)

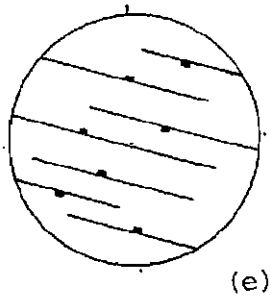
(e)

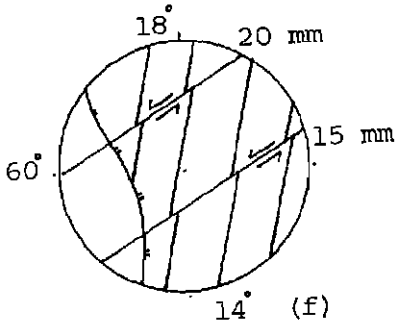

(f)

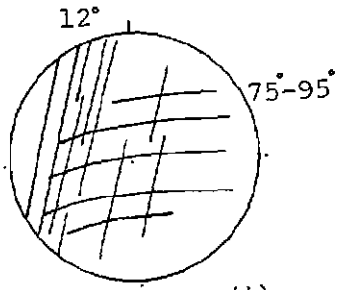

(i)

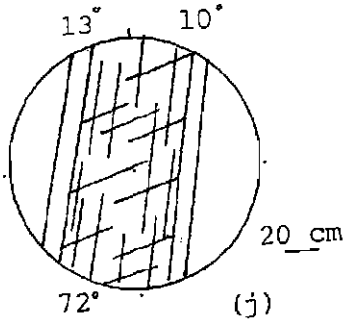

(j)

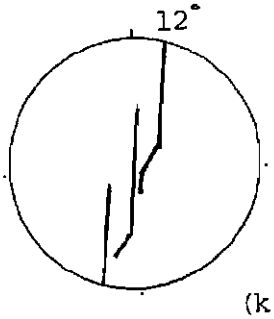

(k)

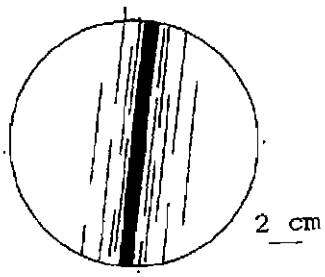

(l)

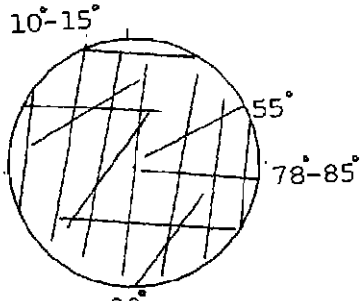

(m)

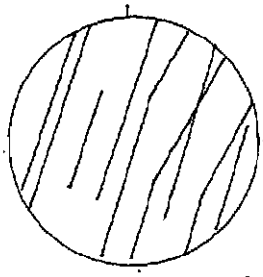
(n)

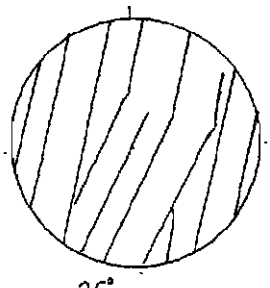

(o)

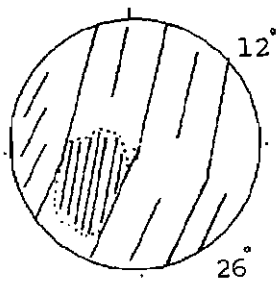

(p)

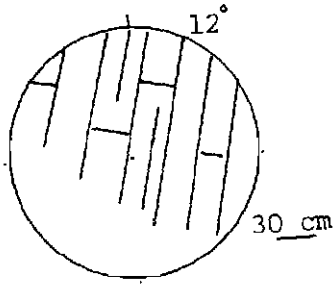

(q)

Clifton South (Outcrop 6)

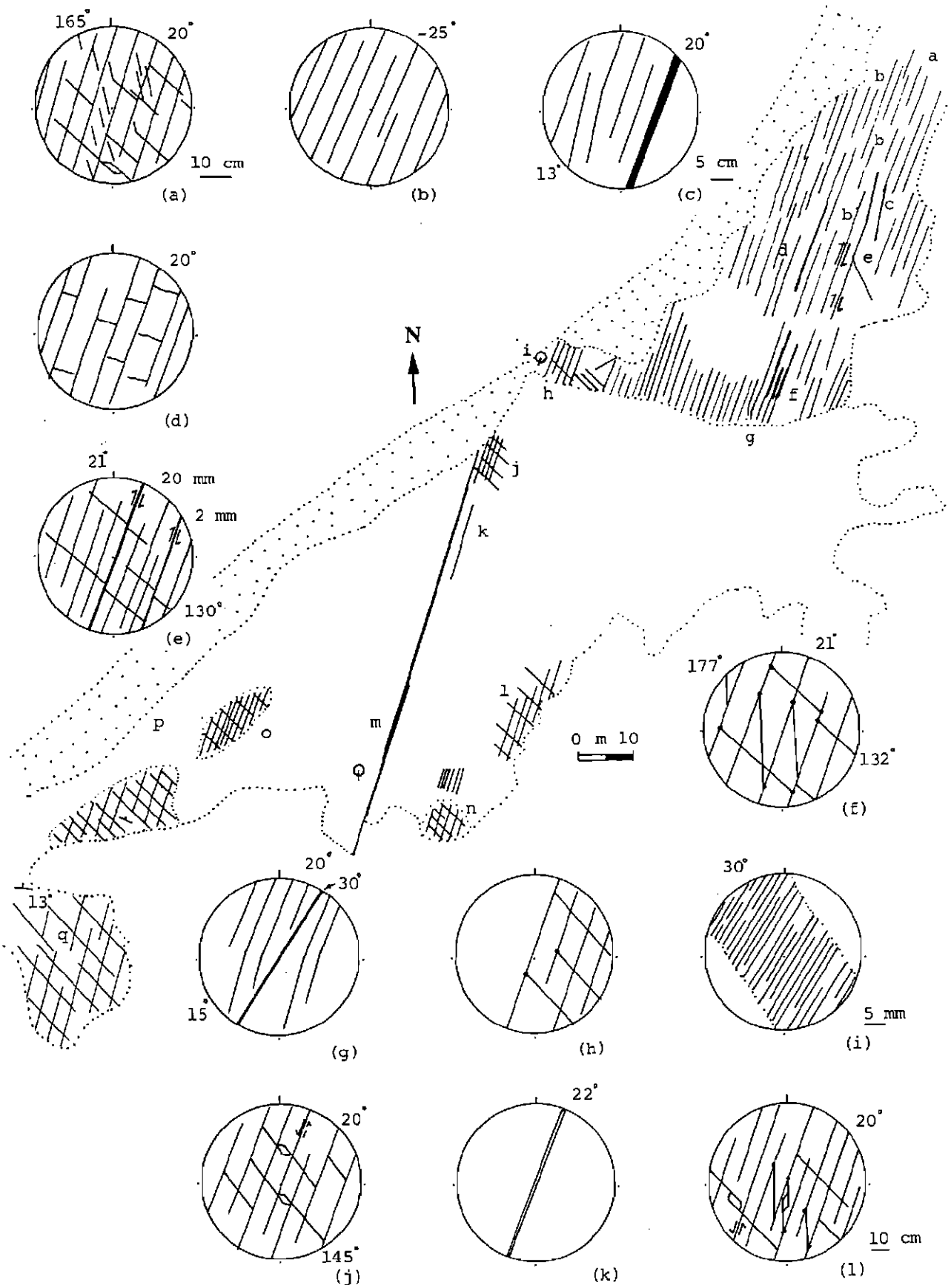

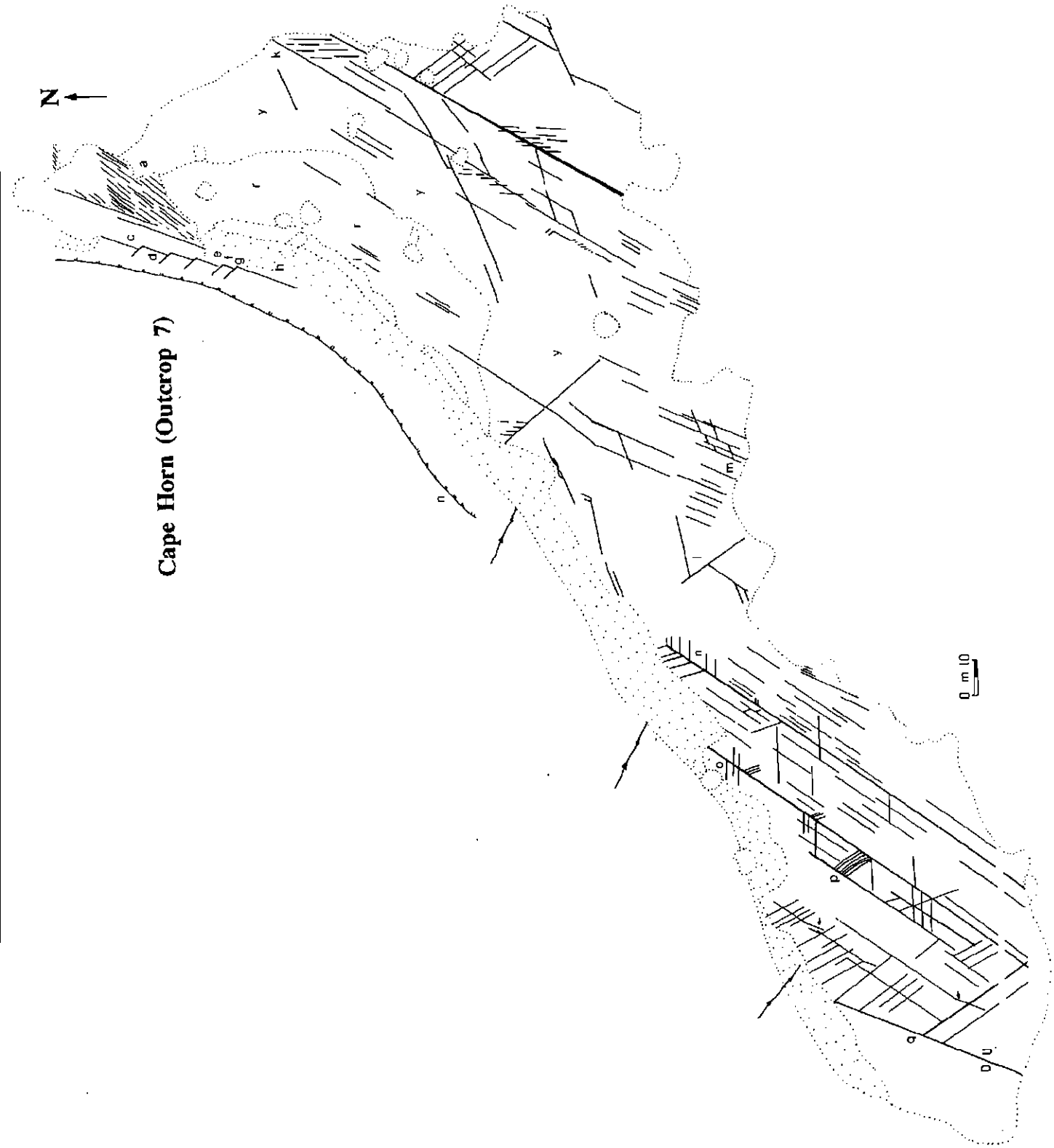
N
Cape Horn (Outcrop 7)
0 m 10

Cape Horn
(Outcrop 7)

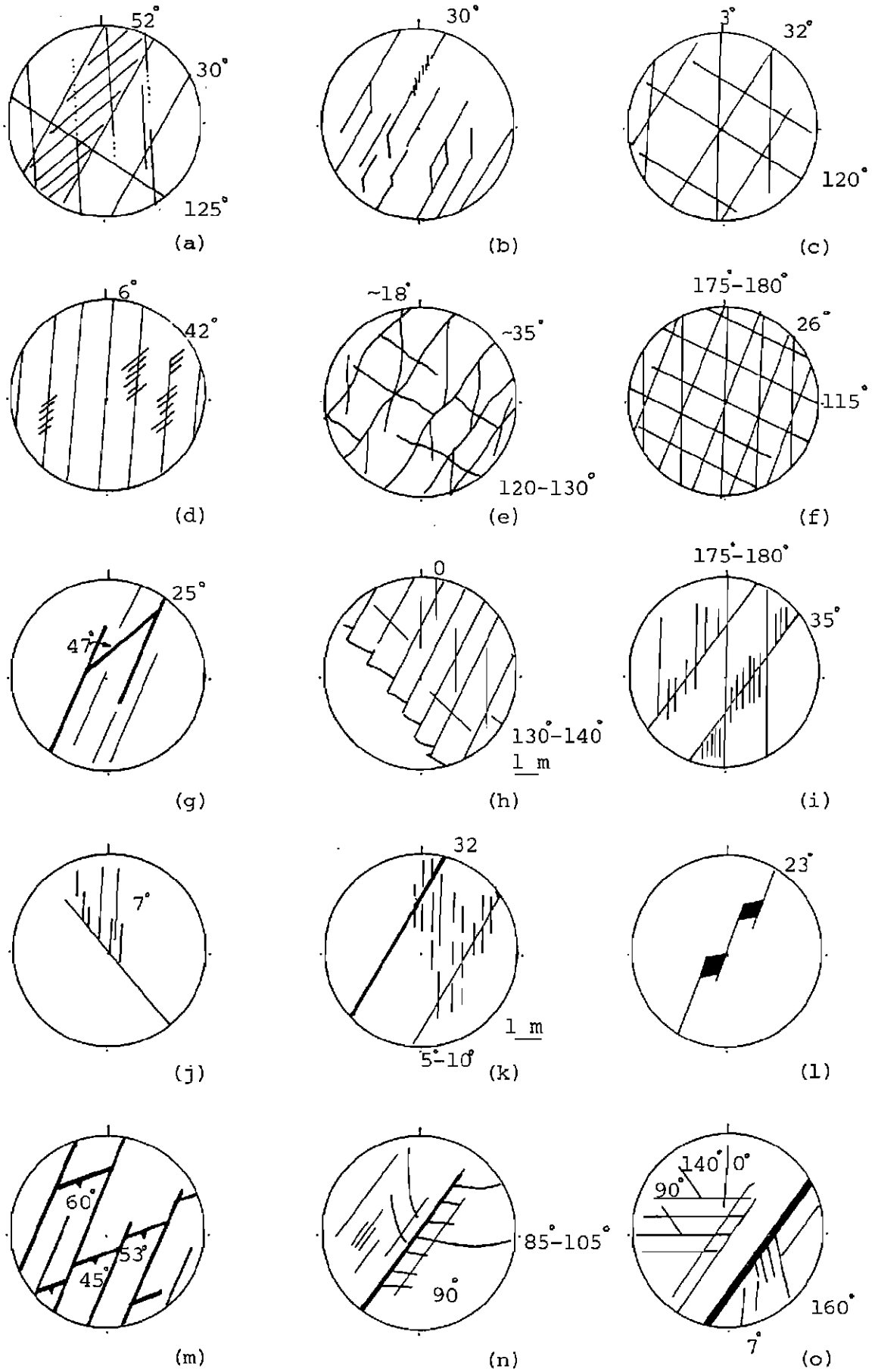

Scarborough South (Outcrop 8)

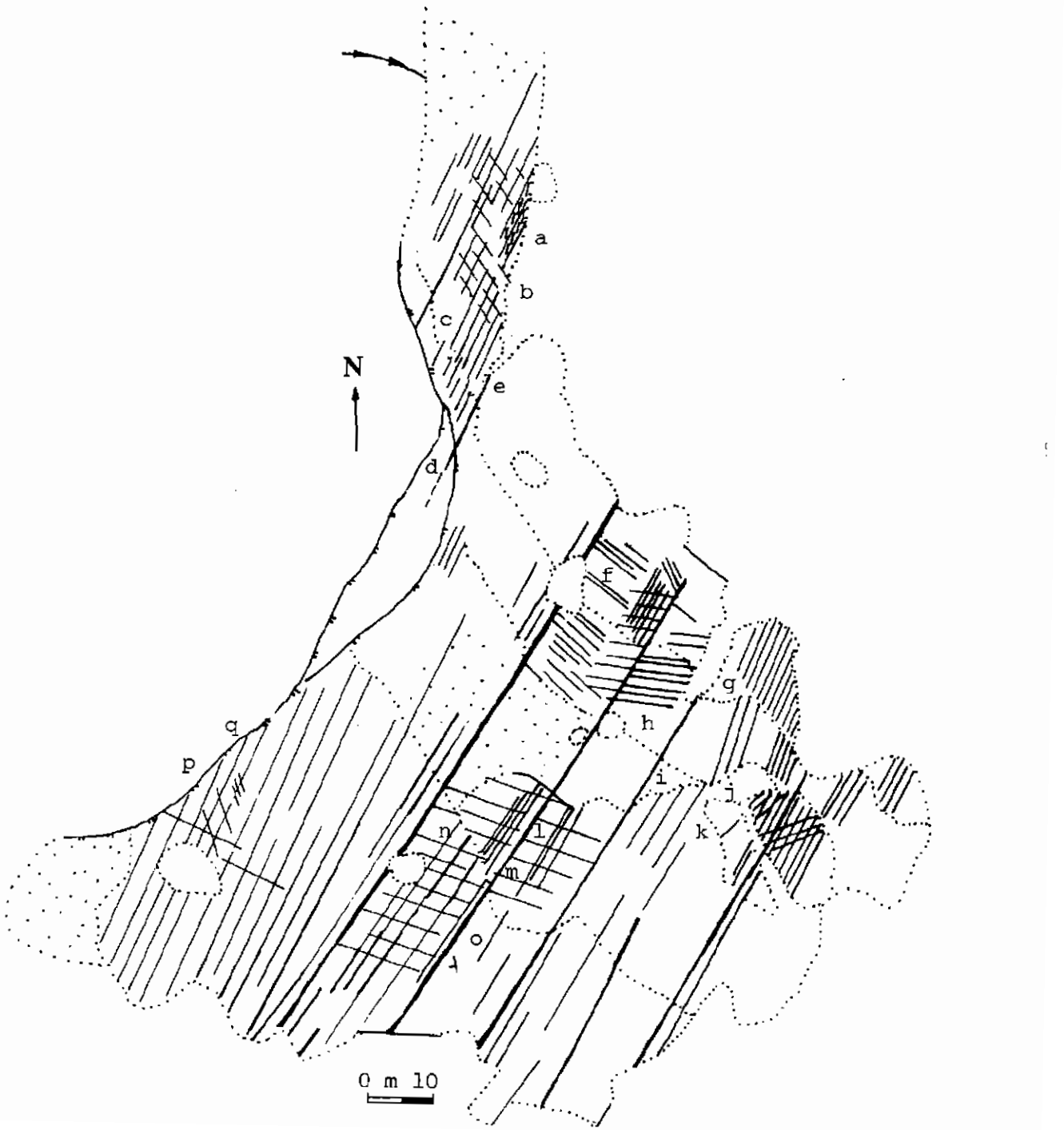

Scarborough South (Outcrop 8)

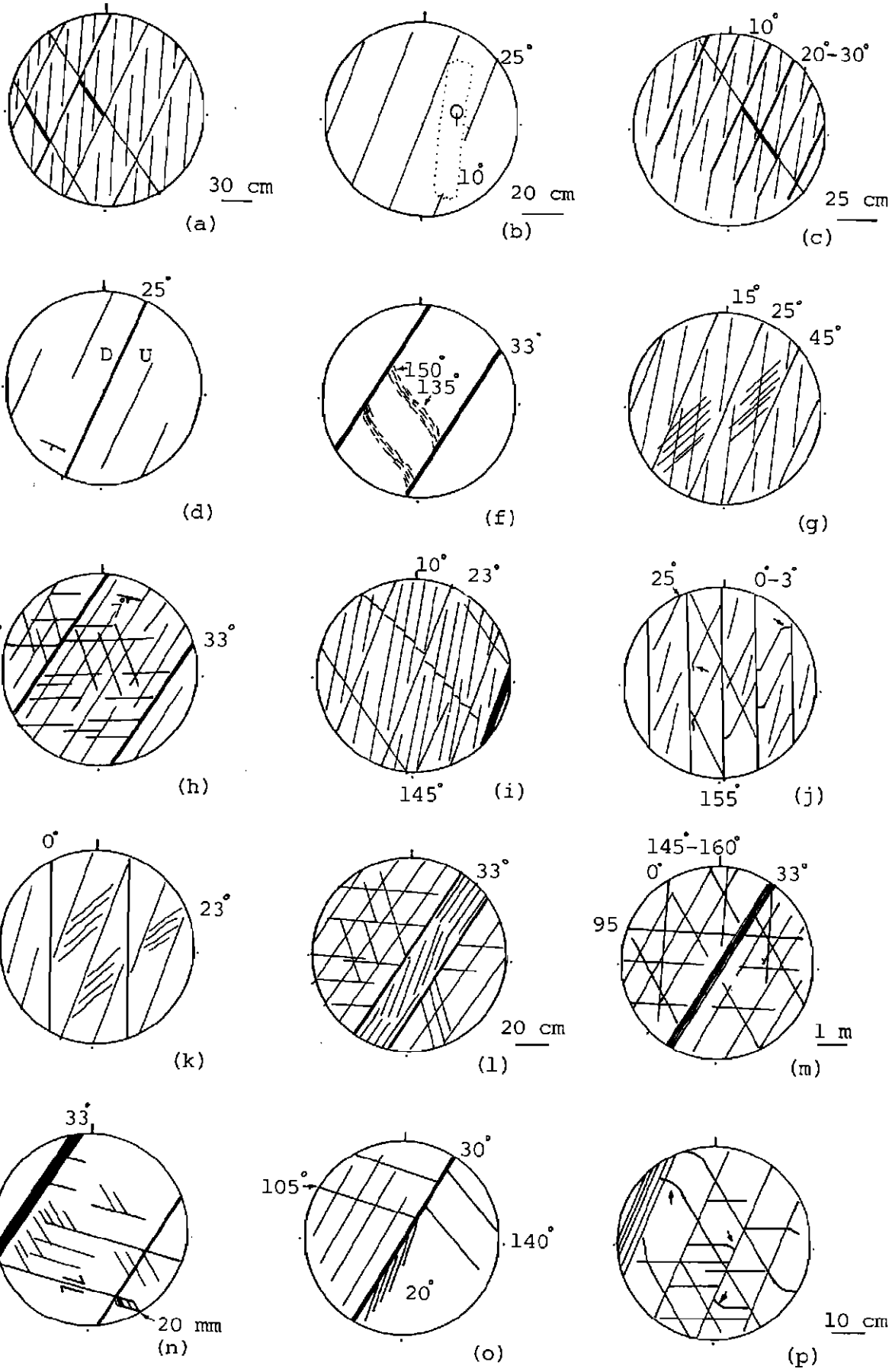

Scarborough South (Outcrop 9)

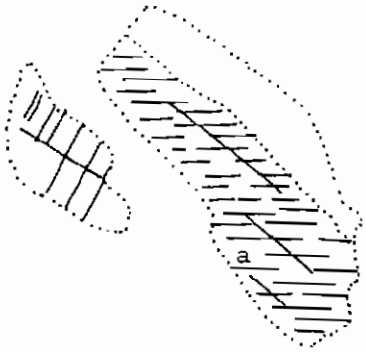

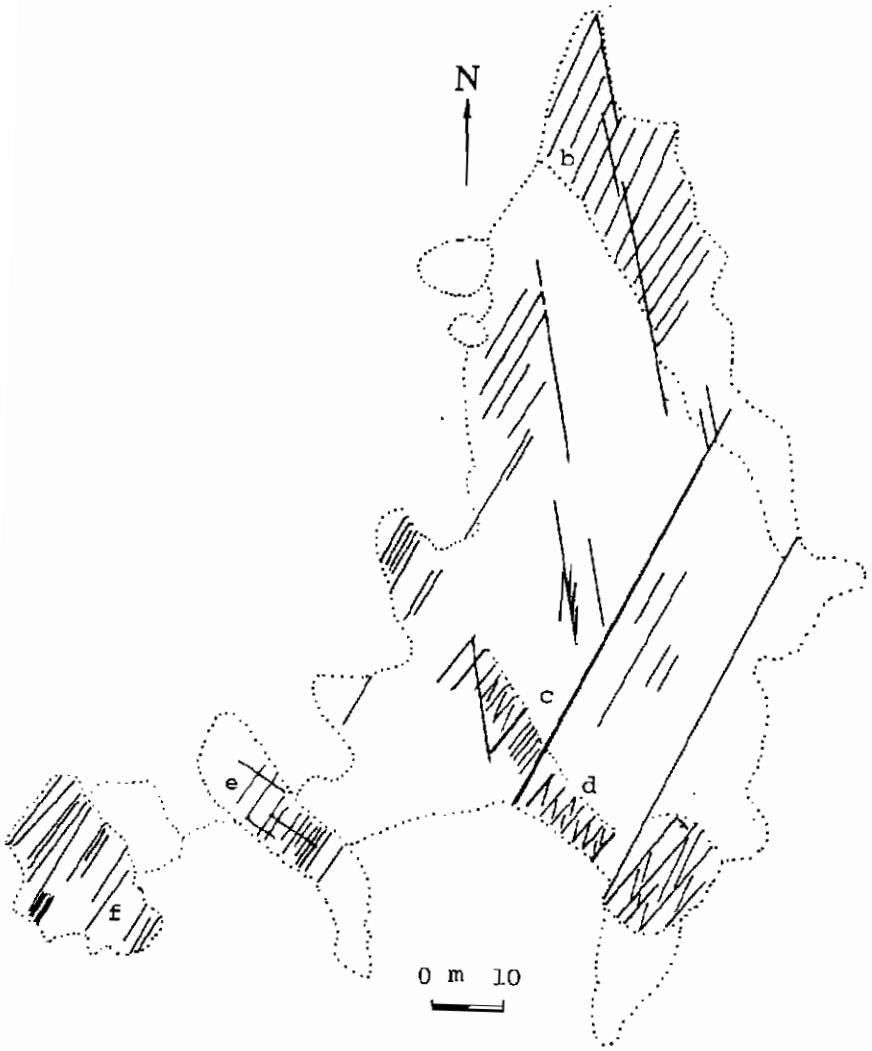

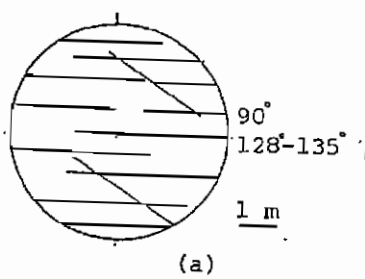

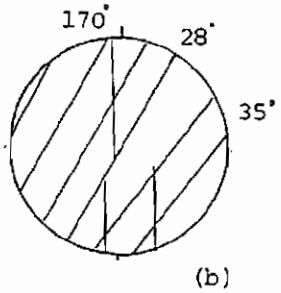

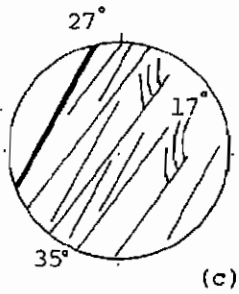

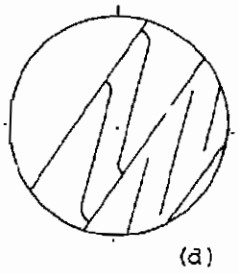

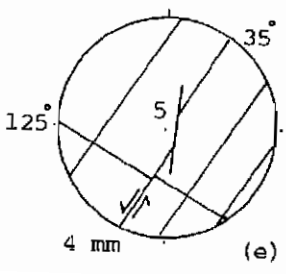

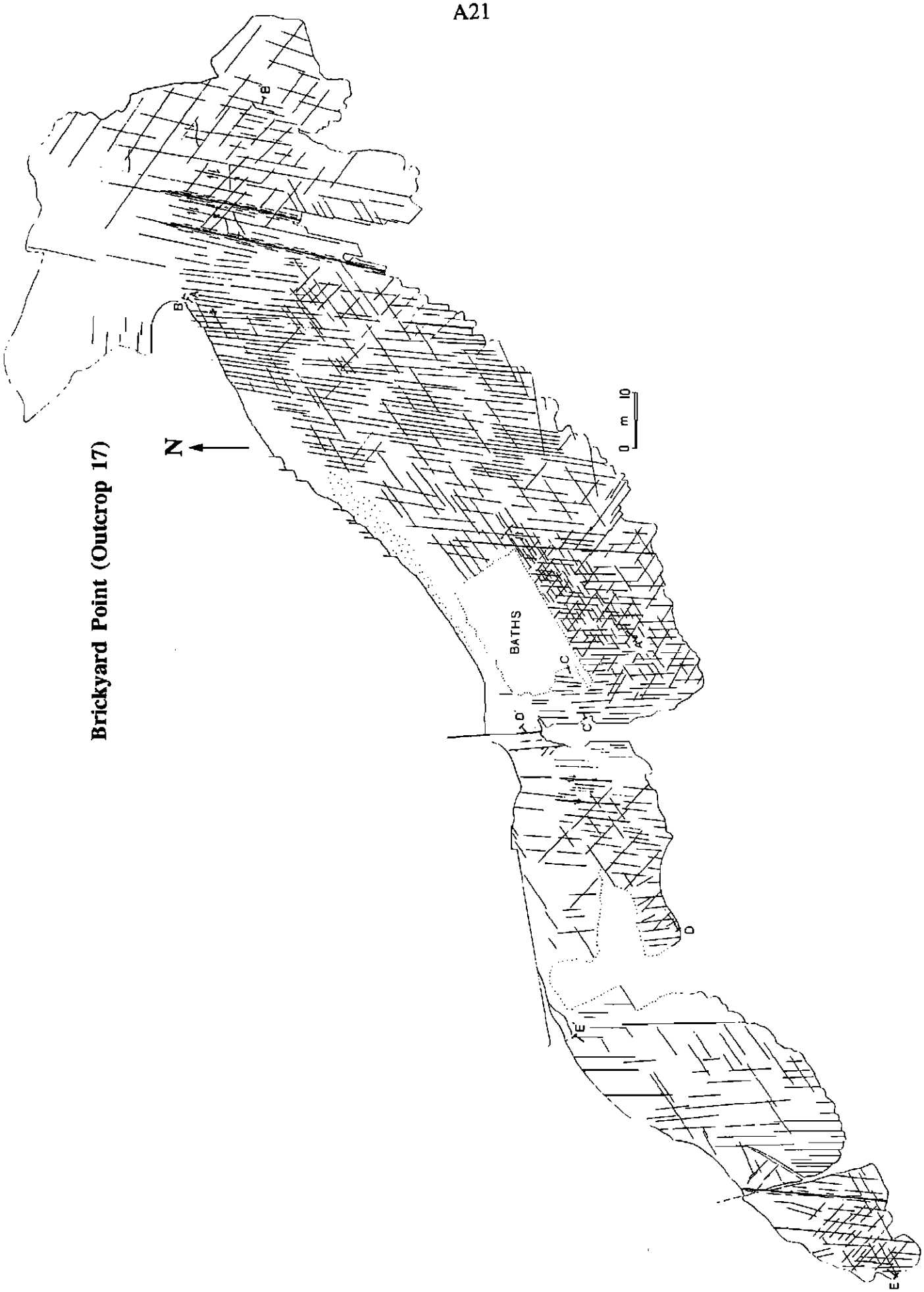
Brickyard Point (Outcrop 17)
N
0 m 10
BATHS
A
A'
B
B'
C
C'
D
D'
E
E'

(4) Scanlines

11-HH' (Wombarra South)

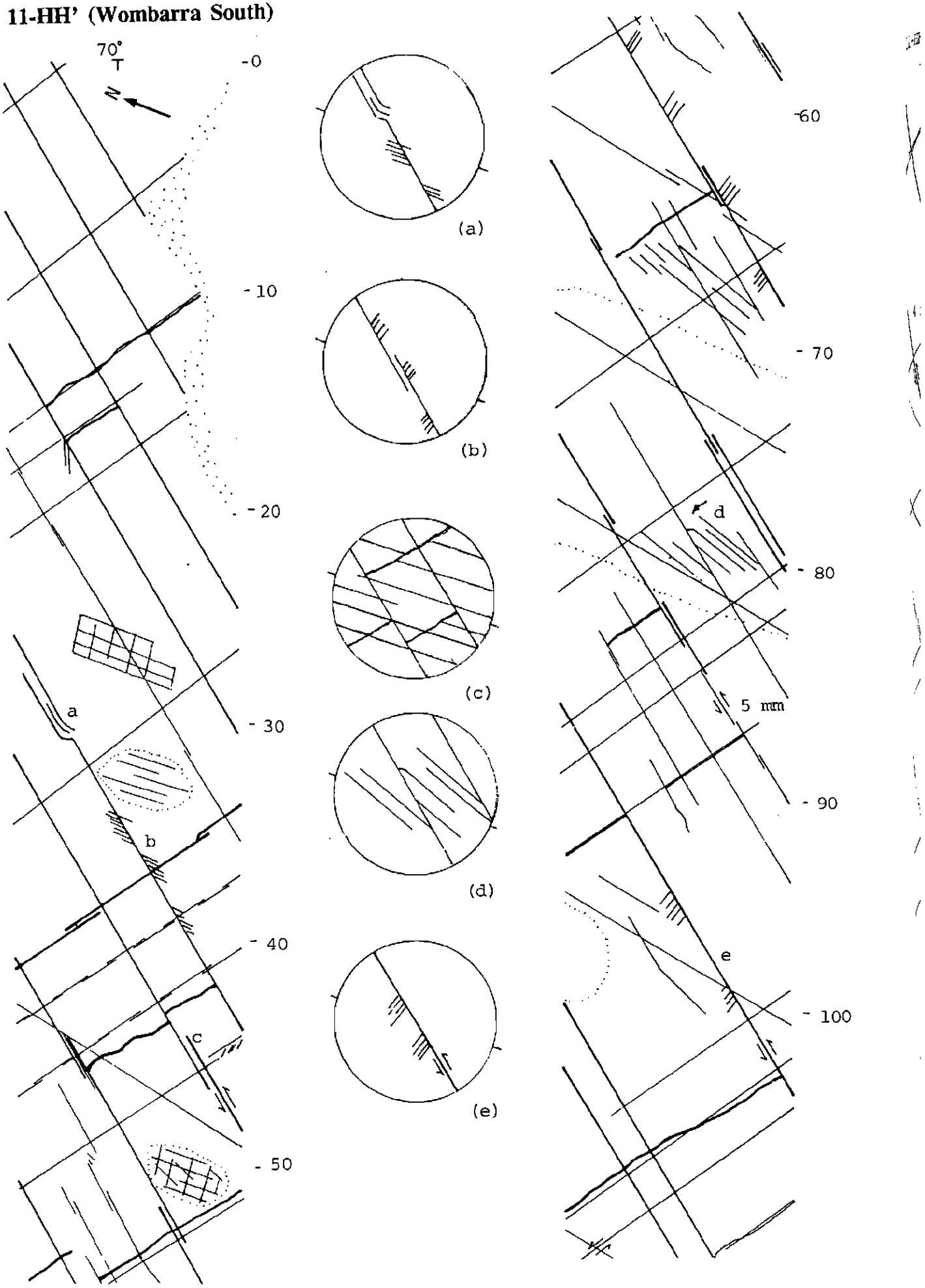

11-HH' cont.

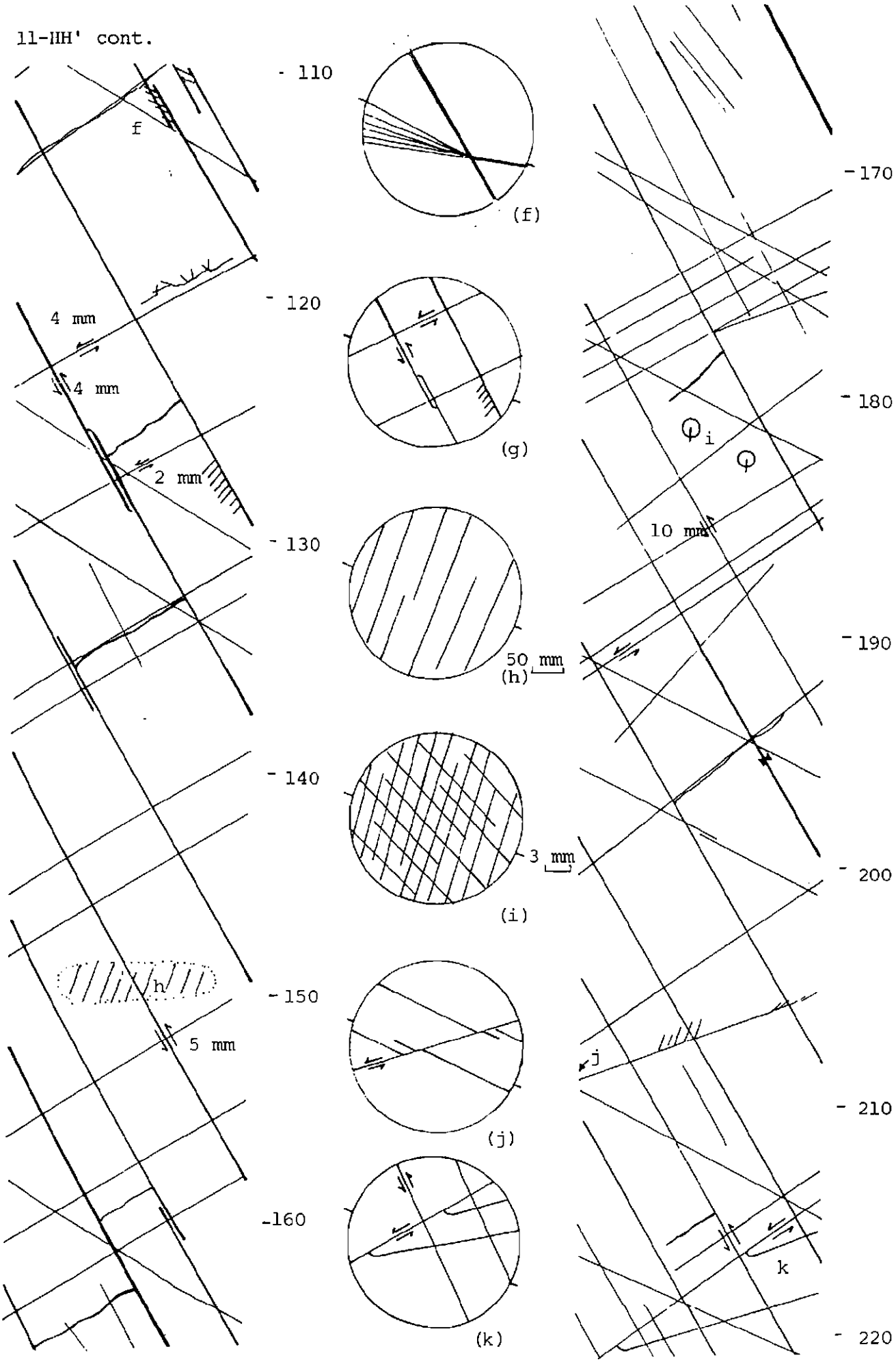
110
120
130
140
150
160
170
180
190
200
210
220
f
4 mm
4 mm
2 mm
h
5 mm
(f)
(g)
(h)
50 mm
(i)
3 mm
(j)
(k)
Q_i
Q
10 mm
j
k

11-HH' cont.

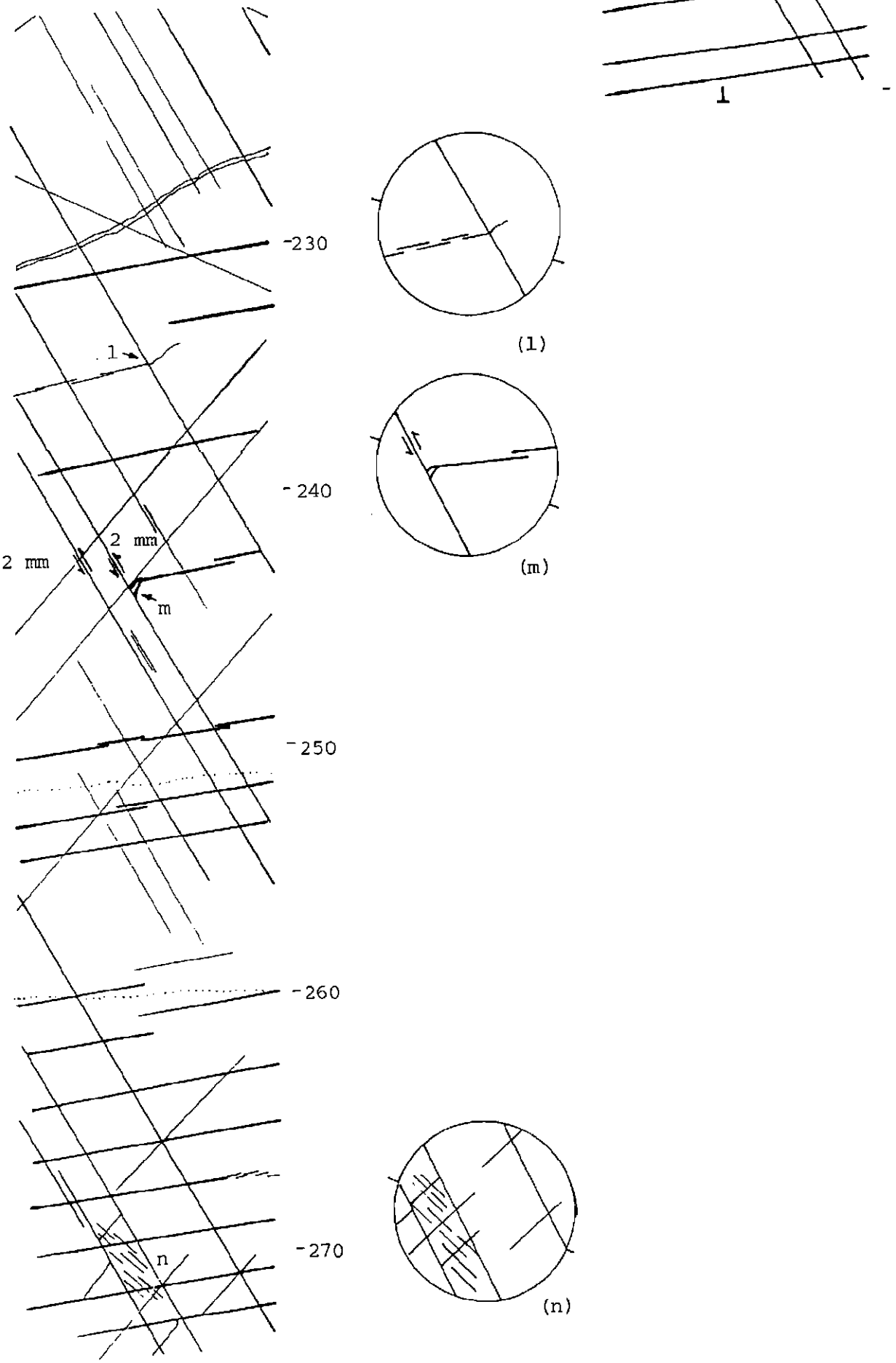

11-II' (Wombarra South)

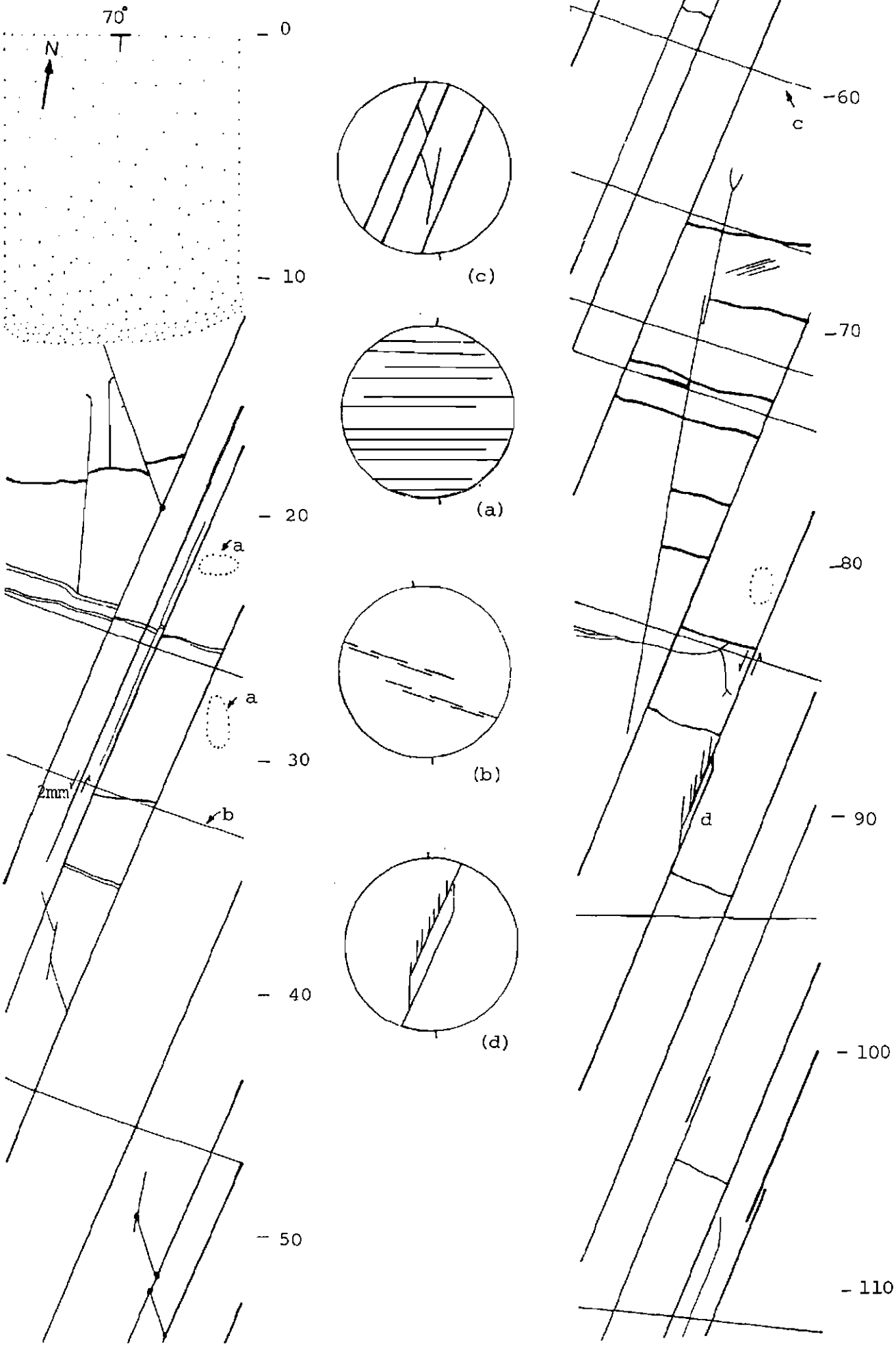

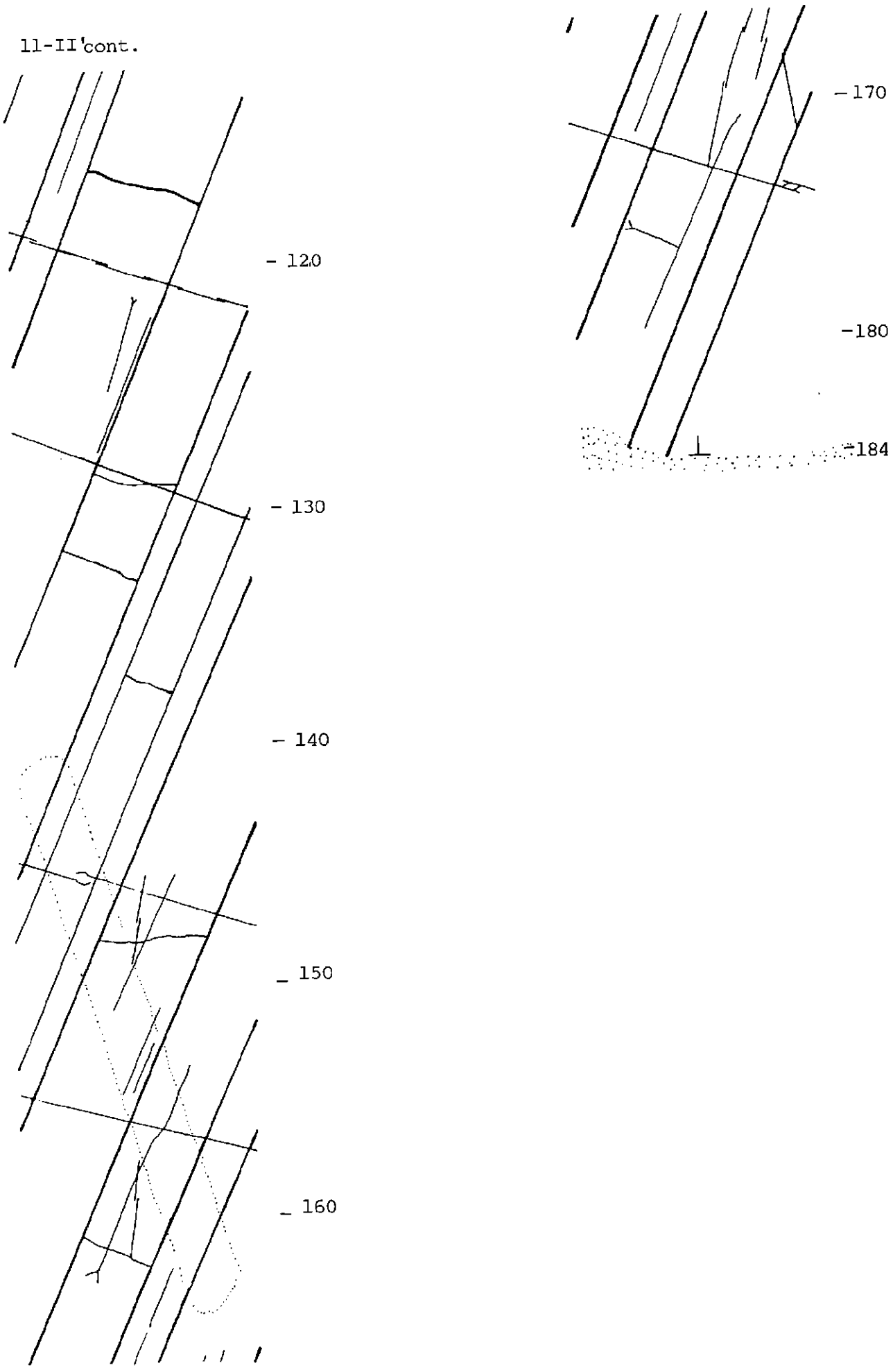
11-II'cont.
- 120
- 130
- 140
- 150
- 160
- 170
- 180
- 184

12-CC' (Wombarra South)

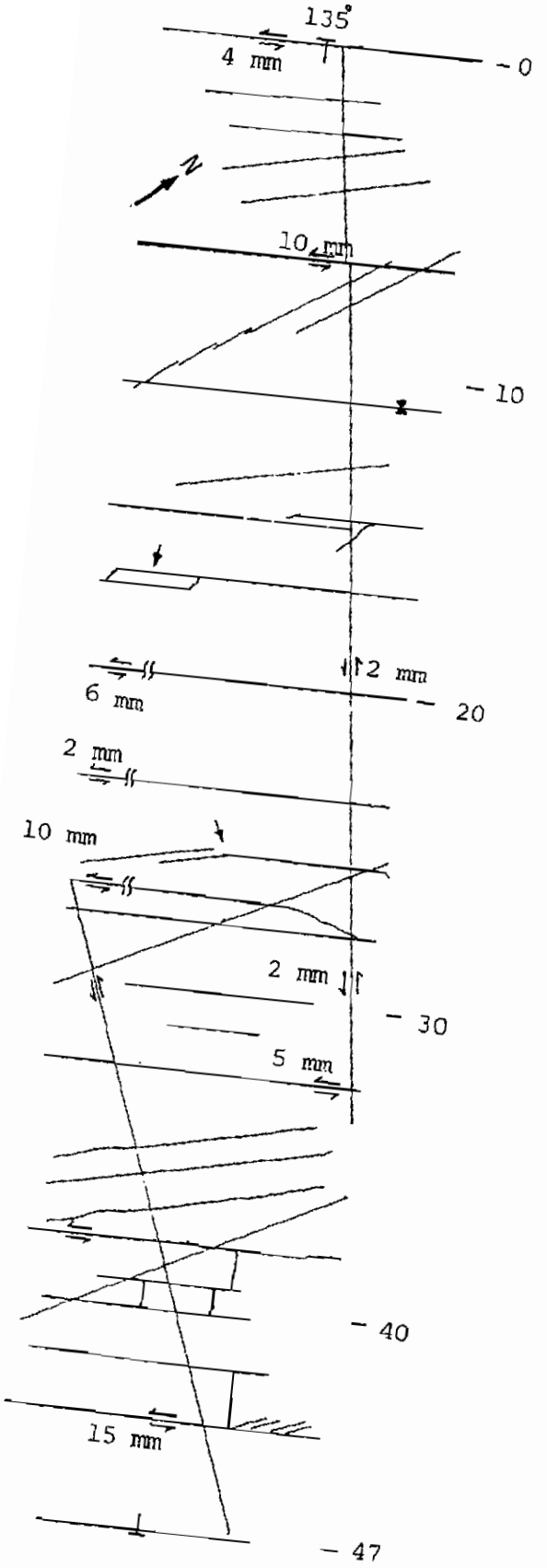

12-DD' (Wombarra South)

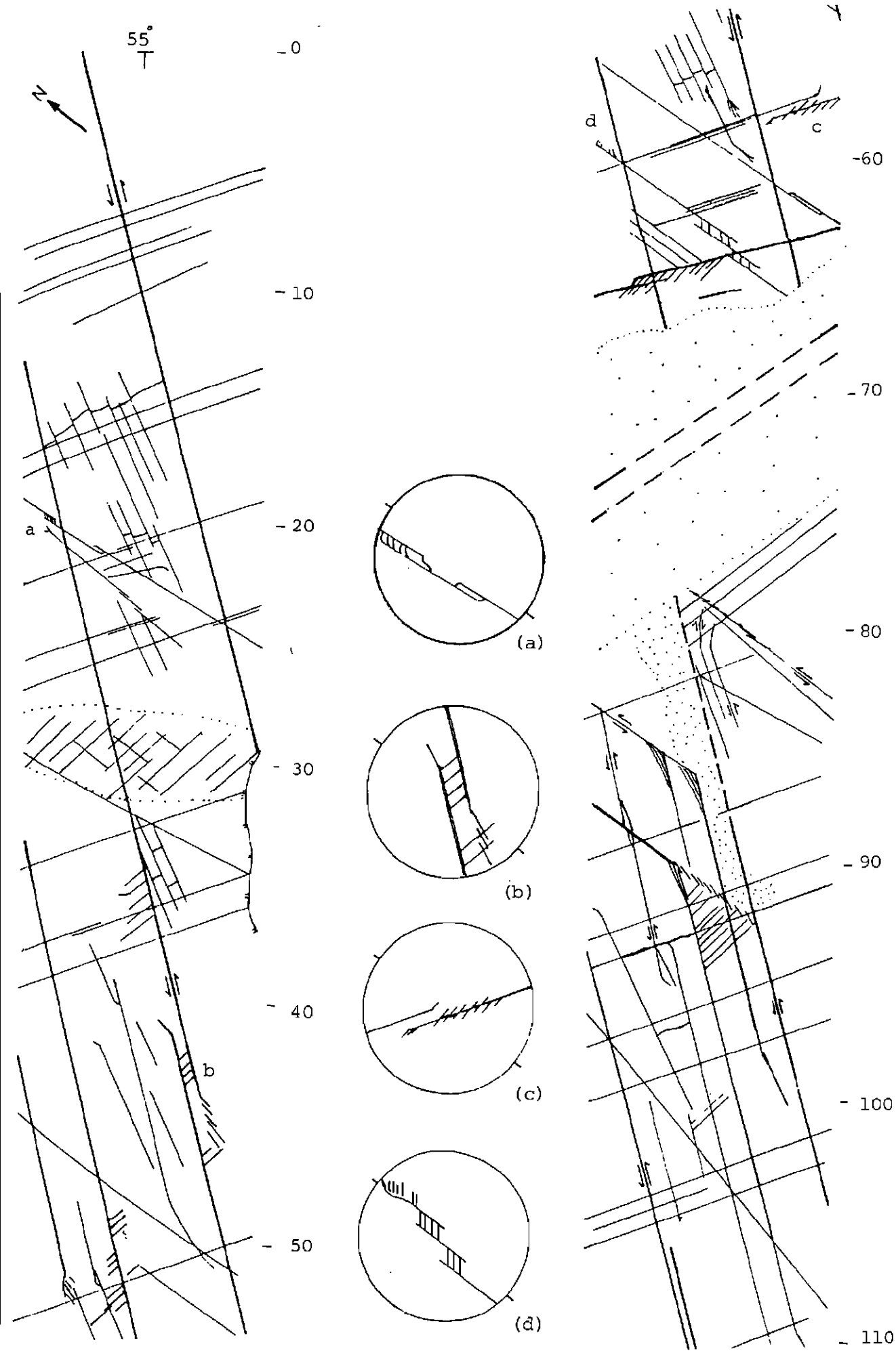

12-DD' cont.

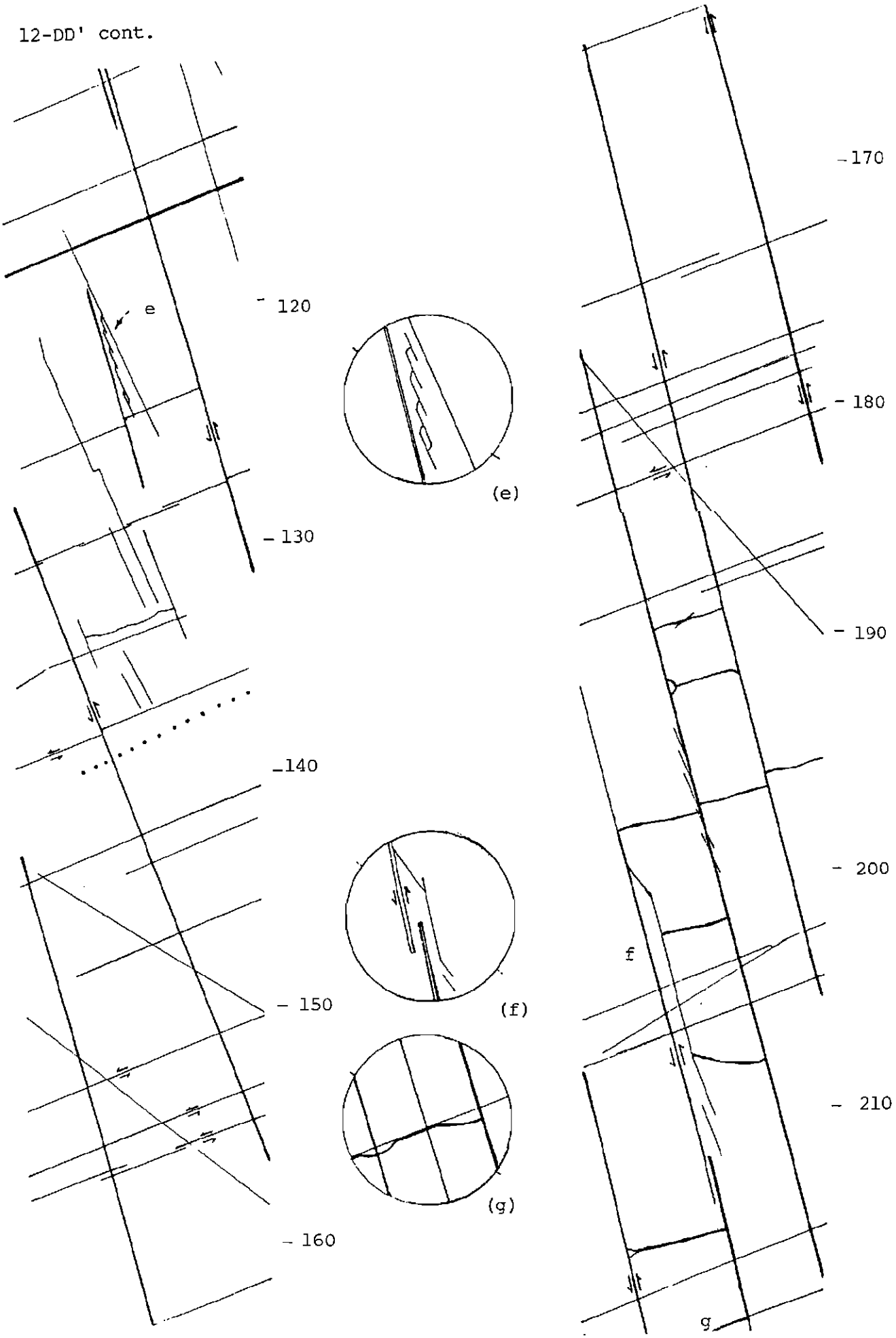

12-DD' cont.

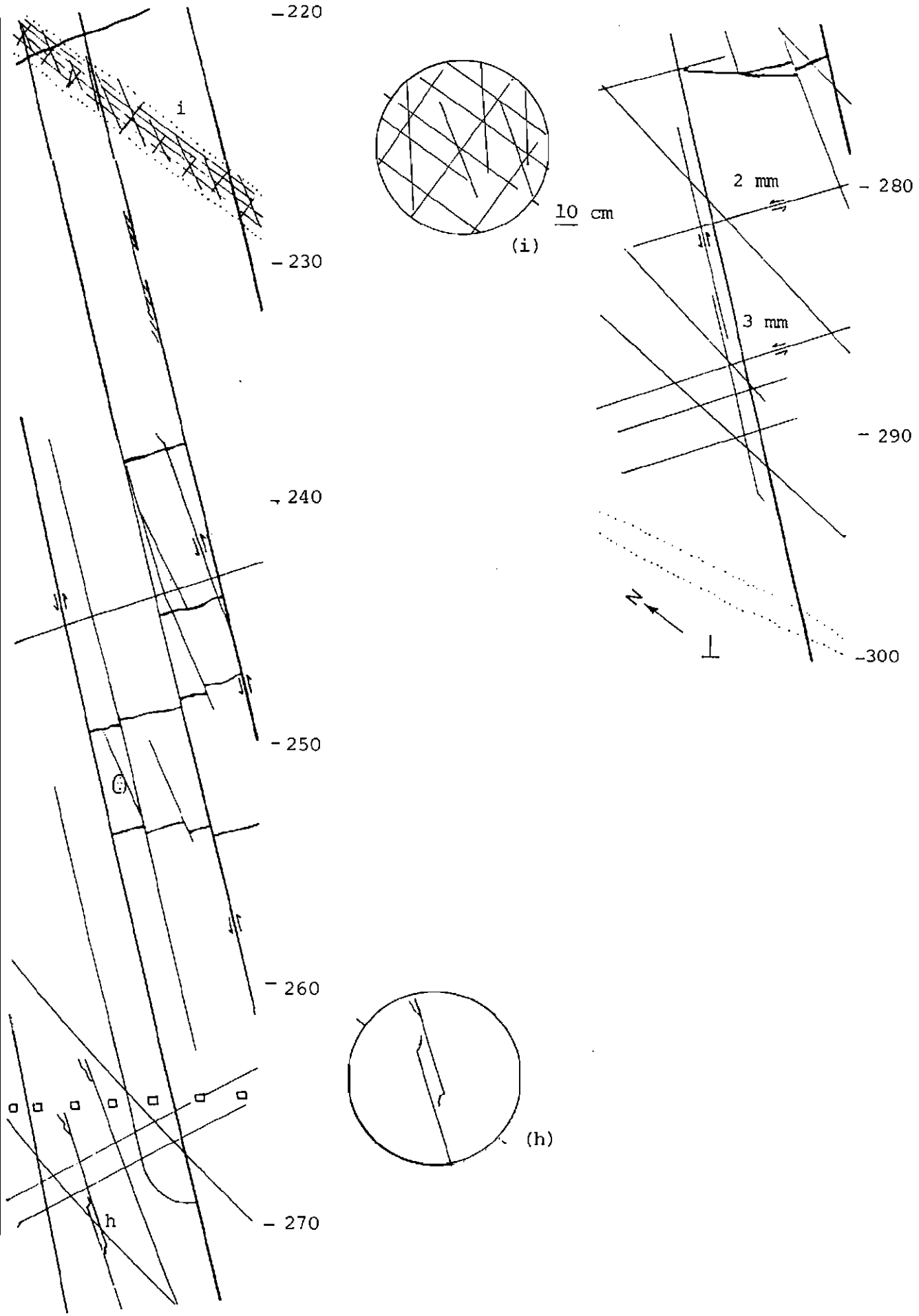

12-EE' (Wombarra South)

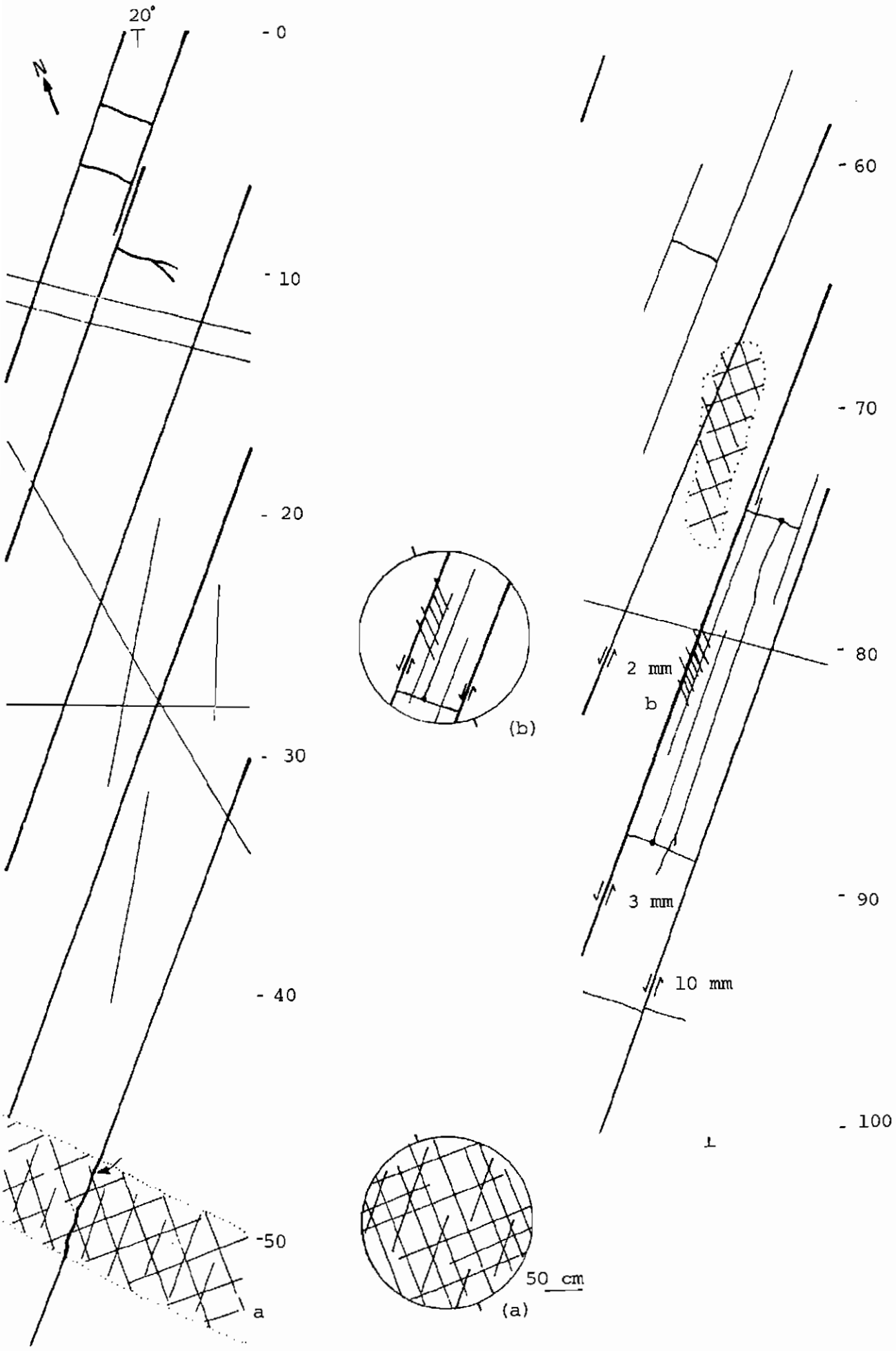

12-GG' (Wombarra South)

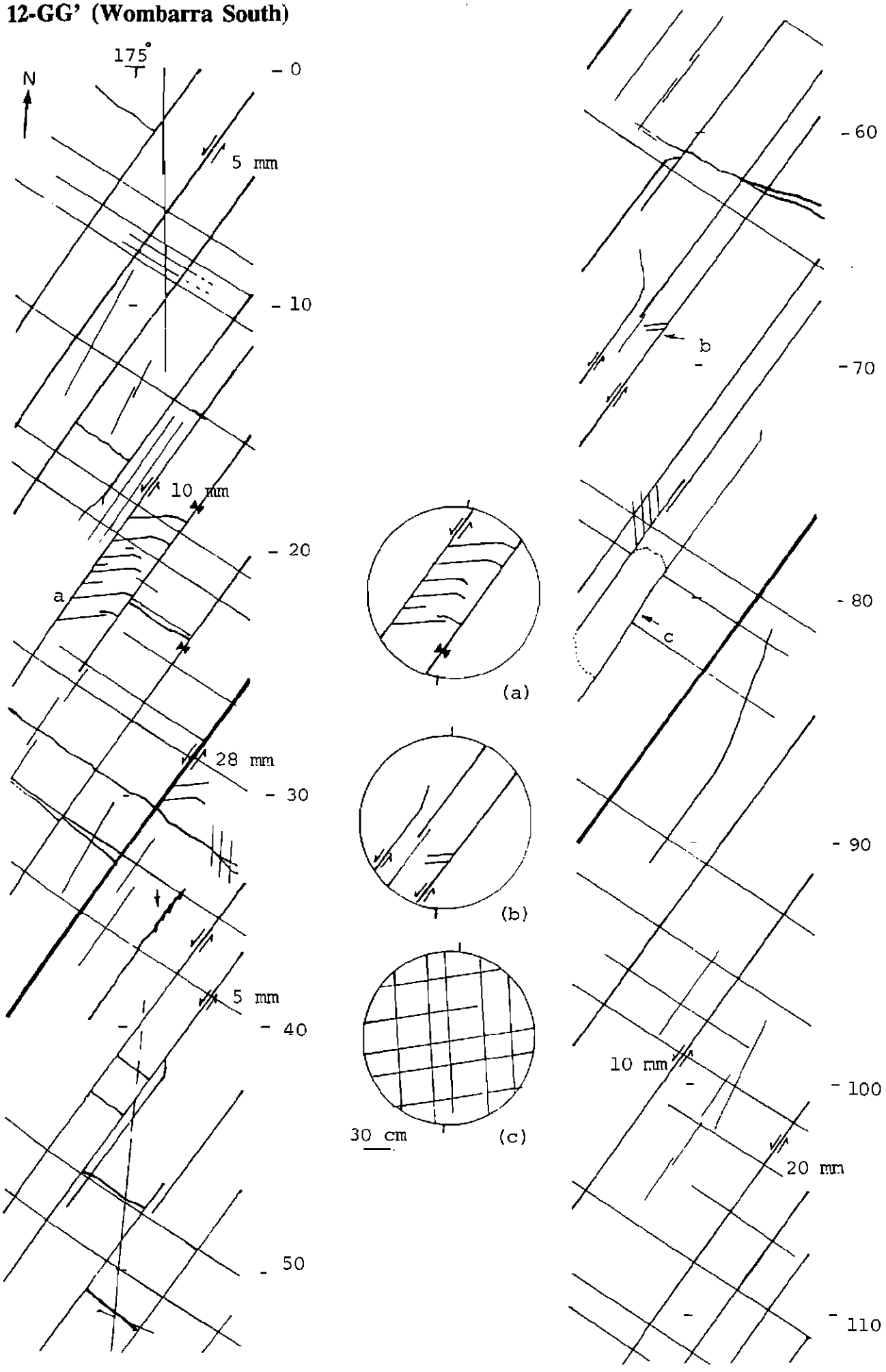

12 -GG' cont.

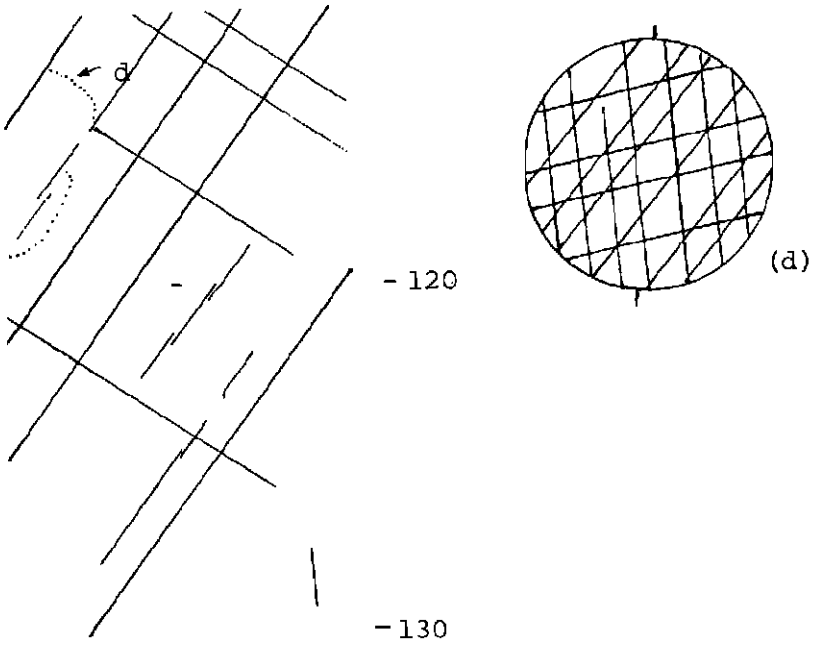

13-AA' (Coledale North)

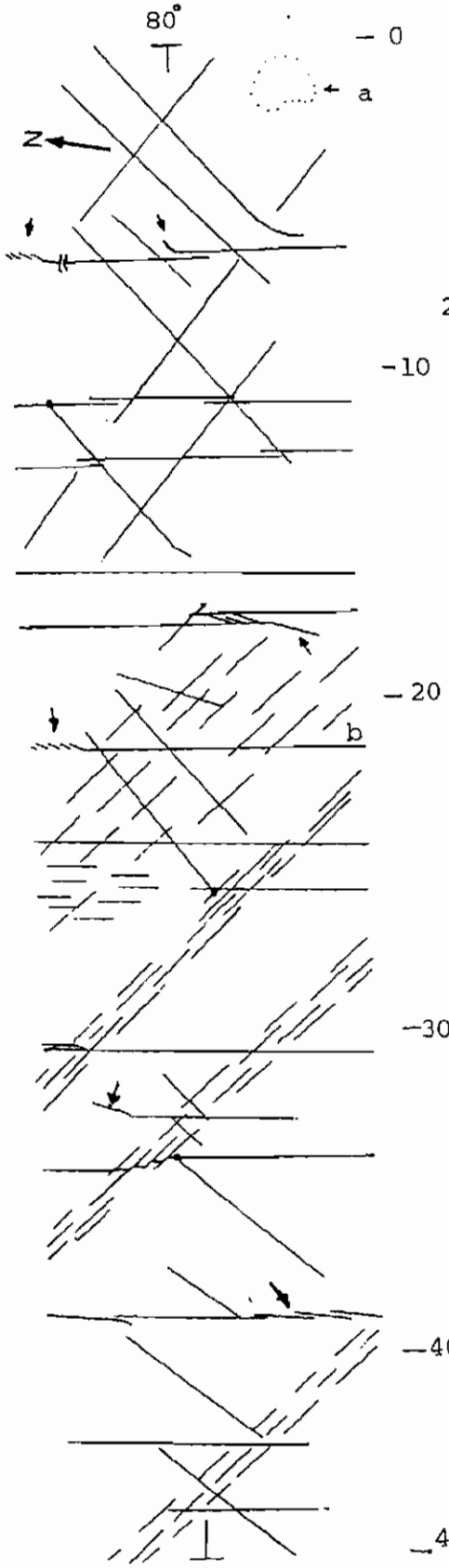

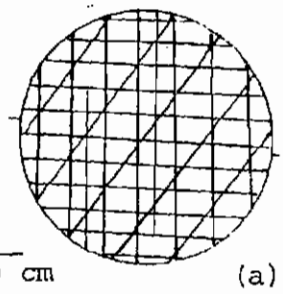

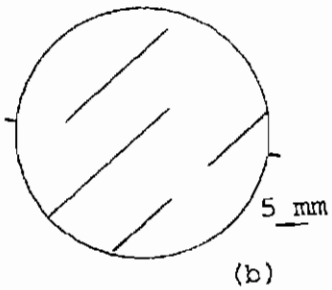

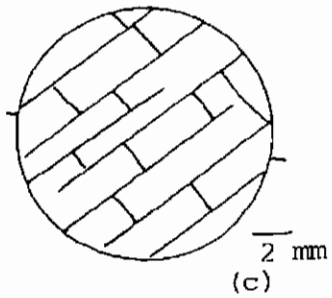

13-BB' (Coledale North)

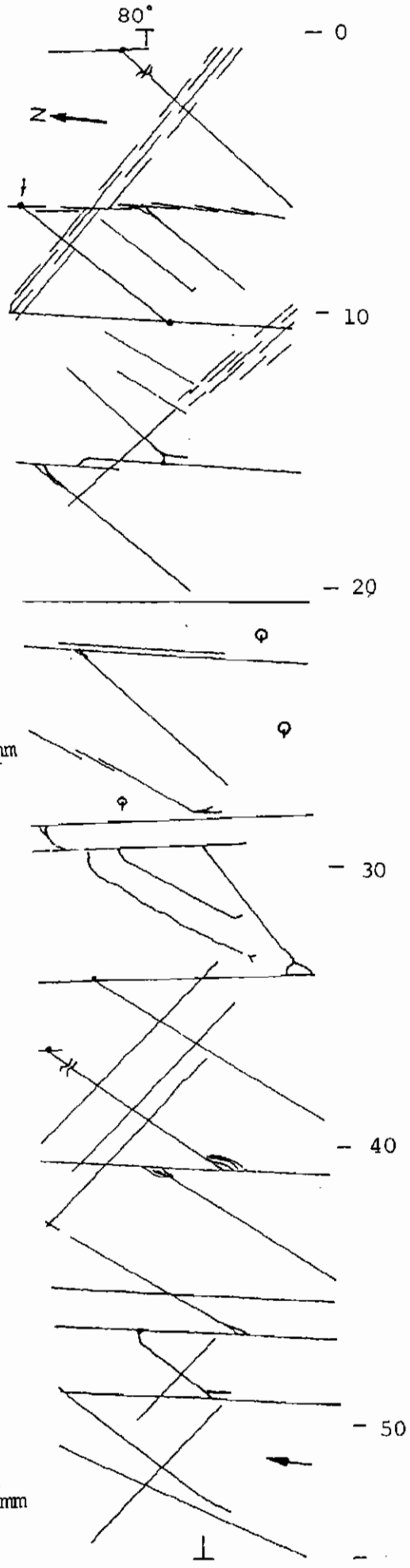

13-CC' (Coledale North)

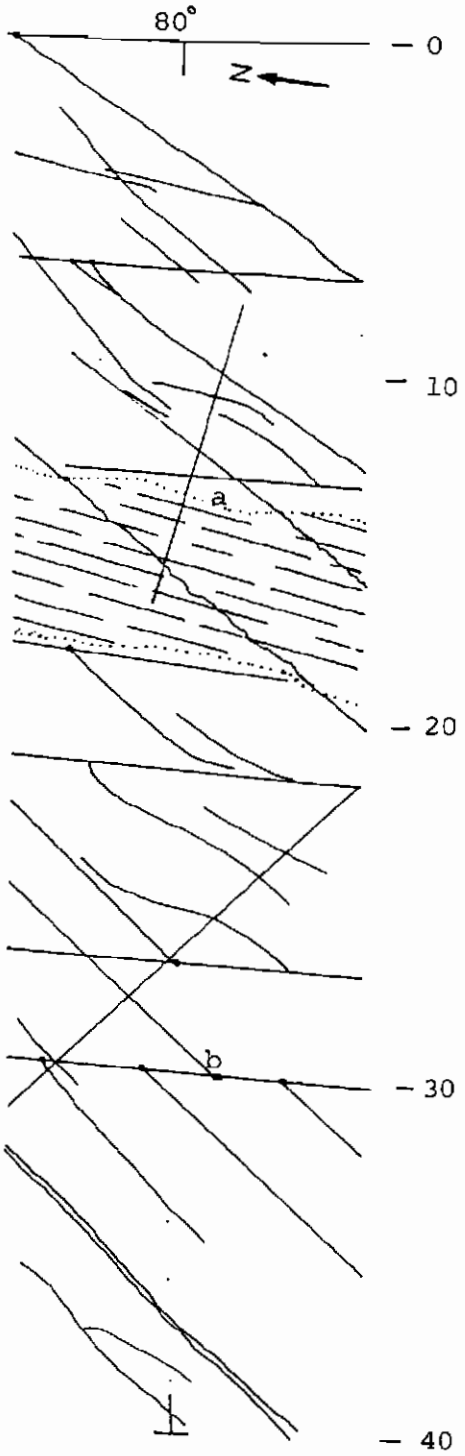

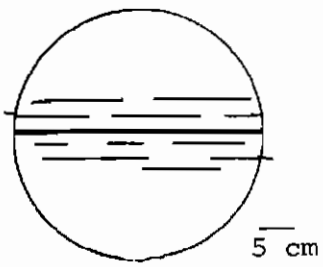

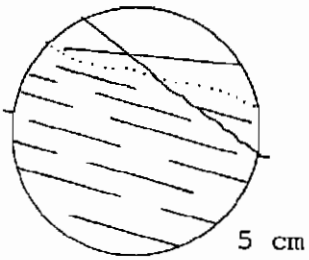

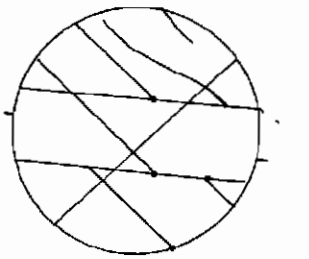

13-DD' (Coledale North)

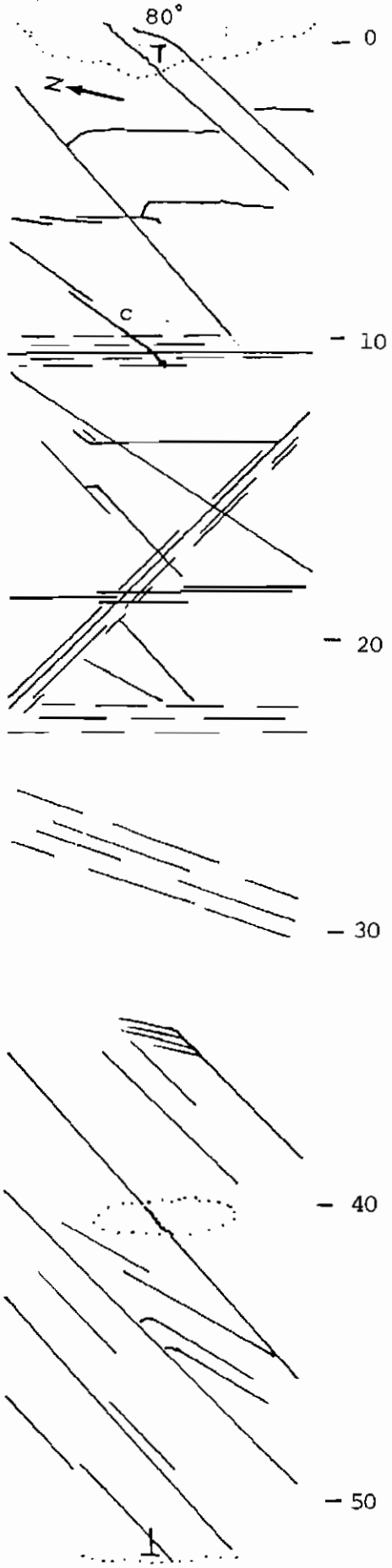

13-EE' (Coledale North)

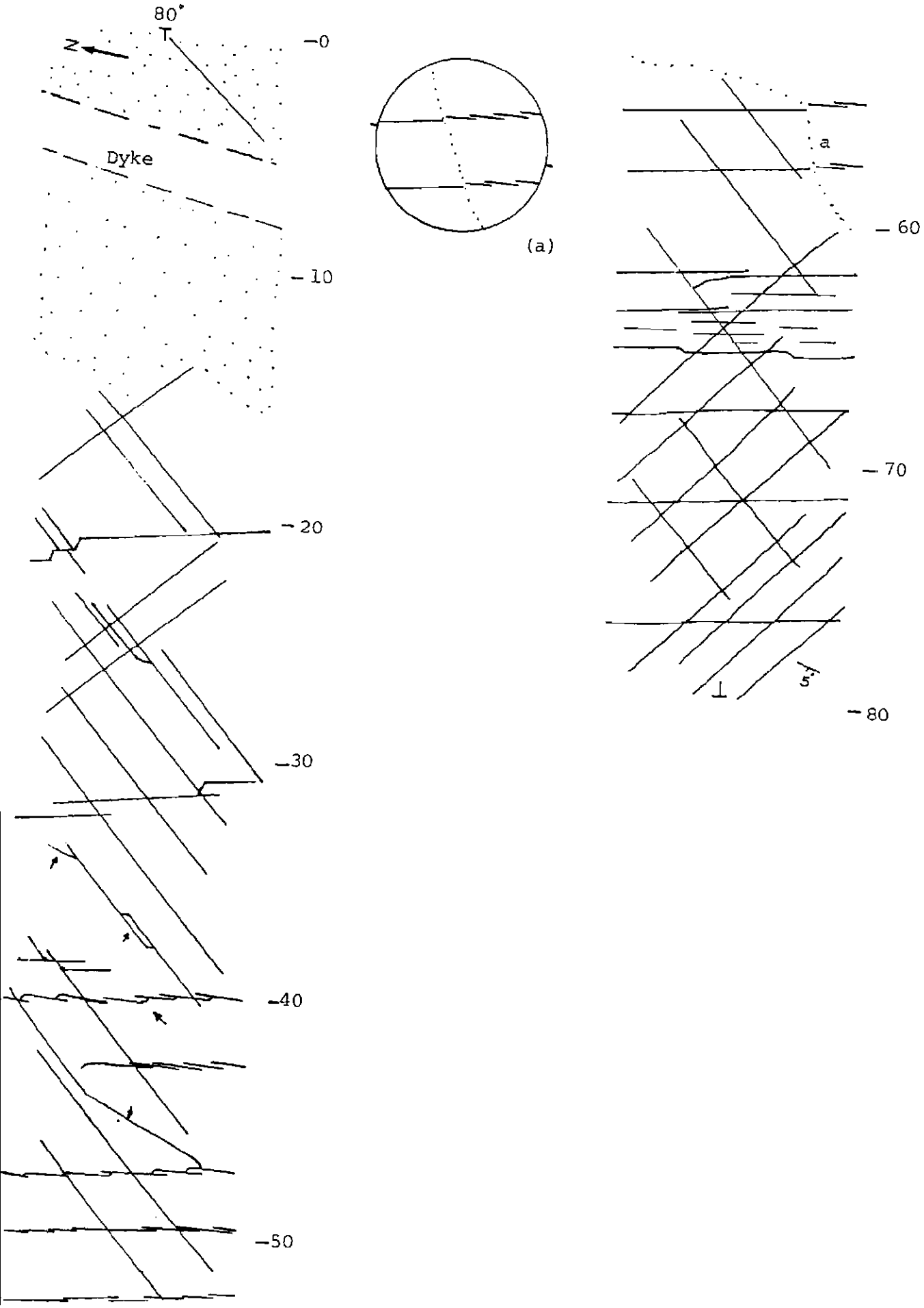

13-FF' (Coledale North)

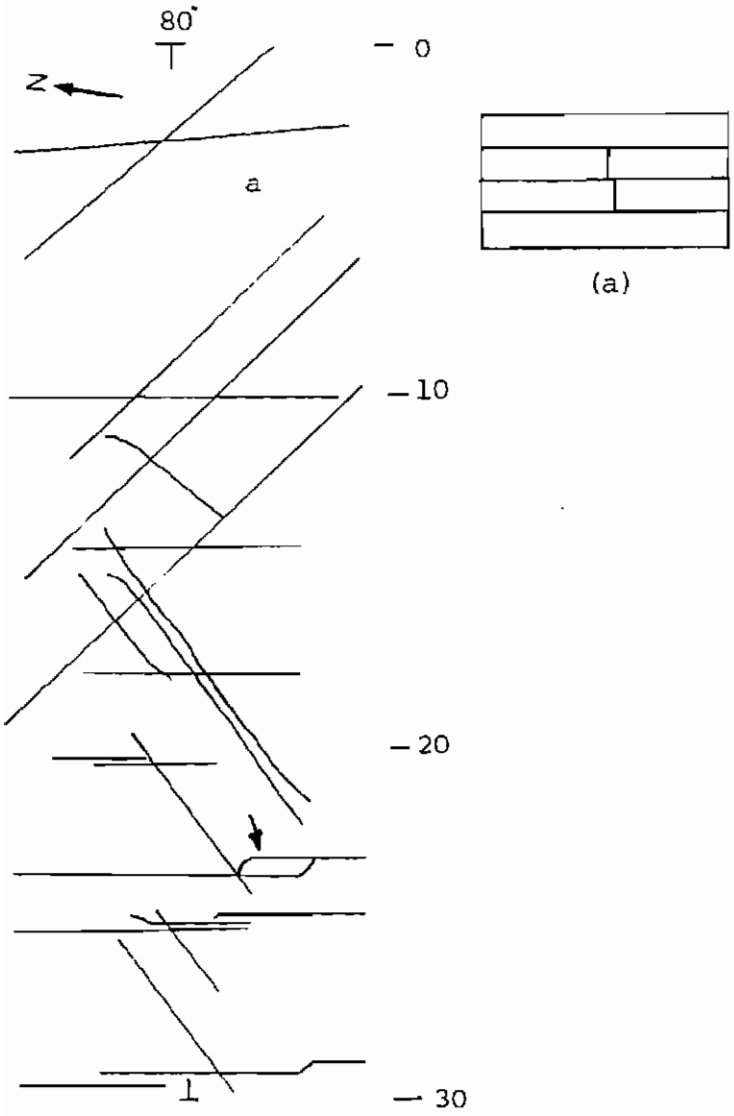

(a)

13-HH' (Coledale North)

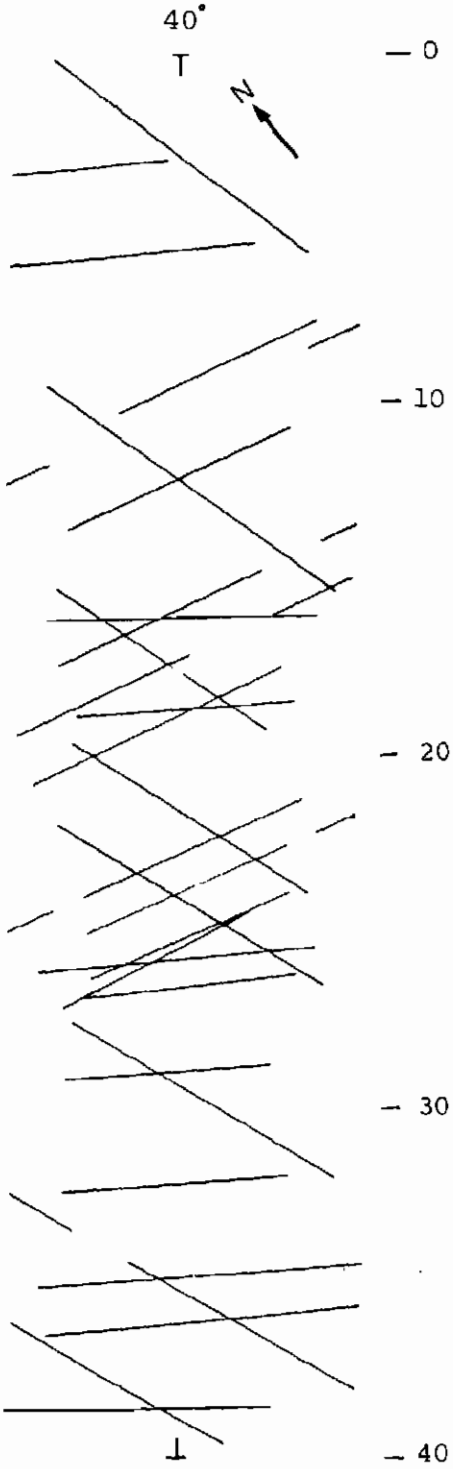

13-GG' (Coledale North)

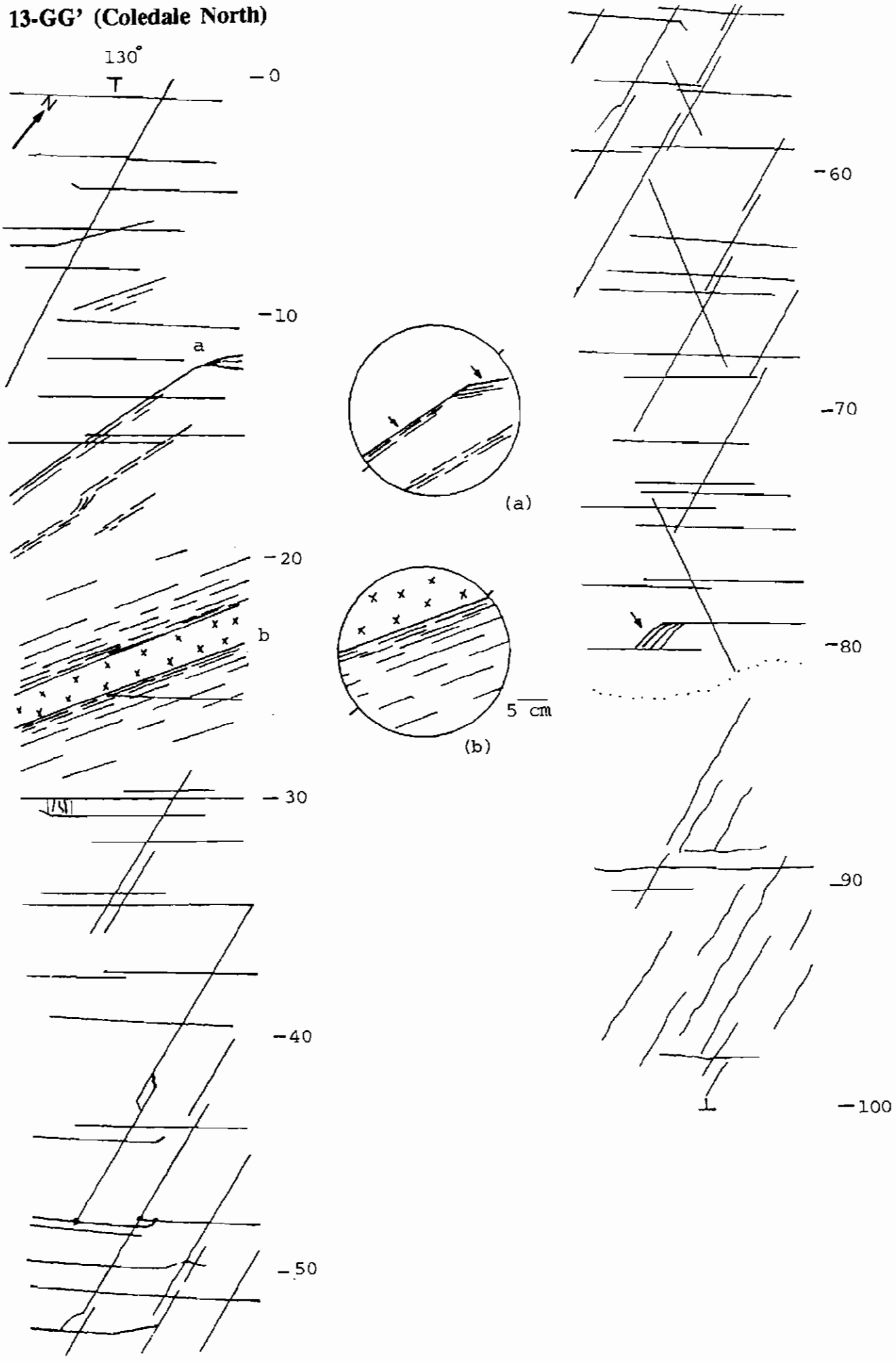

14-II' (Coledale Pool)

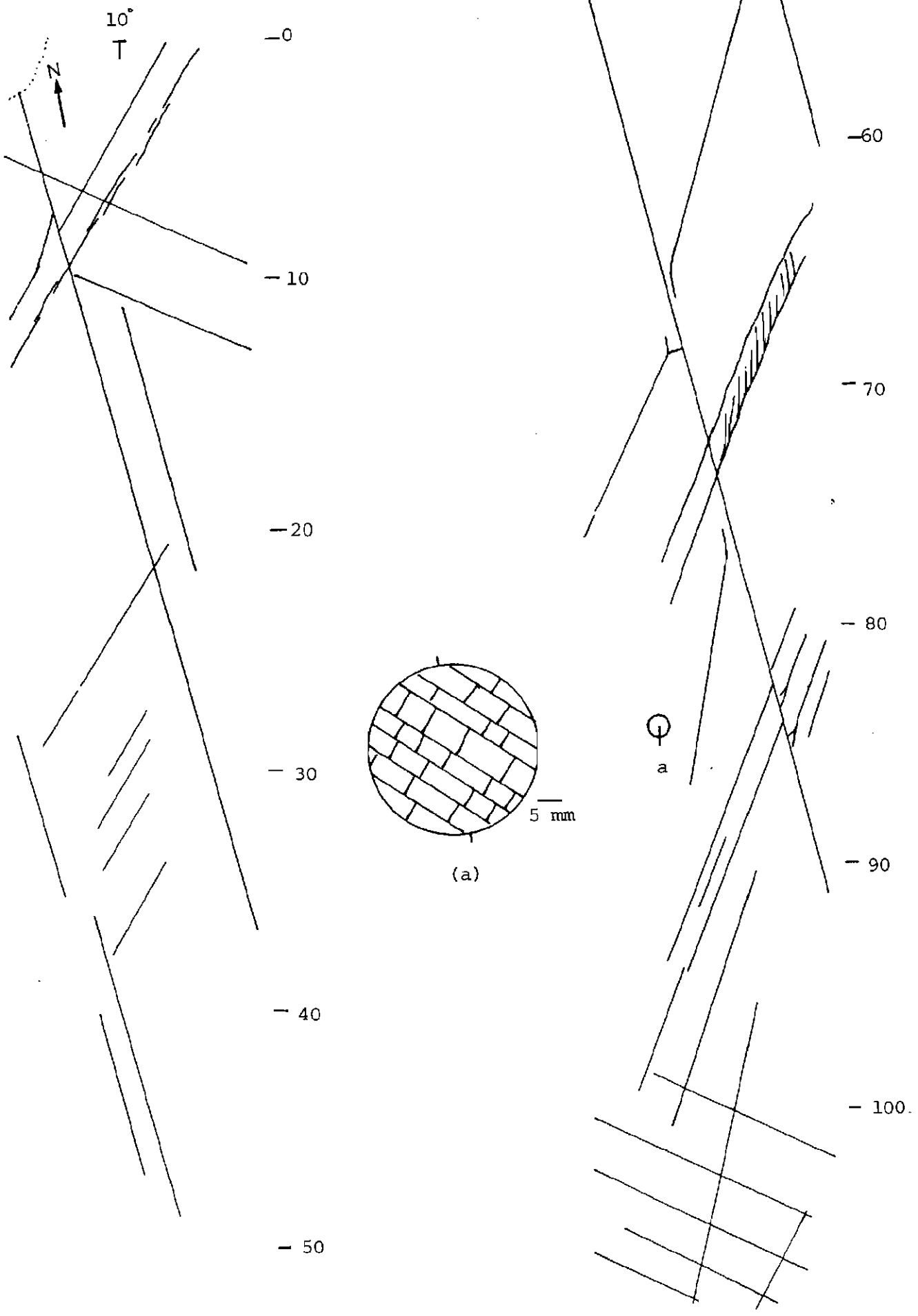

14-II' cont.

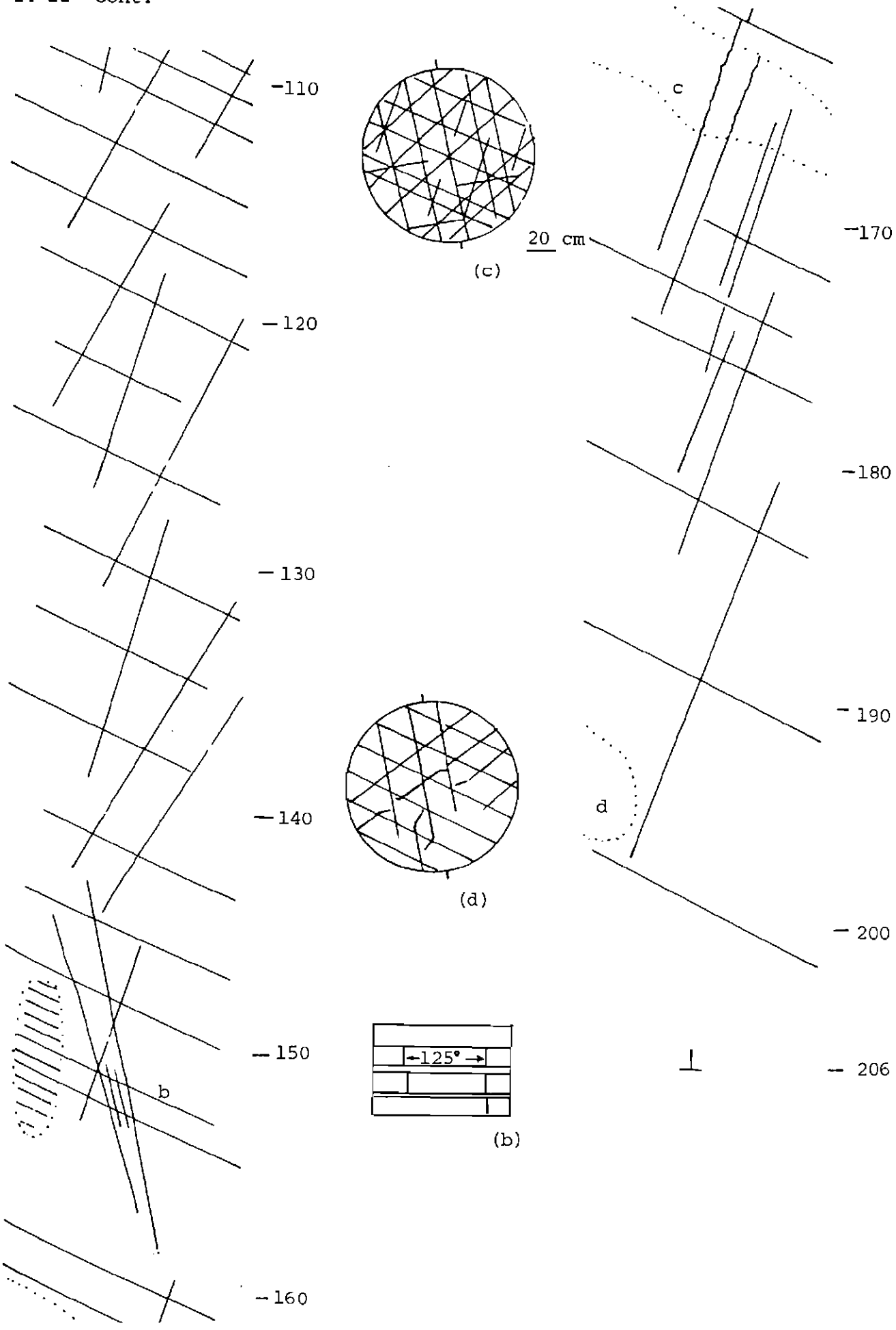

14-KK' (Coledale Pool)

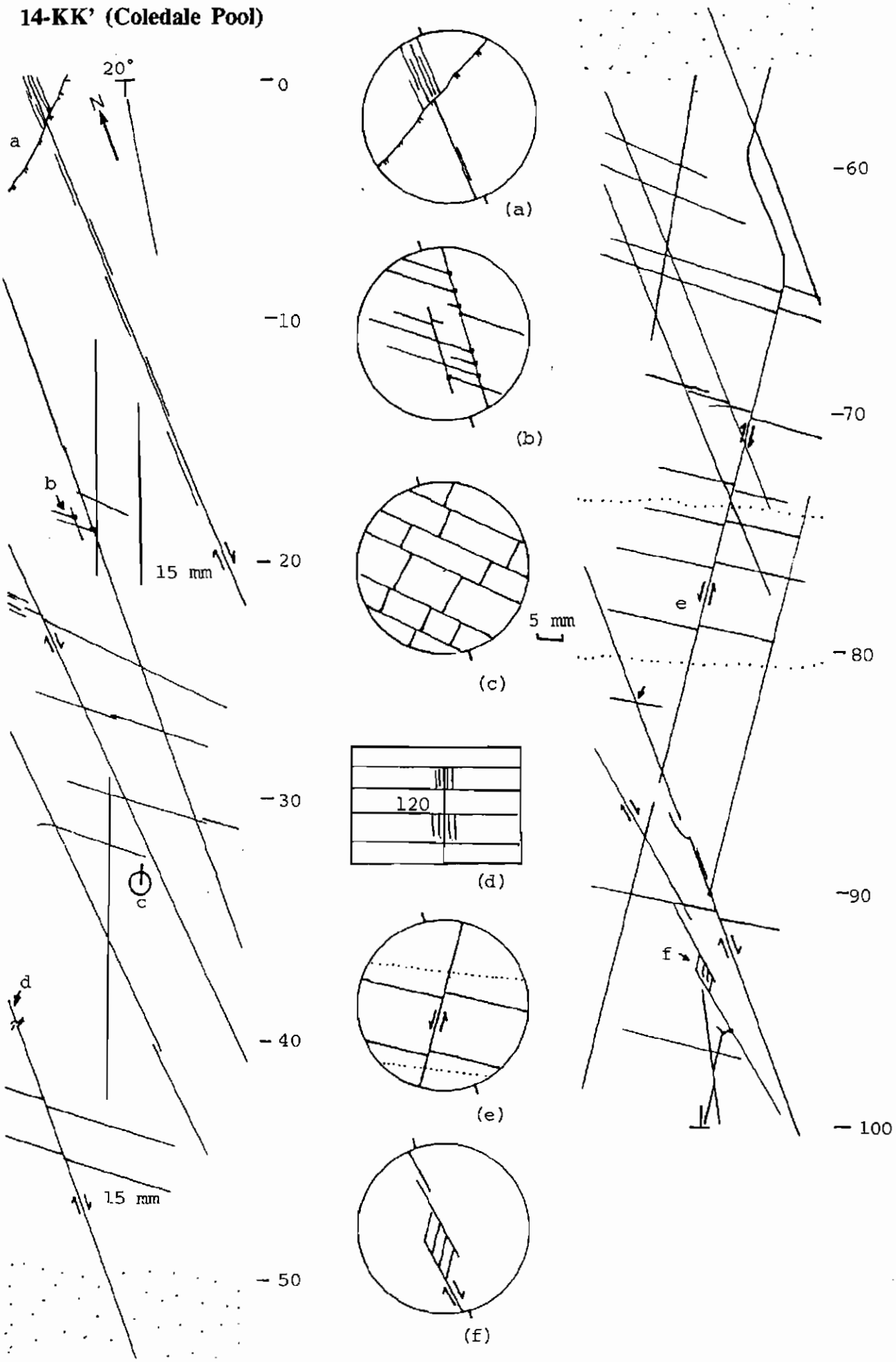

14-LL' (Coledale Pool)

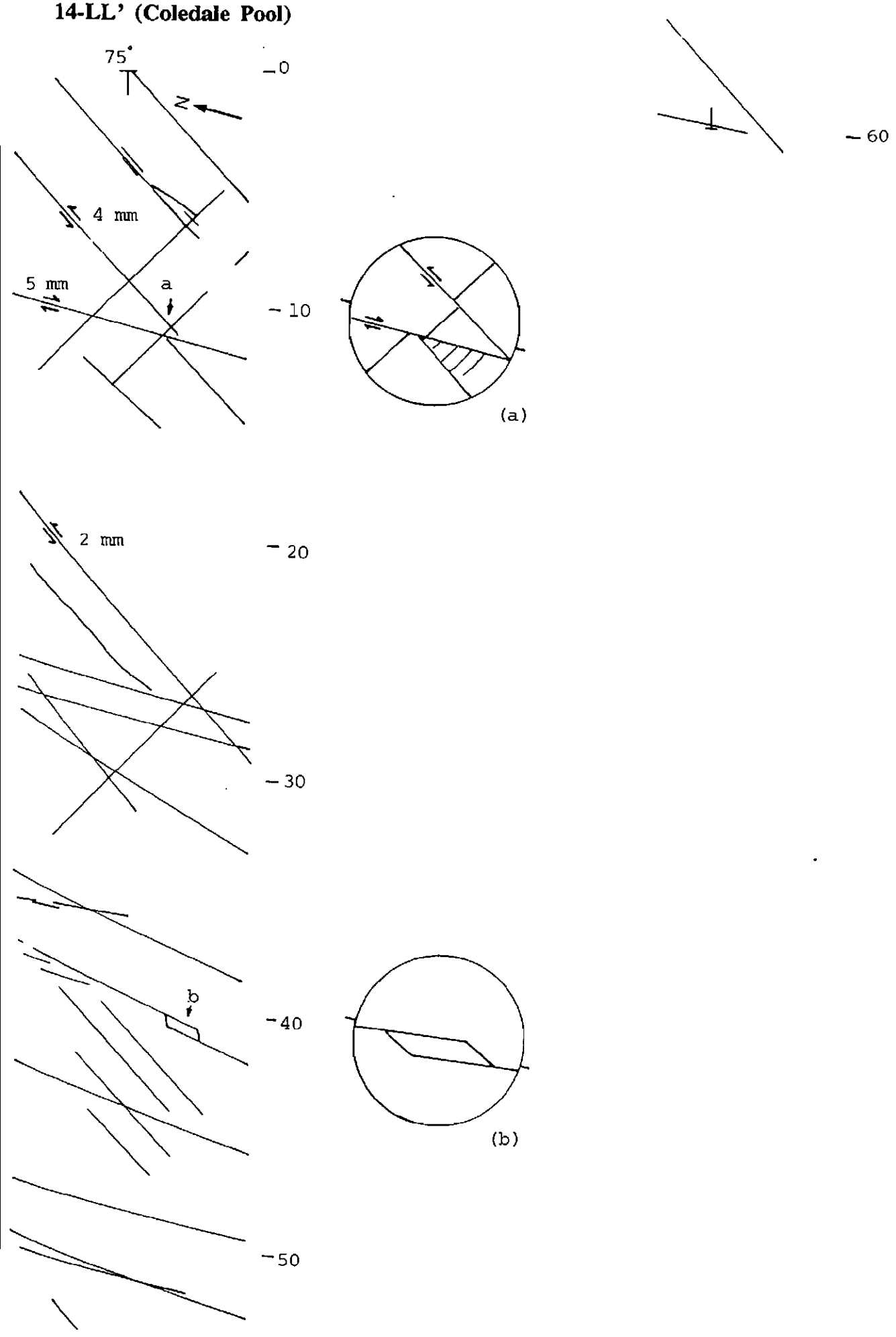

15-JJ' (Coledale South)

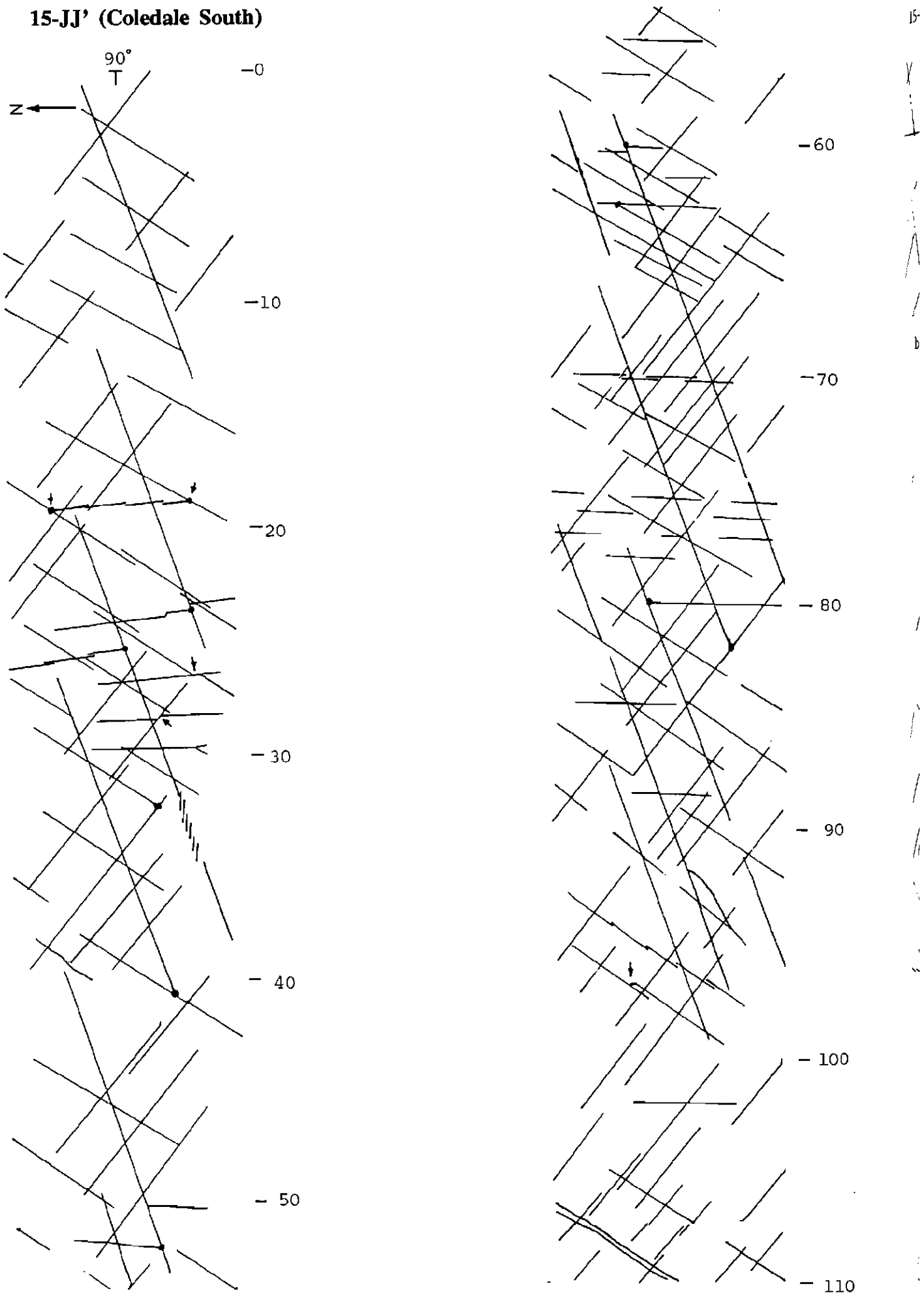

15-JJ' cont.

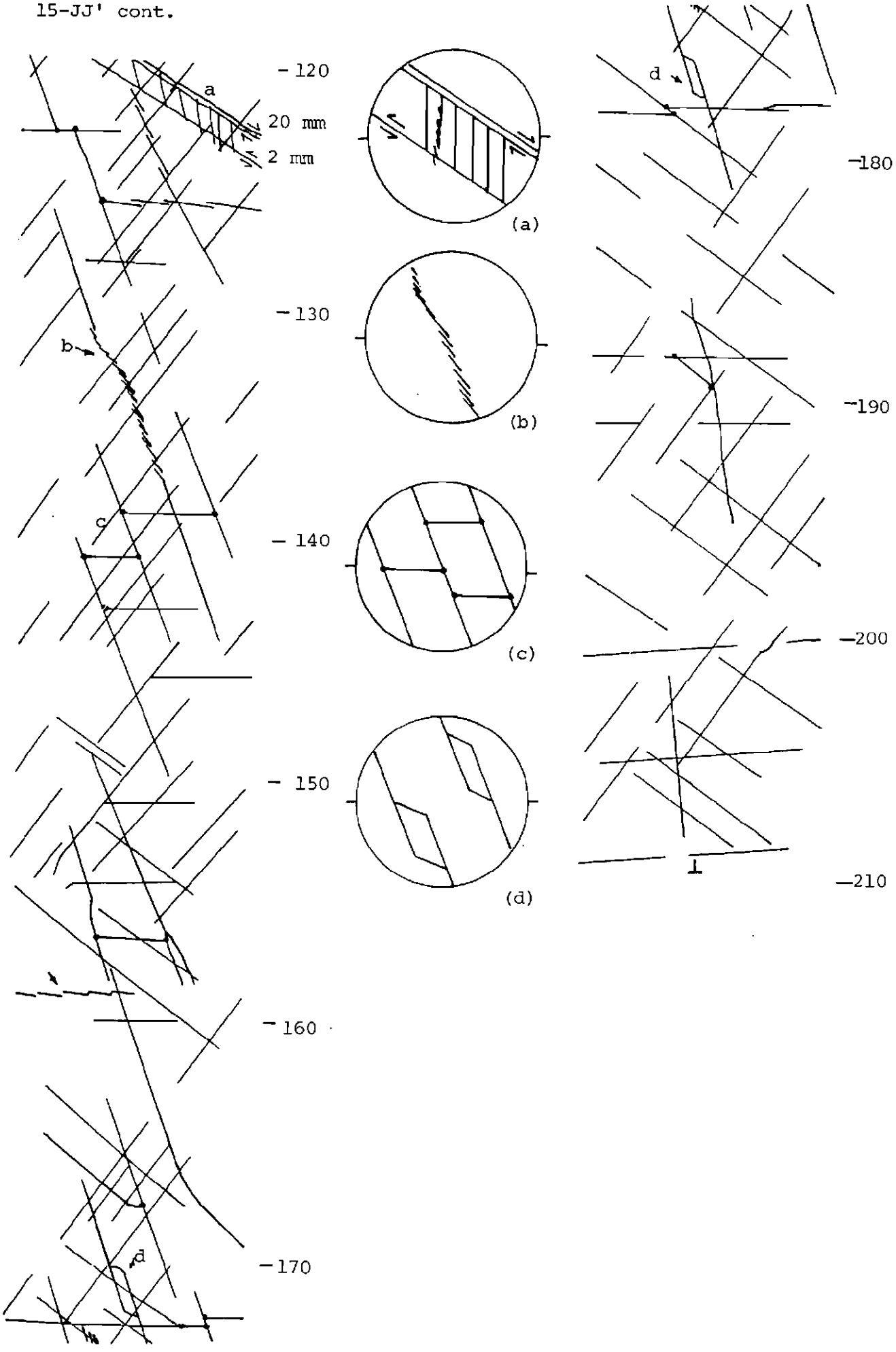

15-MM' (Coledale South)

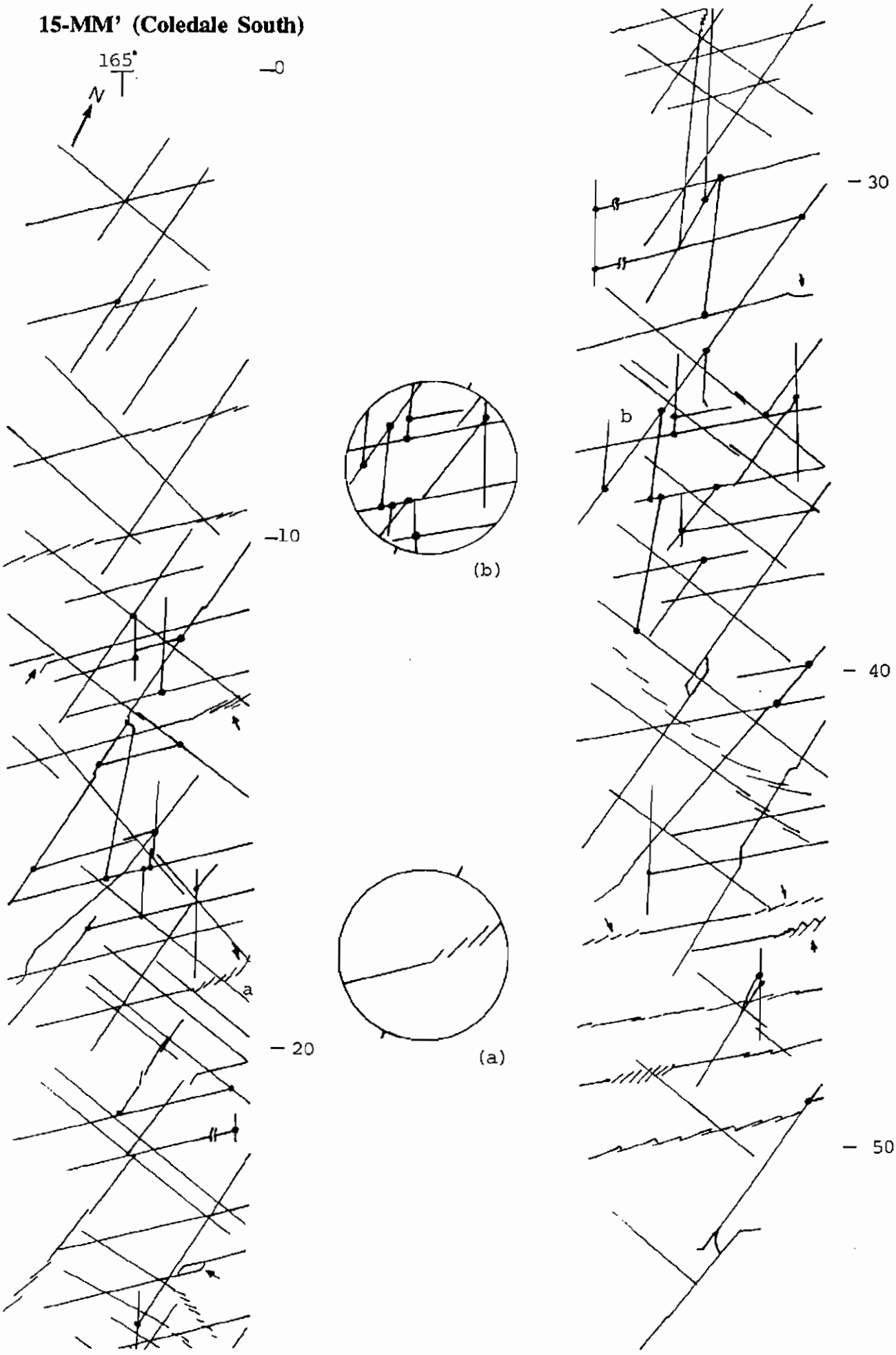

15-MM' cont.

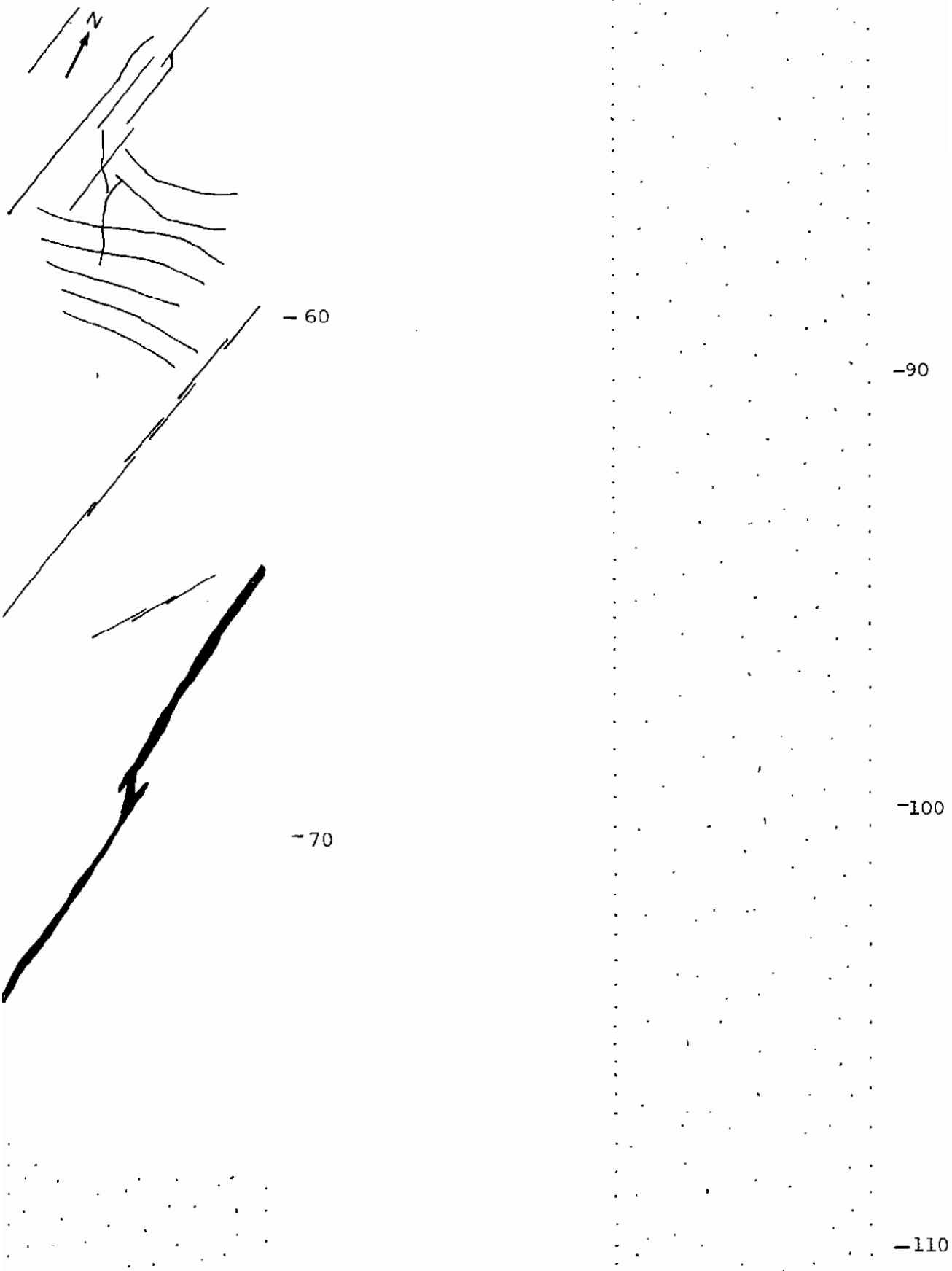

15-MM' cont.

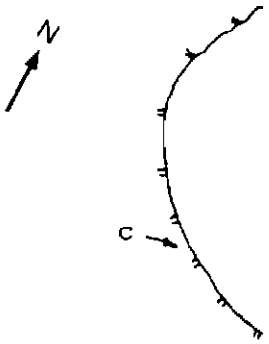

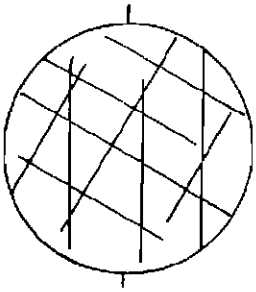

(c)

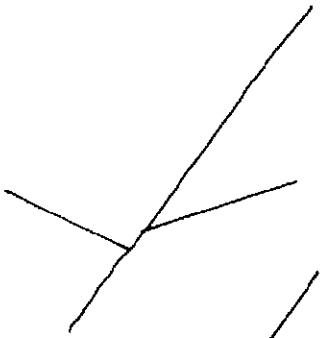

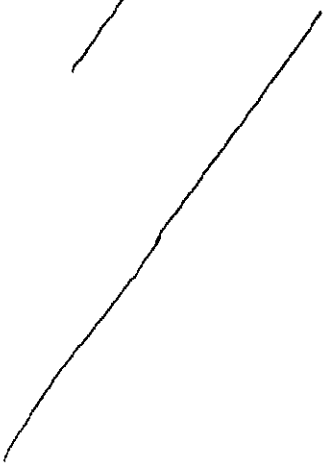

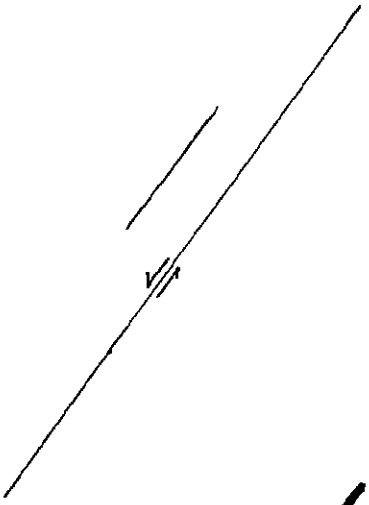

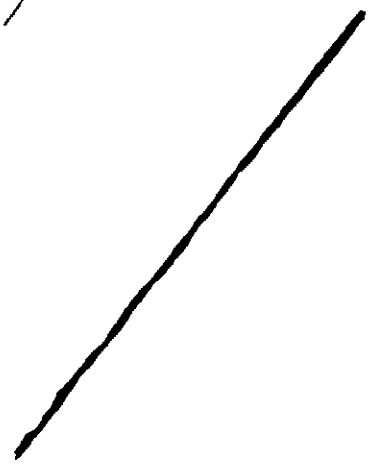

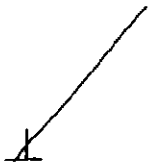

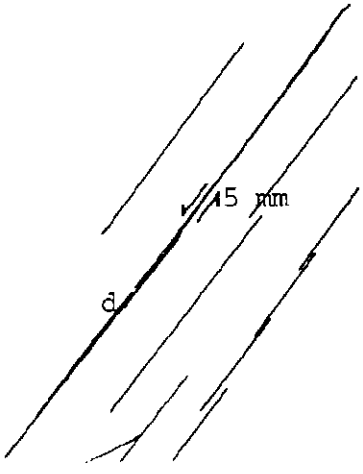

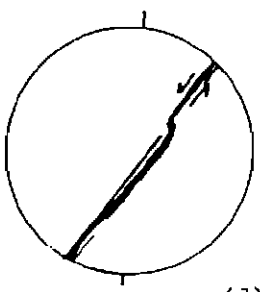

(d)

16-AA' (Brickyard North)

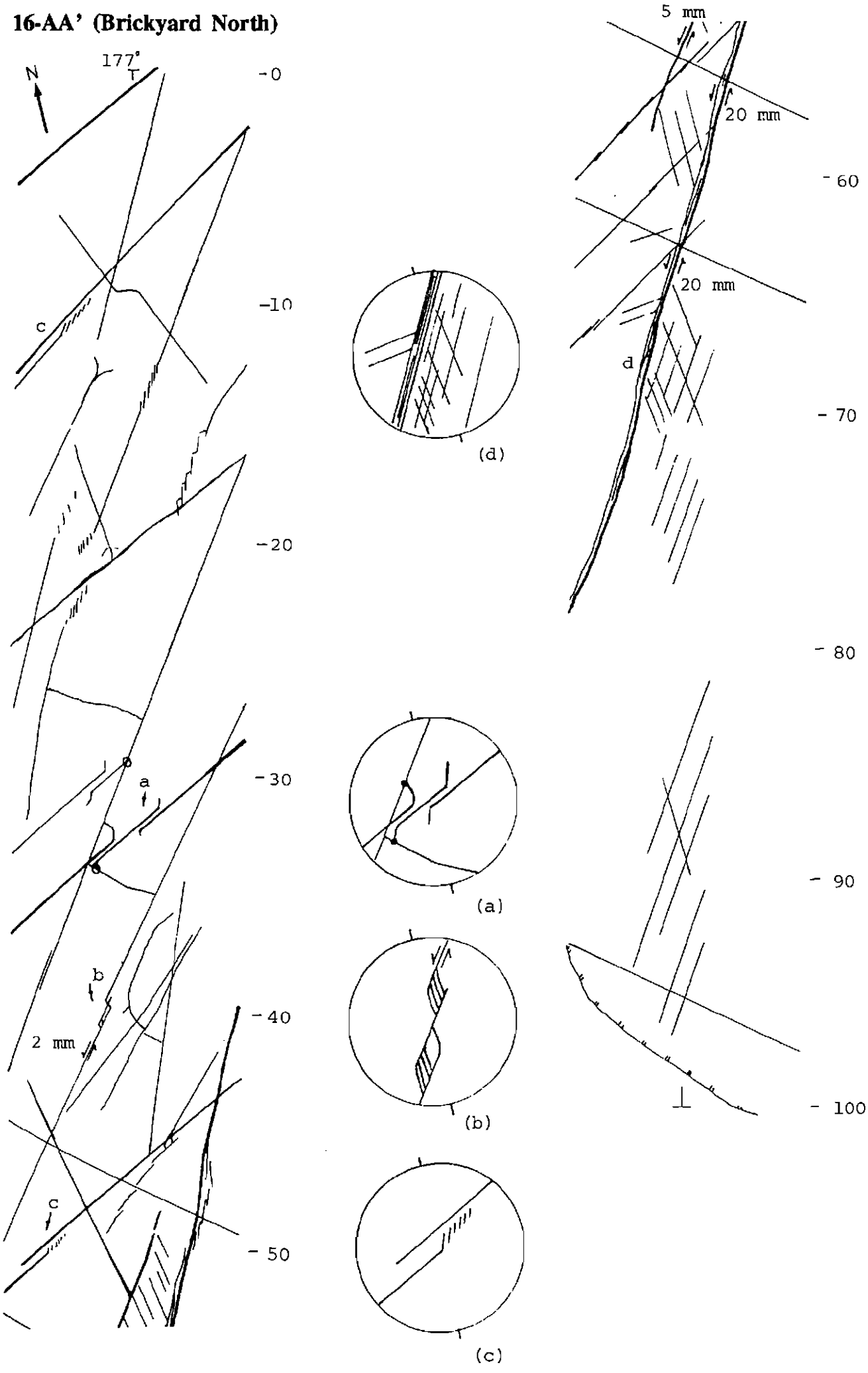

16-BB' (Brickyard North)

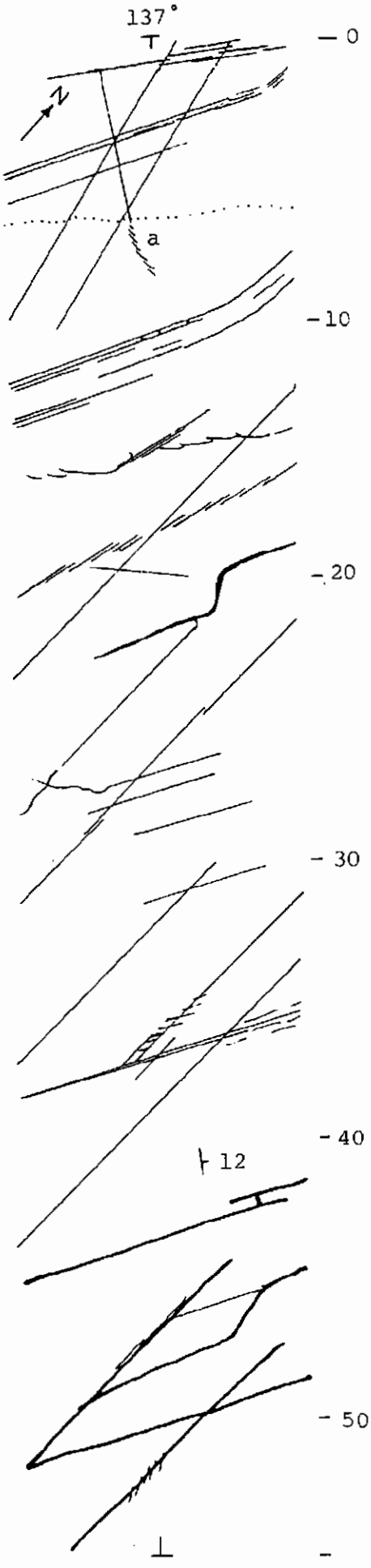

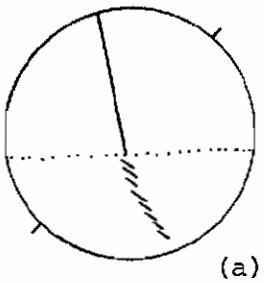

16-CC' (Brickyard North)

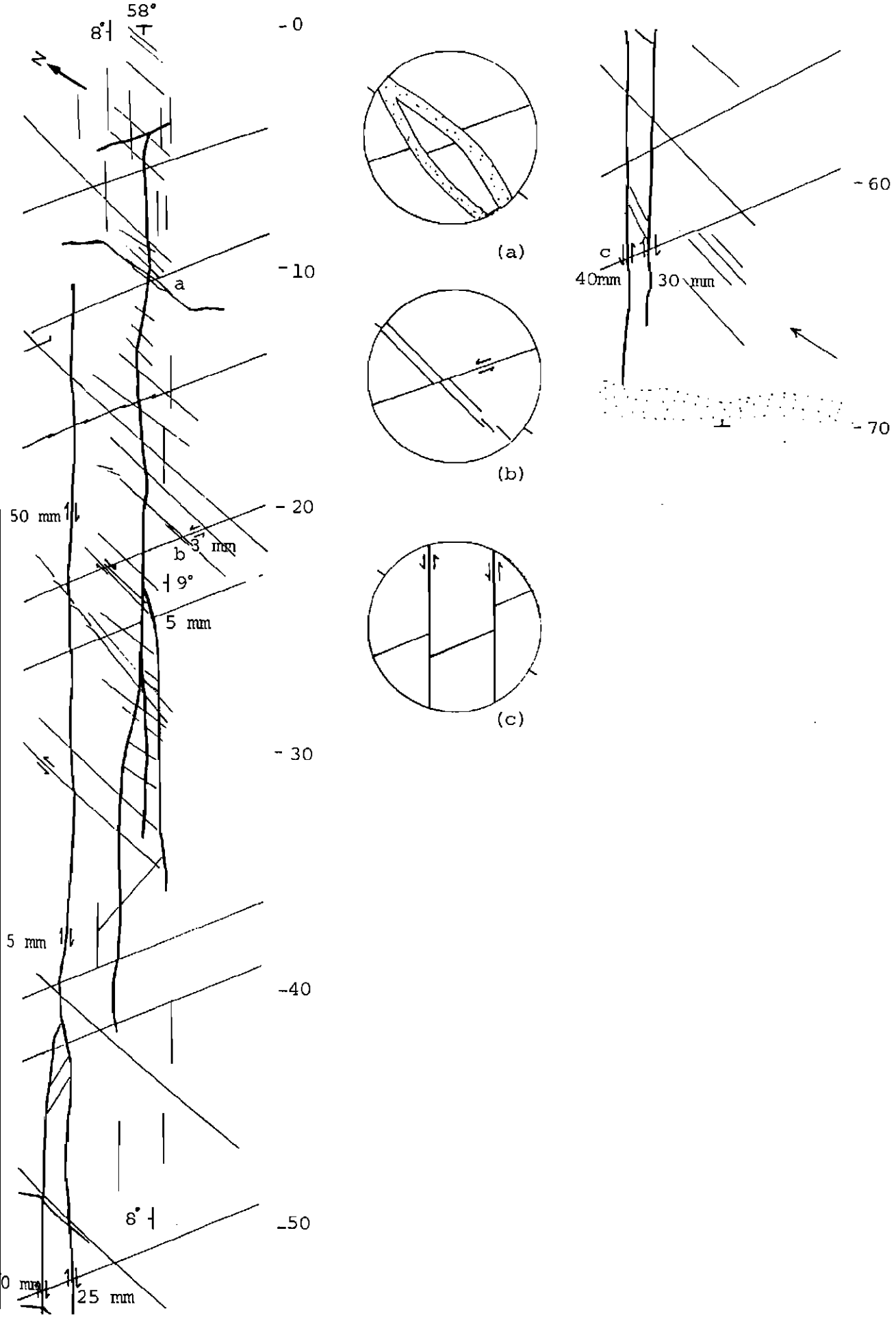

16-DD' (Brickyard North)

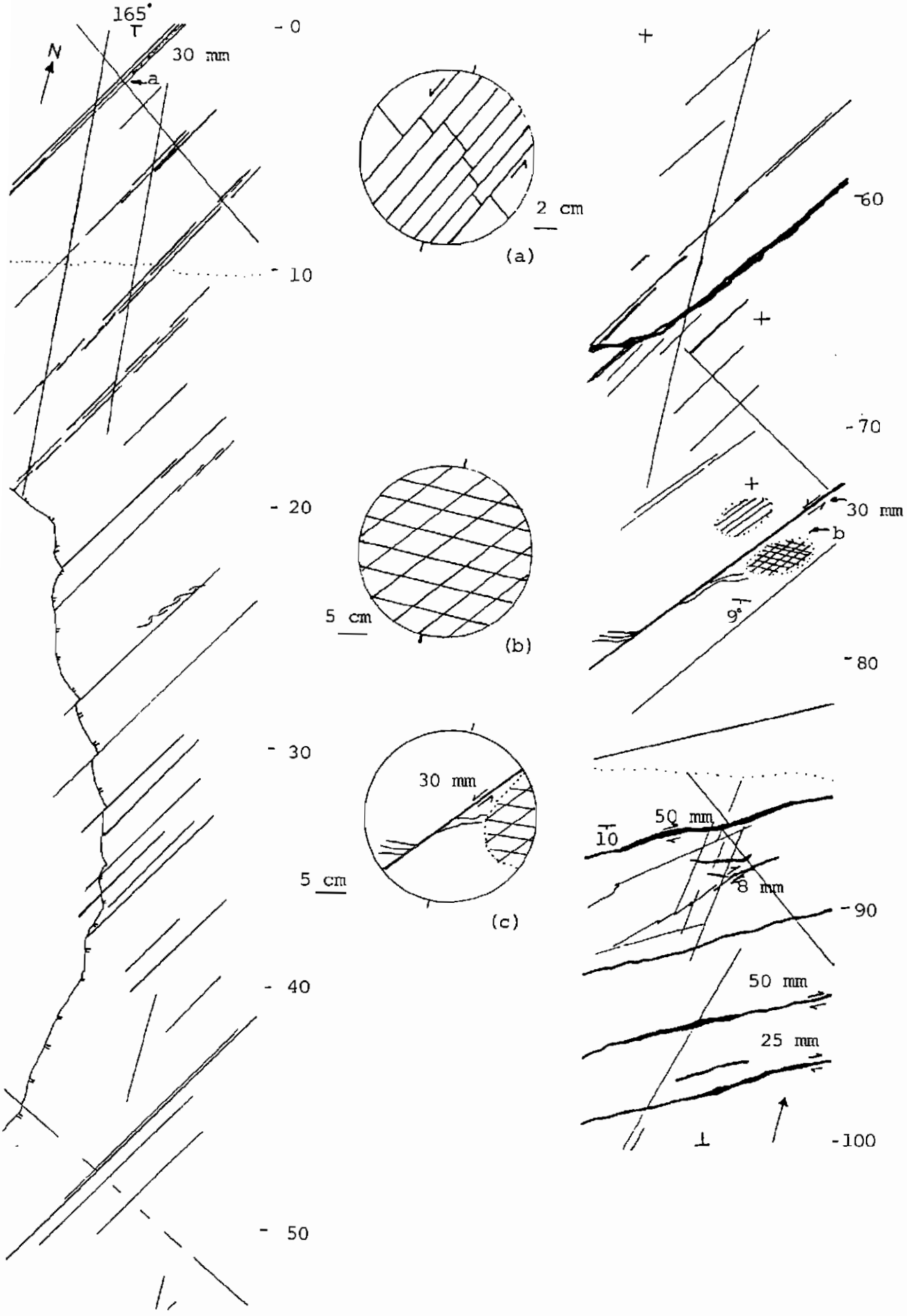

16-DD'2 (Brickyard North)

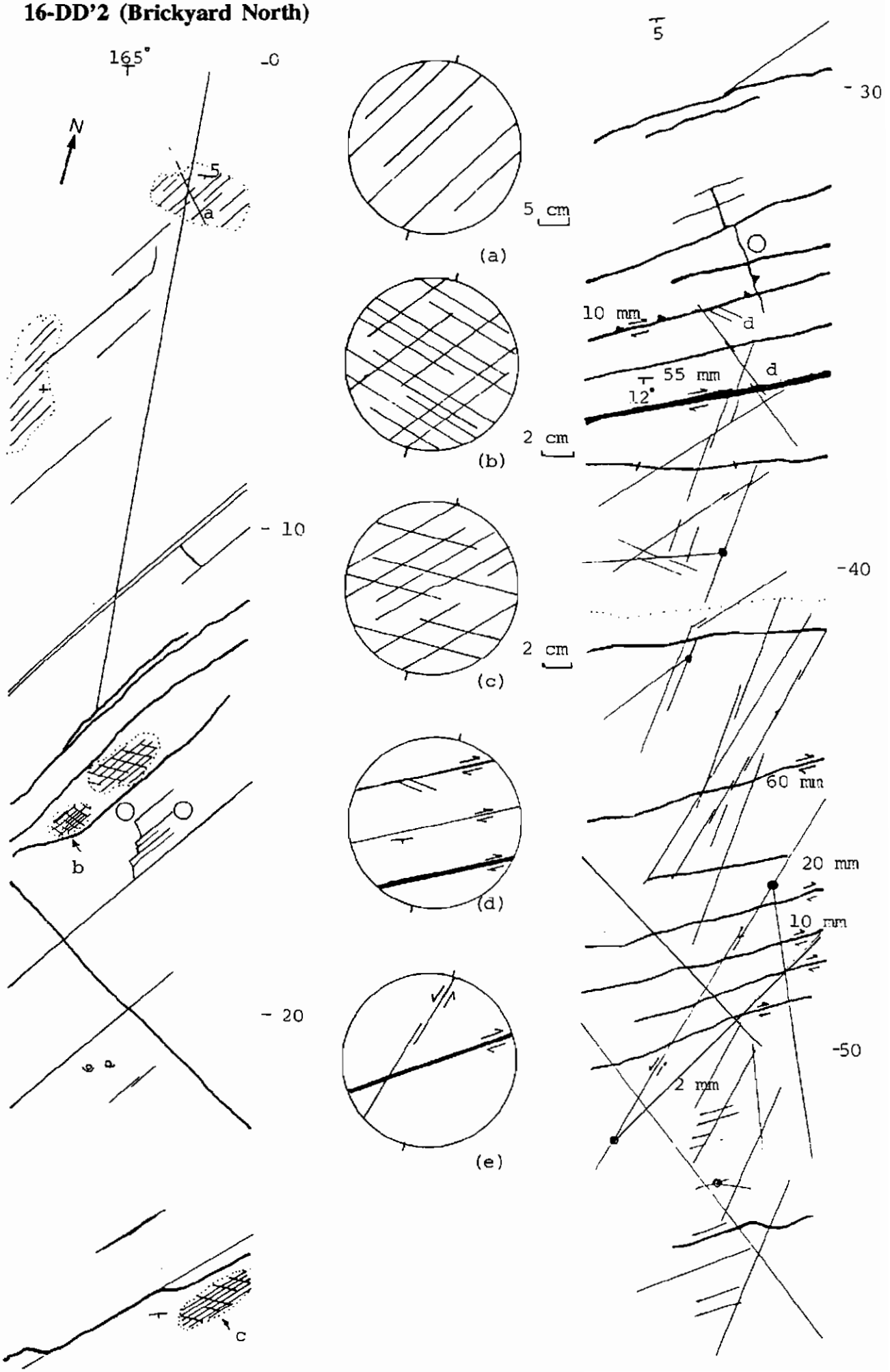

16-DD'2 cont.

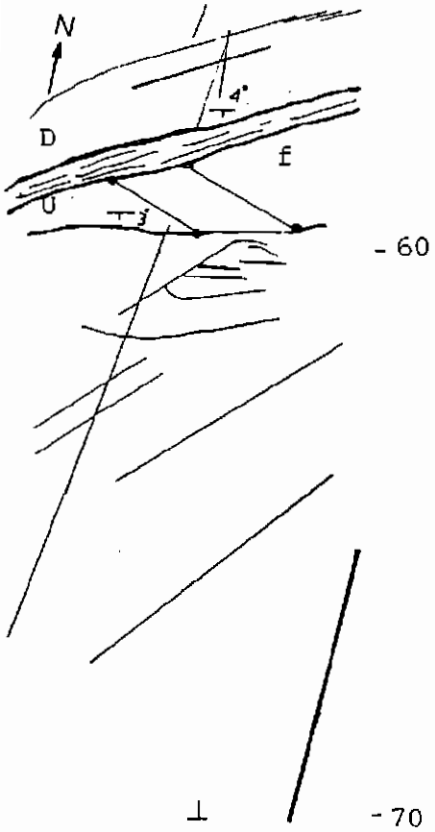

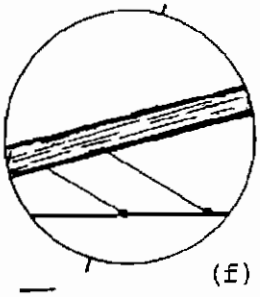

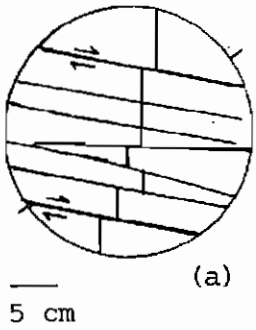

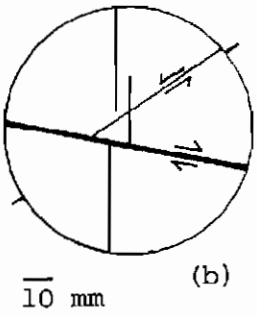

16-EE' (Brickyard North)

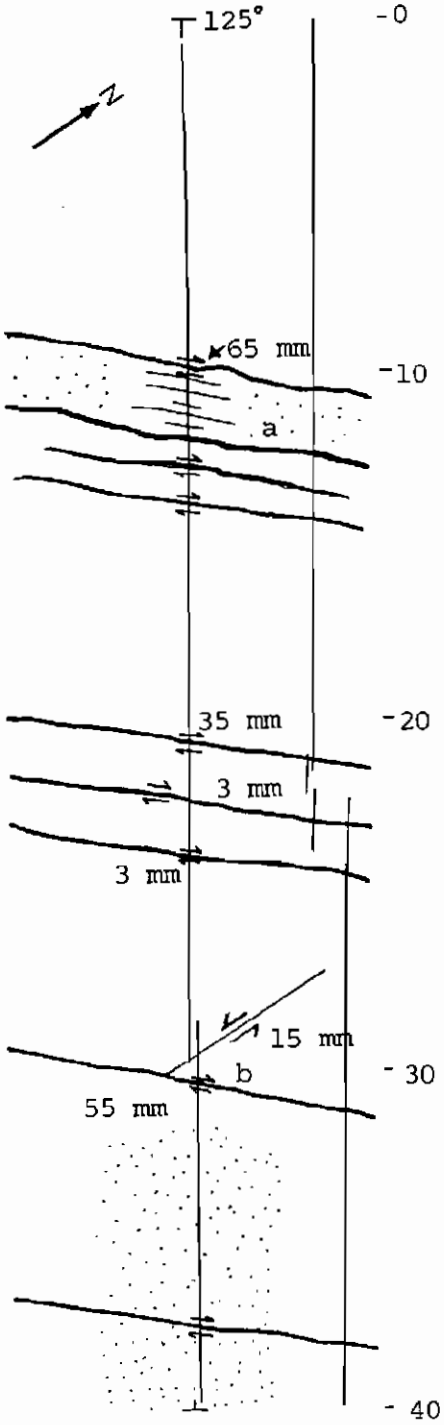

17-AA' (Brickyard Point)

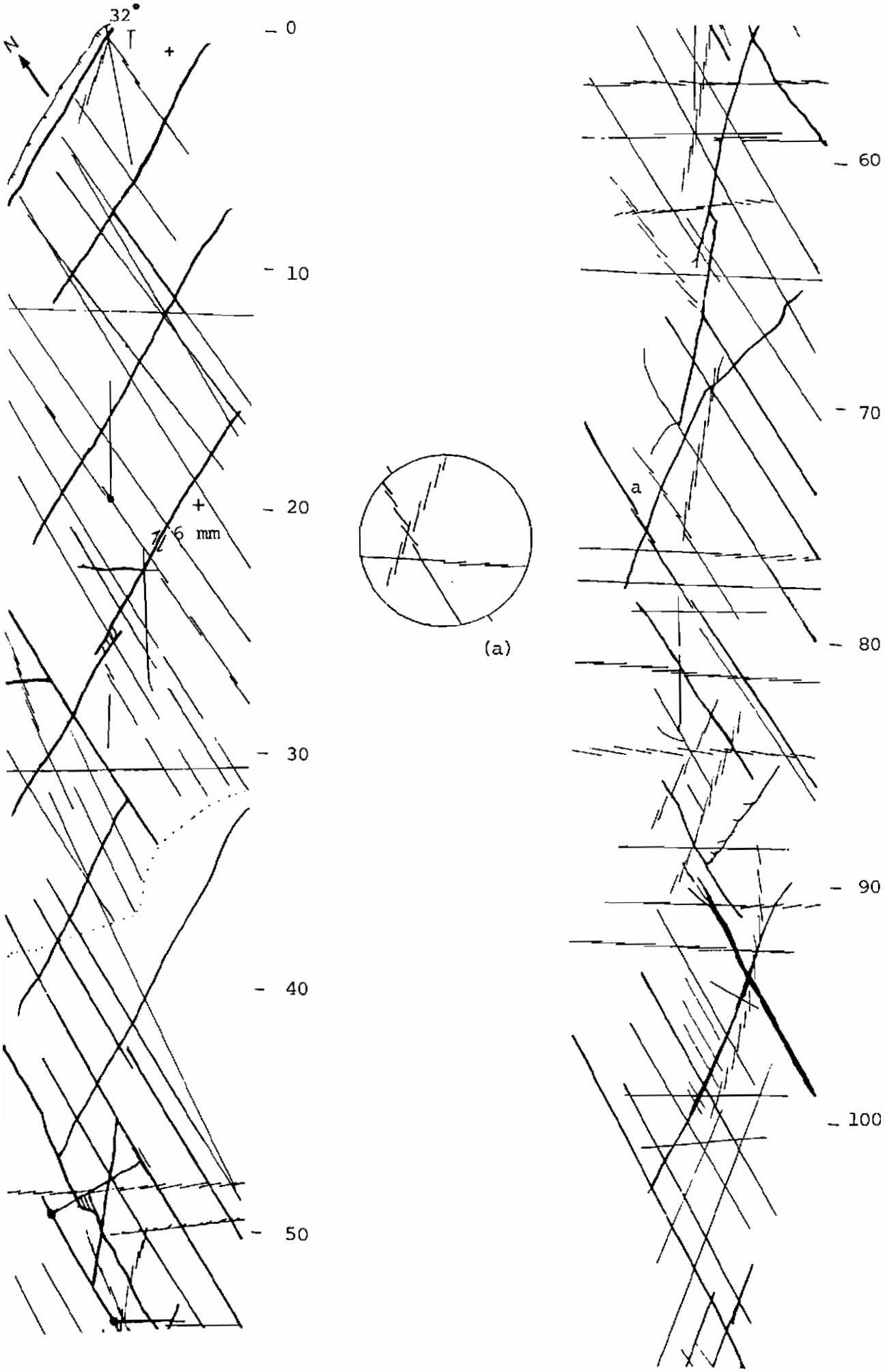

17- AA' cont.

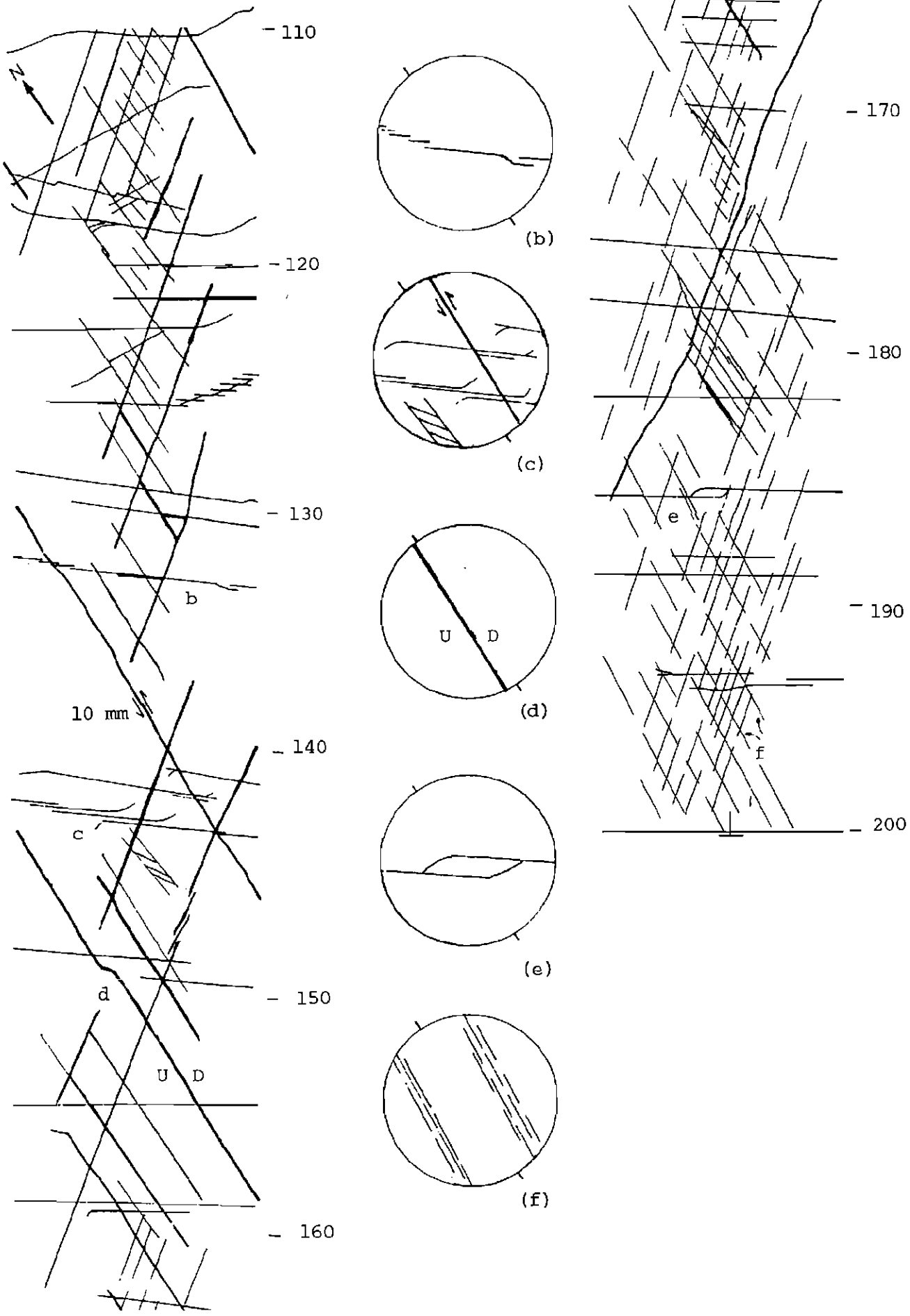

17-BB' (Brickyard Point)

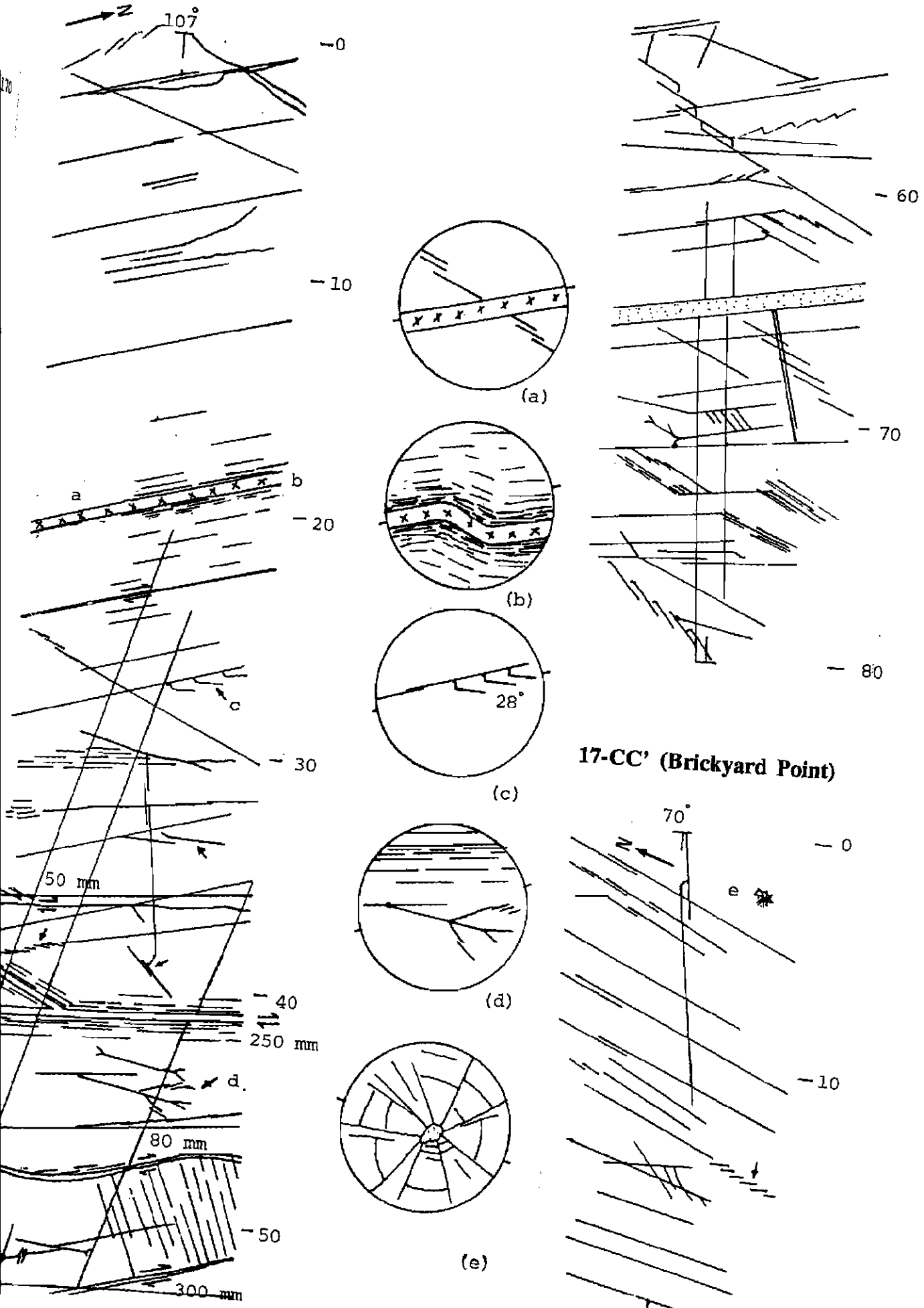

17-CC' (Brickyard Point)

17-DD' (Brickyard Point)

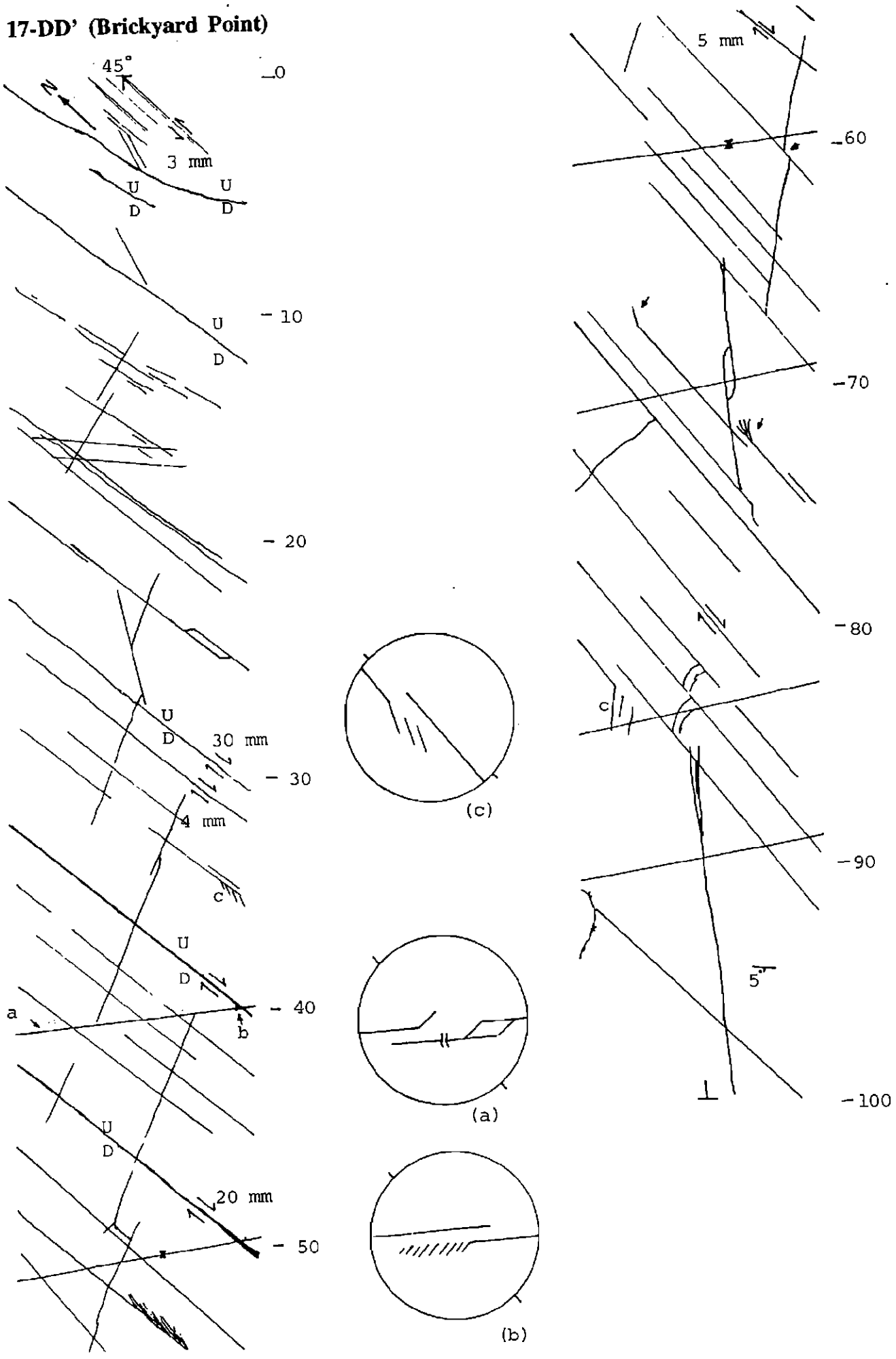

17-EE' (Brickyard Point)

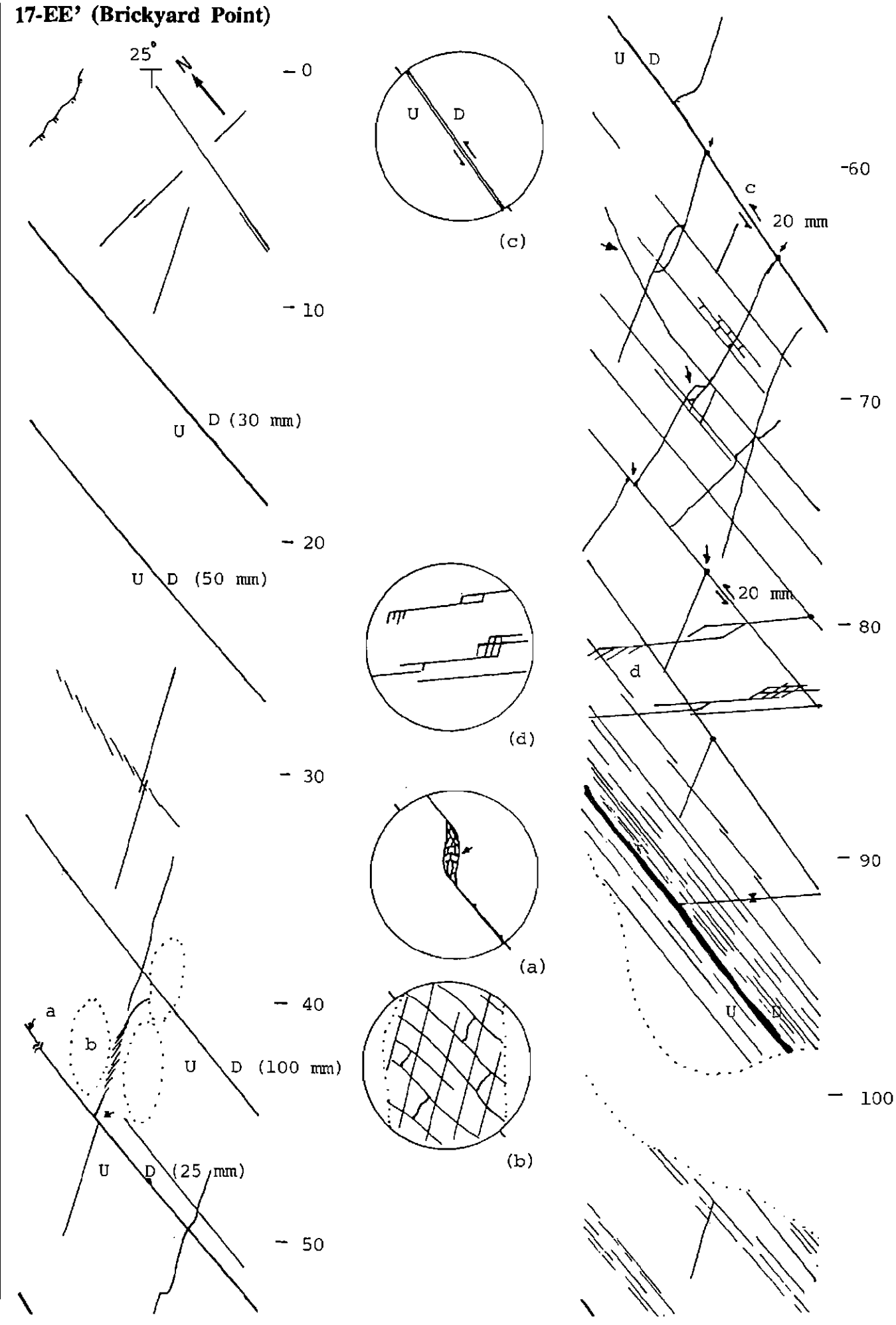

17- EE' cont.

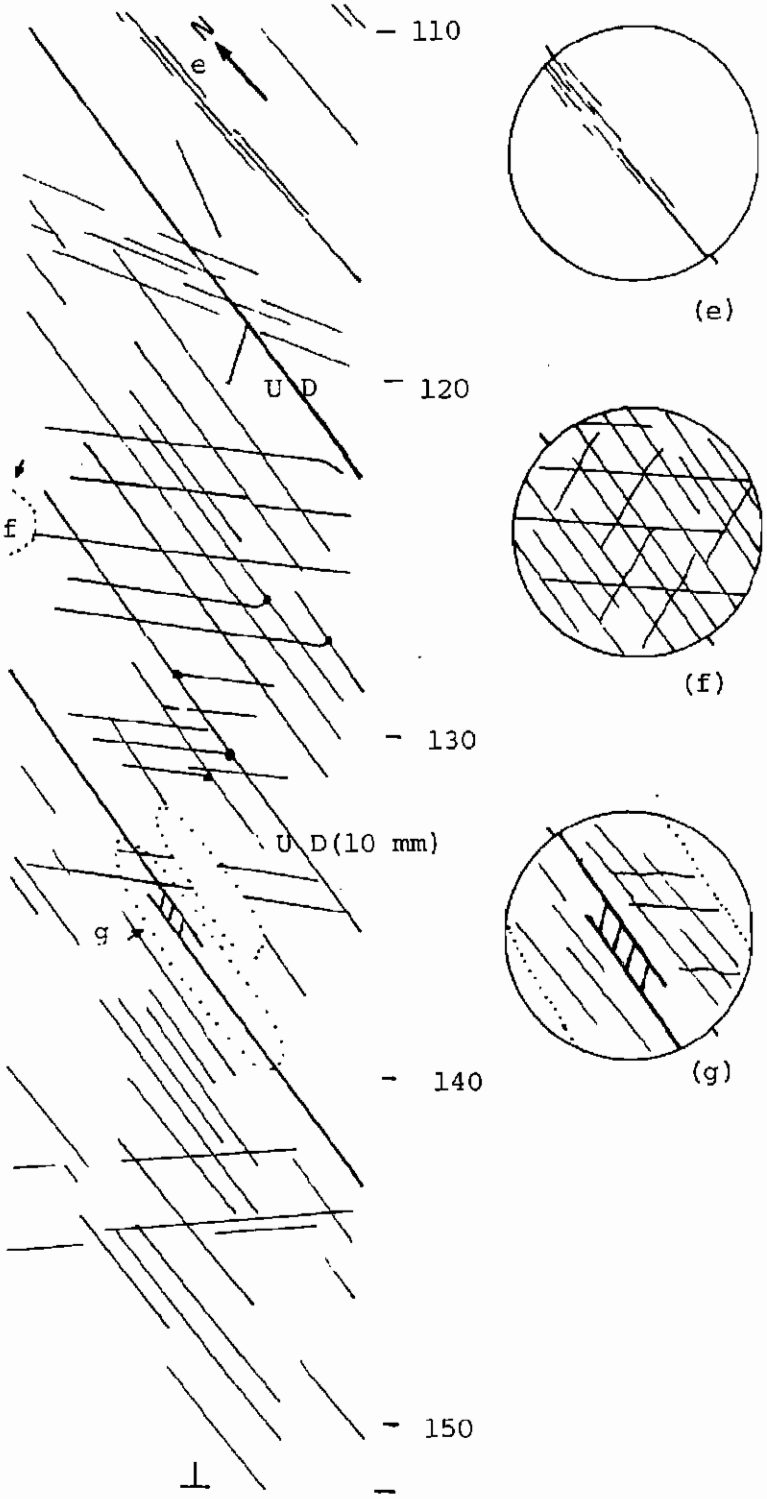

(e)

(f)

(g)

18-AA' (Bell Point)

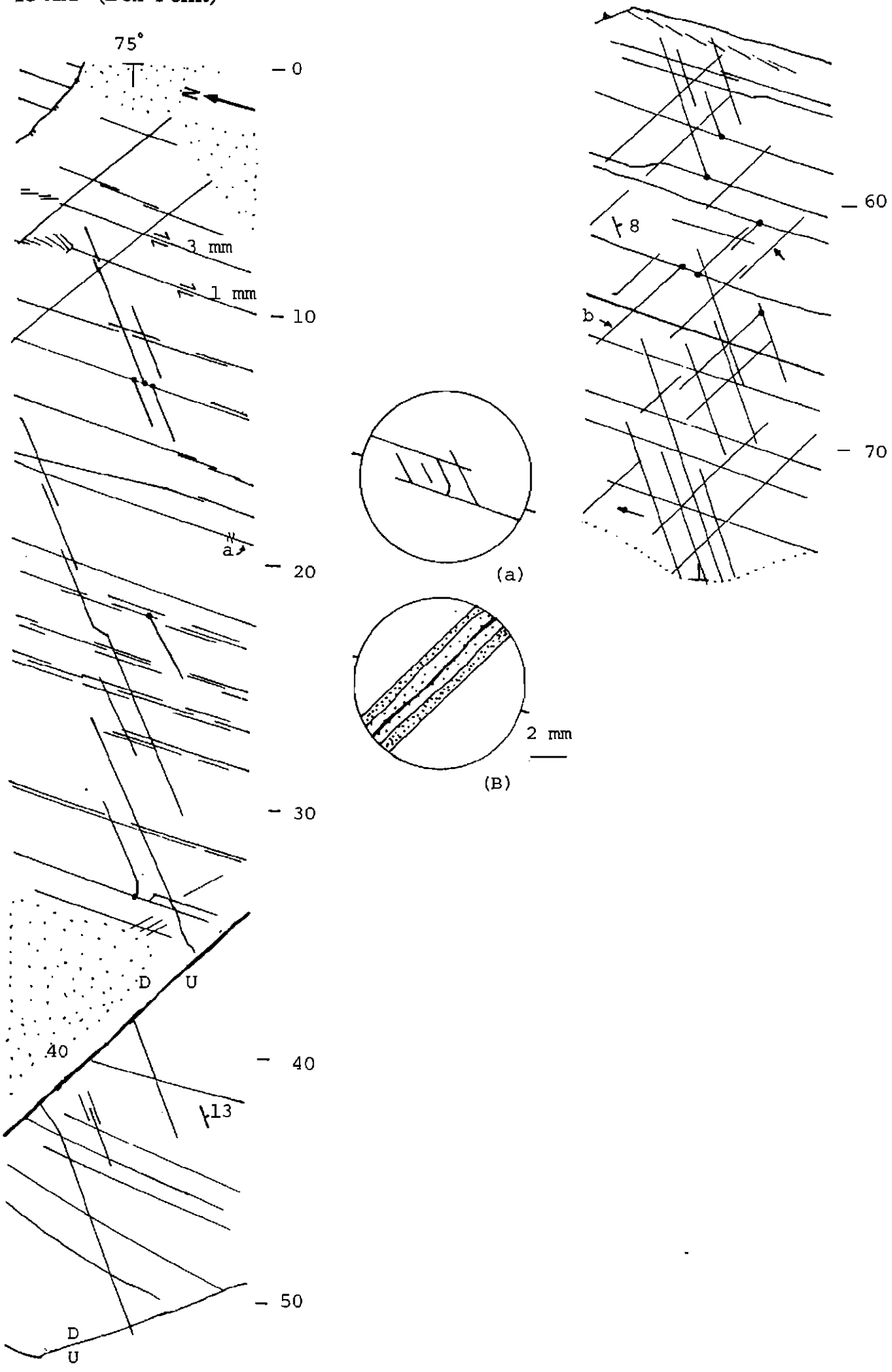

18-BB' (Bell Point)

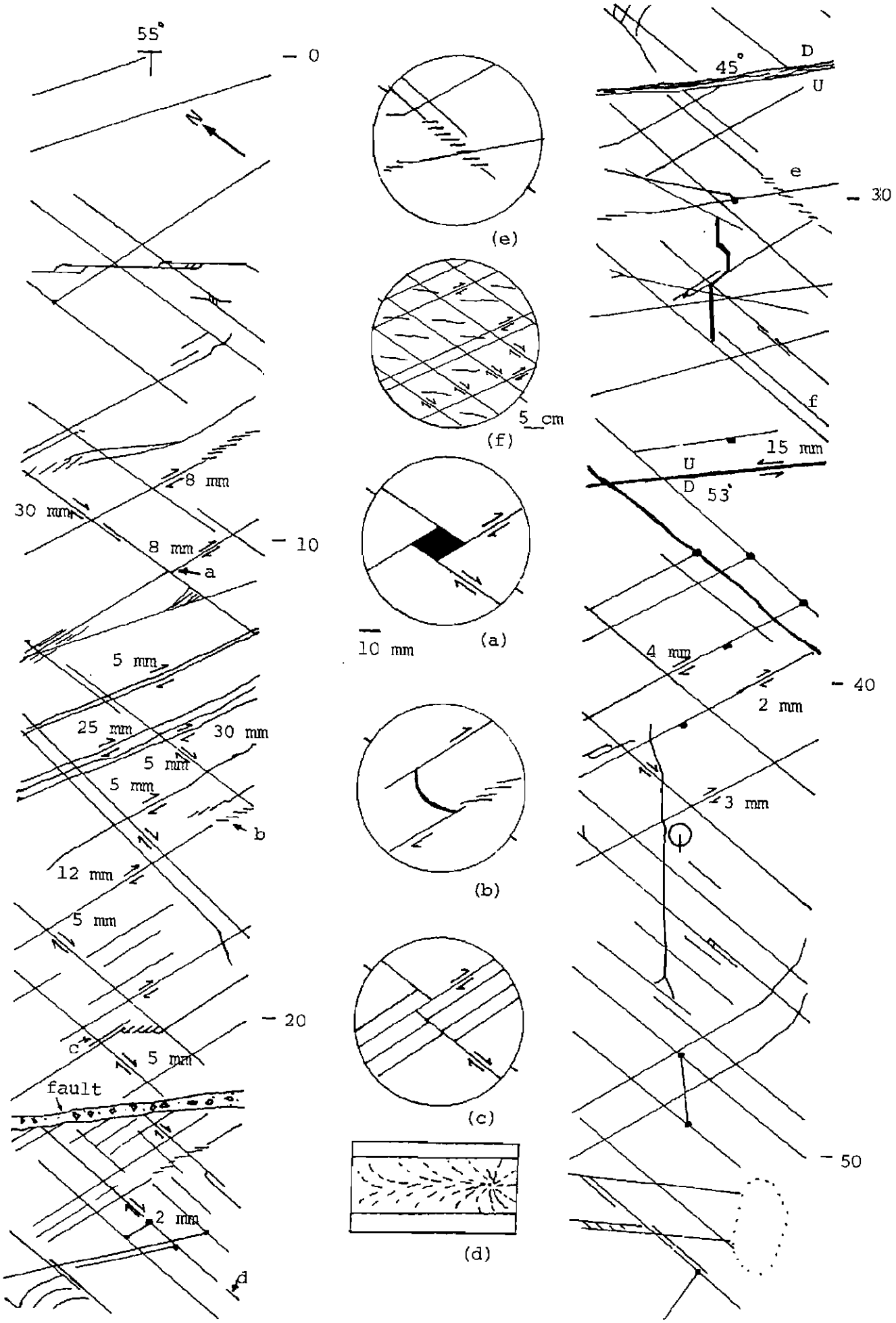

18-BB' cont.

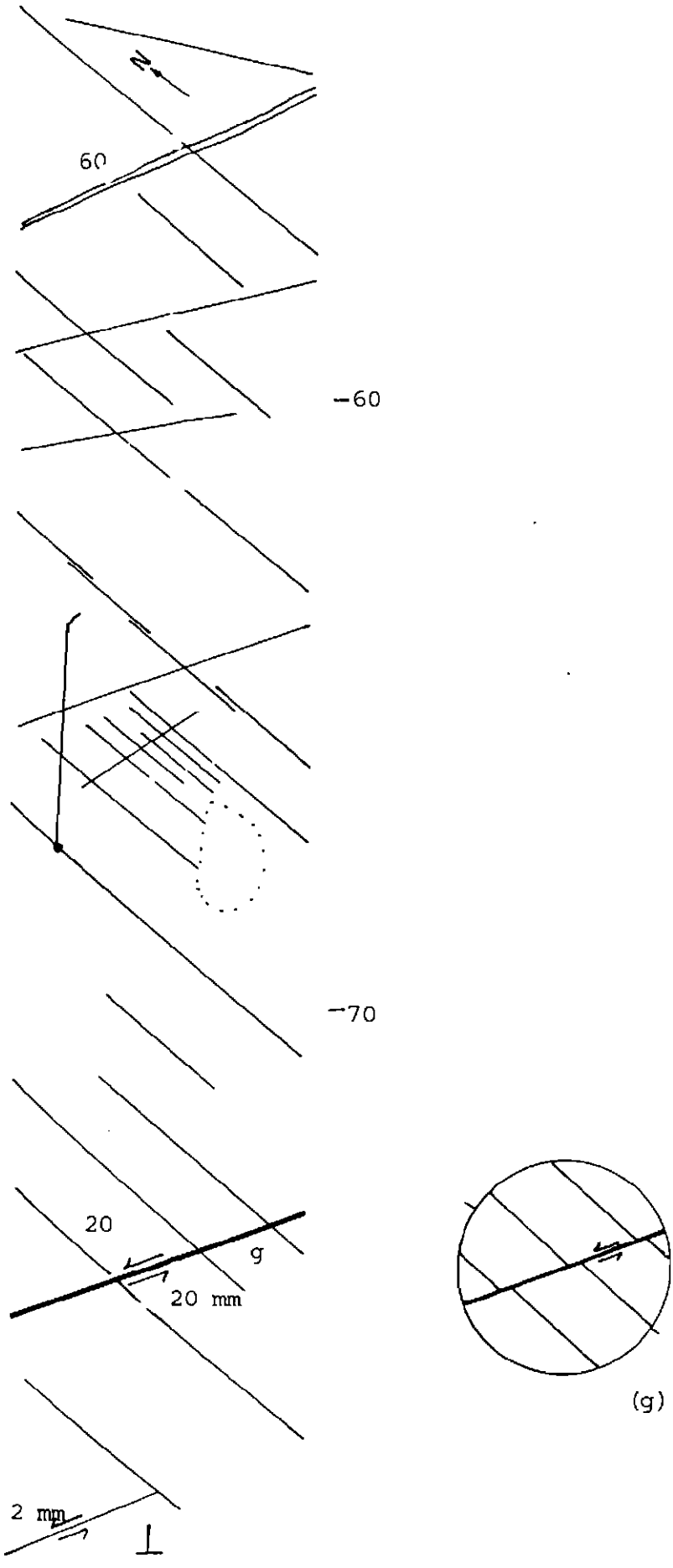

(g)

18-CC' (Bell Point)

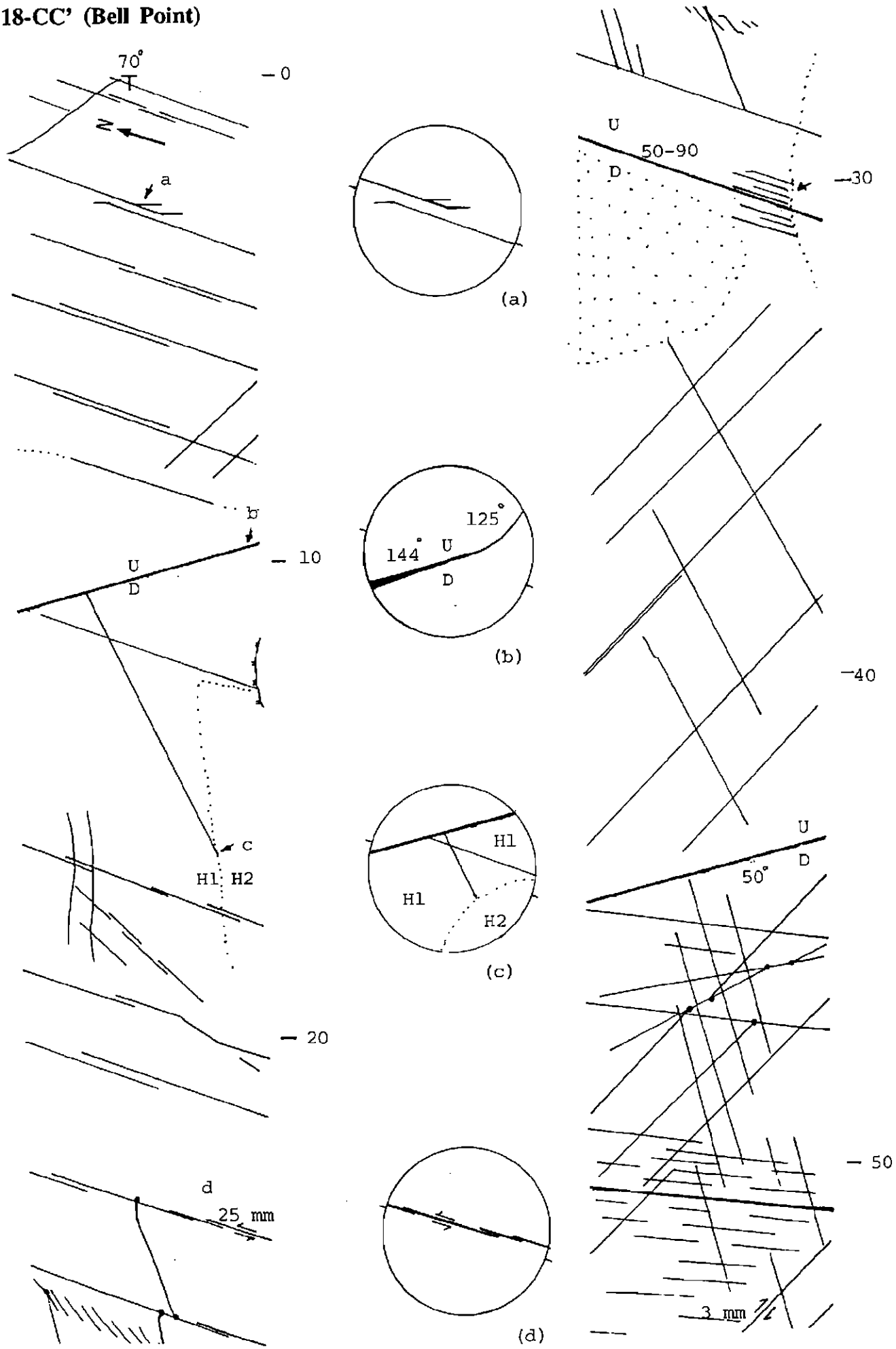

18-CC' cont.

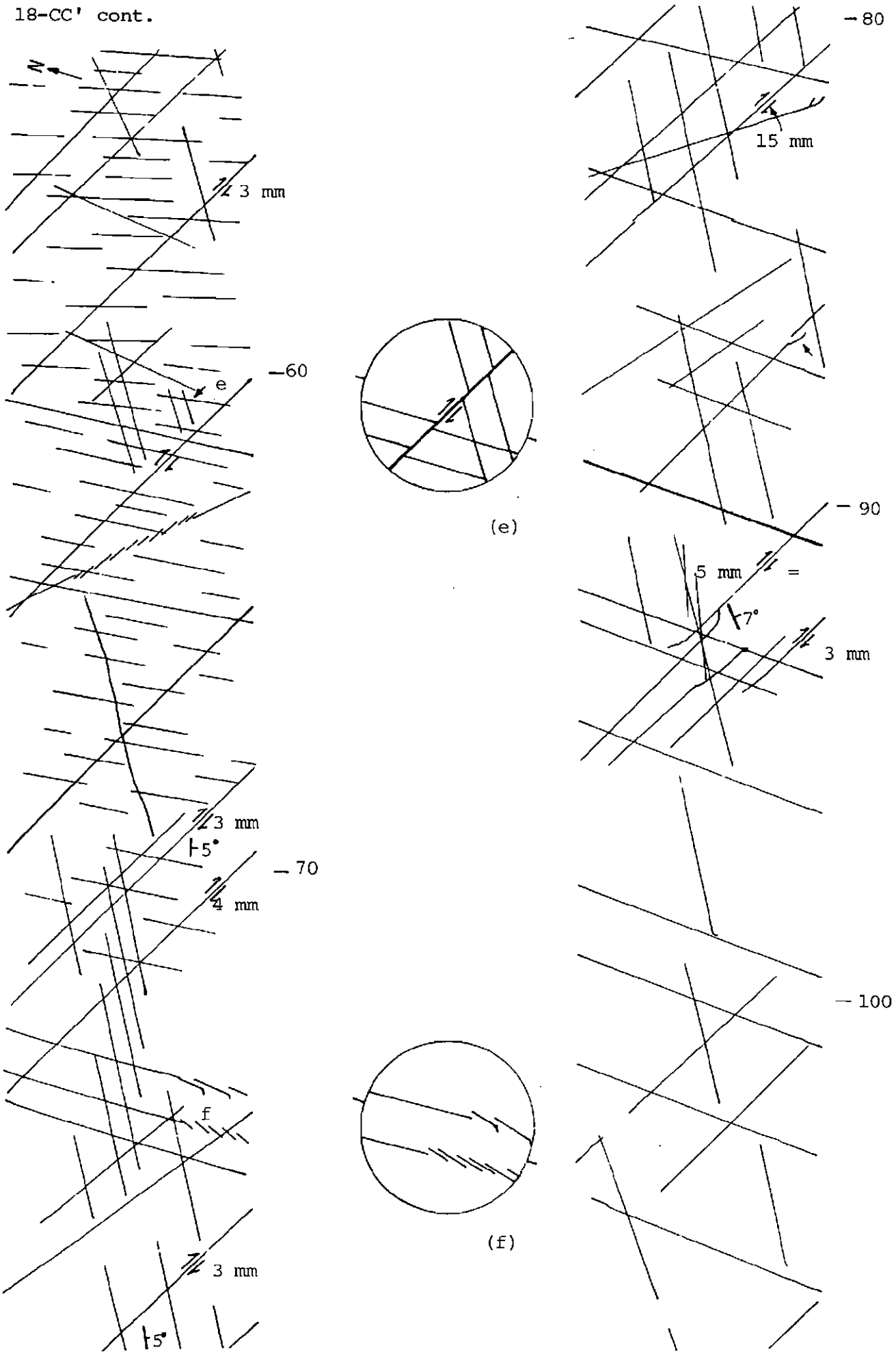

18-CC' cont.

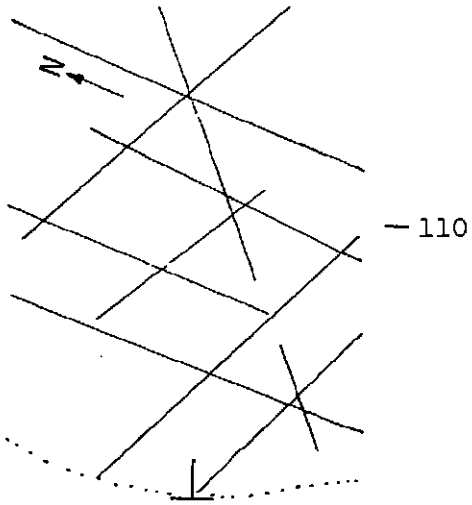

19-AA' (Austinmer South)

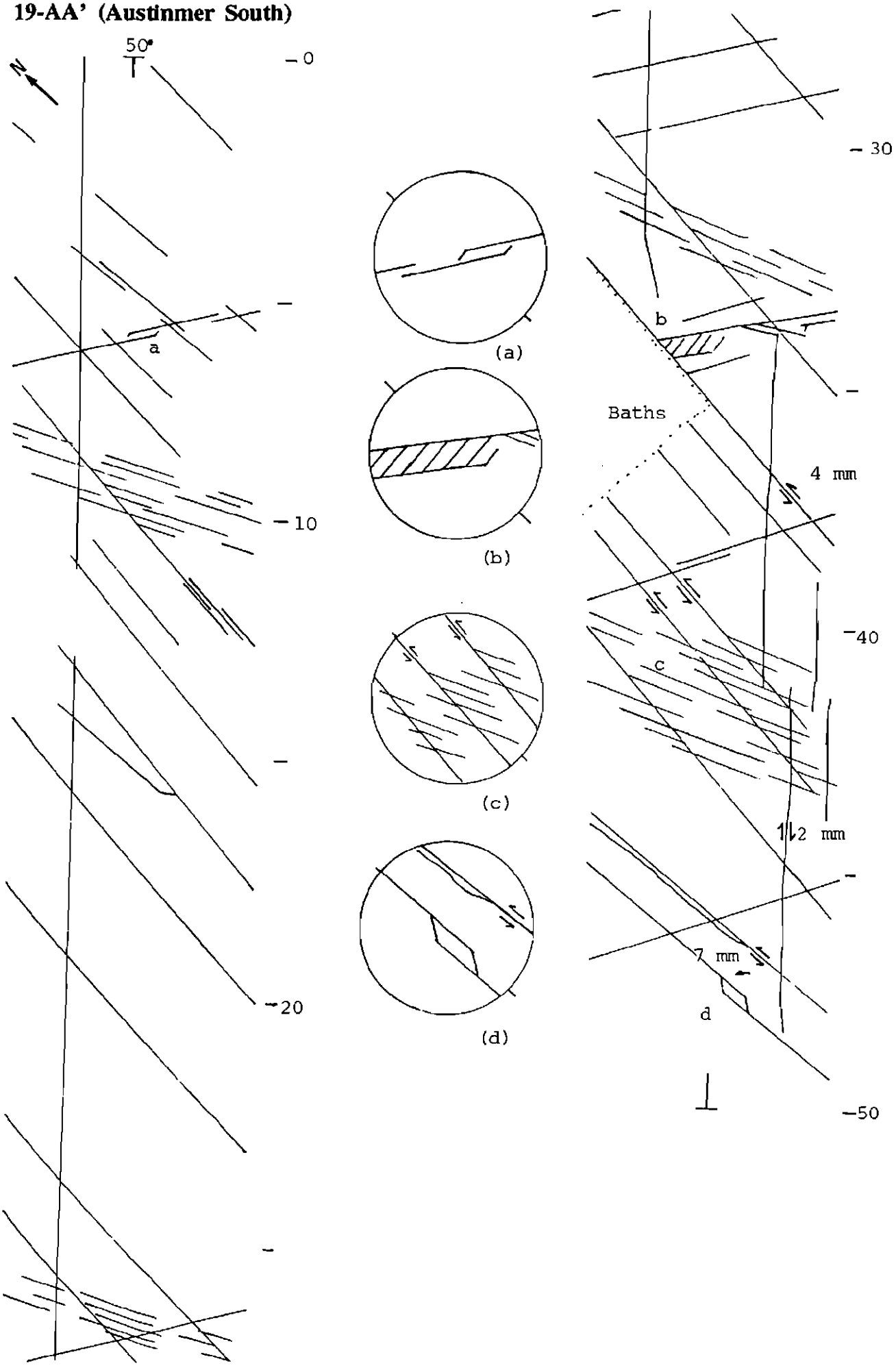

19-BB' (Austinmer South)

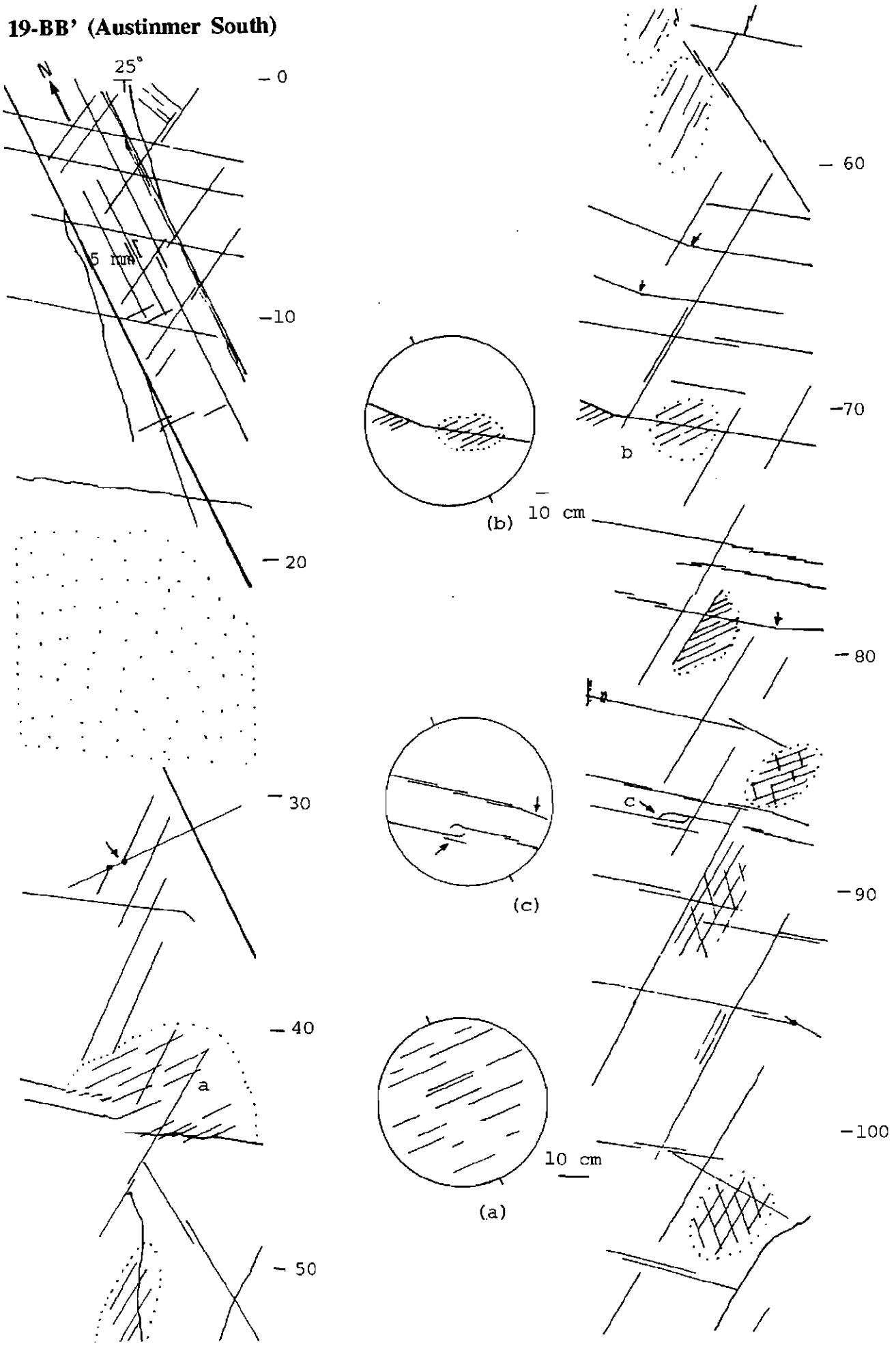

19-BB' cont.

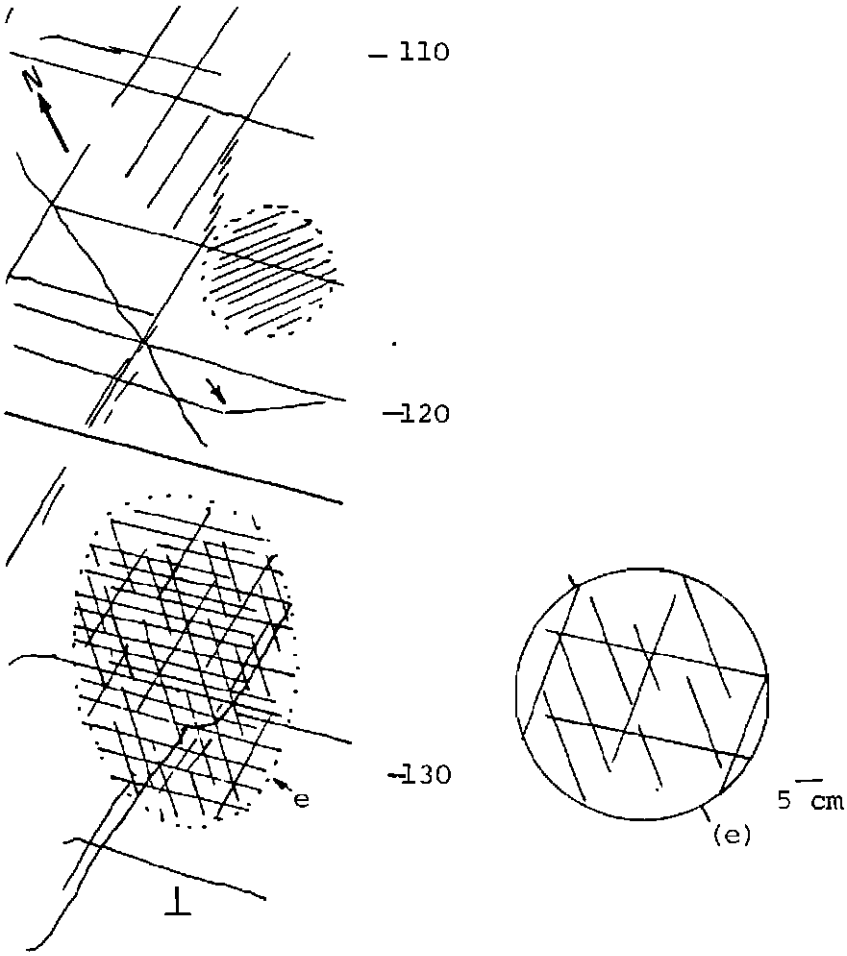

19-CC' (Austinmer South)

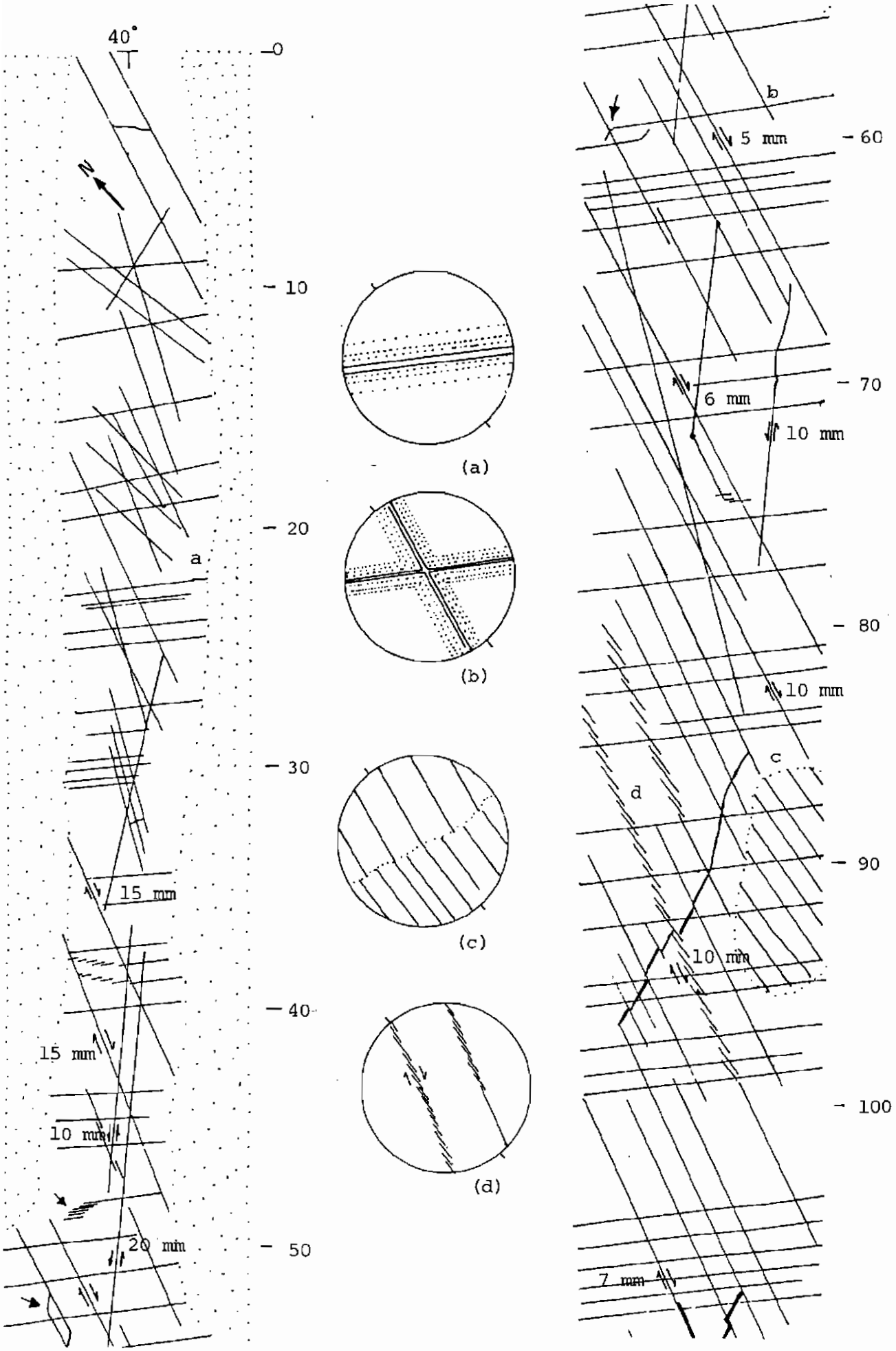

19-CC' cont.

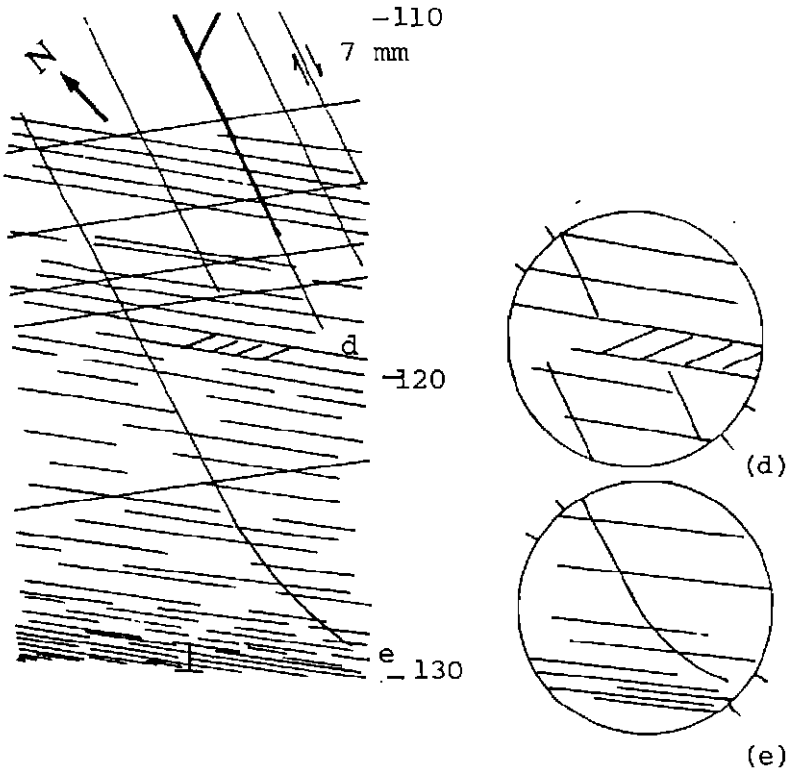

19-DD' (Austinmer South)

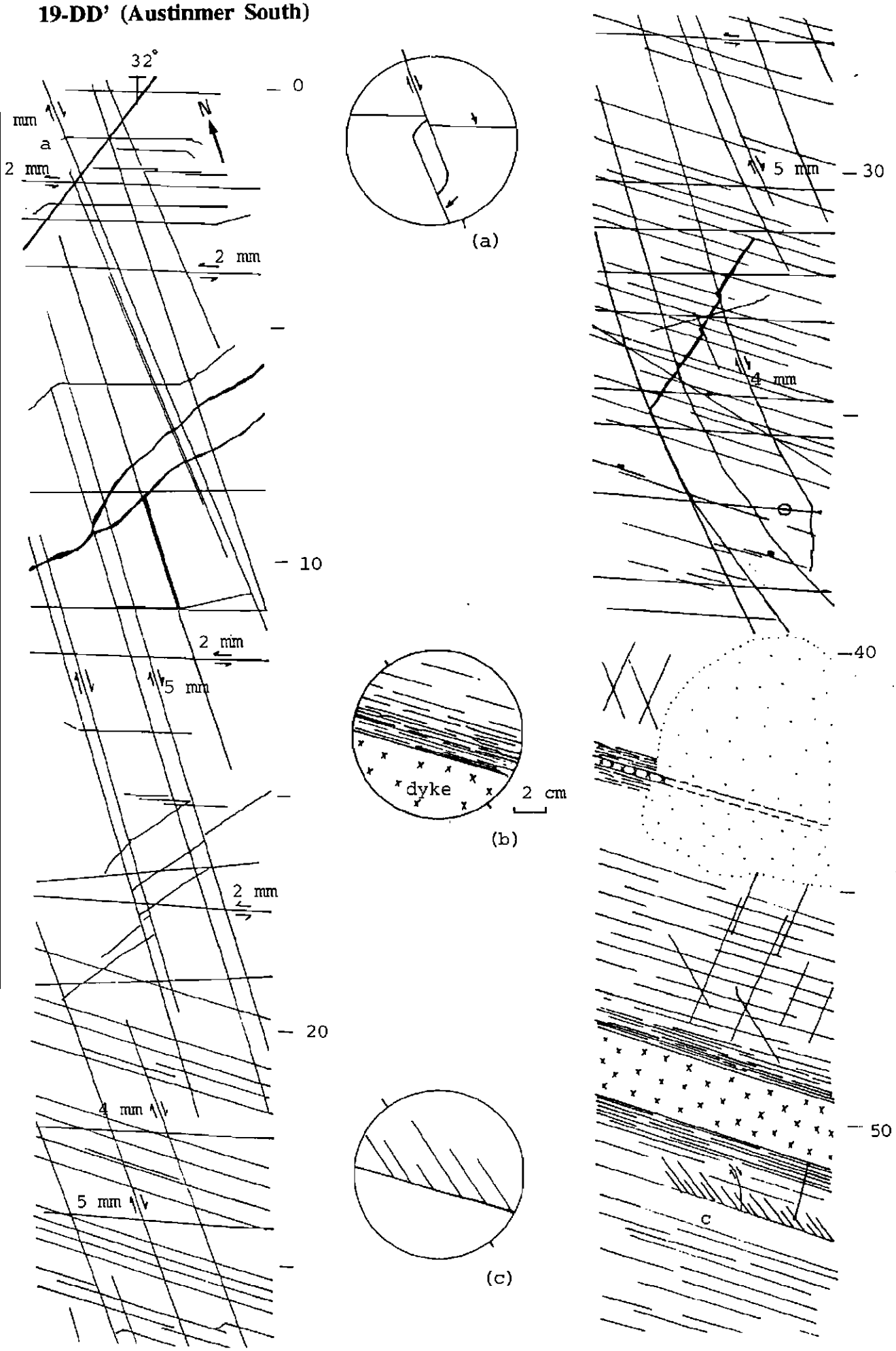

19-DD' cont.

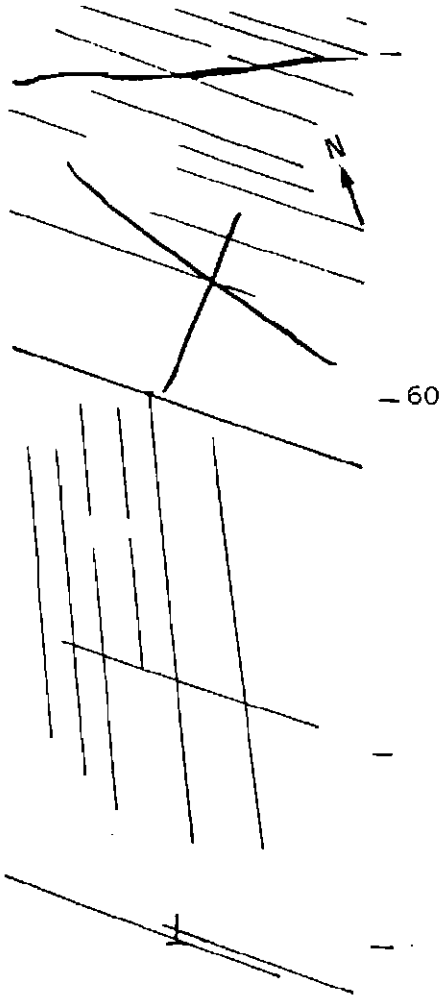

19-EE' (Austinmer South)

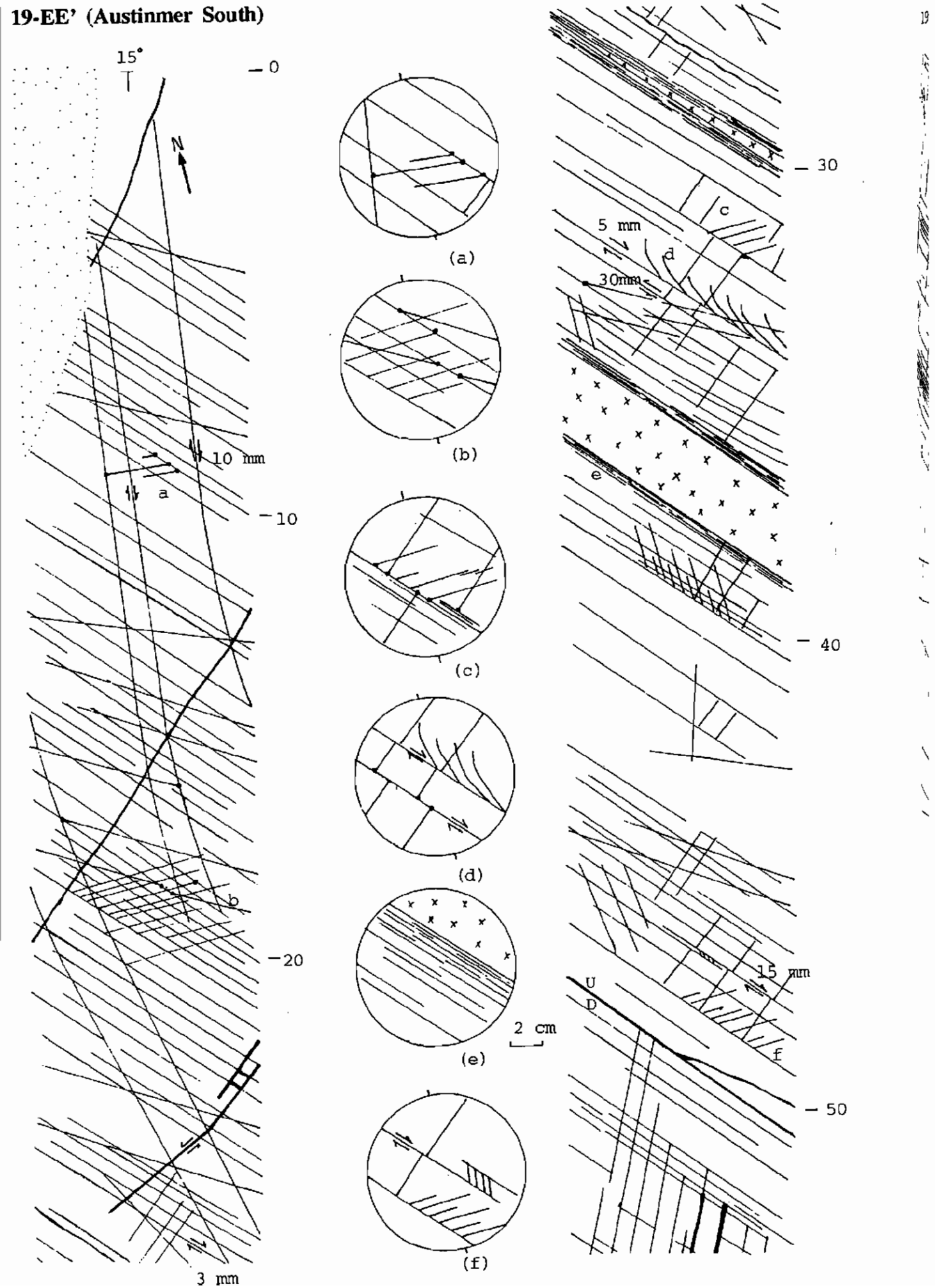

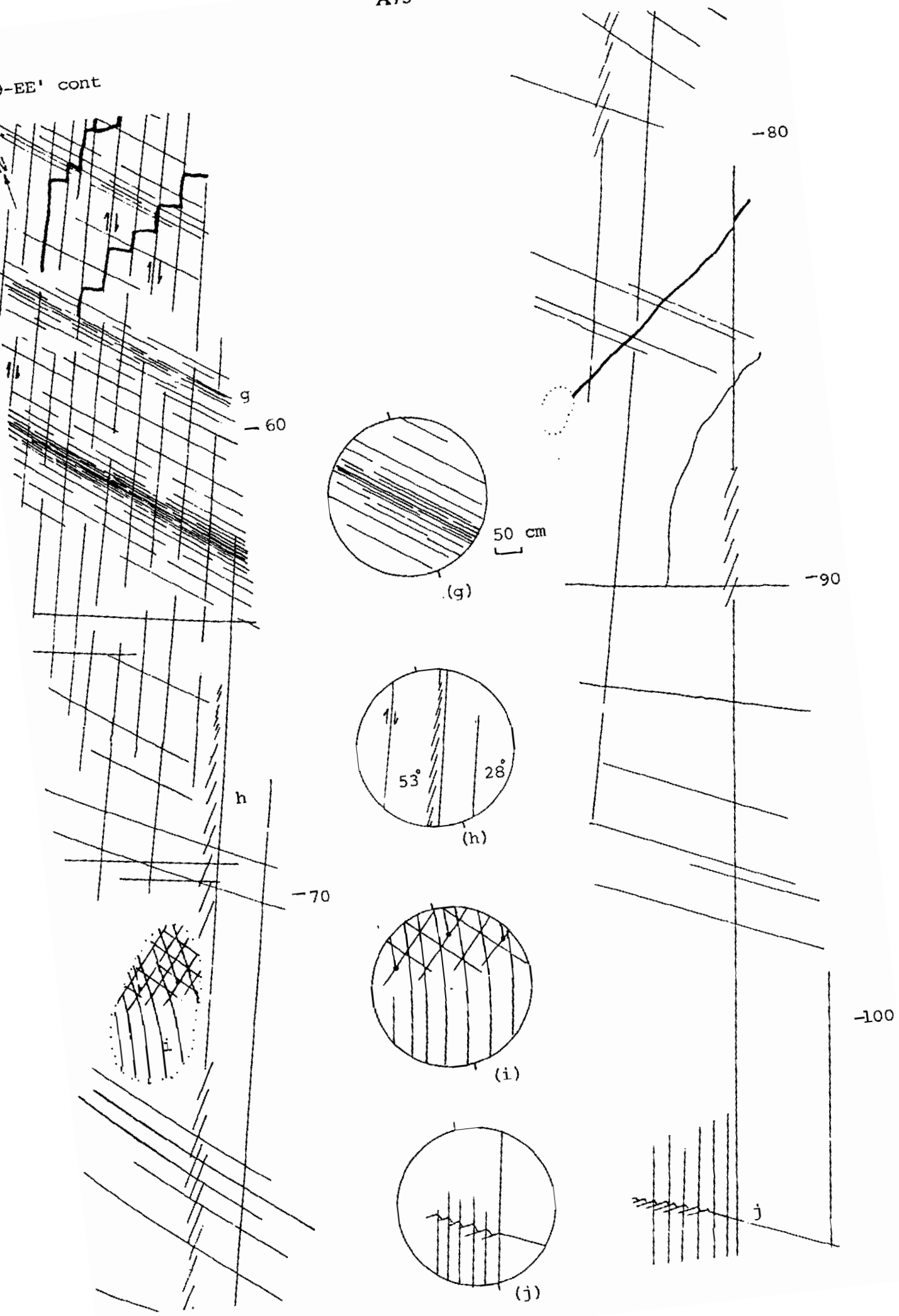
-EE' cont
g
60
50 cm
(g)
80
90
h
53°
28°
(h)
70
(i)
100
j
(j)

E' cont.

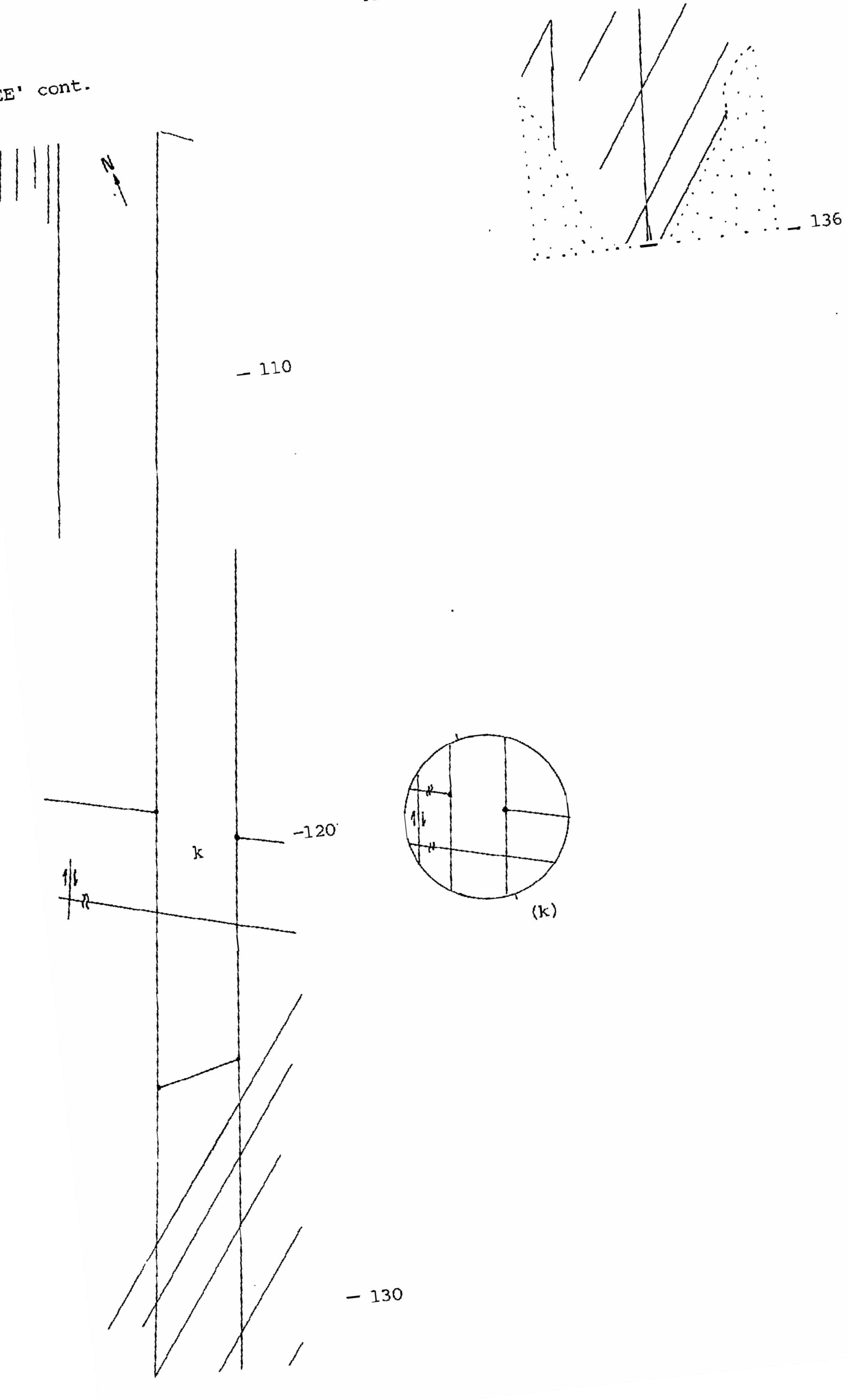

(Thirroul Rail)

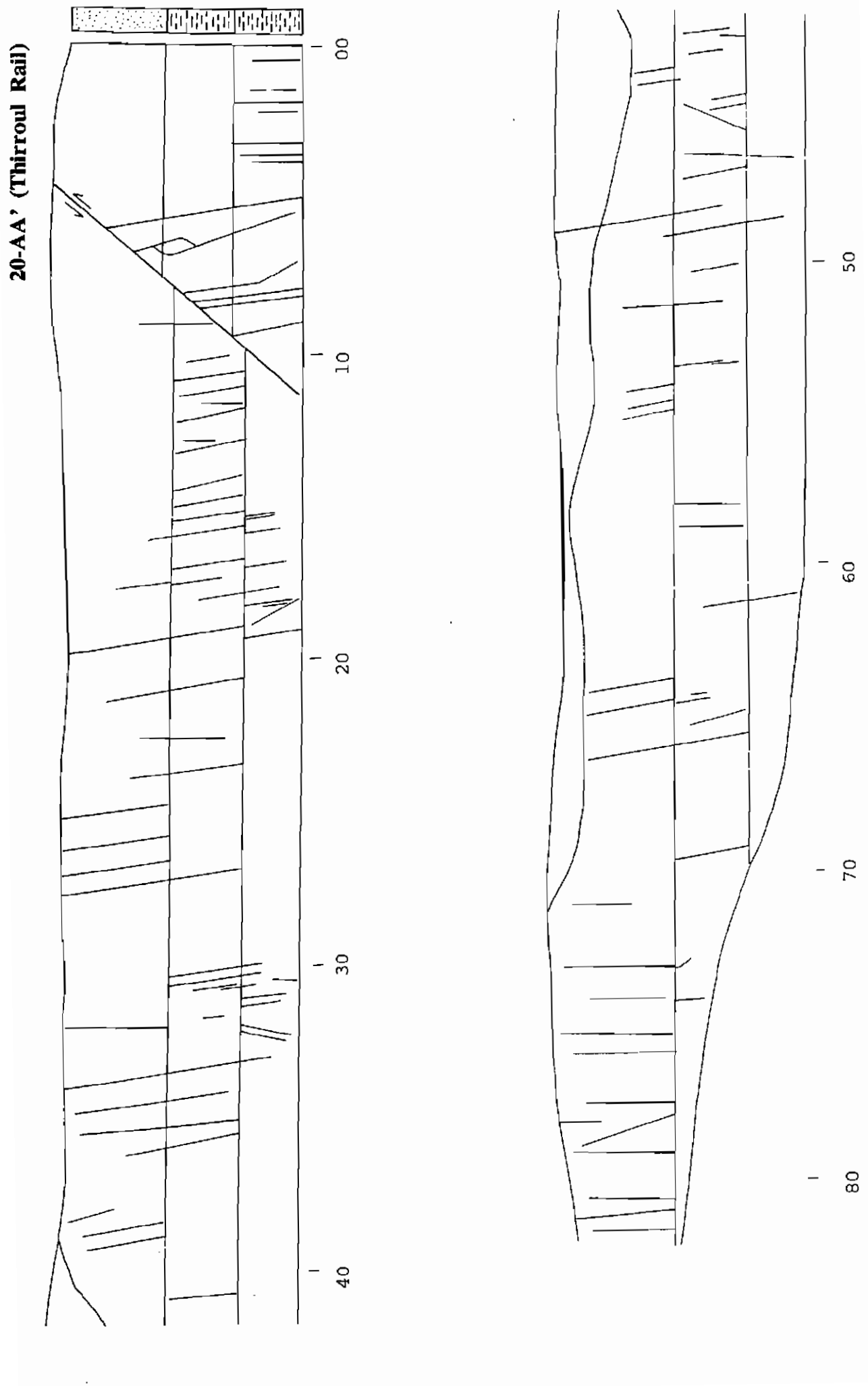
20-AA' (Thirroul Rail)
00
10
20
30
40
50
60
70
80

21-AA' (Thirroul)

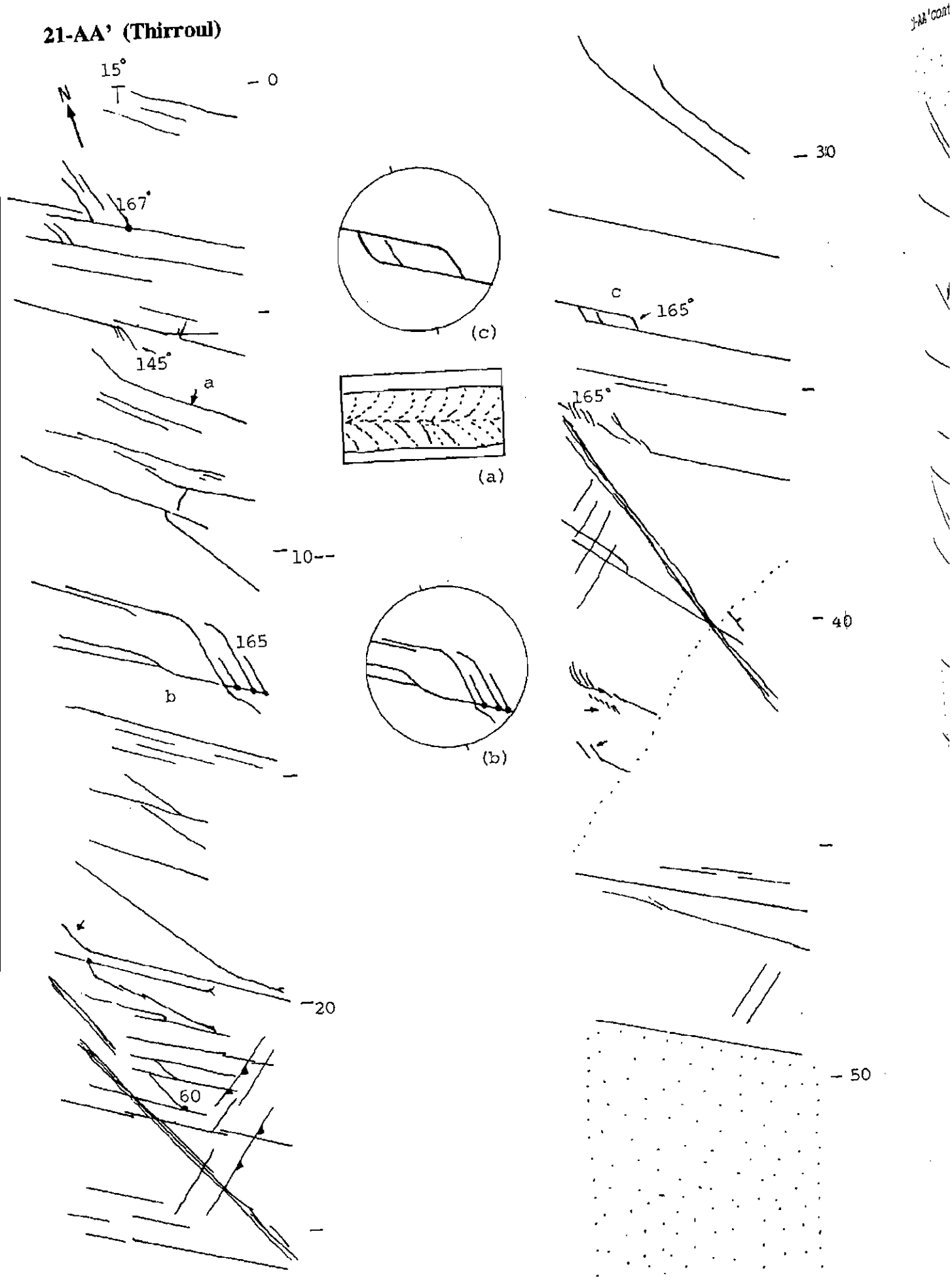

21-AA'cont.

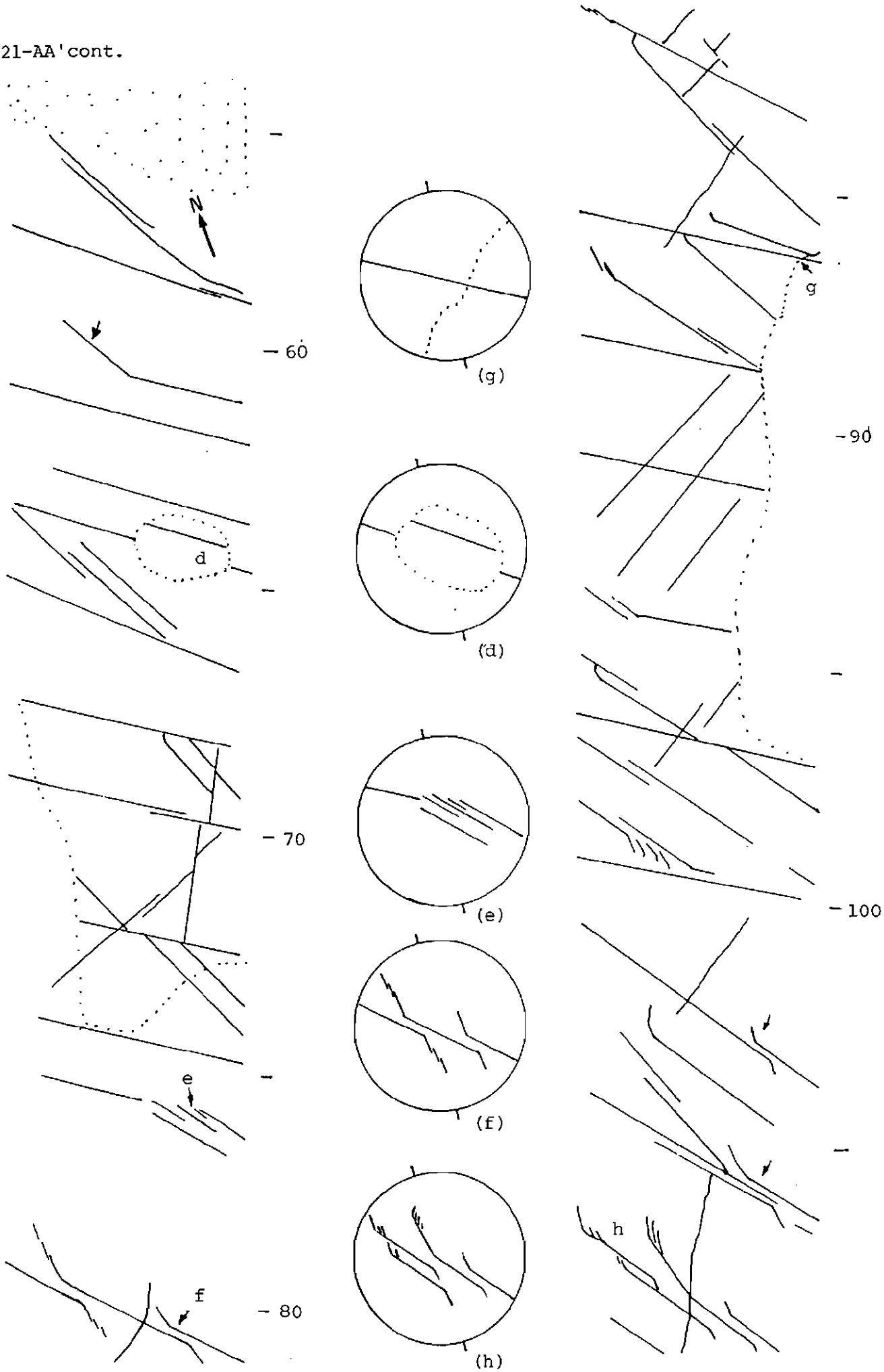

21-AA' cont.

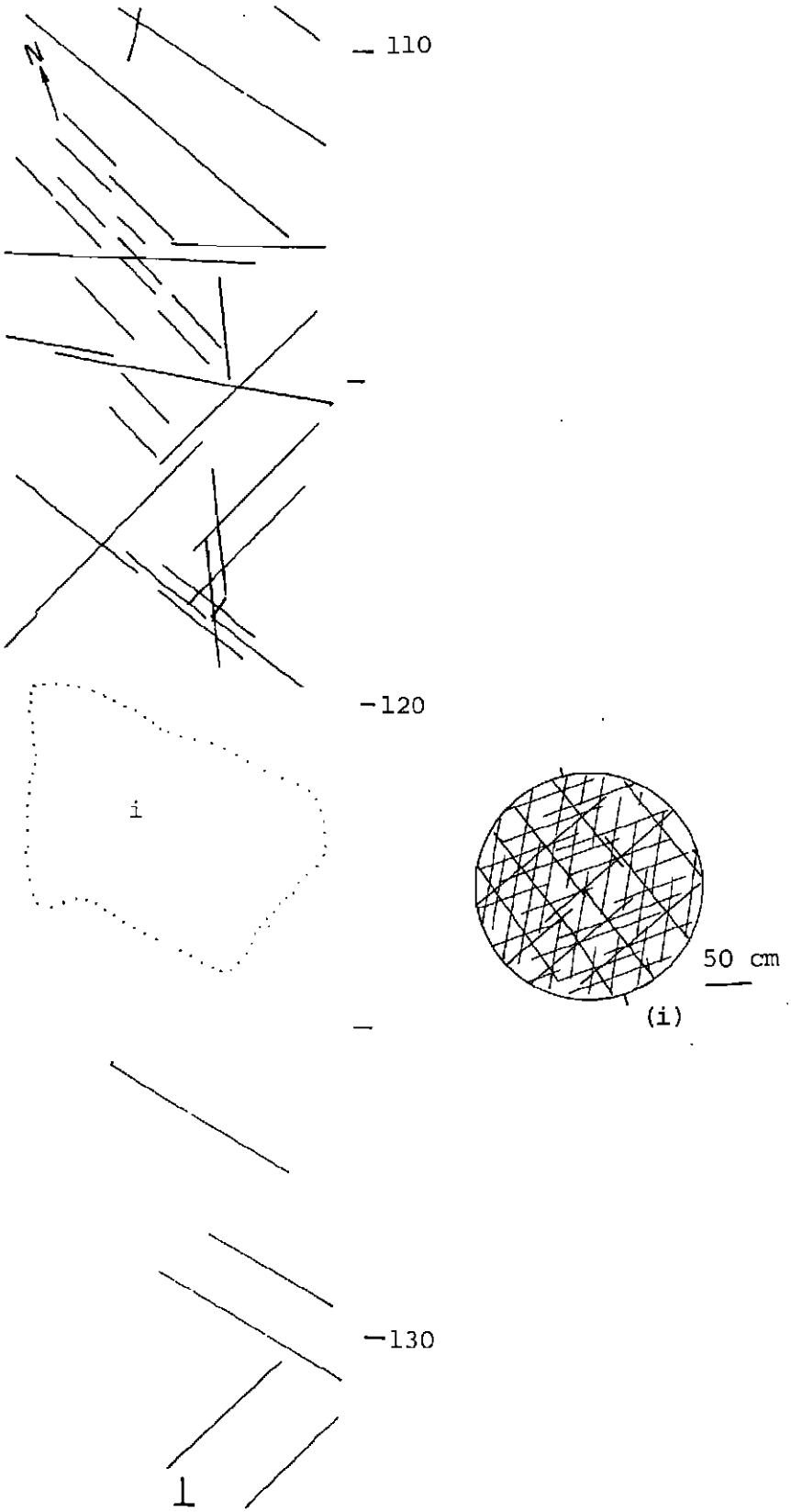

22-AA' (Bulli)

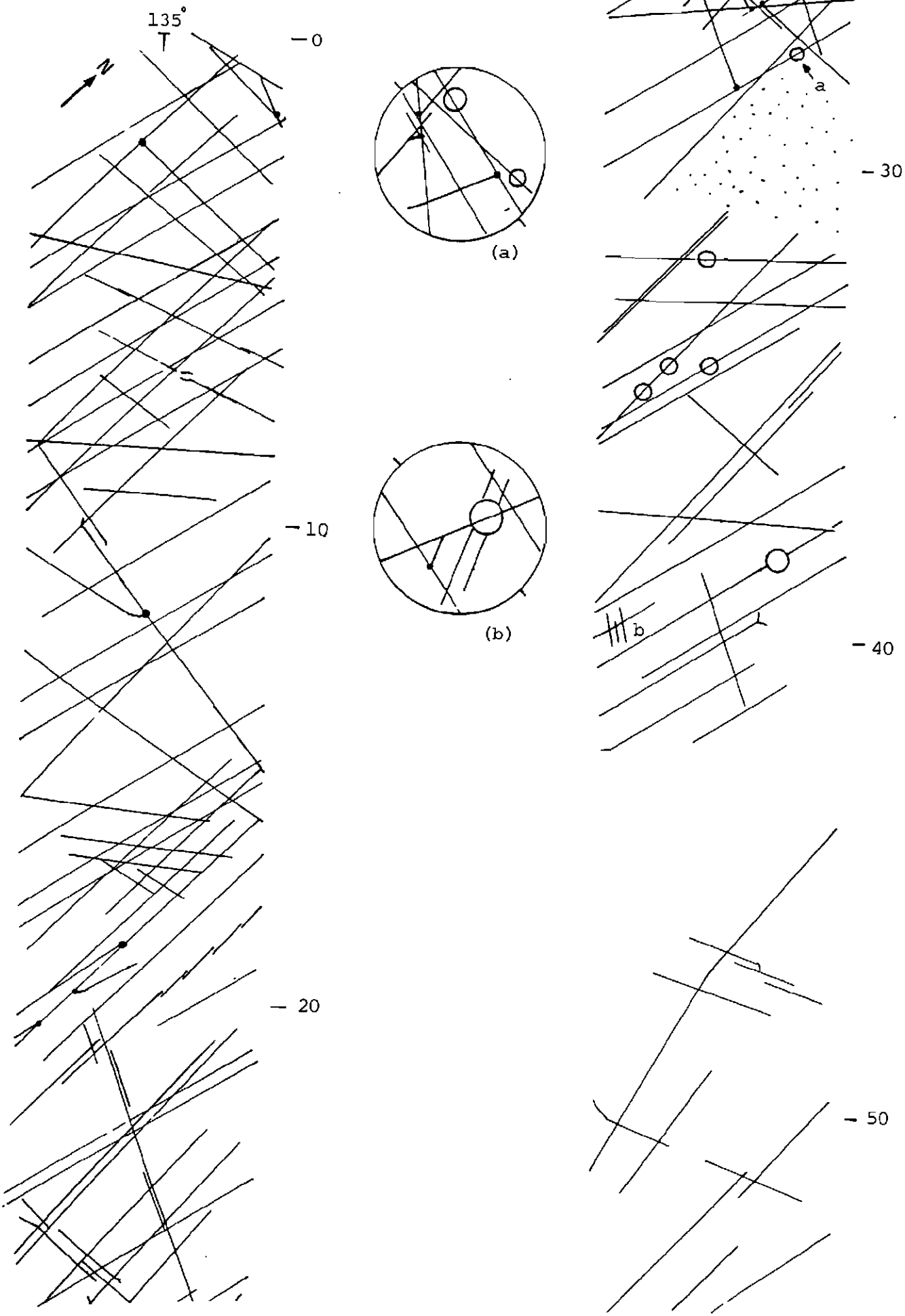

22-AA' cont.

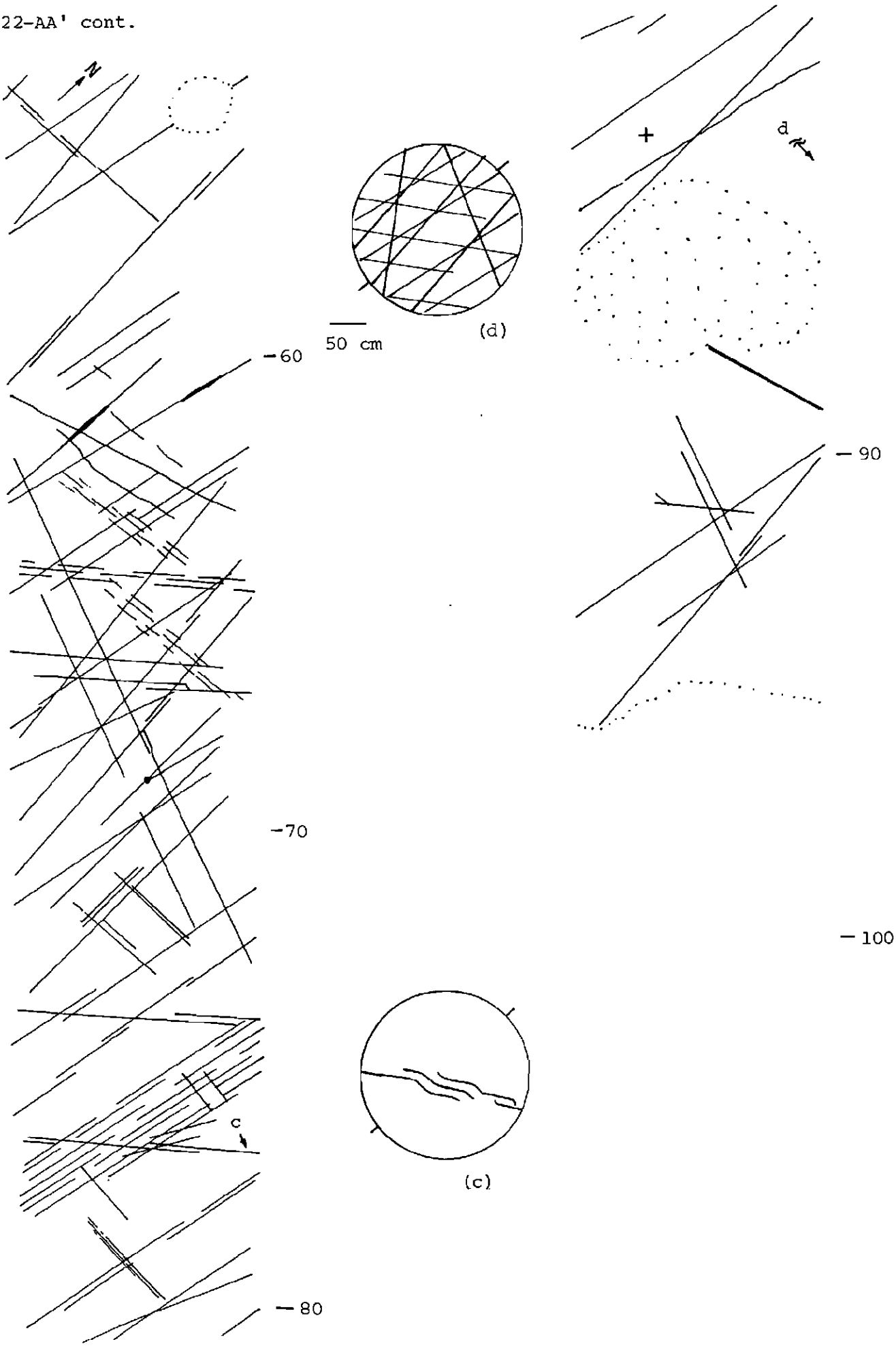

22-AA' cont.

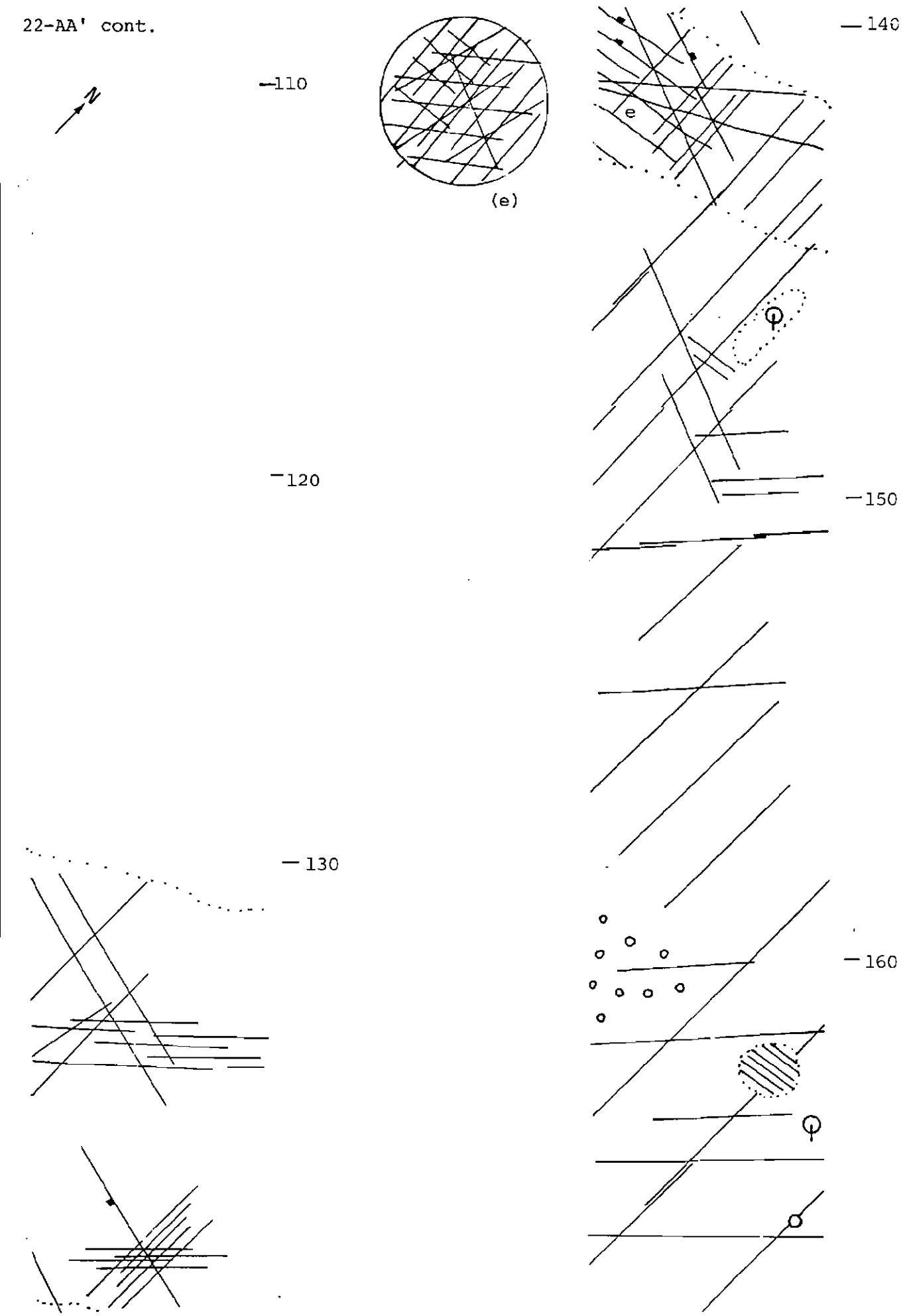

22-AA' cont.

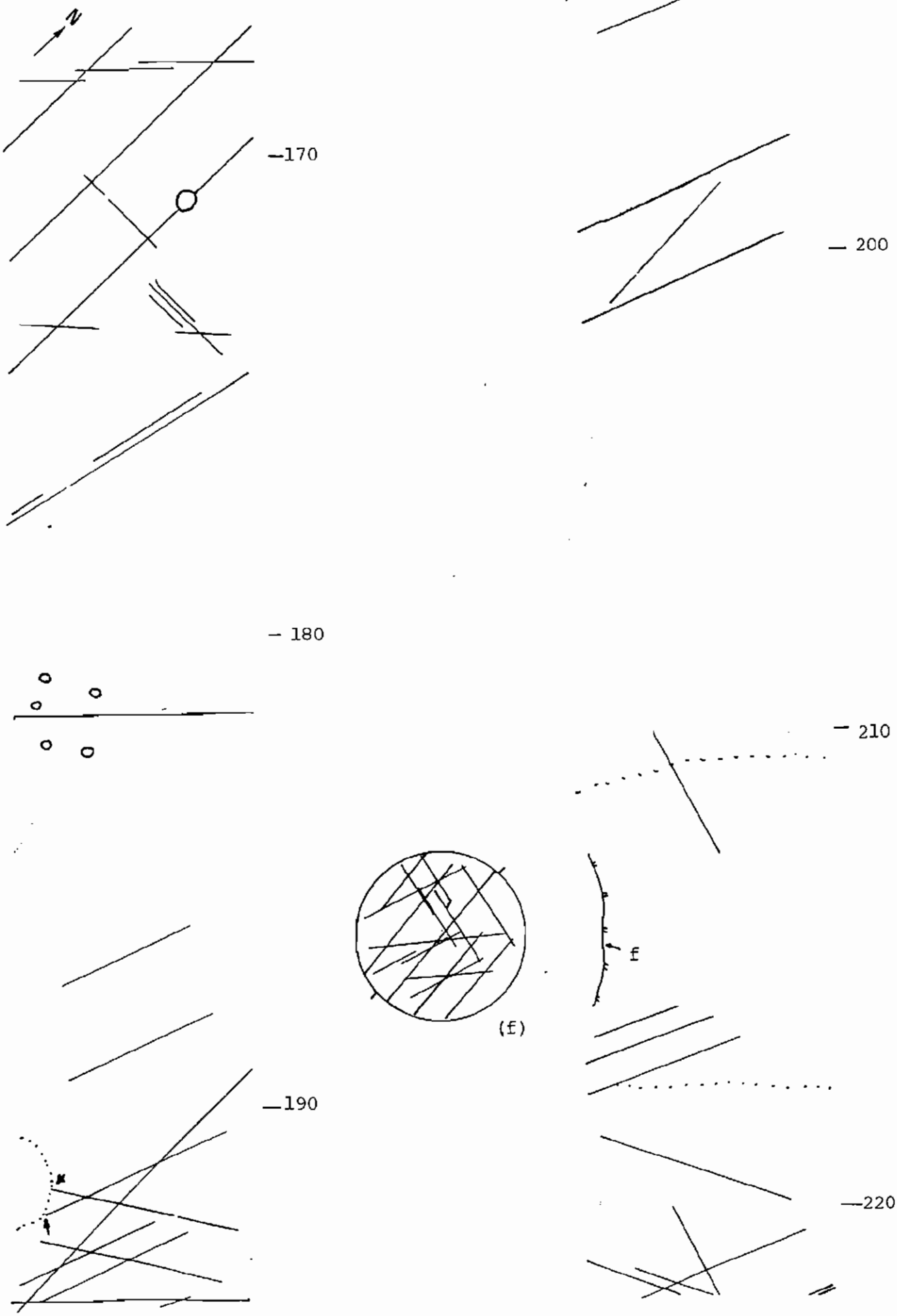

22-AA' cont.

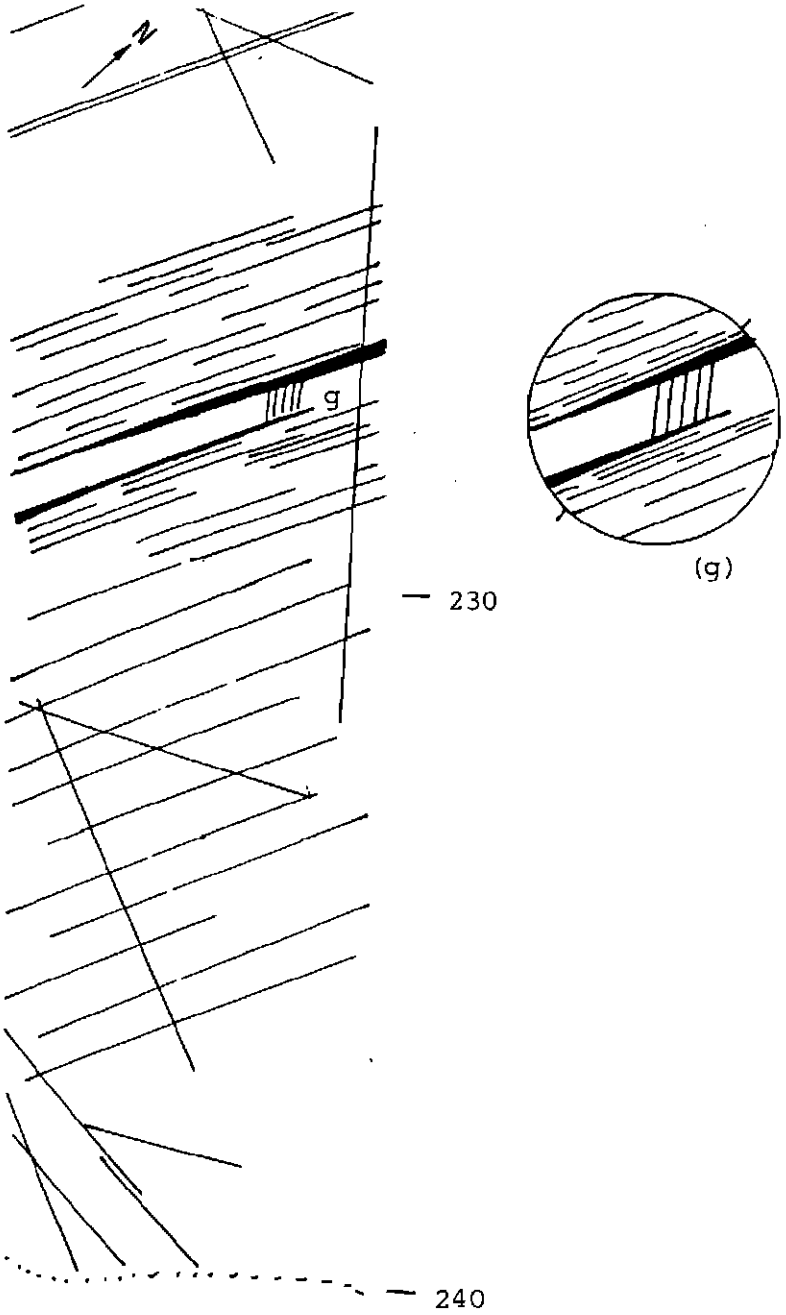

(g)

22-BB' (Bulli)

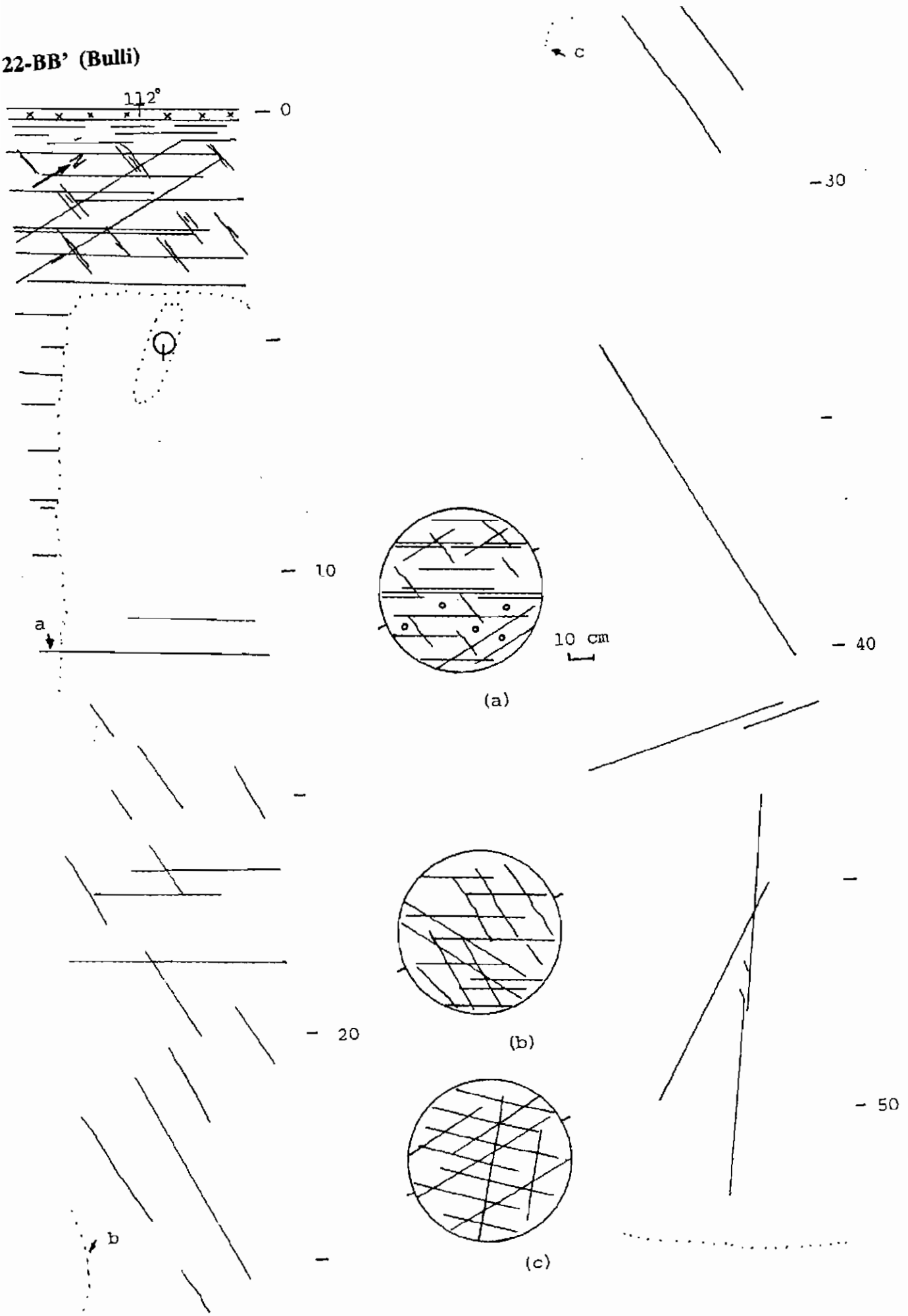

22-BB' cont.

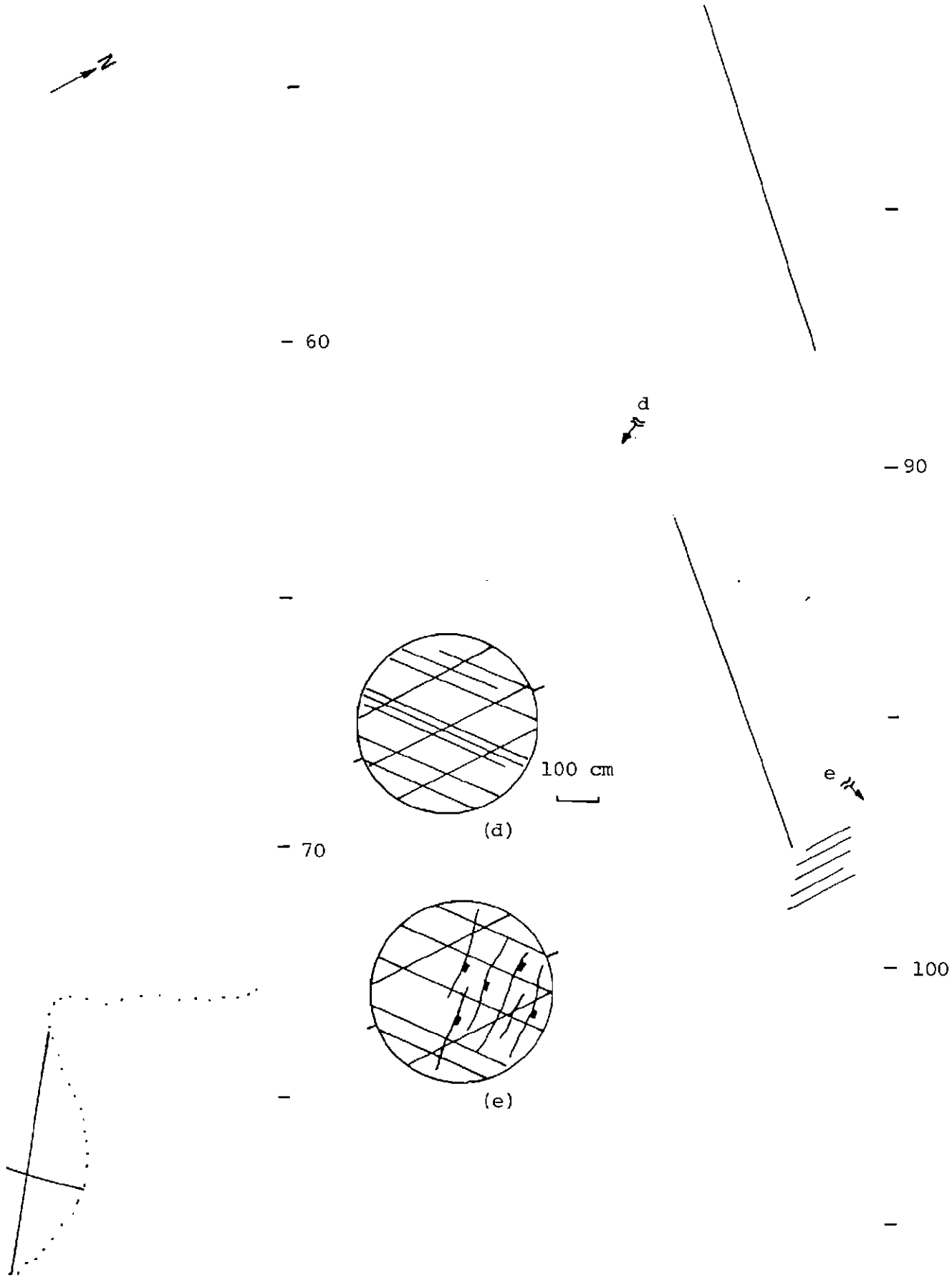

22-BB' cont.

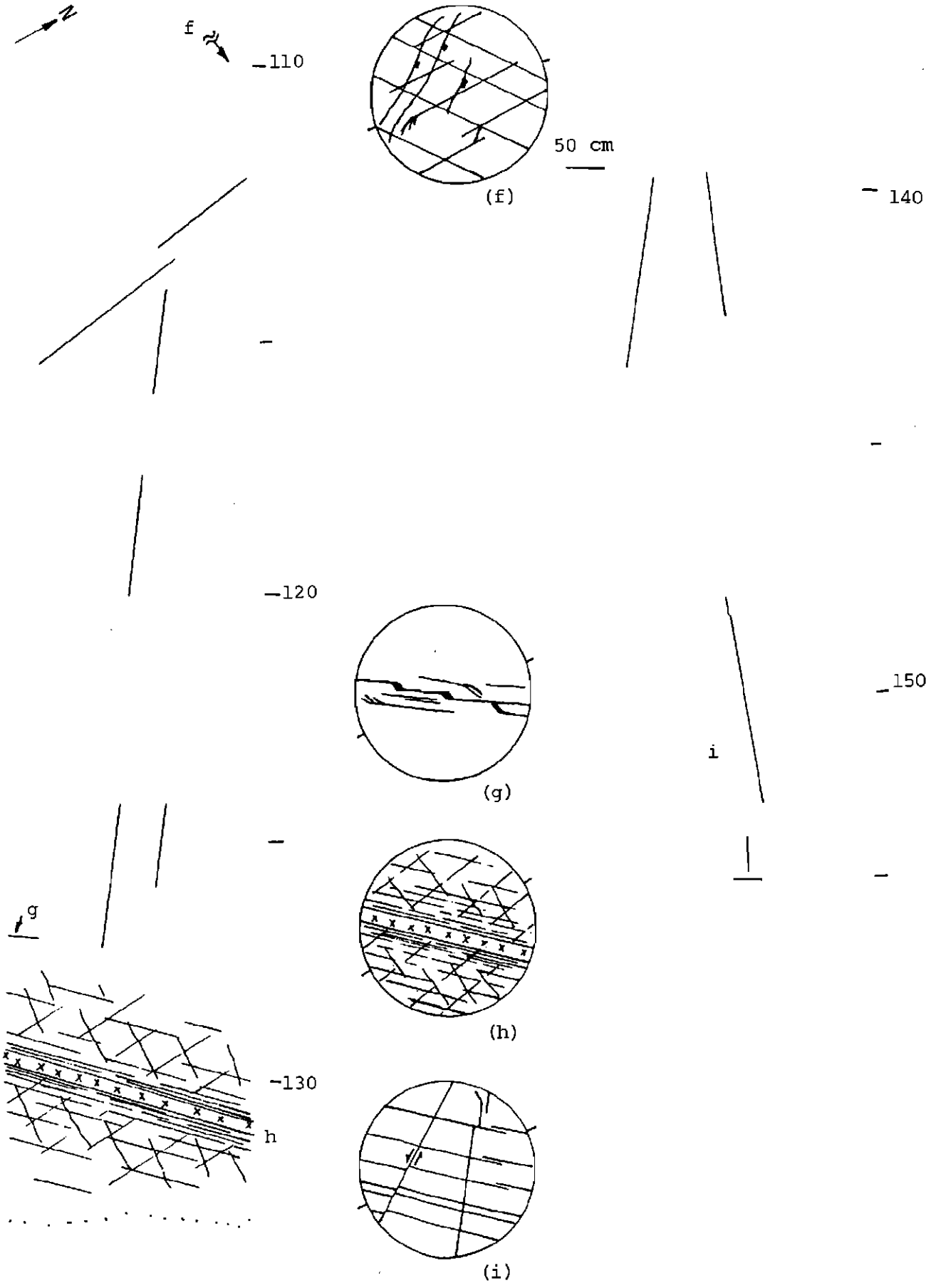

22-CC' (Bulli)

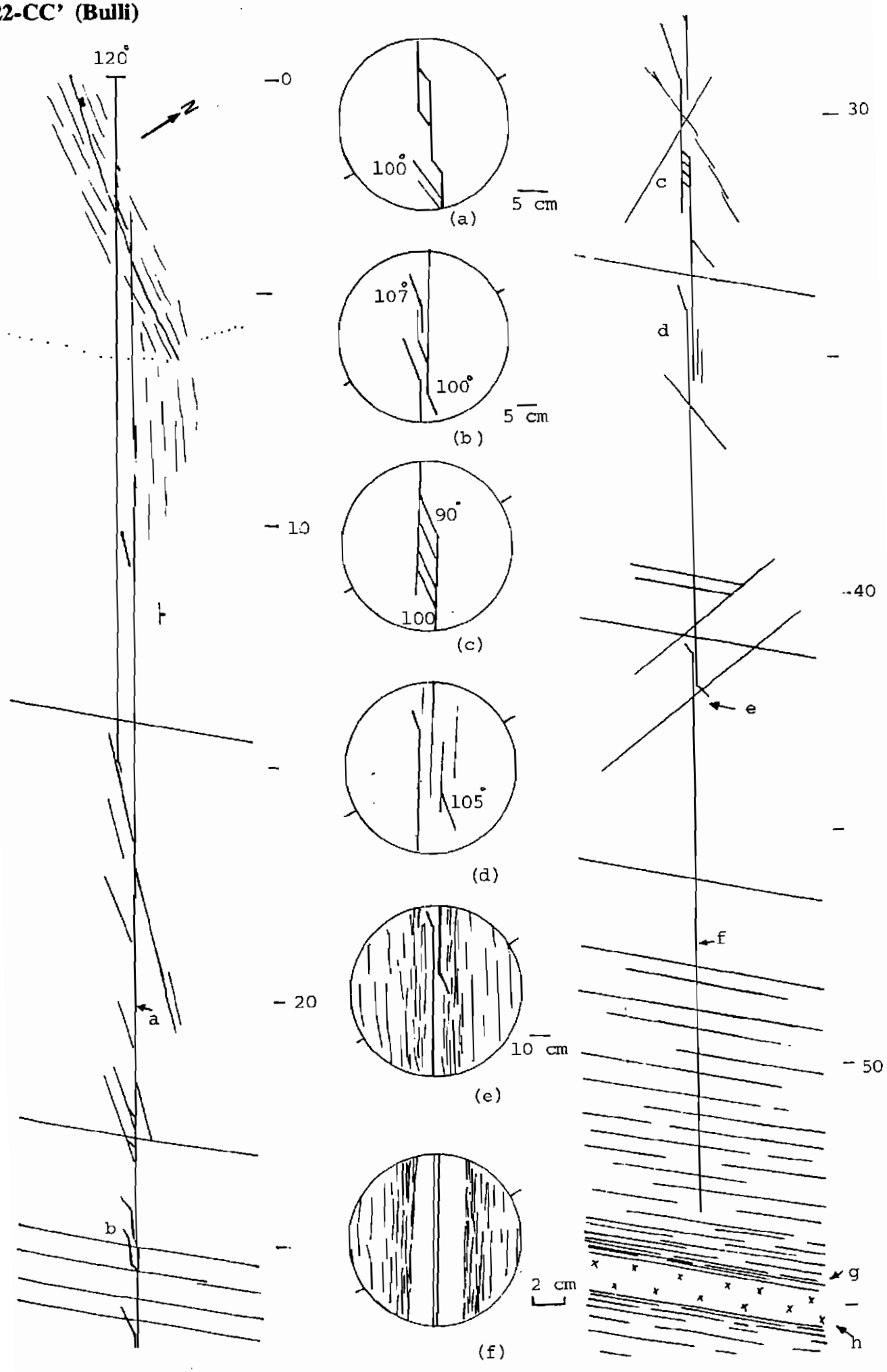
120°
N
0
10
20
30
40
50
a
b
c
d
e
f
g
h
100°
5 cm
(a)
107°
100°
5 cm
(b)
90°
100
(c)
105°
(d)
10 cm
(e)
2 cm
(f)

22-CC' cont.

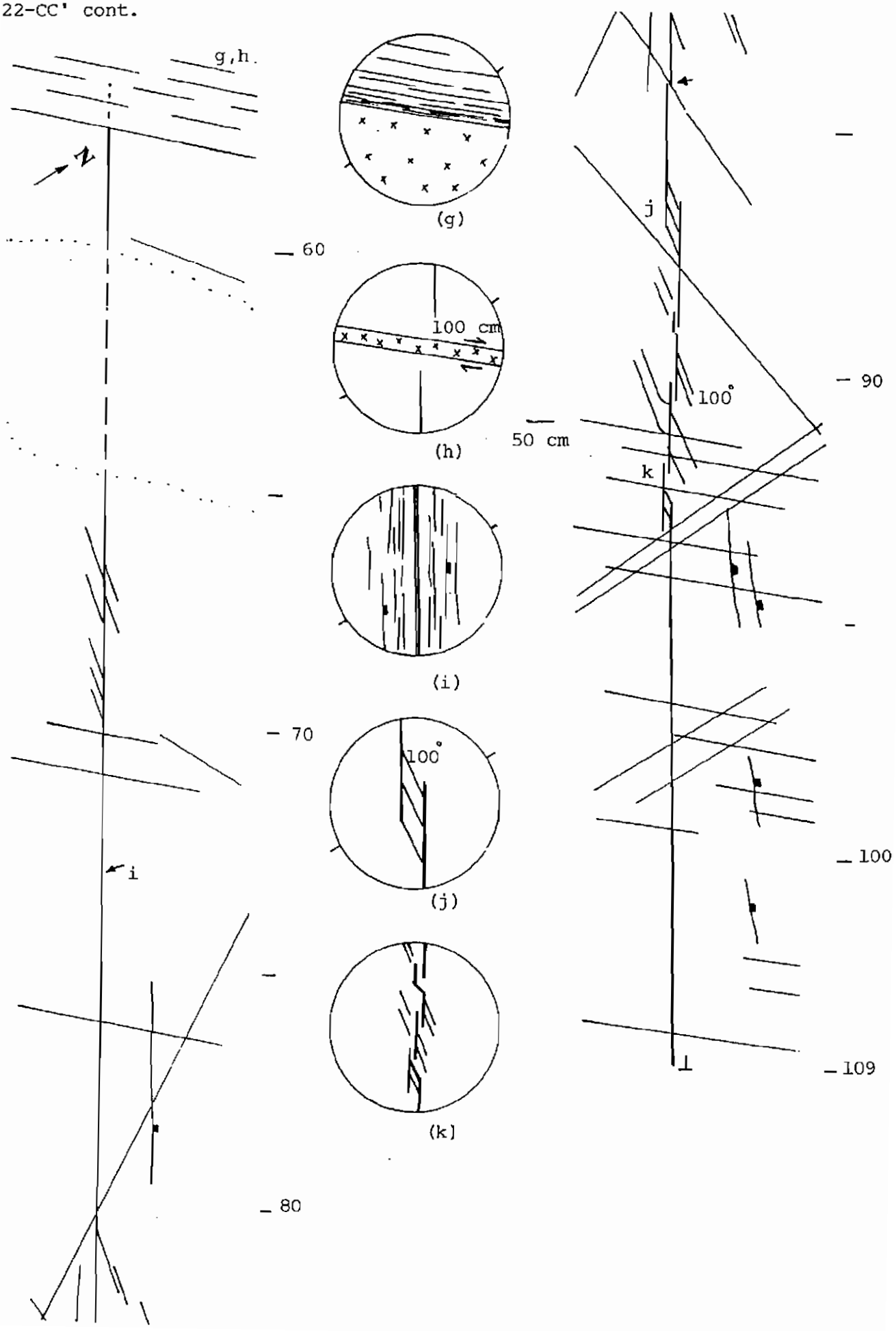

22-DD' (Bulli)

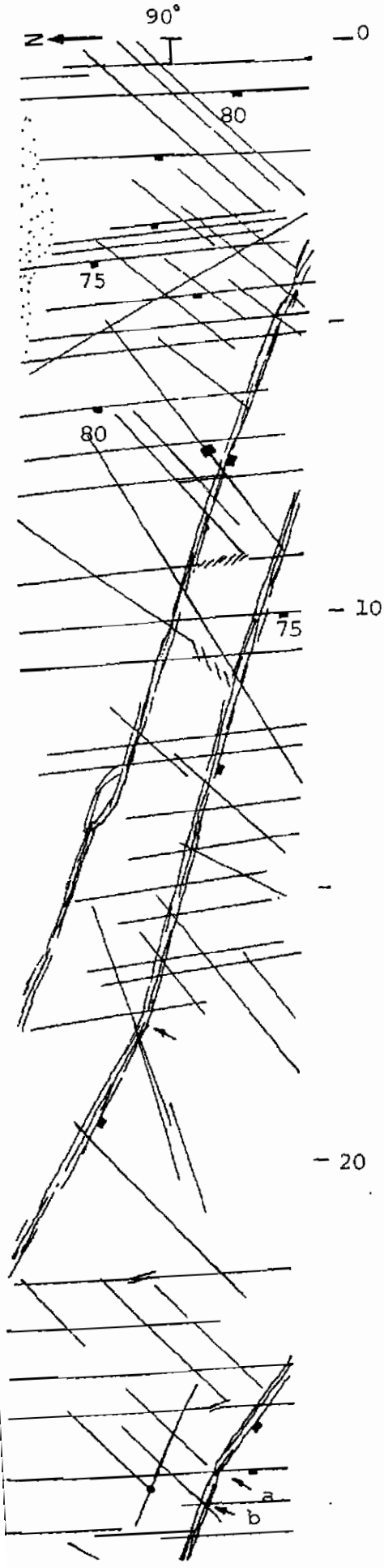

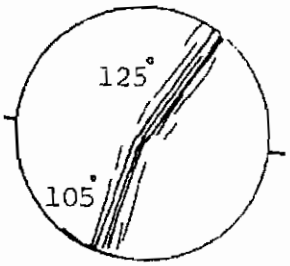

(a)

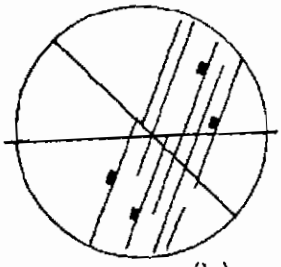

(b)

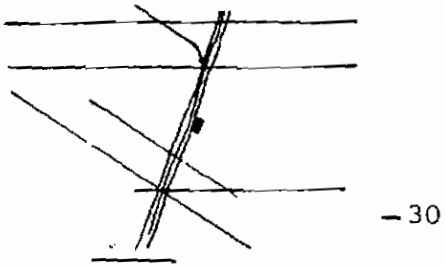

22-EE' (Bulli)

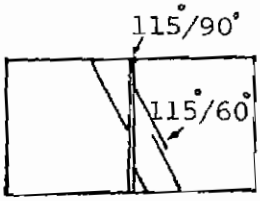

(a)

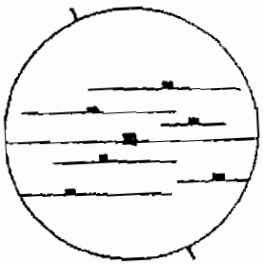

(b)

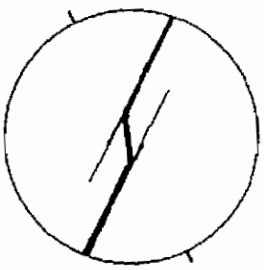

(c)

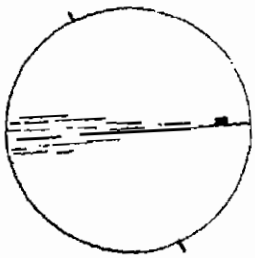

(d)

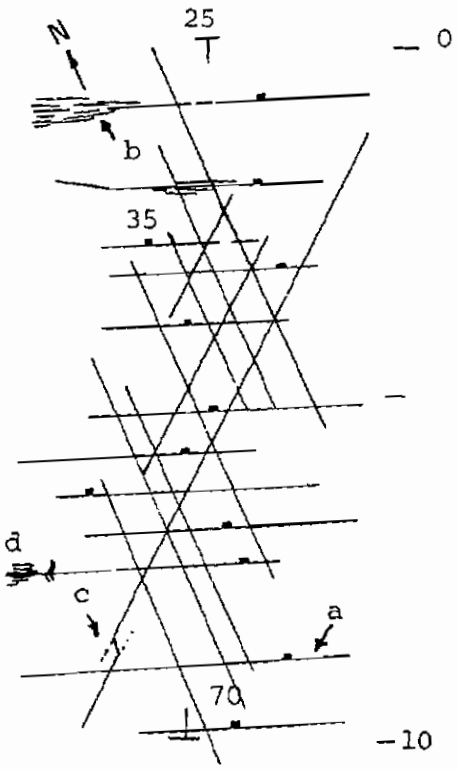

22-FF' (Bulli)

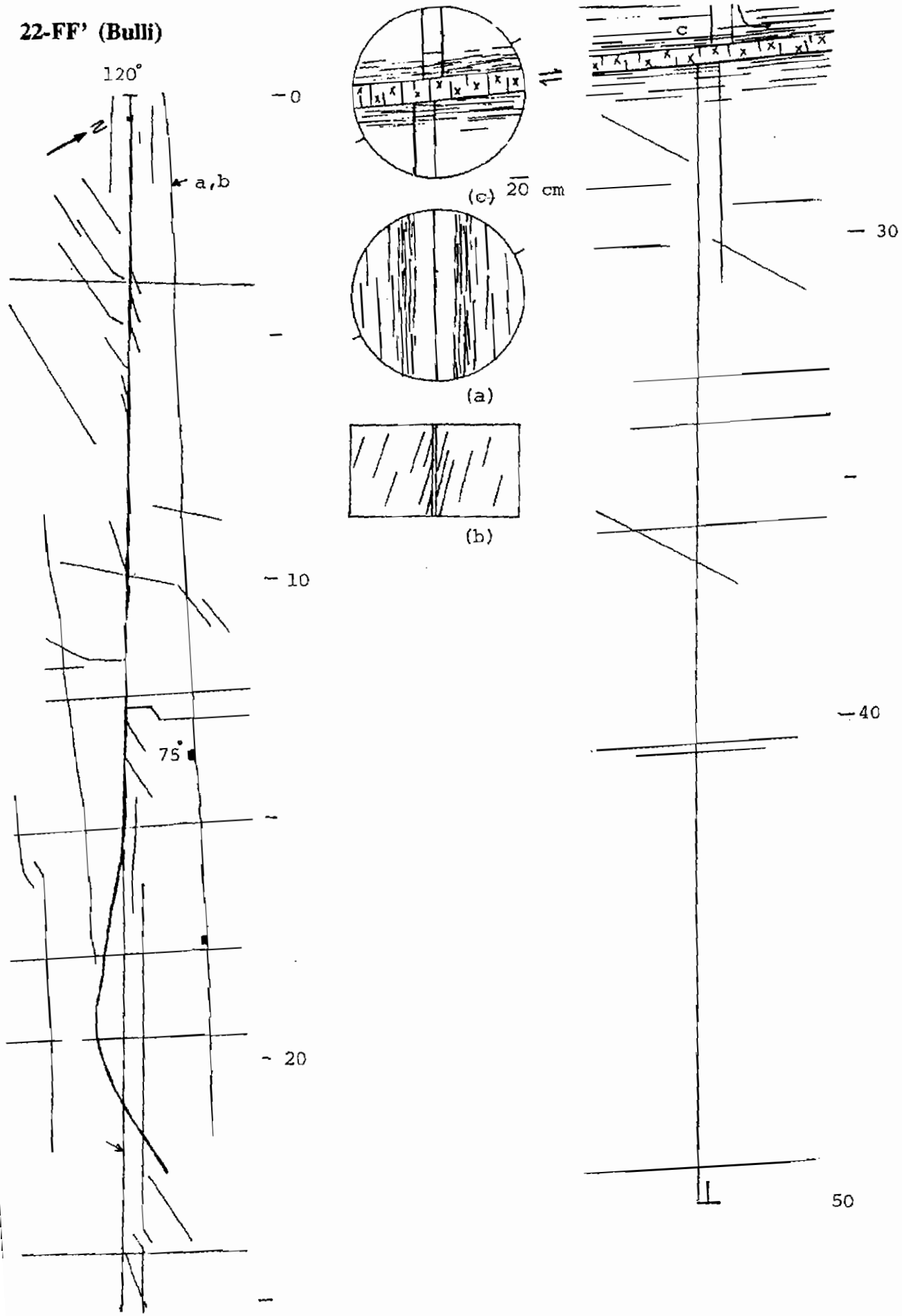

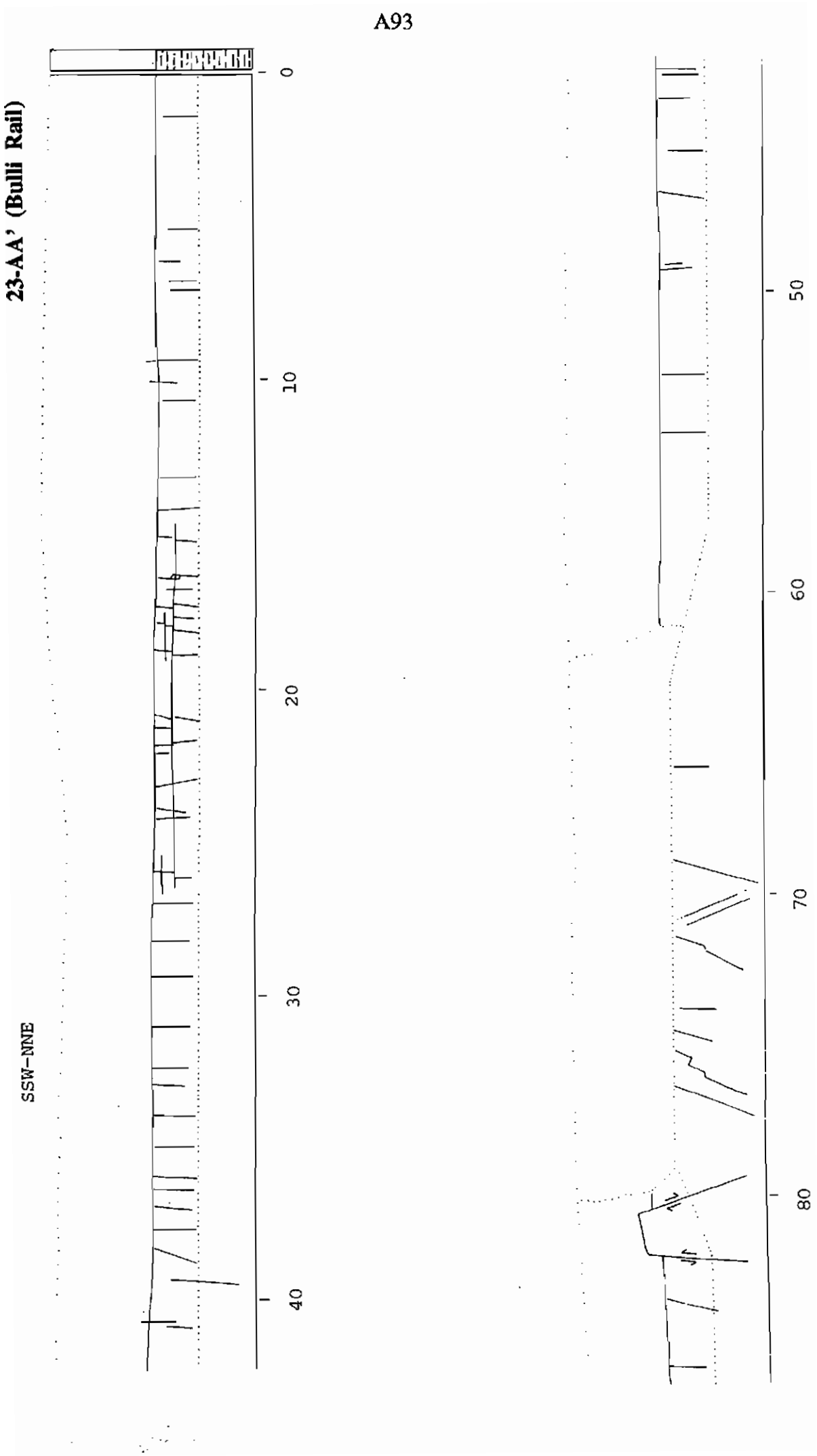
23-AA' (Bulli Rail)
SSW-NNE
0
10
20
30
40
50
60
70
80

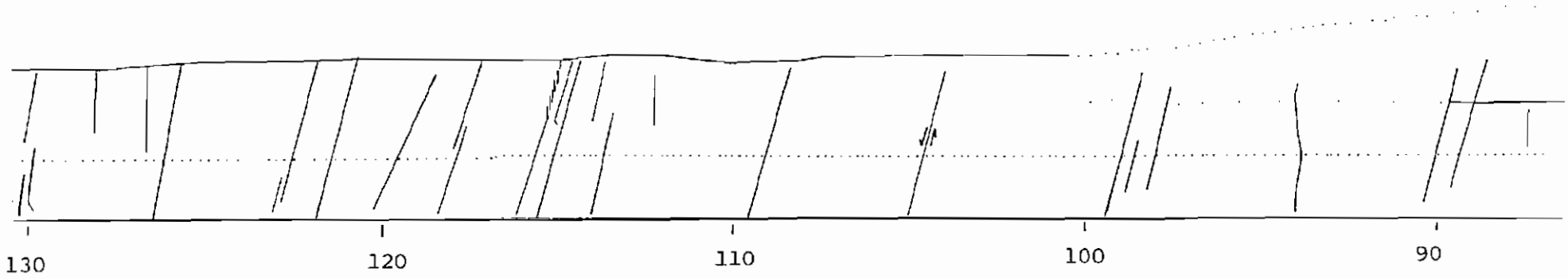
130
120
110
100
90

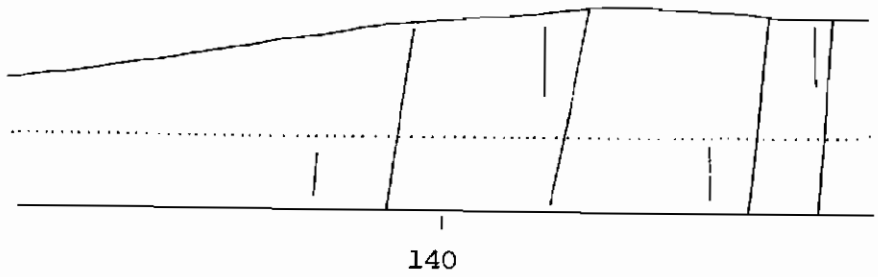
140

25-AA' (Woonona)

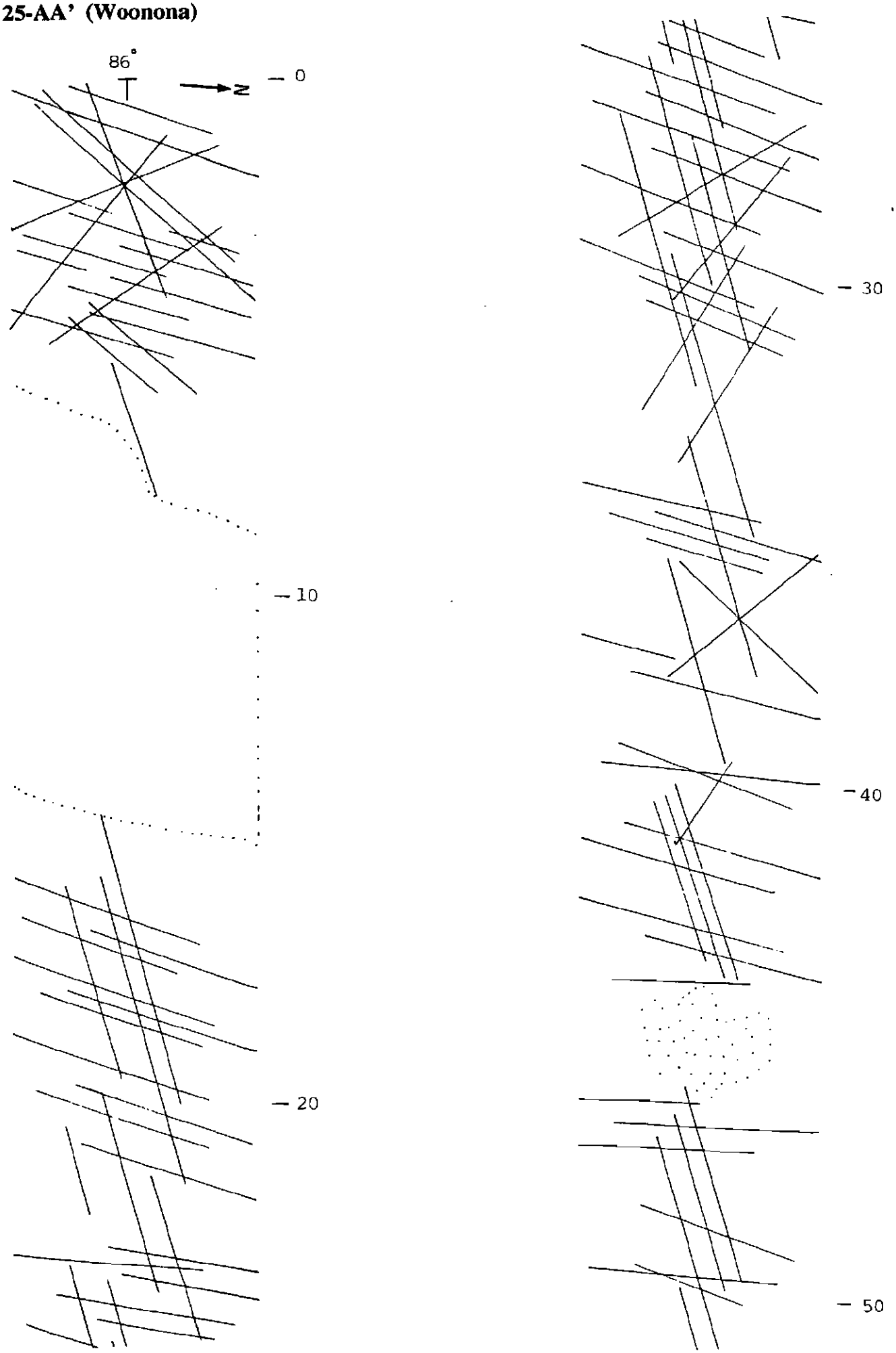

25-AA' cont.

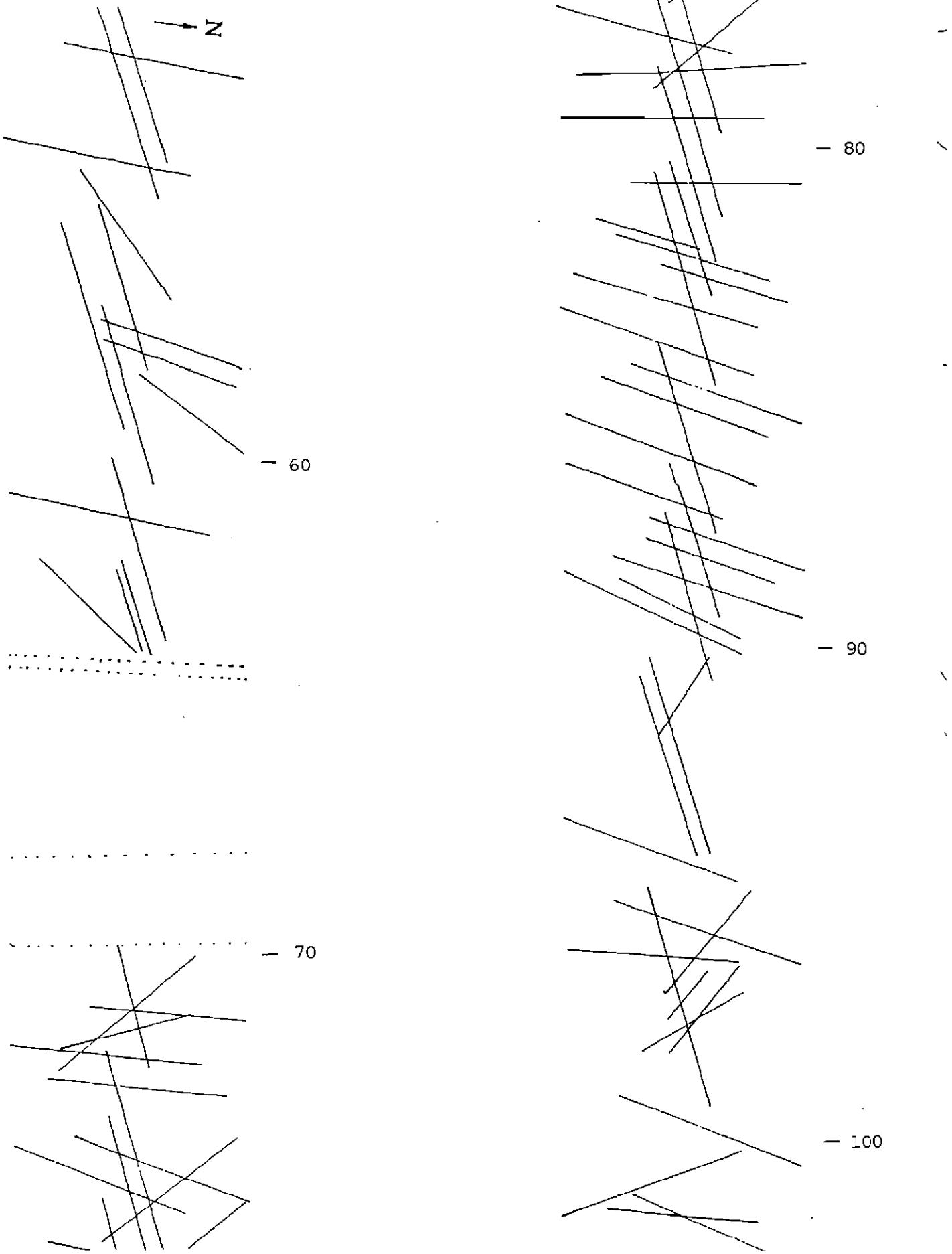

25-AA' cont.

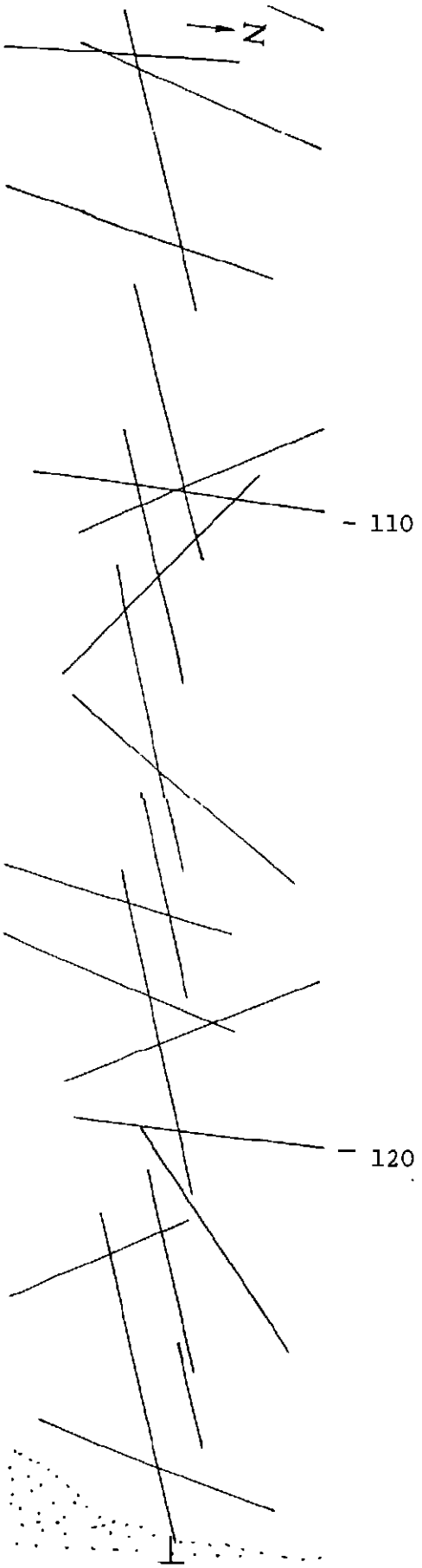

25-BB' (Woonona)

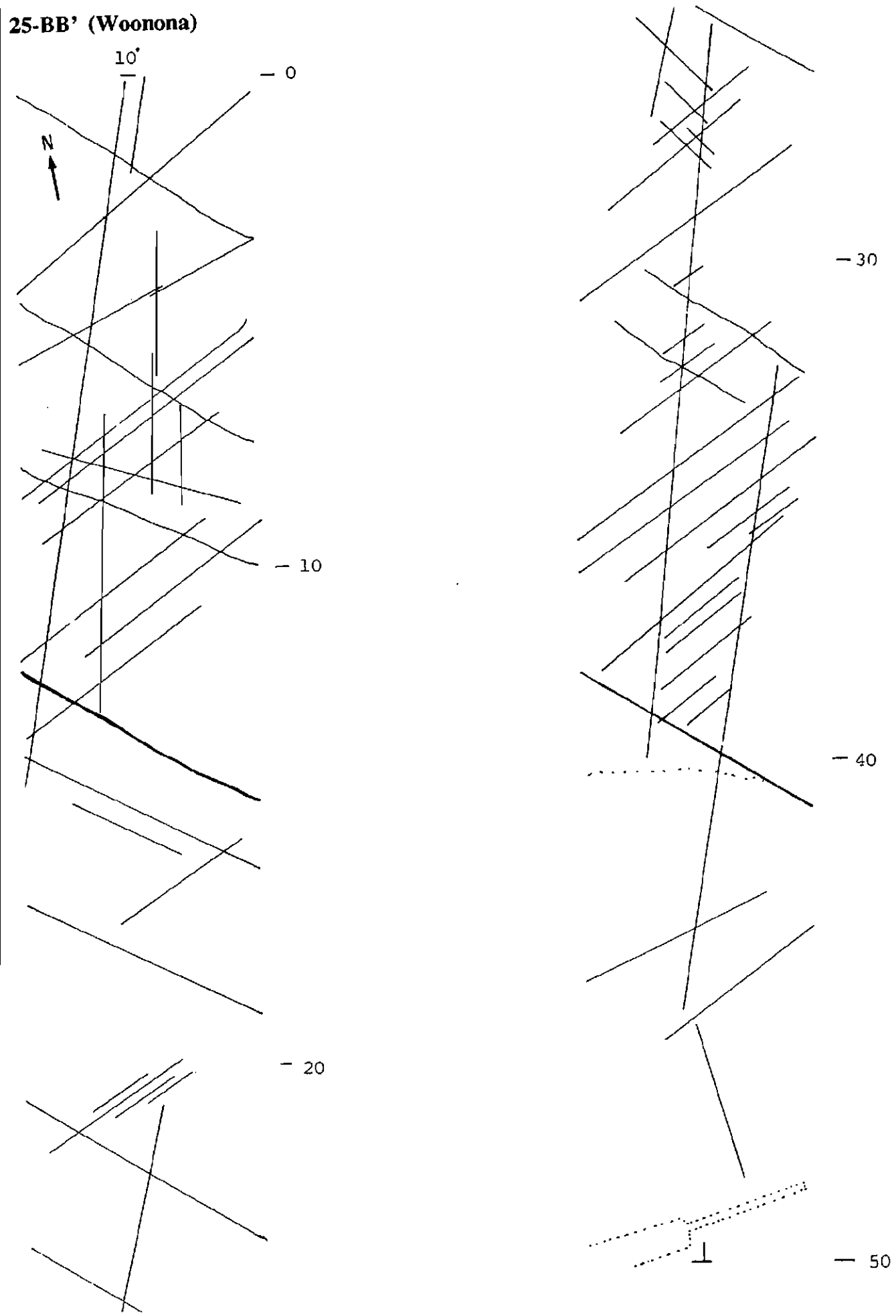

25-CC' (Woonona)

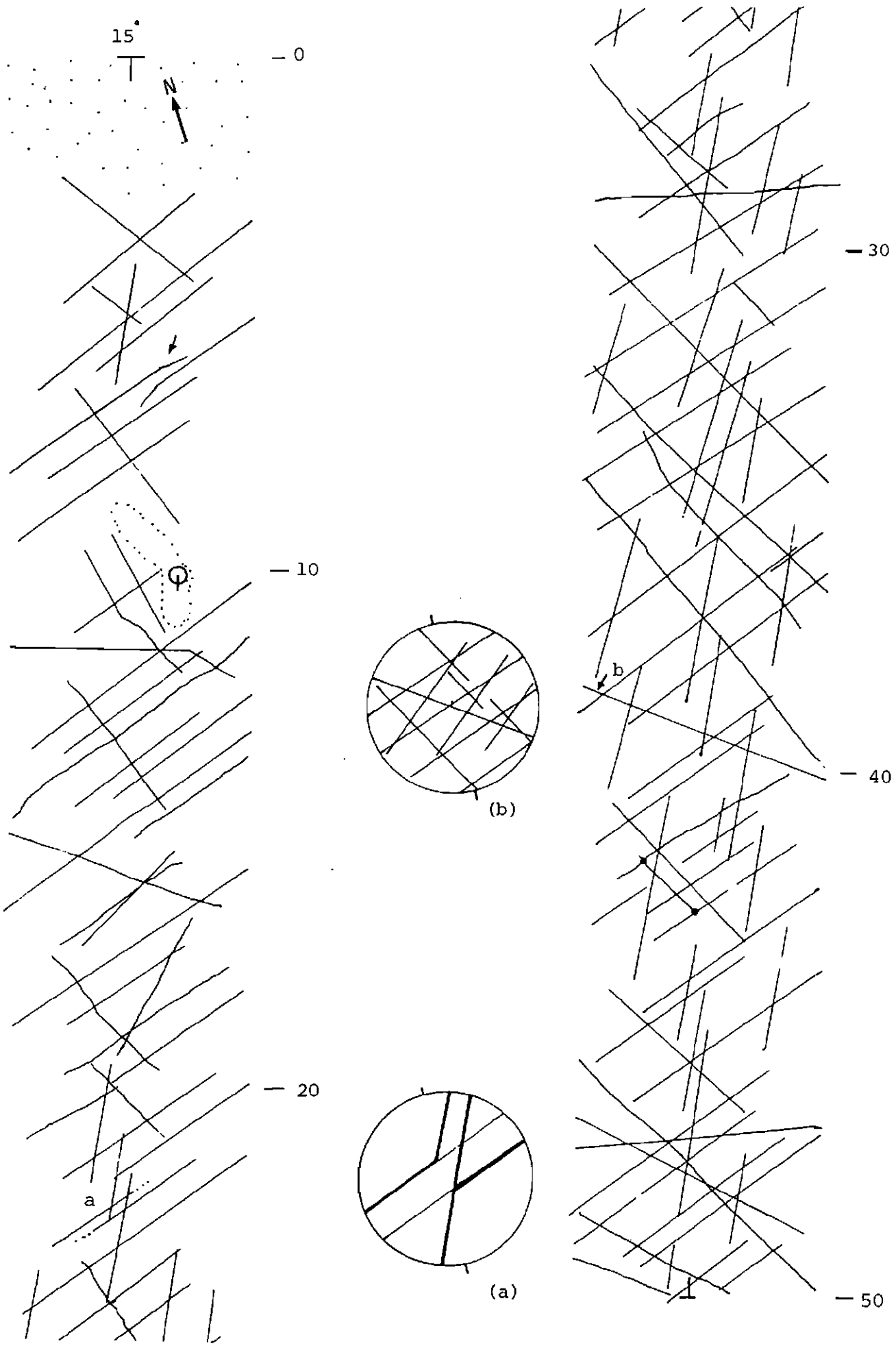

26-AA' (Bellambi)